HAL
open science

Tectono-stratigraphic evolution of the northern margin of the Amu-Darya basin in Uzbekistan (Bukhara-Khiva and Southwestern Gissar regions)

Dmitriy Mordvintsev

To cite this version:

Dmitriy Mordvintsev. Tectono-stratigraphic evolution of the northern margin of the Amu-Darya basin in Uzbekistan (Bukhara-Khiva and Southwestern Gissar regions). Earth Sciences. Université Pierre et Marie Curie - Paris VI, 2015. English. NNT : 2015PA066198 . tel-01559824

HAL Id: tel-01559824

https://theses.hal.science/tel-01559824v1

Submitted on 11 Jul 2017

HAL is a multi-disciplinary open access archive for the deposit and dissemination of scientific research documents, whether they are published or not. The documents may come from teaching and research institutions in France or abroad, or from public or private research centers.

L'archive ouverte pluridisciplinaire **HAL**, est destinée au dépôt et à la diffusion de documents scientifiques de niveau recherche, publiés ou non, émanant des établissements d'enseignement et de recherche français ou étrangers, des laboratoires publics ou privés.

Université Pierre et Marie Curie

Ecole doctorale (398)

Géosciences, Ressources Naturelles et Environnement

Institut des Sciences de la Terre de Paris

Tectono-stratigraphic evolution of the northern margin of the Amu-Darya basin in Uzbekistan (Bukhara-Khiva and Southwestern Gissar regions)

Par : **Dmitriy Mordvintsev**

Thèse de doctorat de l'Université Pierre et Marie Curie

Spécialité : Géosciences et ressources naturelles

Dirigée par Marie-Françoise Brunet et Eric Barrier

Présentée et soutenue publiquement le 9 juillet 2015

Devant un jury composé de :

M. Christian Blanpied	TOTAL S.A.	Examinateur
M. Sébastien Castelltort	Dpt. Earth Sciences Univ. Genève	Rapporteur
M. Philippe Huchon	ISTeP UPMC	Examinateur
Mme. Irina Sidorova	Geology Geophysics Institute Tashkent	Examinatrice
M. Marc Sosson	GéoAZUR CNRS-Univ. Nice-Sophia Antipolis	Rapporteur
Mme Marie-Françoise Brunet	ISTeP CNRS-UPMC	Directrice de thèse
M. Eric Barrier	ISTeP CNRS-UPMC	Directeur de thèse

Acknowledgements

Before to start doing my Ph.D. thesis in the University of Pierre and Marie Curie, I even did not dream, that once I will be in such great place as the Sorbonne is. But this would not be possible without help and support of a lot of people. And I would like to thank all of them. But how to say "thank you" if you need to thank so many people?

At first these are my directors Marie-Francoise Brunet and Eric Barrier. And my first sincere gratitude is for Mme. Brunet for her patience and kindness with me (as I was a hard student), for her limitless knowledge of all geological domains, which she tried to give me and her amazing attention even to the small details, which has risen my thesis to a high level of the European standards. Another "thank you" is for M. Barrier for his knowledge and energy, which he gave me on the long way to the end of the thesis.

Also I would like to thank my Uzbekistan co-director, senior scientist of the "Geology and Geophysics Institute" Irina Sidorova for her assistance and heavy support in my Uzbekistan part of the thesis.

I say "thank you" to my French and German colleagues Raphael Bourillot and Franz Fürsich for all that experience, which they have given me during our common fieldworks in the Southwestern Gissar Mountains.

I thank M. Christian Blanpied and Hermann Munsch from the "Total" company for their wise advices in the geophysical part of my work.

Another gratitude is for the "Total" company at all, as it has funded my thesis. I am really grateful to the University of Pierre and Marie Curie for my accommodation and, anyway, I was really proud to be a student of it.

I also would like to gratitude the team of the "Quai de la Loire" residence, as they have given me a place to live during my work period in Paris.

M. Vitaliy Troitsky, the professor of the "Russian Oil and Gas Academy, named after Gubkin", my old teacher, also gets my gratitude for his advises and assistance in the sphere of the global tectonic and the Southern Tien-Shan tectonic development.

I thank a lot the members of the jury, as they have spent their time "judging" me and my thesis, especially Sébastien Castelltort and Marc Sosson to have accepted to review my work and Philippe Huchon to examine it.

Another big thank I send to the chief of geophysical department of the "National University of Uzbekistan" Dilshod Atabaev for his assistance and support. It would be fair to thank all the geological faculty of this University for all knowledge, I have obtained there during my study.

My gratitude also goes to the members of the department of experiments and methods of the "Uzbekgeofizica" company for their assistance in the data collection and to the laboratory of "Oil and gas objects" of the "Oil and Gas Institute" for their help with the Lower-Middle Jurassic stratigraphy of the Bukhara-Khiva region.

I also would like to thank the direction of the "Geology and Geophysics Institute" and personally vice-director Bakhtiyar Nurtaev, for their support and assistance to me in Uzbekistan. I thank Ilya Kremnev, senior scientist of this Institute for his help with the work in the Central Geological Archives.

One more my gratitude is for all my friends, who has supported me and believe in me and my success.

And at last, but not least, I would like to express my gratitude to my parents, who believe in me, who support me and who loved me all my life. And a special thank for my father, who has left us in 2013, but who was one of the cleverest geophysics, I have ever known. And I would like to dedicate this thesis to the memory of my father.

ABSTRACT: Tectono-stratigraphic evolution of the northern margin of the Amu-Darya basin in Uzbekistan (Bukhara-Khiva and Southwestern Gissar regions)

by Dmitriy MORDVINTSEV

The main aim of this thesis is reconstructing the tectono-stratigraphic evolution of the northern margin of the Amu-Darya basin and northwestern part of the Afghan-Tajik basin in southwestern Uzbekistan (Bukhara-Khiva and Southwestern Gissar regions).

For these works, we have investigated the Southwestern Gissar range, subsurface data of the Bukhara-Khiva region (seismic and well data), and isopachs and isohypse maps.

The most interesting part of the evolution is registered by the Mesozoic sedimentary sequence. This complete section is composed at the base of an undifferentiated unit of Permian-Triassic rocks, not identified in our work, a Lower-Middle Jurassic terrigenous unit, a Middle-Upper Jurassic carbonate unit, an Upper Jurassic evaporite unit and the Cretaceous-Cenozoic sediments. In our study, we focused on the Jurassic system, which constitutes a complete petroleum system.

The first part of this work is dedicated to the geological-tectonic structure of the Bukhara-Khiva region. This area consists of two main tectonic steps – the Bukhara step in the north-east and the Chardzhou step in the south-west. These steps are separated by the south-east oriented Uchbash-Karshi Flexure-Fault Zone, which is a huge tectonic break.

A lot of geological-geophysical data enlightens the structure of the region. We have used seismic time sections, well data and isohypse maps for the construction of 8 geological-geophysical sections. Two lines are running parallel to the Bukhara and Chardzhou steps from the north-west to the south-east. The other six lines cross these steps from the north to the south.

On these lines, we distinguish the principal features of the following surfaces: the pre-Mesozoic, the terrigenous Jurassic, the carbonate Jurassic, the evaporite sequence of the Upper Jurassic and the Cretaceous. The main faults, highs and lows were also determined. Schemes of the lithological-facial regionalization for each unit (terrigenous, carbonate and evaporite) have been constructed. An important object, which influenced the sedimentation in the area, is a Middle-Upper Jurassic reef system that probably grew on tectonic highs.

Another part of the study is the tectonic subsidence analysis, performed through 15 wells of the Bukhara-Khiva region, and 3 of Southwestern Gissar. We present and discuss the detailed data for each well. The comparison of the tectonic subsidence rates shows an active tectonic subsidence during the late Early Jurassic to Middle Jurassic, and minor events during the Early Cretaceous and the Turonian.

The third part of the work concerns the fault tectonic analysis. This part of the thesis includes fieldworks, which we have performed in the Southwestern Gissar Mountains. We mainly analysed the faults population in the Middle-Late Jurassic carbonates. The results indicate that normal faulting developed during the Mid-Late Jurassic associated with the NE-trending extension that developed in the northern margin of the Amu Darya basin.

Finally, in the last part we synthetize and discuss the results of our study of the Bukhara-Khiva and Southwestern Gissar regions. The tectono-stratigraphic evolution of the northern margin of the Amu-Darya basin is expressed and linked with the Southwestern Gissar and northwestern part of the Afghan-Tajik basin. These areas are replaced in the general Mesozoic geodynamic context of the evolution of the northern margin of the Tethys domain.

All of the results show that the Amu-Darya basin evolution is strongly connected to the Mesozoic development of the northward subduction of the Tethys Oceanic domain beneath the Central Asia margin. During the Jurassic, after the final closure of the Paleo-Tethys Ocean, the northward subduction of the Neo-Tethys beneath Eurasia generated extensional stress fields in the overriding Turan platform which originated the Amu-Darya basin.

Résumé: Evolution tectono-stratigraphique de la marge nord du bassin de l'Amou-Daria en Ouzbékistan (régions de Boukhara-Khiva et du sud-ouest Ghissar)

par Dmitriy MORDVINTSEV

L'objectif principal de cette thèse est la reconstruction de l'évolution tectonique et stratigraphique de la marge nord du bassin de l'Amou-Daria et du nord-ouest du bassin Afghan-Tadjik dans le sud-ouest de l'Ouzbékistan (régions de Boukhara-Khiva et du sud-ouest Ghissar).

Nous avons utilisé dans ce travail les données géologiques de terrain collectées dans le sud-ouest Ghissar, des données de subsurface de la région de Boukhara-Khiva (données sismiques et puits), et des cartes d'isopaques et d'isohypses.

L'évolution tectono-sédimentaire de la marge nord de l'Amou-Daria est enregistrée par la série sédimentaire Mésozoïque. Cette série complète est composée : d'une séquence indifférenciée du Permo-Trias à la base non identifiée dans notre travail, d'une unité terrigène du Jurassique inférieur à moyen, d'une unité de carbonates d'âge Jurassique moyen-supérieur, d'une unité évaporitique du Jurassique supérieur et des sédiments du Crétacé-Cénozoïque. Dans notre étude, nous nous sommes concentrés sur le Jurassique, qui constitue un système pétrolier complet.

La première partie de ce travail est consacrée à la structure géologique et tectonique de la région de Boukhara-Khiva. Cette zone qui constitue la marge septentrionale du bassin de l'Amou-Daria est composée de deux grandes zones – la zone de Boukhara au nord-est et la zone de Chardzhou au sud-ouest, séparées par la zone de faille d'Uchbash-Karshi, qui est un important accident tectonique d'orientation NW-SE.

Un grand nombre de données géologiques et géophysiques ont été étudiées. Elles nous informent sur la structure de la région. 8 coupes géologiques et géophysiques ont été reconstruites à partir de sections sismiques et de cartes d'isohypses. Deux de ces coupes, orientées NW-SE sont parallèles aux zones de Boukhara et Chardzhou, les six autres coupes, orientées N-S coupent ces zones perpendiculairement aux principales structures de la marge.

Sur ces coupes, les principaux réflecteurs ont été caractérisés: le pré-Mésozoïque, les toits du Jurassique terrigène, du Jurassique carbonaté, des évaporites du Jurassique supérieur et du Crétacé. Les failles principales, les hauts et dépressions ont également été déterminés. Des schémas de la répartition des faciès ont été construits pour chaque unité (terrigène, carbonates et évaporites). Un élément important qui a influencé la sédimentation dans la marge est un système récifal qui s'est développé au Jurassique moyen-supérieur. Les alignements de récifs semblent en partie se superposer aux failles normales qui structurent la marge septentrionale du bassin de l'Amou-Daria.

La seconde partie de la thèse est consacrée à l'analyse de la subsidence, réalisée à partir de 15 puits de la région de Boukhara-Khiva et de 3 puits du sud-ouest Ghissar. Nous présentons et discutons les données utilisées pour chaque puits. La comparaison des taux de subsidence montre une phase tectonique principale active pendant le Jurassique inférieur et moyen et des événements mineurs au cours du Crétacé inférieur ainsi qu'au Turonien.

La troisième partie de la thèse porte sur une analyse de tectonique cassante. Cette partie comprend des travaux de terrain dans la chaîne du sud-ouest Ghissar. Des populations de failles ont été mesurées dans les carbonates du Jurassique moyen-supérieur. Les résultats indiquent que les failles normales sont associées à une extension de direction NE qui s'est développée dans la marge nord du bassin de l'Amou-Daria au cours du Jurassique moyen supérieur.

La dernière partie est une synthèse des résultats qui sont discutés et replacés dans le cadre de l'évolution régionale du domaine téthysien au Mésozoïque. L'évolution tectono-stratigraphique de la marge nord du bassin de l'Amou-Daria est décrite ainsi que ses liens avec le sud-ouest Ghissar et la partie nord-ouest du bassin Afghan-Tadjik. Nos résultats montrent que l'évolution du bassin de l'Amou-Daria est liée au développement de la marge nord de l'océan néo-téthysien au Mésozoïque. La fermeture définitive de la paléo-Téthys et l'accrétion des blocs cimmériens au Trias ont provoqué un saut de la subduction vers le sud. La subduction vers le nord de la Néo-Téthys sous la marge méridionale de l'Eurasie a induit un régime extensif dans la plaque chevauchante et l'ouverture de bassins sédimentaires dont le bassin de l'Amou-Daria.

Content

Acknowledgements I
Abstract III
Résumé IV
Content V

Foreword 1

Chapter 1 The Bukhara-Khiva and Southwestern Gissar regions: Overview 3

1.1. Geographic framework 5

1.2. Regional geological structures 6

1.3. Previous works 13

1.4. Late Paleozoic tectonics 15

1.5. The Pre-Mesozoic structures in the Bukhara-Khiva and Gissar regions 18

1.6. Examples of reconstruction of Central Asia evolution during the Paleozoic 20

1.7. Conclusion 26

Chapter 2. Deposits of the Bukhara-Khiva and Southwestern Gissar regions 27

2.1. General setting 29

2.2. Pre-Jurassic 30

2.2.1. Southwestern Gissar 30
2.2.1.1. Lower Cambrian 30
2.2.1.2. Carboniferous 30
2.2.1.3. Permian 31
2.2.2. Bukhara-Khiva region 31
2.2.2.1. Pre-Cambrian to Devonian 31
2.2.2.2. Carboniferous 32
2.2.2.3. Permian-Triassic 32

2.3. Jurassic 35

2.3.1. Terrigenous unit 39
2.3.1.1 Lower Jurassic - Toarcian (Sanjar Formation) 42
2.3.1.2. Aalenian-Lower Bajocian (Gurud Formation) 45
2.3.1.3. Upper Bajocian (Degibadam Formation) 47
2.3.1.4. Lower Bathonian (Tangiduval Formation) 51
2.3.1.5. Middle Bathonian-Lower Callovian (Baysun Formation) 51
2.3.2. Carbonate unit 54
2.3.2.1. Middle Callovian (Kandim Formation or XVI horizon) 57
2.3.2.2. Upper Callovian-Middle Oxfordian (Mubarek Formation or XV-a and XV-UR horizons) 57
2.3.2.3. Upper Oxfordian-Kimmeridgian (XV, XV-R and XV-AR horizons) 59

2.3.2.3.1. Barrier reef system model 60
2.3.2.3.2. Reefal type (Urtabulak and Kushab formations) 62
2.3.2.3.3. Lagoonal type (Gardarya Formation) 66
2.3.2.3.4. Basinal type (Khodjaipak Formation) 68
2.3.3. Evaporite or salt-anhydrite unit (Tithonian Gaurdak Formation) 72
2.4. Cretaceous 75
2.4.1. Lower Cretaceous 75
2.4.2. Upper Cretaceous 77
2.5. Cenozoic 79
2.5.1. Paleogene 79
2.5.2. Neogene 81
2.5.3. Quaternary 82
2.6. Petroleum systems 82
2.6.1. Petroleum resources in Uzbekistan 82
2.6.2. Petroleum system 84
2.6.2.1. Source rocks 84
2.6.2.2. Reservoir rocks 85
2.6.2.3. Seal rocks 86
2.6.2.4. Trap types 86
2.7. Conclusion 88
Chapter 3. Geological-geophysical sections through the Bukhara-Khiva region 89
3.1. Methodology 91
3.2. NE-trending geological-geophysical lines through the Bukhara and Chardzhou steps 96
3.2.1. Line A-A' 96
3.2.2. Line B-B' 100
3.2.3. Line C-C' 104
3.2.3.1. Line 01970595 in the Bukhara step 105
3.2.3.2. Line 51880688 in the Chardzhou step 106
3.2.4. Line D-D' 110
3.2.5. Line E-E' 112
3.2.6. Line F-F' 117
3.3. NW-trending geological lines parallel to the Bukhara and Chardzhou steps 118
3.3.1. Line G-G' 119
3.3.2. Line H-H' 123
3.4. Review of the features along the sections 126
3.4.1. Review of the Jurassic thickness 126
3.4.1.1. Jurassic terrigenous unit 126
3.4.1.2. Jurassic carbonate unit 127
3.4.1.3. Jurassic evaporite unit 131
3.4.2. Review of the lithology. 132
3.4.2.1. Terrigenous unit 132
3.4.2.2. Carbonate unit 133

3.4.2.3. Salt-anhydrite unit 137

3.5. Conclusions 137

Chapter 4. Tectonic subsidence analysis 141

4.1. Methodology 143

4.1.1. What is the tectonic subsidence? 143

4.1.2. Method of subsidence reconstruction 144

4.2. Subsidence reconstructions for some wells of the Bukhara-Khiva and Southwestern Gissar regions 149

4.2.1. Yangikazgan-Baymurad western area 153

4.2.1.1. Yangikazgan 10 well 153

4.2.1.2. Ashikuduk 1 well 157

4.2.1.3. Baymurad 1 well 159

4.2.2. Kimerek-Chandir area 162

4.2.2.1. Synthetic well 1 165

4.2.2.2. Kimerek 4 well 167

4.2.2.3. Khodji 1 well 171

4.2.2.4. Chandir 2 well 174

4.2.3. Divalkak-South Alan area 176

4.2.3.1. Buzatchi 2 well 179

4.2.3.2. Karim 2 well 182

4.2.3.3. Synthetic well 2 184

4.2.3.4. Divalkak 1 well 187

4.2.3.5. Kruk 1 well 189

4.2.3.6. Pirnazar 2 well 192

4.2.3.7. South Alan 2 well 195

4.2.4. Shurtan-Amanata, eastern area 198

4.2.4.1. Shurtan 25 well synthetic column 201

4.2.4.2. South Tandircha 14 well 204

4.2.4.3. Pachkamar 3 well 207

4.2.4.4. Amanata 3 well 210

4.3. Correlations of the studied wells and comparison of the tectonic subsidence rates 212

4.3.1 Correlations of the Jurassic thicknesses and subsidence events 212

4.3.2 Correlation of the wells columns for the Cretaceous 214

4.3.3 Correlations of the thicknesses and subsidence events during the Mesozoic and Cenozoic 216

4.4 Evolution of the tectonic subsidence during the Meso-Cenozoic 218

Chapter 5. Fault tectonic analysis 223

5.1. Methodology 225

5.1.1. Paleostress reconstructions 225

5.1.2. Methods of analysis of a population of faults 227

5.1.3. Fault slip analysis and measurements 228

5.1.3.1. Dating of meso-scale faults 228

5.1.3.2. Conjugate system of fault population 230

5.1.3.3. Faults and displacements indicators 233
5.2. Field study 236
5.2.1. Area of investigation: the Southwestern Gissar region 236
5.2.2. Field work: the fault sites 236
5.3. Study of the sites 240
5.3.1. Langar 240
5.3.2. Derbent 241
5.3.3. Sayrob 243

Chapter 6. Mesozoic-Cenozoic evolution of the northern margin of the Amu-Darya basin 247

6.1. Pre-Jurassic evolution: the Late Paleozoic and Triassic tectonics 249
6.1.1. The Late Paleozoic collages and the mosaic of blocks 249
6.1.2. The basement of the Amu-Darya and Tajik basins 250
6.1.3. The Late Permian – Triassic post-orogenic rifts 251
6.1.4. The Middle-Late Triassic Cimmerian orogeny 252
6.2. Early-Middle Jurassic rifting 253
6.2.1. Syn-rift sedimentation 253
6.2.2. Early-Middle Jurassic Rifting 255
6.2.3. The Amu-Darya basin: an Early-Middle Jurassic extensional basin 256
6.3. Middle-Late Jurassic post-rift evolution 257
6.4. Cretaceous – Paleogene evolution 259
6.4.1. Early Cretaceous tectonostratigraphy 259
6.4.2. Late Cretaceous-Paleogene subsidence 261
6.5. Neogene Pamir orogeny 262
6.6 Conclusion 264

References 265

Foreword

The northern margin of the Amu-Darya basin, the Bukhara-Khiva and Southwestern Gissar regions, is an interesting area of Central Asia from a geological point of view. The main interest is the existence of significant oil and gas resources in this region. In Uzbekistan the Bukhara-Khiva region is a rich oil and gas province where hydrocarbon explorations initiated as early as the fifties.

Besides this economical aspect, the geological structure of this area is interesting too, especially for the general understanding of the tectonic and stratigraphic evolution of the Amu-Darya and Tajik basins during the Mesozoic. The regional evolution since the Paleozoic is complex and polyphase and different models of Mesozoic tectono-stratigraphic evolution have been proposed. The Mesozoic basins developed on a Hercynian basement constituted of accreted terranes composed of deformed Paleozoic rocks.

This work was integrated in a larger interdisciplinary program (Northern Tethys) dealing with the geological evolution of western Central Asia. This program was funded by Total. In Uzbekistan the activity of the Northern Tethys program also included field investigations of the Mesozoic sequence in Southwestern Gissar in the fields of stratigraphy and sedimentology.

In this work we target to answer and discuss the most important questions concerning the long and polyphase evolution of the northern margin of the Amu-Darya basin. Using a combination of geological-geophysical data and methods we propose a reconstruction of the tectono-stratigraphic evolution of the Bukhara-Khiva and Southwestern Gissar regions during the Mesozoic, and more particularly during the Jurassic.

The first chapter presents the area of investigation in terms of geography, geology, geodynamics, and petroleum systems. It contains a review of the geological and geophysical works, on scales ranging from the whole western Central Asia to the northern margin of the Amu-Darya basin. We have paid a particular attention to the different models of tectono-stratigraphic evolution of the basin. Many interpretations have been proposed for the Paleozoic evolution. We present and discuss the main ideas of the literature, especially in the domains of tectonics and stratigraphy.

The second chapter deals with the deposits over the area, particularly with the stratigraphy, lithology of the Mesozoic. It provides abundant details for a better understanding of the relationships between the different Mesozoic geological units. We describe the three main Mesozoic stratigraphic units, with a particular attention to the Jurassic ones constituting the main petroleum system in the Amu-Darya and Tajik basins. This chapter includes many published and unpublished data including maps of the pre-Mesozoic structure, of the thickness of the Jurassic terrigenous, carbonate units, and of the structure of the Jurassic reefal system. In addition, several stratigraphic columns reflecting the different points of view on the Jurassic stratigraphy are shown.

The third chapter is dedicated to the reconstructed geological-geophysical lines crossing the Bukhara-Khiva region. Four lines out of six perpendicularly cross the Bukhara and Chardzhou steps, while the two remaining lines are parallel to these steps. In this chapter we present a brief analysis of the thickness variations of the Jurassic units in the Bukhara and Chardzhou steps. The study of the lines allowed us to determine the main normal faults active during the Jurassic times and to specify the age of faulting. Some correlations between the Jurassic reefal system evolution and the Jurassic normal faulting are presented, as well as its influence on the sedimentary processes.

The subsidence processes are studied in Chapter 4. 18 wells have been chosen to analyse the subsidence in the Bukhara-Khiva and Southwestern Gissar areas. Detailed information is given about the data used to study the subsidence of each well and of its surrounding area. The periods of main tectonic events observed for each well are described and correlated between the wells in each of our three large domains: the Bukhara and Chardzhou steps with respectively 6 wells and 9 wells analysed and the Southwestern Gissar with 3 wells studied. Two main periods of active tectonic subsidence linked to extension are identified during the Mesozoic: the main one during the Early-Middle Jurassic

and the second one during the Early Cretaceous, a Turonian event is also evidenced. We discuss the timing of these tectonic events which will be replaced in the geodynamic context in the Chapter 6.

Chapter 5 concerns the paleostress analysis. A short brittle tectonic analysis was performed in the Southwestern Gissar mountains. The Middle-Late Jurassic carbonate unit was investigated in order to evidence syn-depositional normal faulting.

Finally, in Chapter 6 we synthetize and discuss the results of our study of the Bukhara-Khiva and Southwestern Gissar regions. The tectono-stratigraphic evolution of the northern margin of the Amu-Darya basin will be expressed as well as its links with the Southwestern Gissar and the northwestern part of the Afghan-Tajik basin. These areas are replaced in the general Mesozoic geodynamic context of the evolution of the northern margin of the Tethys domain.

Chapter 1

The Bukhara-Khiva and Southwestern Gissar regions: Overview

Chapter 1

The Bukhara-Khiva and Southwestern Gissar regions: Overview

The area we study in this thesis, the Bukhara Khiva region and the Uzbek part of the Southwestern Gissar, is located in the northern part of the Amu-Darya basin, and partly in the northwestern part of the Afghan-Tajik basin. Before to consider the tectono-stratigraphic evolution of this domain, we will present the geography of the area and the geological-geodynamical context of Central Asia.

1.1. Geographic framework

The Amu-Darya basin is a large sedimentary basin of Central Asia mainly located in eastern Turkmenistan. The northern margin of this basin is in southern Uzbekistan, while the southern part is in northwestern Afghanistan (fig. 1.1). The main part of the basin (360 000 km^2 out of 400 000 km^2) is located in the Turkmen and Uzbek territories (Ulmishek, 2004). The Amu-Darya basin is parallelogram-shaped. It is bounded by the Kopet-Dagh fold belt in the southwest, the Kuldzhuktau Mountains in the north and the Southwestern Gissar in the east.

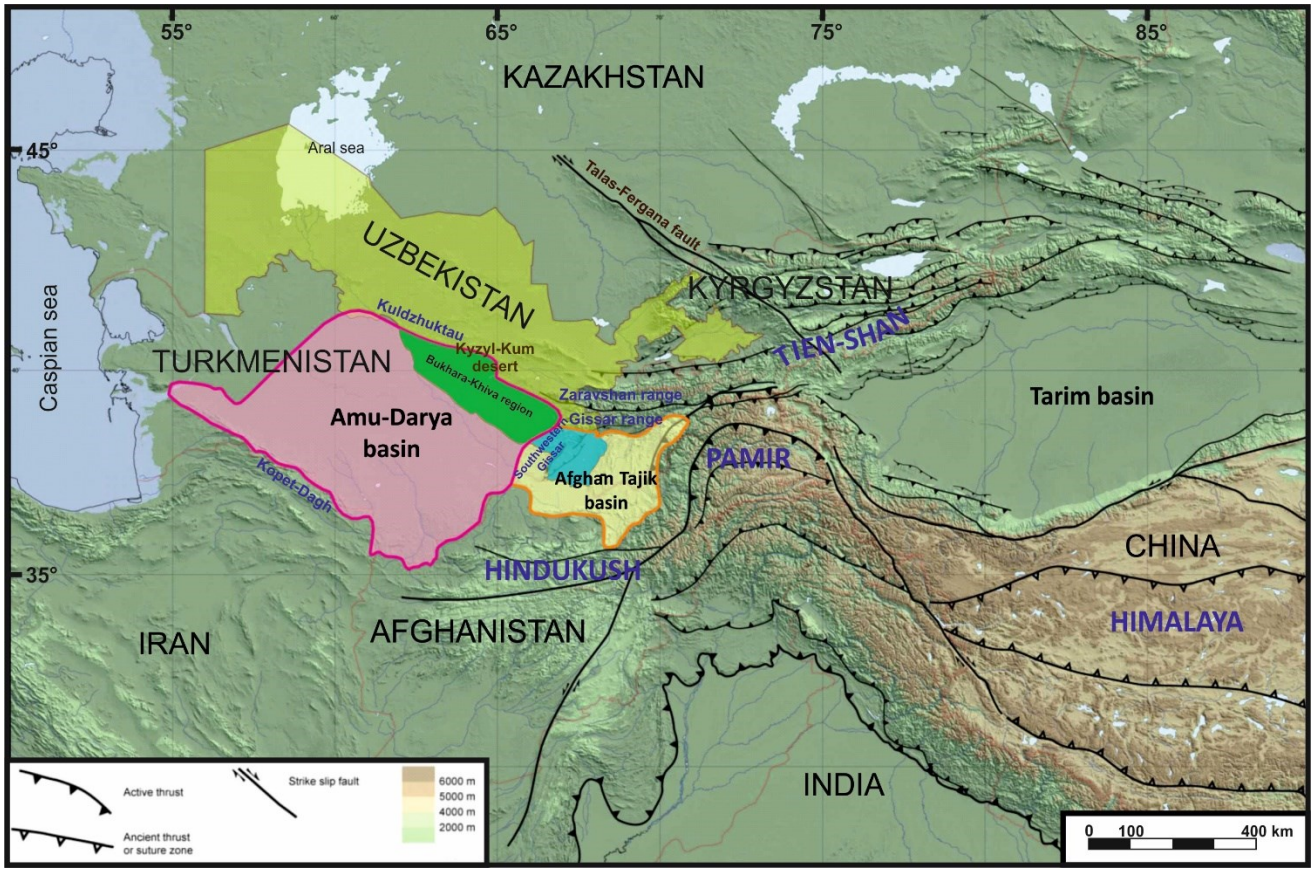

Fig. 1.1. Location of the Bukhara-Khiva and Southwestern Gissar regions in the Present-day geodynamic context of the Amu-Darya and Afghan-Tajik basins and Central Asia orogenic belts.

The Amu-Darya basin is connected to the southeast with the Tajik basin (also called Afghan-Tajik basin in the literature). This latter basin is surrounded by high mountains ranges, i.e. the Southwestern Gissar Range in the west, the Gissar Range (or western segment of the Southern Tien-Shan) in the north, the Pamir in the east, and the Hindu-Kush in the south (fig. 1.1). It covers an area of 100 000 km^2 on the Tajik, Uzbek and Afghan territories (Li, 2011). Most part of the Tajik basin belongs to Tajikistan and Afghanistan. Only a small part is located in Uzbekistan.

Our area of investigation is essentially located in the northern part of the Amu-Darya basin and marginally in the northwestern part of the Afghan-Tajik basin in Uzbekistan (fig. 1.1). It covers the Surkhandarya, Kashkadarya, and partly the Bukhara provinces of Uzbekistan (fig. 1.2). The provincial capitals are the cities of Termez, Karshi and Bukhara respectively.

Geographically, the southern Kyzyl-Kum desert occupies the majority of the Bukhara province. The Kashkadarya province is centred on the Kashkadarya River valley, on the western slope of the Pamir-Alay Mountains. The Surkhandarya province is mainly a mountainous region, bounded by the Gissar Range in the north, the Southwestern Gissar Range in the west and northwest, and the Babatag Ridge in the east. The southern part of the province is a flat land belonging to the Amu-Darya Valley.

The northeastern margin of the Amu-Darya basin in Uzbekistan includes two main domains: the Bukhara-Khiva region and the Southwestern Gissar Range. The Amu-Darya basin itself is mainly located southwestwards in Turkmenistan. The Bukhara-Khiva region, mainly known from sub-surface data, is constituted by two steps, which form the northeastern margin of the Amu-Darya basin (fig. 1.1, 1.2 and 1.4). The Southwestern Gissar Range is an uplifted margin of the Amu-Darya basin (fig. 1.1). It is a 200 km-long and 150 km wide NE-oriented range (fig. 1.1). The elevation of the crests ranges from about 2000 m in the southwest at the Uzbek-Turkmen border and increases towards the northeast to more than 4000 m near the Tajik border.

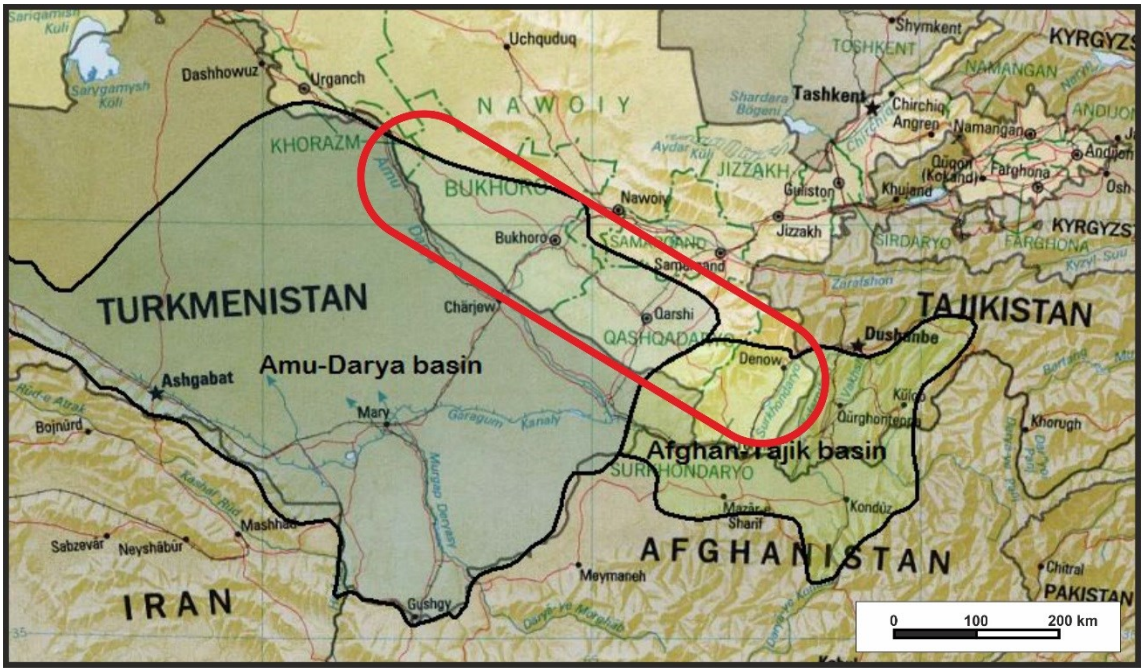

Fig. 1.2. Location of the Amu-Darya and Afghan-Tajik basins in the regional political contours including the administrative division of Uzbekistan (names in green; Qashqadaryo= Kashkadarya).

1.2. Regional geological structures

From a geological point of view the Bukhara-Khiva region corresponds to the northern margin of the Amu-Darya basin and the Southwestern Gissar marks the northern part of the boundary between the Amu-Darya and Afghan Tajik basins. We will provide here the main feature of these two basins before to focus on our area.

The Amu-Darya basin

The Amu-Darya basin is located in the southeastern part of the epi-Hercynian Turan Platform (fig. 1.3) extending westwards into the Caspian Sea and limited to the south by the Kopet Dagh and northwards by the Mangyshlak. To the northeast the boundary differs according to the authors: either it corresponds to the Turkestan suture (Thomas et al., 1999) or much to the north as on Figure 1.3 including a part of Altaids (Talwani et al., 1998; Natal'in and Şengör, 2005; some Russian authors).

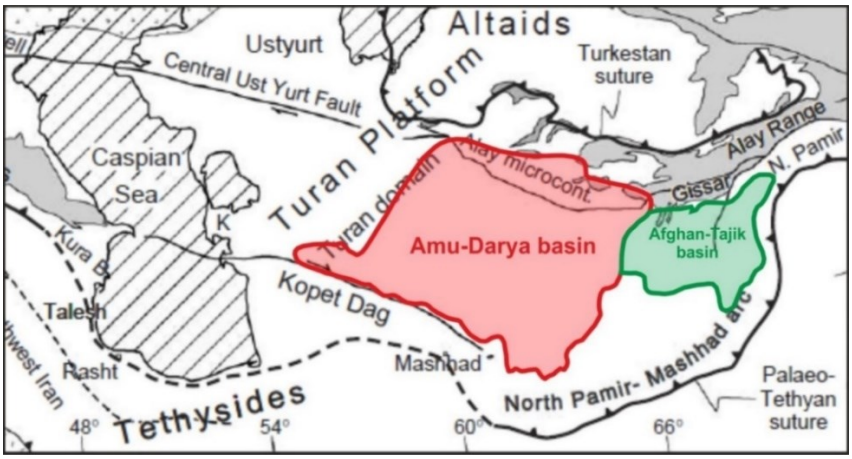

Fig. 1.3. The Amu-Darya and Afghan-Tajik basins in the main regional structures of Central Asia (modified after Natal'in and Şengör, 2005).

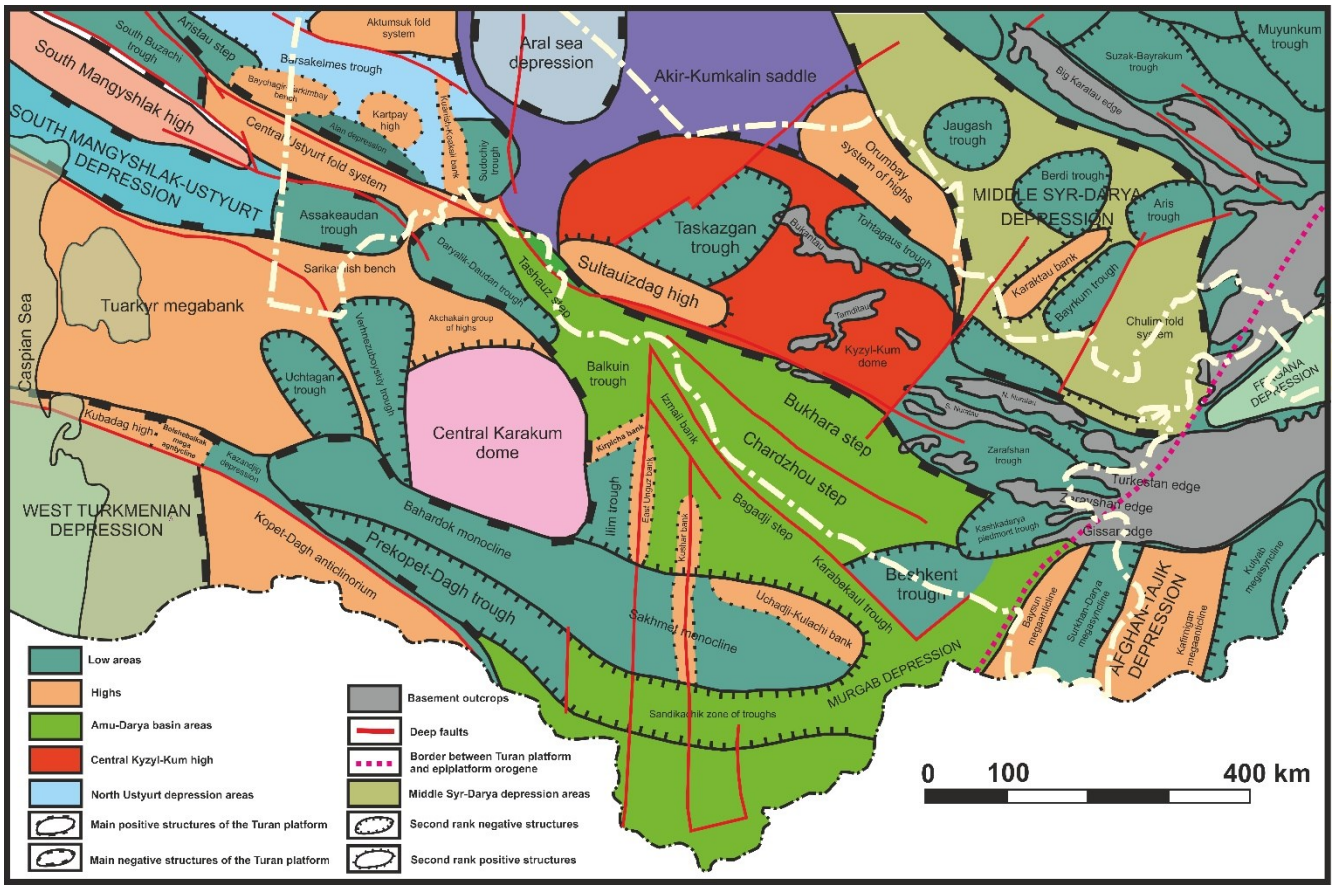

Fig. 1.4. Map of the main tectonic features of western Central Asia (modified after Babadjanov and Rubo, 1991)

The Amu-Darya basin is bordered to the west by the structures of the Balkhan and Tuarkyr which separate the basin from the Caspian Sea, to the southwest and south respectively by the Kopet-Dagh and Bande Turkestan fold belts and to the north by the Kyzyl Kum High (fig. 1.4, 1.5). The Southwestern Gissar marks the northern part of its eastern border, while the southeastern part is continuing into the Afghan-Tajik basin (fig. 1.4, 1.5).

Some papers of the english literature: Clarke (1988), Dyman et al. (1999), Thomas et al. (1999), Brookfield and Hashmat (2001), Ulmishek (2004), Brunet et al. (2015) give a general overview of the stratigraphy and tectonics of the Amu-Darya basin. The Amu-Darya basin is constituted of several structural elements, steps, uplifts and depressions of various orientations (fig. 1.4, 1.5). The main ones are the Central Karakum High in the west, the Kopet-Dagh foredeep in the southwest, the Murgab

depression in the deepest central part of the basin, the Badkhyz-Maimana step is the southern margin of the basin and the northeastern margin is composed of the Bukhara and Chardzhou steps (fig. 1.4, 1.5, 1.6, 1.7), deepening towards the east into the Beshkent depression or trough.

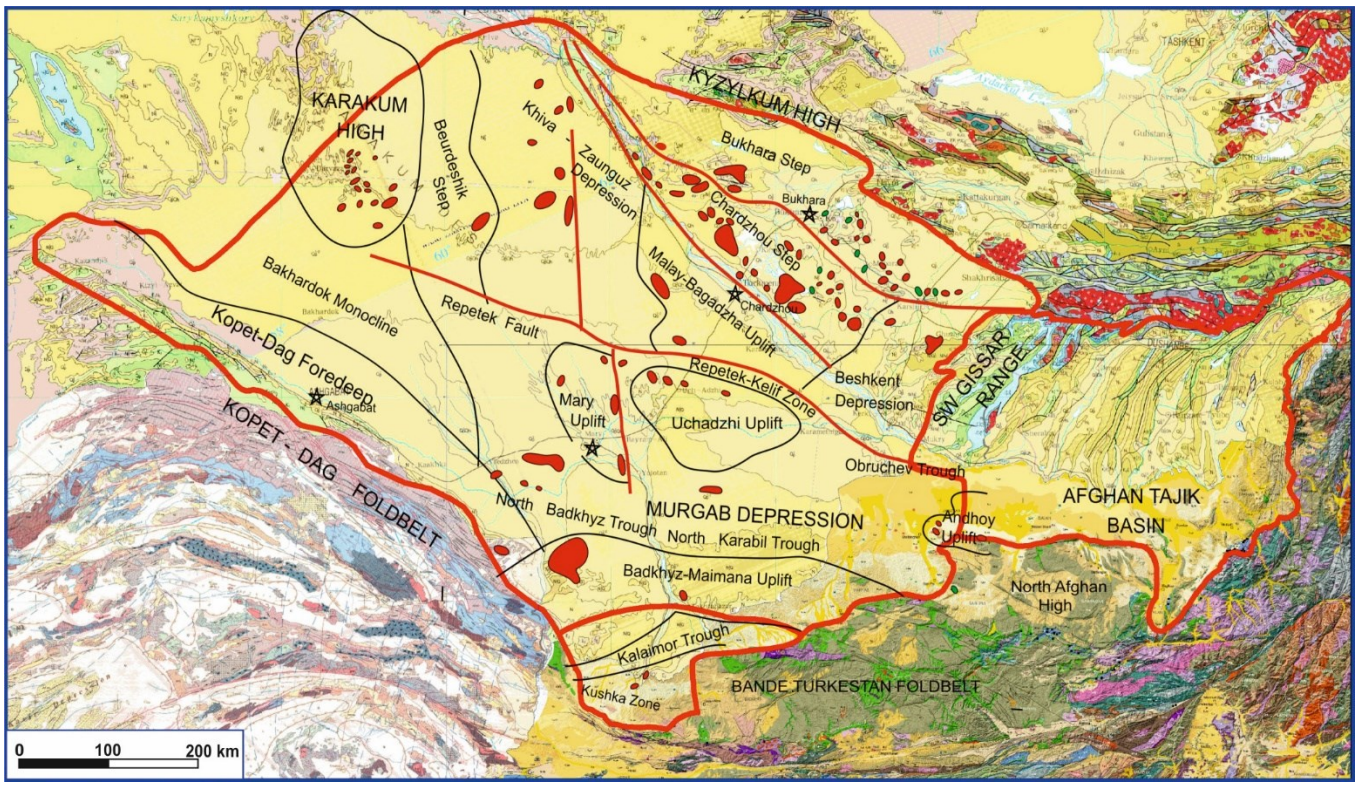

Fig. 1.5. Main structures of the Amu Darya basin. Amu Darya and Afghan Tajik basins are rounded with thick red lines. Detailed location in the Amu Darya basin and small red areas showing some of the oil and gas fields are from Ulmishek (2004) modified. In background geological maps of Caucasus, Iran, Central Asia and Afghanistan are in ArgGis system (after Brunet et al., 2013, modified).

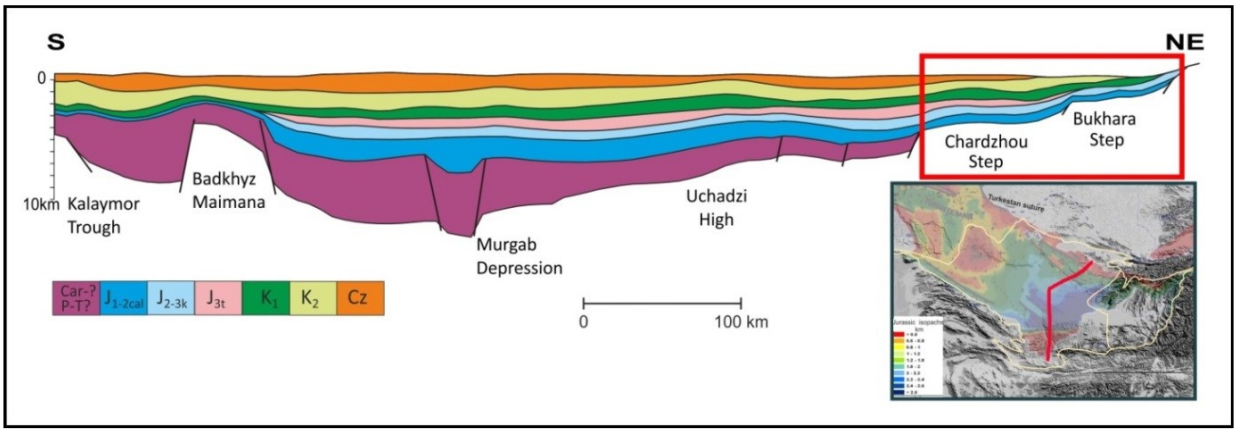

Fig. 1.6. Schematic S-NE-oriented cross-section of the Amu-Darya basin (after Brunet et al., 2014). The rectangle shows the location of our study area=the northeastern margin of the Amu-Darya basin in Uzbekistan.

The basin is underlain by localized troughs (rifts?) filled by up to several thousand metres of continental clastic sediments and possibly volcanics of Late Carboniferous to Triassic age. The geometry and exact depths of these troughs is not well known. The Late Triassic (Cimmerian) unconformity separates this initial basin fill from the Meso-Cenozoic series reaching a thickness of 7 km in the deepest parts of the E-W elongated Murgab depression. The Jurassic begins by Lower-Middle Jurassic sediments at first continental clastics then marine clastics and carbonates reaching more than 1 000 m in thickness. The Upper Jurassic consists mainly of carbonates (500-600 m)

overlain by the evaporites of the Gaurdak Tithonian formation (more than 1500 m in the eastern part). The Cretaceous and Cenozoic piles of sediments may each be more than 2 000 m thick, composed of clastic and carbonate rocks of continental or marine origin.

The Amu-Darya basin is a very rich petroleum province (fig 1.7) and is dominantly gas prone. Several reservoir rocks are recognized: Middle Jurassic, Upper Jurassic carbonates, Lower Cretaceous clastics, Paleogene Bukhara carbonates, the two main reservoirs being the Upper Jurassic carbonates sealed by the Upper Jurassic Gaurdak evaporites, and the Lower Cretaceous clastics when the Gaurdak formation pinches out (Ulmishek, 2004).

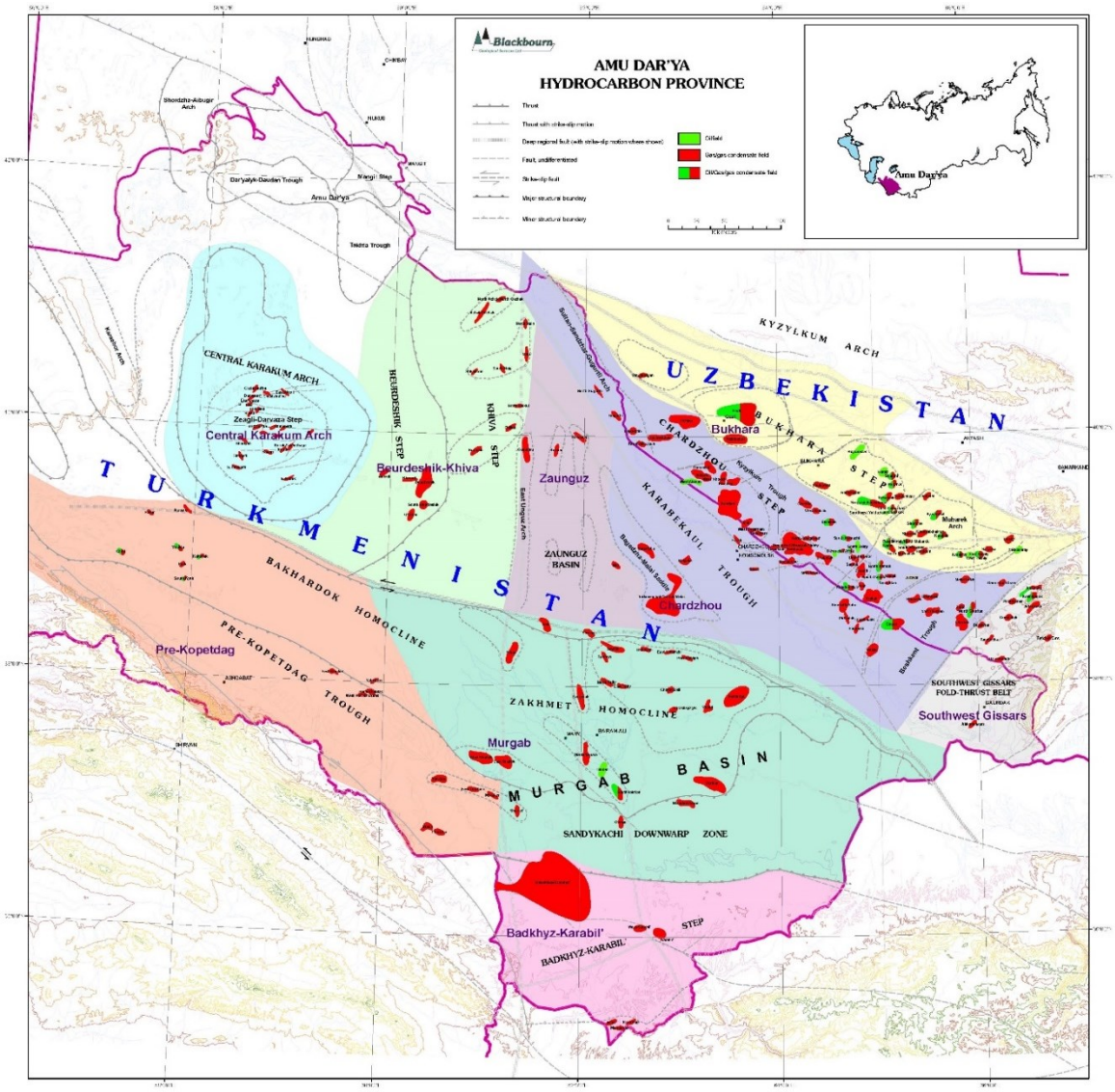

Fig. 1.7. Main geological structures and oil and gas fields of the Amu-Darya basin (Blackbourn, 2008).

The Afghan-Tajik basin

The Tajik basin (or Tajik depression) is a Mesozoic-Cenozoic (possibly Late Paleozoic-Triassic) sedimentary basin inverted during the Late Cenozoic in relationship with the India-Eurasia collision. It mainly corresponds to the western Tajikistan and northern Afghanistan territories (fig. 1.2, 1.5) so it is commonly called Afghan-Tajik basin. The part of the basin located in Uzbekistan comprises the Baysun and the Surkhan mega-synclines in the Surkhan-Darya province.

The present limits of the Afghan-Tajik basin are mainly active boundaries. The northern and northwestern boundaries are the western Tien-Shan and Southwestern Gissar ranges, belonging to the same Paleozoic belt reactivated during the Late Cenozoic. The eastern boundary is the western border

of the Pamir indenter. This latter active boundary is characterized by left-lateral strike-slip displacements and west-vergent thrusting of Pamir onto the eastern Afghan-Tajik basin. The southern boundary in Afghanistan is marked by the strong uplift of the Hindu-Kush. Its western boundary, where the Afghan-Tajik basin connects with the Amu-Darya, is poorly defined and not active.

The sedimentary succession of the Afghan-Tajik basin reaches the thickness of 9000 m. Despite the fact that the Amu-Darya and Afghan-Tajik basins belong to different tectonic units they are filled up by a similar Mesozoic-Cenozoic sedimentary sequence (Brookfield and Hashmat, 2001; Nikolaev, 2002; Ulmishek, 2004; Klett et al., 2006; Brunet et al., 2015). This sequence comprises a Jurassic to Paleogene pre-orogenic part, and a thick Neogene to Present continental molassic sequence. In the pre-orogenic series a major incompetent layer, the Upper Jurassic evaporites, constitutes the main regional decollement layer that plays an important role in the Neogene tectonic evolution of the Afghan-Tajik basin.

The decollement on top of the Upper Jurassic evaporites originates the thin-skinned Tajik fold and thrust belt including the almost entire Tajik basin. The Cretaceous to Recent sequence is detached forming the N- to NE-oriented anticlines of the Tajik and fold and thrust belt (fig. 1.5).

The northern margin of the Amu-Darya basin: the Bukhara and Chardzhou steps

The northern margin of the Amu-Darya basin corresponds to the Bukhara-Khiva oil-gas province, according to the nomenclature used in Uzbekistan. It is the main hydrocarbon province of the Republic of Uzbekistan (fig. 1.7). Its name is based on the names of the two ancient cultural centres of the area, the cities of Bukhara and Khiva (fig. 1.2, Khiva is located in the northwest, south of the city of Urganch). This region is well studied, because of its importance for the oil and gas industry of Uzbekistan.

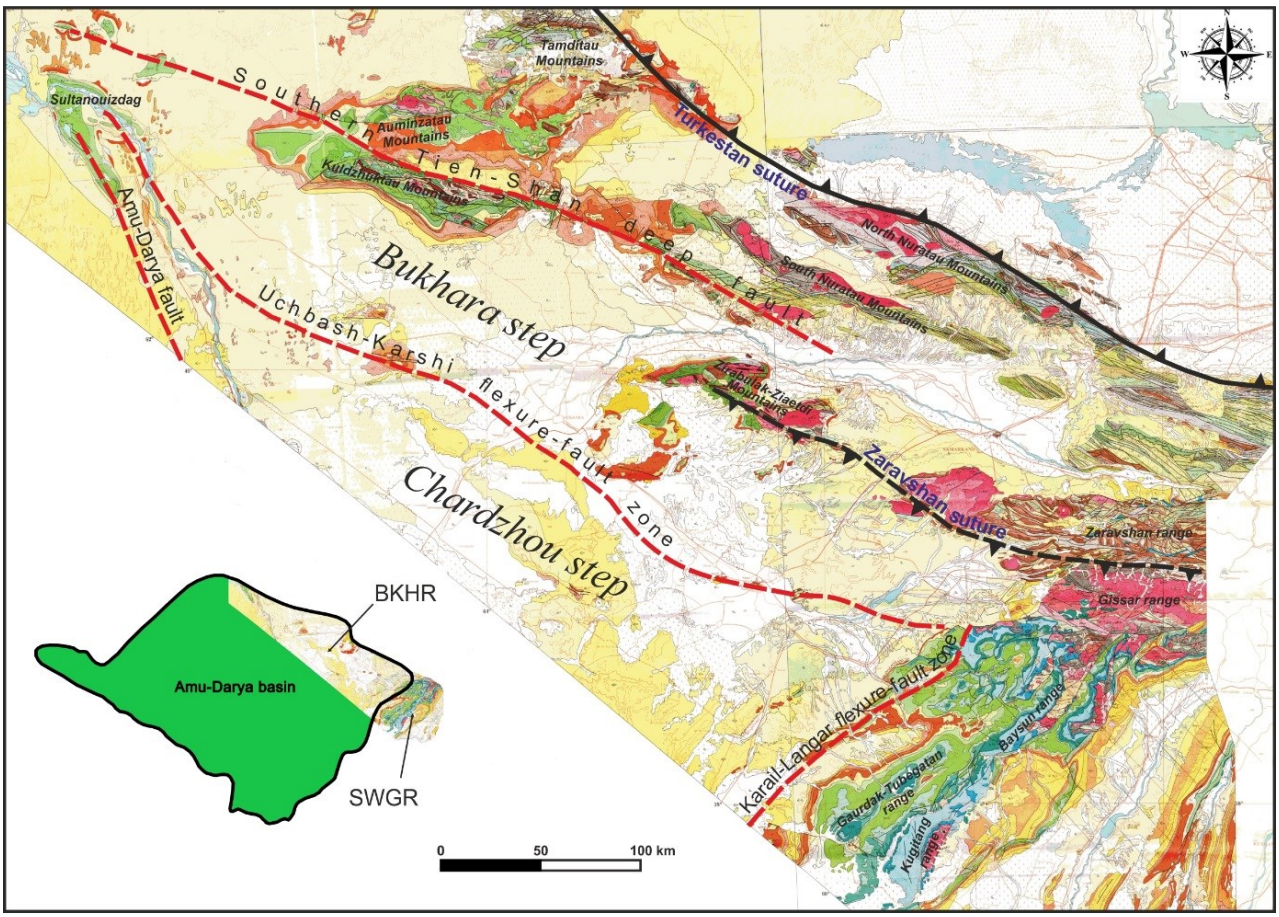

Fig. 1.8. Limits and main structures of the Bukhara-Khiva and Southwestern Gissar areas.
Background: Geological map of Uzbekistan (1998). The colours are usual: red, brown for the basement rocks and Paleozoic, blue for the Jurassic, green for the Cretaceous and orange-yellow for the Cenozoic.

The Bukhara-Khiva region is located in the Central Kyzyl-Kum and forms like an elongated triangle, pointed northwestwards. This region is limited in the north by the South Tien-Shan deep fault and in the northeast by the Zaravshan suture zone (fig 1.8). In the east it is bounded by the Southwestern Gissar Range and the south by the Amu-Darya deep fault (fig 1.8, 1.9) which separates this margin from the deep Amu-Darya basin. The western limit of the area is the Sultanouizdag Mountains. From the northwest to the southeast, the region is 500 km long. Its widest part at the base of the triangle in the east reaches 170-180 km.

As seen before, the Bukhara-Khiva region is divided into two main NW-oriented parallel strips separated by a major fault zone: the Bukhara and Chardzhou steps (fig. 1.4-1.8); the fault zone is the so-called Uchbash-Karshi Flexure-Fault Zone (fig. 1.8, 1.9), a complex zone including faults and flexures. The amplitude of the vertical displacement along this major fault zone is of 1500-2000 m. In the southeast, the Beshkent trough occupies a vast territory in the Chardzhou step, bordering the Southwestern Gissar.

The Bukhara step constitutes the northeastern part of the Bukhara-Khiva region. It is 400 km long and 60-70 km wide in its widest places. The Bukhara step consists of several highs and lows (fig. 1.9). All of them have an almost isometric form. In the western part of the Bukhara step, the broad structures are roughly N-striking. Approaching the Southwestern Gissar, they are more NE-oriented (fig. 1.9).

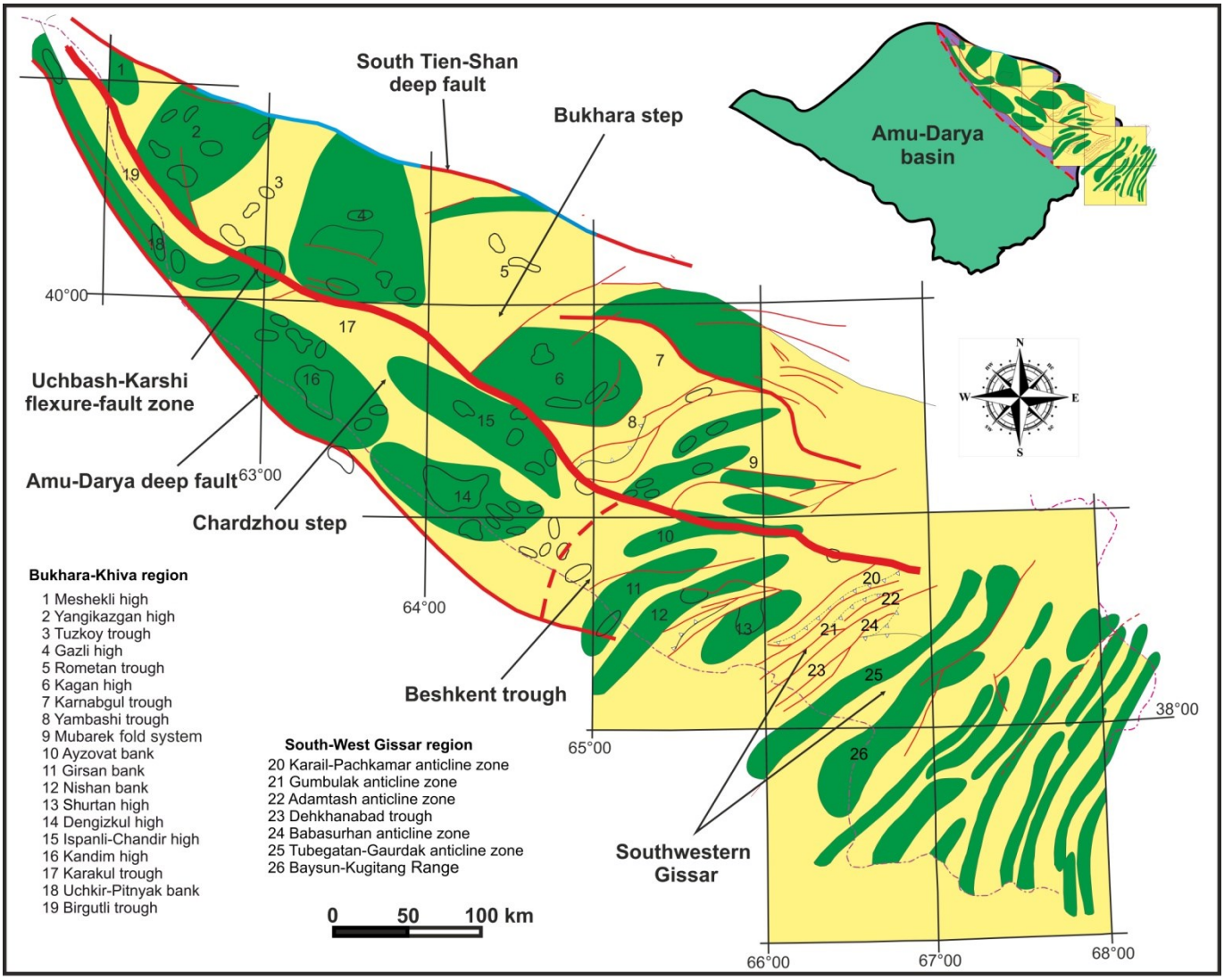

Fig. 1.9. Main sub-surface structures of the Bukhara-Khiva and Southwestern Gissar regions (modified after Abidov and Babadjanov, 1999.). Green = high; Yellow = trough; Red line = Fault.

Paleozoic to Cenozoic sediments cover the Bukhara step. The complete thickness of the Paleozoic, or more correctly the pre-Jurassic sequence, cannot be determined but its roof is 1500-2200 m deep. The Jurassic sediments do not exceed the thickness of 500 m, while the Cretaceous thickness ranges in the 500-1600 m interval. The Cenozoic deposits are around 900 m thick. A more detailed stratigraphy of the Bukhara step is presented in Chapter 2.

The Chardzhou step occupies the southern part of the Bukhara-Khiva region (fig. 1.4-1.9). It is 500 km long and reaches the width of 110 km in its eastern part. As the Bukhara step, the Chardzhou step is constituted of an alternation of lows and highs (fig. 1.9). But, on the contrary of the Bukhara step where they are N-oriented, they are here NW-oriented, becoming ENE-trending in the Beshkent trough, in the neighbouring of the Southwestern Gissar Range.

The Paleozoic is represented by Permian and Carboniferous sequences. The complete thickness of the Paleozoic sequence cannot be estimated, but the depth of its roof varies up to more than 5 km. An almost complete Mesozoic-Cenozoic sedimentary sequence exists in the Chardzhou step. The Jurassic deposits include all the Jurassic sequence (Mirkamalov et al., 2005). They are more than 2500 m thick in the Beshkent trough in the southeast. They are characterized by a thick evaporite pack, which is almost absent in the Bukhara step. The Cretaceous deposits reach a thickness of 2000 m. The Cenozoic sequence is similar to the one of the Bukhara step.

The Southwestern Gissar Range

The Southwestern Gissar range is a 200 km long and 150 km wide NE-oriented broad mountain range (fig. 1.8, 1.9). It constitutes the westernmost extension of the South Tien-Shan. The elevation of the crests of the mountains ranges from about 2000 m in the southwest at the Uzbek-Turkmen border to more than 4000 m in the northeast near the Uzbek-Tajik border. The elevation increases towards the northeast where the Southwestern Gissar Range connects with the E-striking western Tien-Shan Range more than 5000 m high (fig. 1.1).

The Southwestern Gissar is characterized by a NE-SW orientation of the main structures. The folding, Neogene to Quaternary in age, is related to the indentation of the Pamir salient in relationship with the India-Eurasia collision (Shein, 1985). Structurally, the Southwestern Gissar region is expressed by a system of parallel anticlines and synclines. The Southwestern Gissar comprises four main parallel NE-oriented anticlines (fig. 1.10). The most prominent is the Kugitang-Baysun belt, which arms the Southwestern Gissar Range and where is located the stratotype of the Jurassic sections.

The Southwestern Gissar Range is constituted by a Paleozoic to Cenozoic sedimentary sequence covering the basement. In the sedimentary cover one major unconformity separates the Permian (and possibly the Lower Triassic) and the Jurassic (and possibly the Upper Triassic) deposits. This major unconformity is related to a major Late Paleozoic-Early Mesozoic event. We distinguish the pre-unconformity (Paleozoic) sediments and intrusives folded during the Late Paleozoic orogeny, and the overlying Jurassic to Cenozoic sedimentary pile folded during the Late Cenozoic. The pre-unconformity sequence, as well as its basement, outcrops in windows located in the core of the main anticlines (fig. 1.10).

The Southwestern Gissar Range constitutes the NE-oriented extension of the western Tien-Shan (or Gissar s.s.). This latter is a thick-skinned belt mainly constituted of a Paleozoic belt rejuvenated during the Neogene. Unlike western Tien-Shan, in the Southwestern Gissar a Mesozoic-Cenozoic sequence has existed and is well preserved. It covers most of the range. The complete stratigraphic sequence is exposed from the uppermost Neogene to the pre-Jurassic basement. In this sequence the Cretaceous layers are more particularly thick with basinal facies.

As shown on Figure 1.10, the Mesozoic-Cenozoic outcrops dominate in the Southwestern Gissar. There the Jurassic sequence displays a well seen three-stage division: the Lower-Middle Jurassic clastic sequence reaches 500-700 m; the Middle-Upper Jurassic carbonate reaches 1000 m, and the Upper Jurassic evaporites are 1000 m thick (Tevelev and Georgievskii, 2012). The Cretaceous is well developed in the Southwestern Gissar where all the stages of the Cretaceous exist, with a total thickness of 4600 m.

The Southwestern Gissar Range is a thick-skinned belt where the structure is defined by asymmetric fault-related anticlines involving the crystalline basement, the Paleozoic and the Jurassic-Cenozoic sedimentary cover. Potential decollement in the Mesozoic-Cenozoic sequence does not play a major role in the Southwestern Gissar tectonics unlike in the Afghan-Tajik basin. Generally the SE-vergent anticlines prevail displaying an overall southeastern vergence of the range. However, the northern part of the range displays a bi-vergent structure emphasizing a large-scale pop-up structure. Here, the Southwestern Gissar Range is thrusted over the western Afghan-Tajik basin to the southeast and the northeastern margin of the Amu-Darya basin to the northwest. In the central and southern parts of the range the amplitude of deformations decrease and the thrusts are mainly southeast vergent. The fault displacements diminish southwestwards and the range plunges beneath the eastern Amu-Darya basin.

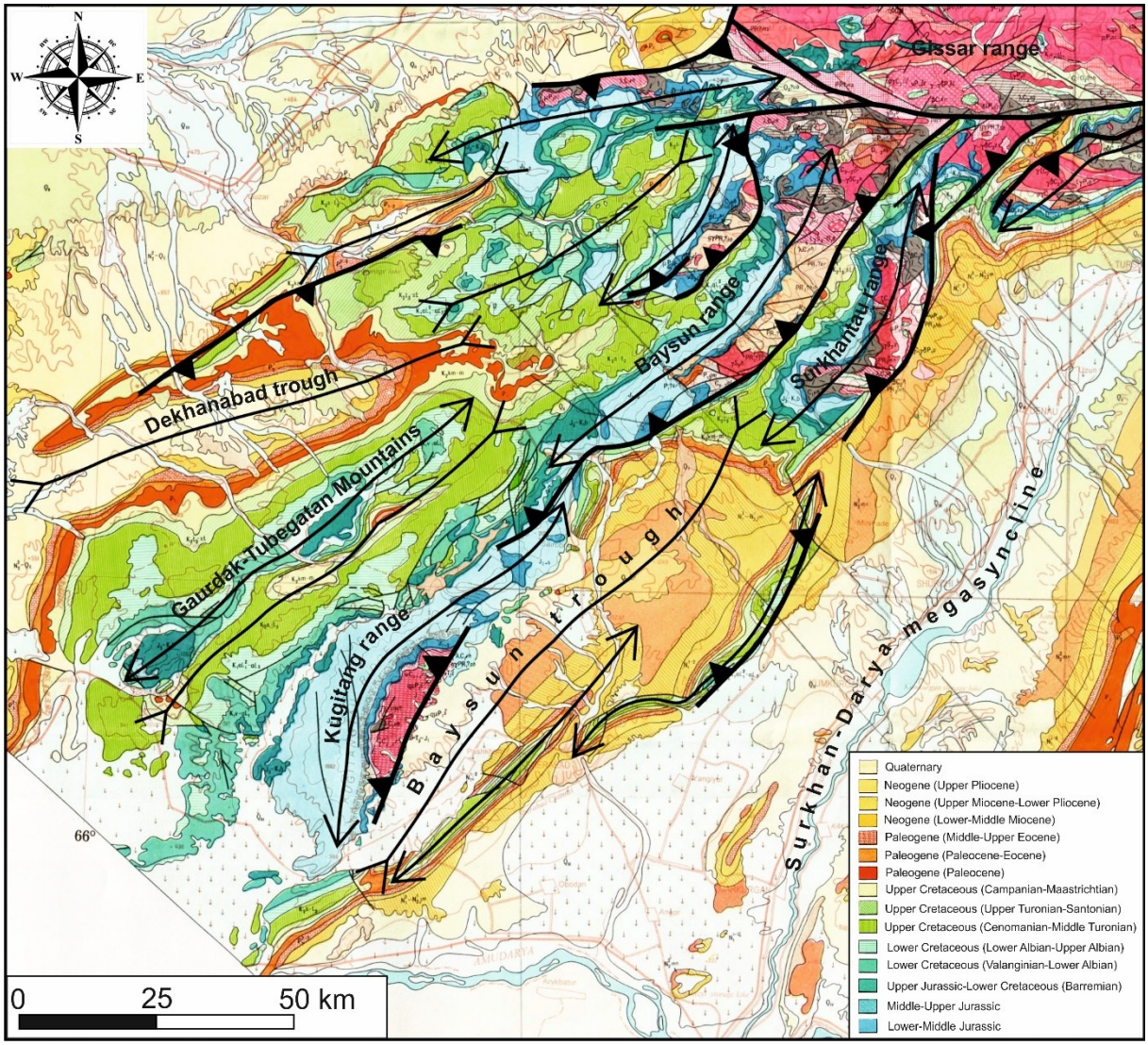

Fig. 1.10. Principal structural elements of the Southwestern Gissar
(modified after Tevelev and Georgievskii, 2012 on the geological background map).

1.3. Previous works

Since more than 100 years many works were dedicated to the geology of the Bukhara-Khiva and Southwestern Gissar regions. The first studies of the northern margin of the Amu-Darya basin, are dated from the beginning of the 20th century. Now almost the whole Bukhara-Khiva and Southwestern Gissar regions are covered by geological and geophysical maps at different scales (except the 3D seismic survey only covering some local areas). This amount of data provides us abundant information

about the deep structure and the geological evolution of the region. The results of these numerous works have been used as a base to develop new ideas about the tectono-stratigraphic evolution of the Amu-Darya margin and basin.

A lot of syntheses are dedicated to the deep geological structures of the Bukhara-Khiva and Soutwestern Gissar regions. Many isohypse, lithologic and tectonic maps of different geological levels have been published (e.g. Tal-Virsky, 1967; Ahmedjanov et al., 1986). A major synthesis is the "Gravimetric map (Bouguer reduction σ=2,3 g/cm^3) 1:200 000 scale", made during the 60's under the coordination of Fuzailov (confidential map, not availalable). One of the most important work in the domain of the deep geological structure of Central Asia was the creation of the "Map of magnetic anomaly of Central Asia (1:1 500 000)", published in 1991 and coordinated by Tal-Virsky and Fuzailov (fig. 1.11). This map synthetizes all the previous magnetometric works. The map shows, in the Bukhara-Khiva area, northwest trending elongated magnetic anomalies, parallel between them and to linear long gravimetric anomalies (Natal'in and Şengör, 2005). Natal'in and Şengör (2005, see also Zanchetta et al., 2013) interpret these anomalies as a set of en echelon-arranged arc fragments of Paleozoic age sheared and stacked together in a large Late Permian-Early Triassic right-lateral strike-slip zone setting the Turan domain (fig. 1.3). The positive and negative magnetic anomalies as well as seismic velocities indicate the presence of intrusives and volcanic rocks (arcs, lenses of ophiolites or basalts?) alternating with areas with a predominance of sediments (accretionary prism, fore-arc basin), separated by faults.

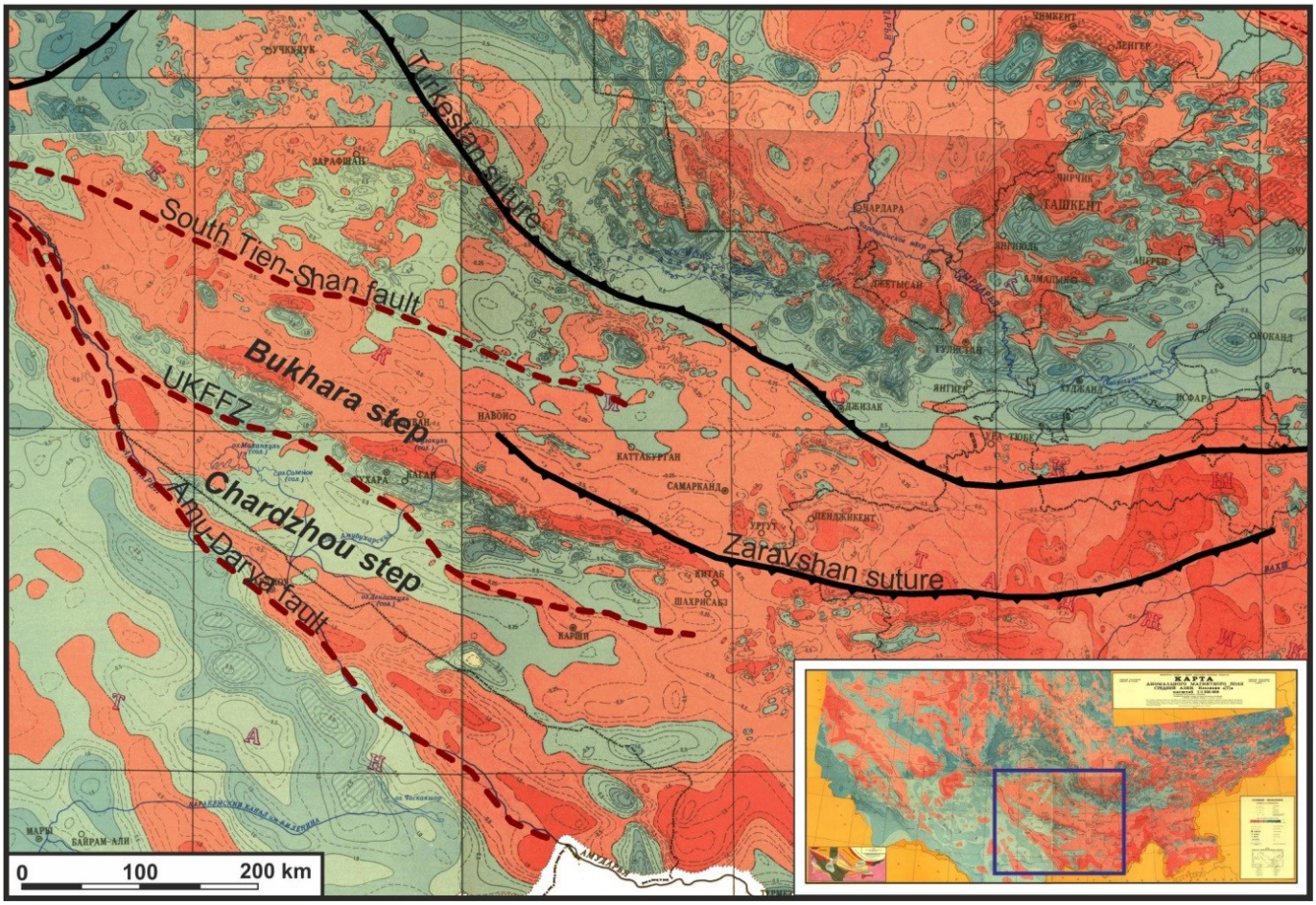

Fig. 1.11. Magnetic anomalies of Central Asia (1:1 500 000) with superimposition of the main sutures and faults (after Tal-Virsky and Fuzailov, 1991, modified). Negative anomalies are in red and positive in blue-grey.

The seismic surveys are other important geophysical approaches. The principal methods of seismic surveys are refraction correlation method (RCM), seismic reflection method (SRM), deep seismic

sounding (DSS) and common deep point (CDP-2D and CDP-3D). The first three methods have been generally used for the deep structure investigations, while the CDP has been used for the oil and gas researches. The RCM and DSS data have allowed to elaborate tectonic and isohypse maps of the pre-Jurassic surface (e.g. Yegorkin et al., 1962; Pikovsky and Cherkashina, 1971; Mitrofanova et al., 1981; Aliev and Cherkashina, 1981). The CDP surveys have allowed discovering several oil and gas fields in the Bukhara-Khiva and Southwestern Gissar regions.

A group of authors, under the direction of Shayakubov and Dalimov (1998) has considered several aspects of the Uzbek geology, including stratigraphy and tectonics. Later, an interesting work has been performed in the "Oil and gas Institute" by Mirkamalov et al. in 2005. They have elaborated a new Jurassic stratigraphy for the Bukhara-Khiva and Southwestern Gissar regions based on the biostratigraphy. Another important report from the "Geology and Geophysics Institute" deals with the Jurassic geology of the Southwestern Gissar (Egamberdiev and Ishniyazov, 1990). In this latter study, from data collected on the field, the authors present the stratigraphic and paleo-geographic features of the Southwestern Gissar during the Jurassic. There are few synthetic papers in the international literature, among them the papers of Thomas et al. (1999), Brookfield and Hashmat (2001) or the most recent synthesis from Ulmishek (2004) are dealing with tectonics, stratigraphy and hydrocarbon potential mainly of the Mesozoic of the Amu-Darya and Afghan-Tajik basins in general but do not detail our area of study.

1.4. Late Paleozoic tectonics

The pre-Mesozoic Central Asia is essentially constituted of a mosaic of continental blocks and volcanic arcs accreted during the Late Paleozoic (fig. 1.12 and 1.13). The Late Paleozoic geodynamic evolution of this vast domain mainly results from the collage of these continental blocks or micro-continents that led at the end of the Permian to the constitution of the northern Pangea super-continent. During the Late Paleozoic the oceanic domain separating the continental blocks was progressively subducted resulting in convergences of the continental blocks and continent-continent collisions.

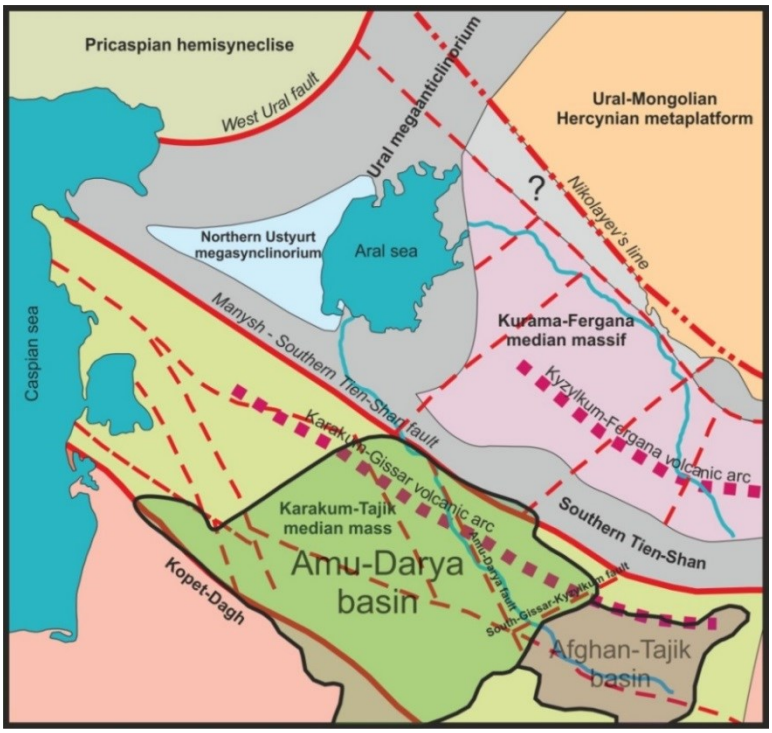

Fig. 1.12. Regional tectonic model of Central Asia at the end of the Hercynian cycle, with the location of the Amu-Darya and Afghan-Tajik basins (modified after Ahmedjanov et al., 1967)

The boundaries between the major continental fragments are constituted of Late Paleozoic orogenic belts. These belts will be eroded during the Early Mesozoic. At the end of the Ordovician, Central Asia was divided into four main oceanic domains: the Uralian, Turkestan, Junggar-Balkash, and Ob-Zaisan oceans (for location see below on fig. 1.17). The Middle to Late Paleozoic history of these oceans ended with their complete closure during the Late Carboniferous to Permian times.

Several geodynamic reconstructions of Central Asia, and more particularly of the western Tien-Shan and Uralian domains, during the pre-Mezosoic times have been proposed (Ahmedjanov et al., 1967; Burtman, 1978, 1980; Abdullaev et al., 1989; Zonenshain et al., 1990; Mukhin et al., 1991; Dalimov et al., 1993; Bukharin, 1999; Heubeck, 2001; Filippova et al., 2001; Natal'in and Şengör, 2005; Troitsky, 2012…). The contradictions in the different tectonic models proposed by many authors did not conducted to a unified scheme of tectonic evolution of western Central Asia. However, most of the models assume a collage of blocks during the Late Paleozoic associated with continent-continent collisions.

The map of Ahmedjanov et al. (1967) that first proposed the block geometry of Central Asia is shown on Figure 1.12. It does not considerably differ from the more recent map of Troitsky (2005) shown on Figure 1.13. The modern regional tectonic model of Central Asia (fig. 1.13) divides western Central Asia into several micro-continents, called median massifs in old works, and blocks in more recent ones. The names of these blocks, orogenic belts, sutures and oceanic domains may appreciably differ according to the authors. Here we selected the terms the most commonly used in the modern literature.

In the area of investigation, in western Central Asia, two main Late Paleozoic orogenic belts are concerned: the N-oriented Uralian and E-oriented Tien-Shan orogenic belts. The Late Paleozoic fold-and-thrust belts of the Urals and Tien-Shan formed as a result of convergences and collisions of the Kazakhstan continent with the east Europe craton in the west, and the Tarim, Alay and Karakum-Tajik/Turan micro-continents in the south respectively. These almost perpendicular belts connect in the region of the Aral Sea and Syr-Darya basin (fig. 1.4, 1.12). The relationship between these two Late Paleozoic orogenic belts is still unknown mainly because the junction is located beneath the thick Mesozoic-Cenozoic sedimentary cover deposited in the Aral-Ustyurt region.

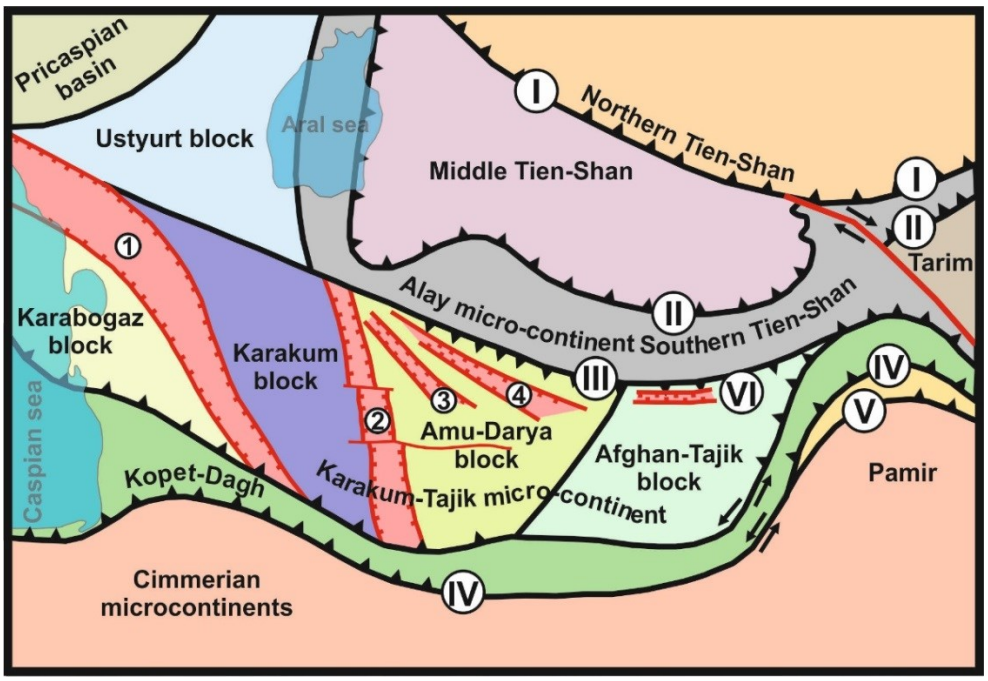

Fig. 1.13. Sketch of the main Paleozoic structural elements of Central Asia (modified after Troitsky, 2005).

I- Kyrgyz-Terskey suture; II- Turkestan suture; III- Zaravshan suture; IV- Paleotethys suture; V- Mesotethys - Rushan-Pshtar suture; VI- Gissar magmatic arc. 1 - Mangyshlak-Tuarkyr paleo-rift; 2 - Khiva-Murgab paleo-rift; 3 - Amu-Darya paleo-rift; 4 - Bukhara-Khiva paleo-rift.

We give here a sketch of the general Late Paleozoic evolution, the reconstructions will be more detailed in the paragraph 1.6.

The convergence between Kazakhstan and East Europe was controlled by the eastward subduction of the Uralian oceanic plate beneath the Valerianovsky volcanic Arc (V on fig. 1.14-a) during the Devonian times. In the Carboniferous the volcanic arc accreted and the subduction jumped to the east. In the north, after all the oceanic lithosphere was subducted beneath the Kazakh continent, the continent-continent collision between Kazakhstan and East Europe initiated in the Middle Bashkirian (at 315 Ma). The diachronous collision propagated towards the south during the Late Carboniferous-Permian times. The Uralides are a N-trending wedge dominated by west-vergent thrust faults deforming Paleozoic sediments deposited on the east European continental margin and platform, and then in a foredeep during the Late Carboniferous - Early Permian times.

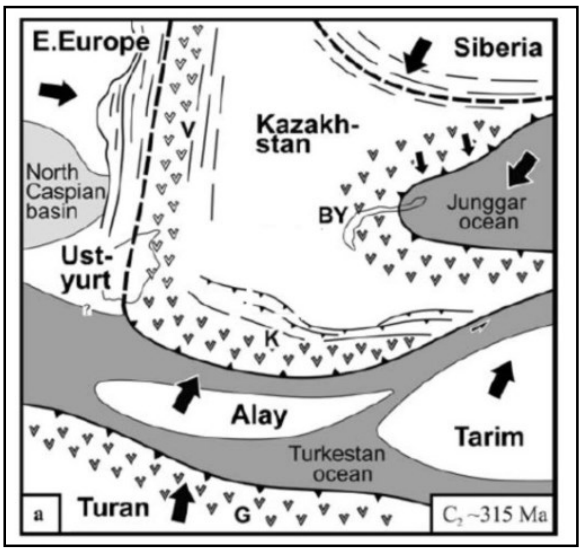

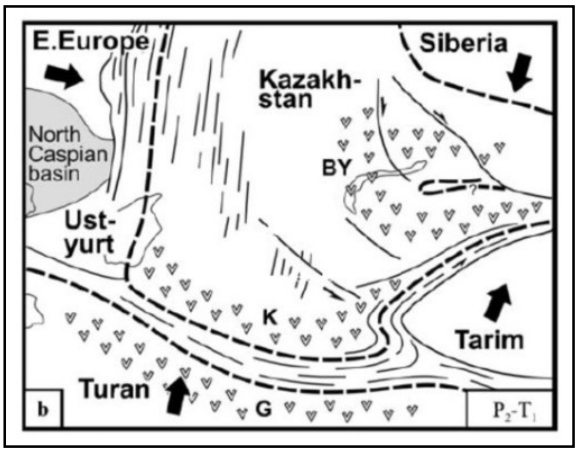

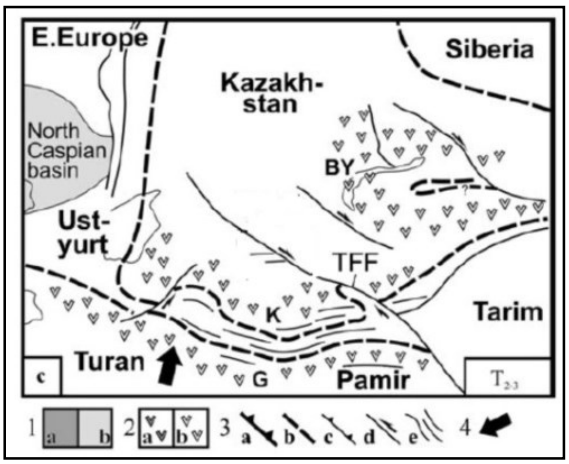

Fig. 1.14. Plate tectonic reconstructions of the Ural and Tien Shan junction for 3 main periods: a: Late Carboniferous; b: Late Permian to Early Triassic; c: Middle-Late Triassic. 1: Basins with oceanic crust (a) and thinned subcontinental crust (b); 2: Volcanic arcs: active (a) and extinct (b); 3: Active subduction zones (a), collisional sutures (b), major thrusts (c), strike–slip faults (d), trends of folds and reverse faults in collisional belts (e); 4: Assumed directions of plate motion with respect to the stable central part of the Kazakhstan continent. Volcanic belts: V: Valerianovsky; K: Kurama; BY: Balkhash–Yili; G: Gissar; TFF: Talas–Ferghana Fault. Aral Sea and Balkhash Lake are shown for reference (from Alexeiev et al., 2009).

The Late Paleozoic orogenic belt of Tien-Shan results from the closure of the Turkestan oceanic domain during the Late Paleozoic (fig. 1.13, 1.15). The western segment of the Turkestan Ocean separated a northern domain composed of Siberia, East Europe (Baltica) and Altaids from an E-W elongated domain composed of continental blocks that extended from northern China in the east to the south Aral Sea in the west through the Tarim and Alay blocks. The Tien-Shan is a Late Paleozoic collision system resulting from the collision of the southern margin of the Kazakhstan continent with the Turan (or Karakum-Tajik), Alay and Tarim micro-continents. It comprises complex fold and thrust belts involving mostly Silurian to Lower Permian sediments and volcanics. The different tectonic models of the Tien-Shan consider both north- and south-vergent subductions. Nevertheless, the geological data suggest a northward subduction of the Turkestan oceanic plate beneath the margin of the Kazakhstan continent during the Late Carboniferous (fig. 1.14, 1.15). The principal structures in

the belt are tectonic nappes and thrusts, which were formed in the Late Carboniferous and Early Permian.

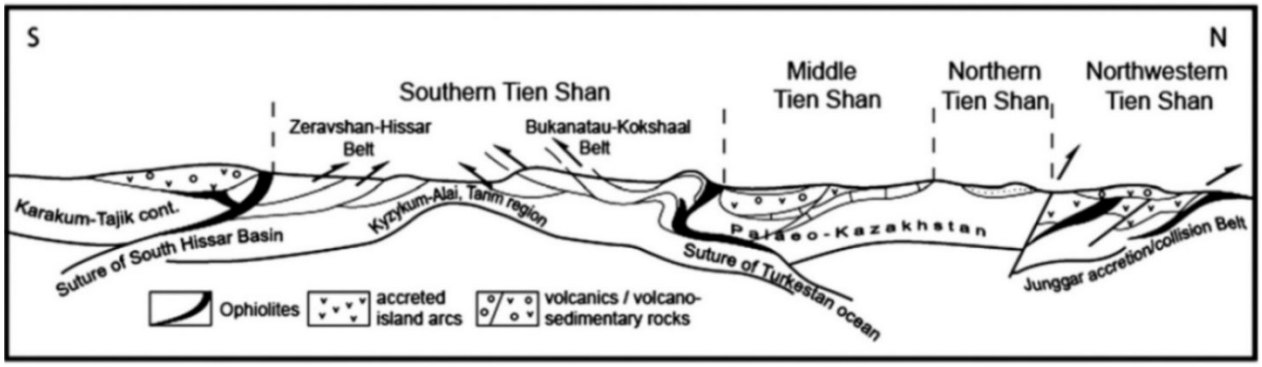

Fig. 1.15. Idealized cross-section of the Paleozoic Tien-Shan: geodynamic model of collision in Karakum–Tien-Shan–Junggar system in Permian. Arrows: direction of thrusting (after Biske and Seltmann, 2010).

The age of the collision is still controversial. According to the different authors it was estimated as Late Devonian to Early Carboniferous (Su et al., 2010; Wang et al., 2011), Late Carboniferous to Early Permian (Gao et al., 1998; Wang et al., 2008; Alexeiev et al., 2009), Late Permian and Triassic (Zhang et al., 2007; Xiao et al., 2008), or diachronous from Early Carboniferous to Permian (Chen et al., 1999). However, recent data (Alexeiev et al., 2009) show that the onset of collision of Kazakhstan with Alay and Tarim micro-continents is dated as Middle Moscovian and latest Carboniferous in age respectively.

1.5. The Pre-Mesozoic structures in the Bukhara-Kiva and Gissar regions

Two suture zones resulting from the Late Paleozoic orogenies border the studied area to the north (fig. 1.16). These sutures are the relics of paleo-oceanic domains closed during continent-continent collisions. In this area the Turkestan suture marks the limit between the Kazakh continent to the north and the Alay block to the south.

The Bukhara-Khiva and Southwestern Gissar regions are located on the southeastern part of the *Turan Platform* (Platform is the name given after the end of the Paleozoic accretion to Eurasia of a series of blocks among which a Turan one). The number, names and Paleozoic positions of the blocks lying below our study area differ according to the authors. For Troitsky (2005) these are the Amu-Darya and Afghan-Tajik blocks, part of the Karakum-Tajik micro-continent (cf. fig. 1.13). The Karakum-Tajik micro-continent (fig. 1.13) named also Turan micro-continent or domain (fig. 1.3; fig. 1.15) spans from the Caspian Sea in the west to the Pamir in the east. The Kopet-Dagh fold-and-thrust belt bounds it to the south, separating the Cimmerian Iranian blocks and the Eurasian related Turan Platform.

In the north, the Alay block is limited by the western extension of the Late Paleozoic Tien-Shan orogenic belt, which occupied a large part of our area of investigation.

The Southern (or western) Tien-Shan extends from the Sultanouizdag Mountains at the western limit of the Bukhara-Khiva region (fig. 1.16) to the Kokshaal Mountains at the Kyrgyz–Chinese border through the southern Kyzyl-Kum Ridge and the Gissar (s.s.) and Alay ranges south of the Fergana depression. It can even be traced as far east as Xinjiang in China (Biske and Seltmann, 2010). The closest to the northern margin of the Amu-Darya basin are the Zirabulak-Ziaetdi Mountains, Nuratau Mountains and Zaravshan-Gissar mountain system (including Southwestern Gissar) of Southern Tien-Shan (fig. 1.16).

A major suture zone has been described between the Alay and Kazakhstan-Kyrgyz (or Middle Tien-Shan) micro-continents (fig. 1.14-1.16). This zone corresponds to the Late Paleozoic Turkestan suture where the Paleozoic Turkestan Ocean closed (Biske and Seltmann, 2010; Troitsky, 2012). The Turkestan suture (the Southern Tien-Shan suture of Nurtaev et al., 2013) has appeared during the Late

Paleozoic (Carboniferous) closure of the Turkestan Ocean (Zonenshain et al., 1990; Kheraskova et al., 2010; Seltmann et al., 2011; Nurtaev et al., 2013). This suture marks the northern limit of the Southern Tien-Shan (Troitsky, 2012). It runs north of the studied region.

According to Biske and Seltmann (2010) and Troitsky (2012) the boundary between the Karakum-Tajik and Alay micro-continents is the Zaravshan suture zone, also called Gissar Suture (Portnyagin, 1974; Burtman, 1976; 2006).

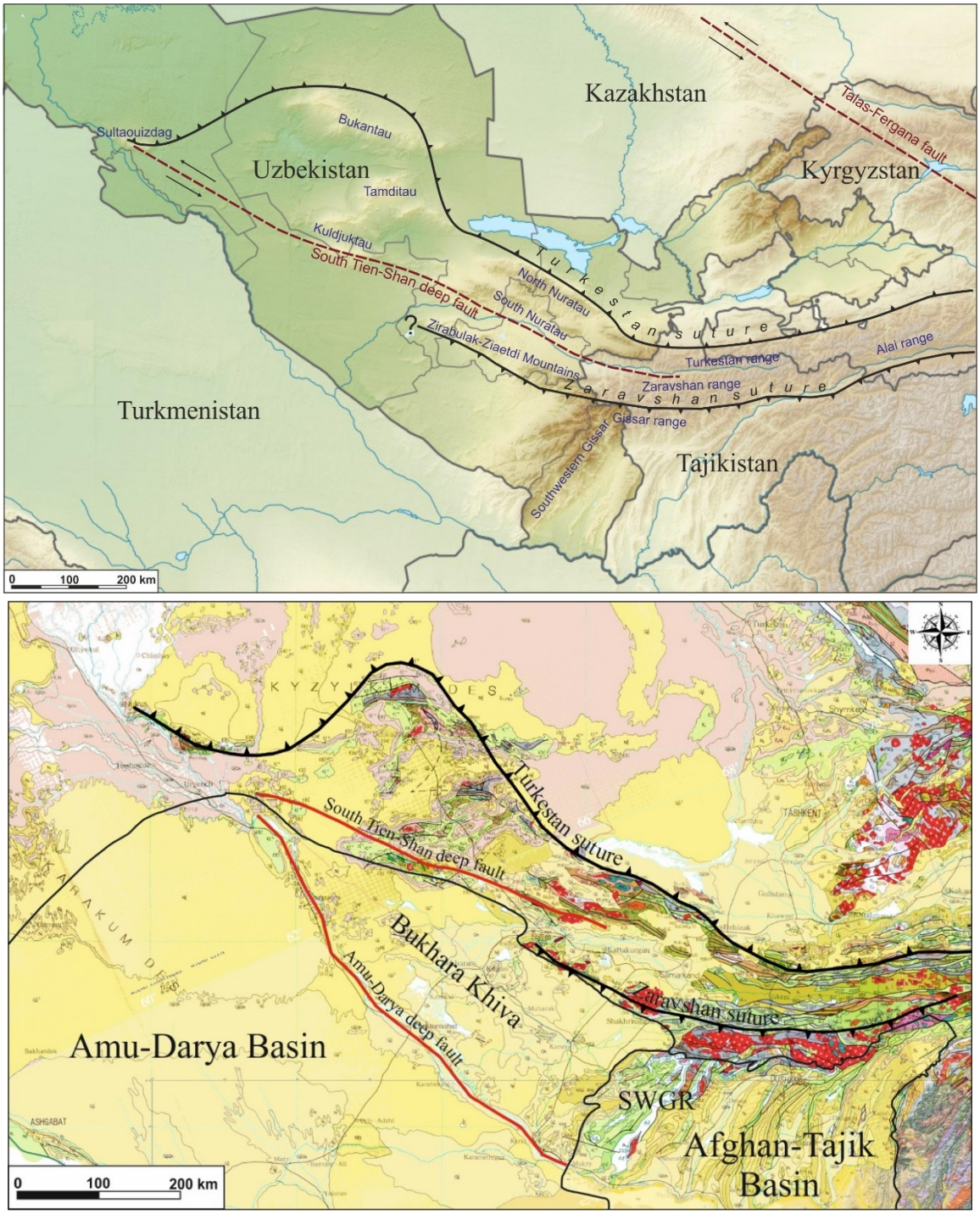

Fig. 1.16. Location of the Turkestan and Zaravshan sutures with respect to the Amu-Darya and Afghan-Tajik basins (modified after Brookfield, 2000; Heubeck, 2001; Biske and Seltmann, 2010; Troitsky, 2012), topography and geology. Bottom map, the continuous thin dark green line marks a schematic contour of the Amu-Darya and Afghan-Tajik basins; SWGR: Southwestern Gissar Region. Background = topography and Atlas of Geological maps of Central Asia and Adjacent Areas (2008).

The presence of a Turkestan Ocean is supported by many data and generally admitted (Brookfield, 2000; Heubeck, 2001; Alexeiev et al., 2009; Biske and Seltmann, 2010; Troitsky, 2012; Nurtaev et al., 2013, and many others), while the existence of the Zaravshan Ocean, corresponding to the eponyme suture, is not clearly evidenced (Troitsky, 2012).

From a tectonic point of view, the Turkestan suture does not floor the Amu-Darya and Afghan-Tajik basins (fig. 1.16, 1.15), as it is located more to the north and runs through the northern limits of the Turkestan range in the Nuratau Mountains where ophiolites crop out in the Sultanouizdag (Heubeck, 2001). We may note that ophiolitic complexes in the Kyzyl-Kum and Nuratau Mountains do not form a continuous section and exist only within different nappes (Troitsky, 2012).

The other suture zone, the Zaravshan suture, is much closer from our area of investigation. It borders the Gissar Range s.s. to the north (fig. 1.16). Its existence is still a point of discussions among the earth sciences community. The ophiolites of the Zaravshan and Zirabulak-Ziaetdi mountains (Brookfield, 2000; Troitsky, 2012) and of the Western Alay further to the east may be considered as a possible remainder of a paleo-ocean or marginal basin between the hypothetical Alay and Karakum-Tajik micro-continents. But, as in the Turkestan suture zone, these ophiolites do not form a continuous belt. It would be situated between the Zaravshan and Gissar ranges (fig. 1.16). Its route towards the west varies according to the authors as well as its position compared to the South Tien Shan fault. This is in relation with the unclear southern boundary of the Alay micro-continent in this area.

According to this, the Zaravshan Ocean is supposed to be a regional structure, which was coeval with the Turkestan Ocean as shown in the reconstructions of Alexeiev et al. (2009). For this group of authors there were two subduction zones, during the closure of the Turkestan Ocean. The Zaravshan suture is not mentioned, but the location of the second subduction zone and suture (located south of the Turkestan suture fig. 1.14), corresponds with the position of the Zaravshan suture zone described in other publications.

1.6. Examples of reconstruction of Central Asia evolution during the Paleozoic

According to Troitsky (2012), the pre-Mesozoic geodynamic evolution of Central Asia consists into two main stages:

The Archean-Proterozoic stage, when the micro-continents were forming. The crystalline basements of the Amu-Darya and Afghan-Tajik sedimentary basins are of this age;
The Paleozoic stage, when the oceanic basins of the Uralian and Turkestan oceans were subducted and finally closed. As a result of this closure appeared the Turkestan and Zaravshan suture zones and the Tien-Shan collision zone bounding the Ustyurt, Alay and Karakum-Tajik/Turan micro-continents.

The limits between the micro-continents, as well as the history of the pre-Mesozoic evolution of this region, have been differently explained. One of the most popular assumptions argues that the Paleozoic evolution of the northern margin of the Amu-Darya basin is connected to the evolution of the nearby oceanic basins. The Turkestan Ocean has appeared in the Middle or Late Ordovician. It has developed during the Devonian (Bai et al., 1987; Klishevich et al., 1992; Biske et al., 1993; Klishevich and Khramov, 1993; Ruzhentsev and Mossakovsky, 1996; Buslov et al., 2001), and started to close in the Carboniferous. The Zaravshan Ocean was developing during the same time (Troitsky, 2012). However, the Zaravshan Ocean could be only a marginal basin, neighbouring the Turkestan Ocean and separating the Karakum-Tajik/Turan and Alay micro-continents (fig. 1.17).

We may divide the tectonic evolution of western Central Asia during the Late Paleozoic into four stages. This is a simplified model of evolution of the Central Asia region. It illustrates the geodynamic processes active before the Mesozoic sedimentation of the Amu-Darya and Afghan-Tajik basins.

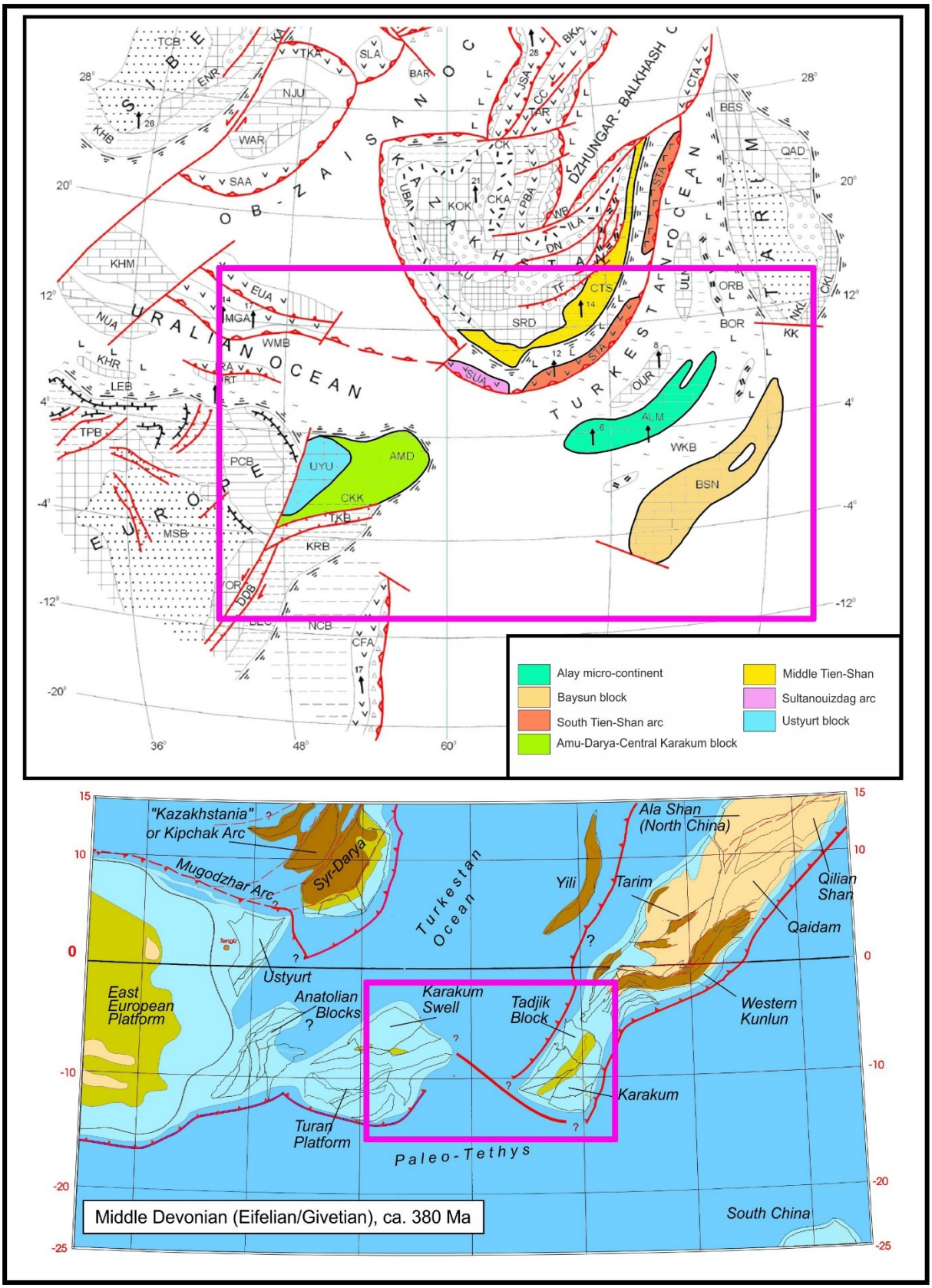

Fig. 1.17. Middle Devonian paleogeography of Central Asia [modified after Filippova et al., 2001, top; Heubeck, 2001 bottom, strike-slip separation between Turan and Tajik is conjectural and is only invoked to avoid excessively southerly position of Turan]. Legend for Filippova et al., 2001, see continuation next page. *Continental paleogeographic and paleotectonic settings*: 1 – orogenic edifice, 2 – denudation plain, 3 – intermontane basin or foredeep with continental sedimentation, 4 – active margin volcano-plutonic chain,

5 – epicontinental nearshore or marine basin, 6 – marginal shelf, 7 – deep water (bathyal) intracontinental basin, 8 – continental slope and rise of a passive margin.
B. Oceanic and backarc basinal paleogeographic and paleotectonic settings: 9 – primitive deeply submerged volcanic arc, 10 – mature volcanic island arc, 11 – accretionary prism, 12 – micro-continent, 13 – carbonate platform, 14 – ocean and backarc basin floor and abyssal plain.
C. Active tectonic structures: 15 – spreading axis, proven or inferred, 16 – principal strike slip or transform fault, 17 – subduction zone, proven or inferred, 18 – overthrust, 19 – rift. D. Other features: 20 – barrier reef, 21 – ocean-floor siliceous sediments, 22 – clay and carbonate sediments, 23 – flysch/olistostrome apron, 24 – ocean-floor tholeiitic basalts, 25 – within-plate subalkaline and alkaline volcanics, 26 – paleomagnetic vectors and mean paleolatitudes, 27 – names of structural units (see list), 28 – names of principal faults (see list).

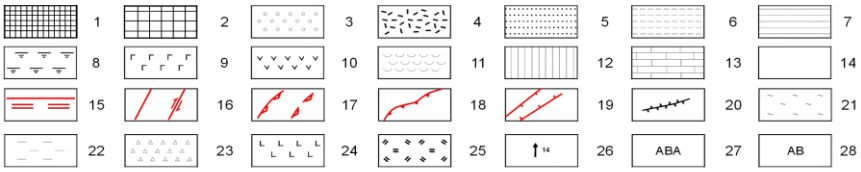

Names of structural units: A. Massifs, micro-continents, blocks, and tectonic zones: ALM = Alay micro-continent, AMD = Amu-Darya block, AMN = Altay–Mongolia block, BAR = Barnaul massif, BDM = Baydaratsky massif, BEC = Bechasyn zone, BEL = Beltau zone, BES = Beishan, BOR = Borkoldoy block, BSN = Baisun massif, CAT = Chatkal, CDZ = Central Junggar Alatau, CHI = Chinghiz, CKK = Central Karakum, CKL = Central Kunlun, CTS = Central Tien Shan, DZF = Junggar foldbelt, ENR = Yenisei Range, EUF = East Urals folded zone, EUR = East Urals, GAL = Gorny Altay, GCM = Greater Caucasus massif, GKT = Greater Karatau, KHM = Khanty–Mansi massif, KHR = Kharbey micro-continent, KOK = Kokchetav massif, KRB = Karabogaz massif, MGZ = Magnitogorsk zone, NDZ = Northern Junggar Alatau, NJU = Nyurolka massif, NKL = North Kunlun, NPM = North Pamir, NTS = North Tien Shan, NUF = North Urals, OUR = Osh–Uratyube block, OZF = Ob–Zaisan foldbelt, PAR = Parapamiz, QAD = Tsaidam massif, RAL = Rudny Altay, SAL = Salair, SDZ = Southern Junggar Alatau, SGM = Southern Gobi massif, SLZ = Salym zone, SRD = Syr-Darya block, STS = South Tien Shan, SUF = South Urals, TAR = Tarbagatay, TIM = Timan, TKO = Tom–Kolyvan zone, TMM = Tuva–Mongolia massif, TUR = Turgay block, UKM =Ukrainian massif, ULN = Ulan block, ULU = Ulutau, URT = Ural-Tau, UYU =Ustyurt, VOR = Voronezh massif, VUR = Volga–Urals arch, WAR = Vartovsk massif, WSN = Western Sayan, ZAZ = Zeravshan–Alay zone. *B. Sedimentation basins*: ACB = Anuy–Chu, AGB = Angara–Lena, ALB = Almantaisky, BOB = Borotalinsky, CSB = Chu–Sarysu, DBB = Junggar–Balkhash, DDB = Dneper–Donets, DZB = Junggar, KAB = Karpinsky Range, KHB = Khatanga, KUB = Kuznetsk, LEB = Lemva, MIB = Minusinsk, MNB = Mangyshlak, MSB = Moscow, NCB = North Caucasus, ORB = Ortosuisky, OZB = Ob–Zaisan, PCB = Peri-Caspian, RYB = Rybinsk, SAB = Sakmara, SDB = Syr-Darya, TGB = Tunguska, TNB = Teniz, TPB = Timan–Pechora, TUB = Tuarkyr, UFB = Uralian foredeep, WKB = Vashan–Kalmakasuisky, WMB = Western Mugodzhary. *C. Island arcs and volcano-plutonic belts:* ALA = Alay, BEA = Beltau, BGA = Bogdoshan, BHA = Barunkhuray, BKA = Barlyk, BSA = Baisun, CFA = Caucasus Frontal Range, CHA = Chinghiz, CKA = Central Kazakhstan, CKL = Central Kunlun, CTA = Chinese Tien Shan, DEA = Denisovsky, EDA = Eastern Junggar, EUA = East Urals, ILA = Ili, IRA = Irendyk, JOA = Zholotag, JSA = Zharma–Saur, KUA = Kurama, MGA = Magnitogorsk, NBA = Northern Barunkhuray, NUA = North Urals, OUA = Osh–Uratyube, PBA = Balkhash, RAA = Rudny Altay, SAA = Salym, SDA = Southern Junggar, SKA = Sakmara, SLA = Salair, STA = South Tien Shan, SUA = Sultan-Uizdag, TAA = Tagil, TKA = Tom–Kolyvan, UBA = Ubagan, VAA = Valeryanovsky. *D. Principal faults*: AK = Akbastau, AB = Altay face, BH = Boro-Horo, CC = Central Chinghiz, CK = Central Kazakhstan, DA = Darbut, DN = Dzhalair–Naiman, ES = Eastern Sayan, EU = East Urals, IR = Irtysh, KA = Kuznetsky Alatau, KK = Karakunlun, KO = Kobda, NE = Northeastern Altay, TF = Talas–Fergana, TK = Tekturmas, WB = Western Balkhash.

The Early Carboniferous stage (fig. 1.18). During this period, the Paleotethys Ocean started to close, subducting towards the north beneath the string of continental blocks bordering the Turkestan Ocean to the south and moving with respect to each other. Simultaenously, the Turkestan oceanic domain was subducting towards the north beneath the southern margin of the Kazakh continent. Along the southern margin of the Turkestan Ocean, according to Heubeck (2001), there was no active-margin. Kravchenko (1979), Leith (1982), Zonenshain et al. (1990), and Mukhin et al. (1989) consider that a Middle Carboniferous marginal basin existed in the Gissar zone. However, in the southern margin of the Turkestan Ocean, Filippova et al. (2001) identify during the Early Carboniferous, a first overthrusting event along the thrust front of the Zaravshan-Alay zone and more to the south, the opening of a southern Gissar oceanic rift (place of the future Gissar or Zaravshan suture) separating this latter zone from the Baysun micro-continent. These opposite viewpoints are caused by the poor

quality of the outcrops and other data concerning the southern margin of the Turkestan Ocean. As mentioned above, the ophiolitic complexes of the Zaravshan suture zone do not constitute a continuous belt.

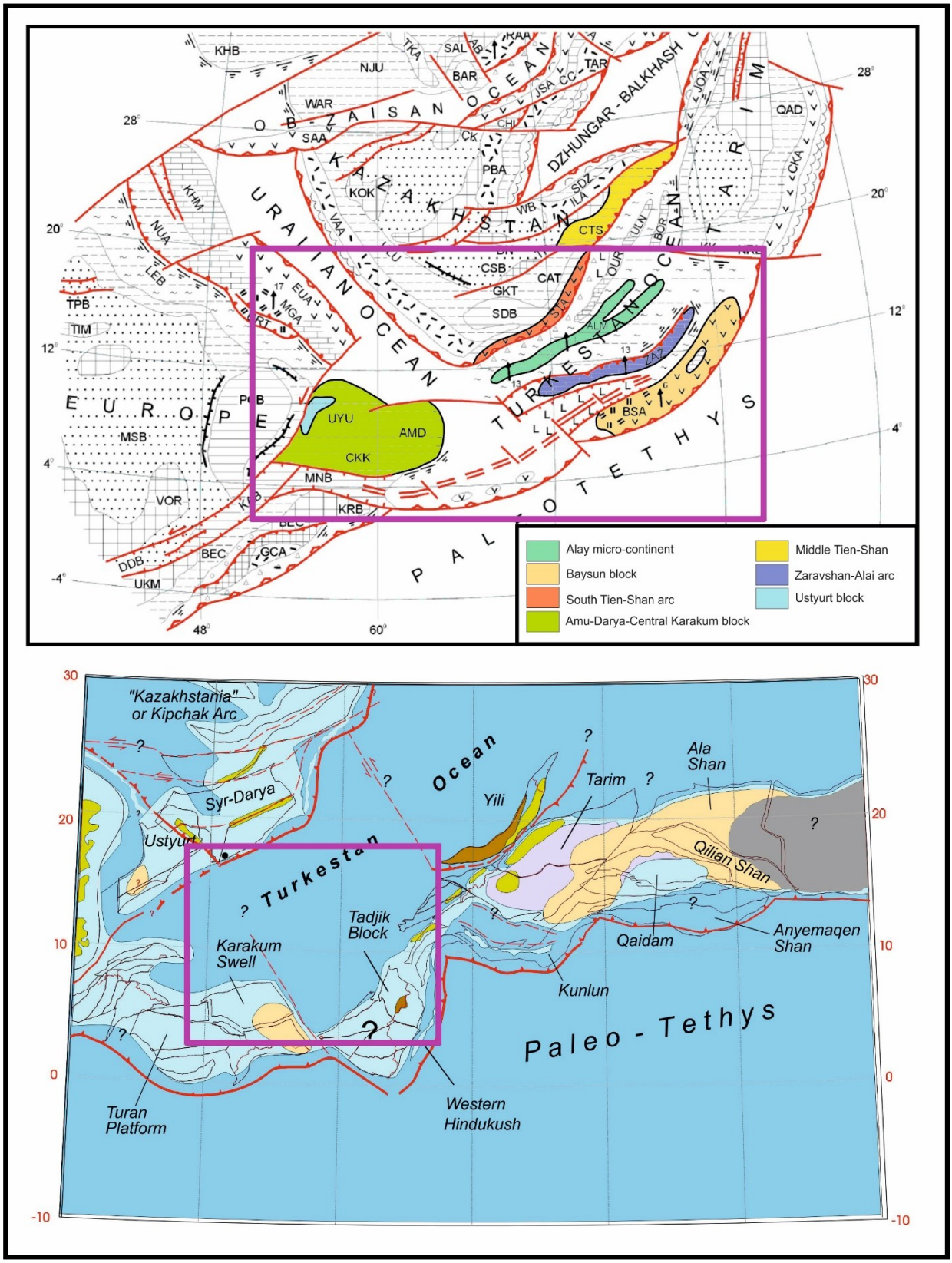

Fig. 1.18. Early Carboniferous paleogeography of Central Asia [modified after Filippova et al., 2001, top; Heubeck, 2001 bottom, strike-slip movement along Aral-Murgab zone is conjectural].

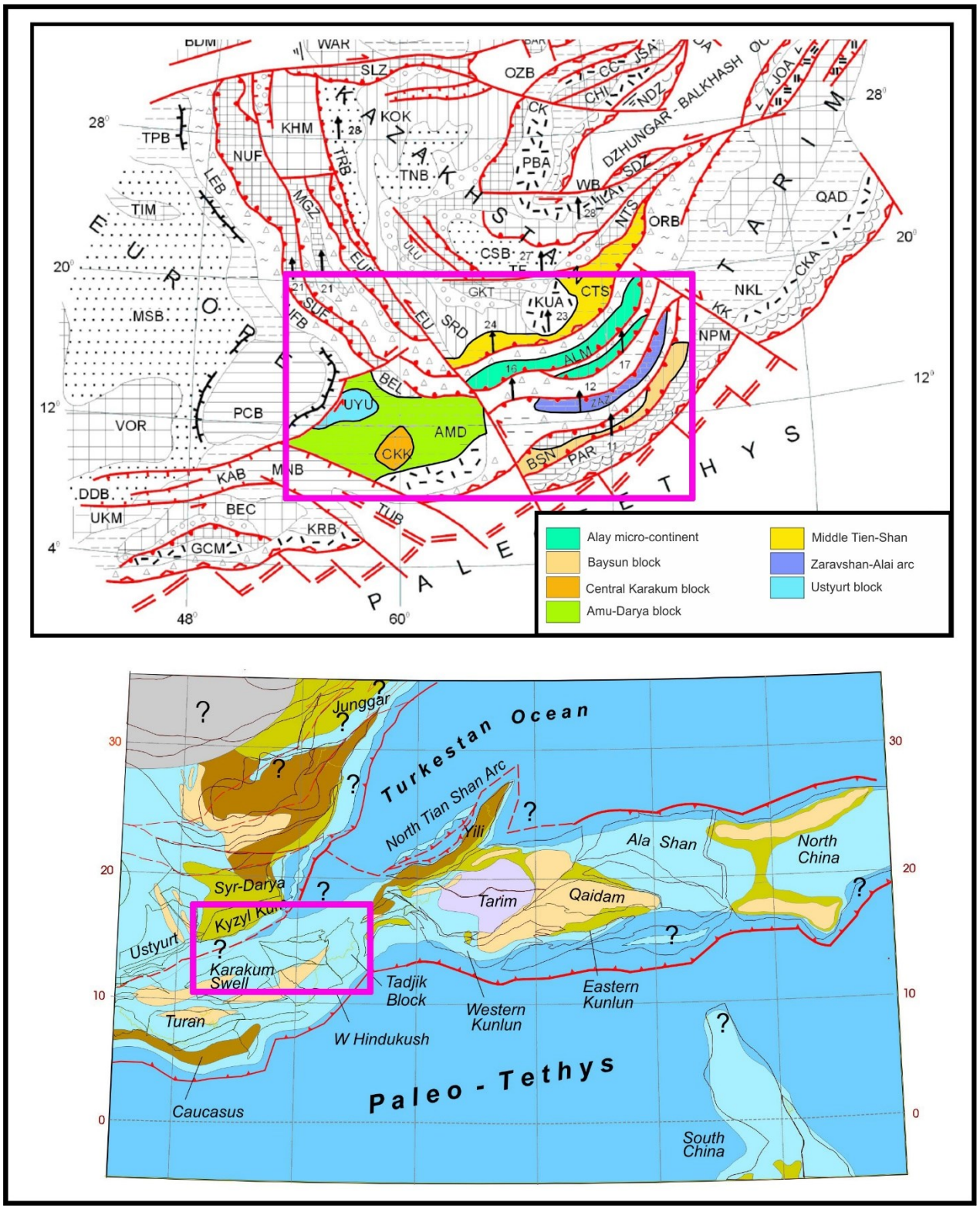

Fig. 1.19. Late Carboniferous paleogeography of Central Asia
(modified after Filippova et al., 2001, top; Heubeck, 2001 bottom).

The end of the Carboniferous – beginning of the Permian stage (fig. 1.19, 1.20). At a wider scale, the beginning of the Permian was characterized by the completion of the Laurasia supercontinent (Zonenshain et al., 1990). In the Central Asia domain it was marked by the entire closure of the Turkestan Ocean and the collision of the Karakum-Tajik, Alay blocks and Middle Tien-Shan. At the end of the Early Permian, the Southern Tien-Shan fold and thrust belt was erecting in response to the

collision of the Alay block with the Kazakh continent (Burtman et al., 1998; Klishevich and Khramov, 1995; Pechersky and Didenko, 1995).

The end of the Permian stage (fig. 1.21). The Late Permian time is marked by the consolidation of the Central Asia structures (Filippova et al., 2001) and by strike slip displacements between the blocks (Thomas et al., 1999; Heubeck, 2001; Natal'in and Şengör, 2005; Nurtaev et al. 2013…). According to the authors, they are either of small or large amplitude, but data are limited to constrain the models.

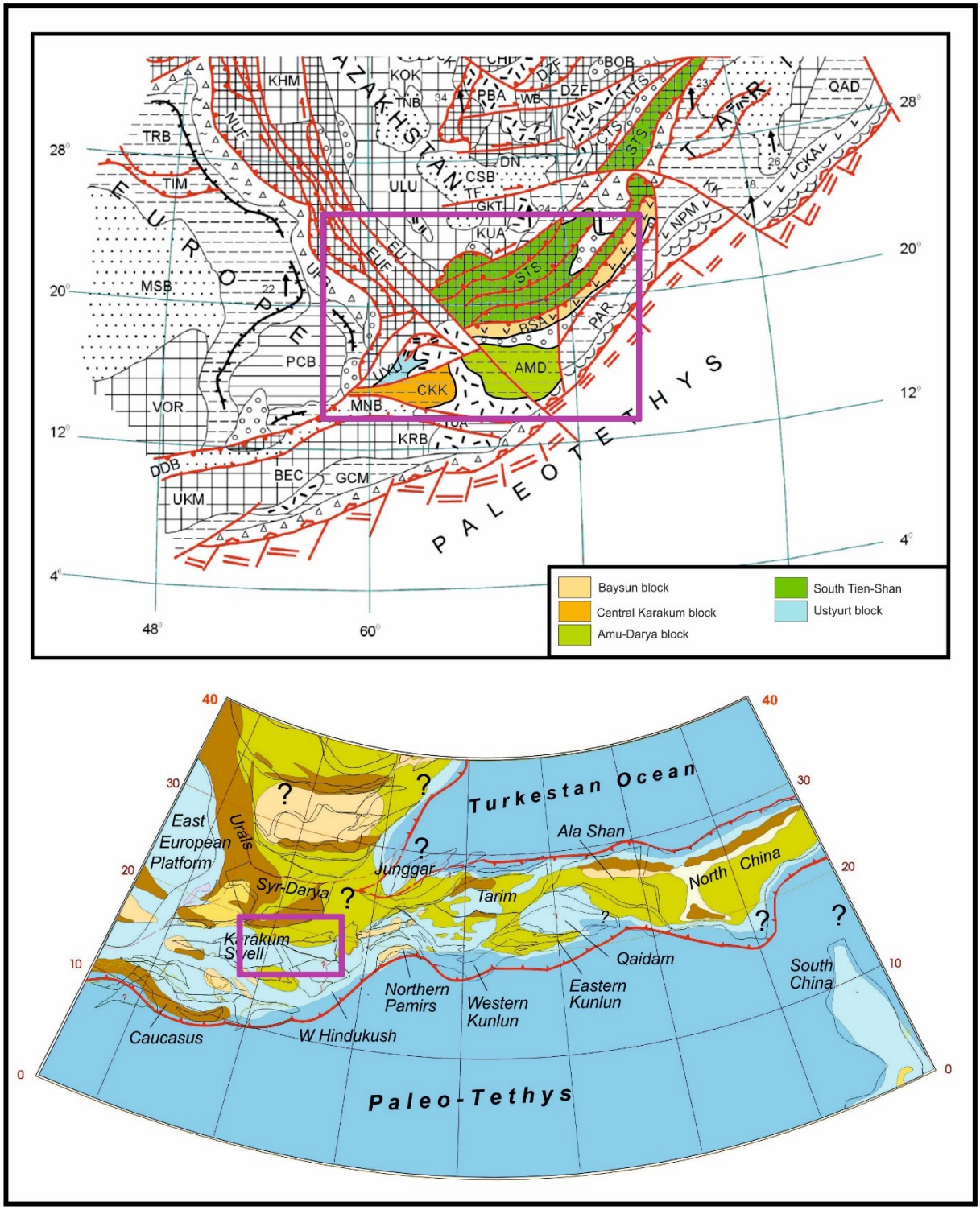

Fig. 1.20. Early Permian paleogeography of Central Asia
(modified after Filippova et al., 2001, top; Heubeck, 2001 bottom).

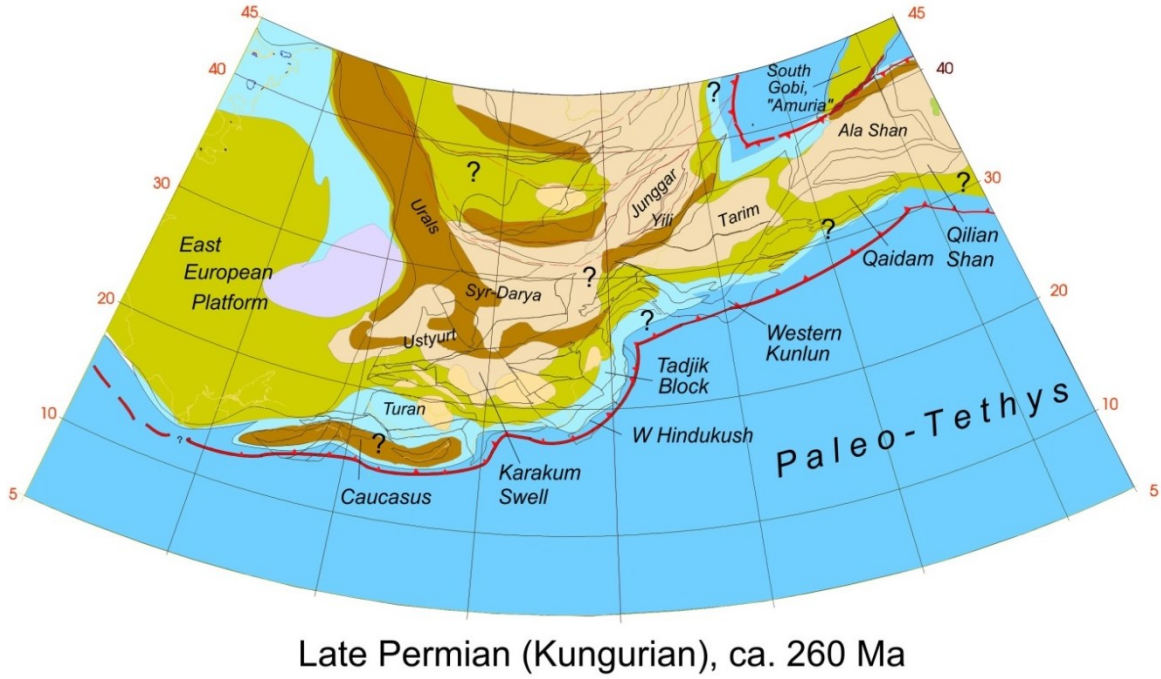

Fig. 1.21. Late Permian paleogeography of Central Asia (modified after Heubeck, 2001).

The end of the Triassic stage. The continuous spreading in the Neo-Tethys, which has begun in the Early Permian, has led to the collision between the Cimmerian continental blocks (North Afghan, Central and South Pamir, Karakorum and Qiangtang micro-plates). These continent-continent collisions have led to the buildup of the about 5000 km long Cimmerian orogen that fringed the southern margin of Northern Pangea during the Middle-Late Triassic. The orogeny resulting from these collisions that initiated in Middle Triassic (and lasted until the Early Jurassic) were relatively short. In some areas like the Bukhara-Khiva region, they had reactivated the Pre-Mesozoic structures and originated the thick molassic sequences deposited in Central Asia (Shein, 1985).

1.7. Conclusion

Our study concerns the northern margin of the Amu-Darya-Basin and the northwestern part of the Afghan-Tajik basin which occupy the southeastern part of the epi-Hercynian Turan Platform. In common, these two basins have a large Mesozoic-Cenozoic sedimentary sequence deposited during the development of the Tethys Ocean's marginal seas and lying on a complex tectonic structure inherited from the Paleozoic evolution which is not well known.

Our objectives are the investigation of the Bukhara-Khiva region in the northern margin of the Amu-Darya basin and of the Southwestern Gissar region, which includes the northwestern part of the Afghan-Tajik basin in order to reconstruct their tectono-stratigraphic evolution. Both regions are important for the oil and gas industry. The Bukhara-Khiva region is the biggest hydrocarbon province of Uzbekistan. As they are economically important, these regions have been well studied by different geological and geophysical methods. The results of the previous studies show a polyphase geodynamical evolution of the area.

The evolutional processes are connected to the development of the Turkestan Ocean and Zaravshan oceanic or marginal domain during the Paleozoic.

Chapter 2

Deposits of the Bukhara-Khiva and Southwestern Gissar regions

Chapter 2

Deposits of the Bukhara-Khiva and Southwestern Gissar regions

2.1. General setting

The most part of the northern margin of the Amu-Darya basin in Uzbekistan is covered by Cenozoic sediments (see fig 1.8). The data about the deep sediments aged from the pre-Paleozoic to the Cenozoic, can be mainly obtained by subsurface investigations.

Outcrops of Paleozoic, Mesozoic and Lower Cenozoic deposits exist in the Southwestern Gissar Range. They are aged from the Early Paleozoic to the Late Cretaceous (fig. 2.1). Most of the principal stratotype sections of the northern margin of the Amu-Darya basin are concentrated in this area.

The pre-Jurassic rocks are metamorphic, magmatic, volcanoclastic or sedimentary formations. The Mesozoic and Cenozoic sedimentary strata are composed of siliciclastics, carbonate and evaporitic rocks, deposited in different environmental surroundings.

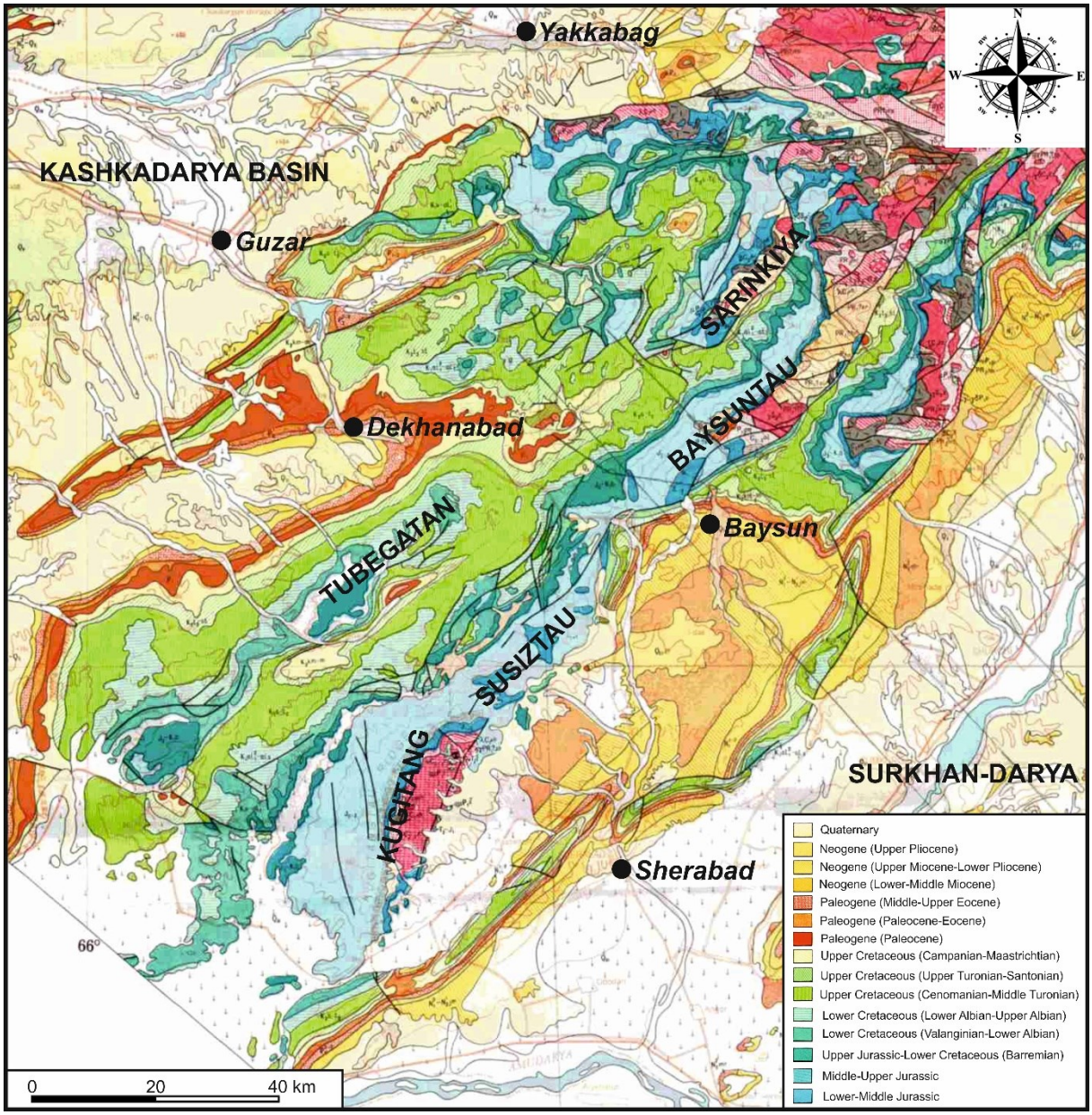

Fig. 2.1. Scheme of Southwestern Gissar. Fragment of the Geological map of Uzbekistan, 1998.

We will shortly and successively describe the pre-Jurassic rocks of the Bukhara-Khiva and Southwestern Gissar. As we mentioned in Chapter 1, the Bukhara-Khiva and Southwestern Gissar regions were belonging to different blocks in Paleozoic time. The Mesozoic and Cenozoic, which are similar for the Bukhara-Khiva region and Southwestern Gissar in a huge united basin, will be described commonly for both areas with the main focus on the Mesozoic.

2.2. Pre-Jurassic

The age of the pre-Jurassic rocks varies in a big interval of time – from the pre-Cambrian to the Permian in the Southwestern Gissar, and from the pre-Cambrian to the Permian-Triassic in the Bukhara-Khiva region.

These rocks have been penetrated by more than 500 wells in the Bukhara-Khiva region. About 280 wells among them have reached metamorphic, sedimentary and volcanoclastic rocks. Intrusive and effusive rocks have been met by more than 220 wells (Babadjanov, 2008).

In Southwestern Gissar, the pre-Jurassic rocks are cropping out in the core of the anticlines, but neither Ordovician, Silurian nor Devonian has been observed or very few, in the north. Meanwhile in the Bukhara-Khiva area only the Ordovician is missing in boreholes data (Tulyaganov and Yaskovich, 1980).

2.2.1. Southwestern Gissar

2.2.1.1. Lower Cambrian

The Paleozoic section of the Southwestern Gissar probably starts with Lower Cambrian sediments (fig. 2.2). It is difficult to more precisely determine the age of this section because of the strong metamorphism of the rocks and poor fauna and flora.

This supposed Lower Cambrian section is constituted by different gneisses and reaches a thickness of 1400 m [here and further descriptions for the pre-Mesozoic rocks of the Southwestern Gissar are taken from Tulyaganov and Yaskovich (1980)].

2.2.1.2. Carboniferous

There is a big stratigraphic gap after the Cambrian. The Paleozoic section is continued by Carboniferous deposits, which overlay the Cambrian metamorphic complexes with a sharp angular unconformity. The Carboniferous is divided into three parts proposed by Tulyaganov and Yaskovich (1980) with an old stratigraphy. Now, the Carboniferous is divided into only two parts.

The first one is the Lower Carboniferous represented by Middle Tournaisian-Lower Visean sediments according to the flora dating. There are conglomerate and sandstone with porphyrite intercalations in the bottom of this interval (t_2-v_1). The thickness of the Lower Carboniferous is 360 m.

The next part of the Lower Carboniferous has a Middle Visean-Early Namurian age [old name from Tulyaganov and Yaskovich, (1980) corresponding to the Serpukhovian and the lower part of the Bashkirian in the present chronostratigraphic chart] and conformably covers the underlying rocks. There are effusives with sandstone and limestone intercalations in the bottom of this bed. The middle part is represented by limestone. The upper part of the described unit, like the bottom part, is effusive rock bearing and has almost the same structure. The common thickness of the Middle Visean-Lower Namurian beds is 1400 m.

The Middle Carboniferous sediments (Upper Bashkirian-Lower Moscovian) are 2000 m thick and are not observed in a stratigraphical contact with the Lower Carboniferous ones. The Carboniferous deposits are represented by isolated outcrops in Southwestern Gissar. Different sandstone, siltstone, tuff-sandstone, limestone and conglomerate constitute the Middle Carboniferous layer.

The next, small bed (only 180 m thick) has a Late Moscovian age and is composed of limestone, siltstone and argillite.

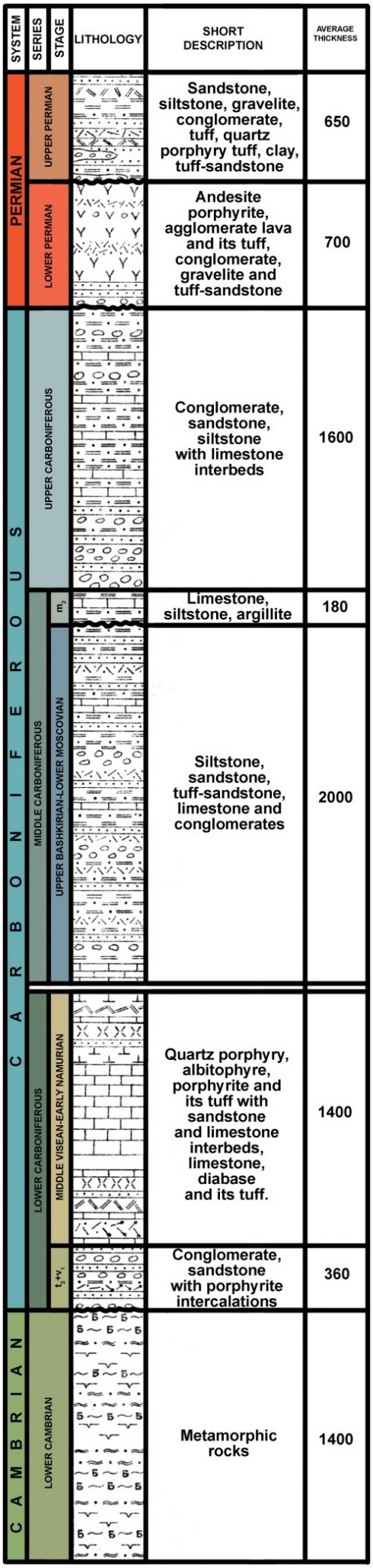

The Upper Carboniferous series is represented by sandstone, siltstone and conglomerate with some limestone intercalations. The observed thickness of this layer is 1600 m.

2.2.1.3. Permian

The Lower Permian sediments unconformably overlay the Carboniferous. This pack is 700 m thick and composed of effusive rocks, conglomerates, gravelites and tuff-sandstones at the base.

The Upper Permian consists of siltstone, sandstone, gravelite, conglomerate quartz porphyry tuff, tuff, and argillite and tuff-sandstone. The thickness of this bed is 650 m

2.2.2. Bukhara-Khiva region

The pre-Jurassic stratigraphy of the Bukhara-Khiva is differing from the Southwestern Gissar one. Its section is more complete and detailed (fig. 2.3). But, even within the Bukhara-Khiva region itself there are some stratigraphic differences between the Chardzhou and the Bukhara steps. On the Chardzhou step, there are pre-Cambrian, Cambrian, Carboniferous and Permian sediments; meanwhile on the Bukhara step all the Paleozoic strata are well determined, (map fig. 2.4), except the Ordovician which cannot be separated from the Silurian.

Another major difference between these two steps is the great amount of magmatic rocks in the Bukhara step, while on the Chardzhou step the deposits are mainly sedimentary.

As seen on the map of the pre-Jurassic surface (fig. 2.4) the most widespread Paleozoic sediments in the the Bukhara-Khiva region are the Carboniferous and Permian siliciclastics.

2.2.2.1. Pre-Cambrian to Devonian

The pre-Jurassic section of the Bukhara-Khiva region starts with a pre-Cambrian complex. This complex consists of amphibolites, amphibolite-sandy orthogneisses and gneisses with shale structure, hard and strongly metamorphosed. The thickness penetrated is around 120 m (see fig. 2.4).

The Cambrian rocks, reached in the Chardzhou step, have not a big penetrated thickness – only 28 m. This stage is represented by strongly metamorphosed sedimentary rocks and, sometimes, effusive rocks.

An undivided pack of the Ordovician-Silurian exists within the Bukhara step and is represented by strongly metamorphosed shales. The maximal drilled thickness is 222 m.

The Devonian system is composed of dolomitized limestone, partly marmorized limestone, and dolomite. The limestone is algal with a lot of organic material. The maximal reached thickness is 337 m.

Fig 2.2. Synthetic section of the Paleozoic in Southwestern Gissar

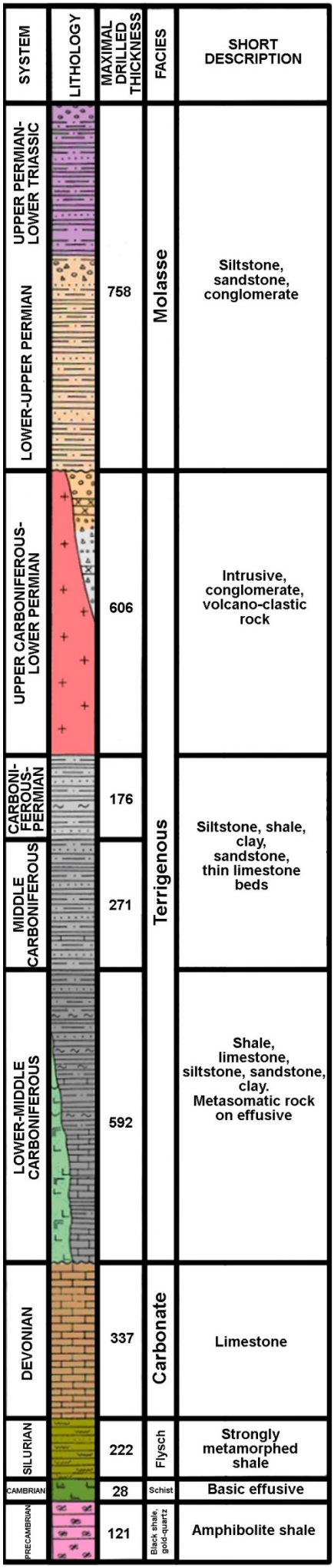

2.2.2.2. Carboniferous

The sediments of the Carboniferous are ones of the most widespread pre-Mesozoic rocks in the Bukhara-Khiva region (fig. 2.3).

The Lower-Middle Carboniferous pack consists of shale, limestone, siltstone, sandstone and clay. There are also metasomatic effusive rocks. The penetrated thickness is 592 m.

The Middle Carboniferous and undivided Carboniferous-Permian pack have almost the same composition (siltstone, shale, clay sandstone with thin limestone beds) and a thickness of 271 m and 176 m respectively. The sediments of these stratigraphic intervals are widely occurring Paleozoic rocks of the area.

We may even include into this pack the undivided Upper Carboniferous-Lower Permian deposits, which are represented by intrusive, conglomerates and volcano-clastic sediments. The most part of the intrusives of the Bukhara step have this age. The maximal penetrated thickness is 606 m.

2.2.2.3. Permian-Triassic

Permian clastics have been met in the Chardzhou step and in the northwestern part of the Bukhara step (see fig. 2.4). They fill Paleozoic troughs and graben structures.

This pack is represented by different types of sandstone, clay, siltstone and conglomerate.

Undifferentiated Permian-Triassic beds have a very limited extension. These sediments have been drilled only in a few wells. As shown on Figure 2.4, most of the Permian-Triassic sediments exist in the Bukhara step, and very locally in the Chardzhou step. They do not constitute continuous massive sequences, unlike the Permian, for example.

The presence of clearly dated Triassic deposits is still under question. In general, the Permian-Triassic rocks, like the Permian ones, deposited in graben structures. They are represented by rudaceous, badly sorted rocks – conglomerates, conglomerate-breccias with effusive rocks pebble and rare limestone innerlayers.
The common thickness of the Permian-Triassic beds is 758 m in the drillings.

Fig. 2.3. Synthetic section of the pre-Jurassic sequence of the Bukhara-Khiva area (modified after Babadjanov and Abdullaev, 2009).

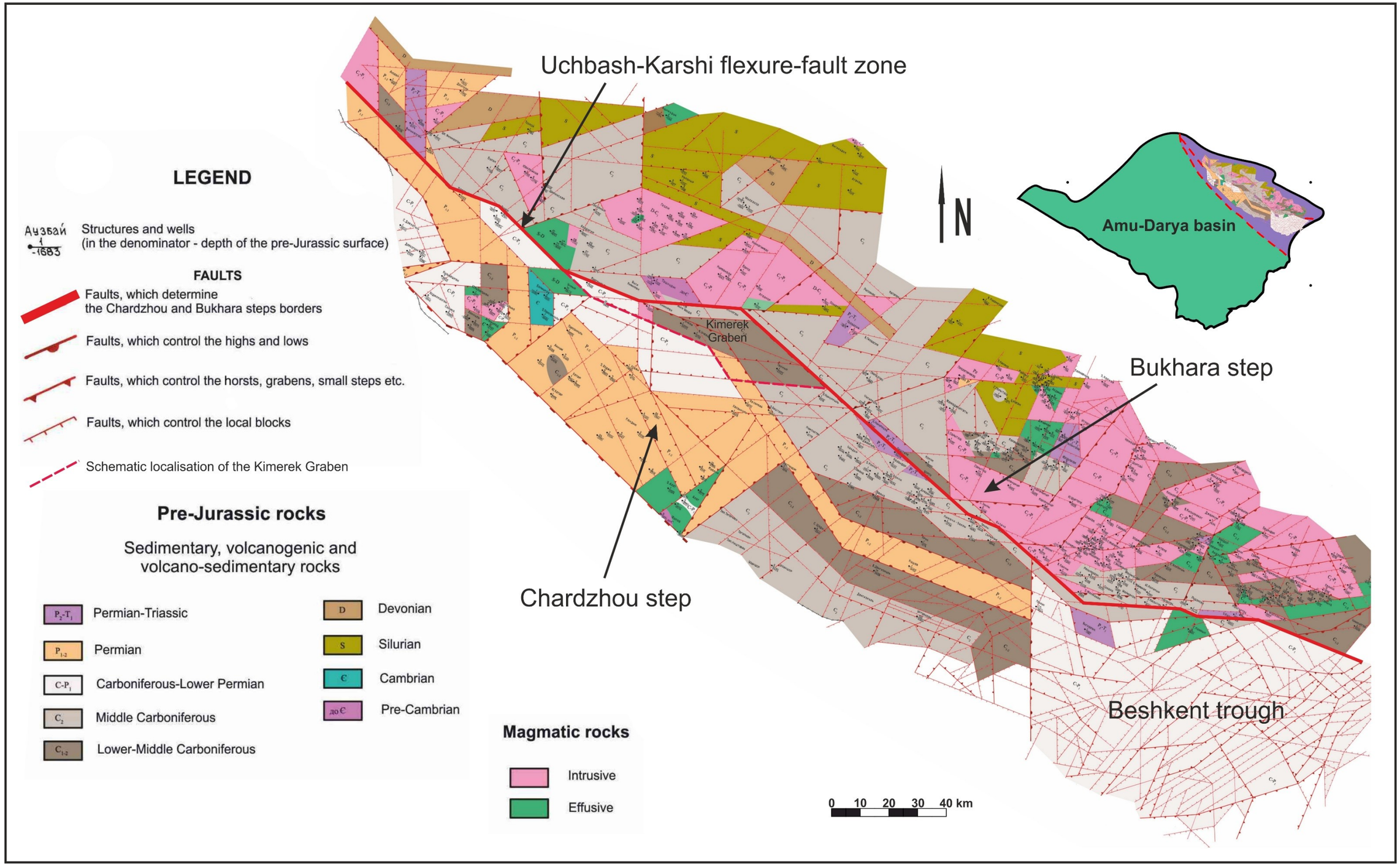

Fig. 2.4. Paleogeological sketch of the pre-Jurassic surface of the Bukhara-Khiva region (modified after Babadjanov and Abdullaev, 2009).

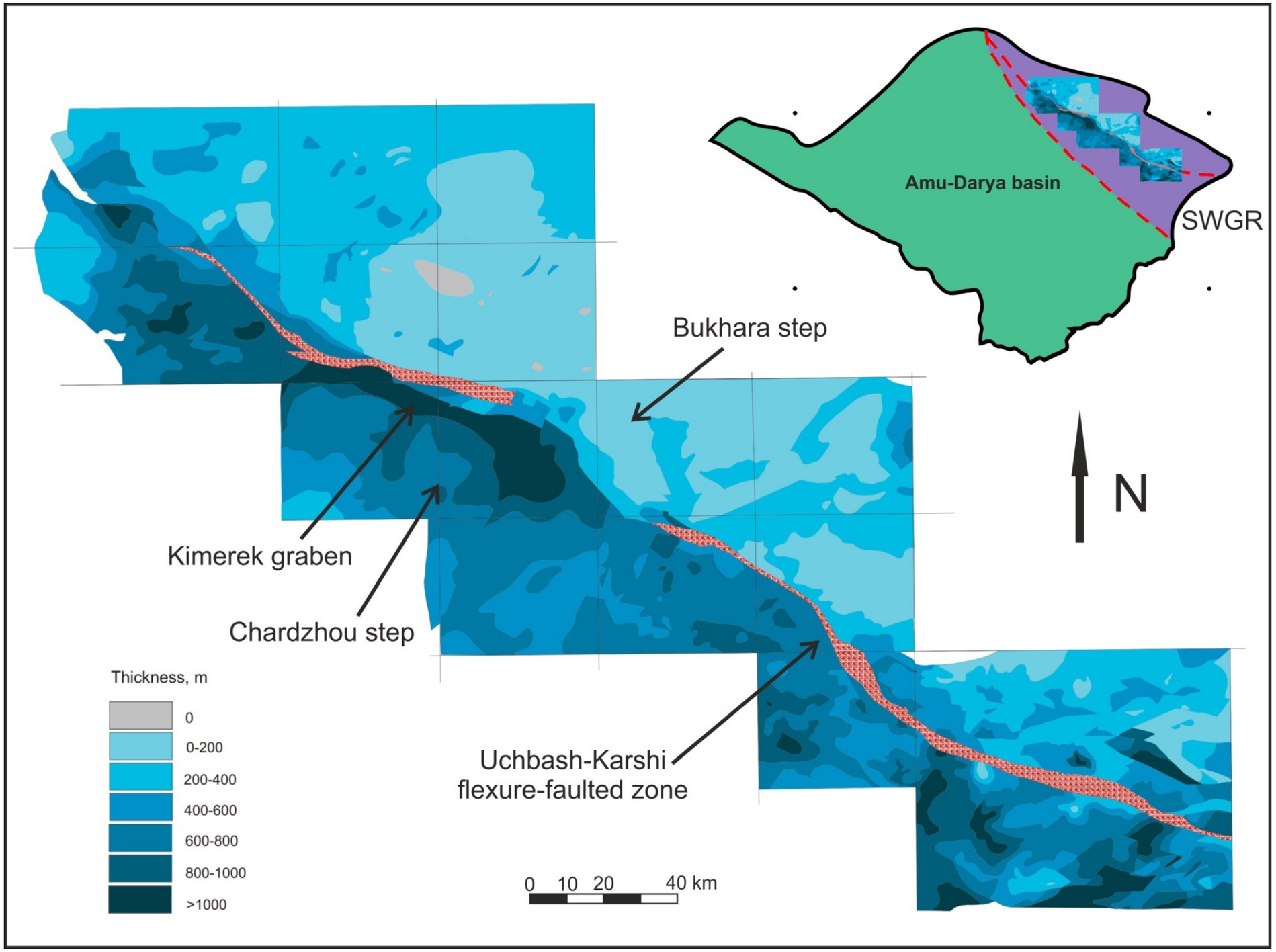

Fig. 2.7. Map of the Jurassic terrigenous and carbonate thicknesses for the Bukhara-Khiva region (modified after Mordvintsev O., 2012 in Babadjanov, 2012).

2.3. Jurassic

The Jurassic sediments unconformably cover the Permian, Permian-Triassic and all the other pre-Jurassic rocks (fig. 2.5).

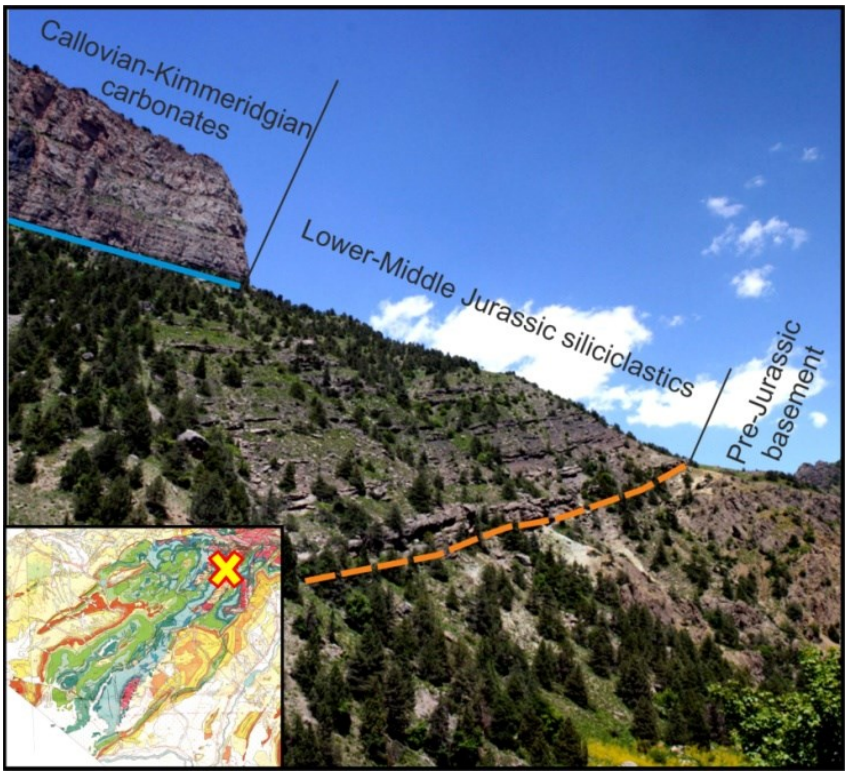

Fig. 2.5. Unconformity between the Jurassic and pre-Jurassic rocks in the northern part of Southwestern Gissar (modified after Bourillot, 2013, personal communication).

Traditionally in Uzbekistan, the geologists divide the Jurassic into three parts (fig 2.6, next page) called here "units": the *terrigenous, carbonate* and *evaporite units,* where:
the terrigenous unit (Surkhantau Group) is a set of siliciclastic beds;
the carbonate unit (Kugitang Group) is generally represented by limestone with different facies;
the evaporite unit (Gaurdak Group) is composed of salt-anhydrite layers.

This scheme, in general, does not depend on the age of the beds, but shows a main lithological differentiation (fig. 2.6). Despite this division is supported by many geologists, there are a lot of discussions about the detailed structure and stratigraphy of each unit because the Jurassic beds non-homogeneously cover the northern margin of the Amu-Darya basin.

Most of the Jurassic is concentrated in the limits of the Chardzhou step of the Bukhara-Khiva region. Thin sections exist on the Bukhara step while the thickest sections are encountered in the southeastern part of the Chardzhou step and in the Southwestern Gissar area.

The thickest Jurassic terrigenous section of the Bukhara-Khiva region has been drilled in the Kimerek graben of the Chardzhou step, a pre-Mesozoic structure (see fig. 2.4), filled also by terrigenous Jurassic sediments (fig. 2.7, previous page).

Figure 2.7 displays the distribution of the Jurassic *terrigenous* and *carbonate units* thicknesses. This scheme was created by drilling and seismic data interpretation. It does not concern the *evaporite unit*, as it was made for the oil and gas industry, for which the *terrigenous* and the *carbonate* Jurassic *units* are the main target.

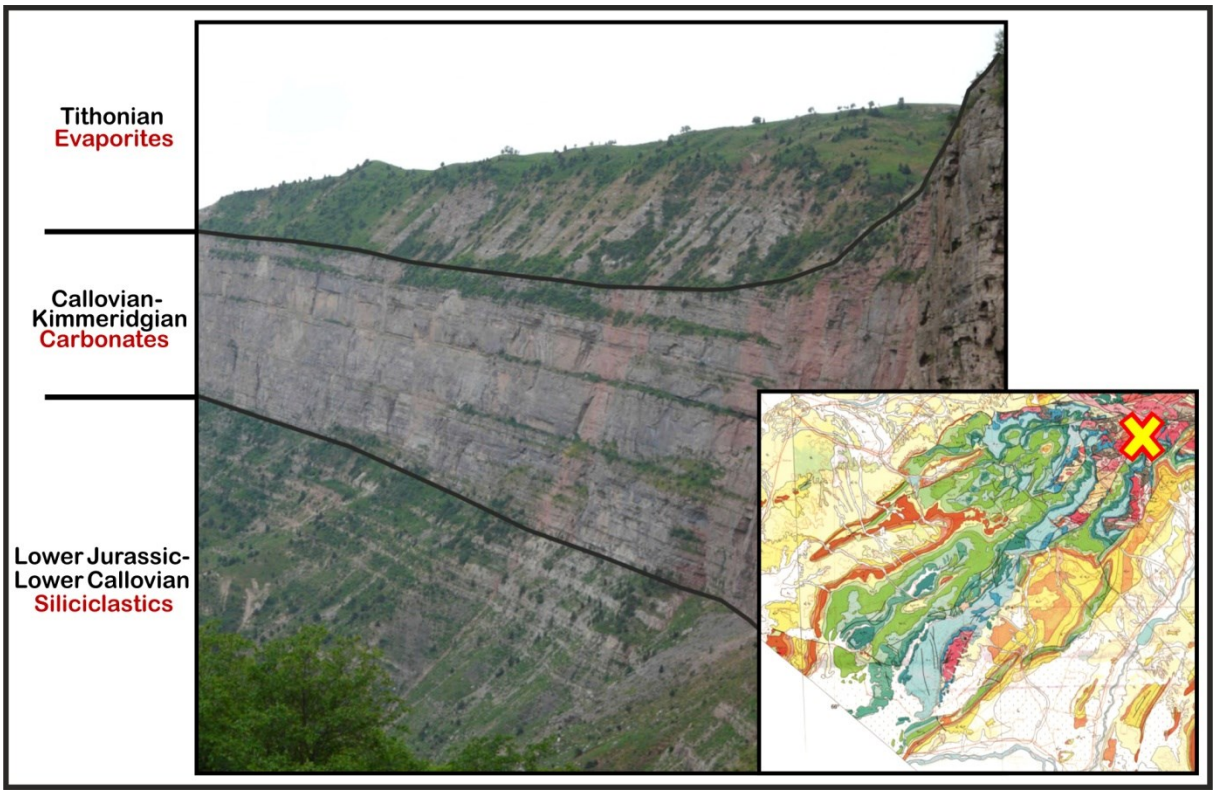

Fig. 2.6. Complete Jurassic section of the northern part of Southwestern Gissar (photo by E. Barrier).

It exists many lithostratigraphic columns/charts, which touch both the entire area and each region separately. Two of them are more important.

The first one was, for a long time, the most used in the Republic of Uzbekistan (fig. 2.8-A). This chart has different stratigraphic subdivisions for the Bukhara-Khiva and Southwestern Gissar. The reason is that the stratigraphic column for the Southwestern Gissar has been established on the basis of analyses of field sections, while the source for the stratigraphic column of the Bukhara-Khiva region was based on well data.

The *terrigenous unit* starts in the upper part of the Late Triassic and ends in the lower part of the Early Callovian. It is divided into five formations: Sanjar, Gurud, Degibadam, Tangiduval and Baysun. This stratigraphy is the same for both the Bukhara-Khiva and Southwestern Gissar regions.

The carbonate unit is continuing from the middle part of the Early Callovian to the top of the Early Kimmeridgian.

For the Bukhara-Khiva area, this unit is represented by three types of section, which exist at the same time, but in different places. These are: the Urtabulak type, the Tubegatan type and the Khodjaipak Formation. Each of them is also divided into subsections, including productive horizons.

This type of stratigraphic division was commonly used because the Bukhara-Khiva region is the biggest oil and gas province of Uzbekistan and most of the geological works, which were performed there, have been dedicated to hydrocarbon studies and explorations. That is why the division of the geological section into hydrocarbon bearing horizons is still widespread, even in the geological literature.

In the Southwestern Gissar, the subdivision of the *carbonate* Jurassic *unit* is a bit different. It consists of different local formations with some overlapping time ranges.

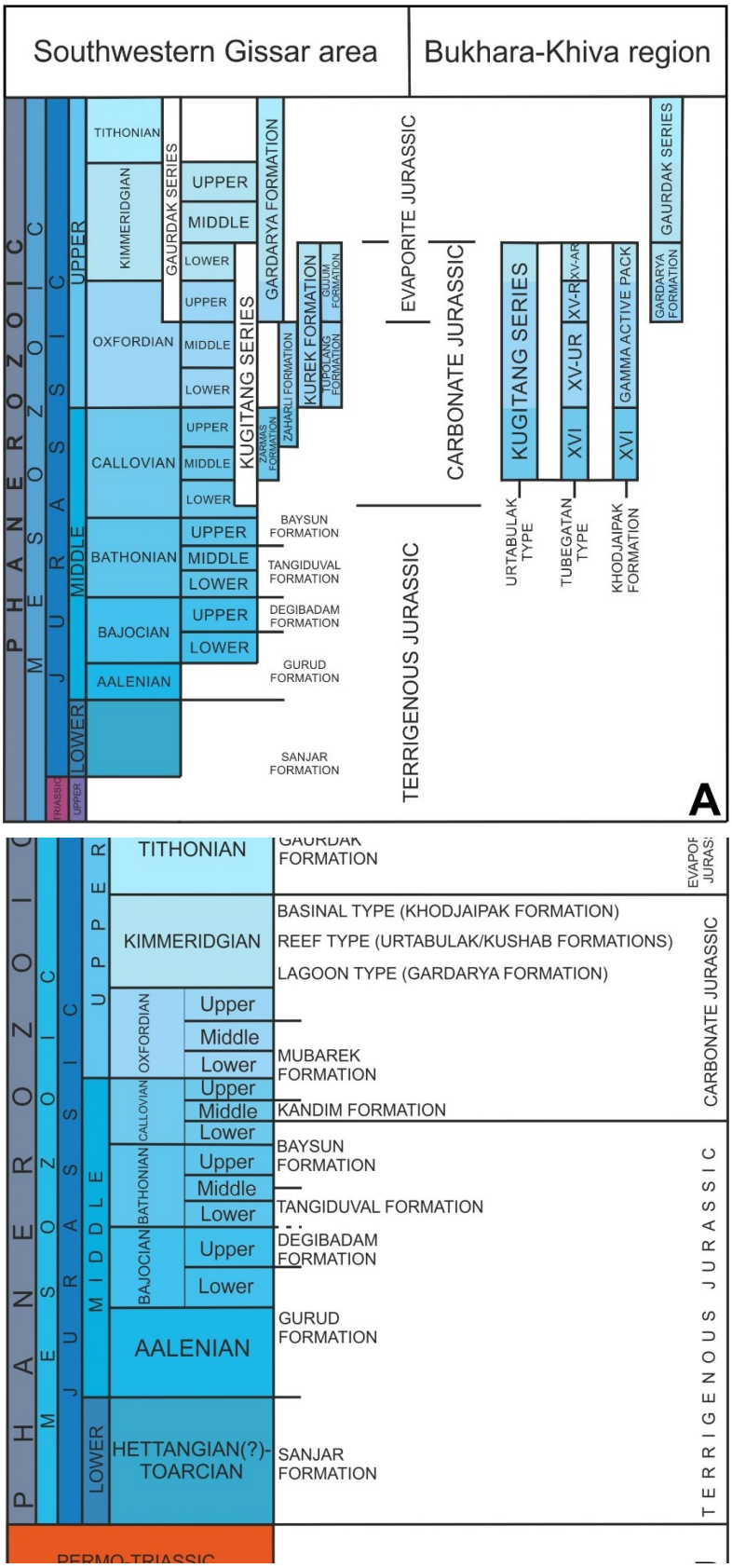

Fig. 2.8. Comparison of Jurassic stratigraphic charts.
A – schematic stratigraphic column modified after Shayakubov and Dalimov (1998); **B** – schematic stratigraphic column, as used in this thesis, modified after Mirkamalov et al. (2005), and Fürsich et al. (2015).

The evaporite unit tops the Jurassic. It has a Late Oxfordian-Tithonian age and consists of the Gardarya Formation for the Southwestern Gissar or the Gardarya Formation plus the Gaurdak series for the Bukhara-Khiva region (Shayakubov and Dalimov, 1998).

One of the difficult points using this stratigraphic chart is that it comprises many local subdivisions. Very often they are not correlated. The complexity of the stratigraphic nomenclature creates many difficulties in the age determination and correlation between the diverse formations of the Bukhara-Khiva and Southwestern Gissar.

That is why we have chosen a more recent and unified stratigraphy after Mirkamalov et al. (2005) (fig. 2.8-B) which covers the whole Bukhara-Khiva and Southwestern Gissar regions. It does not contain too many different local stratigraphic subdivisions.

The stratigraphy of the terrigenous Jurassic is almost the same that in the chart just described, except the beginning and the end of the formation. It does not start in the Late Triassic, but in the Early Jurassic, as the Late Triassic and the base of the Jurassic are not recognized. The second change is at the top of the unit, for which the age of the bottom of the Baysun Formation has been changed from the Late Bathonian to the Middle Bathonian according to Fürsich et al. (2015), because of the presence of the ammonite *Procerites* in the condensed base of the Baysun Formation. Besides this, the rest of the *terrigenous unit* has the same stratigraphy as in the previous chart.

The subdivision of the carbonate Jurassic is different in the new chart. This unit has a Middle Callovian-Kimmeridgian age and is divided into three members: the Kandim and Mubarek formations and the Upper Oxfordian-Kimmeridgian stage. This latter stage corresponds to three types of sections: the basinal, reefal and lagoonal types. These types reflect various sedimentary conditions in the different areas of the Bukhara-Khiva and Southwestern Gissar regions.

The *evaporite unit* has a Tithonian age while it was Late Oxfordian to Tithonian in age in the first chart. In most part of the studied area it is represented by the Gaurdak Formation.

To expose the main features of the Jurassic section, we will use:

Stratigraphic data from the Sultansandjar, Yangikazgan, Uchkir, Kimerek, Uchbash, Parsankul, Gugurtli, Dayahatin, Hodjikazgan, Akkum, Kandim, Alat, Farab wells for the western part of the Bukhara-Khiva region (fig. 2.9);
Data from the Shurtan, Pamuk, Urtabulak, North Kamashi, Zevardi, Ayzovat, Chatirtepe, Buzahur wells for the eastern part of the Bukhara-Khiva region;
Data from the sections of Tubegatan, Gaurdak, Vandob, Shelkan, Tangiduval, Panjob, Sayrob, Derbent, Yukori Machay, Zarmas, Bakhcha, Handiza, Sangardak, Shargun, Chapuh, Tashmush and Shatrut for the Southwestern Gissar region. For this area we have also used the wells data from the Amanata-Koshkuduk group of fields, and the Adamtash and Gumbulak fields (fig. 2.9).
All these sections provide a complete picture of the dispersion and features of the different Jurassic units and their inner structure.

We will also involve in our description some paleogeographical maps. Unfortunately, we did not obtain any paleogeographical map for the Bukhara-Khiva region, so we will show only the paleo-environmental conditions, for some Jurassic epochs, for the Southwestern Gissar and Surkhan-Darya area (location fig. 2.1).

Isopach maps of the Jurassic of the Bukhara-Khiva region will be discussed in Chapter 3 and compared with the thickness observed on the constructed cross-sections of our work.

As the Jurassic is divided into three parts, we will successively describe the stratigraphy of each part according to this division. At first, we will describe the *terrigenous unit* – the thickest Jurassic unit, then the *carbonate unit*, for which we will discuss the differences and correlations between the different types of the carbonate section, and finally, we will describe the lithological-stratigraphical features of the *evaporite unit.*

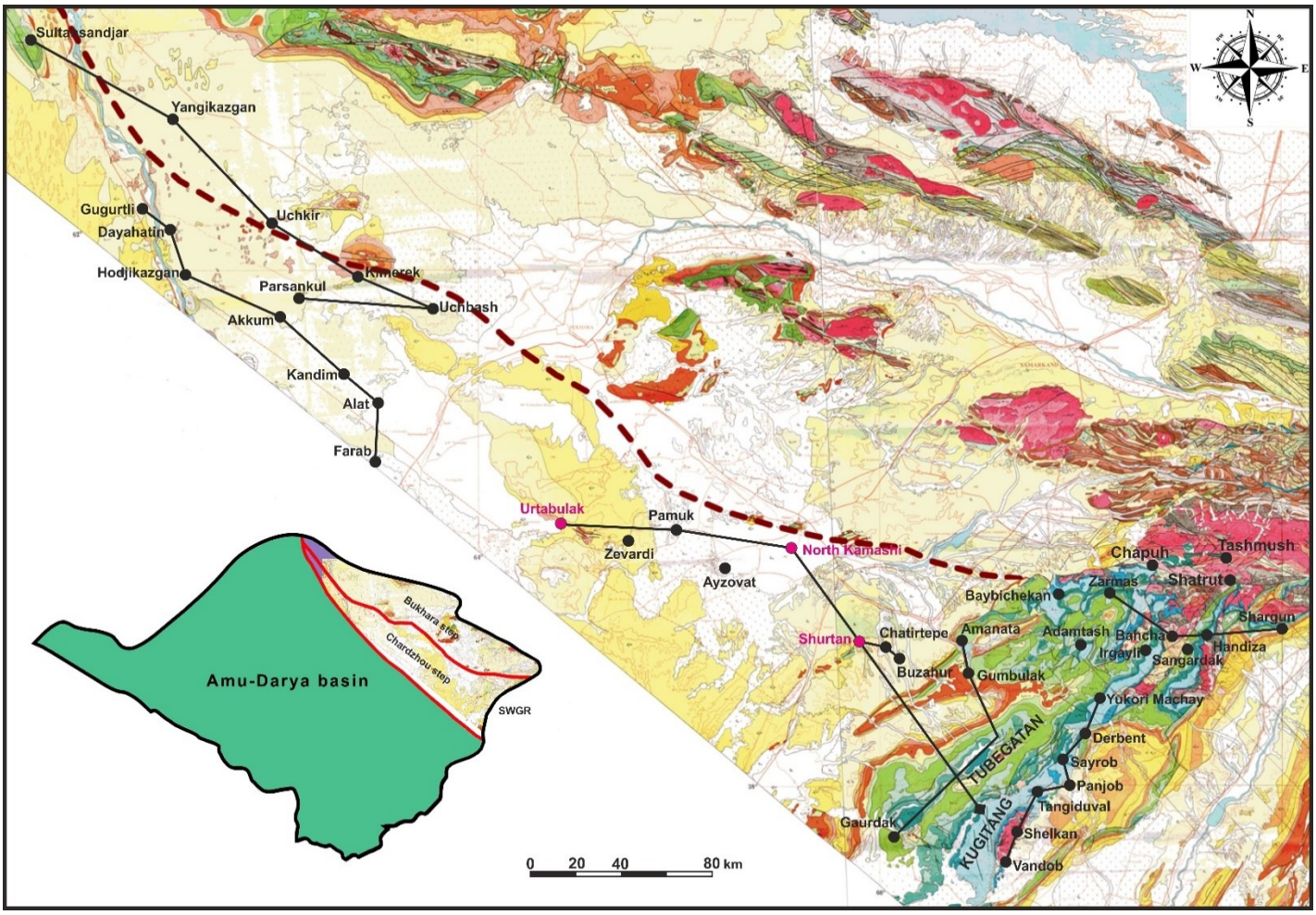

Fig. 2.9. Location of the sections used to show the stratigraphic features of the Jurassic of the Bukhara-Khiva and Southwestern Gissar areas. Magenta points: location of stratotype well sections; dashed thick line: Uchbash-Karshi flexure fault zone. Background = fragment of the Geological map of Uzbekistan (1998).

2.3.1. Terrigenous unit

The *terrigenous unit*, also named Surkhantau Group, is a huge Jurassic siliciclastic unit, which overlaps the pre-Jurassic deposits with an angular unconformity (see fig. 2.5).

The *terrigenous unit* of the eastern part of the Chardzhou step is thicker than the western one, as the sections are more complete in the east. We mostly consider this step, as there is only a very thin Jurassic clastic sequence on the Bukhara step. Generally, the complete Jurassic terrigenous type section concerns the following members, named as formations: Lower Jurassic (Sanjar Formation), Aalenian-Lower Bajocian (Gurud Formation), Upper Bajocian (Degibadam Formation), Lower Bathonian (Tangiduval Formation) and Middle Bathonian-Lower Callovian (Baysun Formation).

In the Bukhara-Khiva region, some of these formations disappear westwards. The complete clastic section is very rare in this area. It exists only in its deepest parts, like in the Kimerek graben for example. As seen in Figure 2.10, the thickness of the terrigenous Jurassic is rather constant in the area near the UKFFZ, except in the Kimerek graben where it is thicker and decreases a lot near the southwestern border of the Chardzhou step. This corresponds to the deep structure of the Bukhara-Khiva region's basement. As it was noted on Figure 1.9, the Karakul and Birgutli troughs border the Uchbash-Karshi Flexure-Fault Zone, while near the southwestern limit of the Chardzhou step exist the NW-oriented Kandim and Uchkir-Pitnyak highs.

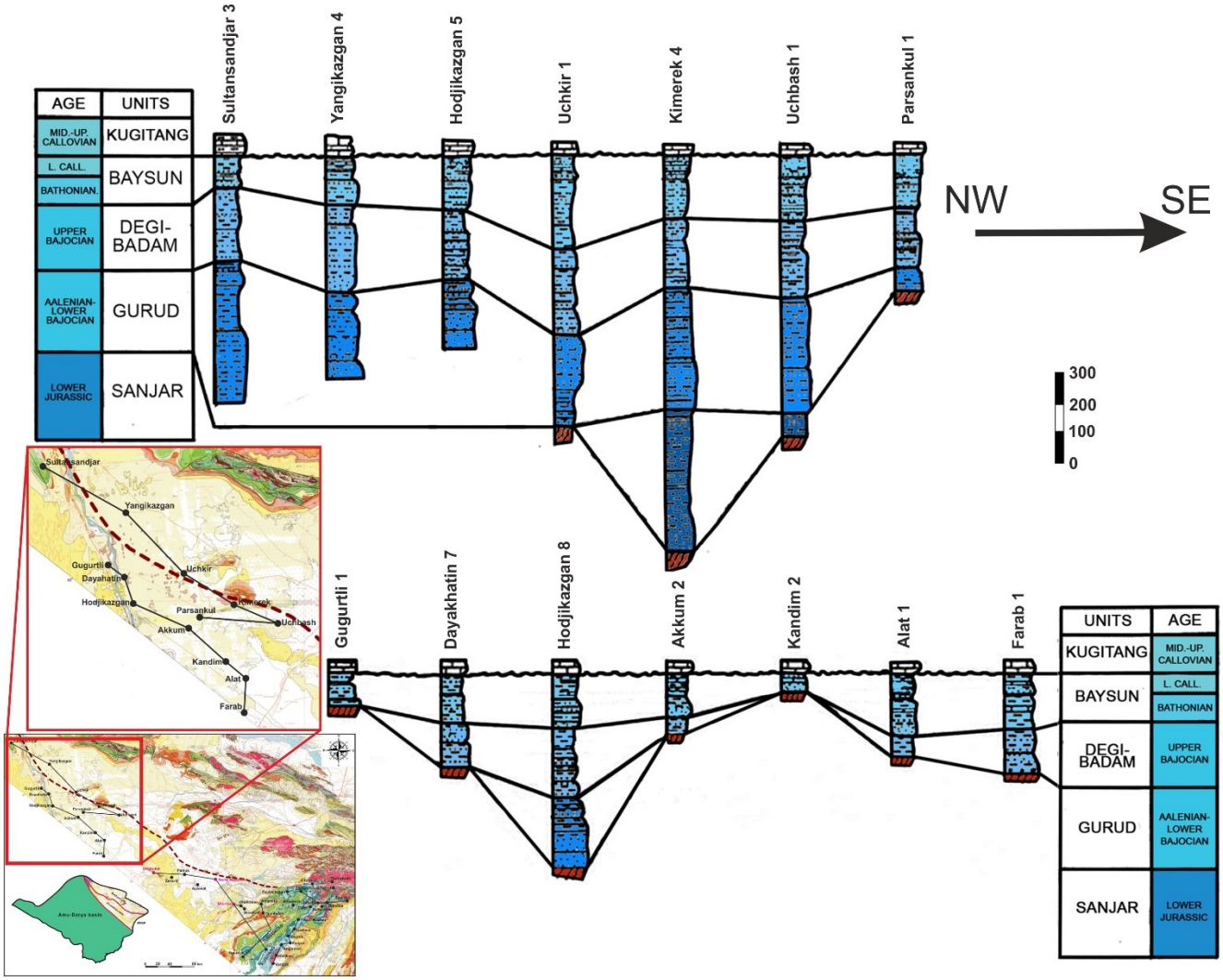

Fig. 2.10. Jurassic terrigenous thickness variations along the western part of the Bukhara-Khiva region (modified after Shayakubov and Dalimov, 1998).

As shown on Figure 2.11, the complete terrigenous Jurassic unit does not exist everywhere in the limits of the Beshkent trough in the southeastern part of the Chardzhou step, but Mirkamalov et al. (2005) propose that this set of sections is enough to recreate a complete picture of the terrigenous Jurassic stratigraphy. The most important sections are: the Pamuk 1 parametric well (fig. 2.11), as it is the most faunistically characterized section of the Bukhara-Khiva region, the Shurtan 25 section (fig. 2.11, 2.12), as it contains the thickest *terrigenous unit,* the Kugitang section, as it is the type-section determined from exposed sections (see fig. 2.11, 2.13). The Pamuk 1 section has been used for correlation between the other sections and the biostratigraphic chart. According to it, the terrigenous Jurassic section starts in the Lower Jurassic.

The maximal thickness of the *terrigenous unit* has been penetrated in the Shurtan 25 well, where it reaches more than 1000 m (fig 2.12). We will study Shurtan 25 as well as Kimerek 4 wells for the subsidence analysis in Chapter 4 because their important thickness registers the Early-Middle Jurassic tectonic evolution.

The most complete and thick terrigenous sections, except the southeastern part of the Chardzhou step (Beshkent trough) exist in the Southwestern Gissar, especially in the Kugitang Mountains (fig. 2.14). Here are the type-sections exposed where the siliciclastics are more than 800 m thick.

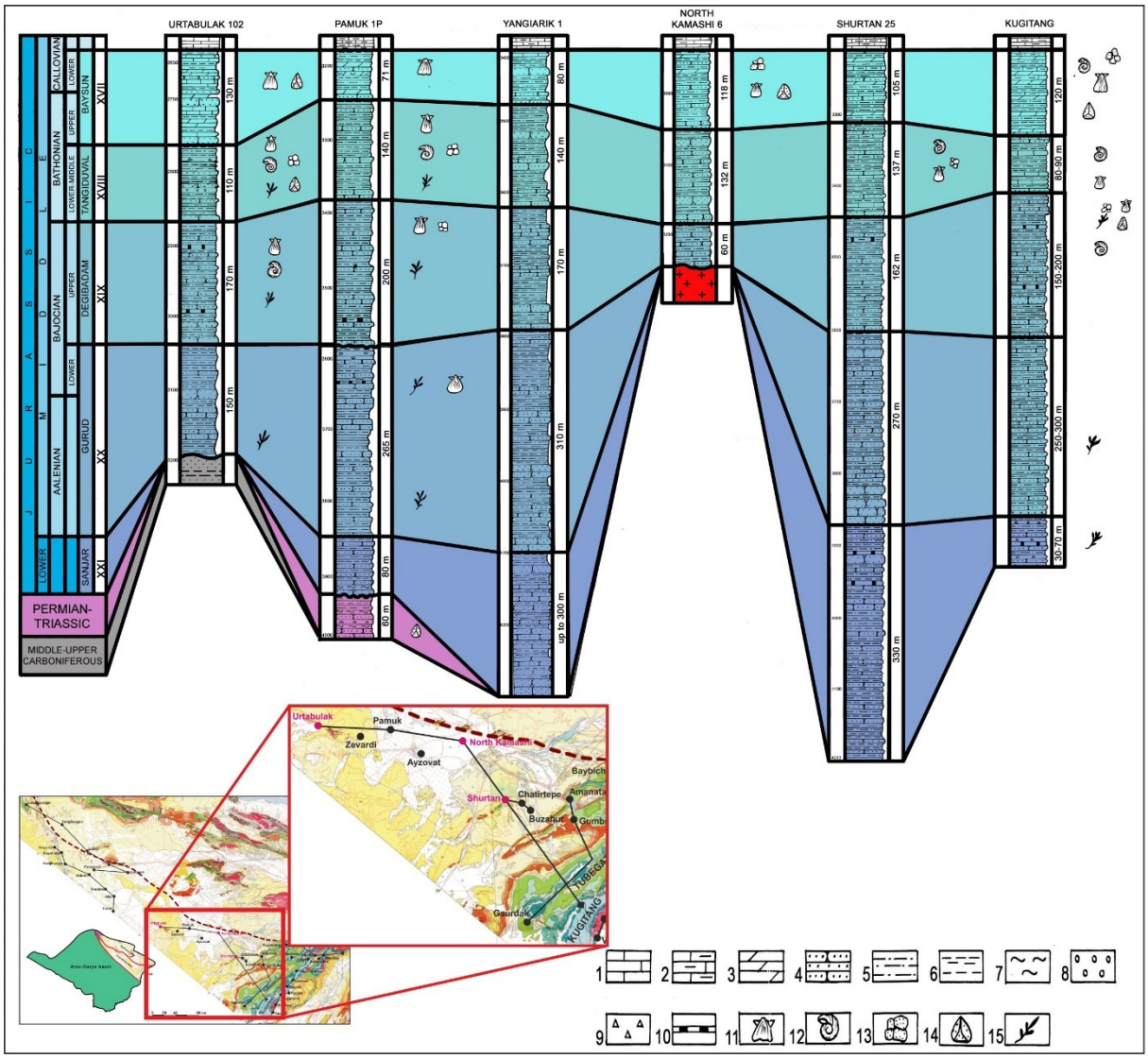

Fig. 2.11. Jurassic terrigenous sections of the south-eastern part of the Bukhara-Khiva region (modified after Mirkamalov et al., 2005). Location on fig. 2.9.

Lithology: 1. Polymict limestone; 2. Clayed limestone; 3. Marls; 4. Sandstone; 5. Siltstone; 6. Claystone; 7. Shales; 8. Gravelite; 9. Breccia; 10. Coal layers.

Fossils: 11. Bivalves; 12. Ammonites; Foraminifers; 14. Spore-pollens; 15. Plant remains.

.

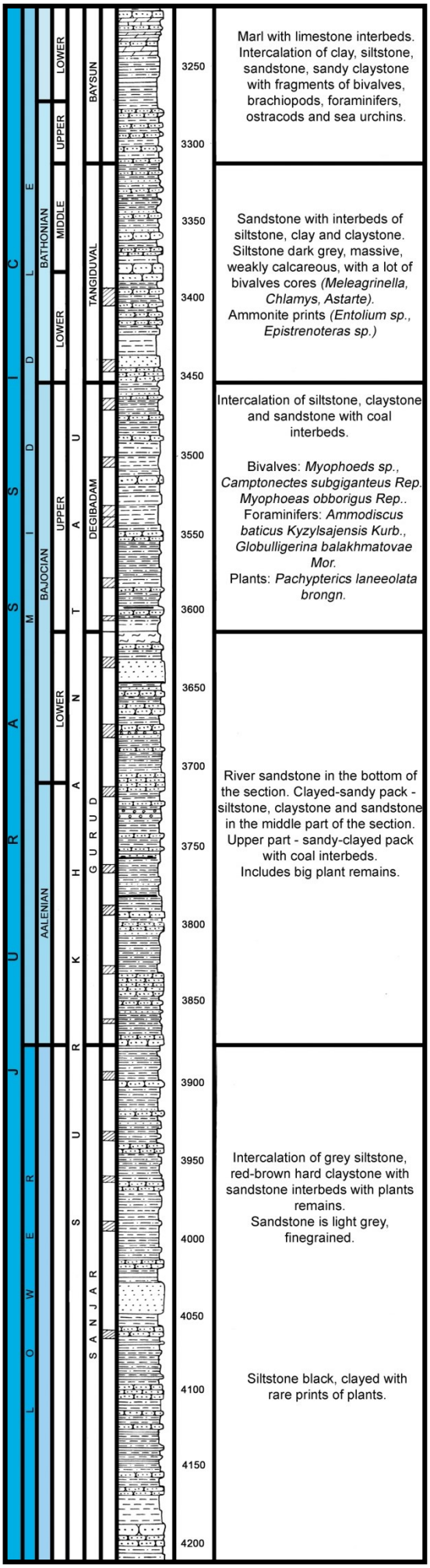

Fig. 2.12. Terrigenous section of the Shurtan 25 well (modified after Mirkamalov et al., 2005). Location fig. 2.9.

2.3.1.1. Lower Jurassic - Toarcian (Sanjar Formation)

The local name of the most ancient part of the Jurassic section is the Sanjar Formation (fig. 2.10 - 2.14). It covers the older, pre-Mesozoic, rocks with an angular and stratigraphical unconformity (see fig. 2.13, 2.14) and fills depressions in the deepest parts of their surface. In the Kugitang Mountains, the Sanjar Formation consists of breccias, gravelites, sandstone, claystone, siltstone and carbonaceous rocks (Mirkamalov et al., 2005).

The precise age of this formation is still a point of discussions, it was previously considered as beginning in the Late Triassic (fig. 2.8-A) but according to the spore-pollens and plant remains analysis of *Sagenopteris phillipsii (Brang), Cladophlebis whitbensis (Brang), Czekanowskia regida Heer.* and *Nilssonia ex gr. orientalis Heer* (Troitsky and Gomolitsky, 1995 in Mirkamalov et al., 2005) it has an Early Jurassic age.

For us, the age of the terrigenous Sanjar Formation is likely Early Jurassic, as the Triassic sediments cannot be separated from the Permian deposits in the most part of the geological sections. That is why, considering the beginning of the Jurassic period we will refer the Sanjar Formation to Early Jurassic, and not to the end of the Triassic.

To confirm this, in the Pamuk 1 parametric well (fig. 2.11), which is one of the most important stratotype section for the Bukhara-Khiva region stratigraphy, the Permian-Triassic sequence has been penetrated (dated with *Cycadophites cf. follicularis Wils., Granulatisporites trisinus Balme.* et *Mallon, Convolutispora hoffmeister Staplin, Verrucosisporites (sp.) Retitriletes sp. Kr.* by Uzakov, 1985*)*. Above this Permian-Triassic bed, deposited azoic sandstone, which was covered by the Aalenian-Lower Bajocian sediments. Mirkamalov et al. (2005) consider that this sandstone could be referred to the Lower Jurassic, according to its stratigraphical position within the section.

The thickness of the Sanjar Formation is ranging from few tens of metres in the low land areas of the Bukhara-Khiva region to 800-900 m in its southeastern parts, where the Paleozoic basement lays very deep. In the western part of the Bukhara-Khiva region this formation disappears from the geological section.

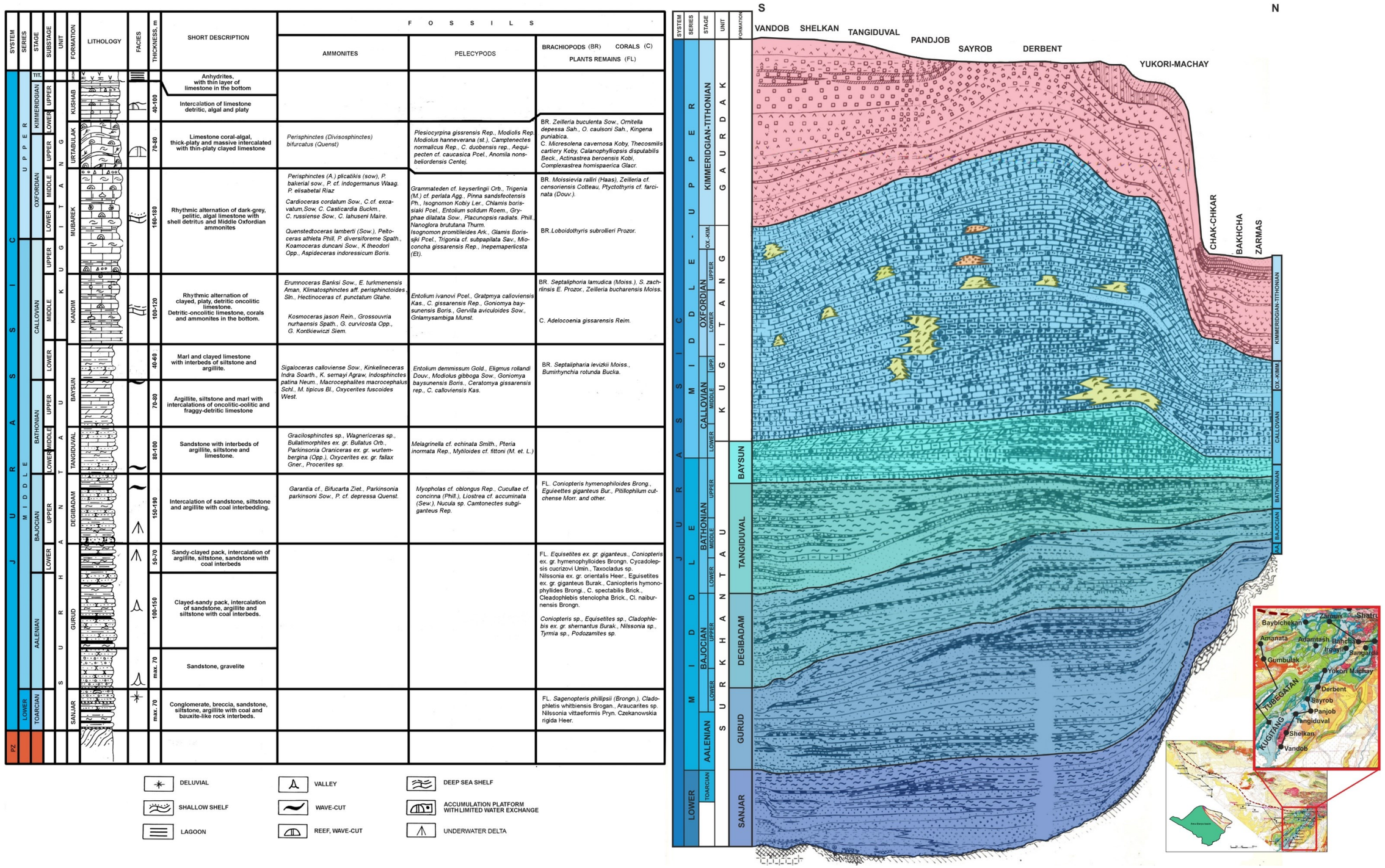

Fig. 2.13. Kugitang type-section of the Jurassic. Lithostratigraphic column (modified after Mirkamalov et al., 2005). SW-oriented geological cross-section along the Southwestern Gissar (modified after Egamberdiev and Ishniyazov, 1990). The authors' original stratigraphy names and ages differ from the chart chosen for this thesis. Reefs are in yellow. Location on fig. 2.9.

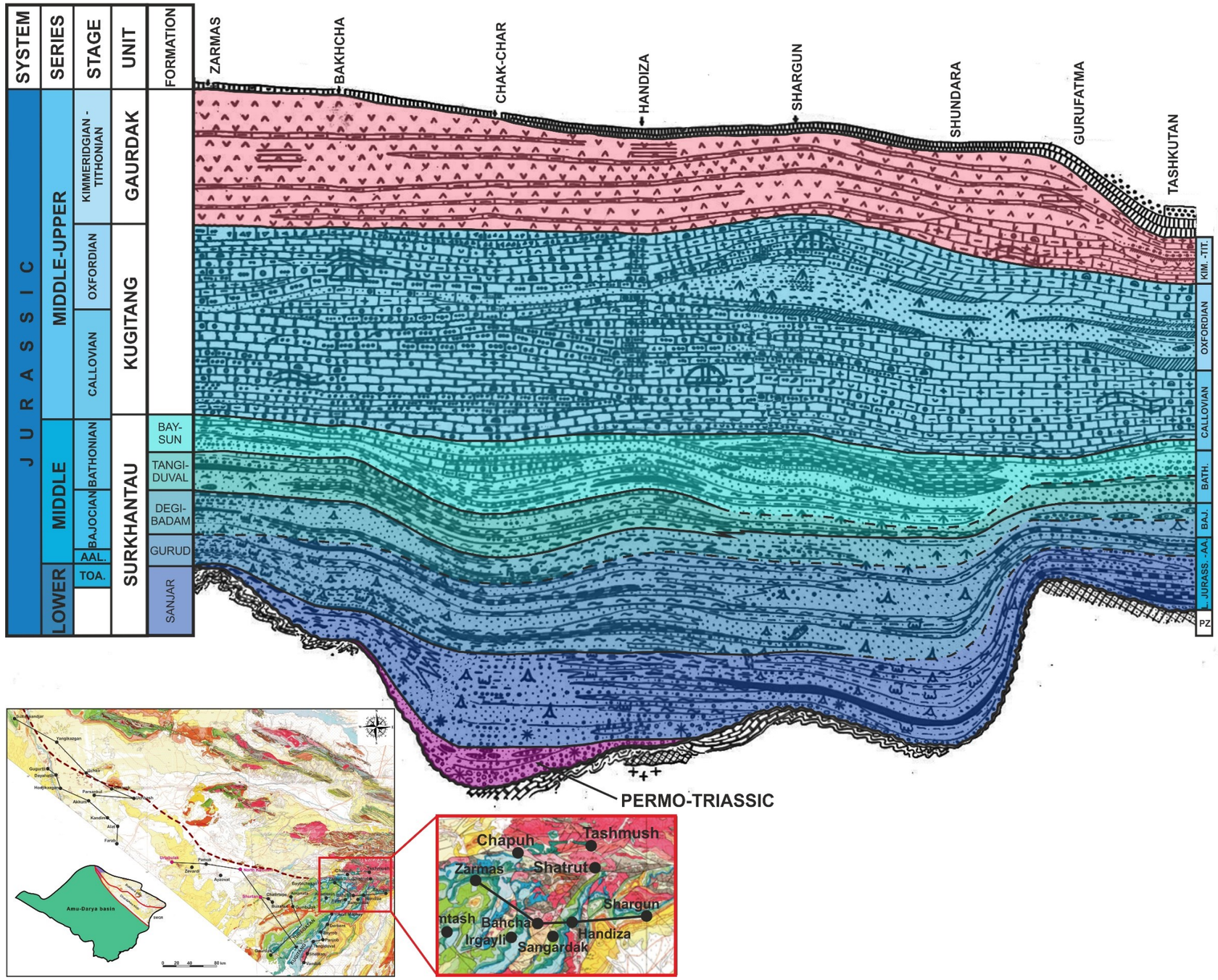

Fig. 2.14. Geological section across the Southwestern Gissar Range. Modified after Egamberdiev and Ishniyazov (1990), with the authors' original stratigraphy, names and ages differing from the chart chosen for this thesis. Location on fig. 2.9.

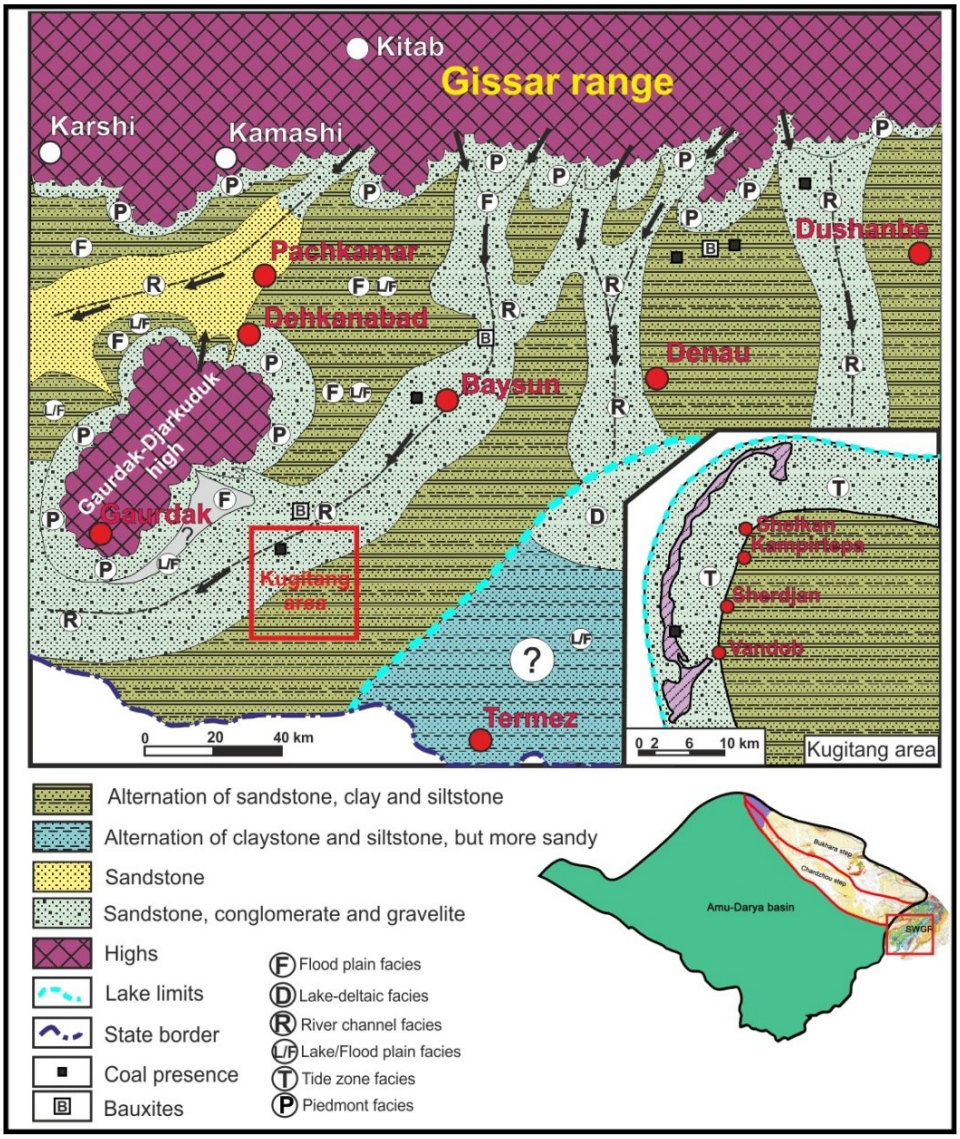

Fig. 2.15. Lower Jurassic paleogeographic map (modified after Egamberdiev and Ishniyazov, 1990).

In the Southwestern Gissar area it is a widespread sedimentary sequence formed in a warm and humid climate (Egamberdiev and Ishniyazov, 1990) (fig. 2.15). The facies of deposition of the Lower Jurassic sediments are divided into five main types: deluvial-piedmont facies, sandstone- clay-siltstone facies of flood plains, sandstone-gravelite underwater deltaic facies, low water lake-flood plain clay-siltstone- sandstone facies and sandstone-gravelite alluvial deposits of ancient rivers.

This variety of facies shows that during the Early Jurassic, the Southwestern Gissar area was a valley with a lot of rivers, a high existed in the region of Gaurdak as well as a huge intracontinental freshwater lake in the southeast, a part of it can be seen near Termez, on Figure 2.15. The freshwater is confirmed by the presence of bivalves *Ferganacocha* and *Unia uzbekistanica* – typical of freshwater (Repman et al., 1972 in Egamberdiev and Ishniyazov, 1990; we will make sometimes the reference in this way when we did not have access to the original work or when the reference was not given in the references list of the report).

2.3.1.2. Aalenian-Lower Bajocian (Gurud Formation)

The next level in the local stratigraphy is the Gurud Formation. It has an Aalenian-Early Bajocian age determined from a flora association (*Equisetites ex gr. giganteus Heer, Conioptris himenophyloides Brang., Cladophlebis stenelopha Brik., Nilssonia ex gr. orientalis Heer)* analysis (Troitsky and

Gomolitsky, 1998 in Mirkamalov et al., 2005). The upper limit of the formation was determined by Upper Bajocian ammonites found in the following Degibadam Formation.
The Gurud Formation is composed of sandstone, siltstones, claystones, conglomerates and gravels. There are some lake-river-bog coals bearing layers within these beds (fig. 2.11-2.16, 2.18).

The thickness of the formation ranges from 200 to 300 m. But, as the Sanjar Formation, it only exists in the deepest domains of the Bukhara-Khiva region (Beshkent trough, Kimerek graben), and in the Southwestern Gissar outcrops. It disappears from the section northwards. It is very thin or absent near the Uchbash-Karshi Flexure Fault zone in the Chardzhou step (fig. 2.10, 2.11) and absent in the limits of the Bukhara step, except in the Yangikazgan area, above a Permo-Triassic graben (see Chapter 4).

Generally, the Gurud Formation is characterized by a continental deluvial-valley facies. Its distribution in the Southwestern Gissar is exposed on Figure 2.16 for the Aalenian and 2.17 for the Lower Bajocian during which still exists an alluvial facies of paleorivers. At the same time, the depth of the surface of the Gaurdak high strongly decreases. The territory of the low-water lake increases and in some places reaches almost the Gissar Mountains. The surface of the underwater deltas increases at the same time. The first carbonate sediments have appeared in the south of the area, which marks the beginning of the marine transgression.

The facies are still the same as in the Lower Jurassic sequence, but with an increase of the lake clayed-sandy facies in the southern and western parts of the Southwestern Gissar.

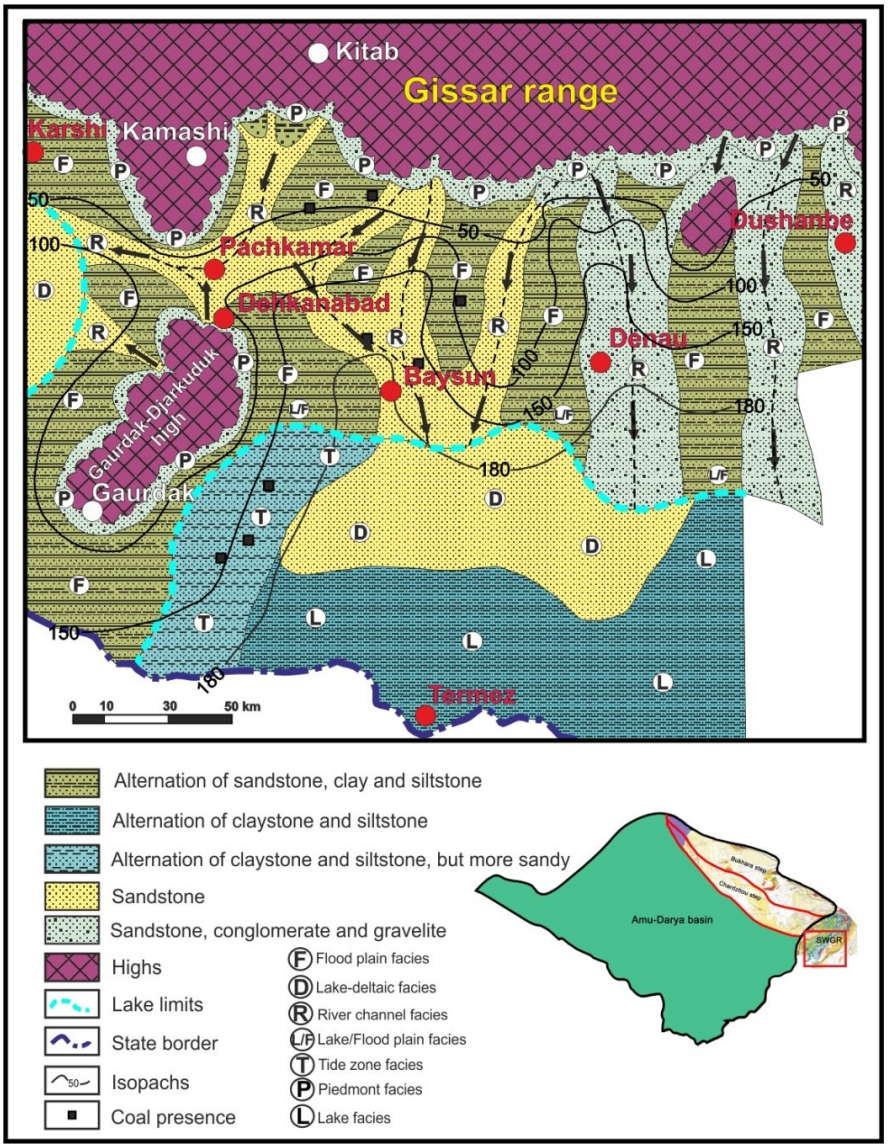

Fig. 2.16. Paleogeographical map of the Aalenian (modified after Egamberdiev and Ishniyazov, 1990).

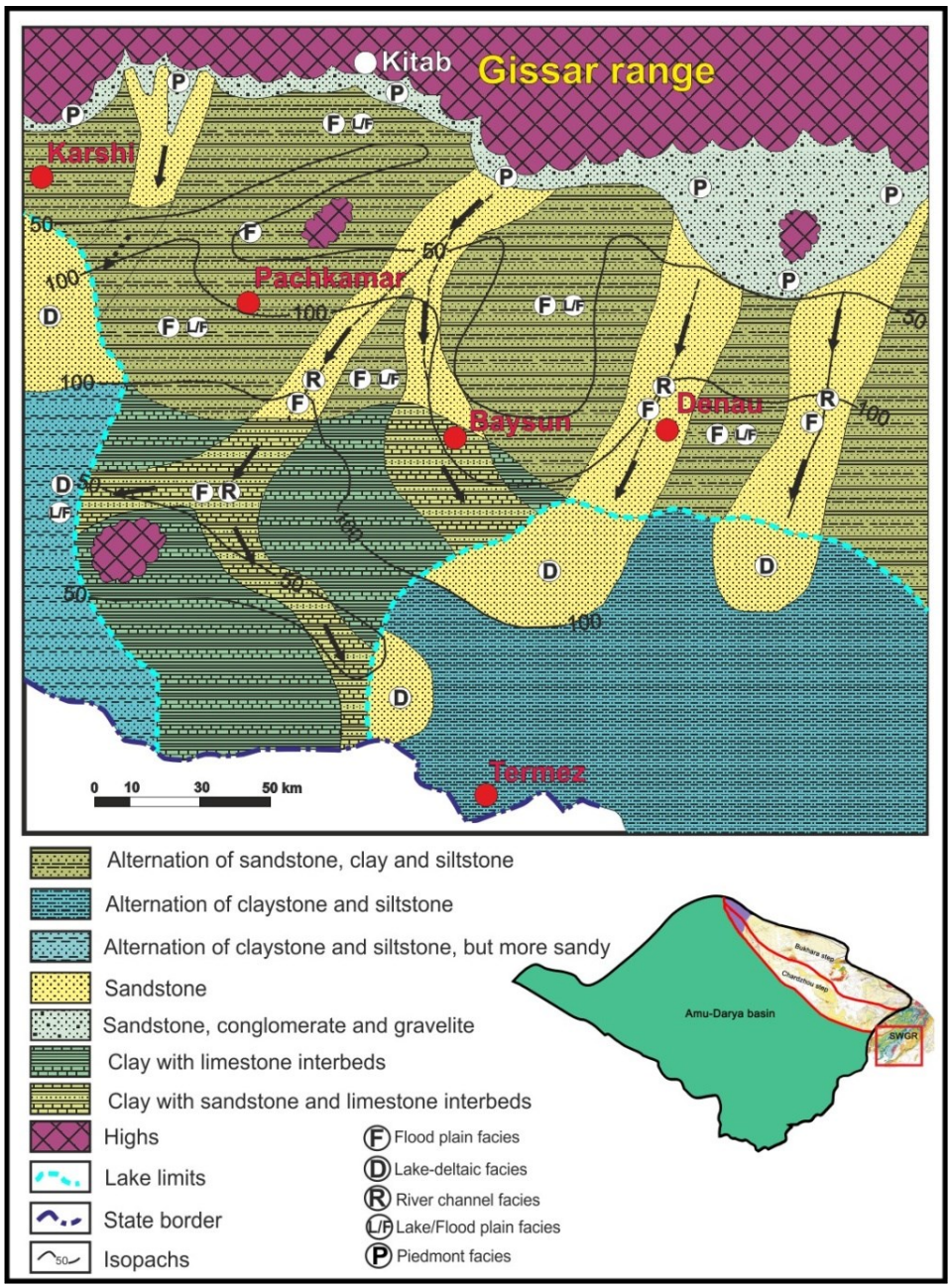

Fig. 2.17. Paleogeographical map of the Lower Bajocian (modified after Egamberdiev and Ishniyazov, 1990).

2.3.1.3. Upper Bajocian (Degibadam Formation)

The deposition of the Upper Bajocian sediments is characterized by environments changing from a continental valley to a marine wave-cut facies. In the Southwestern Gissar region the deposits of this formation are characterized by different types of facies: continental, lagoonal and marine-wave-cut facies (fig. 2.18). In the Late Bajocian time (fig. 2.19), most part of the Southwestern Gissar region was covered by marine clastic and carbonate-clastic sediments. The paleo-rivers facies had almost disappeared. The piedmont deluvial sediments were decreasing too. Another point to mark is the disappearance of the Gaurdak high, at the end of the Bajocian at its place is a carbonate-clastic formation. The limit between the marine and continental deposits is very well seen. The northeastern part of the Southwestern Gissar area is still merged with continental conditions of deposition.

The Degibadam Formation consists of alternations of sandstone, siltstone and claystone with rare beds of coals and limestone (fig. 2.18-2.20).

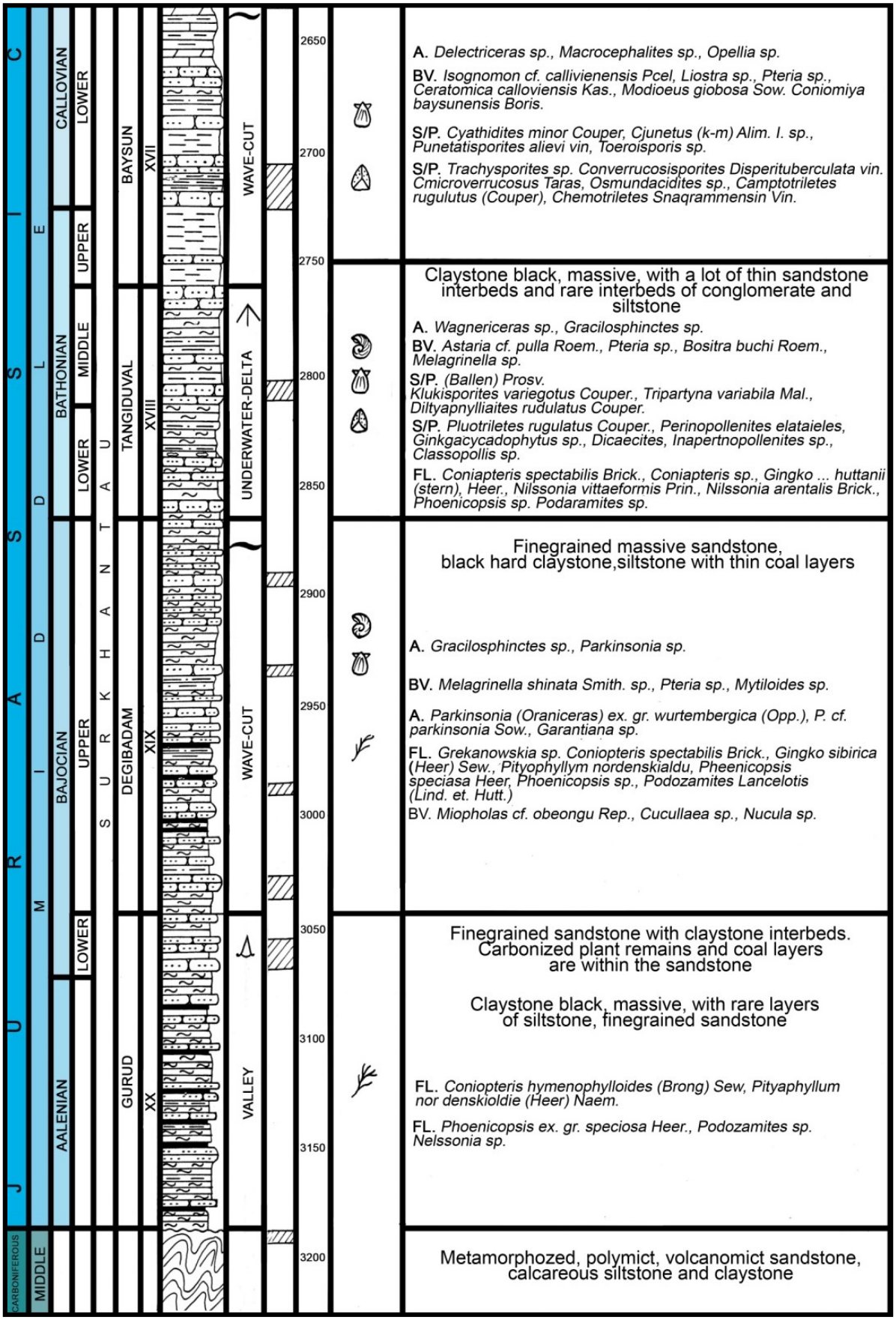

Fig. 2.18. Terrigenous section of the Urtabulak 102 well (modified after Mirkamalov et al., 2005). Location on fig. 2.9.

Letters: **A** – ammonites; **BV** – bivalves; **S/P** – spore-pollens; **FL** – flora.

Freshwater and marine bivalve complexes *(Myopholas oblongus Rep., Camptonectes subgiganteus Rep., Cuculaea aff. concinna (Phiel))* mark the lower limit of the formation and the presence of ammonites typical from the zone of *Parkinsonia parkinsoni Sow., P. depressa Quenst., Garantiana bifureata Ziet. V.V.* (from Mirkamalov et al., 2005) marks the middle part of the formation. The upper limit is determined by the presence of Lower Bathonian ammonites at the base of the following Tangiduval Formation. The thickness of the Degibadam Formation varies from 150 to 200 m.

This formation marks the first marine transgression, which was acting in the southeast of Central Asia (Mirkamalov et al., 2005; Fürsich et al., 2015; McCann, 2015). However, the presence of different types of continental deposits (fig. 2.20) with a lot of plants remains [*Podozamites lanceolata (Lind. et Hutt.), Conioptoris porcina Brick., Nilssonia orientalis Heer., Neocalamites hoerensis (Schimp.)* and others, from Mirkamalov et al., 2005], shows that this transgression has been interrupted several times by continental lake-bog conditions.

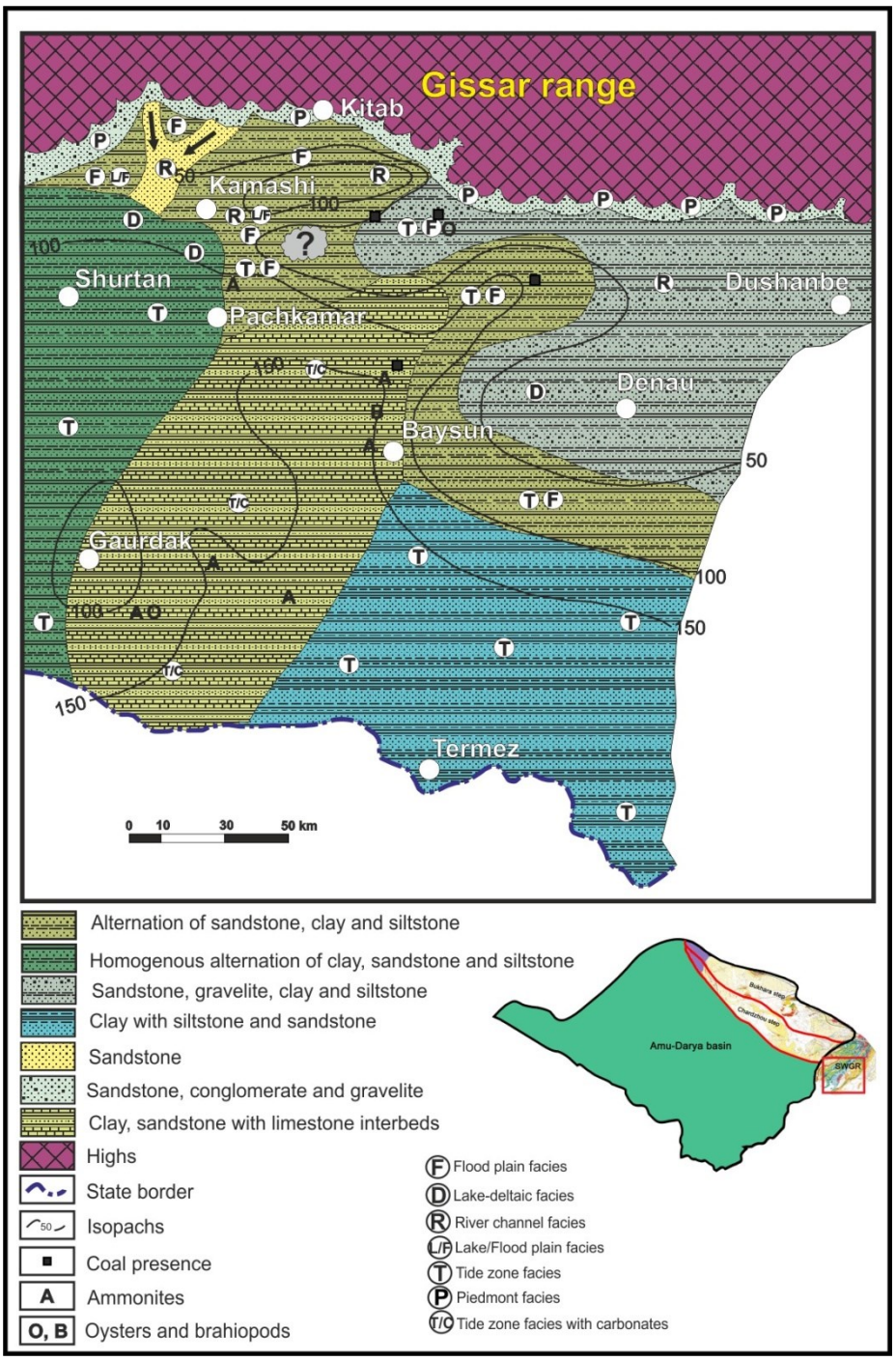

Fig. 2.19. Paleogeographical map of the Upper Bajocian (modified after Egamberdiev and Ishniyazov, 1990).

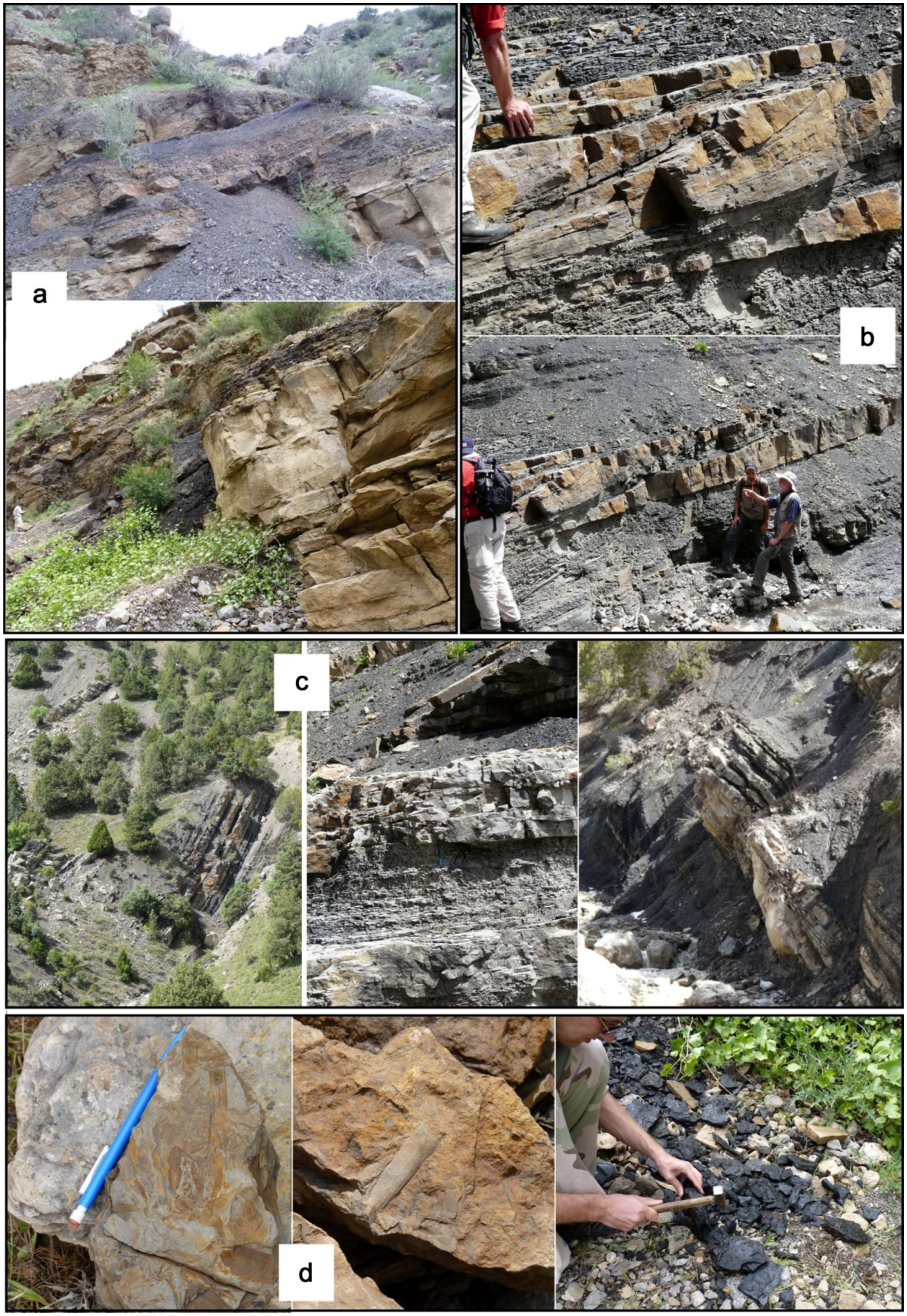

Fig. 2.20. Jurassic siliciclastic facies of the Gurud (Aalenian-Lower Bajocian) and Degibadam (Upper Bajocian) formations in Southwestern Gissar. **a:** Sandstone and black shale in the Baysun section (location on fig. 2.1); **b:** Cross-bedding in sandstone beds; **c:** Black shale with intercalated sandstone beds in the Baysun section; **d:** Plant remains and coals (Barrier and Brunet, 2011).

2.3.1.4. Lower Bathonian (Tangiduval Formation)

The sediments of this formation are represented by wave-cut zone facies. They consist of sandstone, siltstone, claystone and limestone in the Kugitang stratotype section (fig. 2.13), see also the column of Kamashi 6 (fig. 2.21). The limestone beds contain an association of Early-Middle Bathonian age ammonites (*Wagnericeras sp., Gracilosphinetes sp., Procerites sp., Oxycerites sp.)* (Jurassic key sections, 1969 in Mirkamalov et al., 2005). According to the well data, the thickness of this formation is rather constant (80-140 m) in most of the Bukhara-Khiva region.

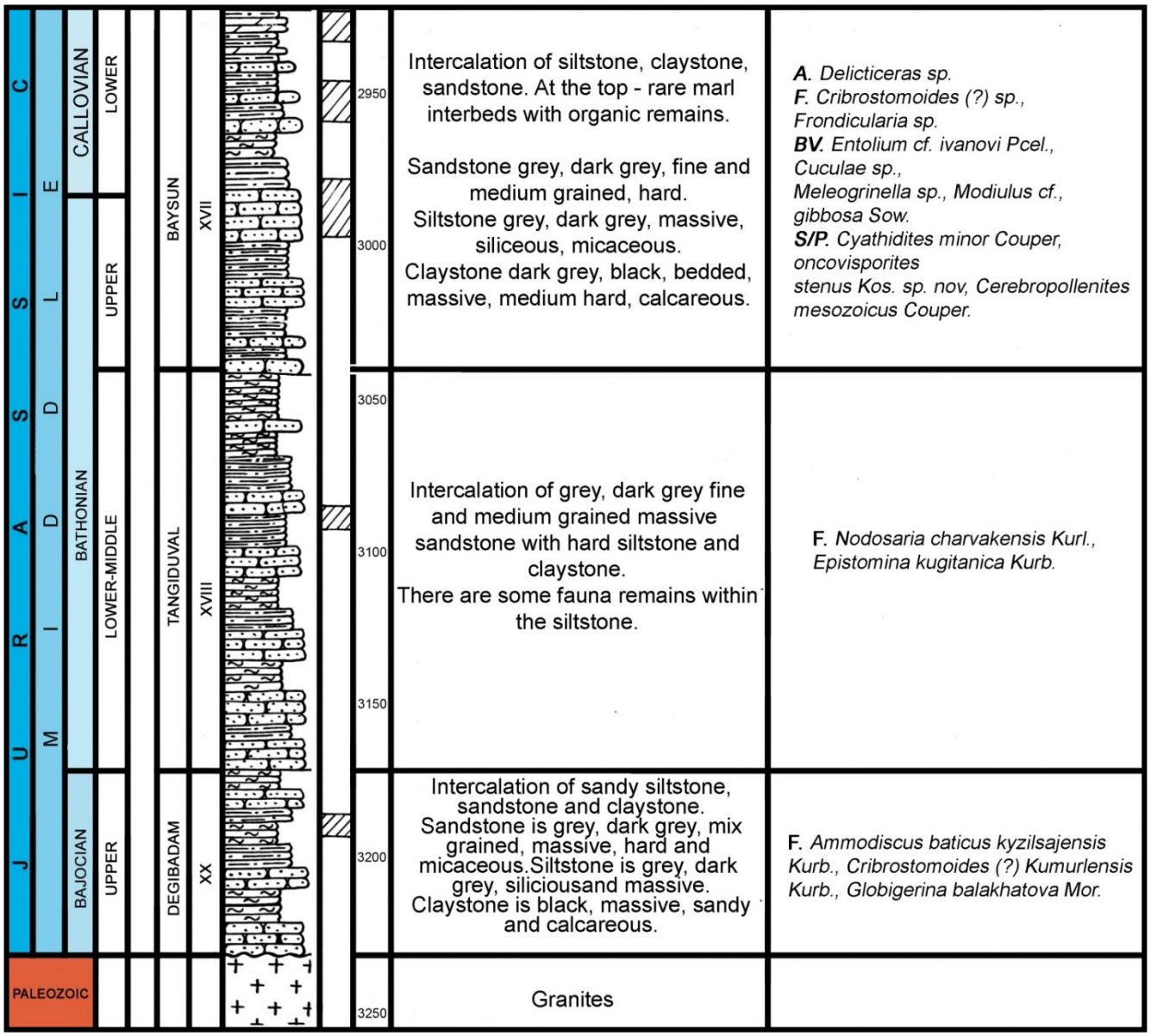

Fig. 2.21. Jurassic terrigenous section of the North Kamashi 6 well. Location on fig. 2.9.
(modified after Mirkamalov et al., 2005).
Letters: **A** – ammonites; **BV** – bivalves; **S/P** – spore-pollens; **F** – Foraminifers.

2.3.1.5. Middle Bathonian-Lower Callovian (Baysun Formation)

The Baysun Formation marks the transition from wave-cut to shallow sea facies and works as a transition zone between terrigenous and carbonate sediments.

Figure 2.22 shows the paleogeographical conditions at the end of the Bathonian. On most of Southwestern Gissar carbonate and clayed-carbonate sediments were depositing. The sea limits are

just near the Gissar range. In the northeastern part of the area there are still sandy-conglomerate-gravelite sediments, but they are already marine.

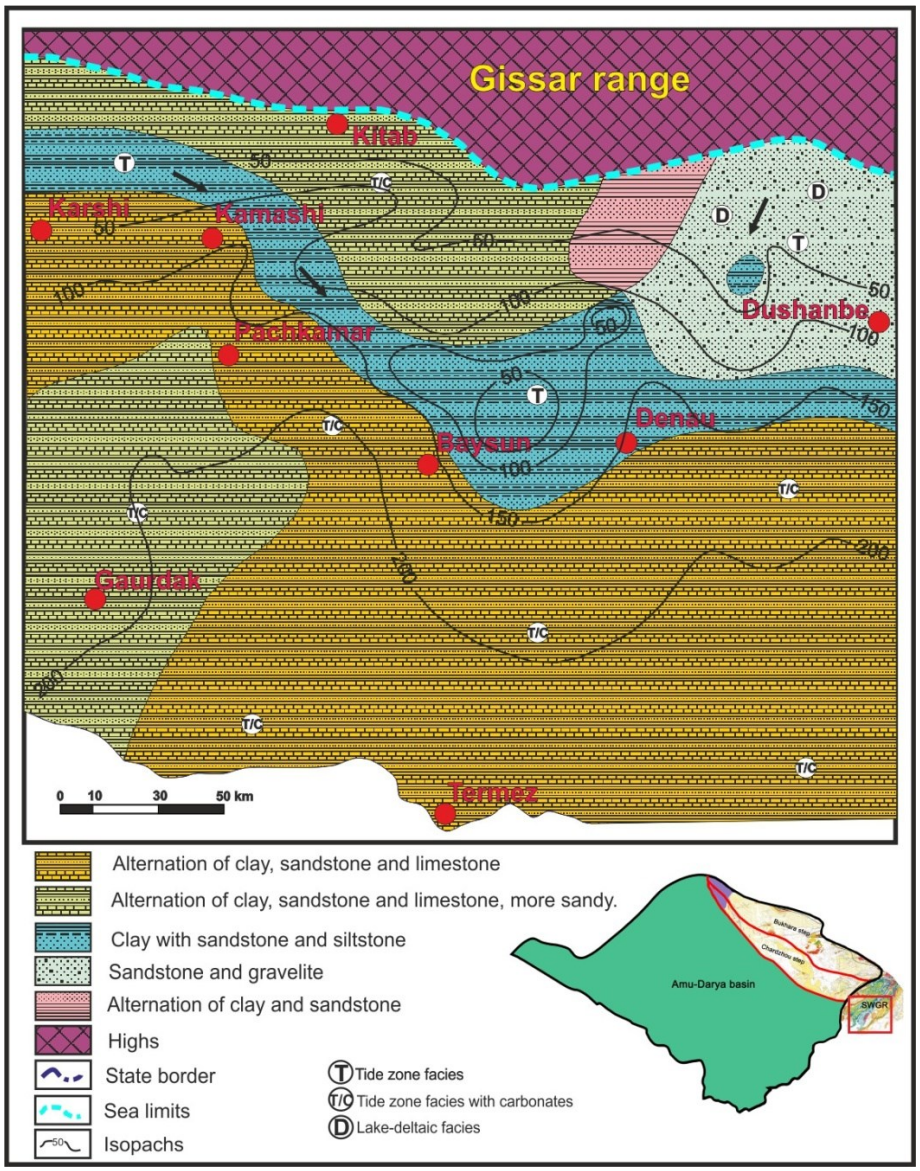

Fig. 2.22. Bathonian paleogeographic map (modified after Egamberdiev and Ishniyazov, 1990).

In the Kugitang type-section, this formation is divided into two parts (fig. 2.13). The lower part consists of claystone, siltstone, marl and beds of detritic limestone (fig. 2.21, 2.23). The upper part has almost the same lithology, but with more marls and clayed limestone. The Late Bathonian-Early Callovian age of the formation was determined from ammonites *Sigaloceras calloviensis Sow. Kinkeliniceras indra Sparth., Indonphinetes patinaNeum., Macrocephalites macrocephalus Schl.* and others (Abdullaev in Mirkamalov et al., 2005). The finding of the ammonite *Procerites* in the condensed lower part of the Baysun Formation in the Shelkan and Vandob sections (location fig. 2.9), led Fürsich et al. (2015) to consider a Middle Bathonian age for the base of the Baysun Formation.

In Southwestern Gissar, the Baysun Formation is 70-140 m thick. On the Chardzhou step, the thickness does not change a lot and is stable within a 60-90 m interval.

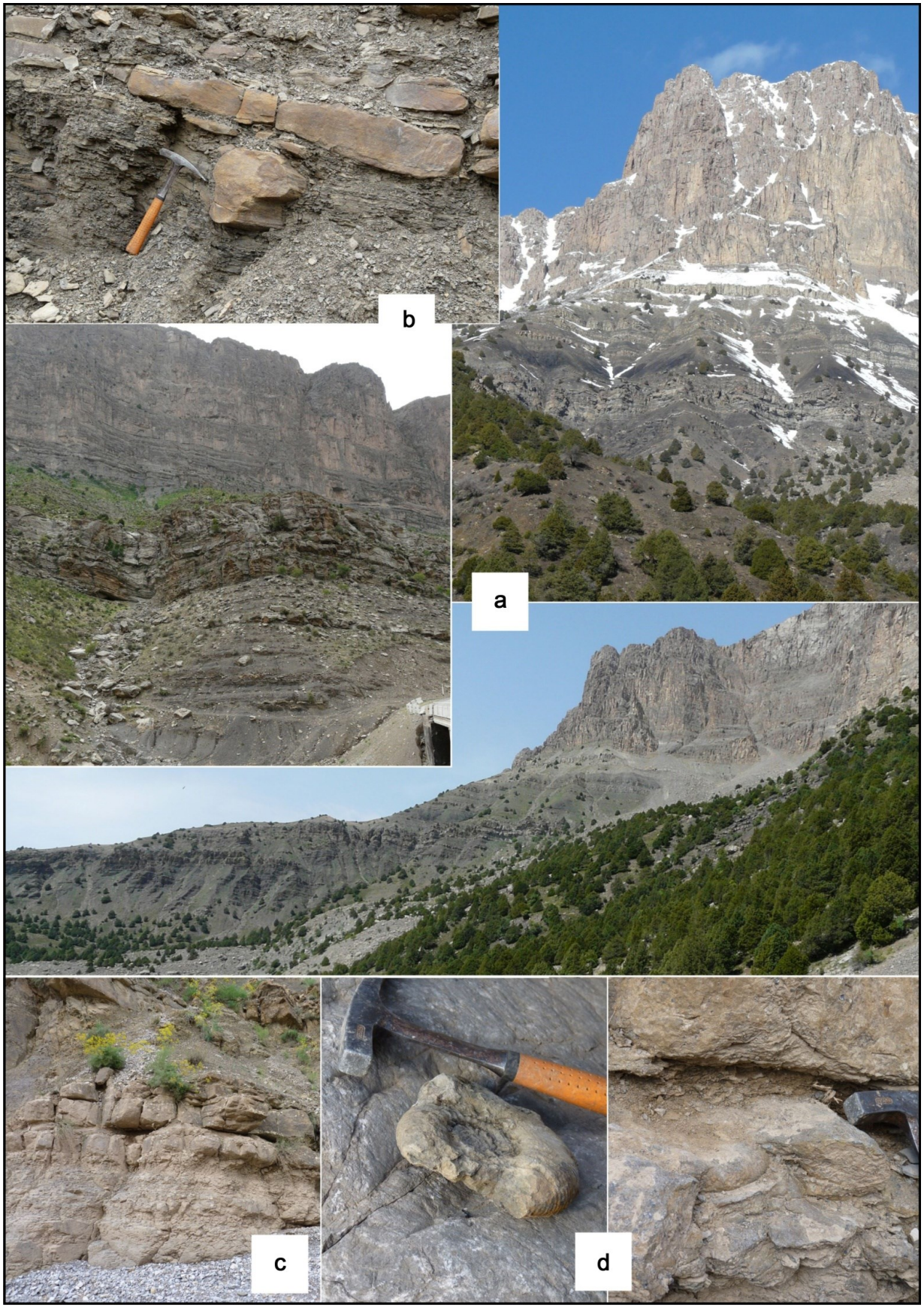

Fig. 2.23. Middle-Upper Jurassic deposits in Southwestern Gissar. **a:** upper part of the Baysun section (location on fig. 2.1) including coal veins; **b:** marine layers in the upper part of the Derbent section (location on fig. 2.6); **c:** marine sandstone and shales; **d:** Ammonite in the indurated shales of the Baysun Formation (Barrier and Brunet, 2011).

2.3.2. Carbonate unit

The *carbonate unit* overlaps the *terrigenous unit* with a sharp lithological contact shown on Figure 2.24.

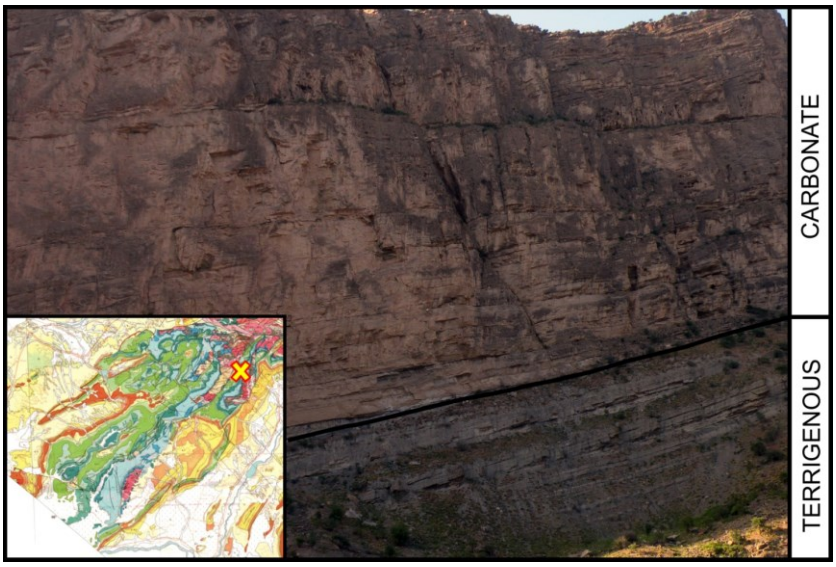

Fig. 2.24. Contact between the terrigenous and carbonate units of the Jurassic in the Sangardak gorge, Southwestern Gissar.

The age of the unit is considered as Middle Callovian-Kimmeridgian, according to the stratigraphy we use in this thesis (Mirkamalov et al., 2005). The thickness of the carbonate unit, as the terrigenous one, varies according to the location. In general the carbonate sediments of the Bukhara step are thinner than on the Chardzhou step.

Nugmanov (2009a) has divided the *carbonate unit* into two parts – the so-called lower carbonates (or Lower Kugitang) and the upper carbonates (or Upper Kugitang), which reflect the different types of limestone and associated paleogeographical environments. According to the chart we use in this study, the lower carbonates correspond to a Middle Callovian-Middle Oxfordian age, and the upper carbonates to a Late Oxfordian-Kimmeridgian one.

The lower carbonates comprise the so-called Kandim and Mubarek formations of Middle Callovian-Middle Oxfordian age (see fig. 2.25).

The structure of the upper carbonates is more complicated. Three types of facies exist: *basinal* (Khodjaipak Formation), *reefal* (Urtabulak and Kushab formations) and *lagoonal* (Gardarya Formation). All of them have a Late Oxfordian-Kimmeridgian age, but are located in different areas and do not overlap each other (except in the transition zones between these formations). Mirkamalov and Abdullaev (Mirkamalov et al., 2005; Abdullaev et al., 2010 …) proposed a model of appearance and development of a barrier reef system in the Late Oxfordian (fig. 2.26). According to this zonation, the three types of facies would develop synchronously in contiguous zones.

<table>
<tr><th colspan="4">BASINAL TYPE</th><th colspan="4">REEFAL TYPE</th><th colspan="4">LAGOONAL TYPE</th></tr>
<tr><td>XV-AR</td><td colspan="2">Khodjaipak formation</td><td>O_3-Km</td><td>XV-AR
XV-R</td><td colspan="2">Kushab + Urtabulak formations</td><td>O_3-Km</td><td>XV</td><td colspan="2">Gardarya formation</td><td>O_3-Km</td></tr>
<tr><td>XV-UR</td><td rowspan="2">Mubarek formation</td><td>Upper</td><td>O_1-O_2</td><td rowspan="2">XV-UR</td><td rowspan="3">Mubarek formation</td><td>Upper</td><td>O_1-O_2</td><td rowspan="3">XV-a</td><td rowspan="3">Mubarek formation</td><td>Upper</td><td>O_1-O_2</td></tr>
<tr><td>XV-a</td><td>Lower</td><td>Cl_3</td><td>XV-a</td><td>Lower</td><td>Cl_3</td><td>Lower</td><td>Cl_3</td></tr>
<tr><td>XVI</td><td colspan="2">Kandim formation</td><td>Cl_2</td><td>XVI</td><td colspan="2">Kandim formation</td><td>Cl_2</td><td>XVI</td><td colspan="2">Kandim formation</td><td>Cl_2</td></tr>
</table>

Fig. 2.25. Correlation between productive horizons, formations of the carbonate unit, stratigraphic chart and different types of the carbonate section (modified after Abdullaev, 2004).

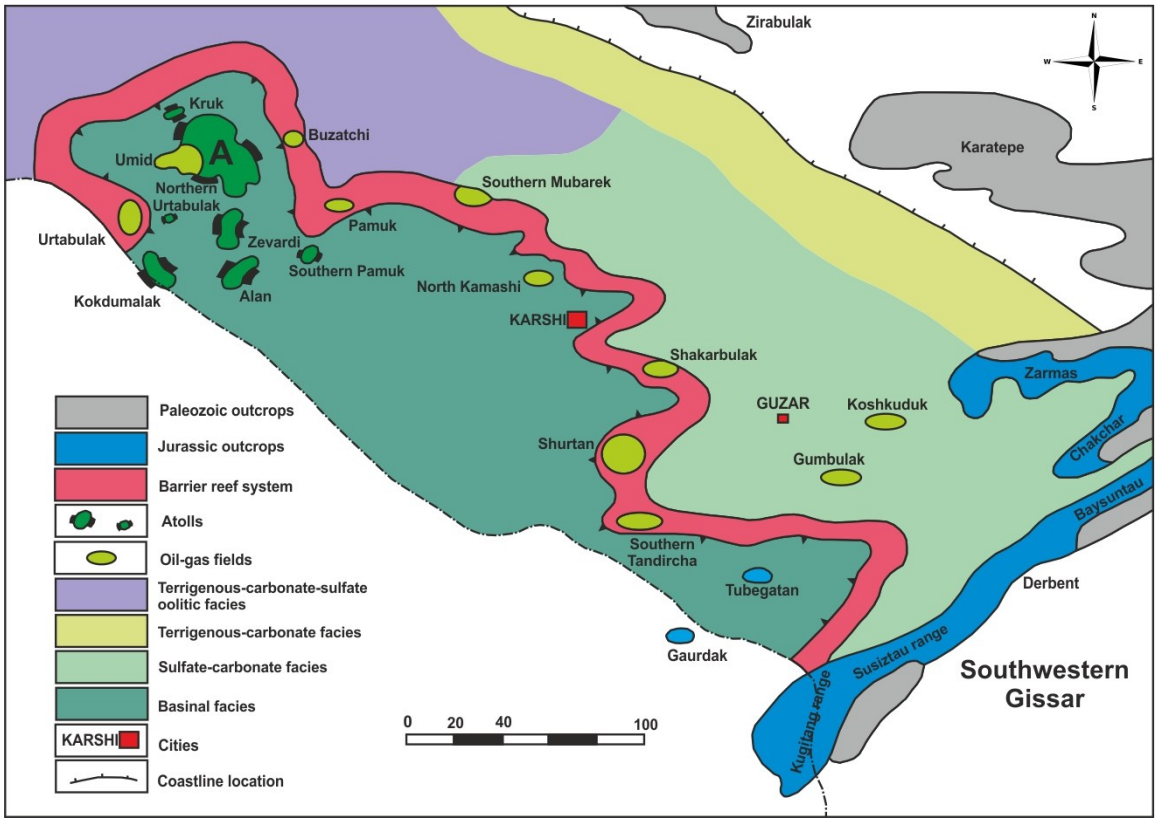

Fig. 2.26. Schematic location of the barrier reef system model of the Bukhara-Khiva region. Lagoon is in the north-northeast of the barrier, the basin in the southwest (modified after Mirkamalov et al., 2005).

As the Jurassic carbonates are one of the most important productive oil and gas bearing horizons of the Bukhara-Khiva region, they are often divided into productive horizons (fig. 2.25). These are, from the bottom: XVI, XV-a, XV-Under reef (XV-UR), XV-Reef (XV-R) and XV-Above reef (XV-AR) horizons. According to the type of the section, some of these horizons may either disappear from the section or are not individualized precisely.

There are many possible correlations between the stratigraphy and the productive horizons. We have chosen the one presented in Figure 2.25, as it corresponds to the stratigraphy we use in this thesis. All types of the carbonate section have a similar base – the Kandim Formation. Then the division changes according to the three types of the reefal system. The third and last set of horizons is more differentiated in each type and gives it its identity.

In the *basinal type* of the section, the Mubarek Formation is represented by the horizons XV-a and XV-"Under reef", so called to show the time equivalent of the reefal type but there is no XV-reefal horizon above. The XV-"Above reef" horizon is expressed by the Khodjaipak Formation, typical of the basin.

The *reefal type* contains all the productive horizons (with this type of the section are connected a lot of oil and gas fields). The Mubarek Formation consists of the XV-a and XV-Under reef horizon, but the lower part (Upper Callovian) of the formation takes not only the XV-a horizon, as in the *basinal type*, but also a part of the XV-Under reef. The XV-Reef (characteristic of the *reefal type*) and the XV-Above reef horizons are represented by the Urtabulak and Kushab formations.

The *lagoonal type* is characterized by a reduced carbonate section. There are the XVI and XV-a horizons, represented by Mubarek and Kandim formations respectively and the undivided XV horizon, expressed by the Gardarya Formation.

The complete carbonate section of the stratotype Shurtan field is exposed on Figure 2.27 exhibiting the three types of deposition and we will give now more details on each period of time.

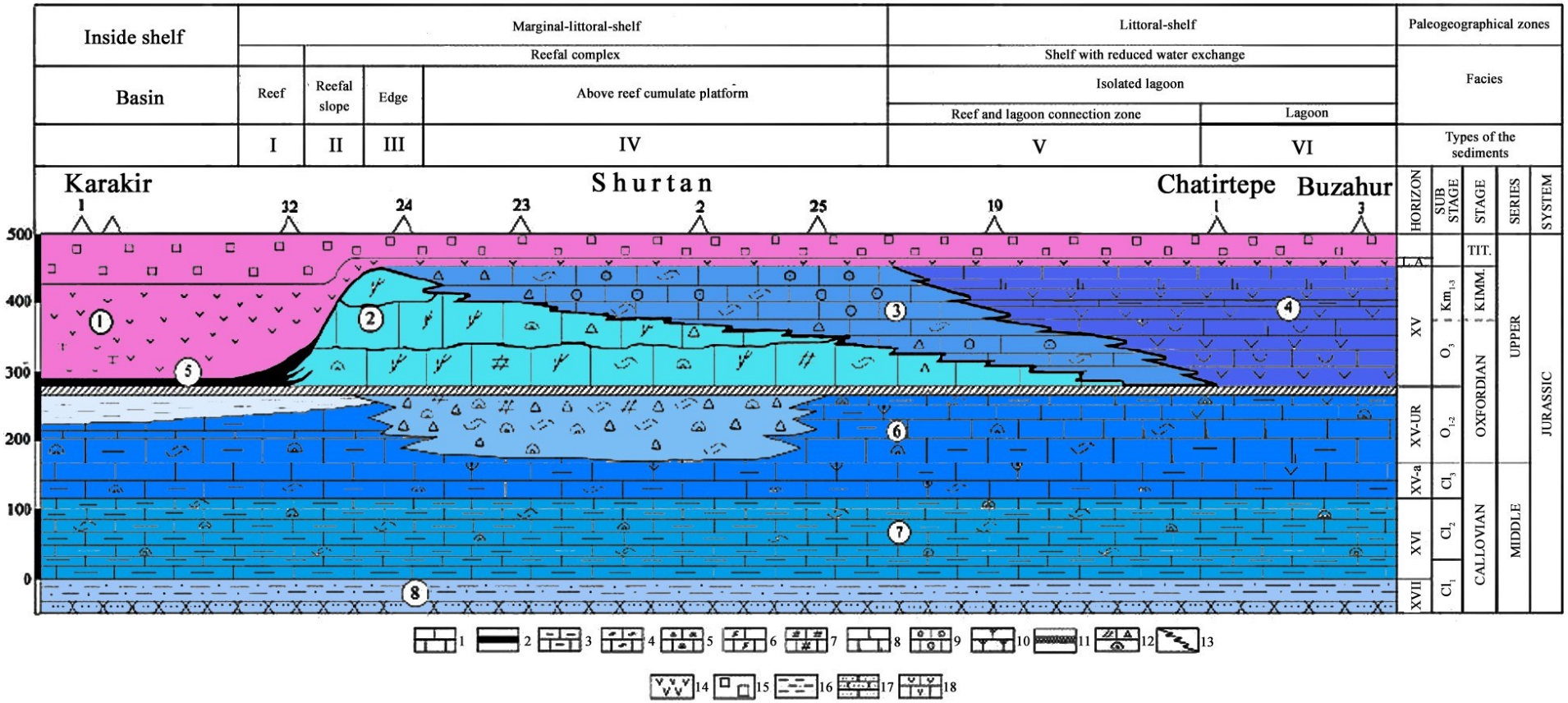

Limestone: 1 - pelitic, 2 - bituminous, 3 - clayed, weakly bituminous, 4 - detritic, 5 - algal, 6 - coral, 7 - bryozoan 8 - dolomitized, 9 - oncolitic, 10 - ballstone, 11 - ammonite-oyster horizon, 12 - reefogenous-cumulative under reef bed, 13 - facial replacement, 14 - anhydrite, 15 - salt, 16 - siltstone, 17 - sandstone, 18 - anhydritized limestone

Numbers in circles: 1 - Gaurdak unit, 2 - Urtabulak formation (XV-R), 3 - Kushab formation (XV-AR), 4 - Gardarya formation, 5 - Khodjaipak formation, 6 - Mubarek formation, 7 - Kandim formation, 8 - Baysun formation.

Fig. 2.27. Cross-section of the Shurtan field, exposing the relationships between the different types of carbonates (modified after Abdullaev et al., 2010). Location of Shurtan field on fig.2.9 and 2.26.

2.3.2.1. Middle Callovian (Kandim Formation or XVI horizon)

Lithologically this formation is represented by dark, non-uniform bedded, pelitomorphic, organogen-detritic limestone, with different clayey grades (up to 20%) (fig. 2.28).

The Middle Callovian age was determined by remains of bivalve, brachiopod and ammonite complexes, belonging to *Chlamys amibiqua (Munaster), Radulopecten subinaequicostatus (Kasans), Melagrinella echinata (Smith), Modiola gibbosa Sow.,Pleuromia balkhanensis Pcel., P. uniformis Sow., Goniomya subsulcata Rep., Grammatadon sp.*, *Guzarella, Zeileria* and *Terebratula, Sigaloceras* and *Cadoceras* (after Abdullaev, Repman in Mirkamalov et al., 2005). Its thickness is 50-100 m.

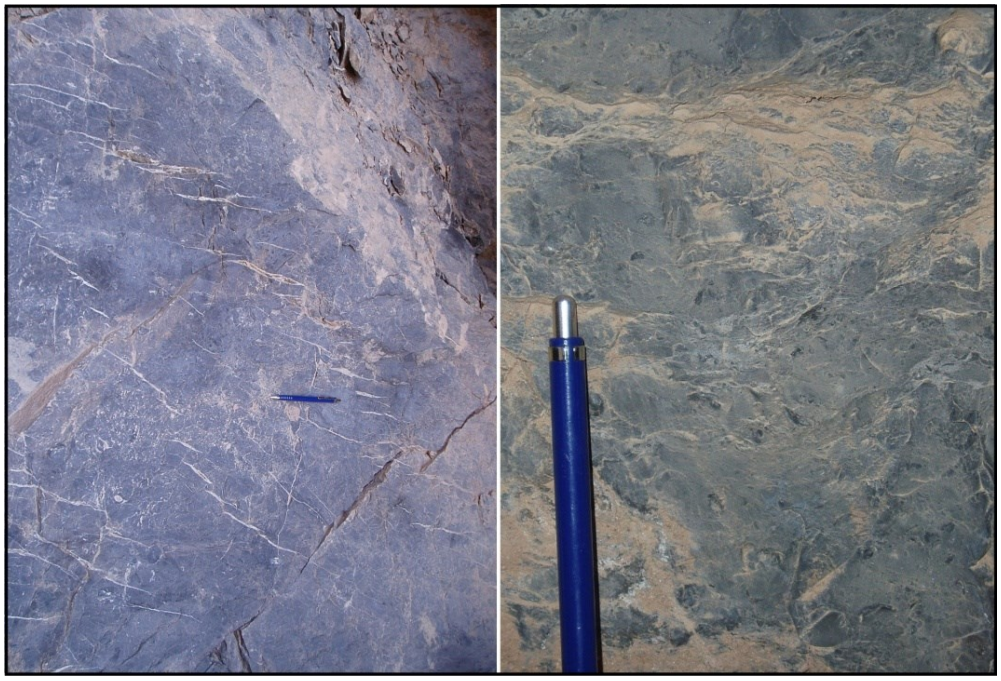

Fig. 2.28. Fine-grained carbonate of the Middle Callovian Kandim Formation in Southwestern Gissar (Barrier and Brunet, 2011).

2.3.2.2. Upper Callovian – Middle Oxfordian (Mubarek Formation or XV-a and XV-UR horizons)

The Mubarek Formation is composed of two relatively big members.

The lower member (Upper Callovian) is roughly the same throughout the Bukhara-Khiva and Southwestern Gissar regions. In the *basinal type* of the section it corresponds to the XV-a productive horizon. In the *reefal type*, the lower member of the Mubarek Formation, in addition to the XV-A, spreads also into the bottom of the XV-UR (see fig. 2.25). In the *lagoonal type*, the XV-a horizon consists of the complete Mubarek Formation.

This lower member consists of fine-micro bedded, low clayey limestone, alternating with crumbling limestone with packs of organogenic-detritic and algal limestone. This limestone is creating thin biostroms, which consist of shells and algal formations. Foraminifers *Textularia aff. agglutinaus Orb., Lenticulina ex gr. foliacea, L. ex gr. evolata Kurb., Treoholina sp., Karaiselea sp.* (from Mirkamalov et al., 2005) have been found in this limestone and confirm the Late Callovian age of the lower part of the Mubarek Formation.

The upper member of the Mubarek Formation is quite different. It is constituted of dark-grey limestones alternating with detritic, cloggy-algal limestone, pelitomorphic limestone, clayed limestone with abundant foraminifers, ammonites, radiolarians. Ammonites *Perisphinctes ex gr. plicatilis Sow.* and also *P. variocostatus Buk* (from Mirkamalov et al., 2005) confirm the Middle Oxfordian age of the upper part of the formation. This part of the Mubarek Formation corresponds to the XV-UR horizon.

A good marker of the top of the Mubarek Formation is the so-called gamma active pack. According to Akramkhodjaev and Egamberdiev (1985, in Abdullaev and Mirkamalov, 2001), the gamma-active pack is located between the top of the Jurassic *carbonate unit* (top of the Mubarek Formation) and the base of the Jurassic evaporites. This pack was determined as the Khodjaipak Formation and also marks the basinal-type facies of the Jurassic carbonate section (Abdullaev et al., 2010), which will be described further. Lithologically, the gamma-active pack consists of clayed-bituminous-shaly limestone. The gamma activity of this horizon is caused by the presence of bituminous material. Its thickness does not exceed few tens metres.

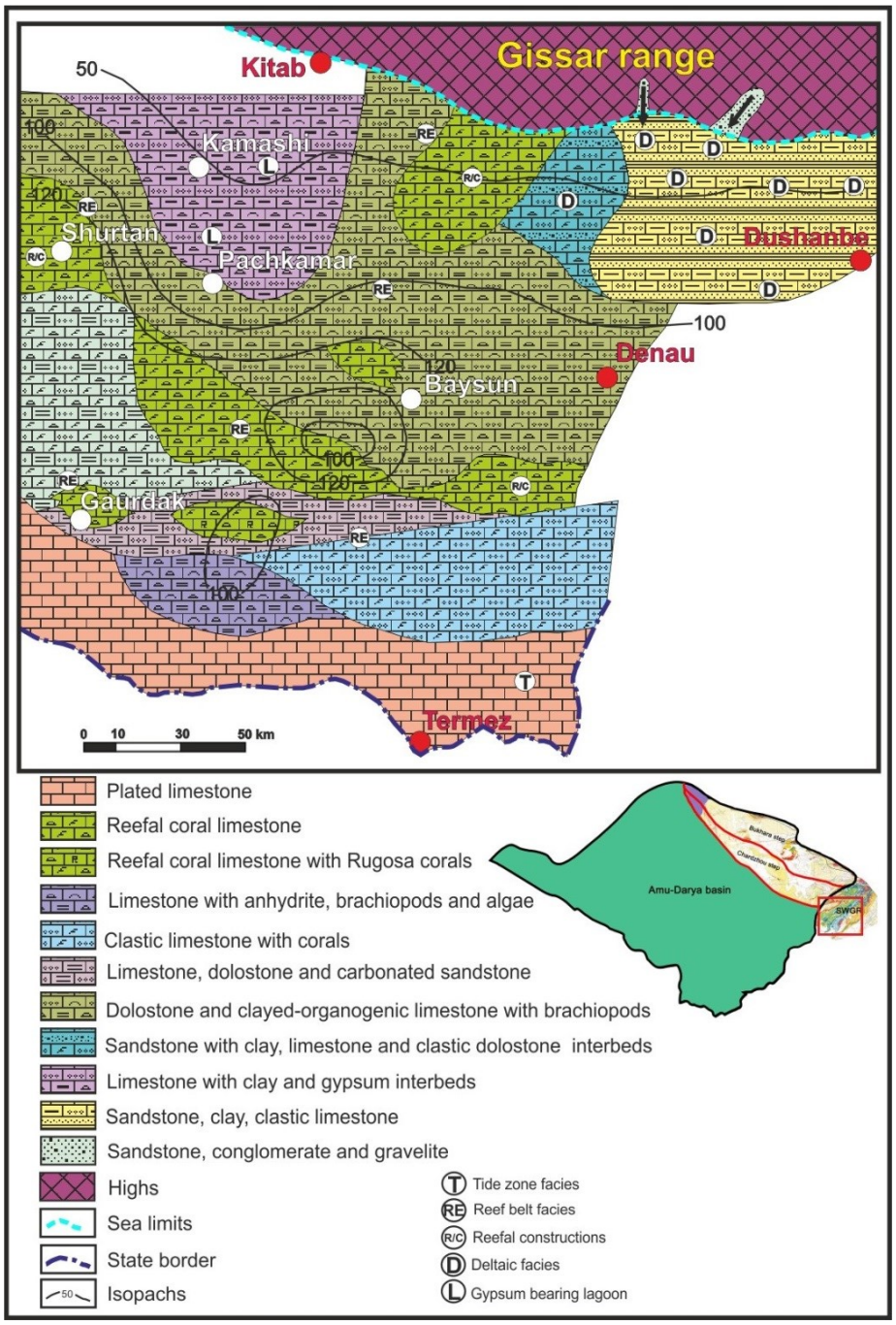

Fig. 2.29. Paleogeographic map during the Early Oxfordian (modified after Egamberdiev and Ishniyazov, 1990).

Another interesting marker of the top of the Mubarek Formation is an ammonite-oyster horizon (Abdullaev and Mirkamalov, 1986, in Abdullaev et al., 2010). If it exists in the areas of the gamma-active pack development, the ammonite oyster horizon underlays it. If not, this horizon marks the top of the Mubarek Formation. The ammonite-oyster horizon is 4-6 metres thick and consists of

organogenic limestone. These limestones contain a lot of ammonites and oysters of Middle Oxfordian age. The most widespread ammonites in this horizon are *Perisphinctes plicatilis (Sow.)*. The oysters, in general, are represented by *Nanogyra sp. (Exogyrinala)* and *Liostrea sp*. (Abdullaev et al., 2010). As the Mubarek Formation exists all over the Bukhara-Khiva region, the ammonite-oyster horizon (or its analogs) exists in all types of carbonate, but the most developed occurs in the *basinal type* (Mirkamalov et al., 2005, Abdullaev et al., 2010)

The complete thickness of the Mubarek Formation is 120-160 m. The sediments were formed in a shallow sea. The paleogeographical situation for the Lower Oxfordian deposits in the Southwestern Gissar area is exposed on Figure 2.29. The most interesting point in this time is that the first coral reef structures appear. They do not construct a barrier reef, but some isolated reefs and bioherms. A lagoon is formed in the northwestern part of the area. The northeastern area still consists of some sandy-clayed deposits of deltaic environment as during the Bathonian (fig. 2.22).

2.3.2.3. Upper Oxfordian-Kimmeridgian (XV, XV-R and XV-AR horizons)

The Late Oxfordian – Kimmeridgian aged sediments have a complicated structure. There are three different types of the section, which have been developed at the same time according to the paleogeographical model of deposition of Mirkamalov et al. (2005) and Abdullaev et al. (2010): these are *the reefal, lagoonal* and *basinal types,*

This division is resulting from the changes of the paleo-environmental conditions in the Late Oxfordian (see fig. 2.30). The paleo-climate became warmer and tropical. As a consequence, good conditions for the organic (as corals) development prevailed. These corals were building reefs and bioherms and other organic constructions, which were forming a reefal area, possibly a barrier reef system. And, as a consequence reefal area, lagoon and basin have differentiated.

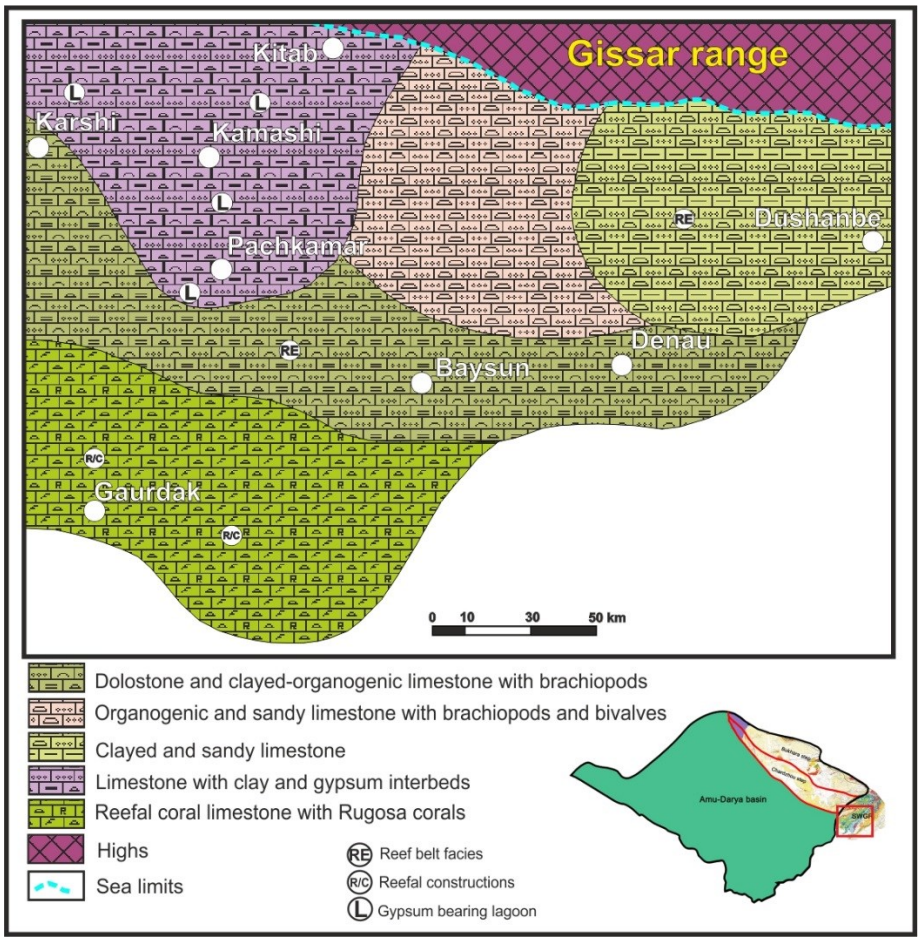

Fig. 2.30. Paleogeographic map during the Late Oxfordian
(modified after Egamberdiev and Ishniyazov, 1990).

2.3.2.3.1. Barrier reef system model

The presence of reefs on the territory of the Bukhara-Khiva region is a confirmed fact by well data. But "Do these reefs form a barrier system or not?" like in the barrier reef model (fig. 2.31) is still a controversial issue. Isolated reefs or bioherms are often discovered even in the Southwestern Gissar, but there is still no confirmation of a continuous reefal structure.

For example, on the location map (fig. 2.32) of the Upper Jurassic carbonates proposed by Nugmanov (2009a), the reefal structures do not create a well expressed long barrier system. There is some kind of a small barrier structure in the western part of the reef but eastwards, there are only some isolated bioherms and reefal structures with another more continuous area of reefs in the surroundings of Shurtan, near the Gissar.

At the same time, Abdullaev et al. (2010) consider that there was a real long barrier reef system, as it is shown on Figure 2.31. The reef system is located in the eastern part of the Bukhara-Khiva region and covers the most part of the Southwestern Gissar. As an argument of the barrier existence they provide the fact, that there is a widespread reefogenous-clastic limestone under the reefal structures, serving as a base for the reefal building. The dark green shows the sediments of the XV-Above reef and XV-Reef horizons, the blue color the basinal black shales, the pink are the bioherms and the light blue the atolls.

As there are still discussions on the continuity of the reefs, we will speak about the barrier reef system as a model.

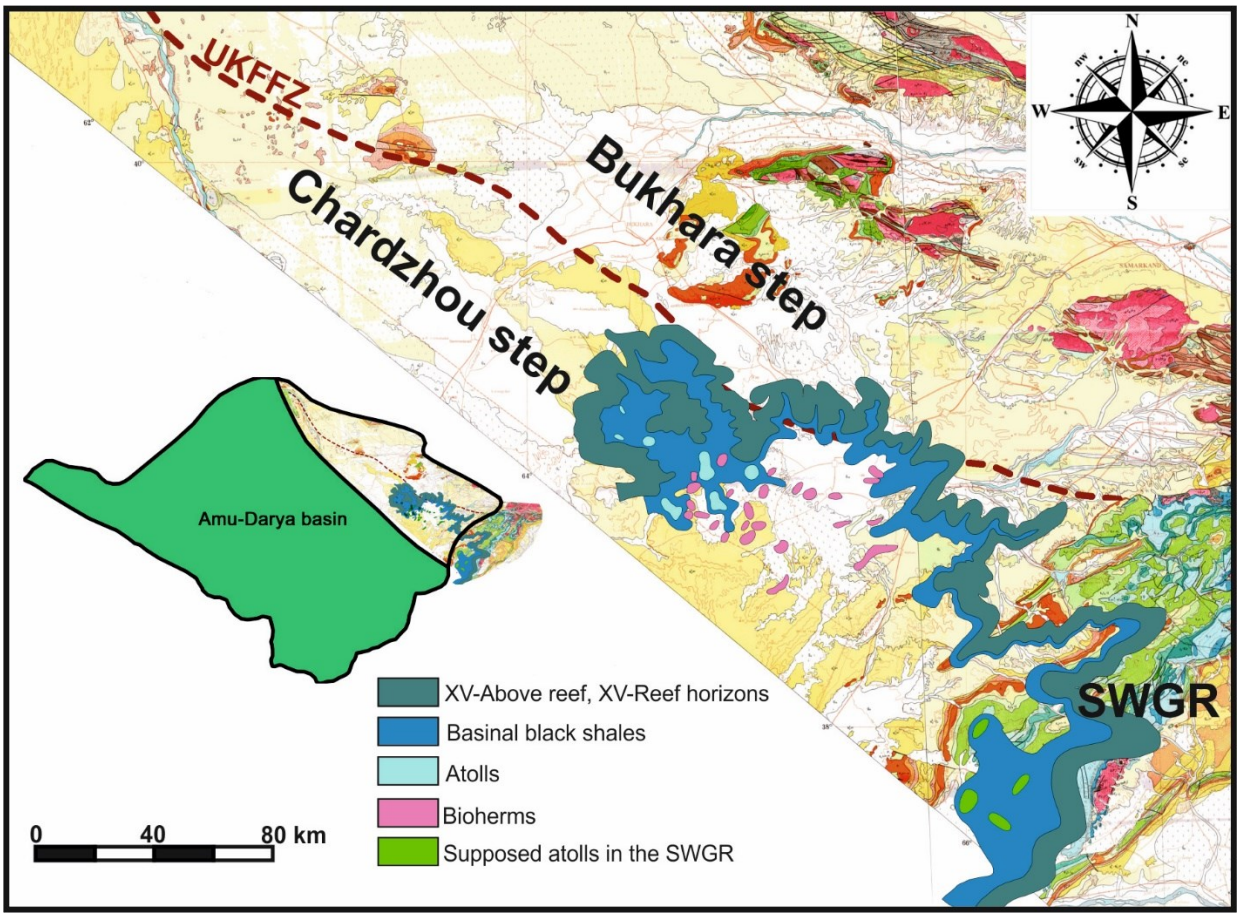

Fig. 2.31. Distribution of reefal Upper Jurassic carbonates. Barrier reef model (modified after Babadjanov, 2012). Here is represented only the location of the reefal carbonates and the basinal black shales situated at the base of the reefs. The lagoon area is located to the northeast of the barrier and the basin to the southwest (see fig. 2.26). Background: fragment of the Geological map of Uzbekistan (1998).

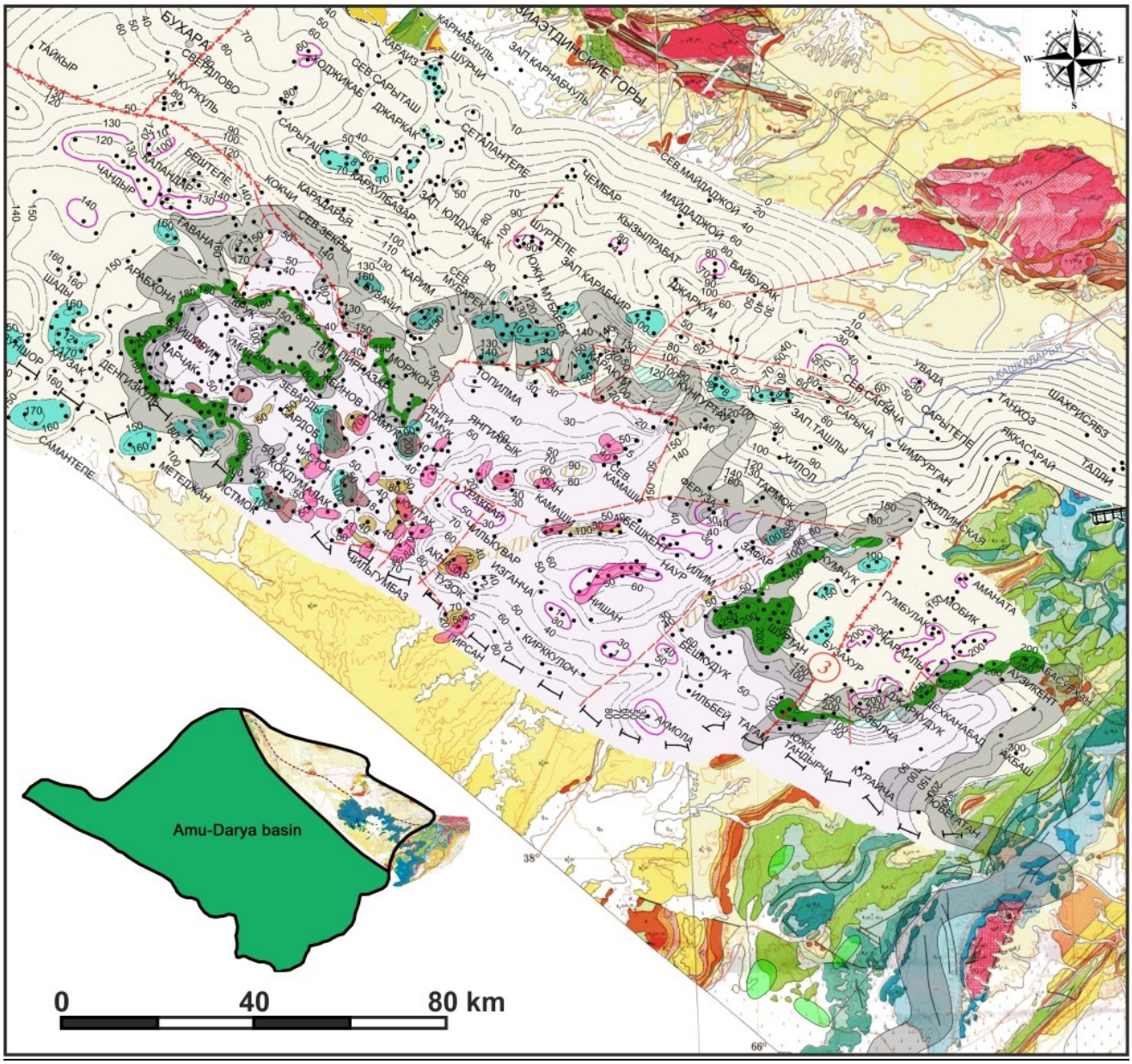

Fig. 2.32. Distribution of reefal Upper Jurassic carbonates.
Location and isopachs of the Upper Kugitang carbonates (modified after Nugmanov, 2009a) showing a non-continuous barrier reef. In green: reef barrier line; in blue green: isolated reefs; in brown: bioherms. Black dots are exploratory wells, pink lines: synsedimentary anticlines. The barrier system model of fig. 2.31 is superimposed in grey (sediments of the reef and above reef horizons) and bioherms in pink surfaces. Background: Geological map of Uzbekistan (1998).

The age of the barrier reef system and the basinal and lagoonal deposits which are more or less synchronous, was confirmed by many corals *[Microsolena agariciformis Etal., M. cavernosa Koly, Comoseris minima Beanvais, Tnecosmilia cartieri Koby, Calamophilliopsis disputabilis (Becker)]* (Husanov, 1995 in Mirkamalov et al., 2005), ammonites *[Progeronia triplex (Quensted)* and *Divisosphinctes bifurcatus (Quenst)]* (Beznosov, 1978 and 1989 in Mirkamalov et al., 2005) and a complex of bivalves [*Chlamys viminea Sow., Velopecten velatus (Goldf), Nucula cf. rieteheni (Loriol), Aequipecten cf. caucasica Pcel, Camptonectes kurganchensis Rep., Parallelodon lutugini Boris]* (from Mirkamalov et al., 2005).

As this reefal system has different carbonate complexes or types (i.e. *basinal, reefal*, *lagoonal*), we will speak about them separately.

2.3.2.3.2 Reefal type (Urtabulak and Kushab formations)

The geological structure of the reef system is exposed on Figure 2.33. As mentioned before, the *reefal type* of the Upper Oxfordian-Kimmeridgian section is composed of two formations – the Urtabulak Formation and the Kushab Formation (see fig. 2.25).

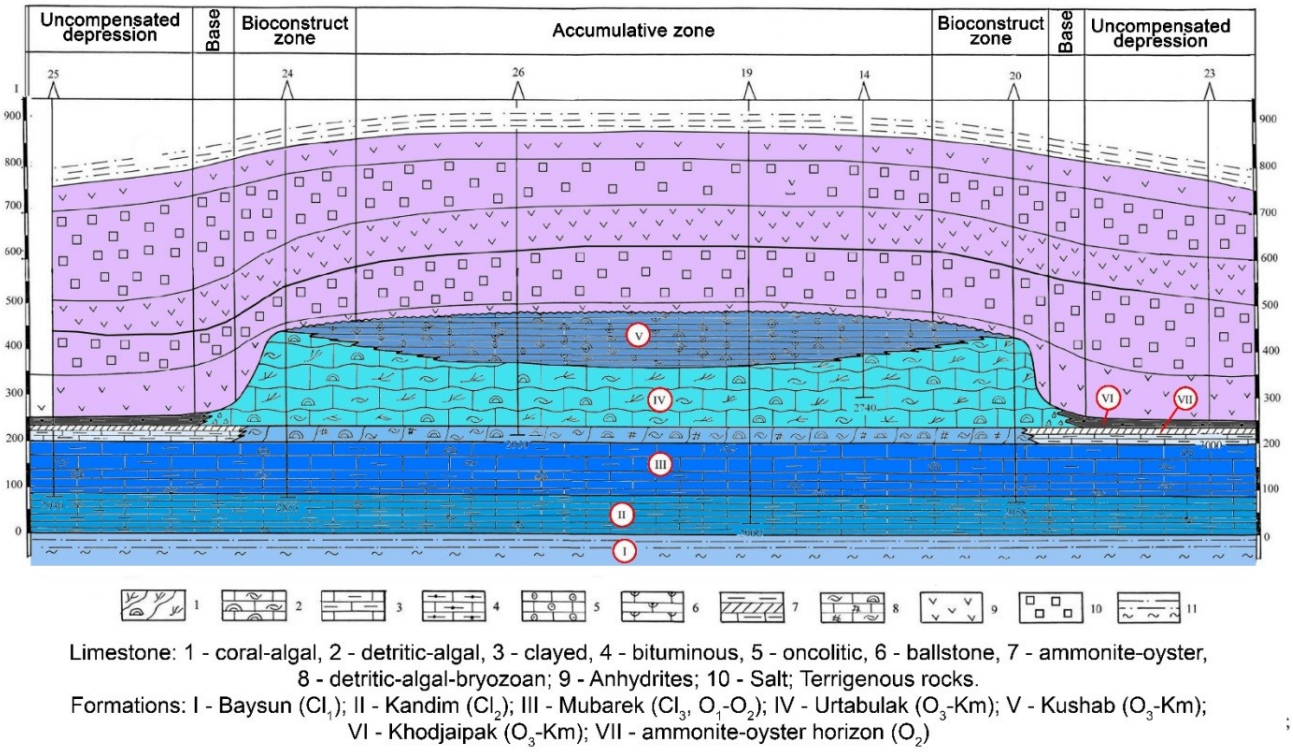

Fig. 2.33. Modelled cross-section of the Zevardi field showing the structure of the reef system. Location of Zevardi field on fig. 2.9. and 2.26 (modified after Abdullaev et al., 2010).

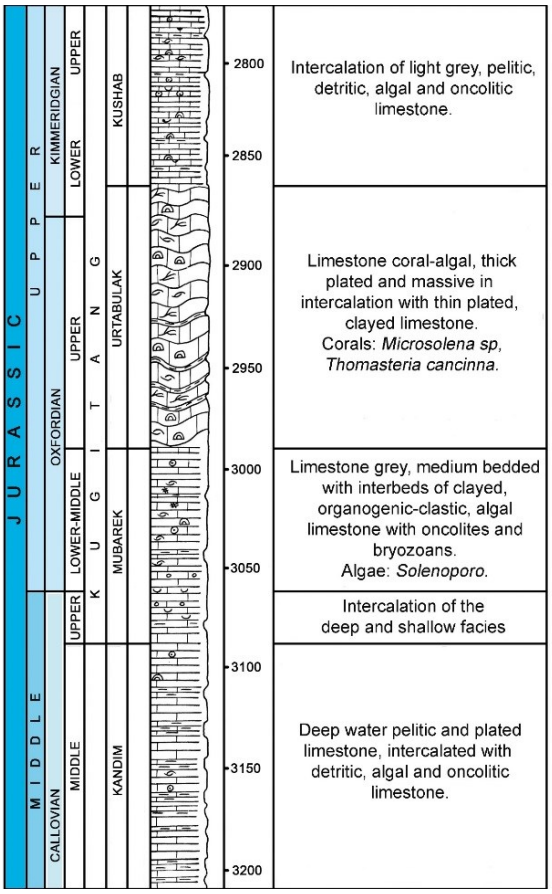

The Urtabulak Formation is the most widespread reefal formation in the Bukhara-Khiva and Southwestern Gissar regions. It is very well represented in the carbonate section of the Shurtan 25 well (fig. 2.34). It forms typical biomorphic constructions (fig. 2.27 and 2.33), which consist of light colored, massive, biomorphic, biomorphic-clastic and detritic limestone. This limestone contains brachiopods, bivalves, gastropods and other fossils (see more details on the synthetic section fig. 2.35). Its thickness changes from 80-90 m to 150-200 m.

The Kushab Formation (less than 100 m thick), which generally covers the previous one, is represented by fine bedded, clastic, organogenic-clastic, detritic, algal limestone, sometimes with intercalated clay beds.

The presence of clastic and clastic limestone in these sections shows that these sediments were deposited in high energy wave conditions.

Fig. 2.34. Carbonate section of the Shurtan 25 well (modified after Mirkamalov et al., 2005).

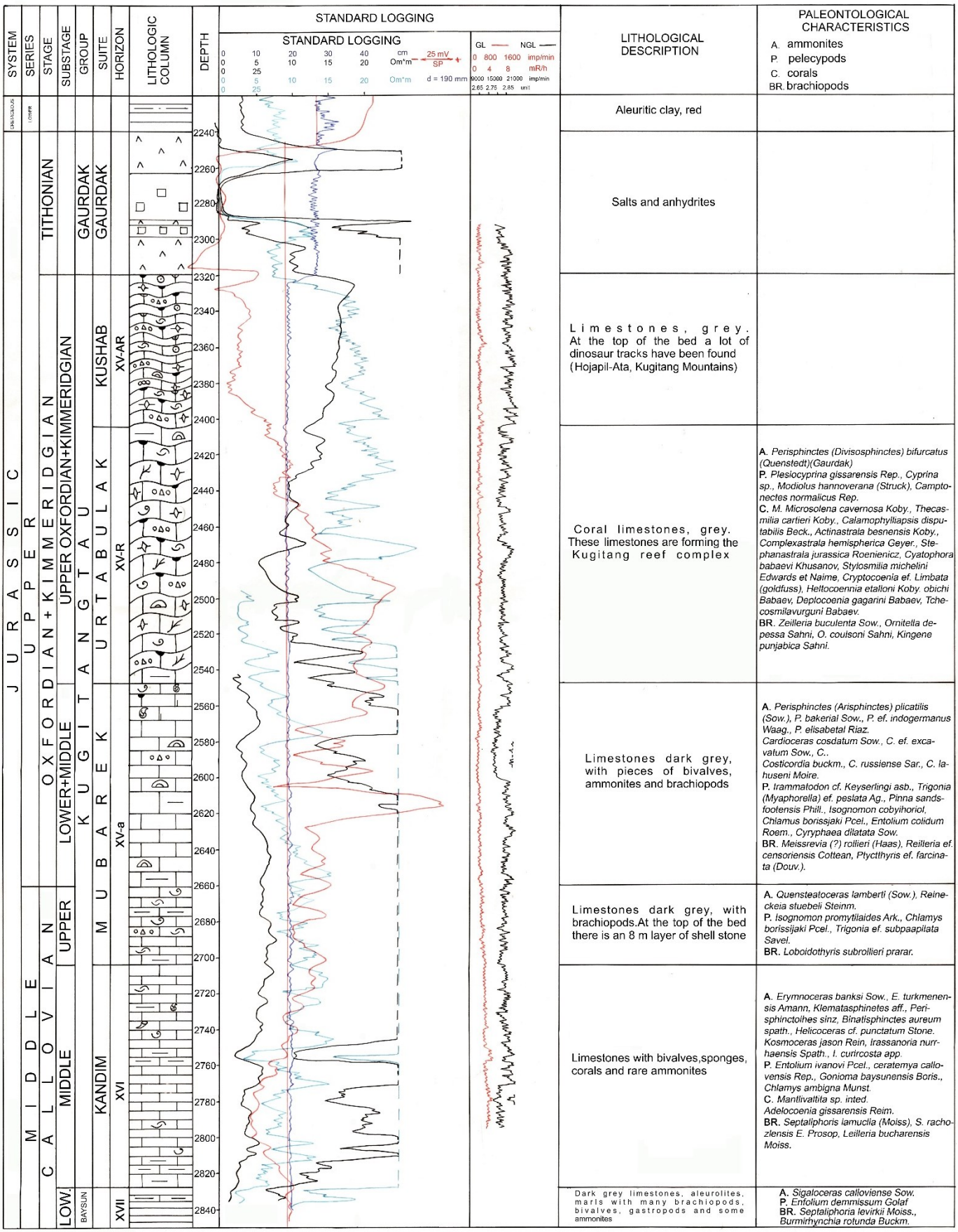

Fig. 2.35. Synthetic carbonate section for the reefal type of the Middle-Upper Jurassic (modified after Kirshin, 2007).

It is interesting to note, that at the top of the Kushab Formation limestone, which crops out in Southwestern Gissar, abundant dinosaur tracks have been reported. In the Uzbekistan part of it, they are exposed in several places, for example in the Derbent gorge (fig. 2.36).

Fig. 2.36. Dinosaur tracks in the Kimmeridgian mudstones of the upper Derbent section (Barrier and Brunet, 2011).

Other footprints are also printed on the top of peritidal Kimmeridgian limestone around the Hojapil-Ata village (northwestern part of the Kugitang Mountains), in Turkmenistan, near the Uzbekistan border (fig. 2.37).

According to Fanti et al. (2013) the level with traces is a 2 cm thick mudstone with a few badly preserved bivalve shells. A stromatolitic layer, which overlaps the mudstone, reflects marginal-marine conditions of tidal flats. The level is situated approximately 20 m below the top of the Jurassic carbonates marking the passage to the evaporites.

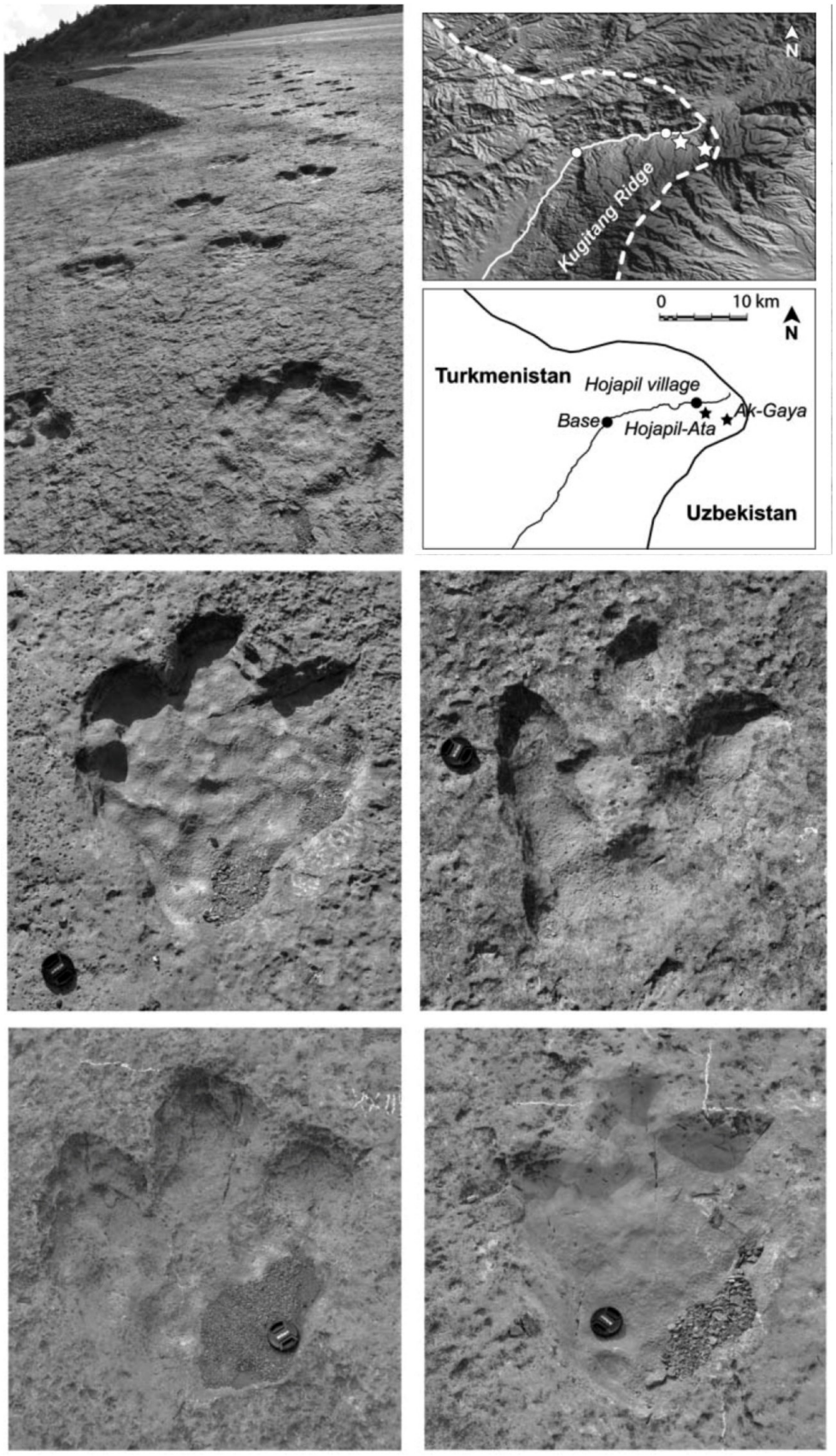

Fig. 2.37. Tracks of dinosaur near the Hojapil-Ata village in east Turkmenistan, northwestern part of Kugitang Mountains, near the Uzbekistan border (after Fanti et al., 2013).

In addition, within the described lithological settings the theropod dinosaur tracks show the presence of nearby emerged landmasses (Fanti et al., 2013) during the Kimmeridgian time.

2.3.2.3.3. Lagoonal type (Gardarya Formation)

The next Late Oxfordian-Kimmeridgian aged formation is the Gardarya Formation (fig. 2.38, 2.39). This unit represents a *lagoonal type* sedimentation. Lithologically it consists of an alternation of limestone (fig. 2.40) and anhydrite beds. Based on fauna, composition and type of deposit, Abdullaev et al. (2010) considered the Gardarya Formation as synchronous of the reef and basin types carbonates.

Anhydrites are grey, dirty white, fine grained, hard and fractured. Limestone is dark grey, pelitomorphic, detritic, algal, weakly dolomitized, with packs of clastic, high porous and fractured limestone inside. The thickness ranges from 60 to 200 m (Abdullaev et al., 2010).

This type of the carbonate section is well exposed in the geological section of the Koshkuduk field (fig. 2.38; see fig. 2.26 for the location in the frame of the barrier reef system model), which is situated near the Pachkamar-Amanata area (see fig. 2.9).

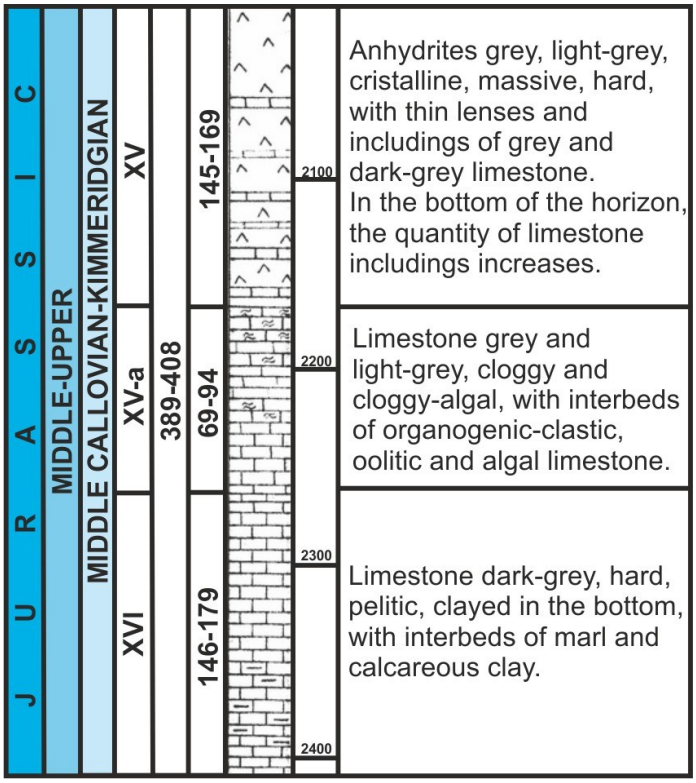

Fig. 2.38. Carbonate section of the Koshkuduk field, exposing the lagoonal-type carbonate facies (modified after Jukovsky, 1993).
See fig. 2.39 for a more detailed age division, and fig. 2.26 for location.

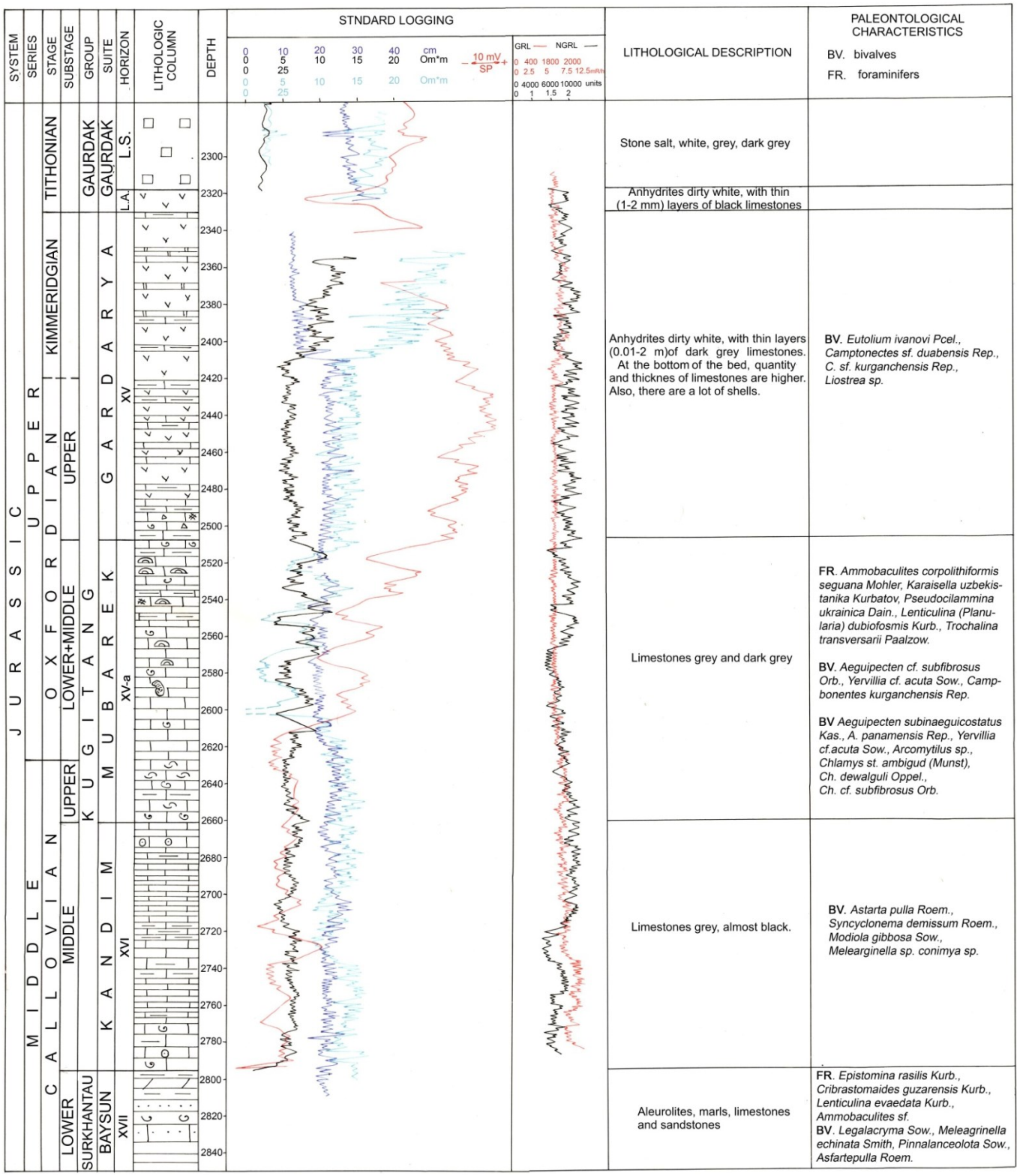

Fig. 2.39. Synthetic carbonate section for the lagoonal type of the Middle-Upper Jurassic (modified after Kirshin, 2007).

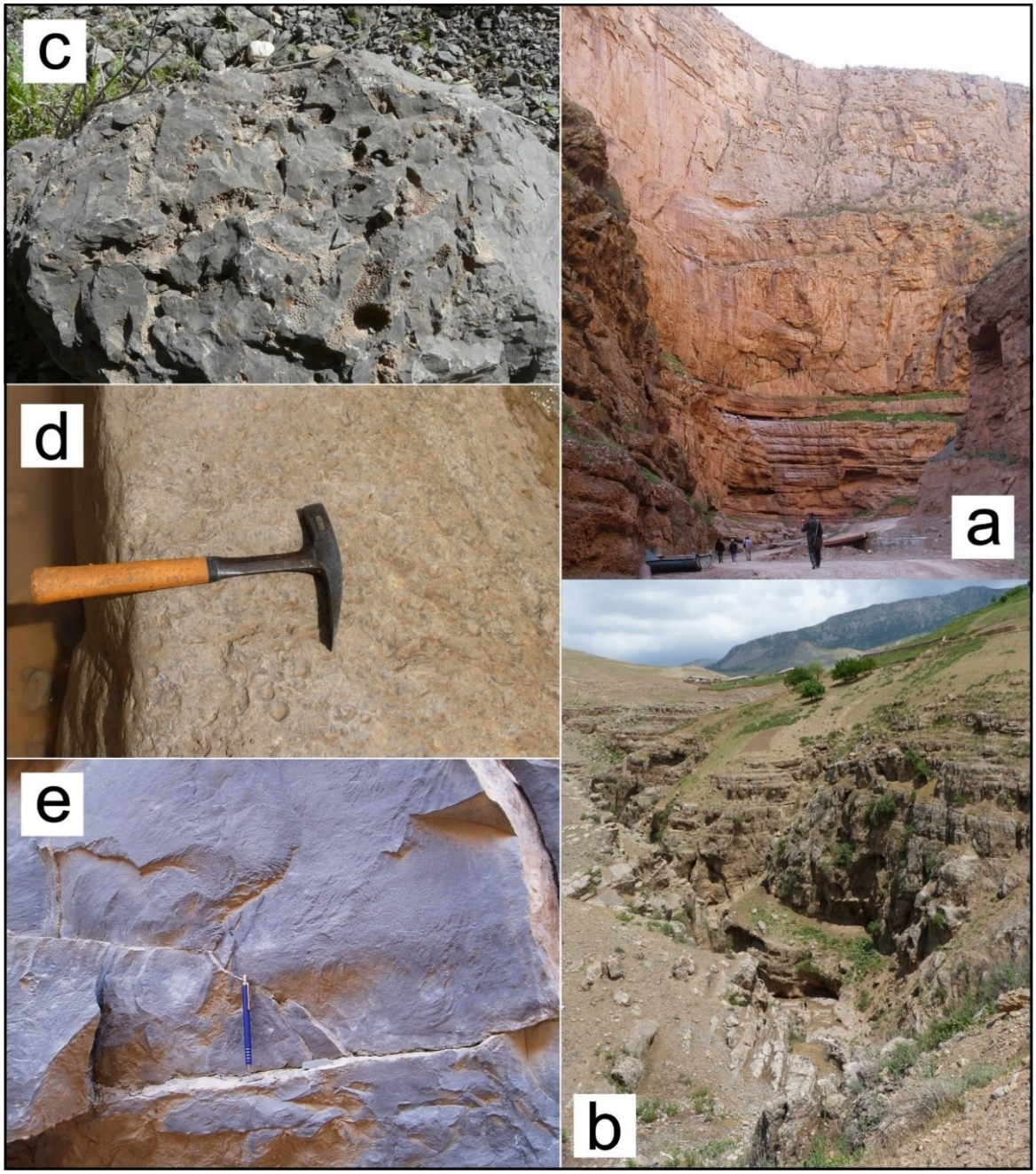

Fig. 2.40: Middle-Late Jurassic carbonates of Southwestern Gissar.
a: Lagoonal carbonate in the Derbent section (location fig. 2.1); **b**: upper carbonate sequence in the Langar section (northern Gissar); **c**: coral in the fine-grained facies in the Derbent section; d: shellstone layers; **e**: fine-grained massive limestone in the Derbent section (Barrier and Brunet, 2011).

3.2.3.2.4. Basinal type (Khodjaipak Formation)

The *basinal type* carbonate section, called the Khodjaipak Formation, consists of deep water sediments (fig. 2.41). They are composed of dark grey, microbedded, strongly bituminous sheeted carbonate-terrigenous rocks and pelitomorphic limestone with packs of clayey limestone inside, which consist of fine grained fragments of fossils.

The formation is only 5-10 m thick, increasing to 30 m near the reefs (fig. 2.27 and 2.33). This increase corresponds to the accumulation of clastic sediments, transported from the reefs and depositing at the foot of the reef (Abdullaev et al., 2010). One of the best examples of this type of basinal carbonates is located in the Tubegatan Mountains, at the Turkmenistan border, near the Khodjaipak spring (fig. 2.41).

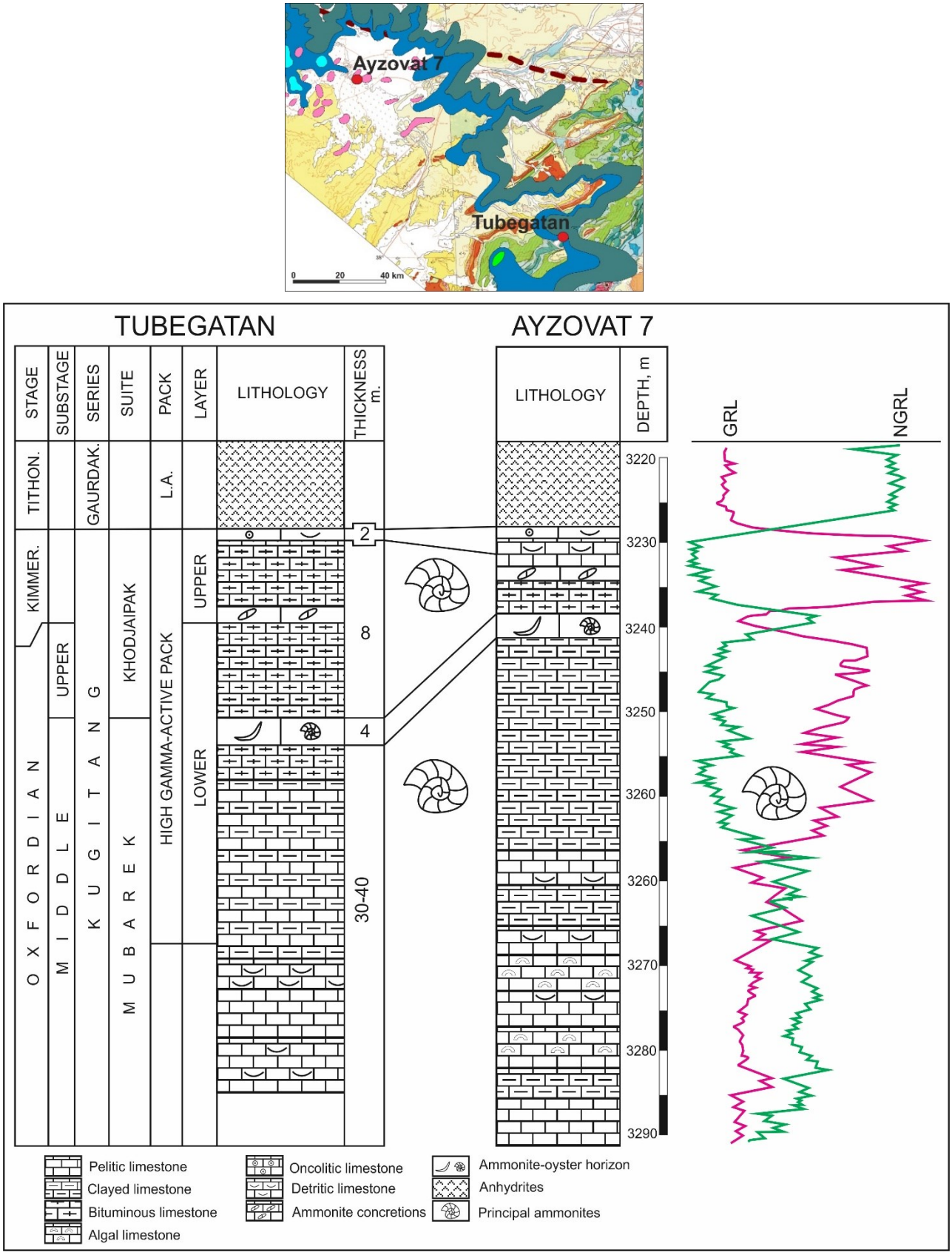

Fig. 2.41. Basinal type carbonate section in Tubegatan Mountain (from exposure) and Bukhara-Khiva Region (from Ayzovat 7 well). Modified after Abdullaev et al. (2010). For location, see also fig 2.9. green line = neutron-gamma ray logging, pink line = gamma ray logging.

The Khodjaipak Formation was penetrated by more than 200 wells in the Beshkent trough area. In this text we provide the carbonate sections of the Urtabulak 102 and North Kamashi 6 wells (fig. 2.42, 2.43).

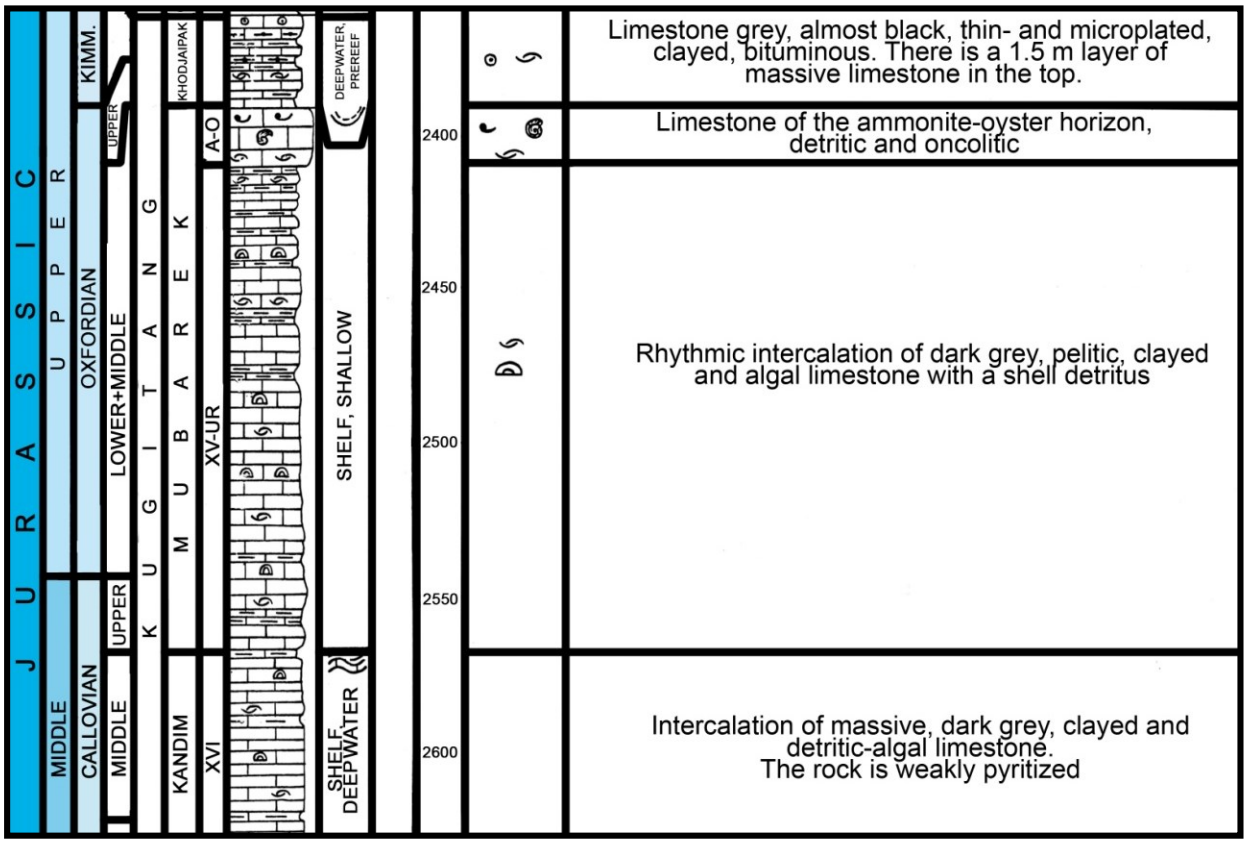

Fig. 2.42. Basinal type of the carbonate section of the Urtabulak 102 well (modified after Mirkamalov et al., 2005). Location on fig. 2.9 and 2.26.

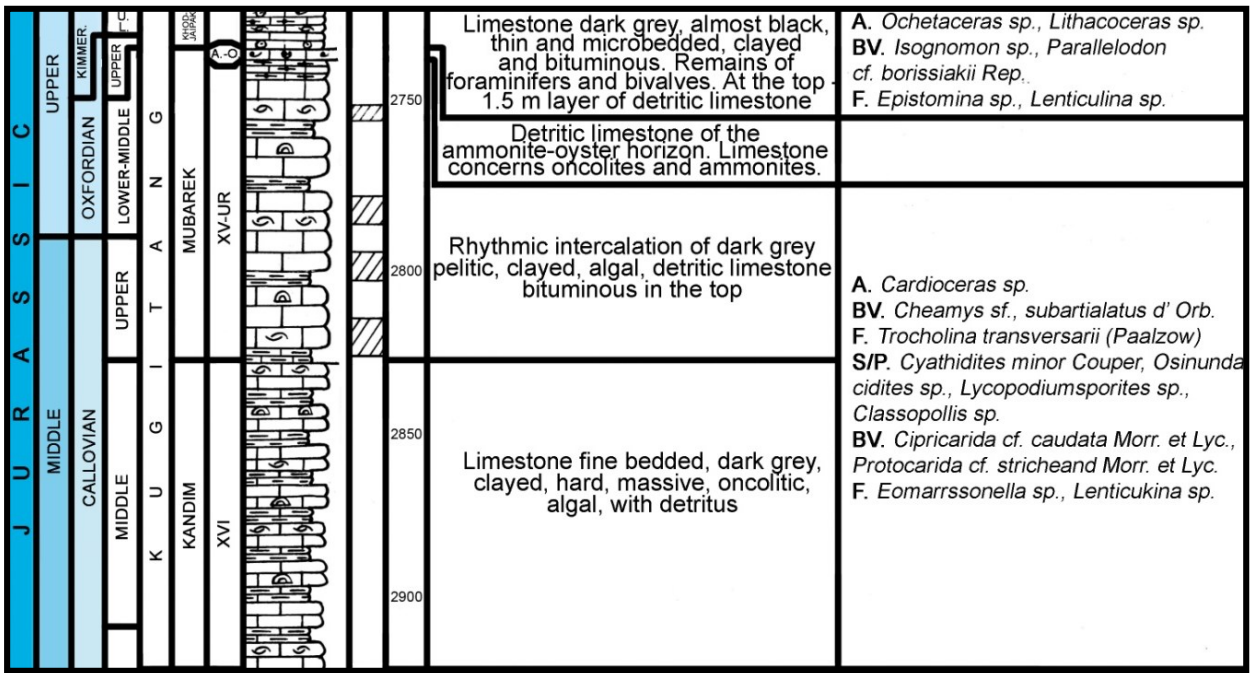

Fig. 2.43. Basinal type carbonates of the North Kamashi 6 well (modified after Mirkamalov et al., 2005). Location fig. 2.9. **A** – ammonites, **BV** – bivalves, **F** – flora, **S/P** – spore-pollens, **A-O** – ammonite-oyster horizon.

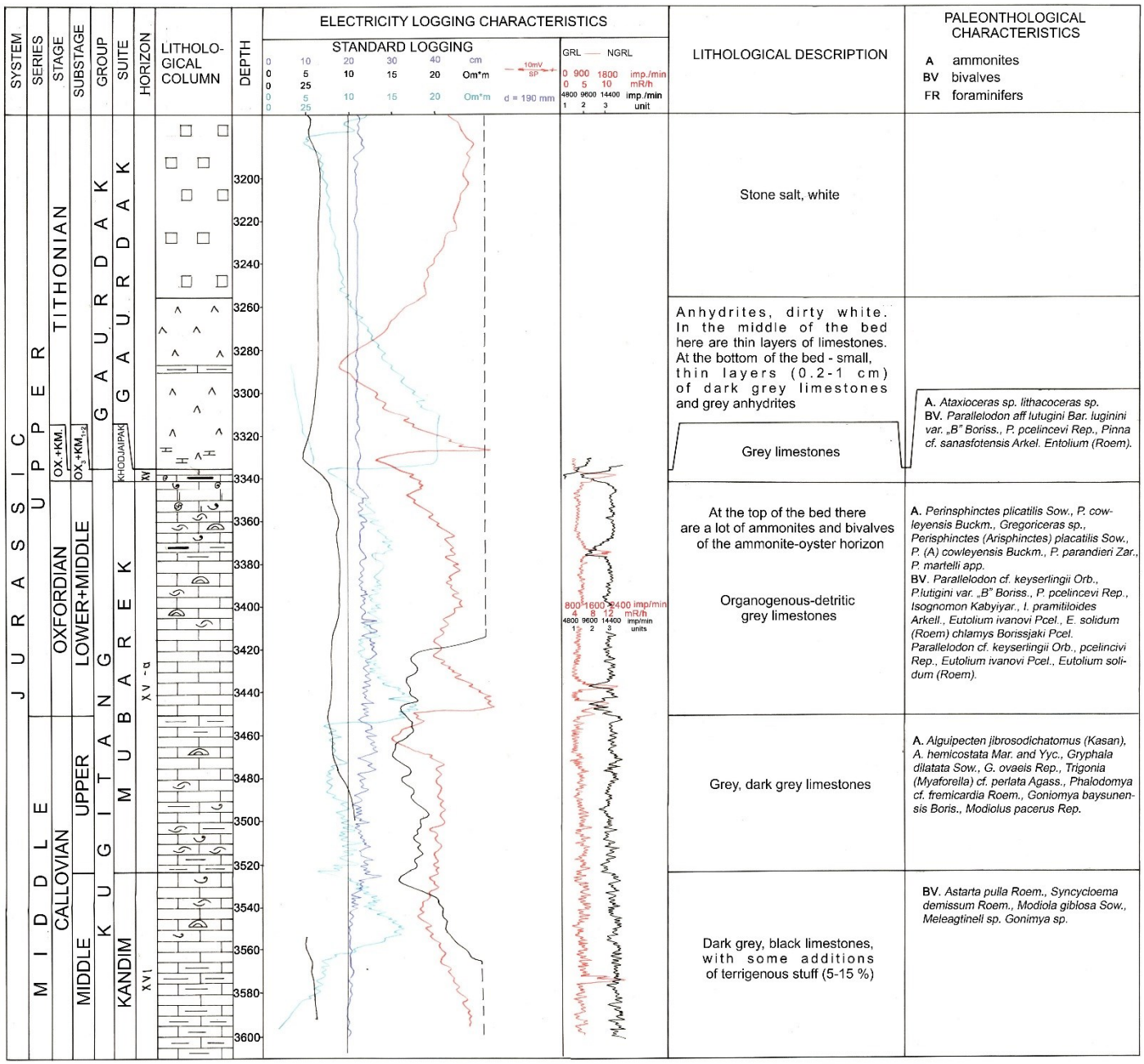

Fig. 2.44. Synthetic section of the Middle-Upper Jurassic basinal-type carbonate section (modified after Kirshin, 2007).

Figure 2.44 shows a synthetic section of the basinal type with details on the fossils names allowing to attribute a Late Oxfordian-Kimmeridgian age to the Khodjaipak Formation.

An interesting point concerning the basinal-type carbonates, as noted in the paragraph 2.3.2.2, is the presence of a high gamma-active pack. This pack is located above the top of the Mubarek Formation and marks well the basinal type of the carbonate. In the Mubarek Formation description above, we wrote, that the gamma-active pack lays above the ammonite-oyster horizon which is at the top of the Mubarek Formation, but according to Abdullaev and Mirkamalov (2001) there could be some gamma-active layers under this horizon inside the Mubarek Formation (see fig. 2.41). The thickest gamma-active packs present below the ammonite-oyster horizon, are determined in the areas where there are no bioherms and in this case these gamma-active packs could be the stratigraphic analogs of the Middle Oxfordian bioherms.

2.3.3. Evaporite or salt-anhydrite unit (Tithonian Gaurdak Formation)

Despite the fact that the *evaporite unit* is well studied, its age is still a controversial issue. For a long time the Gaurdak Formation was commonly dated as Kimmeridgian-Tithonian and some geologists still endorse this age. But, in the light of new data and the reinterpretation of the age of the top of the *carbonate unit*, we support a Tithonian age for the *evaporite unit*.

This proposition is based on the stratigraphical position of the sediments located between the Kimmeridgian black shales (well dated) of the *carbonate unit* (*basin type*) and the red sandstones of the Lower Cretaceous. The second point is that, in 1964 Repman has determined a Tithonian bivalves complex from thin limestone interlayers in the lower part of the *evaporite unit* (Mirkamalov et al., 2005).

The salt-anhydrite unit covers the carbonate one with several erosional surfaces. This unit is widespread on the Chardzhou step and in Southwestern Gissar area, but its structure considerably varies by region.

Actually, there are two main types of *evaporite unit*. The first one, which is called the Baysuntau Formation exists only in the Southwestern Gissar area (Abdullaev and Mirkamalov, 2006), in the northern and central parts. This formation was distinguished in Zarmas (fig 2.45), Derbent, Shuror, Irgayli and many other locations. The type-section is the section of Irgayli (located roughly 35 km North of Baysun, see small-map on fig. 2.45) This section mostly consists of gypsum with some intercalated limestone beds. In the limestone, Repman (1964 cited in Abdullaev and Mirkamalov, 2006) has found the following bivalves: *Camptonectes cf. normalicus Rep., C. duabensis Rep., Plesiocyprina cf. gissarensis Rep., Modiolus aff. Subhannoverana Phel., Isognomon causasicus Phel., Pteria duabensis Rep., Astarte cf. carinata Rep., Chlamys mantonensis Etall., Parallelodon lutugini Boris.*

The second type of *evaporite unit* (Gaurdak Formation) was distinguished in the Gaurdak and the Tubegatan areas. It has a quite different structure with alternations of salts and anhydrites.

In Southwestern Gissar (fig. 2.45) the Gaurdak Formation is divided into four members: the lower anhydrite, halite-anhydrite, stone salt and upper anhydrite members (Abdullaev and Mirkamalov, 2006). The thickest sections are found in the southwestern part of the area, thinning towards the east. Some of the members disappear from the section. Locally the salt is so well developed that it is exploited in salt mines (fig. 2.46, fig. 2.47 c-e).

In the Bukhara-Khiva region exists the Gaurdak type of the *evaporite unit*. Here it is composed in general, of five members. The thickest sections are located in the southeastern part of the Bukhara-Khiva region. Here, the salt-anhydrite unit consists of five lithological members: lower anhydrite, lower salt, middle anhydrite, upper salt and upper anhydrite.

The first one is the lower anhydrite member. It flattens the roughness of the top of the *carbonate unit* and consists of light and dark grey anhydrites. Its thickness ranges from 10 to 150 m.

The lower salt member covers the lower anhydrite. This member essentially consists of halite. Its thickness varies from 0 to 400 m.

The middle anhydrite member is the most widespread horizon of the *evaporite unit* in the Bukhara-Khiva and Southwestern Gissar areas. It is composed of white, grey anhydrites with thin halite intercalations.

The upper salt overlaps the previous horizon. Its thickness reaches 600 m. This member is represented by colorless halite.

The upper anhydrite of the Upper Jurassic is the top horizon of the Jurassic. It consists of white anhydrite with clay intercalations. Its thickness is of 8-20 m (Mirkamalov et al., 2005).

Summing up, there are two different types of evaporites in the northern margin of the Amu-Darya basin. The first one, called Baysuntau Formation, is located only in the north and central part of Southwestern Gissar and is divided into two parts. The second type of the section is the Gaurdak

Formation. This type is the most widespread evaporite section, found both in the Southwestern Gissar and Bukhara-Khiva regions.

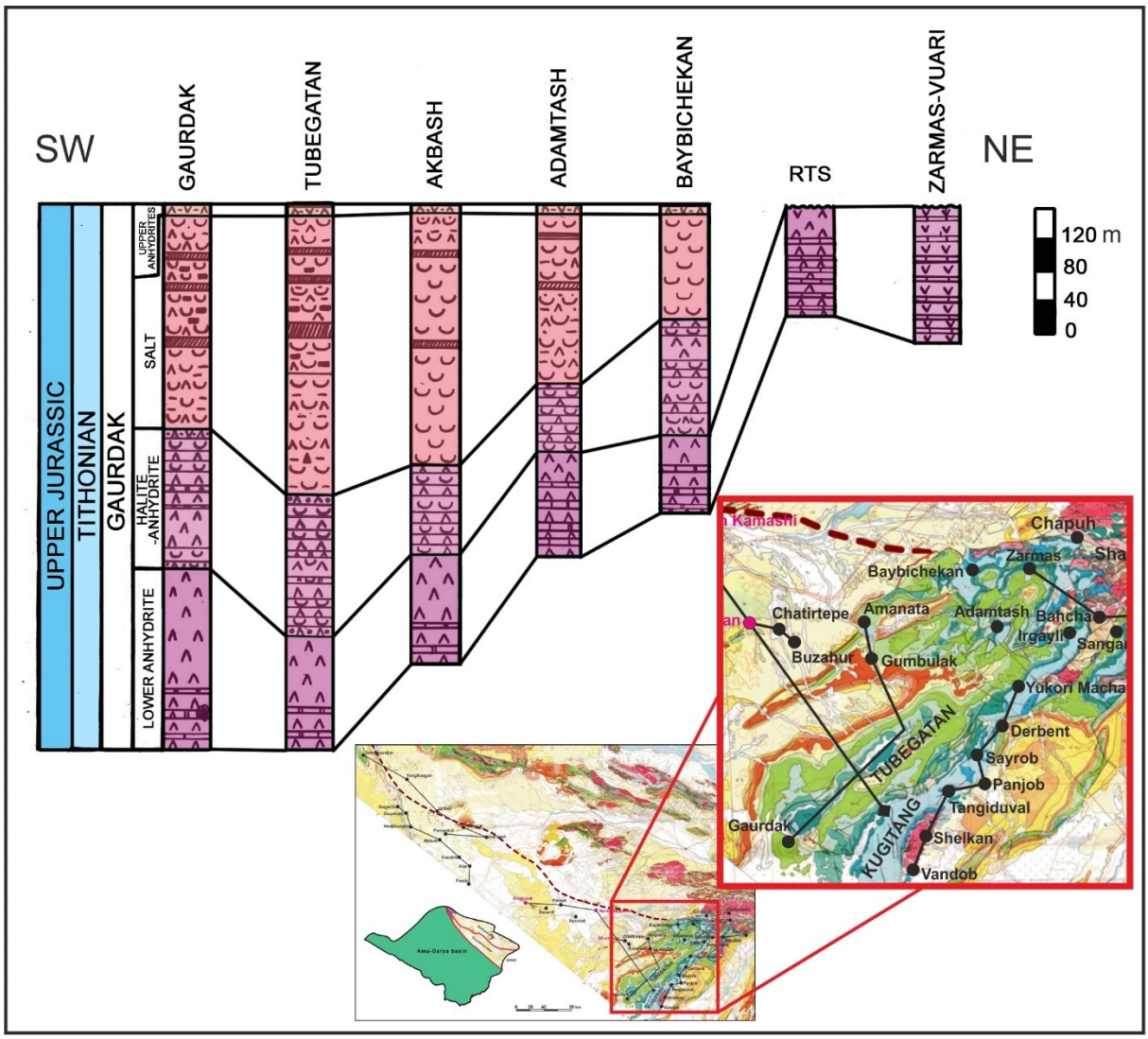

Fig. 2.45. Correlation of evaporites of Southwestern Gissar. The red points on the inset map show the location of four of the columns (modified after Egamberdiev and Ishniyazov, 1990).

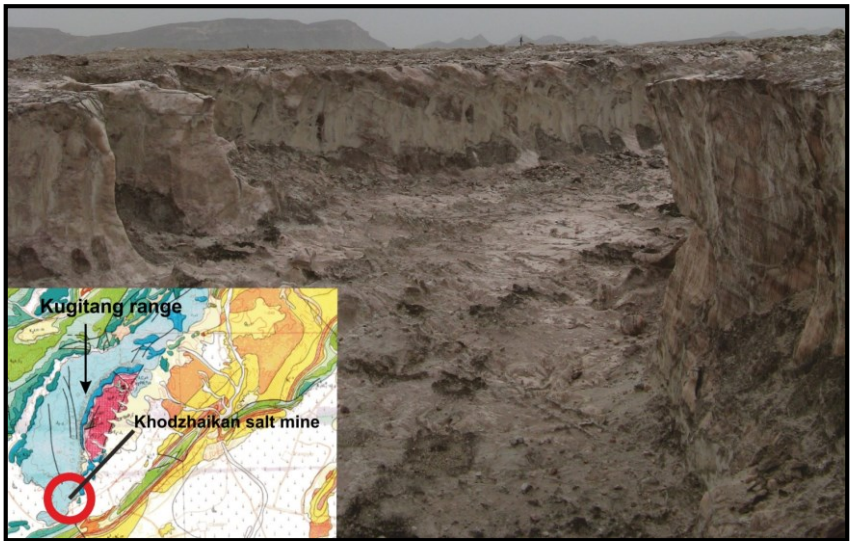

Fig. 2.46. Khodzhaikan salt mine in the south of the Kugitang Mountains.

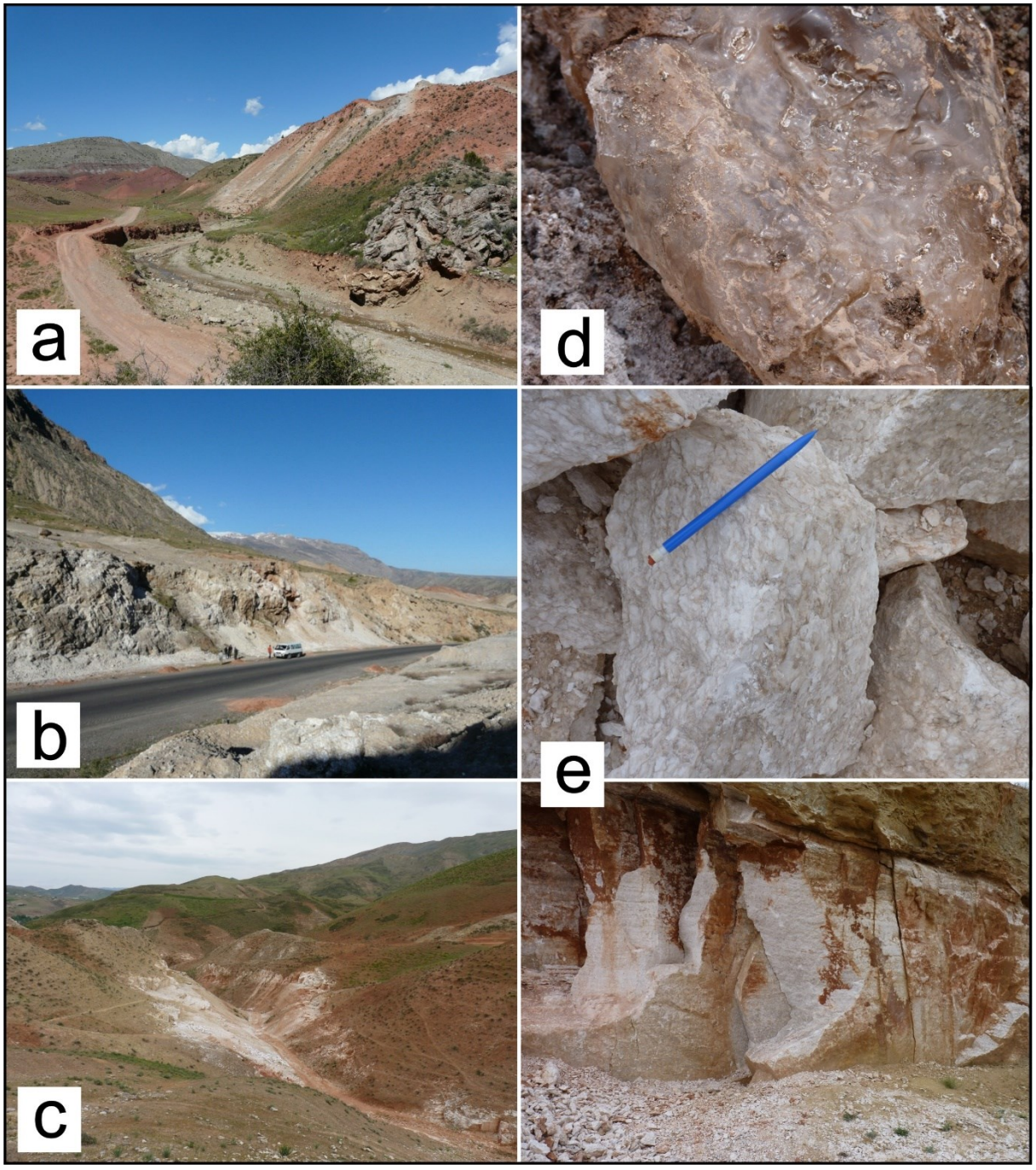

Fig. 2.47. Late Jurassic evaporites in Southwestern Gissar.
a: Evaporite in the northern limb of the Baysuntau anticline, Derbent section (location fig. 2.1). Here the salt overlies the uppermost folded layers of the Kimmeridgian carbonate, and underlies the red bed (background). Note the fold in the limestone related to third order decollements on salt layers; **b**: Evaporite cropping out along the Guzar-Termez highway on the southern limb of the western ending of the Baysuntau anticline; **c** to **e**: Evaporite near the Langar salt mine (NW Southwestern Gissar); **d**: Halite; **e**: Gypsum and anhydrite (Barrier and Brunet, 2011).

2.4. Cretaceous

The Cretaceous sediments overlap the Jurassic ones with an erosional surface. The principal outcrops are located in the Southwestern Gissar area. The main facies are continental, lagoonal, and marine. The marine facies are the most widespread. They contain abundant fauna (names are mainly taken from Mirkamalov, 1975 and Kim et al., 2007), and they are more studied than other facies of the Cretaceous.

2.4.1. Lower Cretaceous

The Lower Cretaceous starts with red colored conglomerates. They conformably cover the Upper Jurassic evaporites, and if this latter unit is eroded, they directly lay on the Jurassic carbonates (Khayitov, 2006).

The Lower Cretaceous is composed of the undivided Berriasian-Valanginian, the Hauterivian, Barremian, Aptian and Albian stages (fig. 2.48). The section is characterized by intercalations of different types of continental and marine rocks. The principal ones are gravelite, sandstone, clay, siltstone, limestone and clayed limestone, marl and gypsum.

The Berriasian and Valanginian are represented by red colored clays and siltstones with intercalated sandstones, dolomites and gypsum. Some badly preserved fauna show that there were short time existing lagoons during this period of time. These layers contain ostracods *Cypridea brevirostrate Martinsand,* which confirm the Berriasian age and bivalves *Lima tombeckiana Orb., Pterotrigonia caudate (Ag.), Astarte beamonti Orb.*, which characterize the Valanginian. The thickness of this formation is around 310 m.

Above, the Hauterivian sediments are represented by a continental sequence of red clay in the lower part and grey sandstone with some gravelite intercalations at the top. *Trigonioides kodairaiformis Mart., Limnocyrena Ghissarica Mart.* bivalves and *Malzevia ex gr. pellucida (And), M. Malzi Andrv.* ostracods were found in this pack ranging in thickness from 50 to 260 m.

An undivided Barremian-Lower Aptian sequence conformably lays on the Hauterivian sediments. These deposits are 230 m thick. They are represented by clay, sandstone, siltstone, some shellstone and limestone beds containing an abundant fauna. They were deposited in a shallow sea-lagoonal environment.

The Upper Aptian beds are composed of clay, limestone and sandstone. They are still deposited under marine conditions (confirmed by the presence of ammonites). They are 95 m thick.

The Albian stage is divided into three parts. All of them have a marine origin and consist of intercalations of clay, sandstone, limestone and shellstone. These shellstone and limestone contain assemblages of ammonites (*Hypacanthoplites jacobi Coll., H. Karlukensis Lupp., H. Elegans Frit., Hoplites dentatus Sow., H. cf. baylei Spath., Epihoplites trapezoids Lupp., Mortoniceras inflate gibbosa Spath., Hysteroceras carinatum Orb., Semenovites michalskii Sem),* bivalves (*Nucula longa Vinok., Linotrigonia Ghissarensis Vinok, Exogyra localis subtypica Mordv.),* ostracods *(Oncocytheridea socialis Andrv.et Mand.)* and gastropods *(Haustator kamprekensis Djal.i.),* which provide an Albian age. The common Albian thickness is 545 m.

The complete Lower Cretaceous section of the Southwestern Gissar is shown on Figure 2.49.

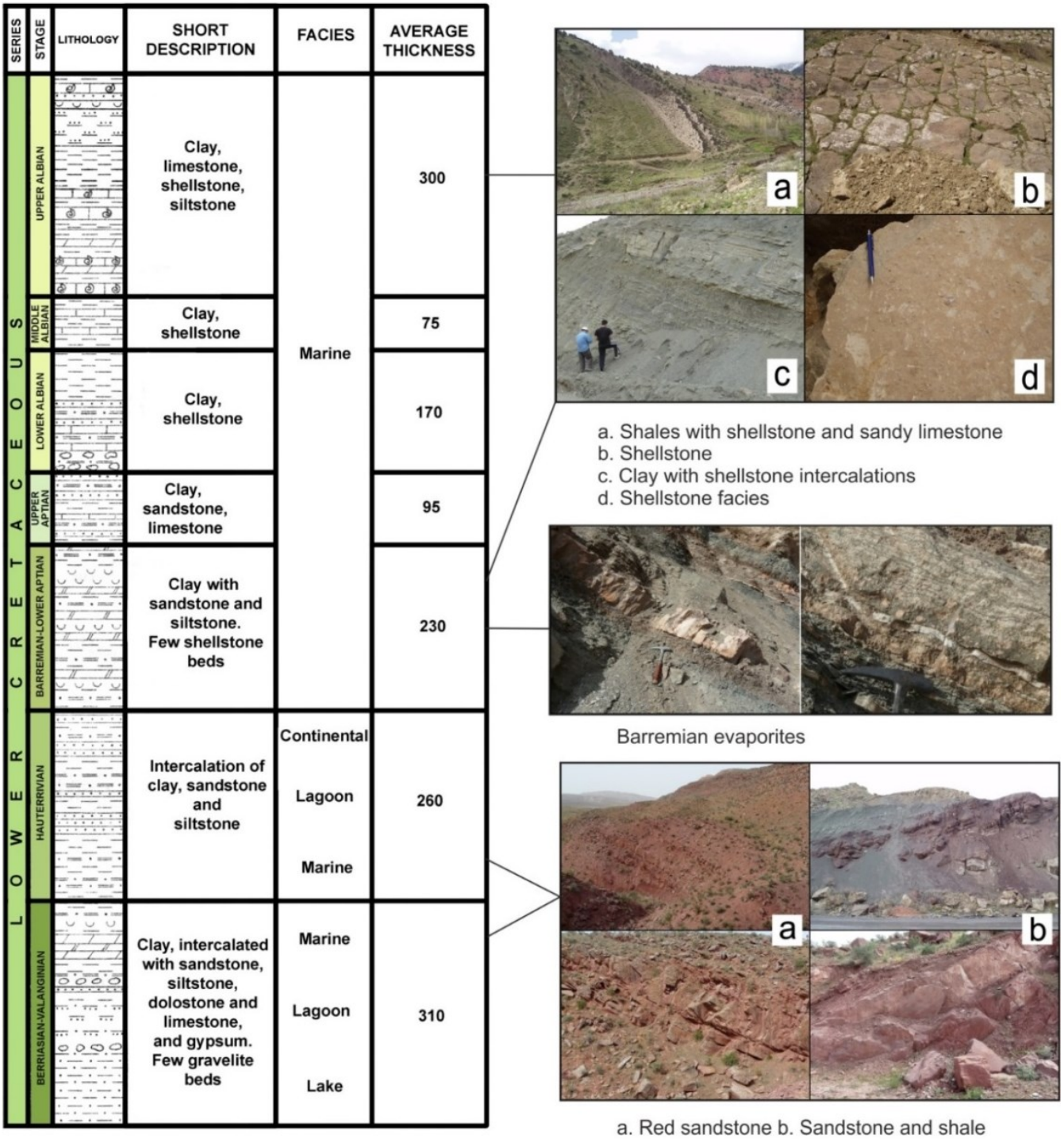

Fig. 2.48. Synthetic section of the Lower Cretaceous in Southwestern Gissar.
Stratigraphic column modified after Tulyaganov and Yaskovich (1980); photos in the Tubegatan and Baysun sections, location on fig 2.1, after Barrier and Brunet (2011).

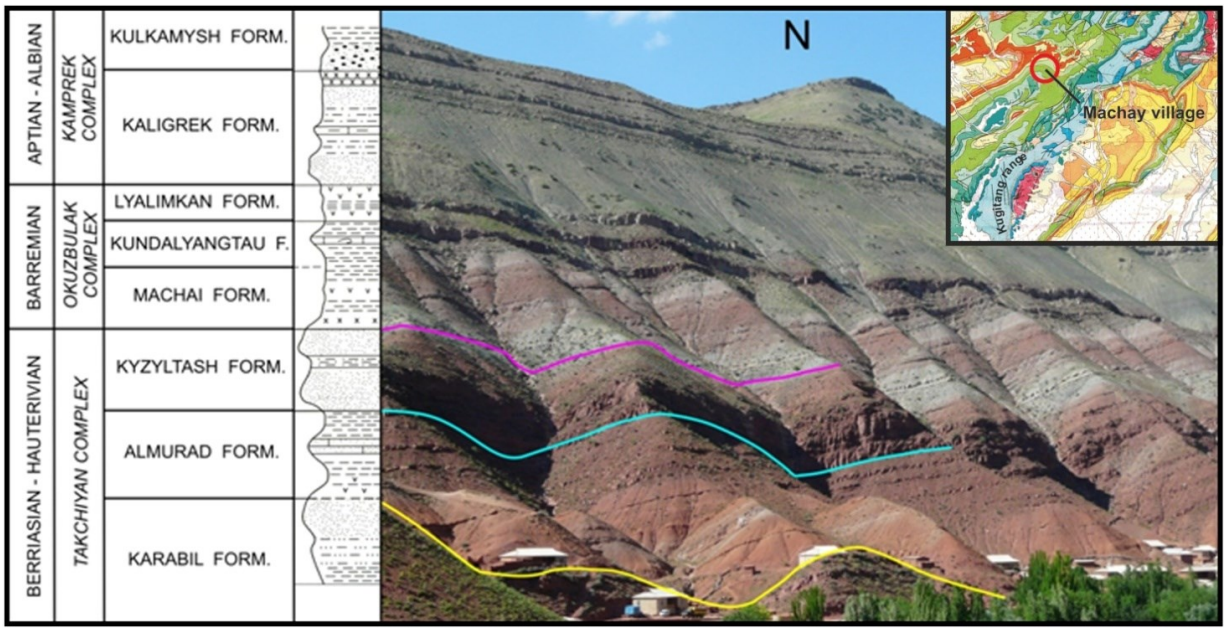

Fig. 2.49. Lower Cretaceous section near the Machay village in the northern part of Southwestern Gissar (Barrier and Brunet, 2011), Formations subdivision after Mirkamalov, 1975.

2.4.2. Upper Cretaceous

The Upper Cretaceous deposits are expressed, in general, by marine facies, but lagoonal and continental ones can be met too. The main composition is a clayed-marly-sandy complex with some limestone and shellstone interbedded layers (fig. 2.50). The Upper Cretaceous is represented by Cenomanian, Turonian, Coniacian, Santonian, Campanian and Maastrichtian stages.

The Cenomanian stage conformably covers the Albian sediments. It is divided into two parts, Lower and Upper, representing a shallow warm sea facies.

The Lower Cenomanian sediments (290 m) consist of clay, sandstone, shellstone, limestone and conglomerate beds. The limestone beds contain ammonites: *Karamaites gaurdakense (Lupp.), Mediasiaceras beliakovae Iljin,* bivalves *elongates Lam., Korobkovitrigonia gaurdakensis Beliak., Lopha dichotoma Bayle, Rhynchostreon columbium (Lam.),* and *Rh. chaperi (Bayle).*

The Upper Cenomanian (155 m) overlays the Lower Cenomanian layers without discontinuity and consist of detritic limestone, sandstone and clay with limestone interbeds. The age was determined by remains of ammonites *Karamaites aktaschense Iljin, Calycoceras batyophalum Kossm., Sciponoceras romanovski*, bivalves *Spondylus balakhanensis Bobk., Korobkovitrigonia darwaseana* and foraminifers.

The Turonian stage has a common thickness of 300 m. It is represented by a calcareous section – limestone, shellstone, calcareous clay, marl and clay intercalations. It contains remains of ammonites *Proplacenticeras orbignyanum Gein., Lewesiceras ex gr. perampium Mant., Coilopoceras Ghissarensis Iljin* and bivalves *Inoceramus lamarckii Park., Liostrea rouvillei Coq.*

The Coniacian stage is expressed by dark-grey clay with interbeds of limestone and siltstone in the bottom of the section (90 m) while in the upper part (120 m) calcareous clay, marl with white limestone and sandstone interbeds are observed. The Coniacian sediments were deposited in an open, normal salty sea, which is confirmed by the fauna: ammonites (*Barroisiceras akrabatense Iljin, Placenticeras orbignyanum Iljin, Proplacenticeras ex gr. proplanum Iljin*.), bivalves (*Inoceramus ex gr. lamarckii Park., Costeina akrabatense*), sea urchins (*Echinobribeus markovi Faas, Hemiaster fourneli Desh., H. Integr. Lamb., H. Amudariensis Schmidt),* foraminifers *(Ammomargulina sixtelae Arap., Am. aulatensis Arap., Gaudryina variabiliformis N.Byk., Gavelinella moniliformis),* and ostracods *(Cytherella facila Mand., Bairdia derooi Andrv., Brachycytere dotata Mand., Cosfa tadjikistanica Andrv. Bythocytheremorpha porrecta Vronsk).*

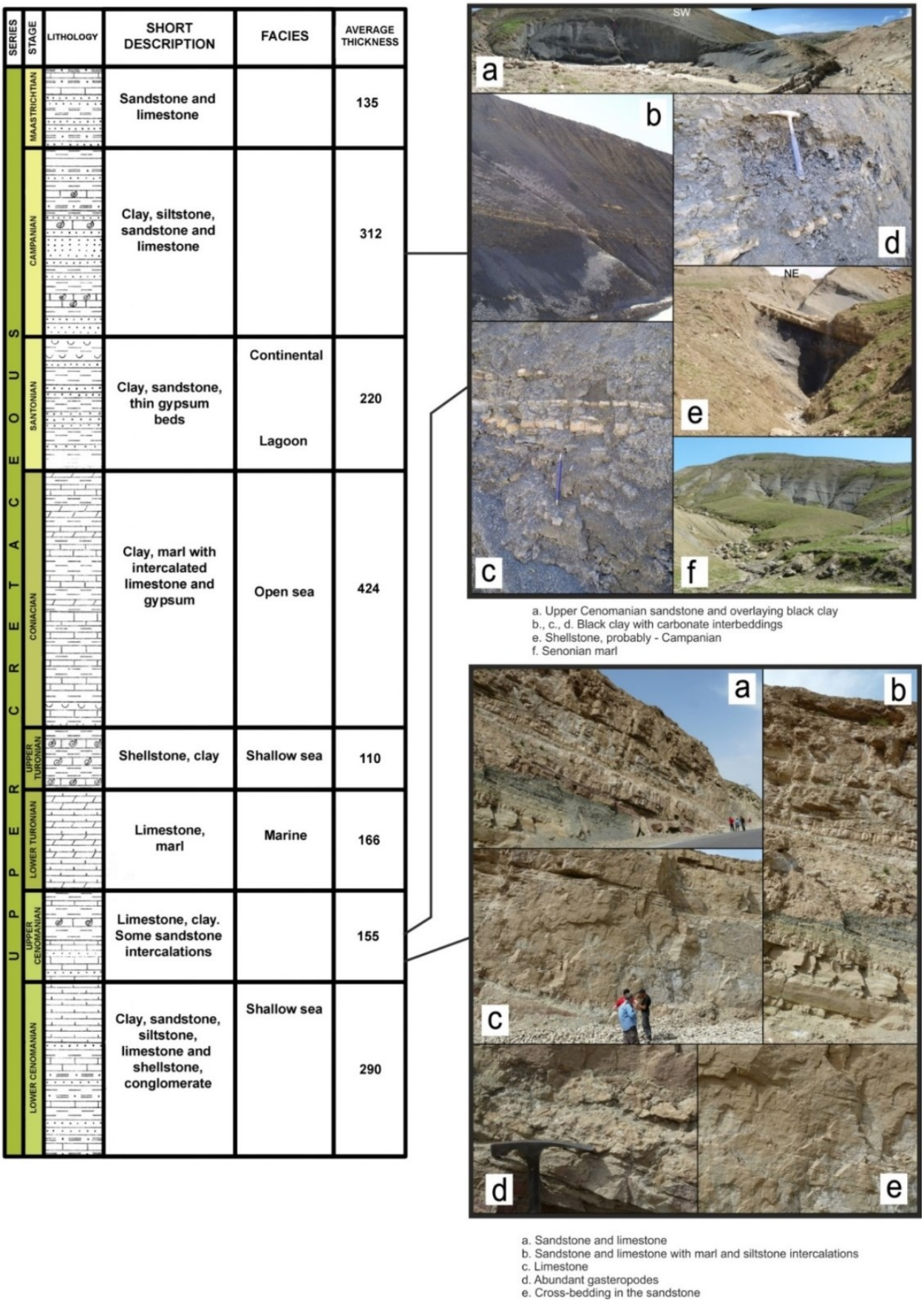

Fig. 2.50. Synthetic section of the Upper Cretaceous in Southwestern Gissar.
Column modified after Tulayaganov and Yaskovich (1980). Photos in the Tubegatan and Baysun sections, location on fig 2.1 (from Barrier and Brunet, 2011).

The Santonian deposits (around 150 m) are composed of clays and sandstones with rare gypsum intercalations, characterized by the transition from continental to lagoonal facies. The following fauna remains were found there: ammonites *Stantonoceras guadolupae asiaticum Iljin, Asiatostantonoceras tagamense Iljin,* and bivalves *Fatina kugitangensi, Born.*

The Campanian level, which covers the Santonian sediments, can be divided into two parts. The lower part (around 212 m) is represented by clay, sandstone and limestone. The upper part is thinner (only 100 m) and composed of sandstone, siltstone and limestone. These sediments contain ammonites: *Hoplitoplacenticeras marroti Coq., Bostrychoceras polyploccum Roem., Trachyscaphites spiniger Schiit.*), and bivalves *Ostrea tecticostata turkmenica Borm., Lopha (A) falcate Mort., L. luppovi Bobk., Gyropleura gaurdakensis Renng.,* and *G, renngarteni Pojar.*

The Maastrichtian stage is represented by a sandy-calcareous sequence, 135 m thick. Its age was determined by the presence of bivalves *Liostrea lehmannii Rom., Chlamys dujardini Roem.*

2.5. Cenozoic

The Cenozoic sediments cover most part of the northern margin of the Amu-Darya basin. They constitute a huge sequence, mainly of continental origin. The marine facies exist in the lower part of the Cenozoic. The common thickness of the Cenozoic deposits is around 4000 metres. The contact between the lower part of the Cenozoic and the Cretaceous is unconformable.

2.5.1. Paleogene

The Paleogene beds overlap the Cretaceous with traces of emersion. They are divided into the Paleocene, Eocene and Oligocene (fig. 2.51).

The Paleocene is represented by intercalations of marl, limestone and gypsum. The most widespread is the Upper Paleocene: the so-called Bukhara beds (fig. 2.52), which are one of the principal geological-geophysical markers of the area that can be traced (where it exists) on the most part of the seismic lines. It contains bivalves *Musculus elegans (Sow.), Brachydomtes jeremejevi (Rom.)* and nummulites (*Nummulites solitarius de la Harpe, N. deserti de la Harpe*). The common thickness of the Paleocene is of around 100 m.

The Eocene deposits cover the clayed-calcareous deposits of the Paleocene. Two parts can be distinguished in the Eocene marine sequence.

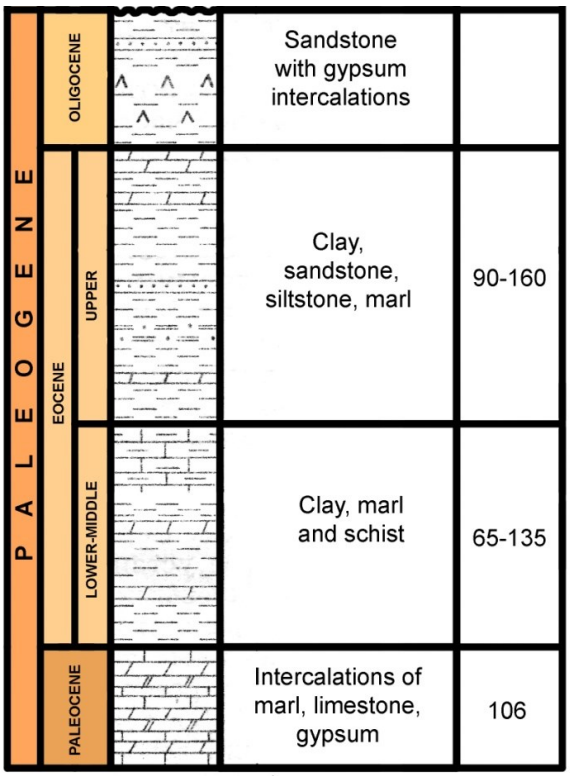

The Lower-Middle Eocene (from 65 to 135 m thick) consists of intercalations of clay, marl, limestone with some shale intercalations. The age of the formation was determined by the bivalves *Musculus elegans, Glycy meris ex. gr. polymarphus (Desb.)*, oysters *Ostrea hemiglobosa Rom., Liostrea Neussu (Netsh.)* and foraminifers typical of the Early Eocene, *Globorotalia subbotinae* and *Gl. Araganensis* and *Acarinita pentacamerata Subb., Globorotalia turkmenica* typical from the Middle Eocene.

The Upper Eocene is composed of siltstone, sandstone and marl. The age of this unit 90-160 m thick, is confirmed by the foraminifers *Bulivina longa Balakh,* and *Cribrononion rischtanicum.*

Fig. 2.51. Synthetic section of the Paleogene in Southwestern Gissar

Where it exists, the Oligocene conformably covers the Eocene deposits and consists of sandstone with gypsum intercalations (fig. 2.53). These rocks contain foraminifers *Cibicides lobatulus (Wulkereticob.), Nonionqrani berus Terquem* and bivalves *Cordiopsis sp.* and *Balames sp.* The Oligocene deposits are very rare in the Cenozoic sections of the Bukhara-Khiva area.

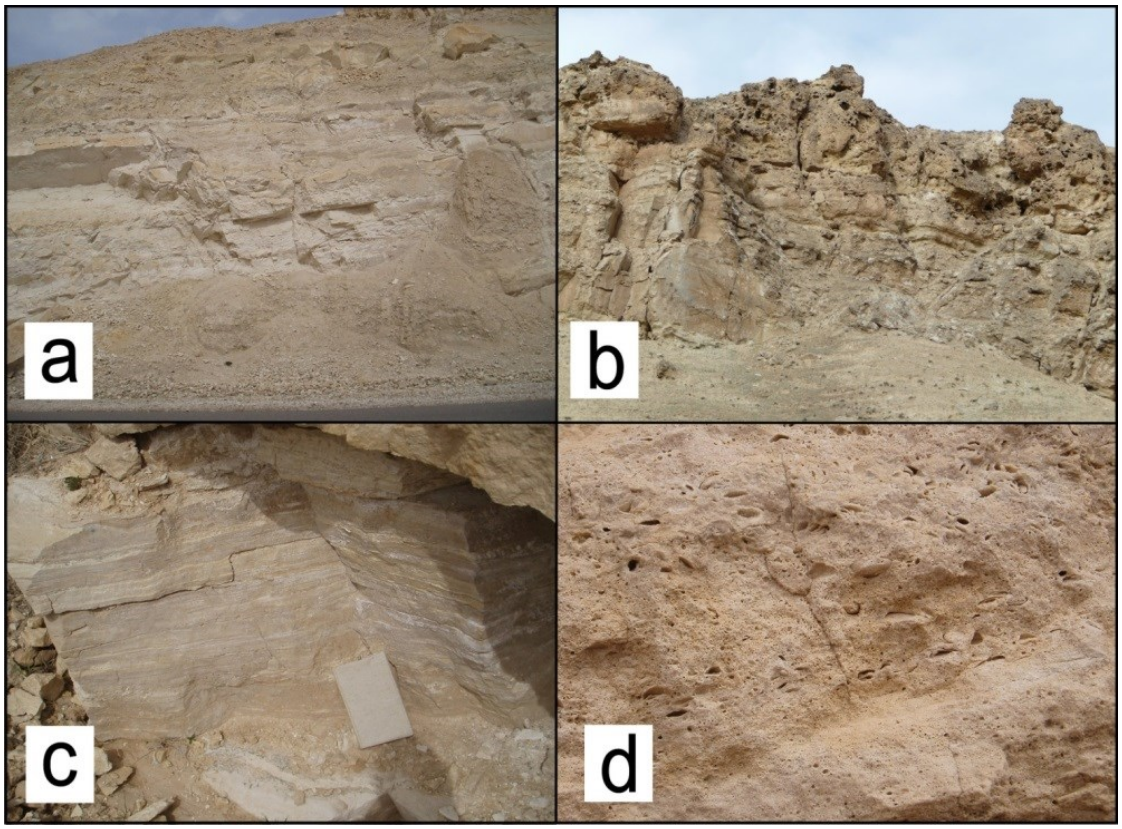

Fig. 2.52. Upper Paleocene Bukhara beds in Southwestern Gissar:
a: White dolomitic limestone; **b**: Cargneule; **c**: Marly layers;
d: Cargneule resulting from the dissolution of salt.

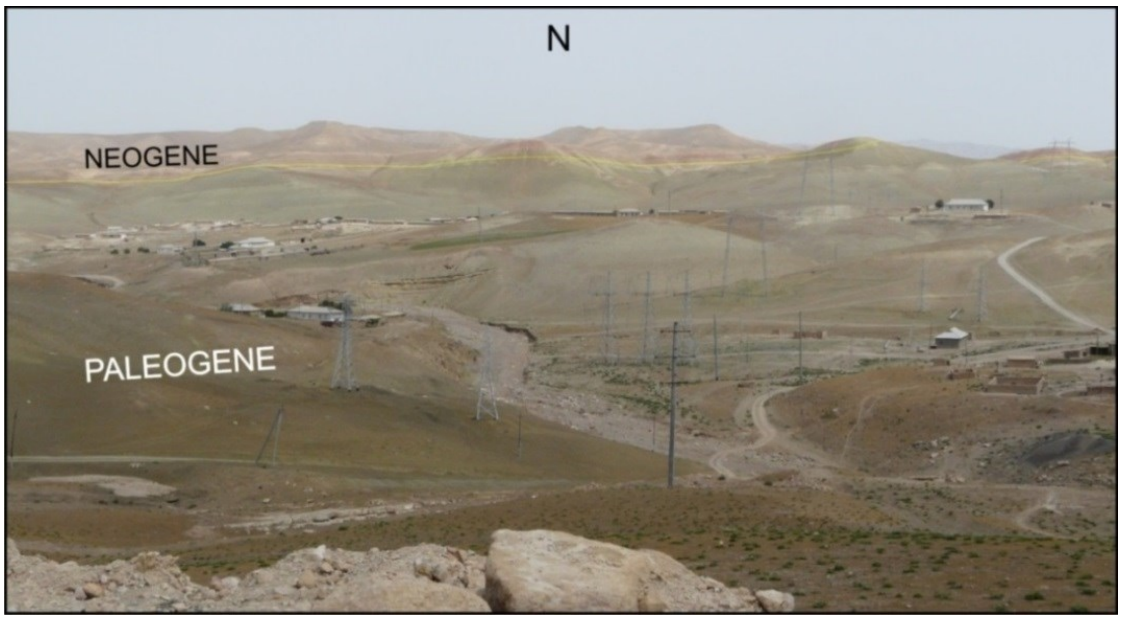

Fig. 2.53. Eocene to Oligocene-Lower Miocene marine clay, siltstone and marl in Southwestern Gissar, south of Dekhanabad.

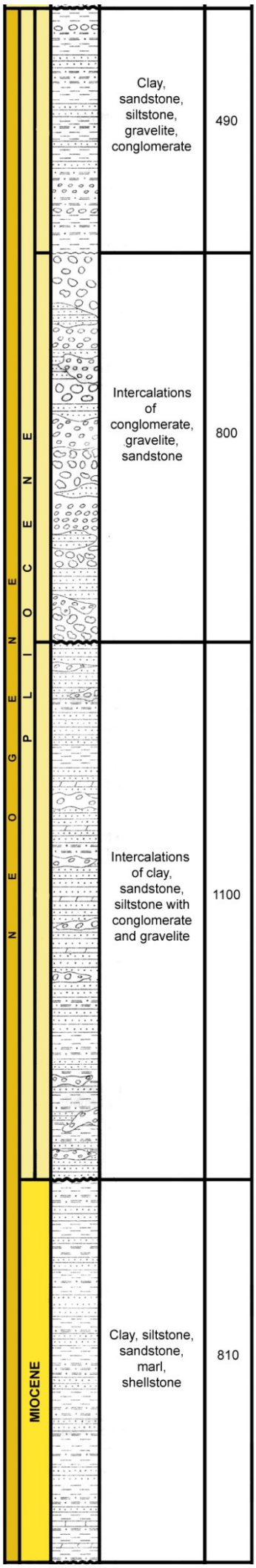

2.5.2. Neogene

The Neogene (fig. 2.54, 2.55) unconformably overlays the Paleogene. Where the Paleogene is eroded the Cretaceous sediments are directly covered by the Miocene and Pliocene deposits.

Fig. 2.55. Neogene molassic red beds in Southwestern Gissar, near Baysun. Location on fig. 2.1.

The Miocene strata are composed of intercalations of clays, sandstones, shellstones, limestones, marls and siltstones. The total thickness of the Neogene sequence is of about 810 m.

The continental Pliocene formations unconformably cover the Miocene. The Pliocene is divided into three members.

The lower part (1100 m thick) is composed of intercalations of sandstones, clays and siltstones with some conglomerate and gravel intercalations.

The middle part consists of conglomerates, gravels, and sandstones. It is 800 m thick.

The upper part of the Pliocene lays on the middle part with traces of erosion. Its thickness is of about 490 m. It consists of clays, siltstones, with some intercalated conglomerates, sandstones and gravel bodies.

Fig. 2.54. Synthetic section of the Neogene in Southwestern Gissar

2.5.3. Quaternary

The Quaternary sediments unconformably (and rarely conformably) cover the Neogene strata (fig. 2.56). They consist of pebbles, clays, sandstones, breccias, conglomerates and other alluvial and deluvial deposits. The common thickness of the Quaternary deposits ranges between 40 and 300 m.

Fig. 2.56. Quaternary river terraces unconformably overlying Neogene continental red beds in Southwestern Gissar near Dekhanabad, location on fig. 2.1.

2.6. Petroleum systems

The Amu-Darya basin is a highly productive petroleum province. In Uzbekistan the northern margin of the Amu-Darya basin is the largest petroleum province. The main hydrocarbon reserves are gas. Only a few small oil fields have been discovered in the basin, as well as in the Bukhara-Khiva region.

2.6.1. Petroleum resources in Uzbekistan

According to the "Oil and Gas Geology Institute" and "Uzbekgeofizika" Joint Stock Company 165 hydrocarbon fields were opened in the Bukhara-Khiva region to the beginning of 2015. These fields include 78 oil, oil-gas and oil-gas condensate fields, 81 gas-condensate fields and 6 gas fields. In Southwestern Gissar, at the same date, 19 fields were opened, including 5 oil, oil-gas and oil-gas-condensate fields, 13 gas-condensate fields and one gas field (after "Oil and Gas Institute" and "Uzbekgeofizika" Joint Stock Company, unpublished data).

The Bukhara-Khiva region is the most important petroleum province in Uzbekistan. From the 163 fields opened to the beginning of 2013 (we have not obtained more recent details), 36 are in the Bukhara step and 127 in the Chardzhou step (fig. 2.57).

There are 25 fields out of 36 in the Bukhara step, which have hydrocarbon deposits within the Jurassic carbonate unit. From these 25 fields, only 9 of them bear hydrocarbon deposits within the Jurassic terrigenous unit. 24 fields out of 36 belong to the Lower Cretaceous sediments. Only 3 fields out of 24 have hydrocarbon deposits within the Upper Cretaceous rocks. There is only one field in the Bukhara step located in the Upper Cretaceous sediments.

According to the lithostratigraphy (fig. 2.58), in the Bukhara step the terrigenous unit concerns 9 fields with gas deposits and one field with oil-gas or oil-gas-condensate deposits; 13 fields have oil-gas and oil-gas-condensate in the Middle Jurassic carbonates, 7 fields have only gas in the carbonate unit, and

5 fields have oil deposits in the J_{2-3}. The Lower Cretaceous rocks host 12 fields with gas/gas-condensate deposits, 6 fields with oil-gas or oil-gas-condensate deposits, and 6 fields with oil deposits. All the fields in the Upper Cretaceous bear gas-condensate and gas.

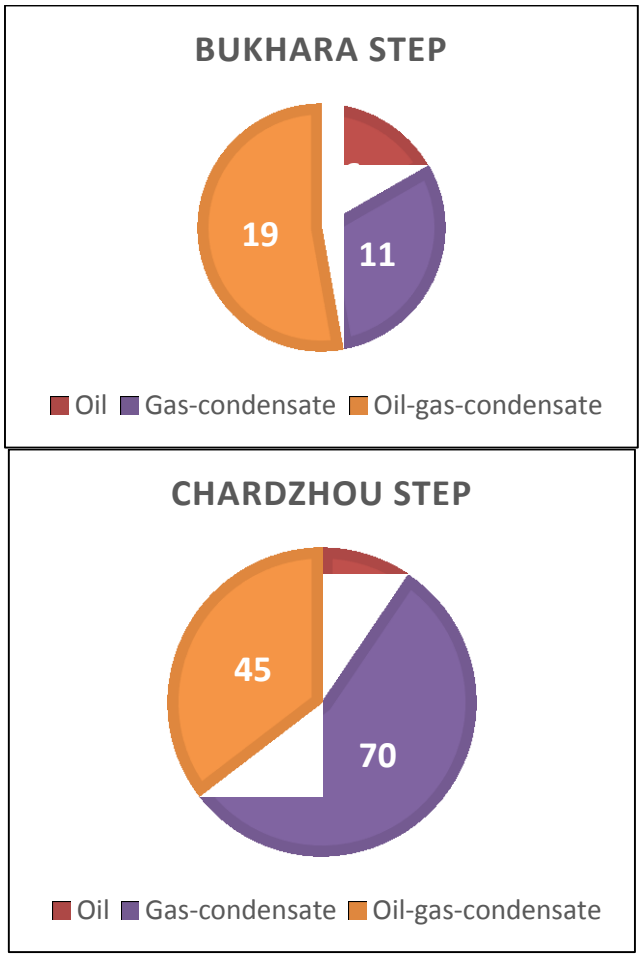

Fig. 2.57. Diagram showing the oil and gas field correlation in the Bukhara and Chardzhou steps. Numbers in diagrams = number of hydrocarbon fields (modified after "Oil and gas geology institute" and "Uzbekgeofizika" Joint Stock Company, 2013, unpublished data).

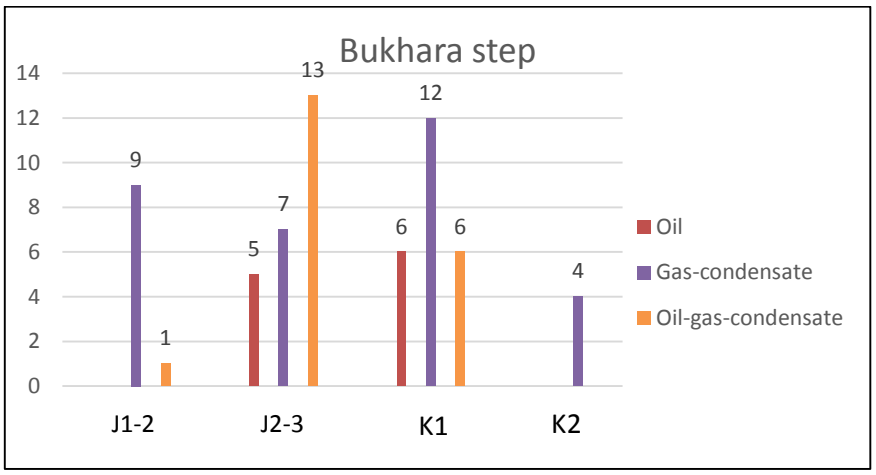

Fig. 2.58. Stratigraphic distribution of the oil and gas deposits in the hydrocarbon fields of the Bukhara step. Numbers = quantity of hydrocarbon deposits, K=Cretaceous (modified after "Oil and Gas Geology Institute" and "Uzbekgeofizika" Joint Stock Company, 2013, unpublished data).

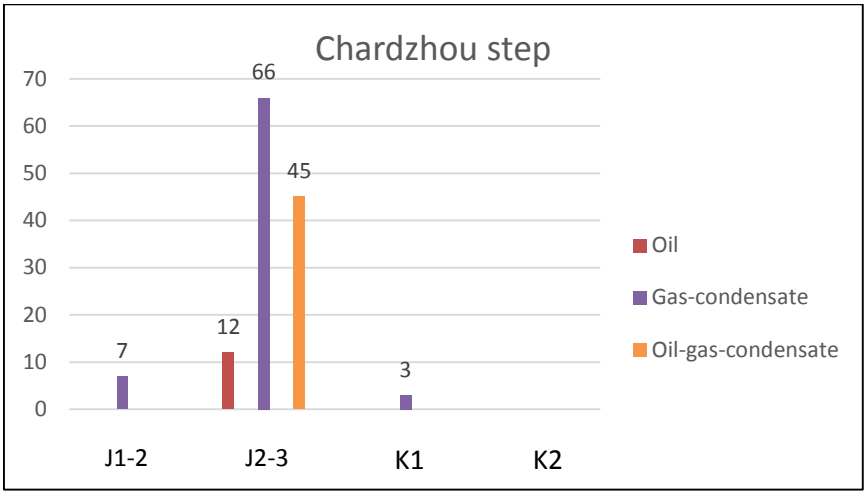

Fig. 2.59. Stratigraphic distribution of the oil and gas deposits in the fields of the Chardzhou step. Numbers = quantity of hydrocarbon deposits (modified after "Oil and Gas Geology Institute" and "Uzbekgeofizika" Joint Stock Company, 2013, unpublished data).

In the Chardzhou step (fig. 2.59), from the 127 hydrocarbon fields, 123 have their hydrocarbon in the Middle-Upper Jurassic carbonate unit. In 7 fields the reservoirs are in the terrigenous unit too and only in 3 fields are in the Lower Cretaceous rocks. There are no field with oil and gas in the Upper Cretaceous.

Most of the fields in the carbonate unit (66) are gas/gas-condensate fields. 45 fields in the carbonate Jurassic have oil-gas or oil-gas-condensates. In addition, there are only 12 fields with oil deposits within the Middle-Upper Jurassic rocks. All the deposits within the terrigenous unit are gas/gas-condensate, as well as within the Lower Cretaceous (fig. 2.59).

2.6.2. Petroleum system

A single main petroleum system was identified in the Amu-Darya basin. This system is primarily gas prone. Most of the reserves are concentrated in two stratigraphic levels (Ulmishek, 2004).

2.6.2.1. Source rocks

Petroleum source rocks are almost all in the Jurassic-Cretaceous strata. The principal source rocks in the Bukhara-Khiva region are: (1) the Lower-Middle Jurassic coaly shales and coals with dominantly type-III gas-prone kerogen, and (2) the Upper Jurassic basinal marine black-shales with type-II kerogen. Both source-rocks are in the gas-generation window over much of the region. The productive fields probably contain a mix of hydrocarbons derived from both sources.

The dominance of gas is related to the gas-prone character of the Lower-Middle Jurassic source rocks, and to the great depths of burial and high degree of maturation of the Upper Jurassic source rocks. Most of the hydrocarbons are highly mature condensates. The biomarkers indicate that many condensate accumulations were generated in the thermal gas-window and that the source rock contains terrestrial organic matter (Sokolova et al., 1993). The thick Lower-Middle Jurassic clastic sequence contains generally thin coal beds. The coal beds become thicker in the margins of the Amu-Darya basin where they are mined (in Southwestern Gissar in Uzbekistan, Gissar in Tajikistan, Alay Range in Kirghizstan, and northern Afghanistan).

The basinal black-shales have been penetrated on the Chardzhou step and are exposed in a single outcrop in Southwestern Gissar. They are composed of intercalations of black argillaceous bituminous limestones and marls with limestone. These Upper Jurassic black-shales of basin type (Khodjaipak Formation) are contemporaneous of the reef and platform carbonates deposited on the periphery (see the reef system in fig. 2.26, 2.31, 2.32) and juxtaposed (fig. 2.60, Urtabulak field).

Migration of hydrocarbons into Lower Cretaceous sandstones took place on the margins of the Amu-Darya basin where the Upper Jurassic salt seal pinches out as in the Bukhara step.
Some beds in the Lower Cretaceous Berriasian-Aptian or Albian are also potential source rocks (Khayitov, 2006, 2013).

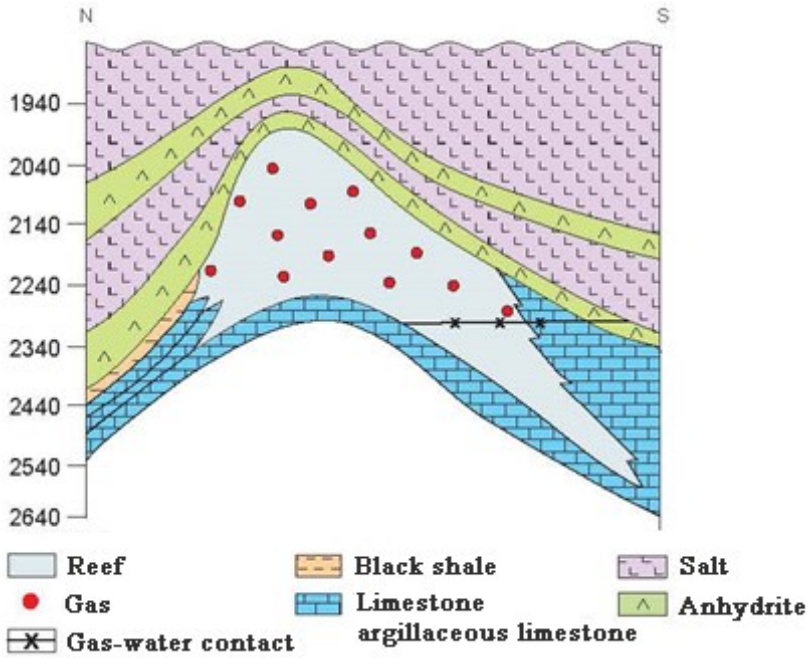

Fig. 2.60. Cross-section through the Urtabulak gas field (Ulmishek, 2004, modified after Dikenshteyn et al., 1983). Horizontal scale not available; the cross section is several kilometres long. Location of Urtabulak field on fig. 2.9, 2.26; terrigenous Jurassic section on fig. 2.18 and basinal carbonate on fig. 2.42. Note that Ulmishek use a stratigraphic chart where the evaporites are Kimmeridgian-Tithonian in age, and not only Tithonian.

2.6.2.2. Reservoir rocks

The principal discovered gas reserves are in (1) the Middle-Upper Jurassic reef and shelf carbonates overlain by the thick evaporites of the Tithonian, and (2) the thick red clastic rocks of the Lower Cretaceous. The major part of the reserves is concentrated in the two narrow stratigraphic intervals – Callovian-Kimmeridgian carbonates and Hauterivian sandstones that are separated by the thick salt deposits of the Upper Jurassic. Other parts of the sedimentary succession, from the Lower-Middle Jurassic to the Upper Cretaceous are locally productive on the basin margins where the evaporites are absent.

Very often one field has its petroleum deposits in different stratigraphic levels (in the Middle-Upper Jurassic carbonates and in the Lower Cretaceous sediments for instance). Most part of the oil and gas fields are connected to several petroleum horizons of the Jurassic carbonates: the XVI, XV-Under Reef, XV-Reef and XV-Above Reef horizons (see fig. 2.25).

According to Troitsky (1967) most of the reservoirs belong to the Lower Callovian carbonates. In the limits of the Bukhara step the sandy-silty limestone reservoirs have a porosity of 16-20% and a permeability of 50-200 mDarcies. In the deeper areas of the Chardzhou step the reservoir rocks in the J_2 sediments become worth with 5-18% of porosity, while the permeability reaches only 10 mDarcies.

The carbonate unit is generally located in the Bukhara-Khiva region, Southwestern Gissar region and Surkhan-Darya Hydrocarbon province. However the carbonates are of industrial importance only in the Bukhara-Khiva and Southwestern Gissar regions.

When the Upper Jurassic evaporites are absent, Lower or Upper Cretaceous can be productive (Ulmishek, 2004). For instance, the oil and gas productivity of the Gazli field is located in the Cretaceous sediments (fig. 2.60 to 2.63). Gas deposits are found in the Cenomanian (IX and X

horizons), Albian (XI, XIa and XII horizons; XII horizon is usually Aptian to Early Albian in other wells), and there are oil and gas in the Berriasian to Aptian (XIII horizon). The common thickness of the mining horizons is 560 m. They are separated from each other by impermeable rocks of various thicknesses (from 7 to 100 m).

Reservoir rocks are also locally present in Lower-Middle Jurassic sandstone beds. In addition, clastics and some carbonate reservoir rocks are productive throughout the Cretaceous sequence.

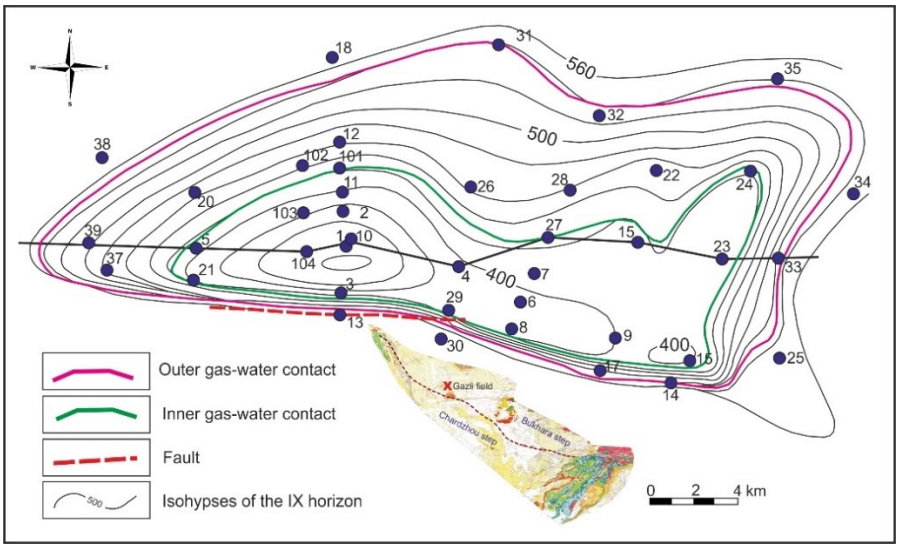

Fig. 2.61. Isohypses of the IX horizon (Upper Cenomanian) of the Gazli field (modified after Shayakubov and Dalimov, 1998).

2.6.2.3. Seal rocks

The main seal rock is formed by the Upper Jurassic evaporite unit (Gaurdak Formation). As much as several hundreds of metres of these evaporites provide a regional top seal for the reservoirs in the Middle-Upper Jurassic carbonates. The evaporite seals extend all over the Chardzhou step. The Urtabulak field shown in Figure 2.60 is a good example of a reefal reservoir sealed by evaporites.

Upper Cretaceous marls, mudstones and clays provide secondary top seals for reservoir where the evaporite unit is missing, particularly in the Bukhara step.

2.6.2.4. Trap types

Most of the accumulations discovered until now in the Bukhara-Khiva region are within (1) elongated anticlines or flexure zones, and (2) barrier-reef carbonates.

The structural traps were formed during the Neogene-Pleistocene folding, although some of them might have formed as early as the Cretaceous. Combination traps are in barrier-reef carbonates intersected by tectonic structures. The Urtabulak field is an example of combination trap (fig. 2.60). These traps are isolated pinnacles and atolls in the Callovian-Kimmeridgian reef carbonates sealed by the Upper Jurassic evaporites. The reef-core carbonates have excellent reservoir properties. All have been discovered in the Chardzhou step.

In summing up, the analyses made for the determination and location of the oil deposits in the Middle-Upper Jurassic carbonates in the Bukhara-Khiva region show that they are mainly located in areas where:

- the top of the carbonate is about 3000 m deep;
- the carbonates are highly fractured or have a high porosity (reefal facies);
- the oil traps in the carbonate unit are separated from the rocks beneath by non-penetrated rocks and by tectonic or lithological shield from the surrounding rocks;
- the pressure inside the traps is of about 250-450 atm;

- the oil traps, often but not always, are bounded by a thinned carbonate section topped by the black shales.

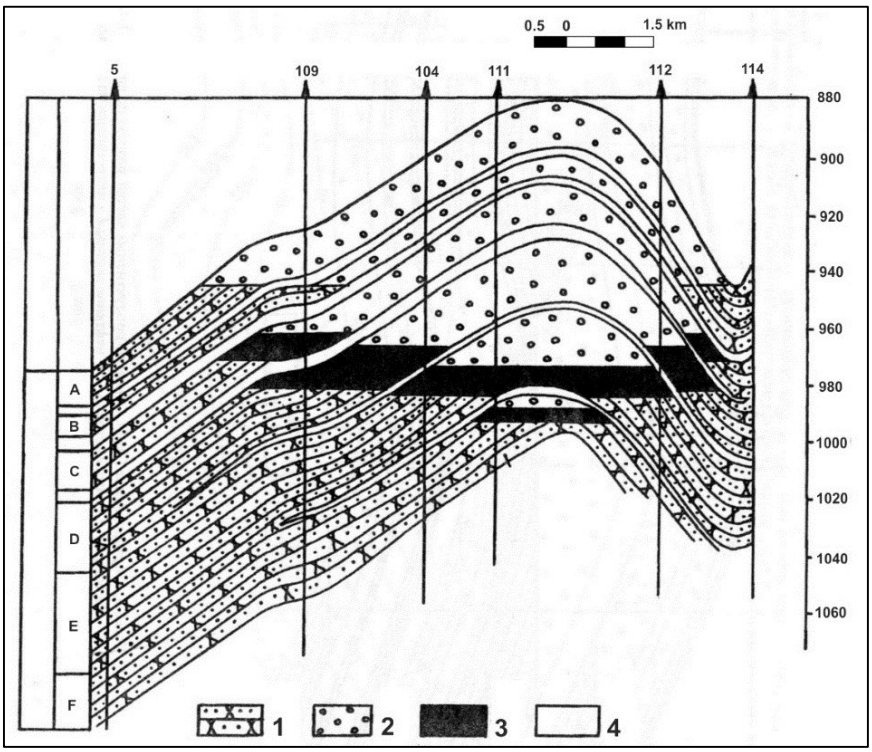

Fig. 2.62. Geological structure of the XIII horizon (in the Berriasian-Aptian interval) of the Gazli field (after Shayakubov and Dalimov, 1998). Location: part of the line drawn in fig. 2.61.
1 – sandstone; 2 – gas deposits; 3 – oil deposits; 4 – impermeable rocks; A, B, C… - reservoir layers

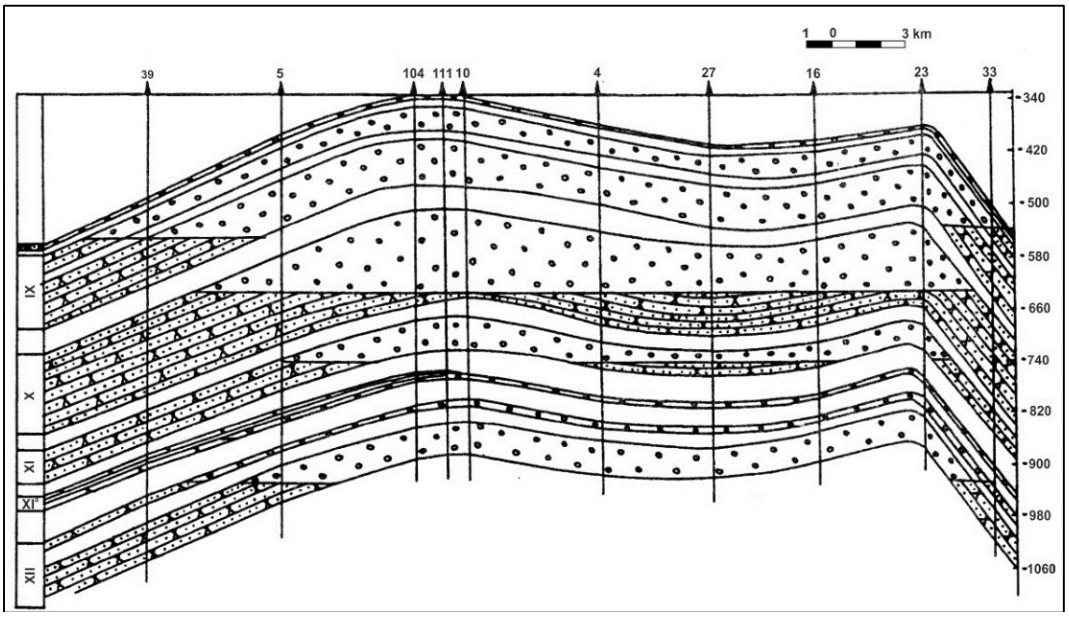

Fig. 2.63. Geological structure of the Gazli field (after Shayakubov and Dalimov, 1998).
Same legend as in fig. 2.62. Location on fig. 2.61.

2.7. Conclusion

In this chapter we have reviewed the main characteristics of the deposits of the Bukhara Khiva and Southwestern Gissar regions by detailing more the Mesozoic part which will be useful in our work.

The distribution of age and thickness of the pre-Mesozoic rocks shows well the heterogeneity of the basement of the area. The three principal tectonic elements of our area of study are already clearly distinguishable: the Bukhara step, the Chardzhou step and the Southwestern Gissar area. Their identity is strongly influenced by their pre-Mesozoic heritage and is then differentiated in the course of their Meso-Cenozoic evolution.

At the beginning of the Jurassic the studied area was belonging to two large tectonic areas lying on the Amu-Darya and the Afghan-Tajik blocks. The Middle Jurassic transgression transformed these two areas into one, huge basin. That is why the Mesozoic stratigraphy of the Bukhara-Khiva and Southwestern Gissar regions are almost the same.

The well determined Mesozoic section starts from the Jurassic, which unconformably overlays the pre-Mesozoic and Permian-Triassic? beds. Traditionally, in Uzbekistan, the Jurassic is divided into three lithological units: the terrigenous Jurassic, carbonate Jurassic and evaporite units.

The *terrigenous unit* has an Early Jurassic-Early Callovian age and is composed of different siliciclastics with some coal-bearing beds intercalations. Their facial changes mark well the sea transgressions. This unit is well distributed in the Chardzhou step and Southwestern Gissar region, where it is very thick, and less – in the Bukhara step, where it has a reduced thickness.

The *carbonate* Jurassic has an Early Callovian-Kimmeridgian age and is represented by different limestone facies. According to them, three types of the carbonate unit have been determined: the basinal, reefal and lagoonal types. All of them are connected to a barrier reef system, developed in the Late Oxfordian-Kimmeridgian. These sections have the same bottom (Early Callovian-Middle Oxfordian in age) and then they reflect the paleo-environmental conditions of the reefal system and its surrounding. The Jurassic carbonates is a very widespread formation, it covers the whole Bukhara-Khiva and Southwestern Gissar areas, except several places in the Bukhara step, where the Jurassic does not exist at all. A debate exists about the existence of a real barrier reef of the carbonate unit. Numerous single reefs and bioherms exist, but “Do they construct a barrier system?” is still debated.

The carbonate unit is covered by the *evaporite unit*, which marks climate changes in the area and less connections with the open ocean. The age of the evaporite sequence is usually known as Kimmeridgian-Tithonian in the Amu-Darya basin, but according to the recent interpretation of the paleogeography and of the fauna age in the Uzbekistan margin, the age of the salt-anhydrite unit seems to be restricted to the Tithonian. This unit, traditionally, is divided into five members, represented by salt, anhydrite and gypsum, but lateral variations occur with some missing members. The salt-anhydrite unit is very thick in the eastern and southeastern parts of the studied area (Southwestern Gissar and southeastern part of the Chardzhou step) and pinches out westwards. In the limits of the Bukhara step the thickness of the evaporite unit is very thin and often does not exceed few tens metres.

Cretaceous and Cenozoic series end the Meso-Cenozoic sedimentary pile which constitutes a rich petroleum system.

Chapter 3

Geological-geophysical sections through the Bukhara-Khiva region

Chapter 3

Geological-geophysical sections through the Bukhara-Khiva region

We have reconstructed a network of geological-geophysical cross-sections crossing the Bukhara-Khiva region. The objectives were (1) to evidence the structure of the northern margin of the Amu-Darya basin, and (2) to understand the tectonic-sedimentary evolution of this domain during the Mesozoic, especially during the Jurassic.

3.1. Methodology

The structural interpretation consisted of two phases. At first seismic profiles and borehole data were analyzed. Then the subsurface geometries were reconstructed along particular lines.

Data

To investigate the subsurface structures of the Bukhara and Chardzhou steps, like geometry of the horizons, location of the main faults, inverted structures …, we mainly used well data and seismic profiles.

Because the Bukhara-Khiva area is the main oil and gas province of Uzbekistan, it has been intensively explored during the last 50 years. The geophysical data are abundant in this area, particularly the 2-D seismic profiles (fig. 3.1). Most of them were shot by the CDP method (Common Deep Point). However, some seismic lines were obtained by the DSS (Deep Seismic Sounding) and ECW (Earthquake Converted-Wave) methods. Most of these seismic profiles were shot in the 80-s – 90-s. Some of these profiles (especially DSS and DSS-ECW) were shot for investigating the deep geological structure.

The seismic lines have different reference numbers, like 41910490 for example, where:

41 – is the number of the seismic profile;
91 – is the year of the completion of the seismic works;
04 – is the number of the seismic expedition;
90 – is the year of the beginning of the seismic works.
This number does not depend of the seismic method (CDP and ECW have the same kind of numeration), but helps us to see the age of the seismic line.

Lines position

Six N- to NE-oriented, and two NW-trending reconstructed lines through the Bukhara and the Chardzhou steps form the core of this work. The cornerstones of our interpretation are seismic profiles that allowed the recognition of subsurface geometries. Therefore some reconstructed lines follow trace of suitably located seismic profiles and incorporate well and map data.

From the map of positions of the seismic profiles of the Bukhara Khiva region we have chosen the CDP sections and wells, which roughly correspond to our lines. Then we have corrected the lines direction, corresponding to the existing and available seismic profiles.

According to the available data, we have selected the eight lines shown on Figure 3.2. The seismic data irregularly cover the investigated territory. The non-covered areas correspond to zones of human occupation, covered by water, and other places where it is difficult to perform seismic surveys. The gaps in our sections also correspond to the availability and quality of the seismic profiles.

Seismic profiles

Concerning the quality of the seismic profiles, the principal criterions to select the CDP profiles were their age (the most recent as possible) and their quality (definition). Unfortunately, we could not obtain the most recent seismic profiles. Therefore we have mainly used the seismic lines shot during the 80-s and 90-s.

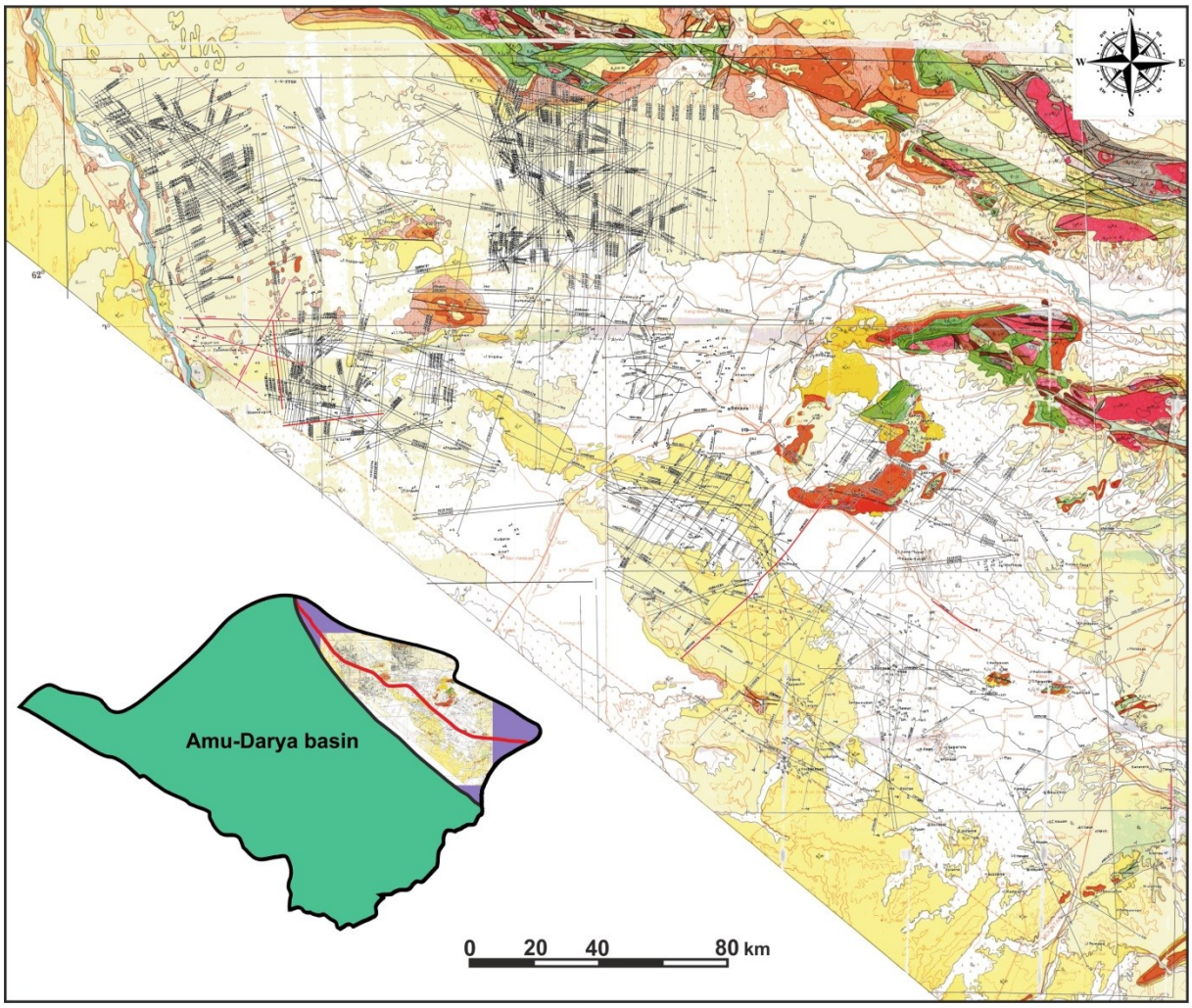

Fig. 3.1. Location of the seismic lines in the Bukhara-Khiva area.
Background – Geological map of Uzbekistan, 1:1 500 000 (1998).

One important point was the presence of wells drilled near the profiles. These wells are used for the calibration of the reflectors, the control of the stratigraphy, and to convert the time-sections into geological depth-sections. More wells we have, more precise results we have obtained.

As the seismic sections were shot to investigate the oil and gas structures (our main use of the term "structure"), they are not accurate enough to perform a detailed stratigraphic analysis. However, they clearly display the main reflectors and are abundant enough to reconstruct geological cross-sections. These seismic profiles are good enough to evidence the main stratigraphic units, structures and faults.

Main reflectors

In the seismic lines the seismic image can be interpreted in terms of stratigraphy. Generally the main reflection surfaces allow identifying the 3 major Jurassic lithologic units, i.e. the so-called terrigenous, carbonate and evaporite units. In the classification established by the Uzbek geoscientists, the main reflectors are referenced from bottom to top: T7, T6, T5, T4 and T3. Their position in the stratigraphic section is shown on Figure 3.3.

The upper part of the Lower to Upper Cretaceous marly sequence is represented by a thick package with strong internal layering.

The uppermost horizon pointed in our time sections is the T2 horizon. It is well traced in all the lines. It corresponds to the roof of the so-called XIII horizon, located inside the Berriasian-Barremian sequence in the Lower Cretaceous. The roman number indicates the position of this horizon in the

stratigraphic column (from the top). The XIII horizon generally corresponds to red-brown sandstone with interbedded layers of clay, siltstone and locally limestone, located in the Berriasian (Neocomian in the reports) to Barremian undivided in age interval, often in the upper part. This mix of continental rocks is distinguishing itself in the Lower Cretaceous sequence by strong and thick reflectors with a transparent interval at the top probably corresponding to the Barremian evaporitic layers.

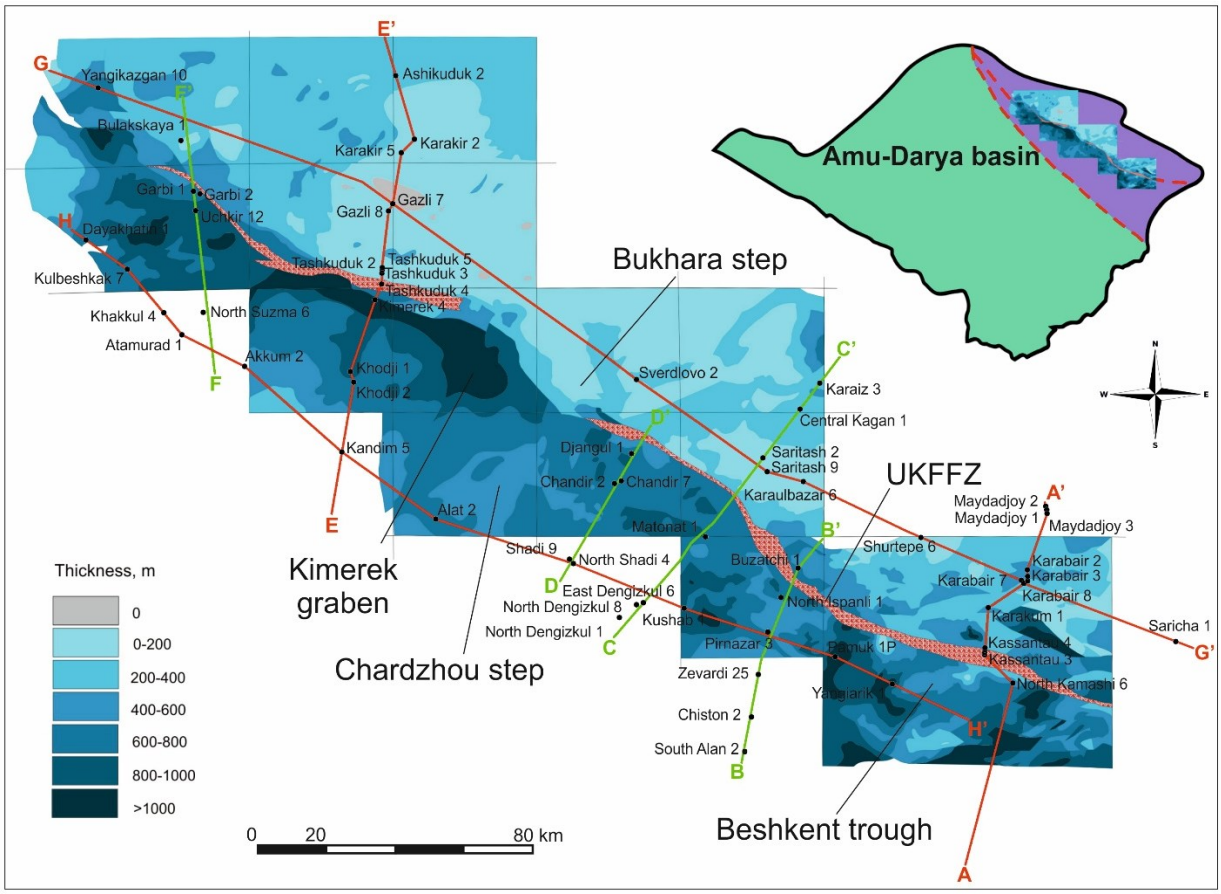

Fig. 3.2. Location of seismic lines and wells used in the reconstruction of the lines.
Green lines = seismic based profiles; red lines = geological data and wells based profiles.
Blue background: thickness map of the Jurassic terrigenous and carbonate (cf. fig. 2.7),
UKFFZ: Uchbash-Karshi Flexure Fault Zone.

The T4 and T3 horizons correspond to the roof of the middle anhydrite and of the upper salt respectively. They were not evidenced in our seismic lines. The T5 horizon corresponds to the top of the lower anhydrite. Broadly speaking the evaporites produce a weak seismic signature.

The next important seismic surface is the T6 horizon. It corresponds to the roof of the Jurassic carbonate unit. The Middle-Upper Jurassic carbonates generally display a moderately thick package of strong and thick reflectors. Commonly only the top (T5) of this unit is well marked as a single strong seismic reflector. However, in some seismic lines this reflector is not well marked. The reason is the interference with the T5 horizon. This interaction is often caused by the small thickness of the lower anhydrite unit.

The T7 reflection horizon corresponds to the roof of the Jurassic terrigenous unit. It is a hard-to-interpret reflector, often with many possibilities for its location. Probably this poor quality is related to the fact that this reflector is generally deep. Because most of the potential productive structures are located above the Jurassic terrigenous unit, the data below the productive horizons have been poorly investigated.

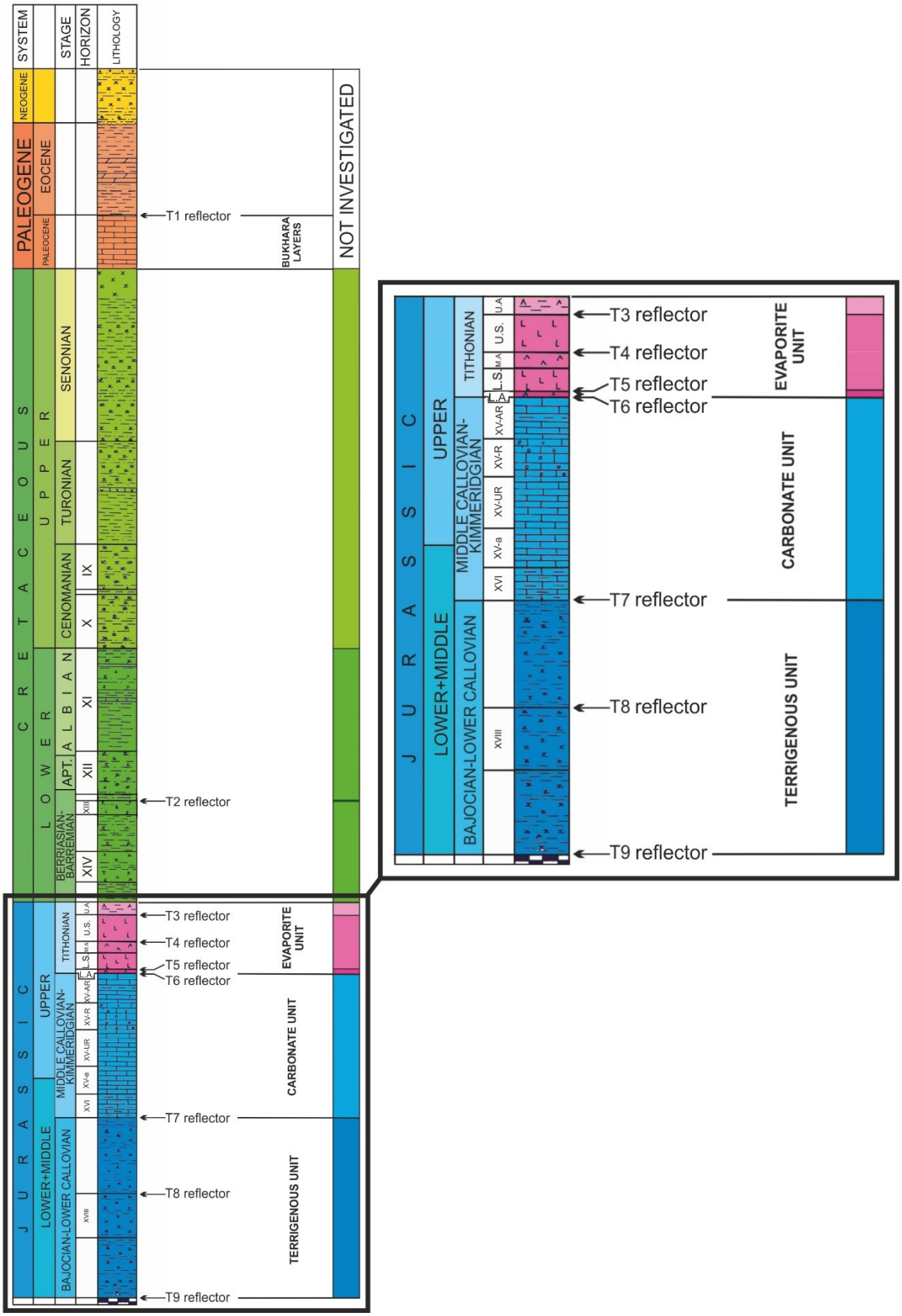

Fig. 3.3. Position of the main seismic reflectors in the stratigraphic column.
Background: lithostratigraphic column of the well Divalkak 1. Same colors in the right column and the geological-geophysical sections (Fig. 3.4 to 3.11). Note than in the Divalkak section the XII horizon corresponds to the Aptian but most of the times it extends in the basal Albian, the same for the base of XII which may begin sometimes in the Barremian or be the base of the Aptian, we show here a general age.

Borehole data

The boreholes selected out of a total of a few hundreds, provide a good coverage along most of the lines. The original logs were only available for some boreholes.

Other data

To take into account the poor quality and irregularity of the seismic information, we have included in our research cartographic information for some areas, in complement to the seismic lines and well data. We have used the following structural maps provided by the "Uzbekgeofizika" company:

Map of pre-Jurassic surface isohypses (depths map in negative isovalues measured below the mean sea-level);
Synthetic map of the isohypses of the Jurassic terrigenous surface;
Synthetic map of the isohypses of the Jurassic carbonate surface;
Synthetic map of the isohypses of the XII horizon roof inside the Berriasian-Aptian-basal Albian interval (fig. 3.3).

These maps have been used to determine the main subsurface relief structures (highs and lows, for example) and the location of the main faults. These results have been incorporated in our CDP interpretation models.

We have used the well data for the stratigraphic calibration of the reflectors and calculation of their depth.

Interpretation

In general, the interpretation was performed according to the following scheme:

1. Stratigraphic reference by vertical seismic profiling (VSP) data. At this stage we determine the location of the searched reflectors on the time section. In some sections, the principal reflectors were already marked;

2. Determination of the reflectors position for those areas, where we have only the stratigraphic columns and no VSP. Then, we draw a first-approximation model of the geological-geophysical section only using the well data;

3. Tracking reflectors by phase correlation method;

4. Drawing the complete line (geological-geophysical section).

For the transformation of time sections into depth sections, we have used the average velocities of the seismic waves for the different horizons. We obtained these data from the VSP. However, taking into account that we have no VSP in some parts of our lines, we have calculated some velocities directly from the time sections, using depth marks located in the sections.

For this we have used the formula:

$$V = \frac{(H + a) \times 2}{t}$$

Where V is an average velocity, H – the absolute marks of the horizon depth, t – the first arrivals time for this horizon, and a – the datum of the seismic profile.

For the pickets, where we had no VSP data, we have calculated the depth mark of the horizon with the formula got from the previous one:

$$H = \frac{V \times t}{2} - a$$

In the case there were significant differences between two nearest wells we have used interpolation of the average velocities meanings. Thus, we have determined horizons surface there, where we have no well data.

One important point, concerning the interpretation of the seismic lines, was the tracking of the faults. The miss of the phase correlation with distortions, diffractions waves and points, changes on the time picture view were the general marks of the break on the time section. To pay attention to this problem was necessary because faults are important indicators of the tectonic activity.

3.2. NE-trending geological-geophysical lines through the Bukhara and Chardzhou steps

We constructed six lines almost perpendicular to the Bukhara and Chardzhou steps. They are NE-SW to N-S oriented. Four out of six (green lines on fig. 3.2) are seismic based profiles, while two lines (red lines on fig. 3.2) have been reconstructed using geological and well data.

3.2.1. Line A-A'

This line is the easternmost line we reconstructed. It is located close to the Southwestern Gissar Range. This NE-oriented line crosses both the Bukhara and Chardzhou steps. It intersects several oil and gas fields, namely the Maydadjoy, Karabair, Karakum, North Kamashi fields, and the Beshkent trough in the south.

This line was reconstructed using geological data only, because no good seismic profile was available in this area (fig. 3.4). We have used the geological and isohypse maps and the borehole data for the reconstructions.

Basically, this line is marked by an important thickening of the whole Mesozoic sequence from north to south (fig. 3.4). The thickness of the complete Jurassic sequence (terrigenous + carbonate + evaporite) increases from 200 m in the north to 1200 m in the south, while the overlying Cretaceous pile passes from 800 m to 2400 m.

One of the main characteristics of this line is that the Bukhara and Chardzhou steps are abruptly separated by a major normal fault zone, the Uchbash-Karshi Flexure-Fault Zone (UKFFZ).

Jurassic terrigenous sequence

The siliciclastic deposits are discontinuous and thin in the Bukhara step, whereas they are widespread and thick in the Chardzhou step. The UKFFZ clearly marks the limit between these two domains. Along the Uchbash-Karshi Flexure-Fault zone the vertical displacement nearly reaches 500 m. The width of the shear zone varies from 5.5 to 7.5 km showing that it is a major normal fault.

In the Bukhara step the maximum thickness of the terrigenous sequence is 300 m. The deposits are restricted to grabens like in the Karabair-Maydadjoy structure where siliciclastics are preserved. The reverse fault located between the Maydadjoy 1 and Maydadjoy 3 wells is possibly a Jurassic normal fault that reworked during the Cenozoic compression. The vertical displacement along this fault that cuts all the horizons is nearly 400 m. Further to the south, the line displays several normal faults with small displacements (around 20-30 m). The second fault with a significant throw is observed in the Karabair structure, more accurately between the wells Karabair 6 and Karabair 1. This north dipping normal fault is interesting because in the hanging wall (to the north) the terrigenous Jurassic exists, while it is missing to the south in the footwall.

The thickness of the terrigenous sequence decreases from 250 m to 50 m in the Karabair 6 well. In fact the Karabair structure is possibly an Early Jurassic horst that extends as far south as the Karakum structure (Karakum 1 well). The J_{1-2} rocks reappear southwards in the Karakum structure. A fault, probably reverse, exists here with a vertical displacement of 40-50 m. The thickness of the siliciclastics increases southwards from 50 m to 300 m. Such a latter thickness is reached near the Uchbash-Karshi Flexure-Fault Zone.

South of the UKFFZ the thickness of the terrigenous deposits growths southwards. It is first almost constant at 150 m (North Kamashi well). Then, it quickly increases to reach 800 m in the middle of the Chardzhou step and 1200 m in the thickest part in the Beshkent trough.

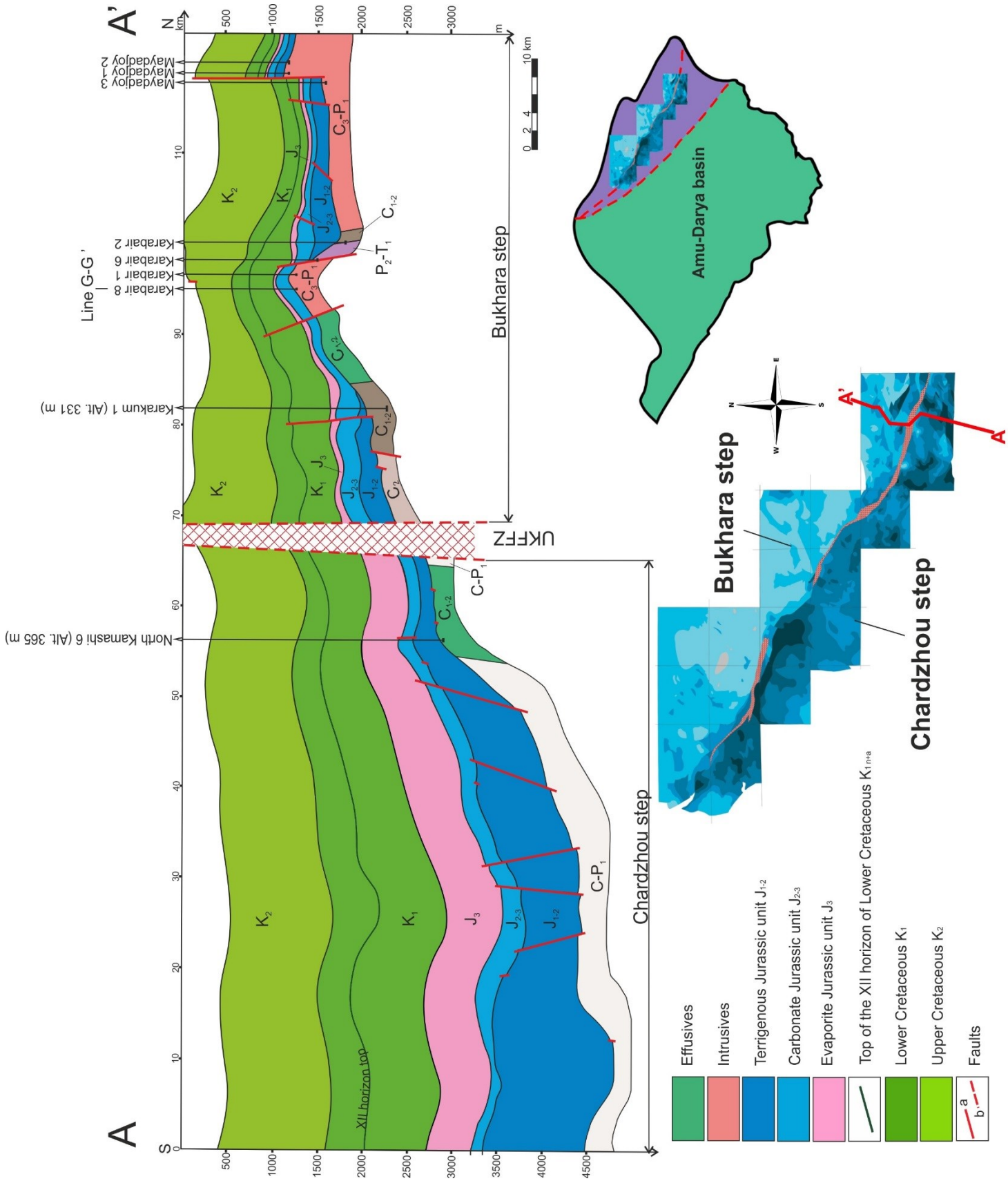

Fig. 3.4. Line A-A'. Cenozoic sediments are left in blank as we have no data.
Sections are drawn from the zero altitude level. UKFFZ: Uchbash-Karshi Flexure Fault Zone.

At the Beshkent area the terrigenous Jurassic surface sharply plunges to the south whereas its thickness increases in the same direction. In this trough, several normal faults have been evidenced forming grabens in the Jurassic units. Their throws are restricted to 20-30 m. At the south-westernmost part of the line, the terrigenous surface rises up and reaches the depth of 3450 m and the thickness of 1300 m.

Jurassic carbonate sequence

The Jurassic carbonate conformably overlays the Jurassic siliciclastics and covers the whole line. In the north the carbonate is very thin (<50 m), whereas it reaches more than 1200-1500 m in the south. In the northern part of the line, south of the Maydadjoy fault, the carbonate surface is 1320 m deep, whereas its thickness is of 40-50 m. All the faults we have noted cutting the terrigenous Jurassic sequence exist in the carbonates. Their displacements in both formations are almost similar. The thickness of the carbonate beds increases in the Karabair graben, where it reaches 100-120 m in the north. The normal fault described before was probably active also during the deposition of the carbonate (Callovian-Oxfordian) because they are thicker in the hanging wall than in the footwall. Its vertical displacement is near 140 m. The thickness of the carbonate remains almost constant on the Karabair high, only increasing southwards up to 200-220 m approaching the Karakum structure.

Southwards, at the limits of the Chardzhou step, the depth of the Jurassic carbonate surface and its thickness are stable at 1450-1500 m and 100-150 m respectively. To the south, the thickness of the Jurassic carbonate increases up to 200 m. The graben-like structure, we have already described in the terrigenous sequence, does not appear in the carbonates. Only two faults, instead of three cut the carbonates. The thickness of the Jurassic carbonate is of 200-220 m and remains constant in the southernmost part of the line. The huge thickening of the siliciclastic sequence towards the south is not observed in the carbonate.

Jurassic evaporite sequence

The evaporite can be traced all along the line, but with severe thickness variations. The thickness variations are rather low in the Bukhara step (around 10-20 m). In the Bukhara step the thickness of the evaporites reaches 80 m. The evaporite thickness abruptly increases south of the UKFFZ. Here, across the UKFFZ, the evaporite thickness increases from about 40 m to 400 m. In the Chardzhou step the thickness of the salt-anhydrite beds is much more important (400-600 m). In the North Kamashi area, J_3 is 400 m thick. Southwards, the evaporite surface plunges towards the south to the depth of 2900 m. The maximum thickness in the deepest part of the Chardzhou step is of 650 m. It is clear that the UKFFZ plays a major role in the deposition of the evaporites. The UKFFZ probably acted as a normal fault during the Late Jurassic, the southern block being downlifted with respect to the northern one.

XII horizon of the Lower Cretaceous

The next horizon we have traced on our section is the roof of the XII horizon located in the Lower Cretaceous sequence. This horizon is a reservoir in this region. Generally, the productive section concerns several horizons, but for the Cretaceous only two are important – XII and XIII. They approximately correspond to the Berriasian-Aptian-basal Albian interval (fig. 3.3). They are parallel to each other. The XIII horizon is an important seismic marker for all the Bukhara Khiva territory. As we have no seismic data for this line, we have used the isohypse map for the roof relief of the XII horizon. To trace this horizon it is important to precise the behaviour of the Lower and Upper Cretaceous roof, as they are not well determined on the seismic lines.

In the Maydadjoy structure limits this horizon is at 820-860 m depth. Further south, its depth reaches 1000-1100 m and rises to 730 m in the Karabair structure. This horizon plunges southwards to 1200 m in the Karakum area. Two main reverse faults, i.e. the Maydadjoy, Karabair, and Karakum faults, cut this interval in the Bukhara step. In the Chardzhou step the regular southward plunging of the XII horizon continues.

Lower Cretaceous sequence

Above the roof of the XII horizon we have traced the roof of the Lower Cretaceous. Because we do not have an accurate map of this bed, we have reconstructed the section only using well data. Then, we have traced the bed's surface parallel to the XII horizon because no significant unconformity has been observed (this is suitable for all the Bukhara Khiva region).

The thickness of the bed is of 200-300 m in the north. The observed surface rises up southwards to the Karabair structure, where the Early Jurassic Karabair normal fault probably reworked as reverse fault during the Cenozoic. In this area the thickness of the Lower Cretaceous bed increases to 400-500 m. Further to the south this horizon plunges and at the Karakum structure it reaches the thickness of 600 m.

The slight and regular southward plunging continues to the UKFFZ, where the thickness of the Lower Cretaceous horizon increases up to 700 m. In the Chardzhou step the explored surface is still plunging and reaches the depth of 1300-1400 m. The thickness is still of 700 m. In the Beshkent trough, the Lower Cretaceous thickness increases to 1000-1200 m.

Upper Cretaceous sequence

The Upper Cretaceous roof is the highest horizon determined in our section. It is almost parallel to the underlying horizons, and regularly and slightly plunges southwards. The thickness of the Upper Cretaceous is of 400-500 m in the north, whereas it reaches 1300 m at the southern end of the line. In the Karakum structure the thickness increases to 800 m. South of the UKFFZ, the thickness is of 1000 m. It seems that during the Late Cretaceous a widespread subsidence origin occurred.

Conclusions

The A-A' line, the easternmost one, is characterized by a significant thickening of the whole Mesozoic sequence from the north to the south (fig. 3.4), increasing from approximately 850 m in the north to more than 4000 m in the south. This thickening is not homogeneous, both in time and space. Here, the Bukhara and Chardzhou steps are here clearly separated by a major normal fault zone, the UKFFZ.

The Jurassic sequence (terrigenous + carbonate + evaporite units) are rather thin in the Bukhara step, ranging from less than 200 m to 600 m, whereas it increases southwards from 700 m to about 2000 m in the Chardzhou step. On the contrary of the Jurassic, the Cretaceous sequence more gently increases southwards from 800 m to about 2400 m without any major break in thickness at the UKFFZ.

In the Bukhara step the thickness of the Jurassic units considerably differs. The siliciclastics were not deposited everywhere and seem to be mainly concentrated in grabens (maximum thickness 300 m). The carbonates deposited on the whole step are rather thin. Their thickness only increases from less than 100 m in the north to 200 m in the south. The evaporite layers are particularly thin (less than 100 m) in the Bukhara step.

In the Chardzhou step the terrigenous and the evaporites units significantly thicken up to 1300 m and 600 m respectively. They commonly reach 1200 m in the Chardzhou step. This thickening may be related to the extensional tectonics that was developing during the Jurassic. Meanwhile, the Middle-Upper Jurassic carbonates sandwiched between these latter two Jurassic units remain relatively thin (around 160 m) and exhibit a rather constant thickness.

The main tectonic feature of this line is the UKFFZ that abruptly separated the Bukhara and Chardzhou steps. It is a major normal fault zone that partly controls the sedimentation during the Jurassic and more particularly during the Late Jurassic when the evaporites were depositing. The thickening in the hanging-wall block (the southern block) of the evaporite unit pleads for a strong normal component during the Late Jurassic faulting. Normal faults offset the Jurassic on both steps. Most of them stop in the evaporites indicating a Jurassic extensional period that lasted until the Late Jurassic. It is not clear on this profile whether or not the normal faulting initiated as early as the Early Jurassic times. Reverse faults cuts all the Mesozoic strata in the northernmost part of the profile in the

Bukhara step close to the Gissar Range. They are probably Cenozoic in age, corresponding to the NE-trending thrusts that frame the Southwestern Gissar range.

The Cretaceous beds conformably overlay the Jurassic ones. The Cretaceous is characterized by a relatively regular thickening along the profile, from 250 m in the north to 1200 m (x 4.8) for the Lower Cretaceous (45 Ma) and from 500 m to 1200 m (x 2.4) for the Upper Cretaceous (34 Ma). It is possible than extensional tectonics prevailed during the Early Cretaceous as suggested by the faults that cut this sediments. On the contrary, the broad thickening during the Late Cretaceous may indicate the prevalence of a thermal or long wavelength subsidence during this period.

3.2.2. Line B-B'

The N- to NNE-oriented line B-B' is located NW from the line A-A'. This line crosses both the Bukhara and the Chardzhou steps, but most of the line is located in the Chardzhou step. From north to south it successively crosses the Buzatchi, North Ispanli, Pirnazar-Markovskoye, Zevardi, Chiston and South Alan structures.

The line was reconstructed from geological and subsurface data because rather good seismic profiles are available in this area. The subsurface data is represented by the time-section 41910490, corresponding to the B-B' profile (fig. 3.5). The geological data we have used are borehole data and isohypse maps.

As in the previous line we have observed a Mesozoic thickening towards the south. In the north the Mesozoic sequences are only 500 m thinner than in the southern part of the line. All the Jurassic formations are well developed and represented. The complete thickness of the Jurassic reaches around 950 m in the northern part of the line, and 1300 m in the south of the profile for the part recognized but more terrigenous Jurassic exists below. The Cretaceous thickness increases regularly from 1500-1400 m in the north of the line to more than 2000 m in the south.

The Uchbash-Karshi Flexure-Fault zone is well reflected on the time section. It is near 3.5 km wide, while the vertical displacement varies in the different Jurassic horizons and completely disappears in the Cretaceous. A strange feature observed in this line and given by the isohypse maps, is the significant southward thinning of the terrigenous unit from 400-500 m in north to 0 in the south. On the contrary, in the same section the thickness of the evaporite unit significantly increases in the same direction from 50-100 m to more than 1000 m.

Jurassic terrigenous sequence

The siliciclastic are well expressed on the both steps. They are relatively thick in the limits of the Bukhara step (600 m), whereas in the Chardzhou step they apparently progressively thin southwards after the isohypse maps. The Uchbash-Karshi Flexure Fault-Zone well bounds the steps. Along this fault zone the vertical displacement of the roof of the siliciclastics is near 300 m. It is strange to note that the siliciclastics are thicker in the northern block of the fault than in the southern one, suggesting a north dipping normal fault active during the deposition of the siliciclastics.

According to the subsurface data, the maximal thickness of the siliciclastics in this line is observed in its northern part. Here it reaches 400-500 m, slowly decreasing southwards.

Two small almost vertical normal faults are observed in the Bukhara step. These faults do not expose a large displacement – few tens of metres - and form a small graben. In the Buzatchi structure the thickness of the terrigenous unit reaches 350-400 m. South of the Buzatchi structure, the Uchbash-Karshi Flexure-Fault zone displaces the roof of the siliciclastics. The vertical displacement along this major structure is near 300 m in the deepest horizons and decreases upwards.

The North Ispanli field is located south of the UKFFZ. It is the northernmost structure of the Chardzhou step in this line. Here, the thickness of the J_{1-2} sequence reaches 200-250 m. A small north dipping normal fault, which crosses the terrigenous layer, is observed south of the North Ispanli 1 well. Its vertical displacement is of 20-30 m. Further to the south, the surface of the Middle-Lower Jurassic siliciclastics plunges southwards, while their thickness regularly decreases (as from the isohypse maps).

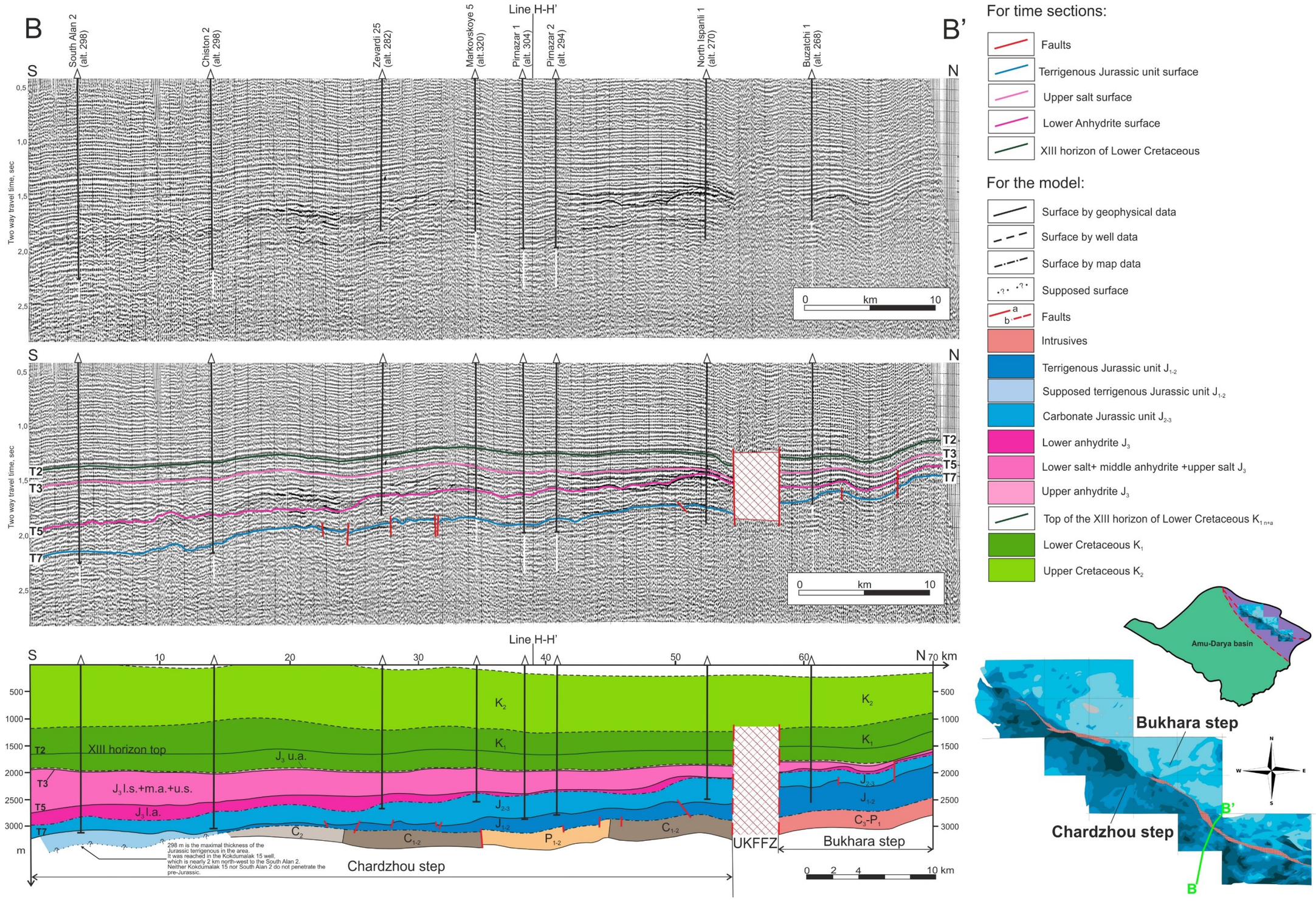

Fig. 3.5. Seismic reflection profile and interpretation for the Line B-B', see fig. 3.3 for the reflectors.

In the Pirnazar-Markovskoye structure the thickness of the J_{1-2} sequence is of 200-280 m (Pirnazar 2 and 1 wells). These wells do not reach the base of the Jurassic terrigenous. The data on the base-terrigenous are issued from the isohypse map. The general plunging of the terrigenous roof continues southwards and finally reaches 2980 m.

As far south as the Chiston structure the J_{1-2} thickness decreases to 50 m. Some normal faults observed near the Zevardi area, north of Chiston exhibit displacements of only few tens of metres. However, they create well visible small steps on the surface of the Jurassic terrigenous.

In the southernmost part of the line (South Alan field area), the roof of the Jurassic siliciclastics plunges to 3100 m as indicated by the Kokdumalak 15 well located two kilometres NW of the South Alan 2 well. In this area it is difficult to measure the thickness of the siliciclastic sequence, as the South Alan 2 and Kokdumalak 15 wells do not penetrate the entire terrigenous sequence, 298 m were drilled in Kokdumalak 15. In addition the pre-Jurassic reflector cannot be clearly evidenced.

Jurassic carbonate sequence

The Jurassic carbonate unit conformably covers the terrigenous sediments. It is well represented all along the line. In general, the carbonate surfaces plunges towards the south. In the northern part, in the Buzatchi structure, the thickness is of 250-270 m. A normal fault, one of those faults described above in the terrigenous sequence in the same area, has a vertical displacement of 50 m.

South of the Buzatchi structure, the UKFFZ marks an abrupt change of thickness of the carbonate of about 300 m suggesting that this normal shear zone was active during the Early-Middle Jurassic. South of UKFFZ the thickness of the J_{2-3} sequence rises up to 400-500 m (North Ispanli area) and slightly decreases southwards. It indicates that the UKFFZ was active during the deposition of the carbonate.

Southwards the thickness decreases to 250-300 m and in the Pirnazar-Markovskoye area rises again to 450-500 m. An increase of the depth of the limestone roof up to 2560 m is observed south of the Markovskoye structure. Nevertheless, the thickness of the carbonates decreases to 250-300 m.

Further to the south the depth of the carbonate roof reaches 2700-2600 m. But this plunging does not seem to affect the thickness, which is still near 250-300 m. In the southernmost part of the line (Chiston and South Alan) the carbonate surface regularly plunges southwards and reaches 3000 m.

Jurassic evaporite sequence

One of the most important features of this unit is its non-uniform presence of evaporite in the Chardzhou and Bukhara steps. The evaporite in the Bukhara step is very thin, while in the south of the Chardzhou step it reaches the thickness of 1000 m.

According to seismic and borehole data, the evaporites could be divided into three different members. The lower one, the lower anhydrite (J3 l.a.) is very thin (few tens metres in the north of the line), while in the Chardzhou step its thickness increases to 250-300 m. The second pack is the undivided lower salt+middle anhydrite+upper salt horizon. It is the thickest evaporite layer, reaching 700 m at the southern limits of the Chardzhou step. The third part is the upper anhydrite layer, a very thin horizon existing on both steps. Its thickness does not exceed few metres.

The surface relief of the salt-anhydrite roof is calm, without sharp drops. The depth of this horizon is rather constant near 2000 m all along the profile in the Chardzhou step. In the northern part of the profile, in the Bukhara step, the thickness of the evaporites is around 100 m. The Late Jurassic activity of the UKFFZ is also demonstrated during the period of deposition of the evaporites. In this latter, the vertical displacement decreases to near 100 m.

To the south of the UKFFZ the salt-anhydrite roof plunges to 1840-1850 m while the thickness increases to 150-200 m, and further south to 400-500 m. The thickness gradually increases southwards in relationship with the general plunging of the carbonate surface. In the limits of the Zevardi field, the evaporite thickness increases to 600-700 m. At the southern end of the profile (Chiston, South Alan structures) the evaporite surface plunges to 2000 m while its thickness increases to 800 m and 1000 m at the very end.

Cretaceous sequence

The Cretaceous sequence has been studied from deep drilling data, except the XIII horizon (in the Berriasian-Barremian interval), which was traced from seismic data (T2 reflector). The Lower and Upper Cretaceous roofs are almost parallel to this horizon.

The average thickness of the Lower Cretaceous fluctuates in the 700-800 m interval, except in the northern and southern parts of the line. To the north, around the Buzatchi structure, the thickness is close to 600 m, whereas to the south (Chiston) it rises up to 900-950 m.

The Upper Cretaceous surface rises from 200 m in the north to 0 in the south. The thickness of the Upper Cretaceous sequence is of 1000 m and is almost constant all along the profile suggesting a period of broad thermal subsidence.

Conclusion

This line is characterized by rather smooth reliefs of the main Mesozoic reflectors. They gently plunge southwards. On the contrary of the A-A' line the southwards thickening of the Mesozoic beds is not so evident. The main role in the thickening of the Jurassic belongs to the evaporite unit. It is interesting to note that the thickness of the main horizons along the B-B' line is smaller than the thickness of the same horizons along the A-A' line. The complete Mesozoic sequence reaches 2300-2400 m in the Bukhara step and increases to 3300 m in the Chardzhou step, for 2400 m and 4500 m respectively in the AA' line. Most of the thickness of the Mesozoic pile is constituted by Cretaceous sediments, which are 1400 m thick in the northern part of the line and reach approximately 2000 m in south.

The Jurassic siliciclastics are thicker in the north in the Bukhara step where they are 400-500 m thick. The thickness gradually decreases southwards in the Chardzhou step along the line and the siliciclactics almost disappear in the southernmost part of the line. On the contrary, the thickness of the Jurassic carbonates does not change a lot through the Chardzhou step (nearly 300 m with some local variations).

The evaporite unit is also represented on both steps. At the northern limits of the Bukhara step it is very thin (only a maximum of 100 m). The thickness gradually increases southwards and reaches more than 1000 m in the Chardzhou step with 100-150 m of thickening where crossing the UKFFZ. The thickness of the evaporite allows determining three packs within the salt-anhydrite formation. The thin upper anhydrite homogenously covers both steps. The evaporites filled up the relief fluctuations possibly originated by deposition of Middle–Upper Jurassic reefal bodies. The overlying horizons and the top of the Jurassic form almost flat surfaces. The overlying Cretaceous sequences have a flat relief and a constant thickness all along the line.

The Uchbash-Karshi Flexure-Fault Zone marks the limits between the steps. It is well expressed in the seismic line. Here, the vertical displacement is nearly 300 m in the terrigenous unit and decreases towards the top of the Jurassic sequence. It completely disappears in the Upper Cretaceous. In any case, it is less important than in the A-A' line. The difference of thicknesses of all the Jurassic units, both north and south of UKFFZ, would suggest an activity of this fault zone with a strong normal component during the whole Jurassic. Nevertheless, the poor accuracy of the seismic profile did not allow to precise the exact timing of the normal faulting within the Jurassic period, although it appears that the fault zone was active during the deposition of the carbonates. Except the UKFFZ few faults were evidenced. Most of them are normal faults with a small throw and are expressed in the Chardzhou step in the terrigenous-carbonate units.

3.2.3. Line C-C'

The NE-oriented C-C' line is located west of the line B-B' and crosses the Bukhara and Chardzhou steps. To reconstruct this line we have used a complex set of data: seismic lines, isohypse maps and borehole data. From the north to the south the line C-C' intersects the following oil and gas fields: Karaiz, Central Kagan, Saritash, Matonat, Hadicha, West Kruk, East Dengizkul, North Dengizkul and Jangul.

There are two seismic profiles, numbered 01970595 and 51880688, which corresponds to this line. The first one crosses the Bukhara step and the second one the Chardzhou step (fig. 3.6). These profiles do not connect each other. There is a 6.25 km gap between them. This and the absence of good quality map and boreholes in the area between the two lines led us to approximately recreate the geological structure here, assuming normal relations (without any breaks and sharp thickness variations) between the strata. Moreover, using the map data we have recreated the relief of the terrigenous Jurassic sequence in the southern limit of the Chardzhou step and the roof of the carbonate unit for the entire Chardzhou step. Further more, we have used the wells data to reconstruct the top of the evaporite sequence.

The C-C' line is rather similar to the B-B' line. Here, we observe thin horizons in the Bukhara step in the northern part of the line. All the Jurassic units (terrigenous+carbonate+evaporites) can be determined in the line. These horizons increase in thickness southwards, in the Chardzhou step south of the UKFFZ. The complete thickness of the Jurassic unit varies from 100 to 350 m in the Bukhara step and reaches 1500 m in the limits of the Chardzhou step. This latter thickness changes in the 500-1700 m interval from north to south along the line. The Jurassic sequence is conformably covered by the Cretaceous sediments.

The Uchbash-Karshi Flexure-Fault Zone is well seen on the seismic line. It is near 3 km wide. The displacement along this fault zone is moderate and almost disappears in the Lower Cretaceous unit.

3.2.3.1. Line 01970595 in the Bukhara Step

This NE-trending line crosses the Bukhara step. It crosses the Karaiz, Central Kagan and Saritash structures. This seismic profile is characterized by thin Jurassic deposits and a set of small faults in the southern part of the profile.

Jurassic terrigenous sequence

The terrigenous siliciclastics are observed all along the line. It is a very thin sequence of few ten metres in the northern part that increases to 200 m in the central part of the line and decreases again southwards.

In the north, there is a nearly 900 m wide fault zone with a vertical displacement of few tens of metres. The terrigenous unit in the northern part of the line is no more than 100 m thick. To the south of the Karaiz structure, the J_{1-2} surface plunges while its thickness increases. In the Central Kagan area the thickness of the terrigenous Jurassic reaches 200 m. Further south, the thickness of the siliciclastics sequence decreases while its surface remains at the same depth of 1100 m. This decrease could be related to the pre-Jurassic surface relief, as there is a high.

The southern part of the line is characterized by a set of faults, which forms a small graben probably inverted. The thickness of the siliciclastics rises to 200-220 m in the limits of the Saritash 2 well in the far south of the line. This borehole does not penetrate all the terrigenous sequence and the thickness here is estimated with respect to the pre-Jurassic surface isohypse map. The fault does not display a significant displacement. The normal faulting could be the result of the Jurassic extension, which was acting in the Amu-Darya basin. Two of the normal faults seem to form a small graben that probably controlled the siliciclastics deposition.

Jurassic carbonate sequence

The carbonate formation has an almost homogenous thickness of nearly 100 m all over the line, except in the southern part, where it decreases to few metres.

The northern part of the line is characterized by nearly 50 m of carbonate sequence. The fault zone that we have described above in the terrigenous paragraph cuts also the carbonate unit. The carbonate thickness increases to 100-150 m. In the Central Kagan structure the thickness is still constant, but starts to decrease southwards. In the southern part of the line it is only few metres thick, but then increases to 200 m in the far south near the Saritash structure. The faults, which were probably active during the deposition of the terrigenous Jurassic, also cut the carbonate.

Jurassic evaporite sequence

The evaporite unit is the thinnest Mesozoic sequence of the line. Its thickness does not exceed few metres.

Cretaceous sequence

The features of the Cretaceous complexes have been determined mainly from the deep drilling data and partly from the seismic lines.

In the northern part of the profile (Karaiz), the roof of the Lower Cretaceous crosses the zero line and plunges southwards to 650 m near the Central Kagan structure. Then the relief of the Lower Cretaceous sequence become flatter and remains at the same depth up to the south of the profile, where it rises to 350 m. The thickness of the Lower Cretaceous reaches 300-350 m and does not fluctuate a lot. The XIII horizon, in the age interval Berriasian-Barremian, was determined from the seismic data interpretation. It is traced at the depth of 300-550 m and gradually plunges southwards to 1450 m. Its thickness is of about 400 m.

The top of the Upper Cretaceous sequence is out of the zero line and it is impossible to determine its real thickness, which is in any case above 700 m.

As we mentioned before, there is a gap between the two seismic lines. This gap was one of the problematic points of our reconstructions, as originally the seismic line 01970595 was badly located. As most of the maps were created according to the position of this seismic line, it was impossible to correctly reconstruct the line in this area. That is why we have reconstructed this area by approximation and hypothesizing that there are no large thickness and depth variations between the lines.

According to our reconstructions, the principal reflectors sharply plunge southwards. The thicknesses of the Jurassic and Cretaceous sequences are nearly 450 m and 1500 m respectively.

3.2.3.2. Line 51880688 in the Chardzhou Step

The second part of the line C-C' is located in the Chardzhou step. It corresponds to the time section 51880688. This line is characterized by a flat relief of the main reflectors. From north to south it crosses the Matonat, Hadicha, West Kruk, East Dengizkul, North Dengizkul and Jangul structures. This sub-line is limited to the north by the UKFFZ, which is 1.9 km wide and cuts the section up to the middle part of the Lower Cretaceous. However, a visible displacement only exists in the terrigenous unit where it is nearly of 300 m.

Jurassic terrigenous sequence

South of the UKFFZ, the terrigenous Jurassic sequence shows a constant southward thickening along the line. The roof of this unit slightly plunges in the same direction, but has a relatively smooth relief. The terrigenous unit was reconstructed using seismic data only in the northern half. The siliciclastics roof of the southern part of the line was recreated using the isohypse map data.

In the northern part of the line, just south of the UKFFZ, the depth of the roof of the terrigenous Jurassic remains constant at 2300-2400 m. The thickness of the Jurassic clastics is around 250 m. It locally rises to 430 m in the Matonat well. There are two small south dipping faults, which frame the Matonat field in north and south. They exhibit small displacements (few tens metres). The thickness of the terrigenous unit increases southwards at the West Kruk and Hadicha structures (to 500-550 m). These two wells do not penetrate the entire terrigenous unit. It is why the thickness was calculated according to the pre-Jurassic roof depth, which was traced from the isohypse map. The thickness increases to 400-450 m. South of the West Kruk, the roof of the siliciclatics has been drawn from the terrigenous Jurassic relief map, alike in the southern part of the line where the wells do not reach the terrigenous unit. According to the map data, the J_{1-2} surface is nearly 2750 m deep. The thickness of the sequence rises to 1000 m near the East Dengizkul well, then decreases to 500 m in the very south of the line.

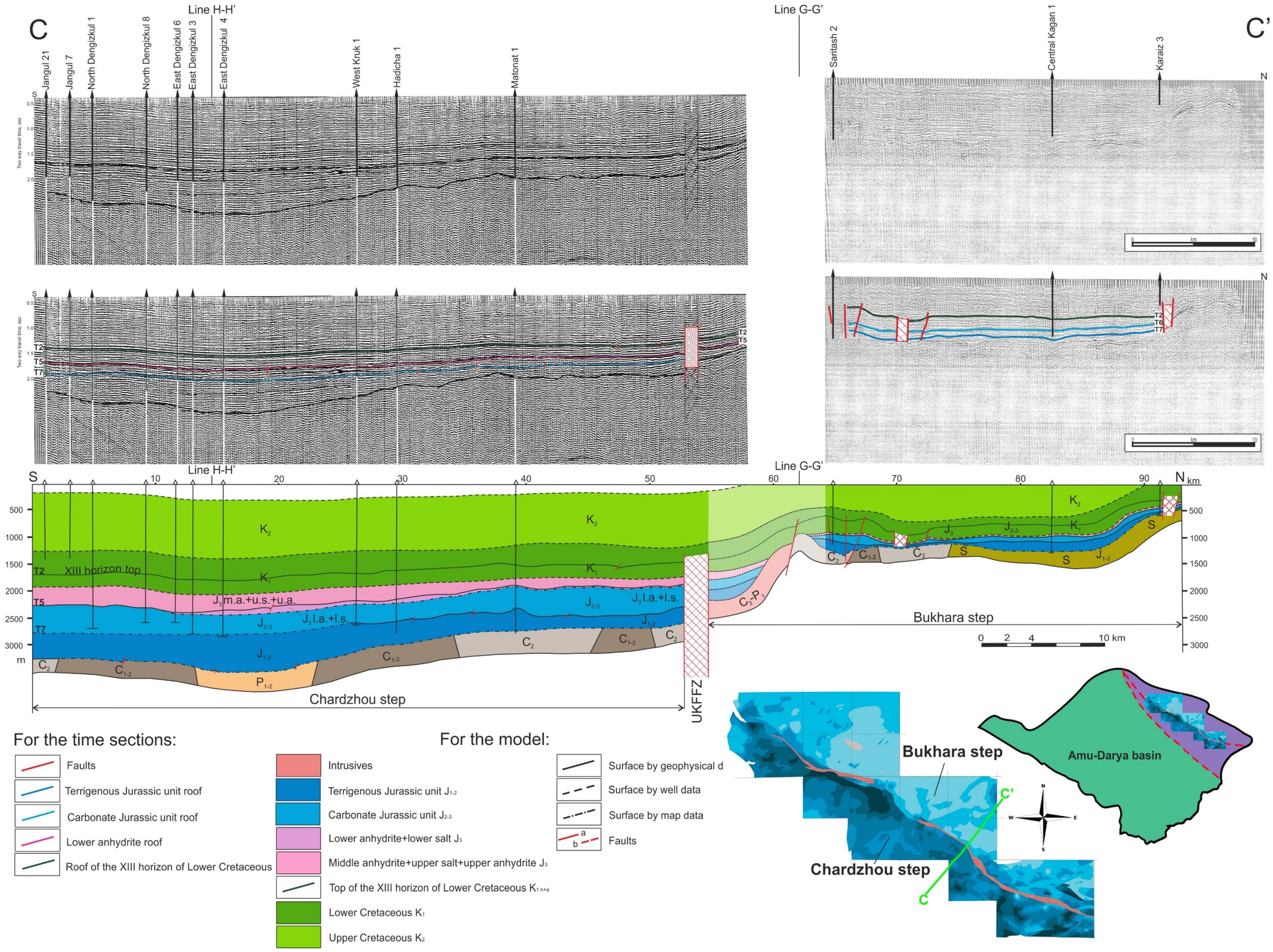

Fig. 3.6. Line C-C'. L.a lower anhydrite l.s lower salt, m.a middle anhydrite; u.a. upper anhydrite.

Jurassic carbonate sequence

The Jurassic carbonate unit is known by well data and map data, which show that there are no big variations in its relief. The carbonate surface, rather flat, slightly plunges southwards. In the northern part of the line, south of the UKFFZ, the thickness is maximal and reaches 500 m. It decreases southwards and at the Matonat structure it is already 400 m thick. Thus, the carbonate surface stays at the same level, except in the small high marking the Matonat structure. Further southwards, the J_{2-3} roof slightly plunges to 2200 m (West Kruk, Hadicha), while the thickness decreases to 300 m. These values remain constant as far south as the East Dengizkul structure. Also, we may point out that no fault was observed in the carbonate sequence.

Jurassic evaporite sequence

In general, the thickness of the Upper Jurassic salt-anhydrite bed regularly increases southwards. Most of this unit was investigated by deep drilling data, except the roof of the lower anhydrite (T_5 reflector) that we easily distinguished on the seismic profiles. These anhydrites are not thick in the north and south, where they reach a maximum thickness of only 100 m in the area between the West Kruk and East Dengizkul fields. In the north of the line (Matonat field) the common thickness is of 120-130 m. In the vicinity of the West Kruk and Hadicha structures, the evaporite thickness increases to 300 m and remains more or less constant up to the end of the line.

Cretaceous sequence

Both the Upper and Lower Cretaceous sequences display a constant thickness. The behaviour of their principal surfaces was mainly explored by the deep boreholes. The thickness of the Lower Cretaceous ranges from 600 m to 650 m all along the profile. The roof slightly plunges southwards. The XIII horizon, reconstructed using seismic data, shows that the main Cretaceous surfaces are almost parallel to the top of the Jurassic. The Upper Cretaceous sediments have a common thickness of about 1000 m (+/- 50 m). Their roof is 200 m deep and slightly plunges to 300 m in the West Kruk and East Dengizkul structures.

Conclusion

To sum up, the line C-C' was the most complex line to reconstruct because of the gap between the two time-sections constituting this profile. Besides that, we have no subsurface or any other data in this area. That is why we have had to trace the Mesozoic reflectors in the missing segment of the line assuming that they should be parallel to the pre-mesozoic surface.

In the northern part of the line corresponding to the Bukhara step, the Jurassic is very thin, but displays a complete section, including the Jurassic terrigenous, carbonate and evaporite units. The common thickness of the Jurassic does not exceed 200 m. The relief of the main Mesozoic surfaces is rather smooth, roughly plunging southwards. Several faults and fault zones have been observed in the Bukhara step. Some normal faults cut not only the Jurassic, but the lower part of the Cretaceous too. We may suppose that these normal faults have appeared during the Early-Middle Jurassic extensional period. We assume that they are related to the opening of the Amu-Darya basin. Some of them reworked as reverse or strike-slip faults during the Late Cenozoic compression, like in the Saritash structure.

In this line the Uchbash-Karshi Flexure-Fault Zone also marks the limits between the Bukhara and the Chardzhou steps. It is well reflected on the seismic profile and exhibits a vertical displacement of about 300 m in the Lower-Middle Jurassic.

In the Chardzhou step all the Mesozoic units are well developed and display smooth reflectors gently plunging southwards. The units are rather thick and well determined on the seismic profiles. The common thickness of the Jurassic in the Chardzhou steps is 100-1200 m, reaching 1400 m in some places. One of the interesting points in this segment of the Chardzhou step is the lack of major normal faults. We only observed some south dipping normal faults, which do not display large displacements (only few tens metres). However, as the maximum thickness of terrigenous sediments is reached

where these faults have been located (between the West-Kruk 1 and East Dengizkul structures) we may hypothesize that they were, at least partly, controlling the sedimentation.

The Cretaceous layers conformably overlay the Jurassic sequence in the C-C' line. The Cretaceous unit exhibits a constant thickness of 1700 m in the Chardzhou step. In the Bukhara step the top of the Cretaceous is poorly determined and the thickness of the Cretaceous sequence is not well determined.

3.2.4. Line D-D'

The line D-D' is the shortest line we have reconstructed. It is a NE-oriented line settled only in the Chardzhou step. On its way, the line D-D' intersects, from NE to SW, the Jangul, Chandir and Shadi structures. This line was reconstructed using the subsurface map data. It corresponds to the 02010598 CDP time-section, which consists of two parts (fig. 3.7). The gap between the two parts of the line was reconstructed using the isohypse maps. The complete Mesozoic section is observed in this line. The Jurassic is represented by well-developed terrigenous, carbonate and evaporite units, which increase in thickness from 500 m in the north to more than 1200 m in the south.

Jurassic terrigenous sequence

In the northern part of the profile, the J_{1-2} terrigenous sequence is about 130-150 m thick, increasing towards the south, while the roof of the siliciclastics plunges in the same direction. In the Jangul structure the thickness of the terrigenous reaches 350-400 m. Here, this thickening seems partly controlled by a normal fault that displaces the top of the pre-Jurassic. Southwards the thickness gently decreases. However, it increases again to 350-400 m in the Chandir structure. South of Chandir field, the terrigenous Jurassic surfaces regularly plunges towards the south up to the southernmost end of the line. The thickness regularly increases and reaches 800 m in the south of the line in the North Shadi structure. A normal fault, or fault zone, with a vertical displacement of 30-40 m, is observed in the seismic profile north of this structure. This fault zone, probably, appeared during the Early-Middle Jurassic extension of the northern margin of the Amu-Darya basin.

Jurassic carbonate sequence

The surface of the Jurassic carbonate unit was reconstructed by using the isohypse maps, as there was no good reflector for this sequence in the chosen seismic line. According to this reconstruction, the Jurassic carbonates cover the siliciclastics all along the line. In general their relief repeats the relief of the top of the terrigenous Jurassic unit. In the northern part of the line, the thickness of the carbonate unit is nearly 200 m and slightly increases southwards. In the vicinity of the Jangul area the thickness is of 375-400 m.

Further to the south the surface of the carbonate unit is relatively flat, while its thickness slightly decreases to 250-300 m in the Chandir field. To the south of this field, the top of the limestone plunges, while the thickness remains almost the same. The vertical fault zone, which was already described in the terrigenous complexes, cuts the carbonates too. But, unlike the siliclastics, it does not exhibit any significant vertical displacement in the carbonates. In the southernmost end of the profile the carbonate thickness reaches 350-400 m (North Shadi area).

Jurassic evaporite sequence

The evaporite formation is non-uniform along this line. The location of the top of the salt-anhydrite was reconstructed by borehole data only, while the lower anhydrite geometry was restored using the seismic profiles. The thickness of the evaporitic layer significantly changes along the line. In the northern part the salt-anhydrite sequence is very thin (nearly 120-130 m). It greatly increases in thickness southwards, where it reaches 300-500 m.

As mentioned before, the data quality allows us to determine two packs in the evaporites: the lower anhydrite and an undifferentiated layer comprising the lower salt, middle anhydrite, upper salt and upper anhydrite. The significant southern thickening of the evaporite formation is mainly related to the thickening of the lower anhydrite, which includes more than half of all the evaporite thickness, except

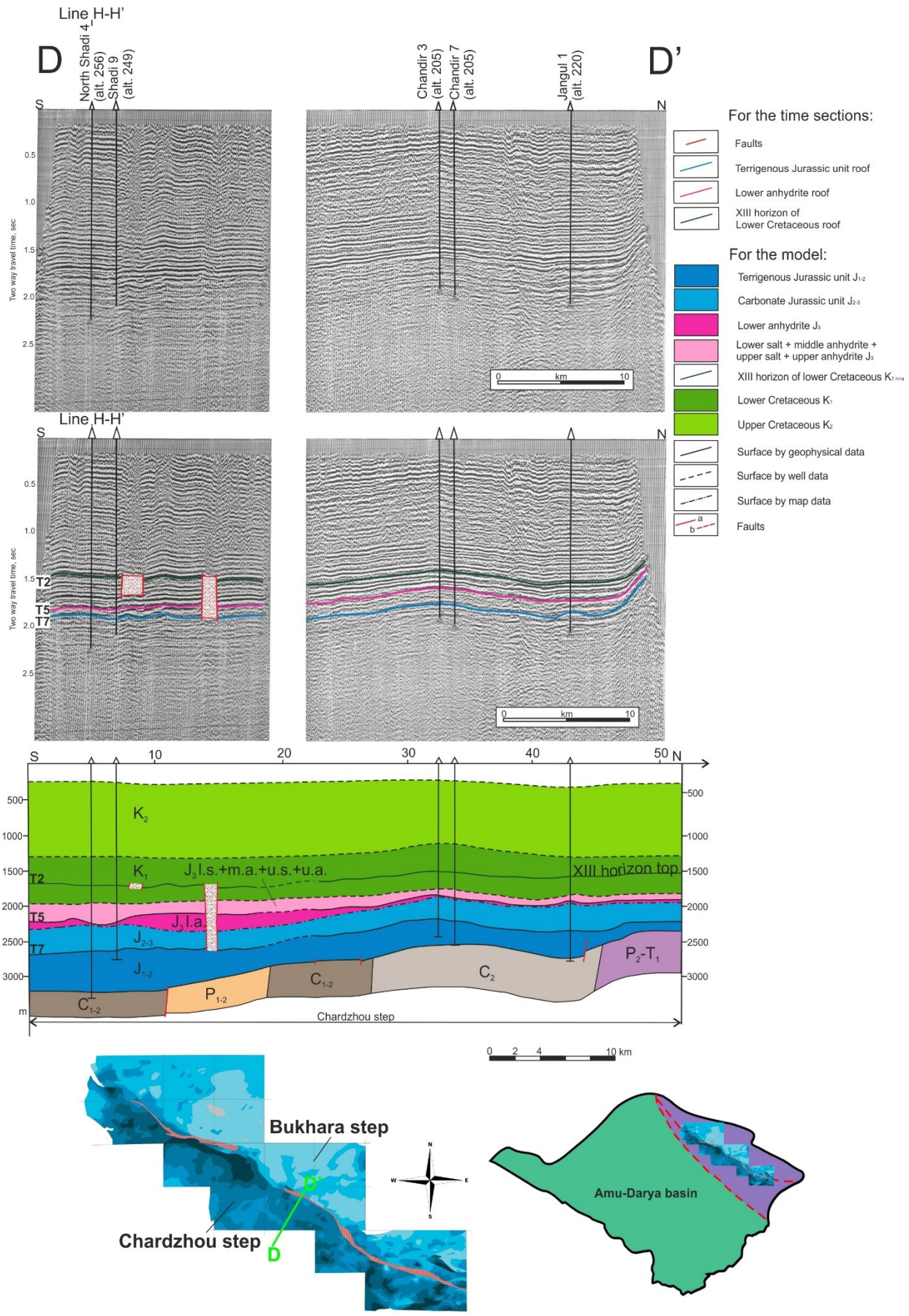

Fig. 3.7. Line D-D'.

in the North Shadi area. In this latter area most of the thickness corresponds to an undifferentiated pack of salt and anhydrite.

The faults zone we have described in the terrigenous and carbonates units, also exists in the evaporite formation but does not show any vertical displacement.

Cretaceous sequence

The Cretaceous sediments have a smooth roof relief. The Cretaceous sediments homogenously cover the Jurassic and have a relatively constant thickness all along the line. The southward increase in thickness is only of 250-300 m. The Lower Cretaceous thickness is of 500-550 m, increasing up to 600 m, while the thickness of the Upper Cretaceous changes southeastwards from 800 m to 950 m along the profile.

Conclusion

The surfaces of the Jurassic terrigenous and carbonate sequences have a smooth wave-like relief, which disappears on the evaporite unit. Above, the main reflectors are rather flat.

The thickness of the Jurassic terrigenous increases from 150 m in the northern part of the line up to 800 m in the south. The carbonate unit, which conformably covers the J_{1-2} deposits, is 350-400 m thick with some thickness locally decreasing to 200-250 m. In the northern part of the line the evaporites are nearly 120-130 m thick and grows southwards. The increase of thickness of the evaporite unit is related to the lower anhydrite sequence, which takes more than a half of the common evaporite thickness. The southern part of the D-D' line is constituted by a 300-350 m thick evaporite layer.

The Cretaceous sequence is relatively constant in thickness and displays smooth reflectors.

In this short section the faults are nearly missing. There is only one small fault cutting the Jurassic carbonate and evaporite. Unfortunately this shear zone does not clearly extend below in the silicilastic unit, and above in the Lower Cretaceous.

3.2.5. Line E-E'

The line E-E' is mainly reconstructed using map and well data, and partly geophysical data. The pre-Jurassic surface was investigated by a gravimetric model, proposed by O.P. Mordvintsev (in Babadjanov, 2008; see below fig. 4.26 in Chapter 4). The carbonate and terrigenous surfaces in the Tashkuduk and Khodji areas were determined from the interpretation of the CDP section 59980496.

The N-S trending E-E' line crosses both the Bukhara and Chardzhou steps. This line intersects the Ashikuduk, Karakir, Gazli, Tashkuduk, Kimerek, Khodji and Kandim structures (fig. 3.8).

This section illustrates the significant thickening of the Mesozoic sequence from the north to the south. The Bukhara step is characterized by an incomplete and/or thin Jurassic section, where the evaporite unit is missing. In some parts of the section there is no Jurassic at all and the Lower Cretaceous sediments directly overlays the Paleozoic. The thickness of the Jurassic in the Bukhara step does not exceed 200 m.

In the Chardzhou step the Jurassic section is thick. In the southernmost part of the step the evaporite unit appears. One important structure of the Chardzhou step in this area is the Kimerek graben, which exhibits an abnormally thick Jurassic sequence. In this graben the Jurassic thickness reaches nearly 1900 m. Most part of this thick sequence is constituted by siliciclastics deposits. Further south, the thickness of the Jurassic deposits decreases to 500-550 m.

The Cretaceous beds are well represented and cover the Jurassic all along the line, except in the Gazli area where the Cretaceous sediments lay directly on the Paleozoic rocks. The Cretaceous is around 1000 m thick in the north of the line and increases to the south to 1500 m.

An important point is that the Uchbash-Karshi Flexure-Fault zone is well expressed in this line as a main south dipping normal fault with a huge vertical displacement of the pre-Jurassic surface (nearly 1500 m). This throw is clearly associated with the thickening of the Jurassic siliciclastic sequence. The

top of the Jurassic terrigenous unit is only displaced of 250 m by the UKFFZ, showing the huge syn-depositional component of the vertical displacement (about 1200 m) during the Early-Middle Jurassic times.

Jurassic terrigenous sequence

The terrigenous Jurassic rocks were non-homogenously deposited in this section. In the Bukhara step these sediments are locally absent. On the contrary they cover the whole Chardzhou step. The thickness of the siliciclastics varies widely in these steps. The terrigenous Jurassic of the Bukhara step is very thin and reaches it maximal thickness (near 100 m) in the northernmost part of the line. In the Chardzhou step the terrigenous cover is 350-500 m thick in average, except in the Kimerek graben area, where it is abnormally thick (1700 m).

In the north of the Bukhara step, the terrigenous Jurassic pile is about 80-100 m thick. It decreases southwards and disappears at the Karakir structure. The terrigenous sequences appear again north of the UKFFZ in the Tashkuduk 4 well where it is only several metres thick.

In this line the UKFFZ separating the Bukhara and Chardzhou steps is a major Jurassic normal fault with a huge vertical displacement of 1200 m at the base of the terrigenous unit (top of the Paleozoic). The Kimerek graben, resulting from the activity of this Jurassic master normal fault is mainly filled with Lower-Middle Jurassic clastic sediments. In the graben the thickness of the siliciclastics reaches a maximum value of 1700 m. It regularly decreases southwards to 600 m, indicating that the Kimerek graben is rather a half-graben framed by the UKFFZ.

The southern part of the section is marked by a high of the Pre-Mesozoic surface in the Khodji area. Here the thickness of the terrigenous beds decreases from 600 m to 200 m, and finally to 150 m in the Kandim area at the southern extremity of the line.

Jurassic carbonate sequence

The overlaying carbonate unit, as the terrigenous one, does not cover all the line. This sequence very thin in the Bukhara step increases southwards, in the Chardzhou step. The thickness of the limestone of the Bukhara step ranges from 0 in the central areas to 150 m near the UKFFZ. In the northern part of the line (Ashikuduk well) the carbonate thickness is near 100 m. To the south, the carbonate surface conformably covers the siliciclastics, while the thickness decreases to 20-30 m. It completely disappears towards the south near the Karakir area. The limestone appears again to the south of the Gazli 8 well, progressively increasing in thickness southwards from a few metres to 100-150 m in the Tashkuduk area. A small normal fault has been identified to the south of the Tashkuduk 3 well. Its vertical displacement is near 20-30 m.

In the Chardzhou step the carbonates are 300-350 m thick and this value changes few along the step. Further south, beginning from the Tashkuduk 4 well the roof of the carbonate unit sharply plunges southwards. Unlike the terrigenous, we did not observe any significant vertical displacement of the roof of the carbonate unit. The carbonate surface stops its plunging in the Khodji area and remains at the same depth up to the southern end of the line. However, the carbonate thickness decreases southwards to 300-350 m.

Jurassic evaporite sequence

The evaporite unit, investigated by the borehole data, only exists in the southern part of the Chardzhou step where its thickness is of 50-60 m.

Cretaceous sequence

The Cretaceous sequence conformably overlays the Jurassic. In the Bukhara step, where the Jurassic is missing it directly and unconformably covers the Paleozoic. The thickness of the Cretaceous sequence is strongly constrained by the numerous wells. The Cretaceous sequence significantly thickens from north to south from 1000 m to 1500 m. The relief of the principle Cretaceous surfaces was determined by the relief of the Early Cretaceous XIII horizon.

In the northern part of the profile, the thickness of the Lower Cretaceous is near 300 m (Karakir well) and remains the same as far south as the UKFFZ area. There, in the Tashkuduk area, the thickness of the K_1 bed increases to 400 m. South of the UKFFZ we observed both a gradual increase of the thickness and a plunging of the roof. In the Kimerek 4 well, the thickness is of 560-580 m. The thickening continues southwards and in the Khodji structure the thickness reaches 600-650 m.

The Upper Cretaceous conformably overlays the Early Cretaceous horizons. The thickness ranges from 600 m in the north to 700 m in the south in the Bukhara step. In the Chardzhou step the thickness increases to 900-800 m.

Conclusion

The E-E' line shows the geological features of the western part of the Bukhara-Khiva region. An interesting point is the incomplete Jurassic section in most part of the line. Fist, the Jurassic sediments are completely absent in some areas of the Bukhara step. In addition, the evaporite unit exists only in the southernmost part of the profile.

The common thickness of the Mesozoic increases from 1000 m in the northern part of the line, to 2300 m in the south. The Jurassic sequence, where it exists, does not exceed 200 m in the Bukhara step, while in the Chardzhou step the Jurassic thickness rises to 1900 m in the Kimerek graben, including 1700 m of clastic sediments. The terrigenous Jurassic is thin (nearly 100 m or absent) in the northern part of the line, whereas in the Chardzhou step it ranges in the 200-600 m interval.

The carbonate unit, like the terrigenous one, is partly missing in the Bukhara step. In the Chardzhou step the carbonate thickness ranges from less than 100 m in the north of the line to 300-350 m in the south where it constitutes an isopach sequence. The evaporite formation is very thin and exists only in the southernmost end of the profile. The Cretaceous thickens southwards (from about 900 m to 1500 m).

This line is interesting because it evidences the structure of the Kimerek graben where the Jurassic sequence is abnormally thick. The Uchbash-Karshi Flexure-Fault zone, well determined on the seismic line, is a large south dipping normal fault limiting the Kimerek graben to the north. Because most of the sediments deposited in the graben are Lower-Middle Jurassic siliciclastics, the UKFFZ, as well as the Kimerek half-graben, were active during this period of deposition of continental sediments. The activity reduced during the Late Jurassic and probably ended in the Kimmeridgian (as the top of the carbonates is of this age).

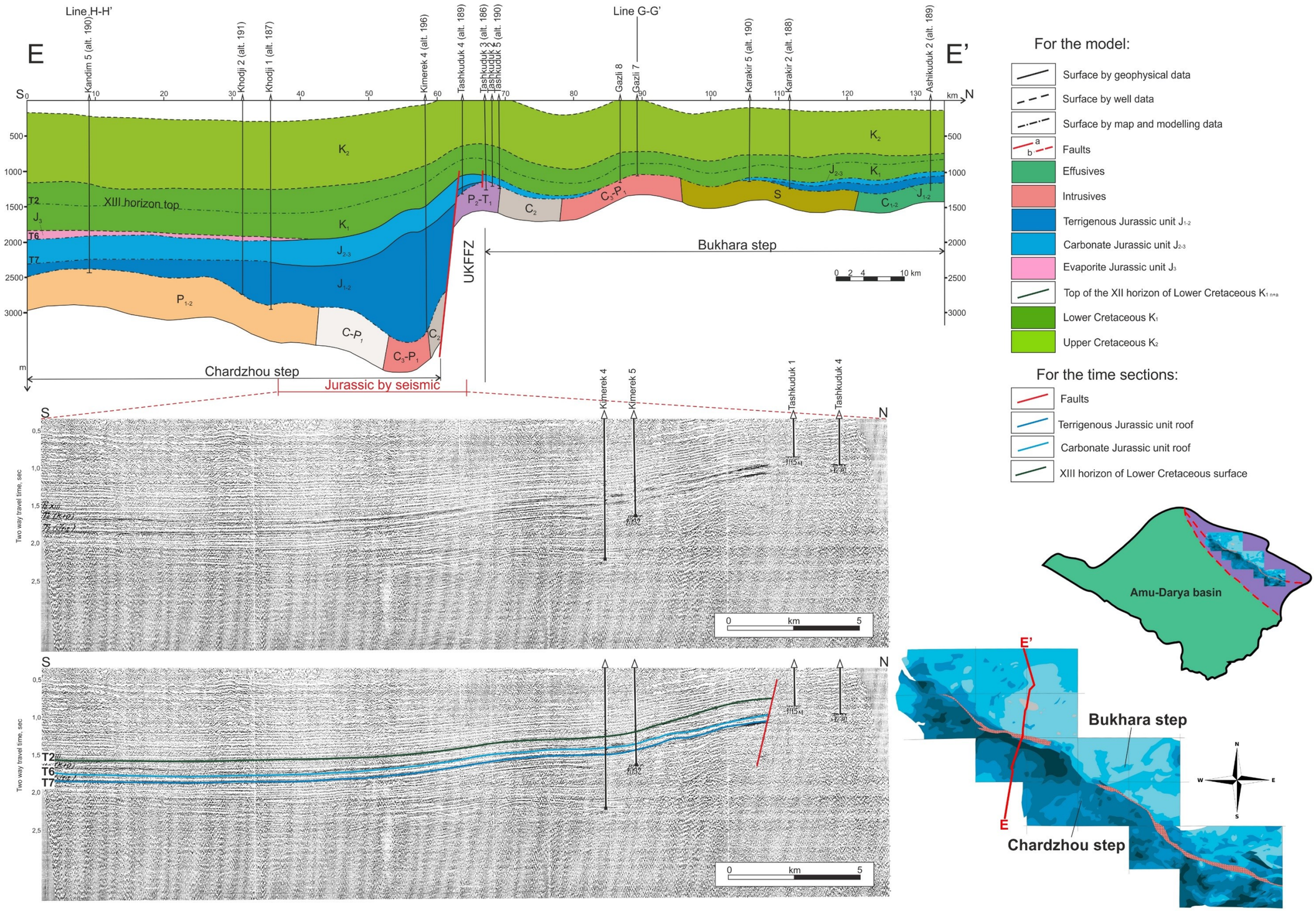

Fig. 3.8. Line E-E'.

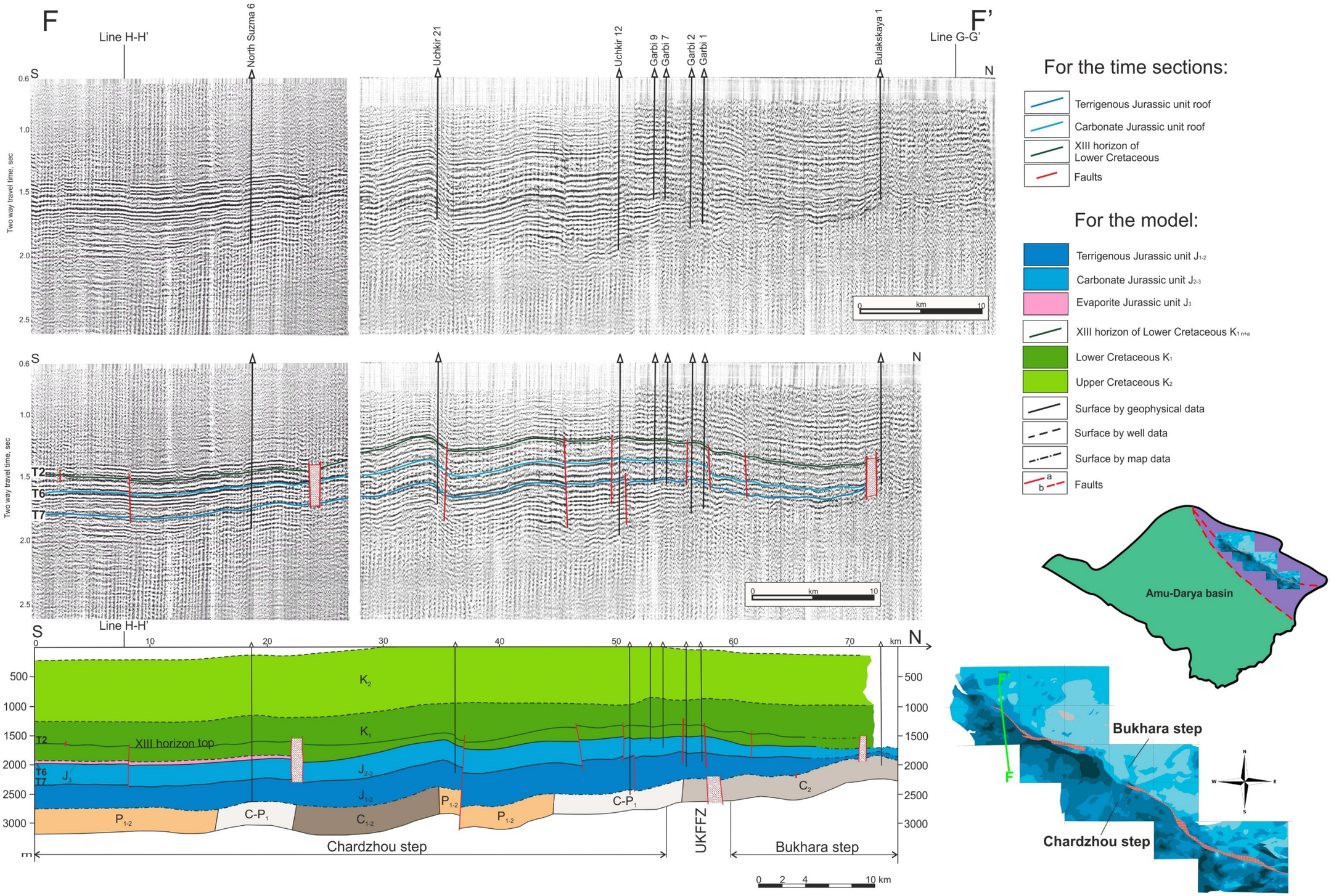

Fig. 3.9. Line F-F'.

3.2.6. Line F-F'

The F-F' line, the westernmost one, was reconstructed, mainly using the seismic data, but wells and isohypse maps were used too. This line crosses both the Bukhara and the Chardzhou steps, where, from the north to the south it successively intersects the Bulakskaya, Garbi, Uchkir and North Suzma structures. The seismic profiles 21840481 and 28813280 frame this line (fig. 3.9). The 21840481 seismic-profile in the north, corresponds to the Bukhara step and the northern part of the Chardzhou step, whereas the 28813280 evidences the southern part of the Chardzhou step. There is a very small gap between these lines. So we have had just to connect the reflectors of both lines. As the gap between these two seismic lines is not significant, we will describe them together, as a single section.

The northernmost end of the profile was reconstructed using isohypse maps, not seismic profile. The time section 28813280 continues to the south in the Chardzhou step the section just described before. There is only one well on this line, the North Suzma 6. The reflectors of the line are characterized by a smooth relief of their surfaces. The thickness of the principal horizons is rather constant, except the very north of the profile, where the Jurassic is very thin.

As in the just described E-E' line, the F-F' line shows an incomplete Jurassic section, where the evaporite formation is missing in the northern part of the profile. A thin evaporite sequence appears only in the southern third of the line. The southern Chardzhou step shows a complete Jurassic section where a thin evaporite unit appears.

The principal horizons are characterized by relatively smooth surfaces, gently plunging southwards with a rather constant thickness. However, a southward thickening of the Mesozoic exists, especially of the Jurassic. The Mesozoic, nearly 2000 m thick in the Bukhara step, gently increases in thickness to 2500 m in the Chardzhou step.

It is important to note that the Uchbash-Karshi Flexure-Fault zone, observed in the 5 lines previously described, does not exist here as a huge fault zone with a significant vertical displacement. It is only represented by a small flexure. It means that there is no clear limit between the Bukhara and Chardzhou steps in this area.

Jurassic terrigenous sequence

The terrigenous Jurassic, unlike the E-E' line, covers the entire Bukhara step in this line. It is very thin in the northern part of the section (Bulakskaya structure) where the thickness is close to 50-60 m. There is a small subvertical fault zone to the south of the Bulakskaya 1 well. This zone is nearly 600 m wide, but does not expose any significant vertical displacement. Southwards, a regular thickening of the siliciclastics is observed. The thickness of the terrigenous Jurassic gradually increases and reaches 500 m near the supposed location of the Uchbash-Karshi Flexure-Fault zone.

The UKFFZ intersects the Uchkir structure, but does not appear as a big shear zone on the seismic-profile. There are two faults near the Uchkir 12 well. The northern fault cuts the terrigenous unit, while the southern one reaches the Lower Cretaceous layers. These small faults correspond to the northwestern extension of the UKFFZ.

The northern end of the Chardzhou step is characterized by another fault with a vertical displacement of 80-100 m. It is a reverse fault that cut the Mesozoic up to the Early Cretaceous. It was possibly a former normal fault active during the Early-Middle Jurassic. The thickness of the siliciclastics is still 500 m.

To the south, near the Uchkir 21 well the J_{1-2} horizon is cut by a reverse fault with a vertical displacement of 100 m. The thickness of the siliciclastics drastically changes near this fault. North of it, the thickness of the siliciclastics is 550-600 m, whereas to the south it is no more than 400 m thick. We propose that this reverse fault was a former syndepositional normal fault during the deposition of the siliciclastics, and reworked as reverse fault during the Late Cenozoic.

In the southernmost part of the profile the roof of the terrigenous Jurassic plunges, while its thickness increases up to 500 m. A main normal fault zone is observed southwards. Its vertical displacement is

around 30-40 m. Here, the thickness of the clastics is near 400 m. In the middle part of the profile it reaches 500 m. In the southernmost part of the section the thickness of the Jurassic siliciclastics decreases to 350 m.

Jurassic carbonates sequence

The carbonate unit of the J_{2-3} lays conformably on the underlying J_{1-2} clastics. In the northern part of the profile (Bulakskaya structure) the limestone are 150-200 m thick. The fault zone, which cuts the terrigenous sequence, also cuts the carbonate unit. The thickness gradually increases southwards and reaches 250-300 m (Garbi structure). The faults traced here have been already observed in the terrigenous Jurassic. The Uchbash-Karshi Flexure-Fault zone does not significantly influence the carbonate deposition. The thickness of the limestone remains constant (nearly 300 m). In the southern part of the Chardzhou step, the J_{2-3} carbonate displays a rather constant thickness of 300 m and the calm relief of the surfaces, gently plunging southwards.

Jurassic evaporite sequence

According to the wells data, the salt-anhydrite sequence of the Bukhara step and the northern part of the Chardzhou step is only a few metres thick along this line. It is out of the scale of the drawing. The well-visible salt-anhydrite bed presence is noted south of the North Suzma 6 well. Its thickness is of 60 m from this well up to the southern end of the line.

Cretaceous sequence

The information about the Cretaceous beds has been obtained mainly from deep drilling data. The roof of the Lower Cretaceous is 900 m deep in the north of the profile and 1150 m in the south. The surface of the XIII horizon in the Berriasian-Barremian is parallel to the relief of the Jurassic roof. The thickness of the Lower Cretaceous sequence is almost constant along the line and close to 600 m.

The top of the Upper Cretaceous sediments is 100 m deep in the northern part of the section and gradually decreases southwards to 120 m. At the wells Garbi 7 and 9 these beds cross the 0 line. They are 700-800 m thick in the north and more than 1000 m in the south.

Conclusion

The F-F' line lights the western part of the Bukhara-Khiva region. The main characteristic of this line is that we cannot clearly distinguish any limit between the Bukhara and Chardzhou steps. The UKFFZ does not appear as a main shear zone in the Mesozoic section where it is restricted to few minor reverse faults, whereas it is well expressed in the previously described NE-oriented lines. It appears that in the northwestern part of the studied area it is impossible to differentiate the Bukhara and Chardzhou steps in the Amu-Darya margin.

The thickness of the siliciclastics ranges in the 400-600 m interval all along the profile. In the northernmost part of the section it is only 50-100 m thick. The carbonates, in average, are 300 m thick, and their thickness ranges from 100 m in the north to 350 m in the middle of the section. The evaporites are not well represented, except in the southern part of the section, where they are very thin (around 60 m).

The Cretaceous layers conformably overlay the Jurassic. Their main surfaces are flat and the thickness (between 1500 m and 1800 m) is relatively constant all along the line.

3.3. NW-trending geological lines parallel to the Bukhara and Chardzhou steps

We have described a set of six lines, which are roughly perpendicular to the main orientation of the Bukhara and Chardzhou steps. To obtain a better view of the structure of the northern margin of the Amu-Darya basin we have constructed two NW-trending lines roughly parallel to the step, and crossing the N- to NE-trending lines (A-A' to F-F'). One of these lines (G-G') is located in the Bukhara step, the other (H-H') in the Chardzhou step. Both lines were constructed using geological and borehole data.

3.3.1. Line G-G'

The line G-G' was reconstructed from well and deep drilling data. It is roughly parallel to the orientation of the Bukhara step. It crosses the step from the northwest to the southeast through the Yangikazgan, Gazli, Sverdlova, Saritash, Karaulbazar, Shurtepe, Karabair, Khodjikuduk and Saricha structures.

One of the main characteristics of this line is the very thin Jurassic section observed in the Bukhara step (fig. 3.10). Another interesting point is the lack of Jurassic deposits in several segments of the line. Besides, the reliefs of the base and top of the Jurassic unit are very rugged, with a lot of sharp drops. These highs and lows are partly connected to the presence of faults sub-perpendicular to the Bukhara step.

The Mesozoic formation is relatively thick, ranging between 1000 m and 2000 m from the north to the south. Most of the Mesozoic thickness is related to the Cretaceous sediment. The Jurassic sequence reaches the maximum thickness of more than 800 m. In general, this formation fills the grabens and other lows. One of the interesting Jurassic features is that it exhibits an incomplete section in the northwestern part of the profile, where the evaporite unit is missing.

Many faults, oblique to the general trend of the Bukhara step, cut the Jurassic units along the line, marking a Mesozoic tectonic activity. These faults, mainly normal, were active during the Jurassic and the Early Cretaceous.

Jurassic terrigenous sequence

The northwestern part of the line (Yangikazgan structure) is characterized by a 250-500 m thick siliciclastics sequence deposited in a NE-oriented graben. This 30 km-wide graben is framed by a NE-oriented normal fault that controls the deposition of the siliciclastics during the Early-Middle Jurassic. This graben is bordered to the southeast by a horst, which constituted a high during the Early-Middle Jurassic where no deposition occurred. Further to the southeast the terrigenous sequence re-appears in a small basin where the deposition is probably controlled by some small normal faults. There, the thickness of the clastics ranges from 0 to 200 m. The vertical displacements of the normal faults, forming this graben, do not exceed 20 m.

There are no Jurassic deposits in the Gazli emerged high that constituted a horst structure during these times. Further to the southeast the terrigenous beds appear again in another small graben about 15 km wide. The terrigenous deposits thickness ranges from 0 to 80 m. Two normal faults of opposite vergence with a 50 m displacement limited this well expressed graben. Another 10 km-wide terrigenous Jurassic accumulation is observed few kilometres southeastwards, between the Gazli and the Sverdlova structures. In this small basin 10 m to 200 m of Lower-Middle Jurassic clastics deposited.

Further to the southeast, in the Sverdlova structure, terrigenous sediments deposited into two sub-basins 35 km- and 15 km-wide respectively. Here the thickness of the clastic deposits does not exceed 50-200 m. Some normal faults with 10-20 m of vertical displacements have been observed in this area. Southeastwards develop another high (Saritash and Karaulbazar structures) about 50 km-wide. The terrigenous unit appears again in the area of the Shurtepe structure where a 40-30 m-thick clastic sequence fills up a small basin.

Between the Shurtepe and the Karabair areas a 80-100 m thick Lower-Middle Jurassic siliciclastic sequence deposited in a 25 km-wide half-graben limited to the southeast by the Karabair normal fault active during the Jurassic. The Karabair structure is located in a horst separating two small basins. The depocenters are located NE and SW of the horst. Southeast of the Karabair 8 well, a main NW dipping normal fault with more than 500 m of vertical displacement cuts the Mesozoic sequence up to the Lower Cretaceous. The terrigenous rocks in both the hanging-wall and foot-wall blocks of this fault are equally nearly 100 m thick. It suggests that this large normal fault post-dates the deposition of the Jurassic clastics. In the southeasternmost part of the line, in the Khodjikuduk-Saricha area, the thickness of the siliciclastics varies between 20 m and 100 m.

Jurassic carbonates sequence

The overlaying Jurassic carbonates are more widespread than the siliciclastics deposits, but did not entirely cover the entire Bukhara step too. At the Yangikazgan structure, the carbonates are 150-200 m thick.

Southeastwards, the J_{2-3} thickness slightly increases to 250 m, and then sharply decreases to 0 partly a small horst where the Lower Cretaceous deposits unconformably overlap the Paleozoic. Few kilometres to the southeast the carbonate beds form a small basin about 40 km wide located in the northwest of the Gazli field. Several faults exist in this area. Some of them are normal faults displaying vertical displacements of 30-40 m. The carbonate unit thickness increases to 250 m and then decreases to 0 towards the northwest of the Gazli structural high.

In the Gazli field there is no Jurassic deposit. This structure was a horst during the Early-Middle Jurassic. Just southeast of it, separated by a normal fault, the carbonates appear again in the small graben describe above. Here, their thickness ranges from 20 to 100 m. Further to the southeast, the carbonates are missing again on a small horst. They re-appear 15 km further to the southeast, where they are 100-50 m thick in the sub-basins. In the 90 km-wide Sverdlova structure the thickness of the siliciclastic deposits reaches 200 m.

Southeastwards, the carbonate thickness grows again to 300 m. In this area some normal faults without significant vertical displacements have been observed. Some of them may have controlled the deposition. Then, in a 40 km-long segment the limestone is only sporadically present (0 to100 m thick) on a broad Jurassic high, unconformably covering the Paleozoic beds.

In the Saritash-Karaulbazar basins the Jurassic carbonate is thin. The thickness sharply grows to 350-400 m in the Shurtepe basin. A normal fault with 50 m of vertical displacement has been determined in this area. In the northern Shurtepe basin the thickness of the Upper Jurassic limestone reaches 200-100 m, to gradually increase southeastwards to reach 300-200 m thick in the Karabair area.

Southeast of the Karabair area a main normal fault with a vertical displacement of 500 m cuts the carbonates (and the siliciclastics as well). The thickness of the carbonate remains (about 300 m) the same on both blocks of the fault, suggesting that the Middle-Upper Jurassic deposits pre-date the main normal faulting. Southeastwards, there is another normal fault with a displacement of few tens of metres seems Late Jurassic in age. In the Khodjikuduk-Saricha area, in the very southeast, the thickness of the carbonate beds varies between 50 m and 200 m, reached at the extremity of the line.

Jurassic evaporite sequence

One of the major characteristics of the Bukhara step is the thin and sporadic evaporitic cover. The salt-anhydrite beds only appear in the southeastern half of the line, in the Sverdlova structure. The maximum thickness of the evaporites is 40 m at the southeastern end of the line. Along the profile they do not exceed the thickness of 20 m. There is no significant thickening of the evaporites related to the normal faults.

Cretaceous sequence

The Cretaceous sequence covers either the Jurassic or the Paleozoic where the Jurassic is missing. We have reconstructed the Cretaceous principal surfaces using the borehole data. For greater accuracy we have used the isohypse map of the XII horizon within the Lower Cretaceous. This horizon, as the XIII horizon, which lies below, is one of the main Cretaceous markers.

In the northwestern part of the line the thickness of the Lower Cretaceous is of 600-800 m and decreases to 400-300 m in the Gazli structure further to the southeast above the Jurassic high. From Gazli to the southeast, the Lower Cretaceous thickness grows slightly to 400-600 m above a small Jurassic graben. Further to the southeast the thickness remains almost constant. In the Sverdlova basin, it is 600 m thick and increases to the southeast to 750 m. In the Saritash-Karaulbazar area the thickness decreases to 400 m to rise up to 650-600 m in the Shurtepe structure. Between the Saritash and Karaulbazar structures three south-dipping faults (probably normal) are observed. Two of them are not very significant. The third fault displays a vertical displacement of 50 m.

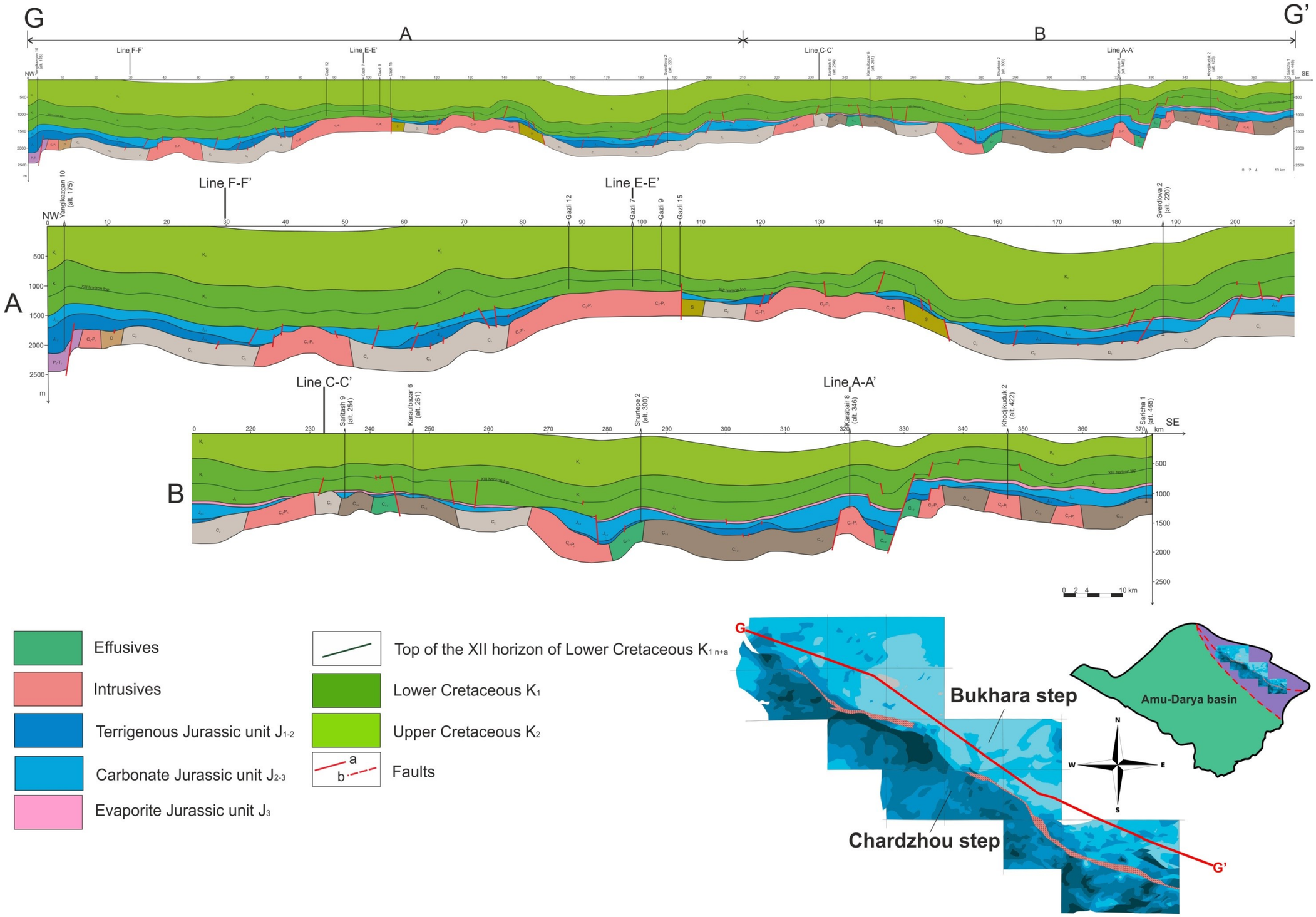

Fig. 3.10. Line G-G.

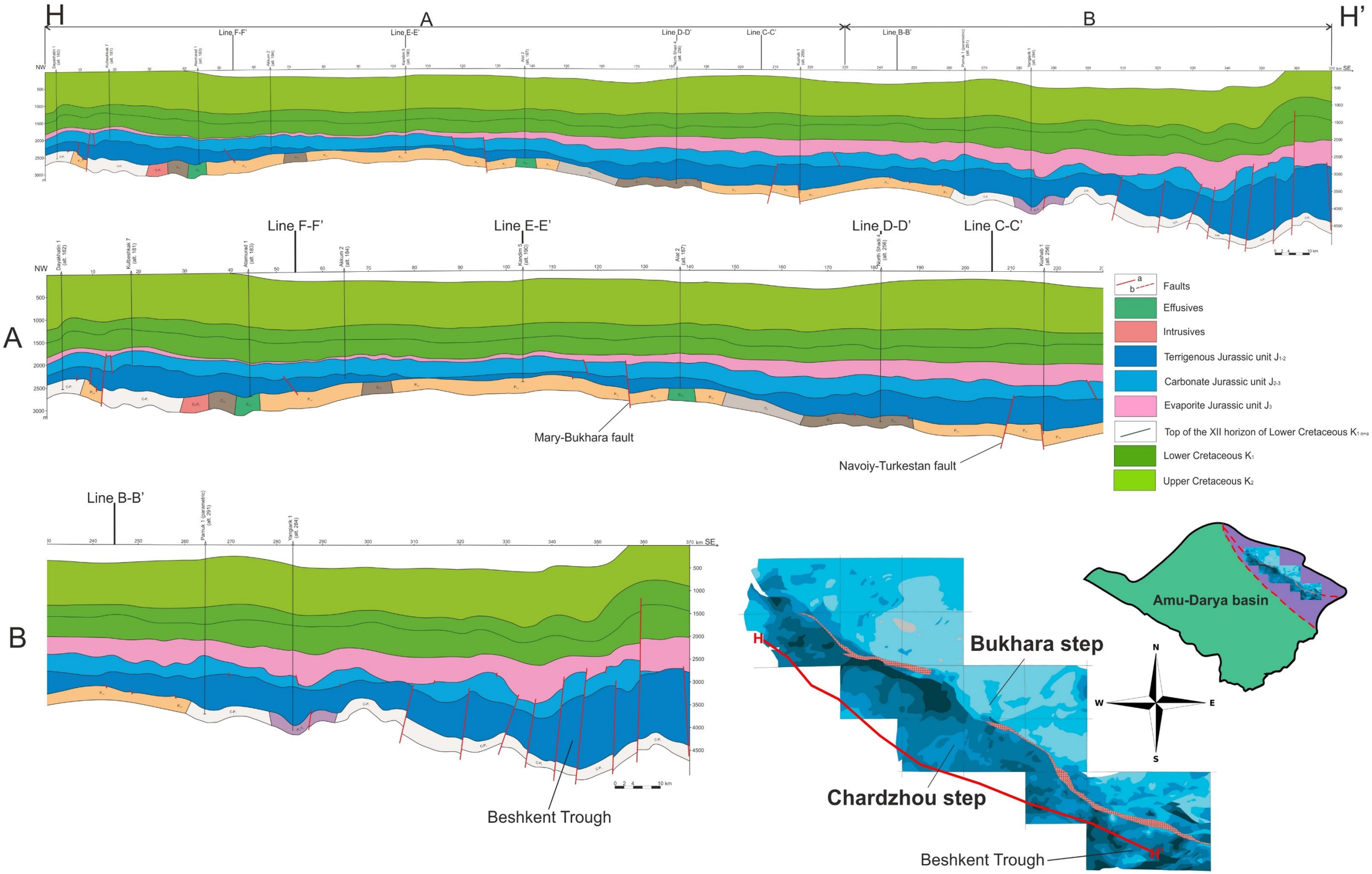

Fig. 3.11. Line H-H'

Southeastwards, in the Karabair structure, the Lower Cretaceous is 550-400 m thick. It appears that the main normal fault that cut the whole Jurassic to Lower Cretaceous sequence is mainly Early Cretaceous in age. Indeed, the thickness of the Lower Cretaceous is of 700 m in the hanging wall, while it is only 350 m in the footwall. In the Khodjikuduk structure it ranges in the 550-650 interval. Several small syn-Early Cretaceous normal faults have been evidenced in the Khogjikuduk area. At the SE end of the line, the Lower Cretaceous horizon is 550-400 m thick.

The Upper Cretaceous beds are relatively thick and their roof is above the zero line on most of the line. In the northwestern part of the section its thickness reaches more than 1000 m. The K_2 relief depth decreases in the Sverdlova structure where it reaches 300 m. The thickness here is of 700 m and decreases to the southeast to 300-350 m. No normal fault affects the Upper Cretaceous sequence.

Conclusion

The G-G' line highlights the structure of the Bukhara step. The most important result concerns the sedimentation during the Jurassic in the Bukhara step, which is highly heterogeneous. The Jurassic deposits are generally thin, discontinuous, and locally absent. This is connected to the complicated geometry of the pre-Jurassic surface.

The Jurassic clastics deposited in depressions, oblique and perpendicular to the main orientation of the Bukhara step. Some of these depressions are clearly Early-Middle Jurassic grabens that controlled the deposition of the clastics. However, not all of the valleys were fault-originated. Some of them do not show real graben structures. They are probably Jurassic paleo-depressions inherited from the Late Permian to Triassic erosion of the Late Paleozoic ranges, comprising large alluvium plain and valleys. These NE-trending Early-Middle Jurassic valleys were probably supplying the Amu-Darya basin in clastics sourced northwards in the remnant Paleozoic reliefs.

The Middle Jurassic transgression invaded the same depressions, where the marine carbonate conformably overlays the siliciclastic layers. The transgression locally extends over the Middle Jurassic reliefs unconformably overlaying the Paleozoic formations. Some of the normal faults were still active during the carbonate deposition but probably much less than during the clastic deposition.

The third point is the lack of evaporite in the northwestern half of the line. In the southeastern part of the line the salt-anhydrite formation is very thin. It generally follows the deposition of the carbonate. During the Late Jurassic regression the sea almost completely retreated from the Bukhara step, except in the southeast.

The Cretaceous sequence is thick and it thickness ranges from 1800 m in the northwest to 800-900 m in the southeast of the line. The relief of its surfaces is parallel to the underlying horizons, but is smoother. The Lower Cretaceous beds often unconformably cover the pre-Jurassic on the Early Cretaceous paleo-highs. The Lower Cretaceous sequence is clearly cut by normal faults oblique to the step orientation. These normal faults may display significant throws like the west dipping NE-trending Karabair Fault. This normal faulting evidences an Early Cretaceous extensional tectonic event observed all along the Bukhara step and in the Southwestern Gissar Range.

The Upper Cretaceous sequence is about 1000 m thick in most of the line. In the eastern part of the line it regularly decreases southeastwards to 300 m. A broad subsidence possibly thermal, originated the thickening of the western part of the Bukhara step.

3.3.2. Line H-H'

The line H-H' is a geological profile, that crosses the Chardzhou step. From the northwest to the southeast it intersects the Dayakhatin, Kulbeshkak, Atamurad, Akkum, Kandim, Alat, North Shadi, Kushab, Pamuk and Yangiarik structures (fig. 3.11). Most part of the line is characterized by a relatively flat relief of the reflectors, except in the Beshkent trough area in the southeast, where the faults are abundant and the thickening sizeable.

On the contrary to the Bukhara step, the complete Mesozoic section with well-developed thick layers is represented in the Chardzhou step. These layers show a significant southeastward thickening of the

Mesozoic sequence. The complete Mesozoic section, more than 2500 m thick in the northwestern part of the line, gradually increases to the southeast to more than 4000 m near Southwestern Gissar. The Jurassic is around 600-700 m thick in the northwest of the line, while in the southeastern end of the profile it reaches more than 2300 m. The Cretaceous sequence also increases southeastwards.
An interesting point is that the faults are rare in the northern and central parts of the section unlike in the southeastern part of the line in the Beshkent trough where the density of the faults highly increases. This latter trough constitutes the foreland of the Southwestern Gissar Mountains. It is mainly framed by blocks separated by reverse faults. Some of them cut not only the Jurassic, but even the Lower Cretaceous.

Jurassic terrigenous sequence

In the northwestern part of the line (Dayakhatin, Kulbeshkak structures) we observe a system of three faults, probably normal, which form a small graben. The thickness of the terrigenous sequence in the structure varies in the 300-500 m interval.

Further to the southeast in the Atamurad structure the thickness decreases from 500-550 m to 400 m. The decrease continues in the same direction, and in the Akkum structure, the thickness of the terrigenous unit is only of 150 m. A south-dipping normal fault cuts the whole Jurassic sequence between the Akkum and Atamurad structures. Its vertical displacement is of nearly 30-40 m. South of Akkum, the siliciclastics decrease in thickness to 10 m or less. Further southeast in the Kandim structure, the thickness of the siliciclastics increases to 100 m. Two normal faults forming a horst are observed southeast of Kandim. One of them has a displacement of 20-30 m, while the second one displays a throw of almost 60 m, cutting the whole Jurassic sequence. Near these normal faults the thickness of J_{1-2} increases from 100 m to 200 m (300 m at the second fault) and progressively increases towards the Alat structure, where it reaches 250 m. This normal fault was active during the deposition of the siliciclastics (and the rest of the Jurassic as well).

In the North Shadi structure the thickness of the siliciclastics increases to 600 m and remains constant as far southeast as the Kushab structure. In this latter structure two normal faults, constituting a horst in the clastics and a half-horst in the carbonate, have been evidenced. The vertical displacement of the NW dipping northwestern fault reaches 60 m, while the southeastern one probably does not display a significant slip in the Lower-Middle Jurassic. The increase of the terrigenous thickness to 740 m in the Kushab structure is connected to the Jurassic normal faulting. Southeast the Kushab structure the thickness of the siliciclastics gradually decreases to 200 m before to rise again to 700 m at the Pamuk structure. Southeast of the Pamuk field, the terrigenous unit regularly grows in thickness, to reache 800 m in the Yangiarik well.

Further southeast the thickness of the Jurassic terrigenous unit locally decreases to 400 m. In the southeastern part of the line, where the profile intersects the Beshkent trough, the thickness of the J_{1-2} quickly grows from 400 m to 1600 m. In the southeastern extremity of the lines we observe a set of reverse faults which constitutes the folded foreland of the Southwestern Gissar Range. The vertical displacements of these faults are around 40-60 m. Despite these reverse faults probably account for a part of the thickening during the Cenozoic, it is clear that most of the thickening of the clastic Jurassic sequence in the Beshkent trough is Early-Middle Jurassic in age.

Jurassic carbonate sequence

The Jurassic carbonate beds are generally parallel to the terrigenous roof, excluding a major intra-Jurassic unconformity. The carbonate shows a relatively constant thickness all along the line, except in the southeastern part, approaching Southwestern Gissar.

In the northeast in the Dayakhatin-Kulbeshkak area the carbonate is 300 m thick. The two normal faults of the Kulbeshkak structure, with a vertical displacement is 20-30 m, cut the carbonate. Between the Kulbeshkak and the Atamurad structures, the carbonate thickness remains almost constant. Further to the southeast of the Akkum structure the carbonate thickness shows some small variations in the 340-300 m interval. In the Kandim field, southeast of the Akkum structure, the thickness remains the same despite the carbonate relief variations. Southeastwards the carbonate unit is cut by two normal faults between the Kandim and Alat structures. They display the same displacements in the carbonate

than in the Jurassic terrigenous sequence, as described before. The thickness of the carbonates is the same in both walls of the normal fault suggesting that this normal fault was not active during the deposition of the limestone.

Further to the south, towards the North-Shadi structure the thickness of the limestone fluctuates between 400 m and 500 m (300 m in average). Between the North Shadi and the Kushab structures the carbonate thickness decreases to 240-250 m. In the Pamuk structure the thickness of J_{2-3} varies from 200 m to 450 m. To the southeast of the Pamuk structure, in the Yangiarik structure, the thickness decreases to 200 m. Further to the southeast the thickness of the carbonates decreases to 60 m then grows to 300 m and then locally disappears.

To the southeast, the thickness rises to 400 m and then increases to 600 m. The southeastern part of the line intersects the Beshkent trough. Most of the faults that cut the siliciclastics also cut the carbonate and extend upwards in the evaporites. Some of these faults have a vertical displacement of 100-200 m. In this area, the thickness of the limestone changes in a wide interval from 200 to 600 m. At the southeastern end of the line the carbonates almost disappear (10-100 m thick). Such a disappearance, not observed eastwards in the Southwestern Gissar Range, may be due to the low quality of the data in the eastern extremity of the line.

These thickness fluctuations observed in the carbonate unit in the southern half of the line are linked to the barrier reef system structure described by Mirkamalov et al. (2005). As we mentioned in the previous chapter, this reefal formation developed during the Callovian-Kimmeridgian time in the Beshkent trough and nearby areas.

Jurassic evaporite sequence

The overlaying evaporite unit covers the entire Chardzhou step. It is very thin (<100 m) in the northwestern part of the line, but significally increases in thickness towards the southeast up to 800 m.

In the northwest, in the Dayakhatin-Kulbeshkak area, the salt-anhydrite beds are 50-60 m thick. The thickness decreases in the Atamurad-Akkum area where it reaches 20-40 m. In the Kandim structure the evaporites are 60 m thick and increase southwards up to 200 m (Alat field). Further southwest in the Kushab structure, the thickness reaches 500 m. From the Kushab to the Pamuk structures the thickness decreases to 400 m and then grows to 500 m whereas in the Pamuk field it decreases again to 350 m. In the Yangiarik structure it reaches 550 m.

In the Beshkent area the salt-anhydrite thickness varies from 600 m to 800 m. In the thinnest places it locally reaches 300-400 m. It is still not clear if this thickening of the evaporite in the Beshkent trough is from stratigraphic (Late Jurassic) or tectonic origin (Cenozoic).

Cretaceous sequence

The Cretaceous sequence conformably covers the Jurassic and exposes a rather constant thickness all along the line ranging in the 1800 m to 2000 m interval. To reconstruct the Cretaceous sequences we have used the same set of data, as for the Bukhara step. The XII horizon of the Lower Cretaceous is the marker of the principal Cretaceous relief fluctuations. In general it is almost parallel to the Jurassic surface.

In the northwestern part of the profile (Dayakhatin-Kulbeshkak area) the Lower Cretaceous is nearly 600 m thick. Its thickness remains constant as far south as the Kushab structure. From Kushab to the southeast, the thickness increases to 700-800 m. In the Beshkent area, the Lower Cretaceous thickness varies in the 800-900 m interval. The main fault of this area reaches the Lower Cretaceous but does not affect the Upper Cretaceous sequence.

The Upper Cretaceous thickness changes from more than 1200 m to 1000 m in between the Dayakhatin and the Alat structures. In the Alat structure its thickness is 1000-1050 m thick. This extends southwestwards to the Kushab area. Further to the southeast in the Pamuk structure, the Upper Cretaceous thickness slightly increases to 1100 m and remains almost the same up to the end of the line.

Conclusion

The H-H' line mostly evidences the structures oblique to Chardzhou step (fig. 3.11). There is a complete Mesozoic section in this step, on the contrary of the Bukhara step. The Jurassic contains all the units, which are conformably covered by a thick Cretaceous sequence.

There is a significant southeastward thickening of the Jurassic from 600 m in the northwest to 2400 m in the southeast. Besides this, the structure of the main Mesozoic horizons is smooth, without sharp drops, except in the southeastern part in the Beshkent trough where Cenozoic reverse faults affect the Mesozoic sequence, strongly modifying the Jurassic configuration.

The thickness of the terrigenous unit ranges commonly in the 300-500 m interval. The maximal thickness of the terrigenous Jurassic (and of the whole Mesozoic sequence as well) is reached in the southeastern part of the profile in the Beshkent trough, where it varies from 400 m to 1600 m.

We may point out an almost constant thickness (300-400 m with minor variations) of the carbonate unit along the line. Some unclear fluctuations appear only in the southeastern end of the line, in the Beshkent trough where most of the Cenozoic reverse faults are concentrated.

Another key point is the development of a reefal system during the Middle Callovian-Kimmeridgian. As mentioned in Chapter 2, the reefal system has been mainly evidenced in the southeastern half of the Chardzhou step where it surrounds the Beshkent trough.

The evaporite formation reaches its maximum thickness in the Beshkent area, which is the deepest part (from the pre-Mesozoic relief) of the Bukhara-Khiva region. The relief of the roof of the salt-anhydrite is flat. This unit, nearly 50 m thick in the northwestern end of the line, gradually increases to 800 m in the southeast.

The Cretaceous beds covering the Jurassic exhibit an almost constant thickness (about 1500 m) and very smooth surfaces, suggesting a large scale subsidence.

3.4. Review of the features along the sections

3.4.1. Review of the Jurassic thickness

We completed the description of the geological structure with an analysis of the thicknesses in the Jurassic units through paleo-thickness maps compiled by Nugmanov and Jdanova (2004) and Nugmanov (2009a). In this paragraph we intend to compare and discuss the thickness data we have obtained from our reconstructed seismic lines with the data of the paleo-thickness maps of Nugmanov and Jdanova (2004) and Nugmanov (2009a).

3.4.1.1. Jurassic terrigenous unit

According to the Nugmanov and Jdanova thickness map (2004), the Jurassic siliciclastics have the following general distribution in the Bukhara-Khiva area (fig. 3.12):

- In the Bukhara step the siliciclastics are thin (0 to 300 m thick, locally 400 m);

- In the northwestern Chardzhou step the thickness varies between 100 m and 1000 m, except in the Kimerek graben where it reaches 1500 m;

- In the Beshkent trough, constituting the southeastern Chardzhou step, the siliciclastics are 700 m to 1500 m thick.

Two major basins are associated to the deposition of the terrigenous sequence in the Bukhara-Khiva region during the Early-Middle Jurassic: the Beshkent trough in the southeast and the Kimerek graben in the northwest.

The Beshkent trough is the major basin of the Chardzhou step characterized by 700 m to 1500 m of terrigenous deposits, reaching locally more than 1500 m. According to our data, in the western part of the trough, especially between the Matonat and East Dengizkul structures (C-C' line, fig. 3.6), the thickness is only of 400-450 m rather than of 700-1000 m in the paleo-thickness map (Nugmanov and

Jdanova, 2004). Southwards, along the B-B' line we observed thickness variations from 50 to 250 m, while the used maps indicate 500 m to 1200 m. More to the east, along the A-A' line, the difference is less important but our thickness is still 200-300 m below the values of the Nugmanov and Jdanova's map. In the Yangiarik 1 well (southeastern H-H' line) the Jurassic terrigenous pile is 800 m thick, whereas in the paleo-thickness map it is 1000-1400 m thick.

The Kimerek graben in the northwestern Chardzhou step is a half-graben characterized by the deposition of 1000 m to 1500 m of siliciclastic deposits during the Early-Middle Jurassic. This half-graben is related to normal faulting along the UKFFZ during the Jurassic. In this structure the values of the thickness of the siliciclastics obtained from our cross-sections (fig. 3.8) and the Nugmanov and Jdanova's map are very similar.

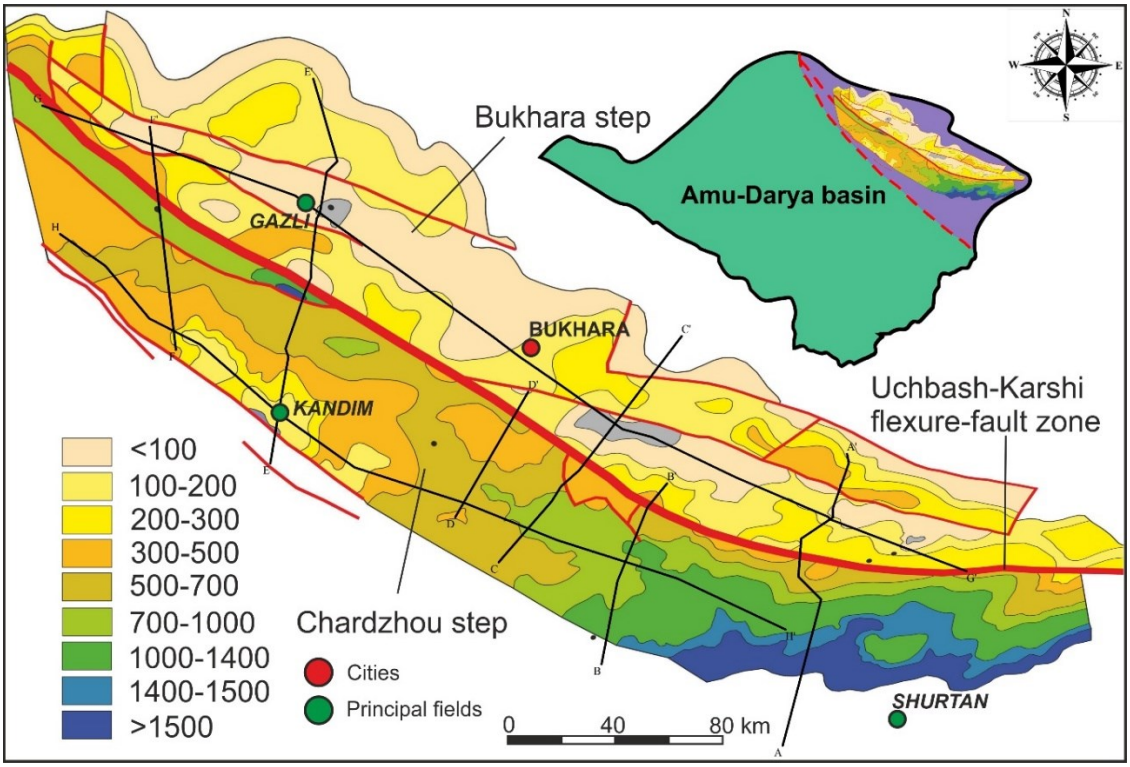

Fig. 3.12. Paleo-thickness map of the terrigenous Jurassic Formation and location of the lines studied (modified after Nugmanov and Jdanova, 2004).

Systematically, and more particularly in the southeastern Chardzhou step, the thicknesses that we have determined from boreholes and seismic profiles are lower than the thickness proposed in the map of Nugmanov and Jdanova (2004). The differences between actual and reconstructed thicknesses are commonly of 300 m to 600 m. This discrepancy may reflect the different approaches between the authors. In fact, the authors have reconstructed paleo-thicknesses, including probably a decompaction of the sediments and no erosion, while we only consider the present-day observed thickness. The Nugmanov and Jdanova's approach systematically raises the actual value of the thicknesses.

3.4.1.2. Jurassic carbonate unit

As mentioned in the previous chapter, Nugmanov (2009a) has divided the carbonate unit into two main formations, corresponding to the Middle Callovian-Middle Oxfordian and to the Upper Oxfordian-Kimmeridgian intervals. He has called them the "Lower Kugitang Formation" and the "Upper Kugitang Formation" respectively.

Lower Kugitang Formation (Middle Callovian-Middle Oxfordian)

One of the most important features of the Lower Kugitang Formation, well featured by the thickness map of Figure 3.13), is a NW-oriented zonation of the isopachs both in the Bukhara and Chardzhou

steps. Generally, the thickness of the carbonate sediments gradually increases from the northeast to the southwest in the both steps, except in the southeast in the Beshkent trough where NE- to E-oriented depocenters appear.

The Bukhara step is characterized by a thickness ranging from 0 to 160 m. In the thinnest parts, in the northern and northeastern Bukhara step, the Lower Kugitang Formation is less than 20 m thick. Its thickness gradually increases to the southwest. The NW-trend of the isopachs corresponds to the general trend of the Beshkent trough controlled by the main normal faults (fig. 3-13).

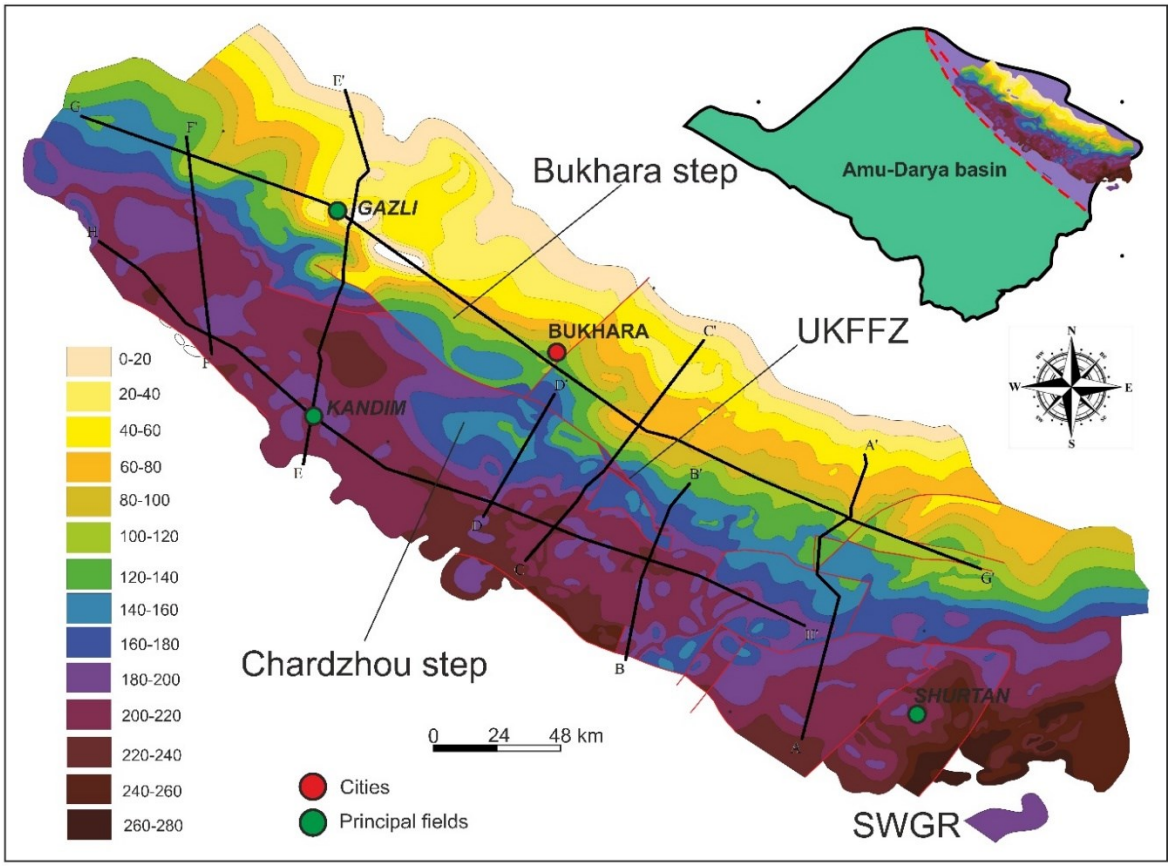

Fig. 3.13. Paleo-thickness map of the Middle Callovian-Middle Oxfordian Lower Kugitang Formation and location of the lines studied (modified after Nugmanov, 2009a).

A similar linear zonation exists in the Chardzhou step, but less expressed than in the Bukhara step, especially where the siliciclastic sequence is more than 160 m thick (fig. 3.13). The thinnest part (140-180 m thick) is located near the Uchbash-Karshi Flexure-Fault Zone, and the maximum thickness (220-240 m) is in the southern areas in the Beshkent trough. The Southwestern Gissar area is characterized by an important value of the thickness of the Lower Kugitang Formation that reaches 260-280 m, associated with the growth of the reefal carbonates. The map of Figure 3.13 reveals the role of the NE-trending faults (presumed to be normal) in the development of the Beshkent trough. It also highlights the role of the UKFFZ as a sharp limit between the Bukhara and Chardhzou steps in the northwestern part of the Bukhara-Khiva region.

Upper Kugitang Formation (Upper Oxfordian-Kimmeridgian)

The area of extension of the Upper Kugitang Formation is smaller than the Lower Kugitang one. In the northwestern Bukhara step (Gazli and Karakir structures) the Upper Kugitang sediments are missing. In addition the Upper Kugitang Formation is thinner. It constitutes on Figure 3.14 very well determined block structures enlightened by sharp thickness variation, especially on the Chardzhou step. This structure is probably related to the activity of two sets of normal faults, NW- and NE-oriented.

The isopachs still roughly exhibit a NW-oriented zonation in the Bukhara step with a minimum (less than 20 m) in the northern part of the step. The thickness gradually increases southwards like in the Lower Kugitang Formation. In the Bukhara step the thickest part (100-140 m) of the Bukhara step, is located near the Uchbash-Karshi Flexure-Fault Zone.

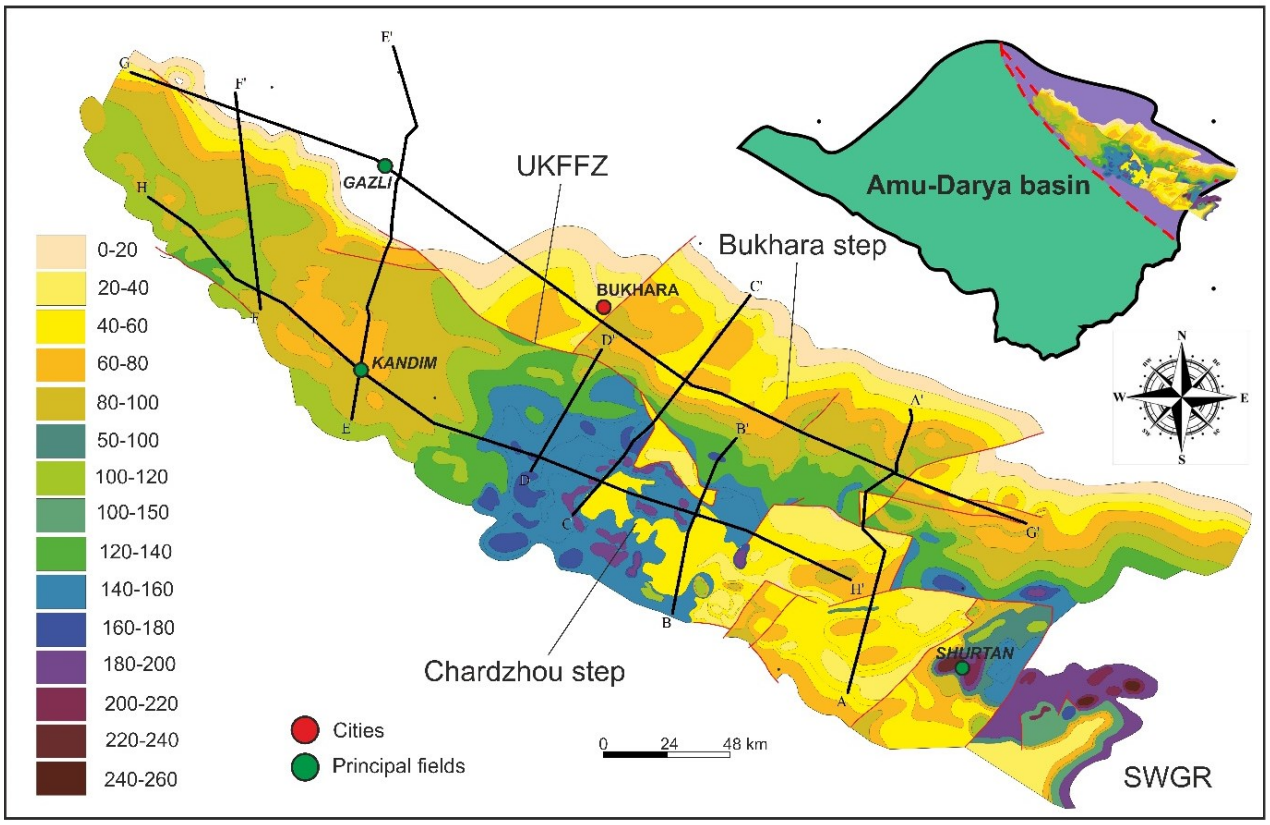

Fig. 3.14. Paleo-thickness map of the Upper Oxfordian-Kimmeridgian Upper Kugitang Formation (modified after Nugmanov, 2009a).

The Chardzhou step is characterized by three main blocks, namely from west to east, the western, central, and eastern blocks. The westernmost block displays a moderate thickness of 80-140 m. This thickness decreases in the central area to 60 m.

The central block is the thickest one and the most interesting. The thickness of the Upper Oxfordian-Kimmeridgian is of 100 m to 160 m, locally reaching 180 m. In this area, Nugmanov (2009a) distinguishes several bioherms characterized by a thickness of 180-200 m. A decrease of the thickness to 40-60 m is observed in the central and northern parts of this block.

Further to the southeast, the eastern block is characterized by a low thickness of the Upper Kugitang Formation (20-40 m to 60-80 m). A maximum of 100 m is reached in only few small areas. In the southeastern part of the block, the thickness changes within the 50-100 m interval, increasing to 140-160 m, and reaching 220 m locally in the Beshkent trough.

The Southwestern Gissar includes all the thickness intervals. The thickness varies from 0 to 140 m in the north, to 40 to 240 m in the south. The trend of the isopachs is controlled by NE-striking faults, probably normal during the Late Jurassic.

The block structure of the Upper Kugitang Formation has been correlated with the barrier reef system model (fig. 3.15) of Mirkamalov et al. (2005), Abdullaev et al. (2010). These authors determined (1) a lagoonal part, the eastern part of the Bukhara step and the northwestern part of the Chardzhou step, (2) a reefal part, the central block and the UKFFZ nearby areas of the southeastern block of the Chardzhou step, and (3) a basinal part, the southeastern block of the Chardzhou step. The map of Figure 3.15, where the reefal barrier is outlined in grey, summarizes the distribution of the three types of Jurassic carbonates.

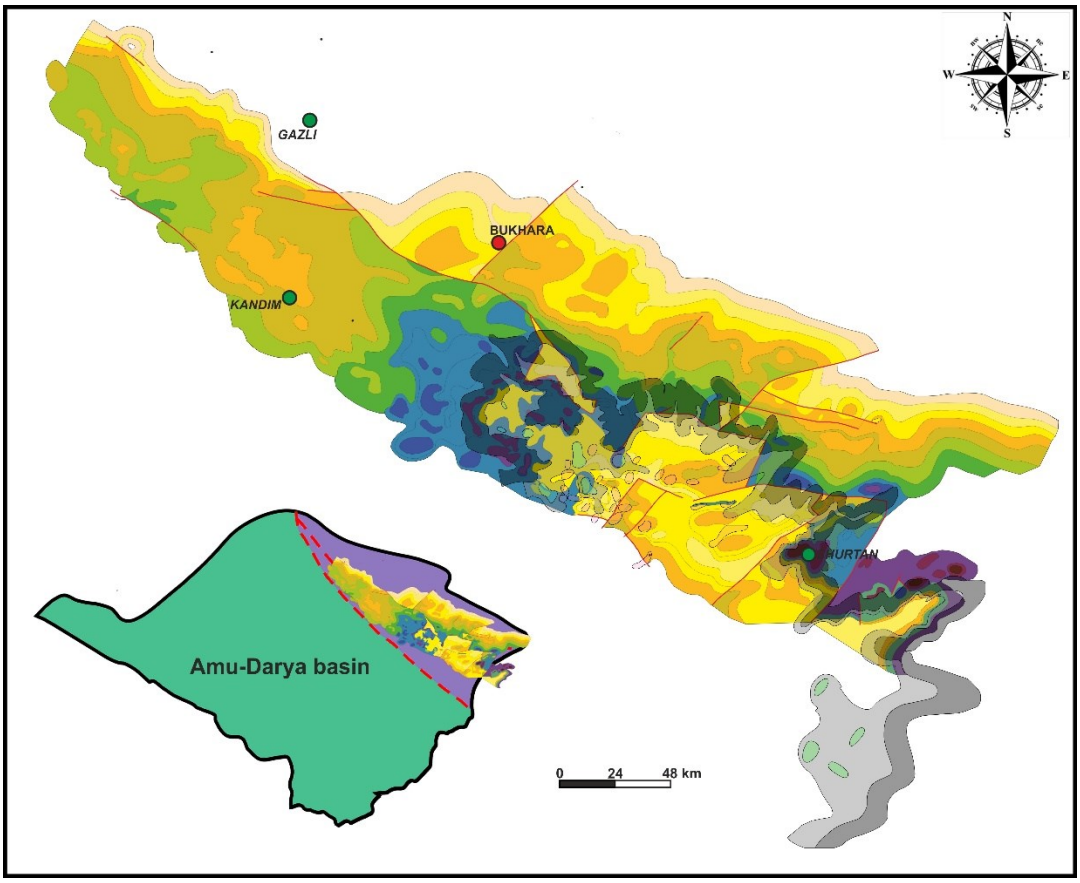

Fig. 3.15. Barrier reef system model (in grey) superimposed onto the paleo-thickness map of the Upper Oxfordian-Kimmeridgian Upper Kugitang Formation (Nugmanov, 2009a). Reef system model modified after Babadjanov (2012).

Total carbonate thickness

Despite we have no thickness of the whole Kugitang Formation we were able to combine the maps of the Lower and Upper Kugitang formations at several points, trying to (1) evaluate the paleo-thickness of the Jurassic carbonates, and (2) compare the data of the maps and of our lines. The comparison enlightened some valuable differences.

In the Maydadjoy structure (northern A-A' line) the carbonate unit is commonly 50-60 m thick. The paleo-thickness reconstructions indicate a thickness of 120-160 m. Likewise southwards the Karabair structure is characterized by a limestone thickness of 200-220 m, while the paleo-tectonic map indicates 260-300 m.

The same situation is observed in the Kassantau structure (central A-A' line) where the thickness of the carbonates is of 100-150 m according to our data, and 280-300 m from the paleo-thickness map. Another difference is observed southwards in the North Kamashi structure. Here, the thickness of the limestone is 400-500 m in our lines and 280-300 m in the paleo-thickness map of Nugmanov (2009a). The Pirnazar-Markovskoe structures in B-B' line show a carbonate thickness of 450-500 m, which is only of 360 m according to the paleo-thickness map.

In the central part of the C-C' line we determine the limestone unit as 500 m thick, where the paleo-thickness reconstruction shows a thickness of only 380 m in this area. In the limits of the Ashikuduk structure (E-E' line), according to the maps data, the J_{2-3} sediments do not exist, while our data shows that in this area the Jurassic carbonates are 100 m thick. The carbonate sediments of the Karakir structure are nearly 20 m thick and pinch out southwards. On the paleo-tectonic map they are not pinching out, but increase in thickness up to 60 m and disappear only in the Gazli area.

In addition, the southern part of the F-F' line is characterized by a 300-350 m thickness (according to the maps of Nugmanov), whereas according to our sections it is only around 300 m. On the G-G' line, in the Karaulbazar-Shurtepe interval, we evidence variations of thickness from 0 to 350-400 m. In the same area, the paleo-thickness maps indicate that the carbonate is no more than 200 m thick.

The thickness of the western part of the Chardzhou step (line H-H') according to the Nugmanov's data is around 260-300 m. According to our data it reaches 300-340 m. Moreover, the Nugmanov's maps (2009a) suggest that the Shadi-Kushab interval is 320-340 m thick, while in our reconstruction it is only 240-250 m thick. In our section the southeastern part of the H-H' line is characterized by variations of the carbonate thickness between 200 m and 600 m, whereas in the paleo-thickness map the carbonate is not thicker than 260 m.

3.4.1.3. Jurassic evaporite unit

We have no map illustrating the thickness variations of the evaporite formation. That is the reason why we only provide a schematic map based on our lines (fig. 3.16). According to this zoning map, we may roughly divide the Bukhara-Khiva region into the northern, eastern, central, and western zones.

The northern zone corresponds to the Bukhara step. It is characterized by a very thin evaporitic cover. The thickness ranges from 10 m to 40 m and the evaporites locally disappear. However, in the southeast, close to the UKFFZ, they increase up to 100 m.

In the western zone the evaporites are generally thin (around 60 m).

The central zone is characterized by a relatively constant thickness. The thickness in this zone reaches 300-500 m in its central part and 100-150 m near the UKFFZ.

The eastern zone (Beshkent trough area) is characterized by a significant increase of the evaporite thickness. In the north of the zone the thickness is of 400-500 m, locally of 150-200 m. It increases southwards up to 800 m. The average evaporite thickness is around 600 m.

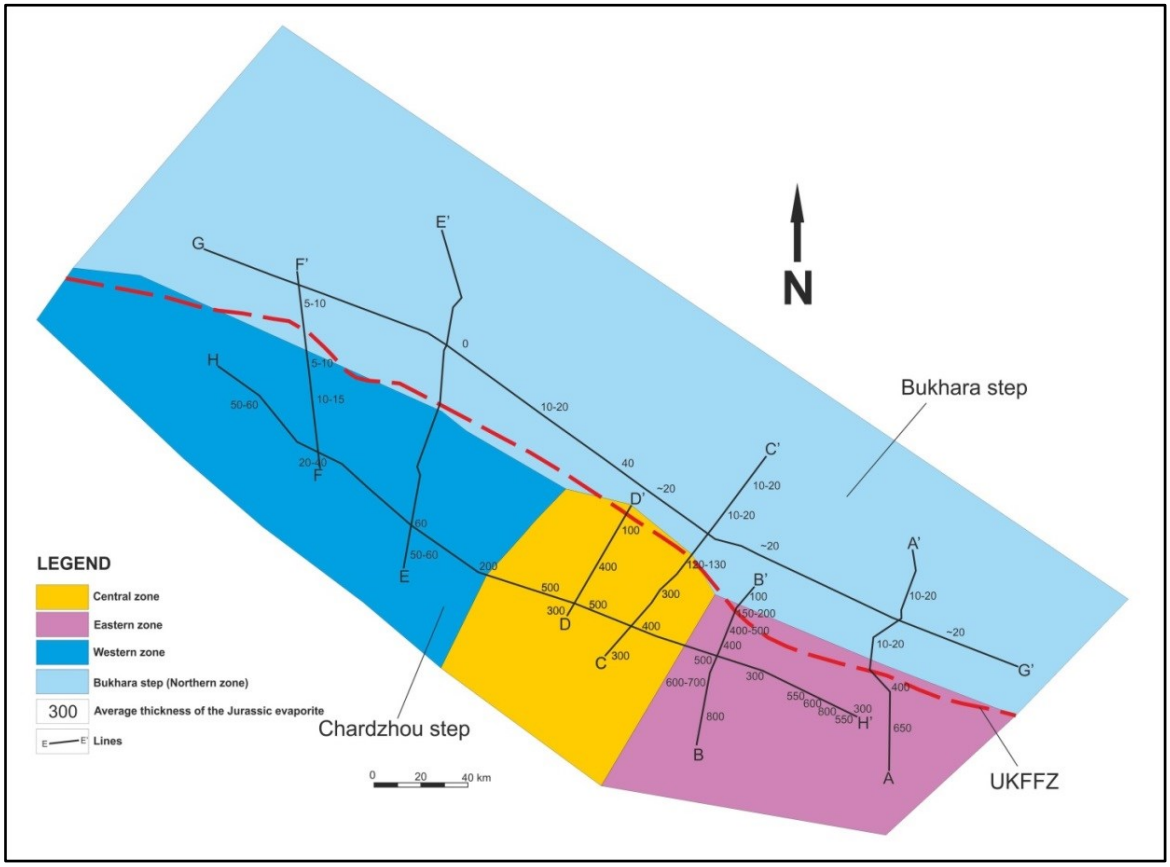

Fig. 3.16. Sketch of the Jurassic evaporite thickness zones

3.4.2. Review of the lithology

This part summarizes the history of the sedimentation. It helps to reconstruct the evolution of the area. This synthesis integrates the lithological data from the boreholes, which are located along the B-B' to F-F' profiles. In this analysis all the different Jurassic units are separately described. It would be more correct to use all the wells from the both steps, but as more than 500 wells have penetrated the Mesozoic sequence, it was impossible to study all of them. First, most of them are not accessible, or have incomplete lithological columns. This is related to the fact that most of these wells were drilled for the oil and gas exploration. Very often only the oil and gas bearing horizon lithology was reported. Second, in many cases only the stratigraphy is available. This is why we have restricted our investigations only to (1) the wells existing in the limits of the lines (fig. 3.17 and 3.19), and (2) the wells where the complete lithology is available.

3.4.2.1. Terrigenous unit

The Jurassic terrigenous unit is the oldest Mesozoic horizon determined in our lines. The terrigenous sequences include continental sediments deposited under a humid climate. They are represented by alternations of clays, argillites and sandstones with common coal veins (fig. 3.17). In general, the Lower-Middle Jurassic is characterized by monotonous lithologies. Most of the sedimentation is continental. However in the upper part of the section the sedimentation is marine.

B-B' line

The terrigenous section of the B-B' profile is the easternmost one where we have lithological data issued from the Buzatchi 1 well. This well did not penetrate the whole Lower-Middle Jurassic siliciclastic sequence. The lithologies mainly consist of sandstones in its northern part. The information about the lithology of the terrigenous formation in the Chardzhou step is issued from the Pirnazar, Markovskoye and South Alan lithological columns. The J_{1-2} beds consist of interbedded grey clay, sandstone and siltstone in the Pirnazar-Markovskoye areas.

There is black solid sandy argillite, partly with interlayers of siltstone in the middle part of the section. Also, they are clayed limestone in the uppermost part of the section. The clay and green-grey, solid argillite, with prints of flora and inclusions of plants with sandstone, siltstone and limestone interlayers, constitute the uppermost part on the South Alan field structure.

C-C' line

The Matonat and West Kruk lithological columns of the C-C' line provided detailed descriptions of the Jurassic terrigenous sequence. The terrigenous section of Matonat consists of beds of black solid argillite with interbedded layers of sandstone and siltstone. In the upper part of the section argillites are interbedded with rare layers of limestone. In the West Kruk area only the upper part of the terrigenous sequence is represented. It comprises interbedded layers of sandstone and siltstone with rare layers of limestone.

D-D' line

Further to the west, on the D-D' line, the Lower-Middle Jurassic sediments have been penetrated in the Chandir 2 well. In the synthetic lithological column of the Chandir field, the upper part of the terrigenous sequence consists in sandstone and siltstone with intercalated layers of clay and limestone. Black clays with rare interlayered light-grey siltstone and sandstone underlay this sequence. Black coal-bearing argillite, grey and light grey siltstone and interbedded sandstone constitute the base of the section.

E-E' line

There is only one lithological column available (Khodji structure) in the line. We have also used the Western Khodji column (near to the latter one). The terrigenous Jurassic comprises intercalations of sandstone, clay, siltstone and argillite. The sandstone is grey, light-grey, green-grey, fine, medium

grained and big grained, hard and partly clayed. The siltstone is grey and dark grey, hard and clayed. The clay and argillite are grey, dark grey, hard, sandy and micaceous. The upper part of the section comprises a pack of grey pelitic, hard solid limestone.

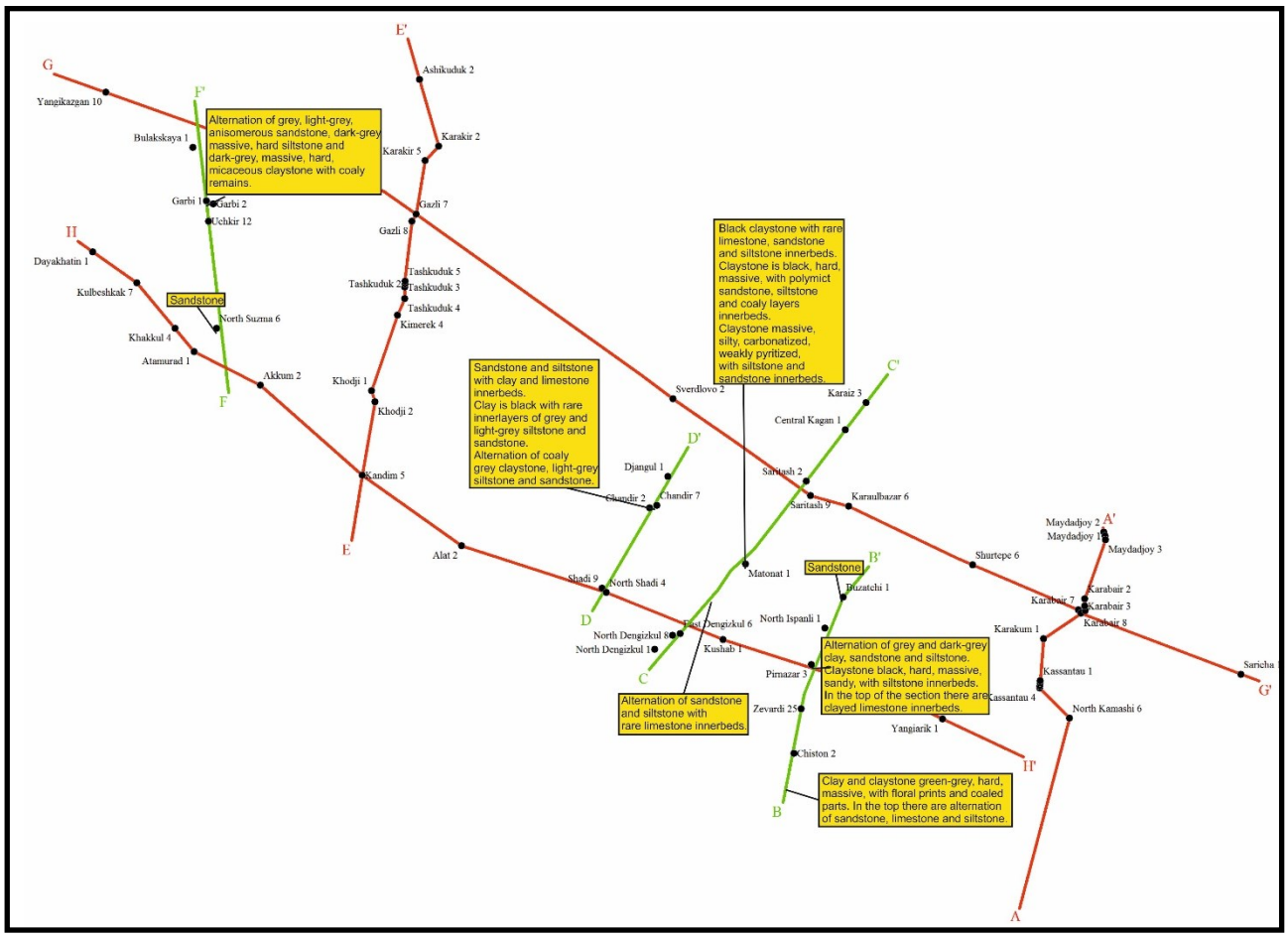

Fig. 3.17. Location of the boreholes used in this study where terrigenous rocks have been evidenced.

F-F' line

The information about terrigenous lithology of the westernmost line F-F' was obtained from the synthetic columns of Garbi field and North Suzma 6 well. The Garbi terrigenous strata are composed of intercalations of heterogeneous grey and light-grey sandstone, dark-grey, solid siltstone and dark-grey, solid, hard, micaceous argillite with charred rests. The North Suzma 6 well reaches the uppermost part of the terrigenous section, mainly consisting in sandstones.

Conclusion

The clastic sequence generally consists of argillite with intercalated siltstone and sandstone beds. The lower part of these sections contains coal veins and coal-bearing beds. The top of the sequence comprises clay with interbedded limestone lenses. The limestone layers interbedded in the top of the J_{1-2} formation mark the beginning of the carbonate sedimentation.

3.4.2.2. Carbonate unit

The carbonate unit, covers the siliciclastics. It is not uniform from a lithological point of view. We distinguish the XVI and XV horizons according to the standard stratification (fig. 3.3).

The XVI horizon is homogenous in all the Bukhara Khiva territory. It is a clear reflector in the seismic profiles. The XV horizon displays some structural features that create some difficulties for its determination. It is separated into the XV-above reef, XV-reef, XV-under reef, and XV-a horizon

(fig 3.3). Their combination and allocation depend on the sedimentation in the different part of the Bukhara Khiva region (fig. 3.18, 3.19). As for the terrigenous unit, we will describe the carbonate lithological features separately for each line.

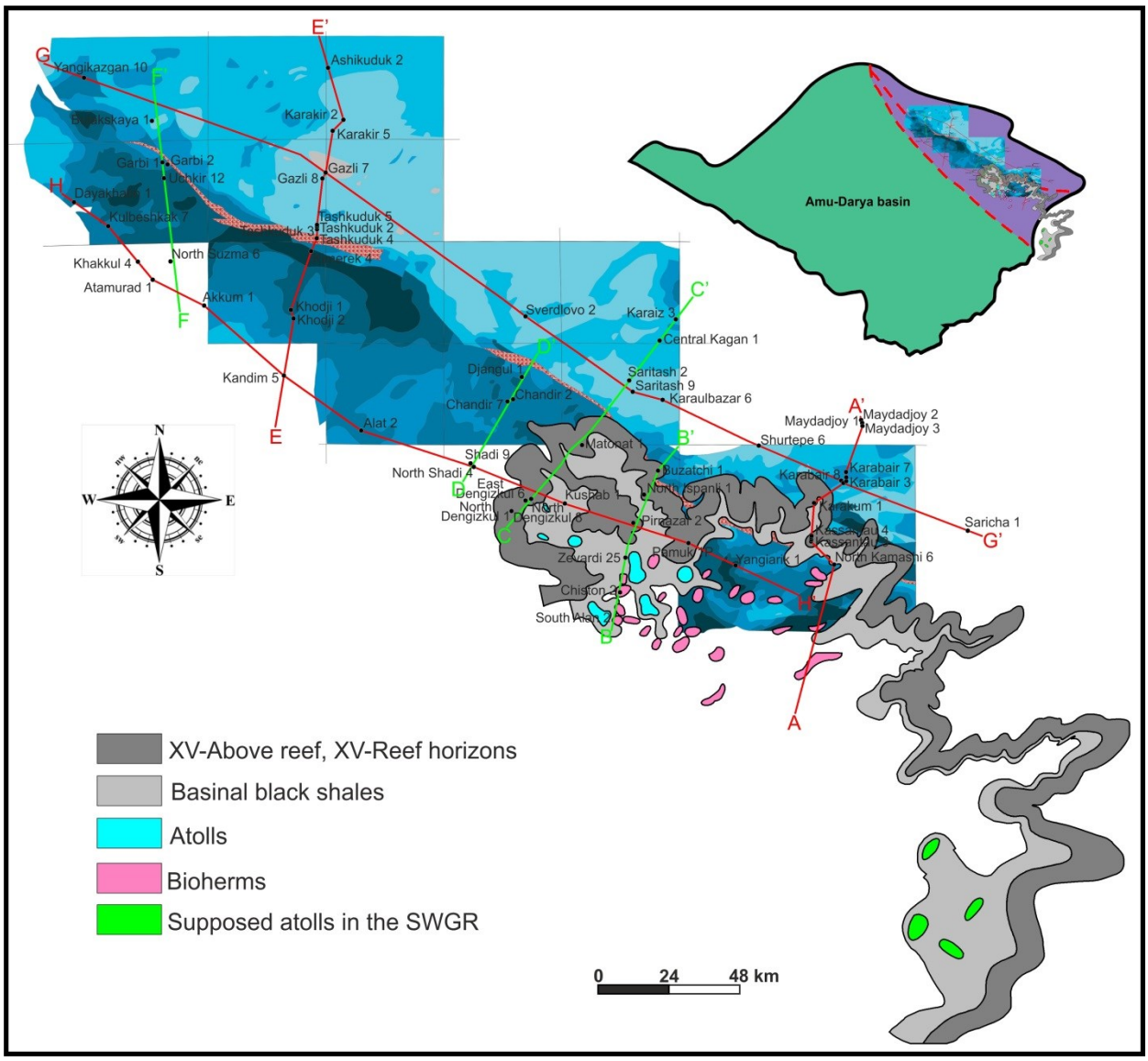

Fig. 3.18. Location of the reefal formations.
Blue background: thickness map of the Jurassic terrigenous and carbonate.

B-B' line

On the B-B' profile at the Buzatchi 1 well (Bukhara step) the carbonate unit comprises different limestones with reefogenous interlayers.

In the south of the Chardzhou step, in the Pirnazar-Markovskoye synthetic section, the carbonate consist in light-grey, grey, solid, pored, big grained limestone with crystalline calcite inclusions. This corresponds to the XV-above reef horizon. Grey limestone, friable, pored, cavernous with fauna rests observed below corresponds to the XV-reef horizon. The XV-under reef horizon is composed of limestone grey, clayey, solid and fine-crystalline. Grey limestone, solid and platy lies below.

The dark-grey, black and very hard limestone, constituting the lower part of the section, corresponds to the XVI horizon.

There is a gamma-active pack of clayey carbonate rocks (XV-above reef) at the top of the Chiston section located more to the south. The pored and cavernous underlying limestone corresponds to the XV-a horizon. The XVI horizon is composed of dark and solid limestone.

There is also a gamma-active pack of black carbonate-bituminous shale at the top of J_{2-3} in the South Alan field. This pack belongs to the XV-above reef horizon. The XV-reef horizon is composed of grey, dark-grey, algal and solid limestone, with pored-cavernous interlayers. This section ends with a pack of solid, dark-grey clayey limestone (XVI horizon).

This non-uniform lithology and structure testifies for fluctuations of the Middle-Late Jurassic paleogeography corresponding to a barrier reef development. For this analysis we have chosen only the wells close to our line, where a complete lithological column of the Jurassic carbonates is available (fig. 3.18 and 3.19).

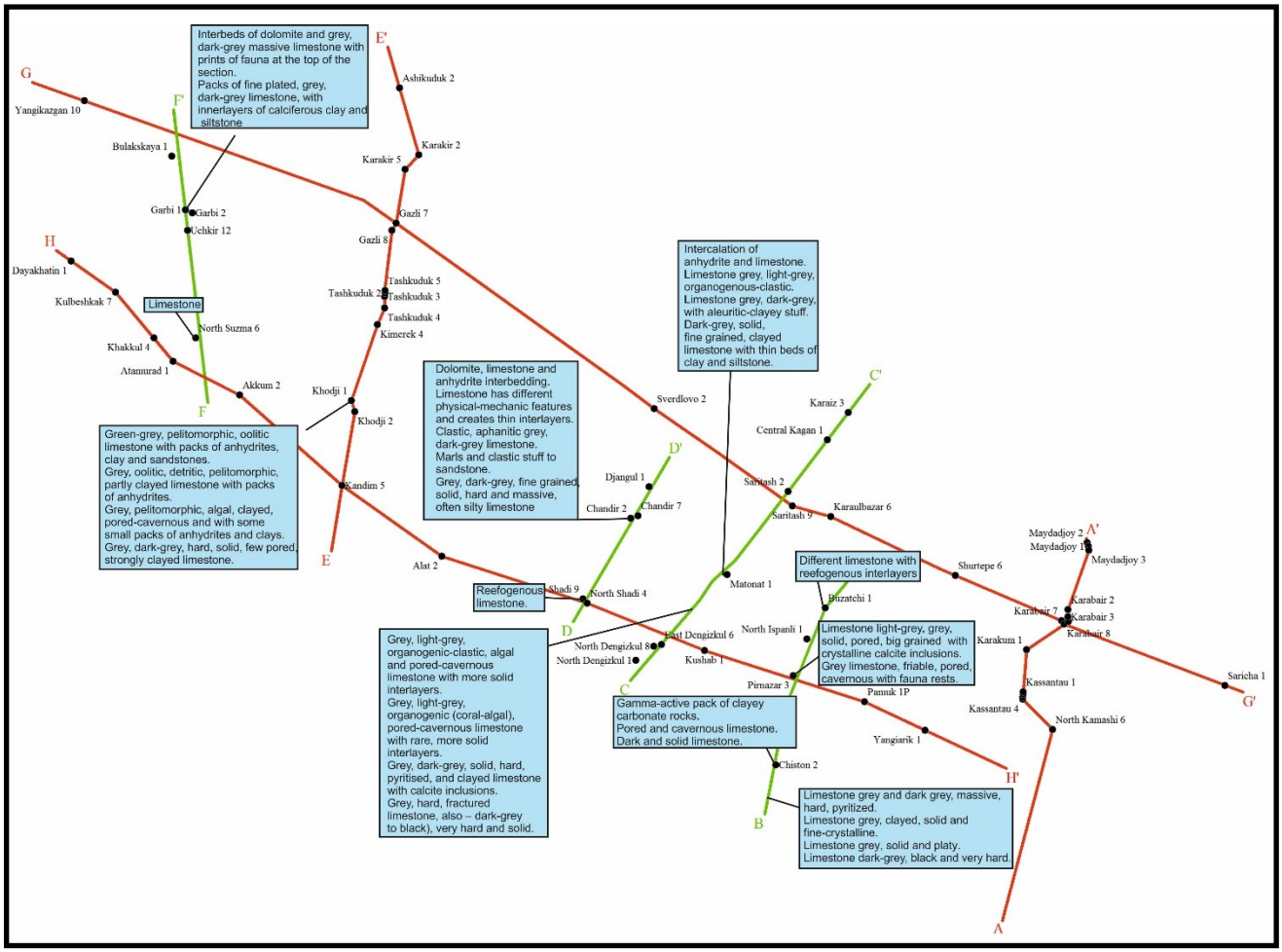

Fig. 3.19. Location of boreholes where the lithology of the carbonate unit is available.

C-C' line

On the C-C' profile the carbonate unit is described on the Matonat and West Kruk synthetic lithological columns. The Matonat carbonate section starts by an intercalation of anhydrite and limestone, which corresponds to the XV-above reef horizon. A grey, light-grey, organogenous-clastic limestone is observed below (XV-reef horizon). A limestone grey, dark-grey, with aleuritic-clayey stuff underlays it and corresponds with the XV-under reef horizon.

A pack of dark-grey, solid, fine grained, clayey limestone with thin beds of clay and siltstone tops this section (XV-a, and XVI horizons). The XV-above reef horizon is composed of grey, light-grey, organogenic-clastic, algal and pored-cavernous limestone with more solid interlayers in the West Kruk

section. A grey, light-grey, organogenic (coral-algal), pored-cavernous limestone with rare, more solid, interlayers is distinguished below. It corresponds to the XV-reef horizon here.

The XV-under reef horizon is composed of grey, dark-grey, solid, hard, pyritised, and clayey limestone with calcite inclusions. The XV-and XVI horizons correspond to a grey, hard, fractured limestone, also – dark-grey (to black), very hard and solid.

D-D' line

The profile D-D' is situated to the west of the reef system. Three lithological columns are available in its vicinity in the Chandir, North Shadi and Shadi structures.

The Chandir carbonate section starts by a dolomite, limestone and anhydrite interbedded pack. Thus, the limestone has different physical-mechanical behaviours and creates thin interlayers. This sequence forms the XV-above reef horizon. This horizon covers the undifferentiated pack including the XV-reef, XV-under reef, and XV-a horizons. They are represented by a clastic, aphanitic grey, and dark-grey limestone. In addition, interlayers of marls and clastic stuff to sandstone were observed.

The XVI horizon consists of grey, dark-grey, fine grained, solid, hard and massive, often silty limestone. At the Shadi-North Shadi fields we cannot provide such an accurate separation because of the quality of the data. However, there are some data evidencing a bioherm.

E-E' line

On the line E-E', at the Khodji field, the XV-above reef horizon is represented by green-grey, pelitomorphic, oolitic limestone with packs of anhydrite, clay and sandstone. A grey, oolitic, detritic, pelitomorphic, partly clayed limestone with the packs of anhydrite corresponds to the XV-reef horizon. The following types of limestone correspond to the XV-under reef horizon: grey, pelitomorphic, algal, clayed, and pored-cavernous, with some small packs of anhydrite and clays. The carbonate formation ends by a grey, dark-grey, hard, solid, few pored, strongly clayed limestone corresponding to the XVI horizon.

F-F' line

The lithology of the F-F', the westernmost profile, is represented at the Garbi and North Suzma sections. There are interbeds of dolomite and grey, dark-grey massive limestone with prints of fauna at the top of the Garbi field carbonate section. This pack represents the XV horizon. However, it is completely different from the same packs in the eastern part of the Chardzhou step because of the distance from the barrier reef system. Below, packs of fine plated, grey, dark grey limestone, with interlayers of calciferous clay and siltstone, which corresponds with the XVI horizon.

Conclusion

We can separate the carbonate into different zones and blocks, as we have done for the Jurassic terrigenous sediments. As it is seen from the description, the zones with the different lithology of the carbonate correspond with zones of different thickness for the Jurassic limestone. However, the lithology-facies composition differs within each block.

Locally, it may differ within one single block. This corresponds to the fact, that there are few different horizons inside the carbonate unit. For example, the XVI horizon, without significant changes, is allocated everywhere in the Bukhara Khiva territory. But, in the XV horizon we can see lateral and vertical facies variations. If its lower part (XV-a, XV-under reef) is just characterized by non-uniform facies, there are three types of section in its upper part, namely reef, lagoon, and basin types.

The massive, light colored, biomorphic, biomorphic-clastic, detritic limestone with a high porosity corresponds to the reefal type of the section. Also, clay beds have been met. The interbeds of the limestone and anhydrite belong to the lagoonal type section. Thus, the limestone is pelitomorphic, detritic, algal, fractured and cavernous. The thin carbonates and the gamma-active pack presence correspond to the basinal type section.

More generally we may say that a barrier reef system has been distinguished. The main feature of it is a reservoir which is represented by organogenic-clastic, pored-cavernous, solid, hard limestone with fauna rests. It is shown on the B-B' and C-C' lines, and corresponds to the eastern zone we have distinguished before.

There are few facial zones that take part in the formation composition. The reefal type of the section is detected at the limits of the B-B' profile (Pirnazar-Markovskoye). However, in the southern section it changes to the depression type confirmed by the occurrence of the gamma-active pack and the general thickness decrease from 400 m to 200-250 m (Chiston – South Alan).

The reef facies are observed at the C-C' line too (West Kruk). In the northern part of this line they pass to the lagoonal type (Matonat). It is possible to allocate the D-D' and F-F' lines to the western zone. There is a lagoonal type (in general) at the limits of both of them. The XVI horizon, the lowest pack of the carbonates, is common for all the profiles, and practically does not change.

3.4.2.3. Salt-anhydrite unit

The lithology of the salt-anhydrite formation is uniform and represented by intercalations of salt and anhydrite beds with some intercalated clayed layers. But, even if it looks like uniform, this formation is "a complicated polyfacial sedimentary complex of a huge salt bearing basin" (Abdullaev et al., 2010).

Generally, the evaporites are characterized by a five-members structure: anhydrite – salt – anhydrite – salt – anhydrite. In the Bukhara-Khiva margin some members are locally missing. For example there is only one thin evaporite bed at the Garbi and Kandim fields and three in the North Suzma field where the lower salt and middle anhydrite horizons are missing.

The evaporite unit is extremely thin in the Bukhara step and represented by a single (undifferentiated) salt-anhydrite sequence. Nevertheless, in some parts of the Bukhara Khiva region where lagoon-type sections have been observed (Chandir, South Alan and Chiston), an increase of the salt-anhydrite thickness exists. The lower anhydrite at the origin of this thickness increase are not so well developed in the reef type sections.

3.5. Conclusions

The cross-sections described above and presented in Figures 3.4 to 3.11, as well as the thickness maps of Figures 3.12 to 3.15 have enabled us to precise the tectonic evolution of the northern margin of the Amu-Darya basin during the Mesozoic. One of the main contributions is the study of the thickness variations in the steps. It clearly appears that a combination of several factors controls the tectono-stratigraphic evolution of the Bukhara-Chardzhou steps. Several points have been clarified but several are still questionable.

In the Bukhara-Chardzhou steps the thickness variations during the Jurassic are controlled by the conjunction of two main directions of thickening: from NE to SW and from NW to SE. It means that the thickness of the Mesozoic sediments is minimum in the NNW and maximum in the ESE.

The Bukhara-Chardzhou steps: thickness variations

A clear northeast to southwest thickening of the Jurassic sequence has been evidenced on the lines A-A', C-C', D-D', E-E' and F-F' (fig. 3.4, 3.6 to 3.9). Generally the terrigenous sediments are thin and scarce in the Bukhara step. They considerably increase in thickness southwestwards in the Chardzhou step. This thickening mainly concerns the siliciclastic sequence that may show huge thickness variations mainly related to the activity of NW-trending normal faults during the Early-Middle Jurassic. In the Chardzhou step some thick depocenters developed during this period in grabens (and half-grabens (e.g. the Kimerek graben), while on highs the sedimentation was reduced or non-existed.

This normal fault activity continued during the Middle-Late Jurassic as shown by the normal faults that controlled the sedimentation of the carbonate and/or evaporite units (e.g. see B-B' and A-A' lines in fig. 3.5 and 3.4). In the Chardzhou step the thickness of the carbonate unit also increases

southwestwards but much less and more regularly than the thickness of the terrigenous unit. Few evaporites deposited on the Bukhara step during the Late Jurassic regression in the Amu-Darya basin (fig. 3.8). They are more widespread in the basins of the Chardzhou step where they have a tendency to thicken towards the southwest and the center of the Amu-Darya basin.

The Chardzhou step and the Beshkent trough

In the southeastern Chardzhou step a roughly east-west trending basin marks the Jurassic deposition. In the so-called Beshkent trough the thickness of the Jurassic sequence reaches 2500 m. This thickening is well documented on the lines H-H' (fig. 3.11) and A-A' (fig. 3.4). On the line H-H' we note a progressive ESE-thickening of the Jurassic sequence. The thickness maps of the figures 3.12 and 3.13 clearly evidence an Early to Late Jurassic ENE-oriented basin. These thickness maps, as well as the lines plead for a period of maximum sedimentation during the deposition of the siliciclastic sequence in the Early-Middle Jurassic. It is still not clear if this Jurassic depocenter is related to a possible rifting in the Tajik basin located southwards and constituting the southeastern extension of the Amu-Darya basin.

The Uchbash-Karshi Flexure-Fault Zone

This near 435 km long major fault zone has been crossed by all of the six NE- to N-trending lines. It constitutes the structural limit between the Bukhara and Chardzhou steps. However, the study of the lines shows that the behaviour of the Uchbash-Karshi Flexure-Fault Zone is far to be homogeneous. Most of the Uchbash-Karshi Flexure-Fault Zone shows a normal fault activity during the Early-Middle Jurassic when the terrigenous sequence deposited. During this period the Kimerek half-graben was developing along the western segment of the Uchbash-Karshi Flexure-Fault Zone (fig. 3.8) as well as small minor grabens. This extensional activity was not restricted to the period of deposition of the siliciclastics but also covered the Middle-Late Jurassic times as indicated by the syndepositional activities evidenced along the Uchbash-Karshi Flexure-Fault Zone during the carbonate (B-B', fig. 3.5) and evaporite (A-A' line, fig. 3.4) deposition. The Uchbash-Karshi Flexure-Fault Zone amortizes northwestwards from the Kimerek graben. On the F-F' line (fig. 3.9) it is soon restricted to a minor fault zone that disappears to the northwest.

The quality and the density of the available data do not allow to more accurately document the normal faulting on the Uchbash-Karshi Flexure-Fault Zone during the Jurassic times. More particularly it seems that only some segments of the fault zone were active together during periods of the Jurassic, while some other segments were inactive. In any case the Uchbash-Karshi Flexure-Fault Zone constitutes one of the major tectonic features of the northern margin of the northern Amu-Darya basin, and undoubtedly the major fault zone of the Bukhara-Khiva region. It played a major role in the development of the Amu-Darya basin during the Jurassic. Our data suggest that the climax of the normal faulting occurred during the Early-Middle Jurassic.

The NE-oriented normal faults

The G-G' and H-H' lines, parallel to the strike of the steps, longitudinally cross the Bukhara and Chardhzou steps respectively. This orientation allows to more easily distinguishing the structures (faults, folds, blocks) perpendicular to the strike of the steps. The G-G' line shows that NE-oriented normal faults and grabens exist in the Bukhara step. They locally control, at least partly, the deposition of the siliciclastics and carbonates in small basins. Some of these Jurassic normal faults were still active during the Early Cretaceous, and more particularly during the deposition of the continental red beds series as indicated by the normal faults bounding the Karabair graben (fig. 3.10).

In the southeastern part of the Chardzhou step, same NE-oriented faults are visible on the line H-H' (fig. 3.11). Some of them cut the Lower Cretaceous layers, others are restricted to the Jurassic beds where they are looking like reverse faults. Taking into account the quality of the data it is difficult to know whether or not these faults were Jurassic normal faults before to be inverted (probably during the Cenozoic) or Neogene normal faults.

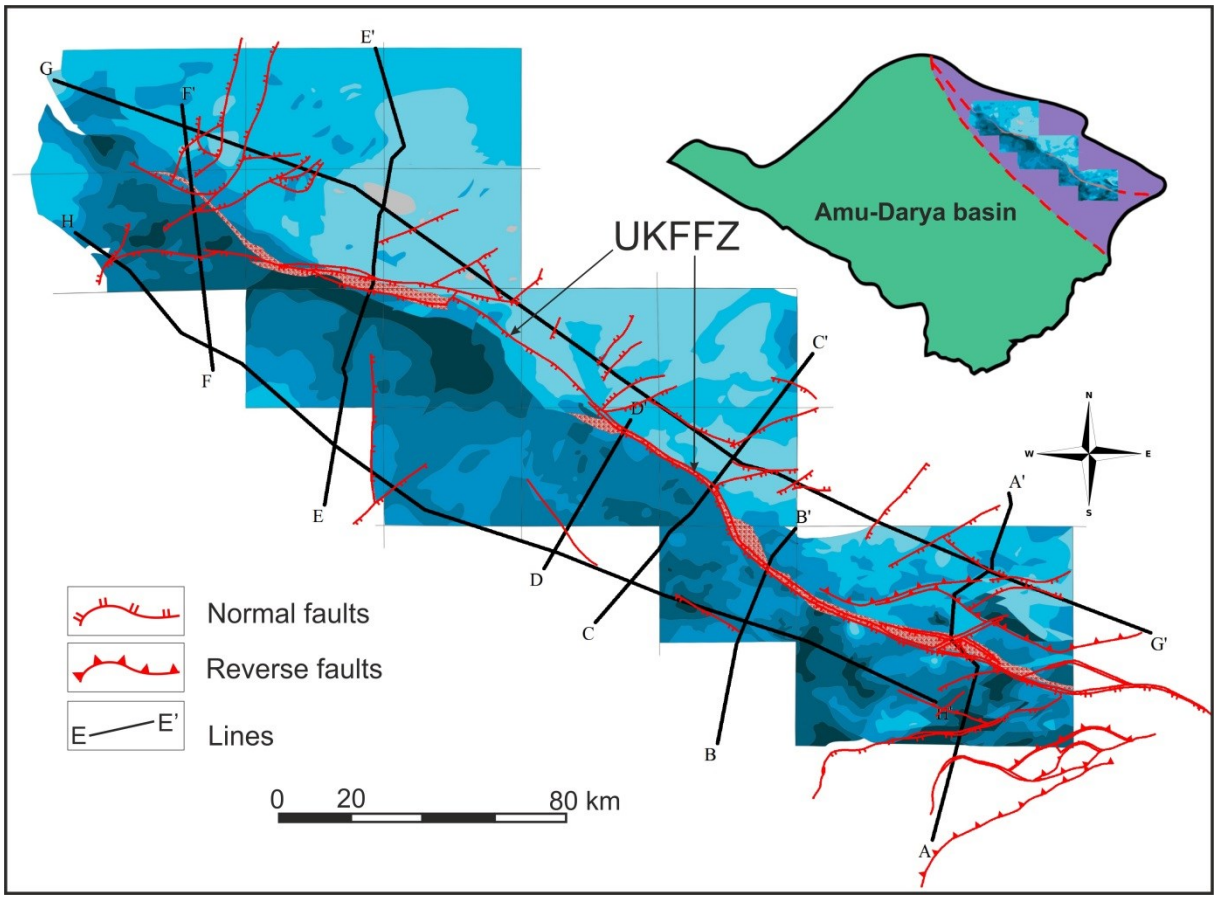

Fig. 3.20. Map of the main faults evidenced in this study
Most of the faults are normal except in the southeast near the Southwestern Gissar Range.

The Middle-Upper Jurassic reefs

Reefal bodies have been reported in the Chardzhou step since the hydrocarbon exploration initiated in the first half of the XX century. Exploration wells crossed such structures in the central part of the Chardzhou step. Some of these reefal bodies crop out in the south of the Southwestern Gissar Range in southern Uzbekistan and eastern Turkmenistan. A model of deposition of the carbonate has been proposed by several authors (Mirkamalov et al., 2005; Abdullaev et al., 2010) to explain the non-uniform deposition of the carbonate on the Bukhara-Chardzhou step during the Middle-Late Jurassic.

During this period, different types of carbonate deposited at the same times: reefal, lagoonal, and basinal on the Bukhara-Chardzhou step. The reefal type is considered by the authors of the model as deposited in a barrier reef system. In their model the lagoonal and basinal types deposited in different paleogeographic conditions, separated by the reef barrier.

In our data, especially in the seismic profiles crossing the reef barrier (B-B' fig. 3.5, C-C' fig 3.6, D-D' fig. 3.7), no large reefal body was clearly identified, except in the B-B' line (fig. 3.5) where such structures were identified.

Consequently, it is difficult with the available sub-surface data to give one opinion on the validity of the reefal barrier model separating lagoonal and basinal environments of deposition. The maps of Figures 3.15 and 3.18 show that the distribution of the reef barrier in the Chardzhou step forms an inverted U-shaped belt with NW- to WNW- and NE-oriented alignments. This particular geometry may suggest that the reef development was controlled by the NW-trending Uchbash-Karshi Flexure-Fault Zone, and NE oriented Jurassic normal faults (fig. 3.20). The reefs could develop on highs marking the crests of the footwalls of the main normal faults. This hypothesis needs to be confirmed by studies of more precise sub-surface data.

The Cretaceous evolution

The Cretaceous units exhibit rather isopach sequences, especially the Upper Cretaceous one. The Cretaceous sediments broadly fill up the steps with a several hundreds of metres thick sequence. Generally speaking they progressively thicken towards the southwest and the center of the Amu-Darya basin. In the Chardzhou steps the Cretaceous units reach the thickness of two kilometres whereas they are 1500 m thick in the Bukhara step. In the Early Cretaceous, clues of extensional activities exist, particularly in the continental lower part of the sequence. The G-G' line (fig. 3.10) shows that NE-trending normal faults control the sedimentation during these times in the southeastern Chardzhou step. In the Late Cretaceous no extensional tectonics has been reported.

Chapter 4

Tectonic subsidence analysis

Chapter 4

Tectonic subsidence analysis

In the previous chapters we have described the geological structure of the Bukhara-Khiva and Southwestern Gissar regions. The main aim of this thesis is, the reconstruction of the geological-tectonic evolution of these two areas according to the main large scale tectonic events which affected Western Central Asia. One of the possible methods to do this is the tectonic subsidence analysis. It allows tracing the subsidence evolution of the area from the very beginning of the sedimentation in the basin to the Present time.

4.1. Methodology

4.1.1. What is the tectonic subsidence?

Before to start the analysis, we may specify what the tectonic subsidence is, how it acts and which factors have influence on it.

The subsidence is one of the important factors of the sedimentary basin evolution corresponding to the vertical movement downwards of the basement of the basin. Three important mechanisms leading to the subsidence are the lithospheric thinning, the cooling and the loading to which we may add the horizontal stresses. The disequilibrium they create in the lithosphere-asthenosphere column is controlled by isostasy, compensated by mantle movements at the boundary lithosphere-asthenosphere and inducing the tectonic subsidence of the crust surface. For a simple analysis and in first approximation, the subsidence is studied in supposing a local isostatic compensation assuming that the lithosphere has no stiffness and responds only to the load directly above it.

Two main models of isostatic equilibrium were proposed by G.B. Airy and J.H. Pratt in the 19th Century (fig. 4.1).

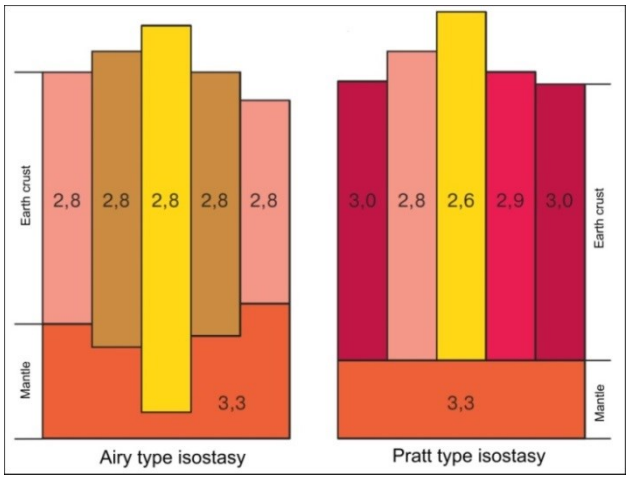

Fig. 4.1. Airy and Pratt isostatic models (after Koronovsky, 2001).

In the isostatic model of Airy, the earth crust has more or less the same density and an excess of topography and the creation of a root in the underlying denser mantle are compensating a crustal thickness variation. At the same time, the Pratt model supposes that the bottom of the crust is flat and the isostatic compensation appears by lateral density variations of the crustal blocks.

When this equilibrium breaks, for example, by changing the thickness or density of the lithosphere column, or by replacing lithospheric mantle by lighter asthenosphere, it leads to the area subsidence or uplift.

The changes in the lithosphere can be caused by its stretching (or only crustal stretching), removing the crust by erosion or tectonic forces, its thickening during compression or emplacing of dense

material into the column (by intrusions, metamorphism, thrust ophiolites..) or replacing the water by sediments (Angevine et al., 1990).

Another factor which has an influence on the subsidence, is the lithosphere temperature changes for example during the lithospheric stretching, when the boundary lithosphere/asthenosphere is uplifted and also the isotherms (McKenzie, 1978).

The thermal changes appear as a consequence of the extensional tectonic movements which initiate the crustal thinning of the future basin area. In this case, the asthenosphere material rises to compensate the lithospheric thinning (fig. 4.2) and, as it is hotter it warms the lithosphere and the crust. During the stretching =rifting, the subsidence is generally fast (deposits of synrift sediments), normal faulting occurs. While the basin subsides, it fills in with water and sediments, which are transported from the margins of the basin. More sediments are deposited, pulling down the basin. Then the lithosphere cools during a phase of postrift slower subsidence. The lithosphere returns to its initial thickness.

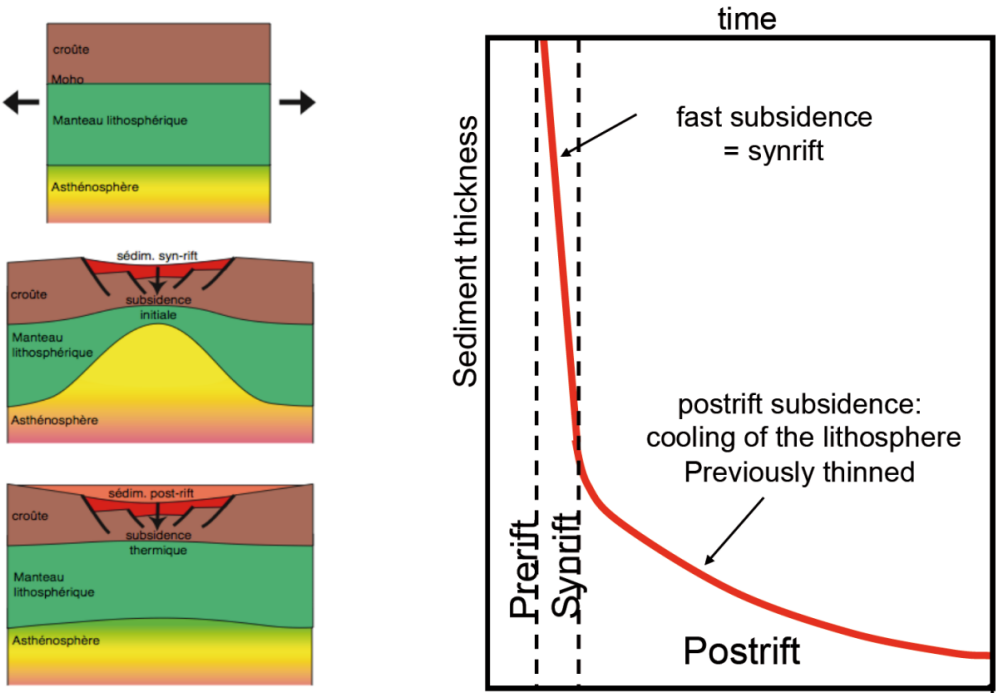

Fig. 4.2. Model of an extensional basin evolution (modified after Séranne, 2014).

The *tectonic subsidence* is amplified by the loading of the water and of the sediments deposited in the basin also balanced by isostasy resulting in the *total subsidence*, corresponding to the basement burial (or paleodeepening) observed in a basin.

4.1.2. Method of subsidence reconstruction

The history of a sedimentary basin is reflected in the sediments, deposited in this basin throughout the time. The geological outcrops exhibit well the sedimentary changes for the facies and lithology but well data are more precise for the thicknesses. These data show the present condition of the sediments, and the goal of the subsidence analysis is to reconstruct the subsidence history of the basin through time since its origin. The result of such analysis is the graphic representation of the vertical movements of the basement through time: the subsidence curve, with respect to a reference present 0 level (fig. 4.3).

The method, which we used for such analysis is called the *backstripping method* to remove the effect of the sediments loading (Steckler and Watts, 1978). The feature of this method is to take out the sediments of the different stratigraphic levels progressively from the present day to the time before the first sediments were deposited and in taking into account the variations of the sea-level.

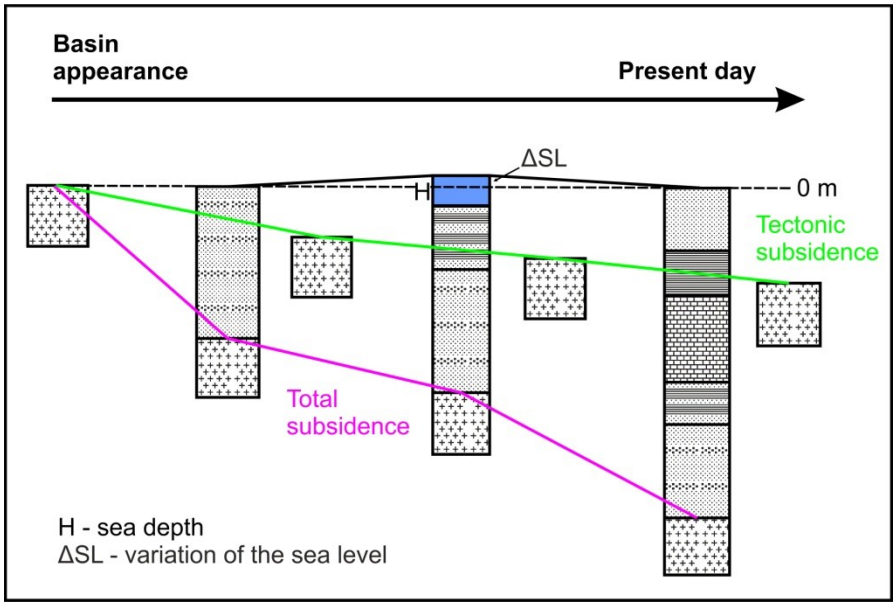

Fig. 4.3. Schematic example of the total and tectonic subsidence evolution of a basin through time (horizontal axis), at four steps from its origin without sediments to the Present day, by using the backstripping method (modified after Brunet, 1989).

For all these calculations and computations we have used the SUBSID computer program (Brunet, 1981), based on the principles of the local isostasy (Airy type) using the backstripping of the sedimentary column and computing the total and tectonic subsidence Y, in free air, through time (fig. 4.4).
The principal formula, which compounds the core of the calculation, is:

$$Y = S\left(\frac{\rho m - \rho s}{\rho m}\right) + H\left(\frac{\rho m - \rho w}{\rho m}\right) - \Delta SL$$

where Y is the tectonic subsidence in free air;
ρm is the density of the mantle material, making the compensation ($\rho m = 3.2$);
S, ρs are the thickness and average density of the sedimentary column;
ρw is the density of the sea water (ρw =1.03);
H is the paleo-water depth (paleo-bathymetry);
ΔSL is the sea-level variation, in relation to the modern mean sea-level = 0 line.

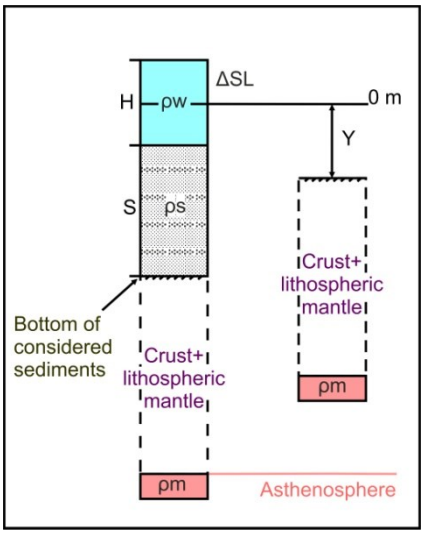

Fig. 4.4. Calculation of the tectonic subsidence in free air (modified after Brunet, 1989).

As the backstripping analysis is closely connected to the geological time, it is necessary to choose a correct time scale. In our reconstructions we have used the recent version of the International Chronostratigraphic Chart (2014), approved by the International Commission on Stratigraphy (2014) (fig. 4.5).

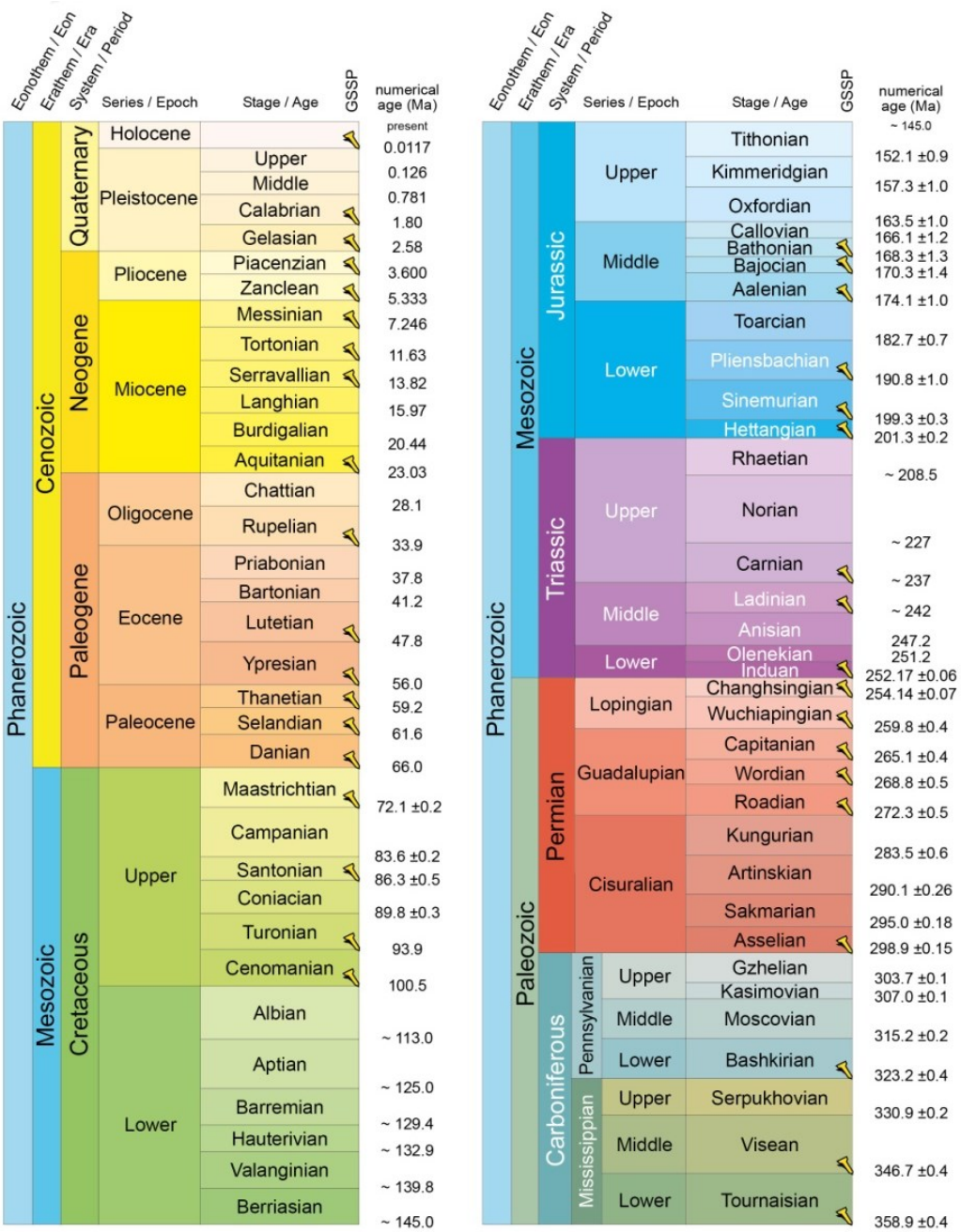

Fig. 4.5. Fragment of the International Chronostratigraphic chart, 2014/10 (International Commission on Stratigraphy, 2014).

The reference level to calculate the subsidence is the present sea-level (0 line). The sea-level fluctuated through time, differing by ΔSL from the present day one. The eustatic (world-wide) variations of the sea-level have been studied by many authors proposing various curves and amplitudes (for example see Figure 4.6). For our calculations we chose the first order curves of Haq 2014 (in Sengör et al., 2014) (fig. 4.7), but calibrated with a maximum of 170 m during the Late Cretaceous transgression (maximum average value of Müller et al., 2008).

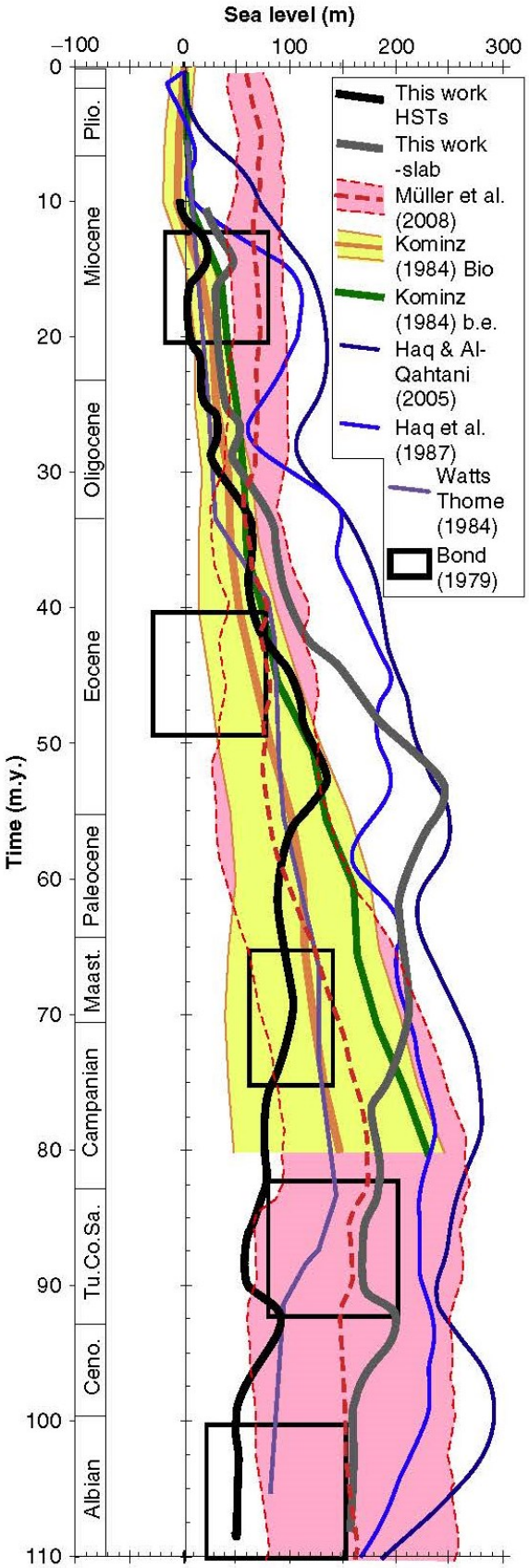

Fig. 4.6. Comparison of some long-term curves of sea-level changes (after Kominz et al., 2008 and references herein). “This work” means Kominz et al. (2008) (Ceno., Cenomanian; Tu.Co.Sa, combined Turonian, Coniacian and Santonian; Maast., Maastrichtian; Plio., Pliocene).

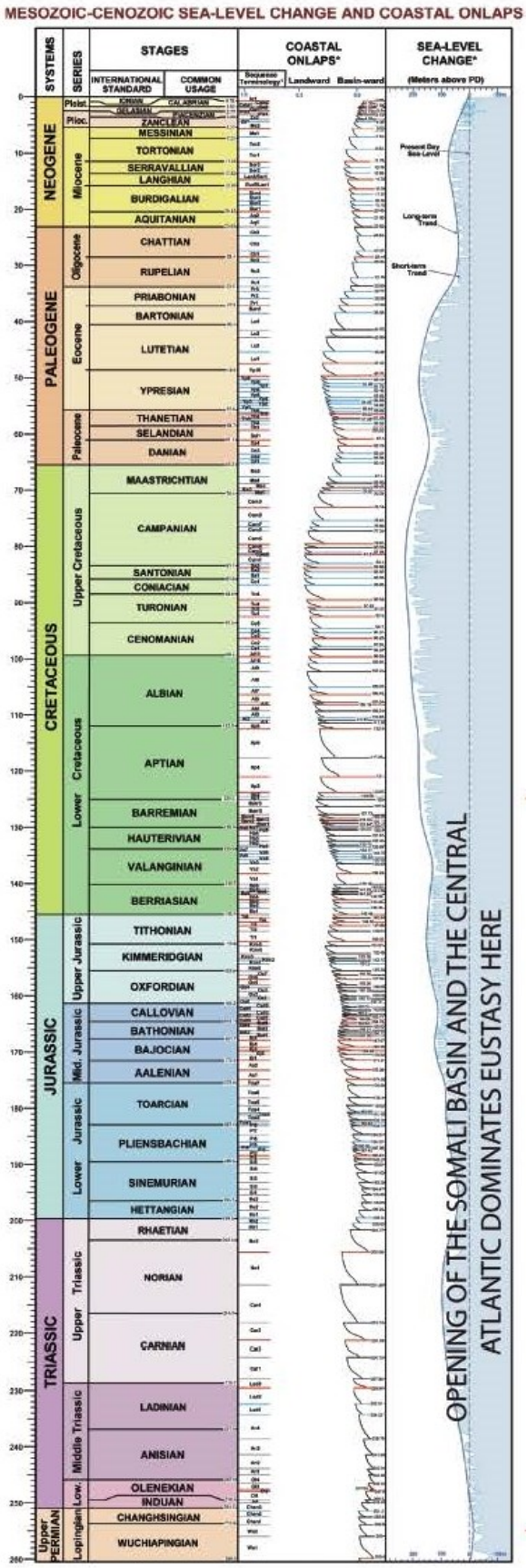

Fig. 4.7. Mesozoic-Cenozoic world-wide eustatic sea-level changes
(B. Haq, written communication September 2014 in Sengör et al., 2014, modified).

At each step of the backstripping, the compaction undergone by the sediments is removed. Indeed when buried, the sediments loose progressively the interstitial water with depth, the porosity and the thickness decrease and the main density of the layer increases.
For calculating the density of the sediments ρ_s, another formula has been used:

$$\rho_s = \varphi \times \rho_e + (1 - \varphi) \times \rho_g$$

where: ρ_s is the density of sediments;
φ is the porosity of the deposits, varying in function of depths and lithology (see Brunet, 1989 for the curves used, mainly with an exponential decay with depth);
ρ_g is the grain density of the deposits, varying with the lithology (table 4.1);
ρ_e is the density of the sea water (1.03).

Rock type	***Grain density***
Anhydrite	**2.96**
Clay 1	**2.65**
Clay 2	**2.71**
Clayed limestone	**2.66**
Conglomerate	**2.65**
Dolomite	**2.87**
Gypsum	**2.31**
Limestone	**2.71**
Marl	**2.75**
Salt	**2.17**
Sandstone	**2.65**

Tab. 4.1. Values of the grain density (parameter ρ_g) according to the lithology.

Once these general parameters are chosen, the data of the basin studied are analysed. They include, the thickness of each sedimentary layer for which the age of the boundaries is known, the lithology and facies to make a hypothesis on the paleo-water depth. The subsidence is computed and curves of total and tectonic subsidence are drawn as well as the velocities of tectonic subsidence. The velocities are compared to each other and described as “high” or “low” but the general evolution of the area has low tectonic subsidence rates in general, as we are on the margin of a basin and not in a basin itself.

The characterization of periods of acceleration of the tectonic subsidence in the history of a basin allows to specify the timing of tectonic events. The tectonic calendar which is then determined, is put back in the geodynamic context of the area to identify the tectonic causes of these events.

We applied this method to some wells of the northeastern margin of the Amu-Darya basin to get information on the Amu-Darya basin geodynamic evolution.

4.2. Subsidence reconstructions for some wells of the Bukhara-Khiva and Southwestern Gissar regions

As the most important evolutional events of the northeastern margin of the Amu-Darya basin have taken place in the Mesozoic, especially in the Jurassic, we have selected for our reconstructions some wells where the Jurassic section was the most complete. No details of thickness exist in the drillings for the pre-Jurassic rocks which were penetrated only for few metres, so we will begin our reconstructions from the beginning of the Jurassic. We tried also to choose a set of points well distributed over our study area to represent the evolution of the main domains. Eighteen wells answer to this criterion: three wells in the Southwestern Gissar, six wells in the Bukhara step and nine wells in the Chardzhou step, including two wells in the eastern deepest part of the Chardzhou step: the Beshkent trough, located near the Southwestern Gissar.

The main source of the wells stratigraphic data has been the wells catalogue of the «Uzbekgeofizika» company. This catalogue concerns the stratigraphic, tests and productivity data about most of the wells of the Bukhara-Khiva and, partly, the Southwestern Gissar regions. The sources of the data about wells lithology, in general, were synthetic lithostratigraphic sections, elaborated for different oil and

gas fields. We had access only to these sections and we will refer to them by the name of their authors and the year of their setting up, indicated on the section, but often we do not have the full information about the titles of the reports in which they are included, most of the time authored by other people. The age of the pre-Jurassic rocks was checked for some wells in the report of Babadjanov (2008).

Very often the wells selection has been complicated because many wells data comprised only stratigraphic details (ages and depths of layers boundaries), without lithology. Where it was possible, we tried to find the complete wells with both the lithology and the stratigraphy, these data come also from the «Uzbekgeofizika» company. For the places, where it was not possible, we chose the wells with the most complete stratigraphy and we took the lithology from the synthetic section of the field the well belongs to, or from the nearby structures. If in some empty areas we had nothing, we constructed synthetic wells, using seismic lines and isohypses data for the stratigraphy and neighbouring wells information for the lithology.

While choosing wells, we paid attention to the following features: their location, the maximum depth and stratigraphic level reached, their lithostratigraphic characteristics, including some peculiar features of each well (absence of some strata, for example). In Chapter 3 concerning the study of sections, the Jurassic terrigenous unit was marked J_{1-2} without precision. Thus, the terrigenous Jurassic will appear in this way on the fragments of cross sections shown to illustrate the location of the wells. We tried to collect, when it was possible, more information on the ages in the chosen wells and in fact only very few contain Lower Jurassic sediments J_1. When it was possible, with available hypothetical cross-sections, we made hypotheses on the total thickness of the terrigenous unit for the wells not reaching the pre-Jurassic beds.

Another point is that most of the wells are old and some stratigraphic divisions are different from the recent stratigraphic chart. This is the case for the lower part of the Lower Cretaceous marked as Neocomian. This stage corresponds to the Berriasian-Valanginian. The Barremian interval is also included in all the wells and even the Aptian for one well. Another united stratigraphic interval exists in the top of the Cretaceous. The four stages, from Coniacian to Maastrichtian, were not divided in the original columns and marked as Senonian.
In our columns, we have converted the Neocomian stage into the undivided sequence of the Berriasian-Barremian and the Senonian stage into the undivided sequence of the Coniacian-Maastrichtian.

The lithological features of the different strata in wells and some depositional environments specified in Chapter 2 allowed us to make hypotheses (the values will be indicated on each column) on the paleobathymetry existing when these layers were deposited. We took for example few metres of paleowater depths when reefal limestone was present and no water at the end of evaporites.

Besides, we have divided the study area into four zones from the northwest to the southeast (fig. 4.8). This allows to show some details of the large maps used in this work for a better understanding of the structural features of the area, where the selected wells are located. We used the scheme of the pre-Jurassic surface ages and the relief maps of the following main levels: the roof of the crystalline basement, the roof of the pre-Jurassic rocks, the top of the terrigenous Jurassic, the top of the carbonate Jurassic and the top of the horizon XII of the Lower Cretaceous (horizon mainly of Aptian age ending in the base of the Albian) (fig. 4.10-A, B, C, D, E, F for the first zone). These maps are isohypse maps in negative values; they have been generated from the zero elevation datum, while our columns expose the depth values measured from the ground surface (data used for the subsidence analysis). Thus, the depth values on the maps do not correspond to the depth marks of the same levels in the wells. To obtain the depths marked on maps, the altitude values must be substracted from the depth marked in the wells.

For each of these areas going from the northwest of the Bukhara area to the southeast in the Southwestern Gissar, we will describe separately the wells' features, at first for the Bukhara step, then for the Chardzhou step. We will show the resulting subsidence curves of each of the selected wells, after a description of the data used as well as of some complementary data allowing to situate the well in the frame of the surrounding structures. In conclusion, we will correlate and compare the main events identified by the tectonic subsidence analysis.

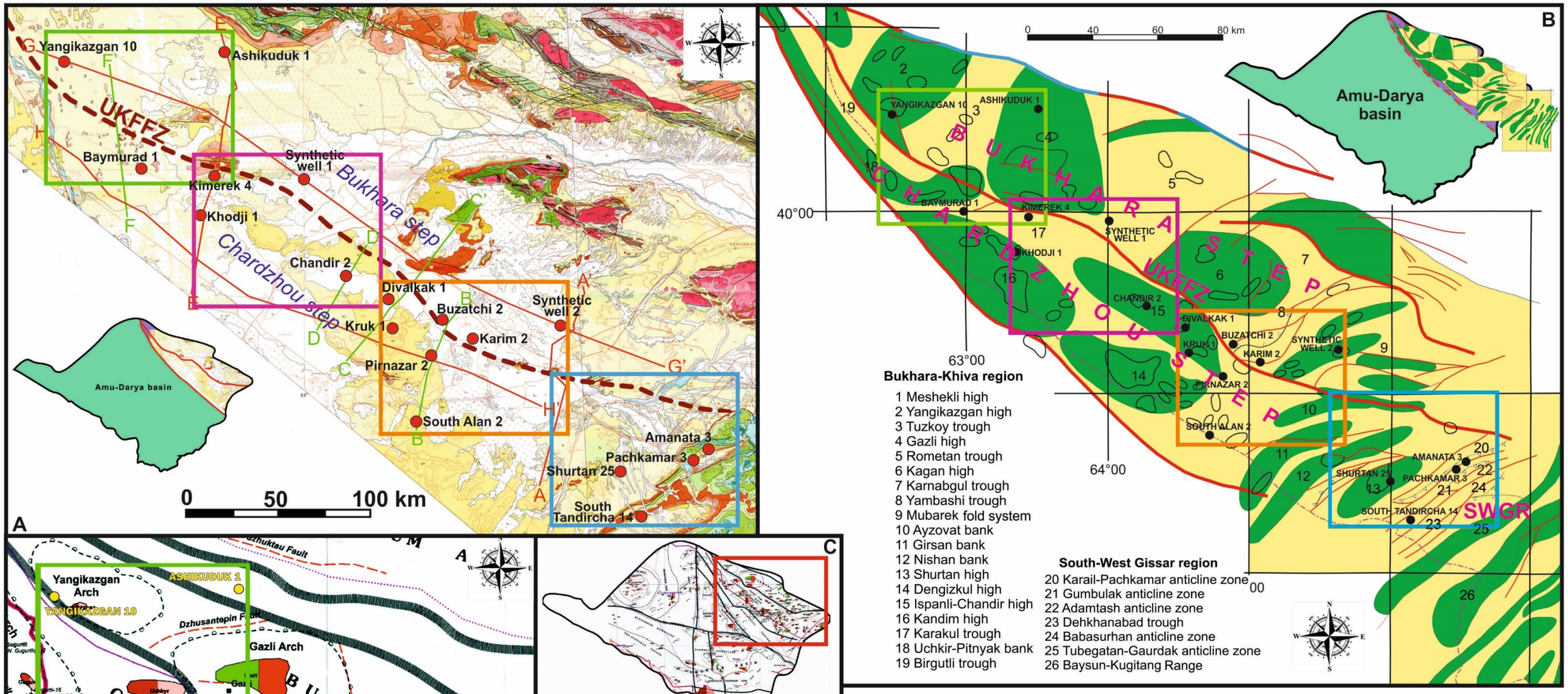

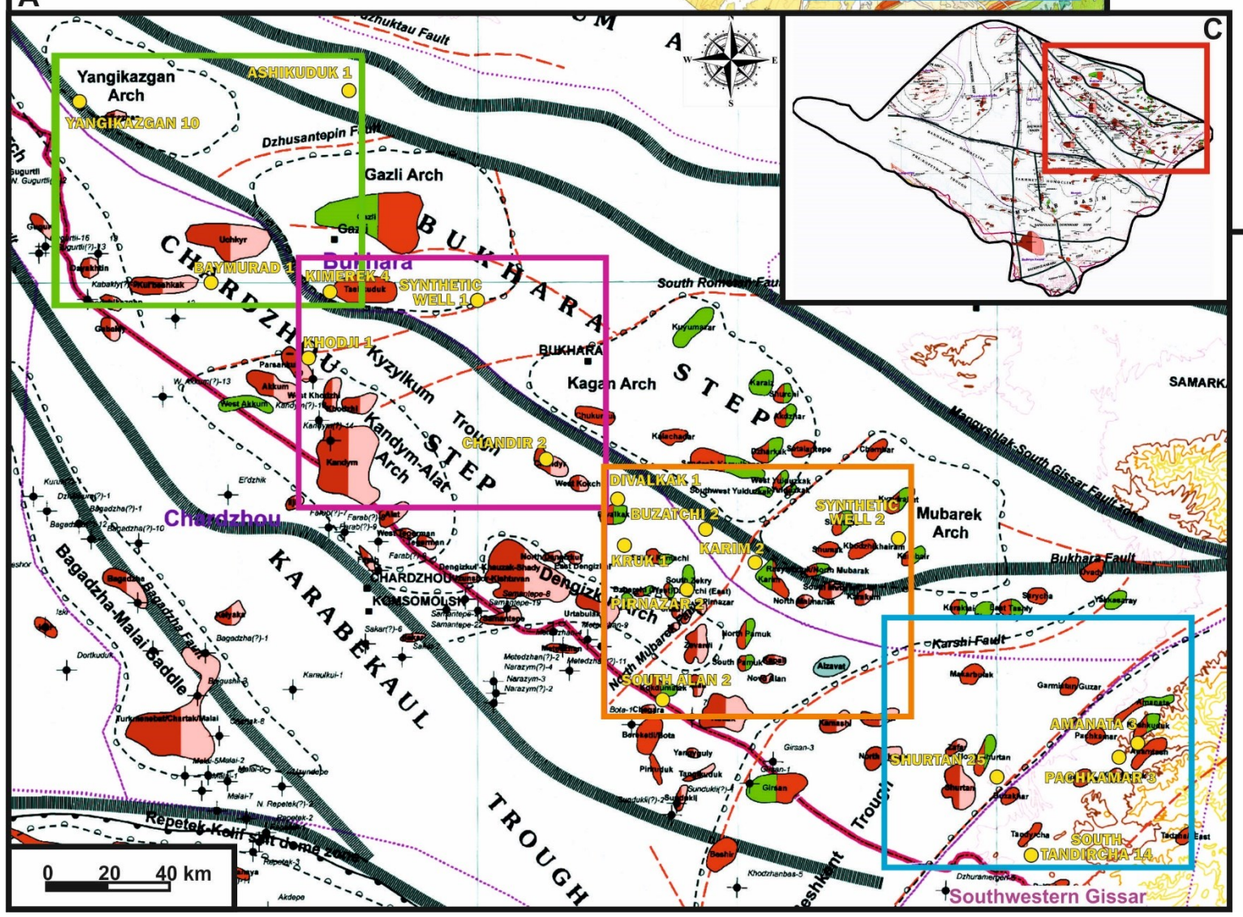

A - Location of wells, selected for the subsidence analysis, with respect to the sections described in Chapter 3. Background = geological map of Uzbekistan, 1998.

B - Location of the selected areas with respect to the tectonic structure of the Bukhara-Khiva and Southwestern Gissar regions. Background = tectonic scheme of the northern part of the Amu-Darya Basin (modified after Abidov et al., 1999). Green = highs, yellow = lows.

C - Location of selected areas with respect to the main oil and gas fields of the Bukhara-Khiva and Southwestern Gissar regions. Background = map after Blackbourn, 2008, modified.

Fig. 4.8. Location of wells, selected for the subsidence analysis and subdivision of the studied region into four areas.

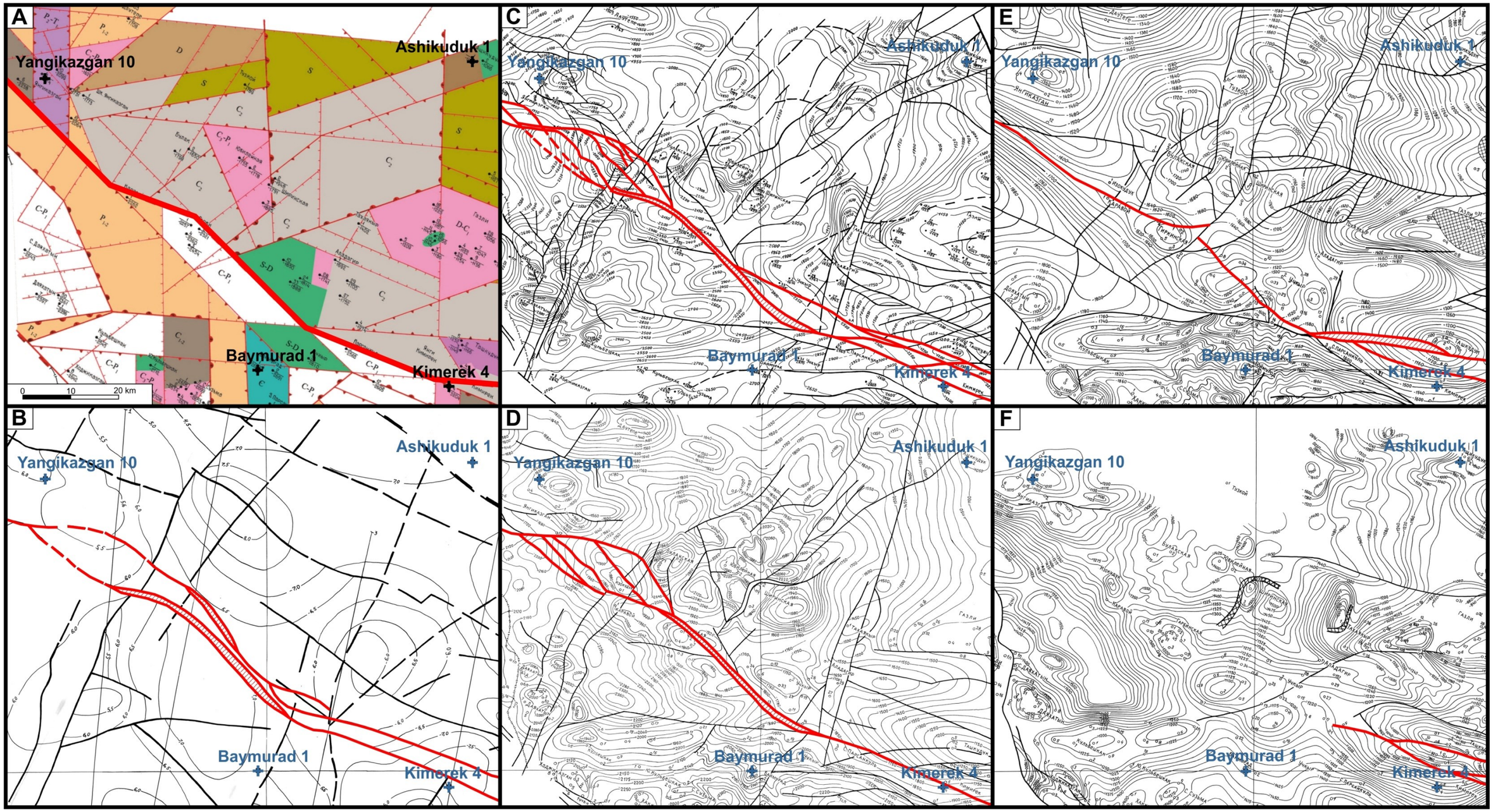

Fig. 4.10. Location of the wells studied in the first westernmost selected area, Yangikazgan-Baymurad and of faults (in red) associated to the Uchbash-Karshi Flexure-Fault Zone.
A – age of the pre-Jurassic surface on a paleogeological scheme of the pre-Jurassic surface of the Bukhara-Khiva region. Є: Cambrian, S: Silurian, D: Devonian, C. Carboniferous, P: Permian, T: Triassic; magmatism: intrusives in pink, effusives in dark green (after Babadjanov and Abdullaev, 2009, modified);
B-F: Isohypse maps (after Mordvintsev O. in Babadjanov, 2008, modified), **B** – relief of the crystalline basement, **C** – relief of the pre-Jurassic roof, **D** – relief of the Jurassic terrigenous roof, **E** – relief of the Jurassic carbonates roof, **F** – relief of the horizon XII roof in the Lower Cretaceous.

4.2.1. Yangikazgan-Baymurad western area

The first selected area is located in the northwesternmost part of the Bukhara-Khiva region. This area occupies a part of the Yangikazgan high, Tuzkoy trough and a part of the Gazli high in the Bukhara step and parts of the Uchkir-Pitnyak bank and Birgutli trough in the Chardzhou step (fig. 4.8-B).
The wells chosen in this area for the subsidence analysis are: Yangikazgan 10, Ashikuduk 2 in the Bukhara step and Baymurad 1 in the Chardzhou step (fig. 4.9). The Kimerek 4 well is located in this area too, but it will be described with the second area.

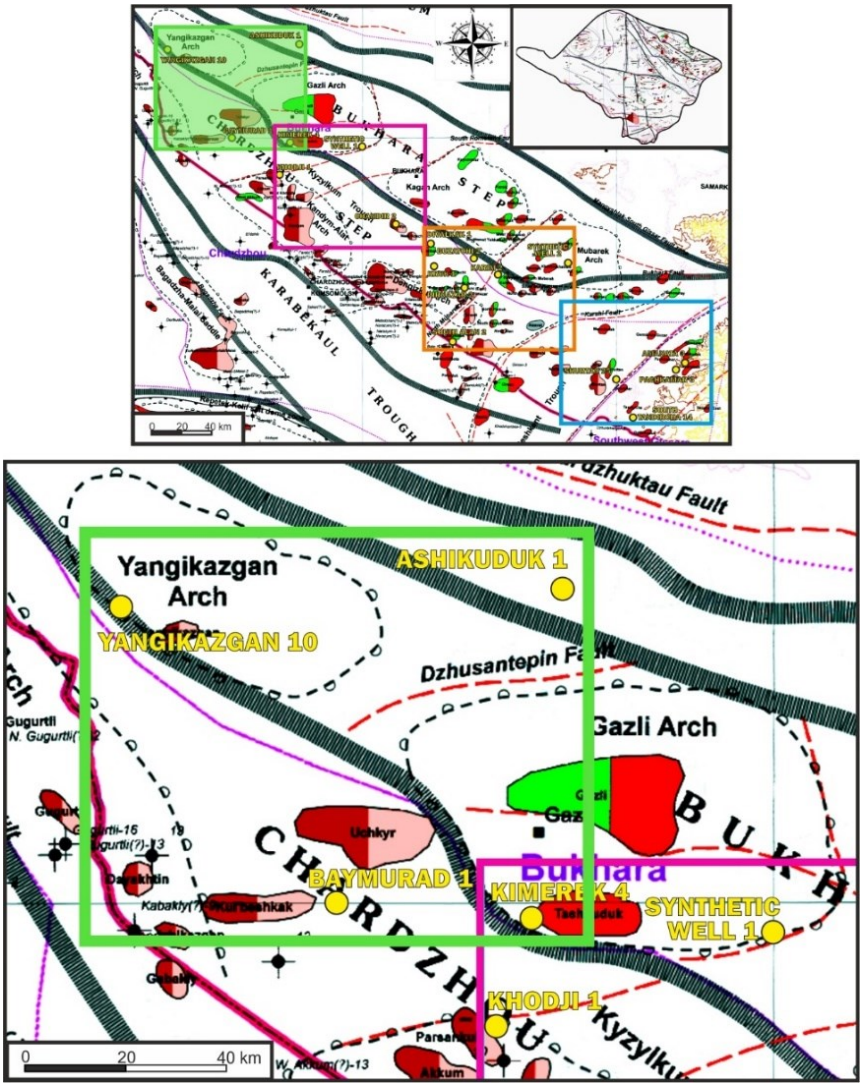

Fig. 4.9. Location of the wells studied in the Yangikazgan-Baymurad area (background map after Blackbourn (2008), modified).

4.2.1.1. Yangikazgan 10 well

The Yangikazgan field, where is located the Yangikazgan 10 well is the westernmost structure of the Bukhara-Khiva region (fig. 4.8). It is located on the Yangikazgan high within the Bukhara step, just to the north of the UKFFZ (fig. 4.8, 4.9).

Unfortunately, we did not found a complete lithostratigraphic column in the list of the available wells, drilled in this field and chose the Yangikazgan 10 well which is one of the thickest. We used the stratigraphy from the wells catalogue of «Uzbekgeofizika» and a simplified lithology from an old geological section (Ostrovsky, 1965) crossing the Yangikazgan field from north to south, but reflecting well the lithostratigraphic relations of the various layers.

We have also used this well in our geological reconstructions of the G-G' line (fig. 4.11).

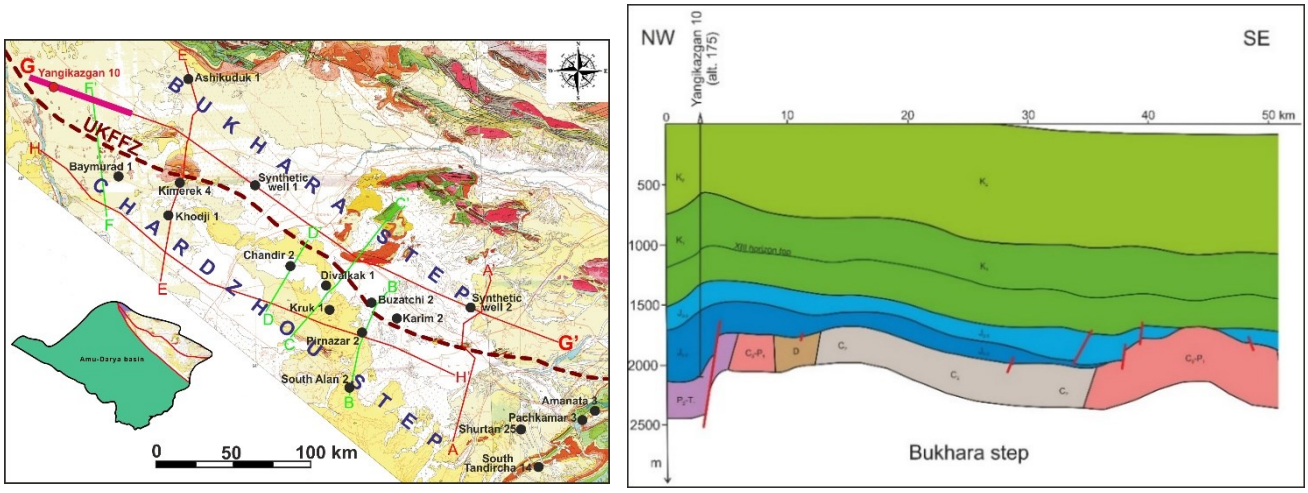

Fig. 4.11. Fragment (thickened part on the map) of the G-G' line, NW-SE oriented along the Bukhara step, showing the Yangikazgan 10 well. See Chapter 3 fig. 3.10, for details on the full line.

According to the column we have selected, there are Jurassic, Cretaceous and Cenozoic sediments in the Yangikazgan area. The Jurassic sequence is incomplete, but rather thick. It is represented by the Lower-Middle Jurassic terrigenous unit and the Callovian-Kimmeridgian carbonates. The precise age of the terrigenous clastics is not given on both lithological and stratigraphic sections as they are marked only as "terrigenous Jurassic". We chose to begin our column (fig. 4.12) with a possible age Pliensbachian coming from a spore-pollen assemblage identified in the interval 2238-2247 m of Yangikazgan 10 (Aliyev et al., 1983) in this analog of the Sanjar Formation; according to the same authors the age could be even older, Late Sinemurian. The Cretaceous starts with a Berriasian-Aptian undivided layer and concerns all the other stages. The Cenozoic part consists of Paleogene and undivided Neogene-Quaternary sequences.

The section we selected touches, but does not penetrate the pre-Jurassic level which is simply indicated Paleozoic in the catalogue of wells of «Uzbekgeofizika» as well on the cross-section of Ostrovsky (1965). The age given in Babadjanov (2008) is Permian. The scheme of the pre-Jurassic ages (fig. 4.10-A) shows that the well is located in a NE oriented graben of Permian-Triassic beds (P_2-T_1), which forms the northwestern flank of the Yangikazgan anticline. This graben-like structure observed in the northwestern end of the G-G' line (fig. 4.11), is bounded on the east by a WNW dipping fault cutting the Permian-Triassic and disappearing upwards in the terrigenous Jurassic. Other faults of the Yangikazgan area are also concentrated in the pre-Jurassic and decrease up to the Lower Cretaceous.

The section of Yangikazgan 10 is 2278 m long. The Jurassic takes 745 m from them, the Cretaceous is the thickest part with 1464 m and the Cenozoic sequence is 69 m thick (fig. 4.12).

From the viewpoint of lithology, the section of Yangikazgan 10 shows a sandy-clayed section, with some carbonate inclusions. The Jurassic terrigenous unit consists of alternating layers of clay and sandstone, the Callovian-Kimmeridgian carbonate is represented by limestone and clayed limestone. The Cretaceous strata expose alternations of sandstone and clay. The Paleogene is composed of limestone and the undivided Neogene-Quaternary sequence of sandstone.

The interesting features of the Yangikazgan 10 well section are a terrigenous unit probably beginning in the Lower Jurassic and the fact that the Tithonian is missing. As we have noted in Chapter 2, the Tithonian is a widespread layer composed of the salt-anhydrite unit which ends the Jurassic in the Bukhara-Khiva and Southwestern Gissar regions, while it is absent of the Yangikazgan 10 section but is represented by a thin sandstone layer in some other wells of the Yangikazgan area (cross section of Ostrovsky, 1965).

For this first set of subsidence curves (fig. 4.13), we give some details, which will be available for all the curves, on how are built the beginning and end of the curves. The origin of the curves is set at zero at the beginning of the Jurassic, but no sediments of this age have been recognized in our study.

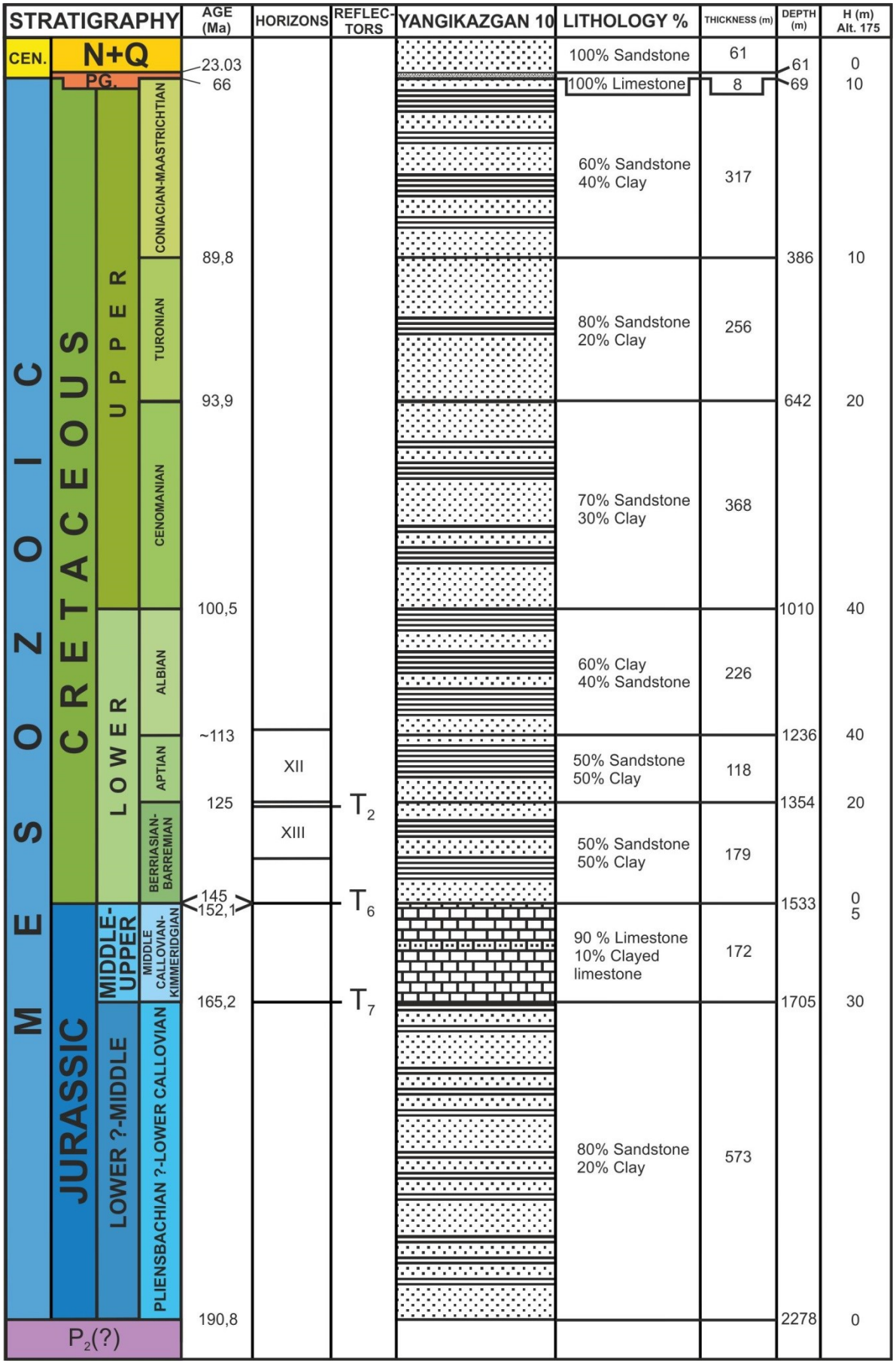

Fig. 4.12. Lithostratigraphic column of the Yangikazgan 10 well.

The second point corresponds to the beginning of the sedimentation for the studied well during the Early or Middle Jurassic. The corrections for this point are made with no bathymetry, as the environment was continental and with the positive sea-level at that time (fig. 4.7). It leads to a level (as an altitude which could be higher) above the present zero sea-level which is represented by the horizontal "x" axis of ages. Thus there is an edge effect with an uplift between the beginning of the Jurassic (set at zero) and the first real point of the column studied. At the end of the curves, the last point observed before Present, is very often the beginning of the Neogene as we do not have many data on the Cenozoic and only few points to draw our curves. The bathymetry is nil for this point as the facies is continental, but also no altitude and a correction of sea-level is made. It is linked to the present state (0 Ma) corrected with the observed present altitude. The last event of the curves is consequently an uplift, but its timing is not representative as we do not have precise age divisions in the continental layers and no paleo-altitudes.

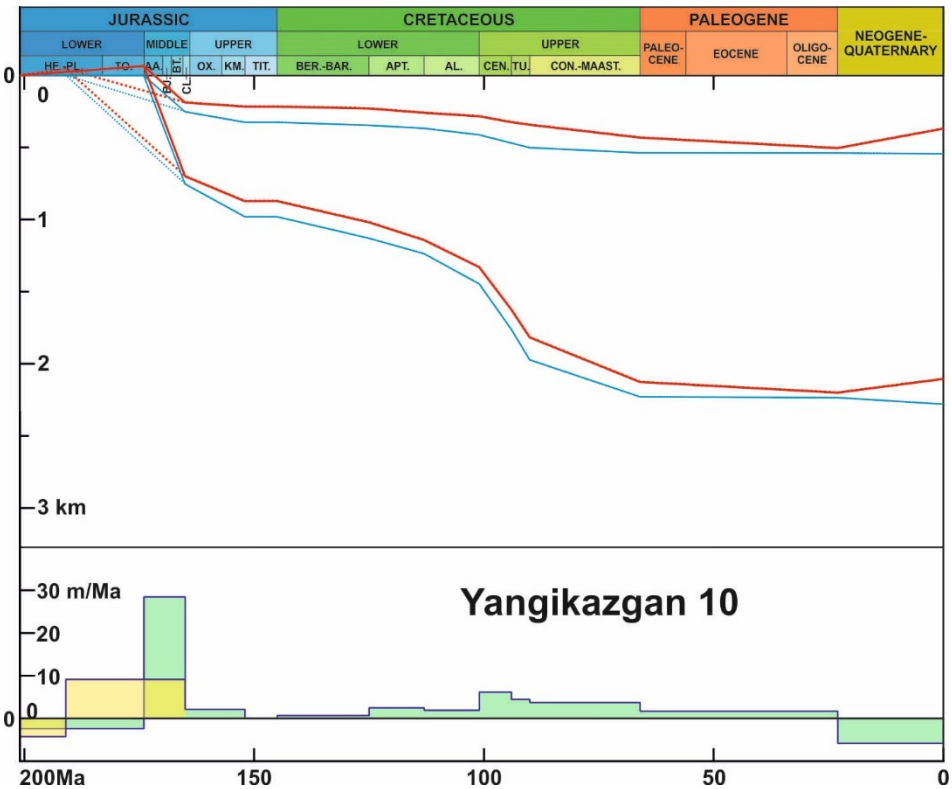

Fig. 4.13. Subsidence curves of the Yangikazgan 10 well.

Two curves at the top = tectonic subsidence in free air. *Two curves at the bottom of the upper part of the figure*= paleo-deepening of the pre-Jurassic "basement", called total subsidence. Blue curves = subsidence without corrections of sea level and bathymetry; red curves = subsidence with corrections; green diagram at the base of the figure = velocities/rates of corrected tectonic subsidence.

Two hypotheses are shown for the age of the beginning of the terrigenous Jurassic: Aalenian with continuous lines and green diagram for the Aalenian-Lower Callovian, and Pliensbachian with dotted lines and yellow part of the bottom diagram. From Middle Callovian onwards, curves and diagrams are identical for both hypotheses.

We will present two hypotheses for the age of the beginning of the Jurassic deposits for three wells. For Yangikazgan 10 the curves are shown for an Aalenian or a Pliensbachian age. The main tectonic subsidence event is observed during the first interval of sedimentation, with a high subsidence rate of 28 m/Ma continuing during 8.9 Ma for the Aalenian-Lower Callovian interval or 9 m/Ma during 25.6 Ma for the hypothesis of a Pliensbachian-Lower Callovian interval. Then the subsidence became slower and during the rest of the Mesozoic its velocities reduced to a range of 2-4 m/Ma. A slight increase is observed during the Turonian stage, where the subsidence velocity reaches 6 m/Ma. The subsidence is very slow during the Paleogene for which we have no subdivision. During the Neogene-Quaternary interval the curve of the tectonic subsidence rises, which marks an uplift of the area with an undetermined timing.

4.2.1.2. Ashikuduk 1 well

The next well chosen, is Ashikuduk 1. It belongs to the northern part of the Gazli high (fig. 4.8-B), one of the northernmost structures of the Bukhara step.

To create this column we have used the stratigraphy from Ashikuduk 1 from the wells catalogue of «Uzbekgeofizika» and the lithology from the Yangikazgan section (Ostrovsky, 1965) as there were no lithological columns for the area, and this latter field is the nearest one with lithological data.

The Ashikuduk 1 well is located very near the northernmost end of the E-E' line, which crosses the Ashikuduk structure through the Ashikuduk 2 well (fig. 4.14, 4.16). According to the isohypses behaviour, the Ashikuduk structure is a well-seen high, which is traced on all the principal surfaces (see fig. 4.10-C, F).

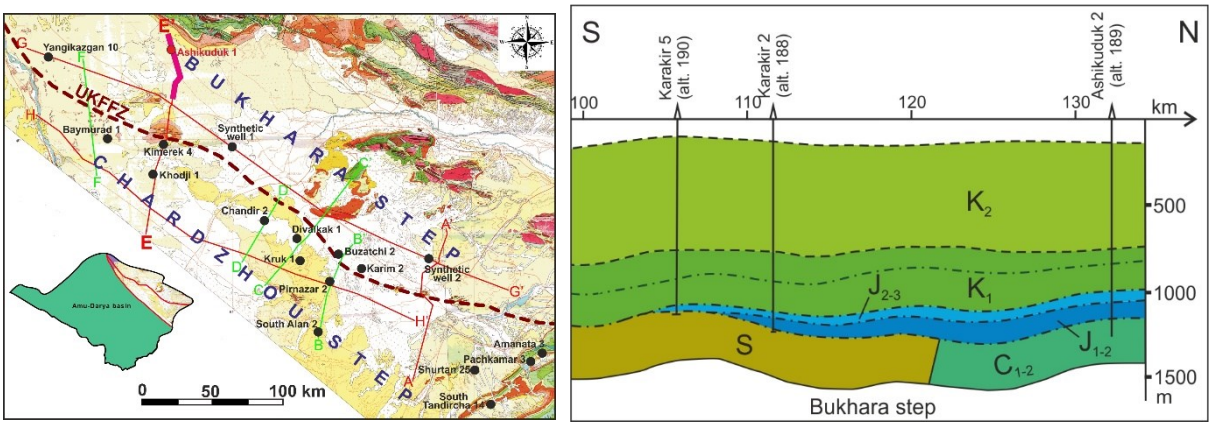

Fig. 4.14. Fragment of the N-S oriented E-E' line, showing the Ashikuduk structure.
See Chapter 3 fig. 3.8, for details on the full line.

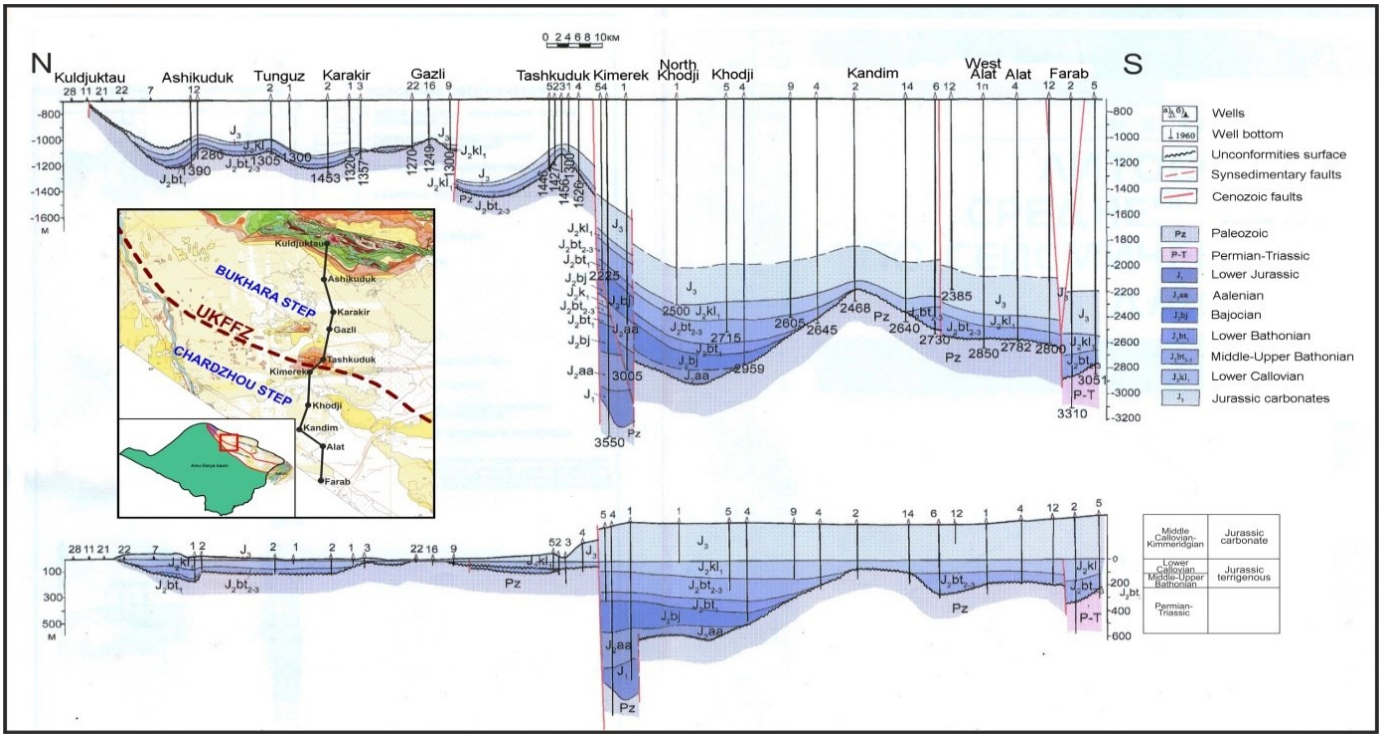

Fig. 4.15. Schematic geological and paleotectonic cross section of the terrigenous and carbonate Jurassic along the line Kuldjuktau-Farab (after Nugmanov, 2009b, modified). Location of the line is partly similar to the E-E' line (see the previous figure). This section crosses the wells Ashikuduk 1, Kimerek 4 and Khodji area, selected for this subsidence study. The reconstruction at the bottom is made with the top of the terrigenous unit flattened.

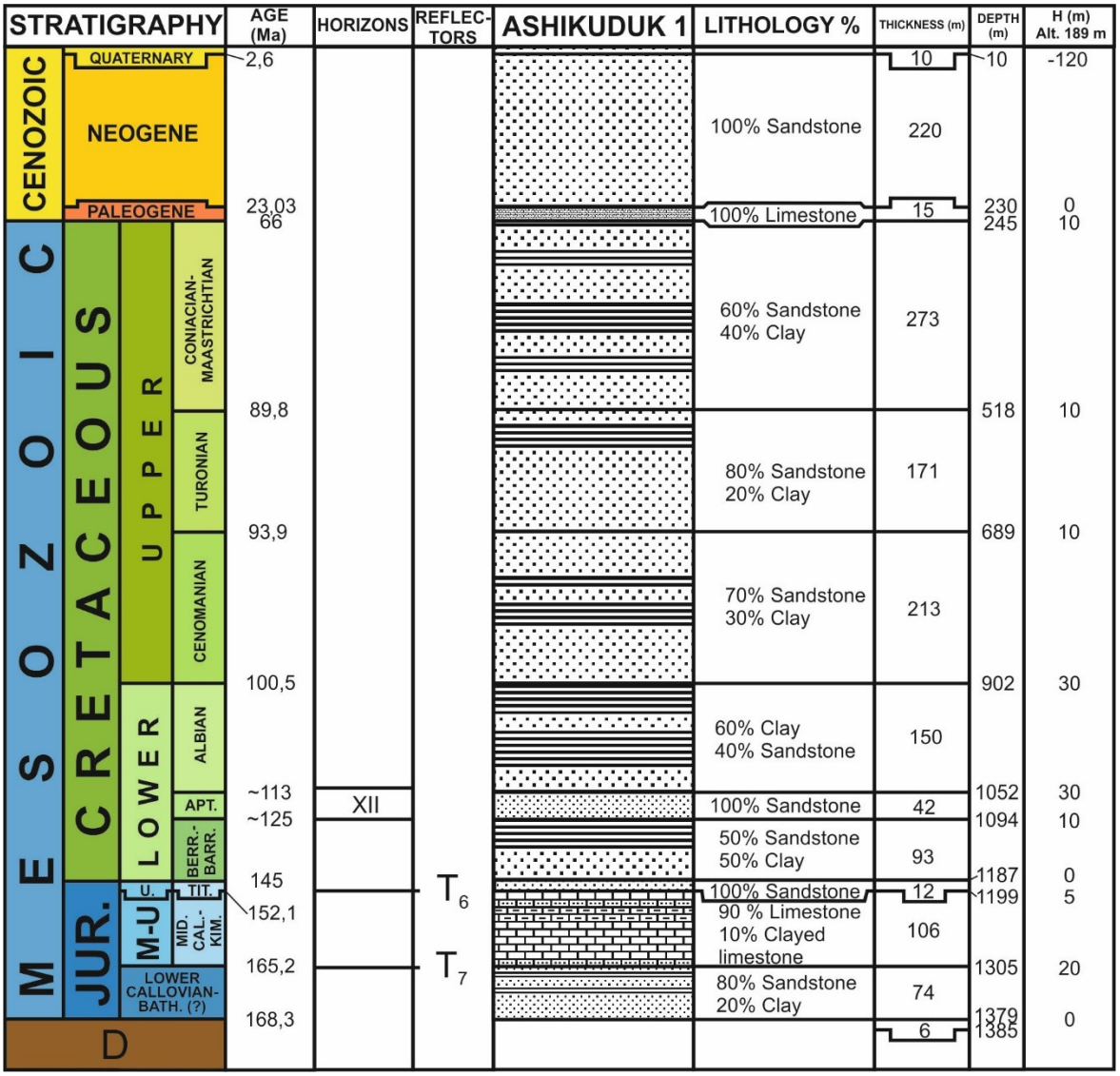

Fig. 4.16. Lithostratigraphic column of the Ashikuduk 1 well.

Despite Ashikuduk 1 and 2 are close, they reach different Paleozoic beds (fig. 4.10-A), Ashikuduk 1 has penetrated Devonian sediments, while Ashikuduk 2 has opened Lower-Middle Carboniferous effusives. The Jurassic concerns the Jurassic terrigenous unit, Middle Callovian Kimmeridgian carbonates and Tithonian siliciclastics. As on the section of Nugmanov (2009b, fig. 4.15) the first Jurassic level is marked Bathonian J_2bt1, we began the column of Ashikuduk 1 (fig. 4.16) by the Bathonian. The Cretaceous is represented by all the Cretaceous strata. The Cenozoic sediments are expressed by the Paleogene, Neogene and Quaternary.

The section of Ashikuduk 1 is not very thick. The well has reached the depth of 1385 m (fig. 4.16) and penetrated six metres of Devonian. The Jurassic is 192 m thick and the Cretaceous 942 m. The Paleogene is thin with only 15 m. The Neogene and Quaternary, in common, have a thickness of 245 m.

Lithologically, as we have taken the lithology of the Yangikazgan field, the section of the Ashikuduk is almost the same. It is represented by a sandy-clayed section, with Callovian-Kimmeridgian and Paleogene carbonates. The peculiarity of Ashikuduk 1 is the Tithonian stage. In the previously described Yangikazgan 10 well, the Tithonian stage was missing. In Ashikuduk it exists, but unlike most part of the Bukhara-Khiva and Southwestern Gissar regions, it is represented by sandstone and not evaporites (according to the section of Ostrovsky, 1965, when Tithonian exists in the Yangikazgan area).

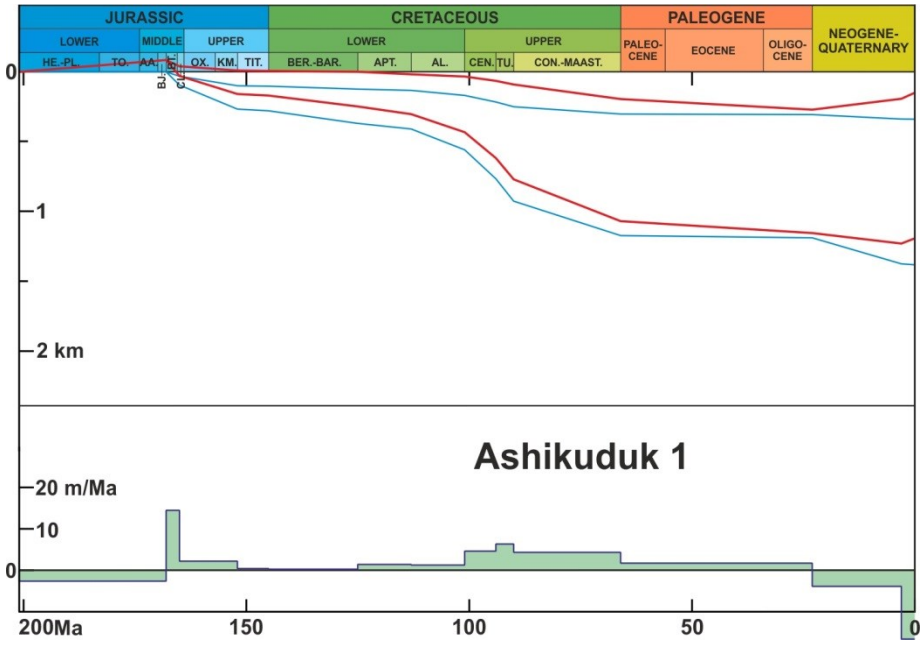

Fig. 4.17. Subsidence curves of the Ashikuduk 1 well. Meaning of the curves see caption of fig. 4.13.

The first and main tectonic subsidence event takes place in the Bathonian-Lower Callovian time interval, when the subsidence rate reaches 15 m/Ma during 3.1 Ma (fig. 4.17). The velocity is very reduced during the remaining of the Jurassic and the Early Cretaceous. It increases during the early Late Cretaceous (Cenomanian-Turonian), where it reaches 5-6 m/Ma and 4 m/Ma till the end of the Cretaceous. During the undivided Paleogene the averaged rate is only 2 m/Ma. During the Neogene-Quaternary interval an uplift of the area is observed. We supposed that a part of the altitude was acquired at the end of the Pliocene but with a very hypothetical value.

4.2.1.3. Baymurad 1 well

The Baymurad field is the northwesternmost structure we have chosen for the Chardzhou step. It is located between the Kandim high and the Uchkir-Pitnyak bank (see fig. 4.8-B).

According to the relief of the principal pre-Jurassic and Mesozoic surfaces (fig. 4.10), the Baymurad field is located in a well-seen WE trending anticline, which disappears in the Cretaceous. To the south of Baymurad 1 there is a roughly NS fault, which cuts the pre-Jurassic and Jurassic.

For the subsidence analysis we have chosen the Baymurad 1 well using the data of the wells catalogue for the stratigraphy and the synthetic lithostratigraphic section of the Baymurad field (Gafurova, 1986) for the lithology. This synthetic section was built on the basis of two wells situated not far from the Baymurad structure (see fig. 4.9): Western Parsankul 1 (Parsankul is a field located outside of the selected area, to the southeast of Baymurad near Khodji) and Uchkir 22 (northeast of Baymurad, fig. 4.9).

The Baymurad 1 well reaches the Paleozoic; according to the scheme of the pre-Jurassic surface ages (see fig. 4.10-A), the well penetrated Cambrian rocks. The Jurassic section concerns the terrigenous, carbonate and evaporite units. We begin the terrigenous unit at the Bajocian age, given by the synthetic section of the Akkum-Parsankul field, very near the Western Parsankul 1 well (Gafurova, 1986, see above) which served as a basis for the lithology. The carbonate unit has a Middle Callovian-Kimmeridgian age. The Tithonian evaporite unit ends the Jurassic section. The Cretaceous concerns all the stages, from the Berriasian to Maastrichtian.

The section of the Baymurad 1 well is 2868 m thick. There is only 44 m of penetrated Paleozoic sediments. The Jurassic sequence is 960 m thick; the overlaying Cretaceous has a thickness of 1666 m. The Cenozoic deposits reach 242 m, where 178 m belongs to the Paleogene (fig. 4.18, next page).

The Jurassic section of Baymurad 1 is represented by a sandy terrigenous unit, limestone of the carbonate unit and anhydrites at the top of the Jurassic. The Cretaceous sequences are expressed by a sandy-clayed section, where clay is predominating. The Paleogene also consists of sandstone and clay, but with a marl addition. The undivided Neogene-Quaternary sequence is represented by different surface continental sediments and marls.

One feature of this column is the Callovian-Kimmeridgian carbonates which are of the “reefal” type (see Chapter 2) with their subdivision into under-reef, reef and above-reef layers in the wells catalogue, while the principal reefal structures are concentrated more to the southeast of the Chardzhou step. We may suppose, that the Baymurad field is located in a stand-alone reef. This hypothesis needs to be clarified as we do not have enough lithological data: in the lithological column (Gafurova, 1986) the carbonate formation was merely noted “limestone” but the same reefal subdivision exists in the wells catalogue for some wells of the nearby productive field of Uchkyr where the reservoir is probably reefal.

Another interesting point of this section is the clastic sediments of the Paleogene. Generally, this stage is represented, either by the so-called Bukhara limestone layers in the lower part and some clastics at the top, or by limestone only.

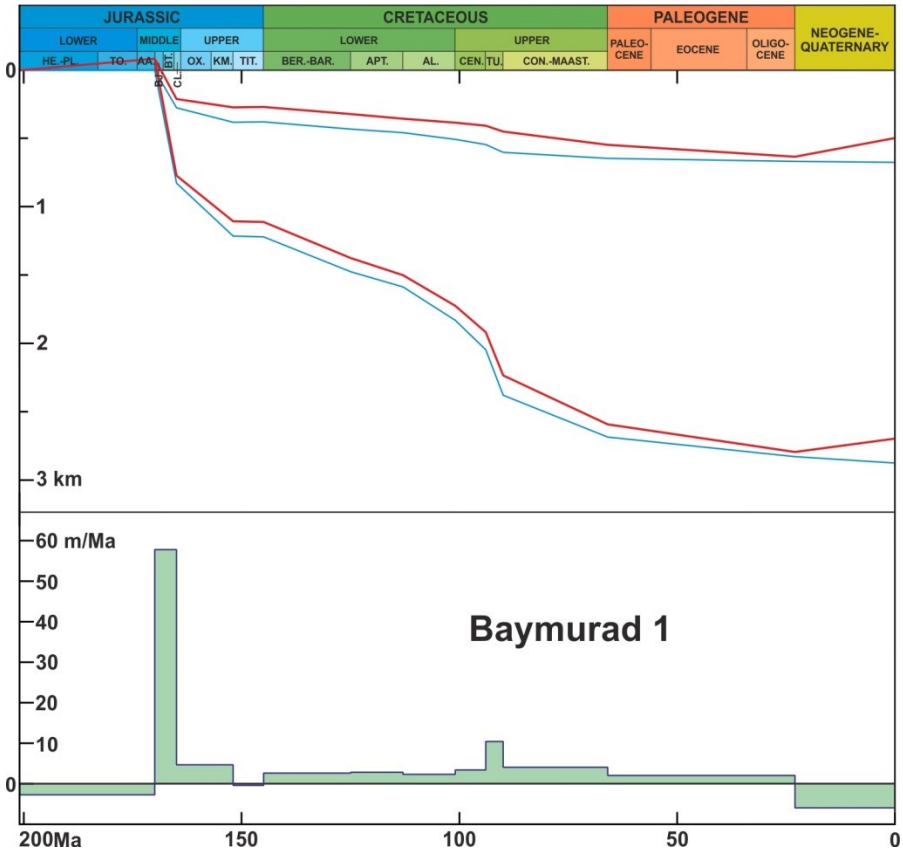

Fig. 4.19. Subsidence curves of the Baymurad 1 well. Meaning of the curves see caption of fig. 4.13.

The main tectonic subsidence event for Baymurad 1 is fixed from the beginning of the Bajocian to the Lower Callovian. The subsidence rate in this time was of 58 m/Ma during 5.1 Ma (fig. 4.19). However this high value is possibly overestimated. Indeed we chose a Bajocian age for the beginning of the Jurassic sedimentation after the synthetic section of a nearby set of fields and not according to data on Baymurad itself. If the sedimentation began earlier, the rate would be reduced. After the Lower Callovian, the subsidence slows down. In the rest of the Mesozoic its velocity is around 2-4 m/Ma, but increases to 10 m/Ma in the Turonian. The velocity is 2 m/Ma during the Paleogene and an uplift occurs during the Neogene-Quaternary interval.

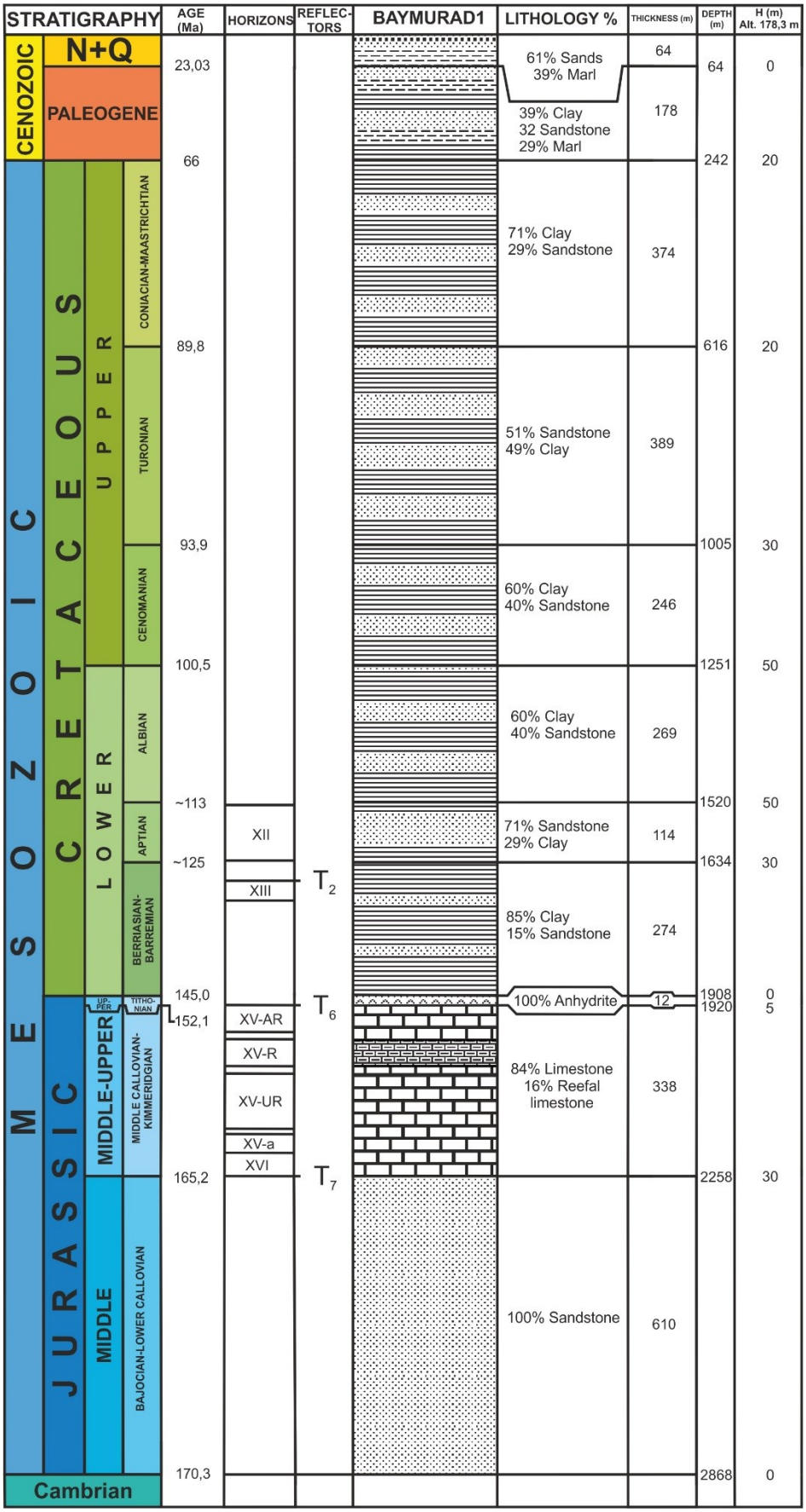

Fig. 4.18. Lithostratigraphic column of the Baymurad 1 well.

4.2.2. Kimerek-Chandir area

The second selected area mostly occupies the Chardzhou step. There it touches the territories of the Karakul trough, Kandim high and Ispanli-Chandir high. In the Bukhara step the selected area takes the southern part of the Rometan trough (see fig. 4.8-B).

We have chosen 4 wells for the subsidence analysis of this territory: the Synthetic well 1, Kimerek 4, Khodji 1 and Chandir 2 (fig. 4.20).

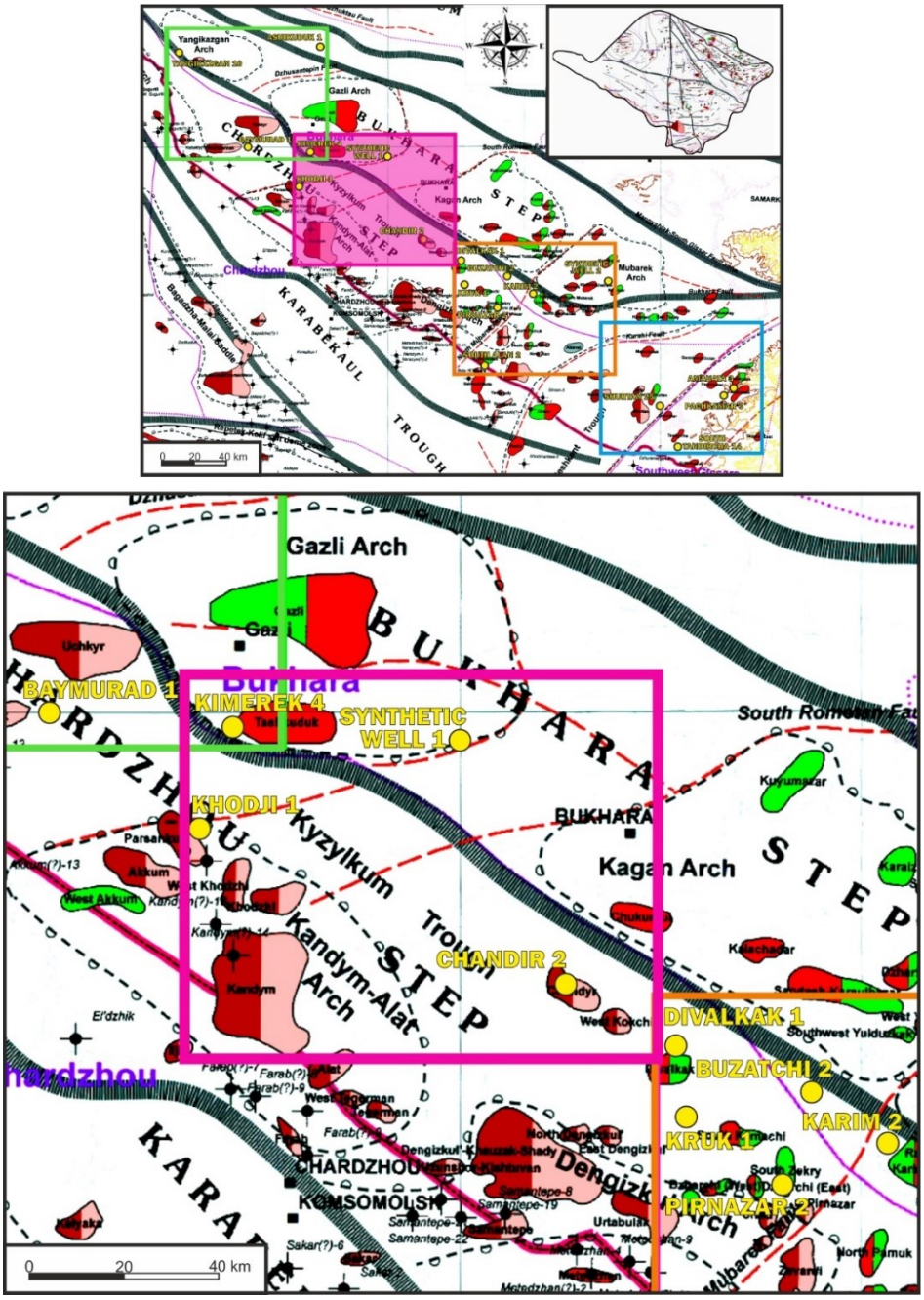

Fig. 4.20. Location of the wells studied in the Kimerek-Chandir area. Kimerek 4 appears on this map to the north of the UKFFZ, probably because of a difference of location of the UKFFZ on the background map but it is well located in the Chardzhou step, to the south of the UKFFZ
(background map after Blackbourn, 2008, modified).

For this area, as for the previous one we also used the isohypse maps of the principal pre-Mesozoic and Mesozoic surfaces and the pre-Mesozoic age scheme (fig. 4.21).

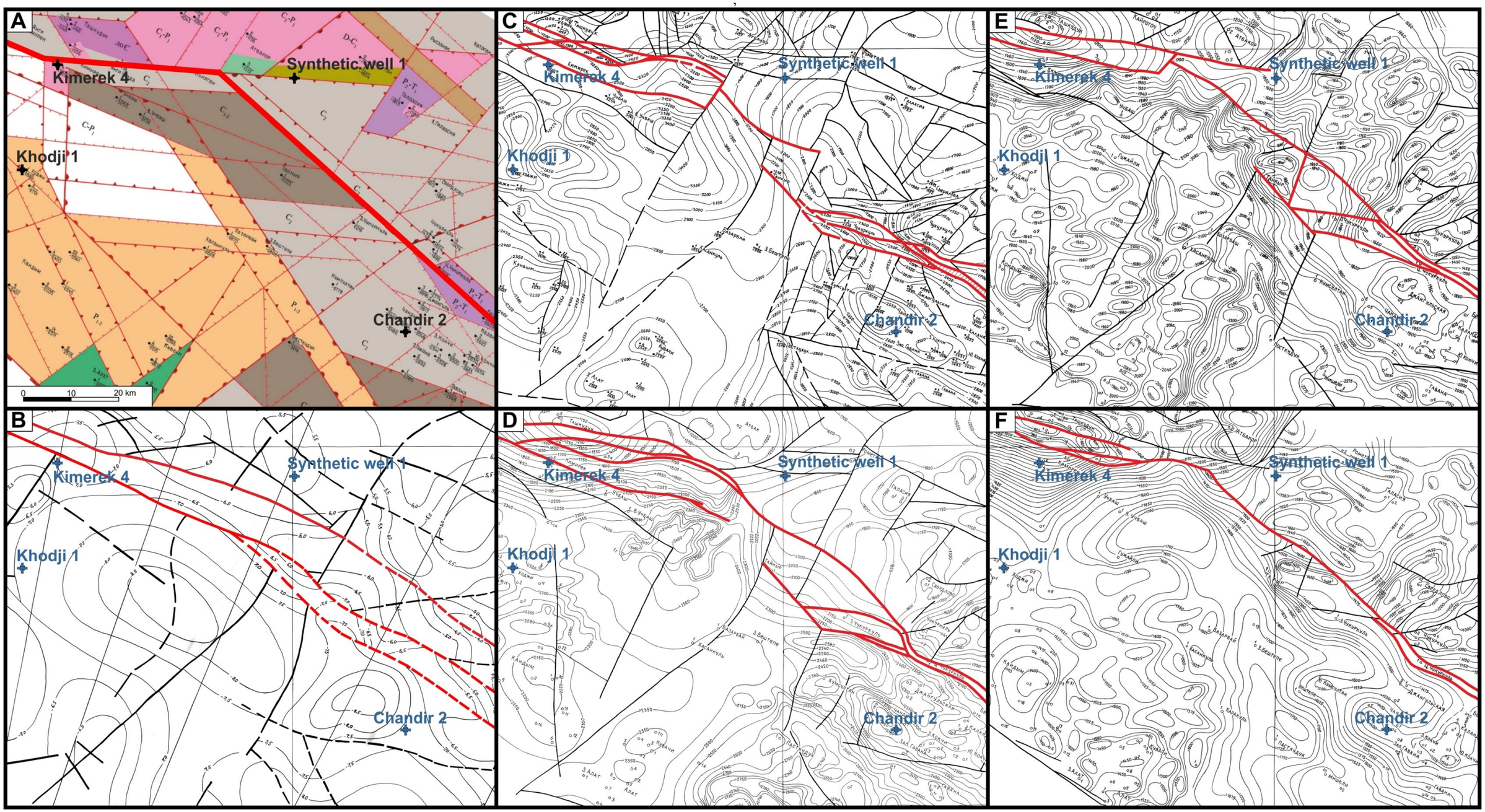

Fig. 4.21. Location of the wells studied in the second selected area, Kimerek-Chandir and of faults (in red) associated to the Uchbash-Karshi Flexure-Fault Zone.
A – age of the pre-Jurassic surface on a paleogeological scheme of the pre-Jurassic surface of the Bukhara-Khiva region. ДоЄ: PreCambrian, S: Silurian (olive green), D: Devonian, C. Carboniferous, P: Permian, T: Triassic; magmatism: intrusives in pink, effusives in dark green (after Babadjanov and Abdullaev, 2009, modified);
B-F: Isohypse maps (after Mordvintsev O. in Babadjanov, 2008, modified), **B** – relief of the crystalline basement, **C** – relief of the pre-Jurassic roof, **D** – relief of the Jurassic terrigenous roof, **E** – relief of the Jurassic carbonates roof, **F** – relief of the horizon XII roof in the Lower Cretaceous

4.2.2.1. Synthetic well 1

In the central part of the Bukhara step we did not have wells available for the subsidence analysis. Thus we have reconstructed a synthetic well, on the basis of the stratigraphic data of the line G-G' (fig. 4.22).

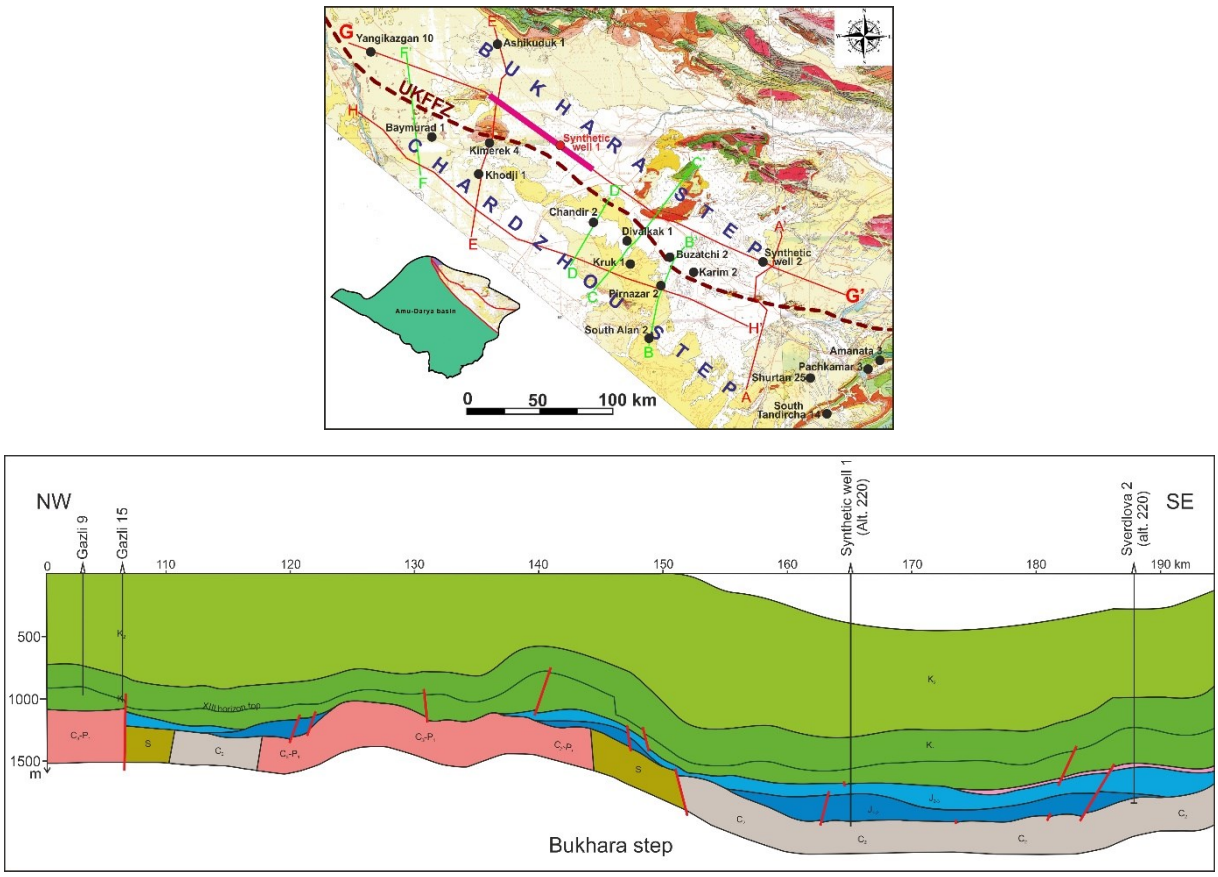

Fig. 4.22. Location of the Synthetic well 1 on the NW-SE oriented G-G' line.
See Chapter 3 fig. 3.10, for details on the full line.

The location of the well was selected in the area of the cross-section where the Jurassic sequence was the thickest. For reconstructing the lithology we have used the lithology of the Ashikuduk 1 and Kimerek 4 wells, as they are the nearest wells with lithological columns.

The Synthetic well 1 is located in the southern limits of the Rometan trough (see fig. 4.8-B). The relief of the main reflectors is relatively calm (fig. 4.21, 4.22), but there are several WE trending faults in the area. These faults cut all the pre-Jurassic and Jurassic strata, but do not expose a big displacement.

As the aim of the geological line G-G' was to show the behaviour and relationships between the main Paleozoic-Mesozoic strata, the stratigraphy of the line is very schematic with only few levels. The pre-Jurassic is represented by the Lower Carboniferous. The Jurassic concerns the Middle Jurassic terrigenous unit and the Middle-Upper carbonate unit. The Tithonian stage is absent. The Cretaceous is divided into two parts: the Lower Cretaceous and the Upper Cretaceous. We suppose that all the stages from the Berriasian to Maastrichtian are represented as in most part of the Bukhara-Khiva region. We have added the Cenozoic from the nearest well.

The thickness of the Synthetic well 1 is 2000 m, of which 300 m belongs to the Jurassic. The Cretaceous is 1320 m thick and the thickness of the Cenozoic reaches 380 m (fig. 4.23).

Very schematically, the lithology of the well is supposed to consist of intercalations of sandstone and clay, in which clay is prevailing for the terrigenous Jurassic, and of limestone with little clay in the

carbonate unit. The Cretaceous consists of siliciclastics, in which most part of sediments are sandstone. The Cenozoic is represented by alternations of clay, sandstone, sand and soil.

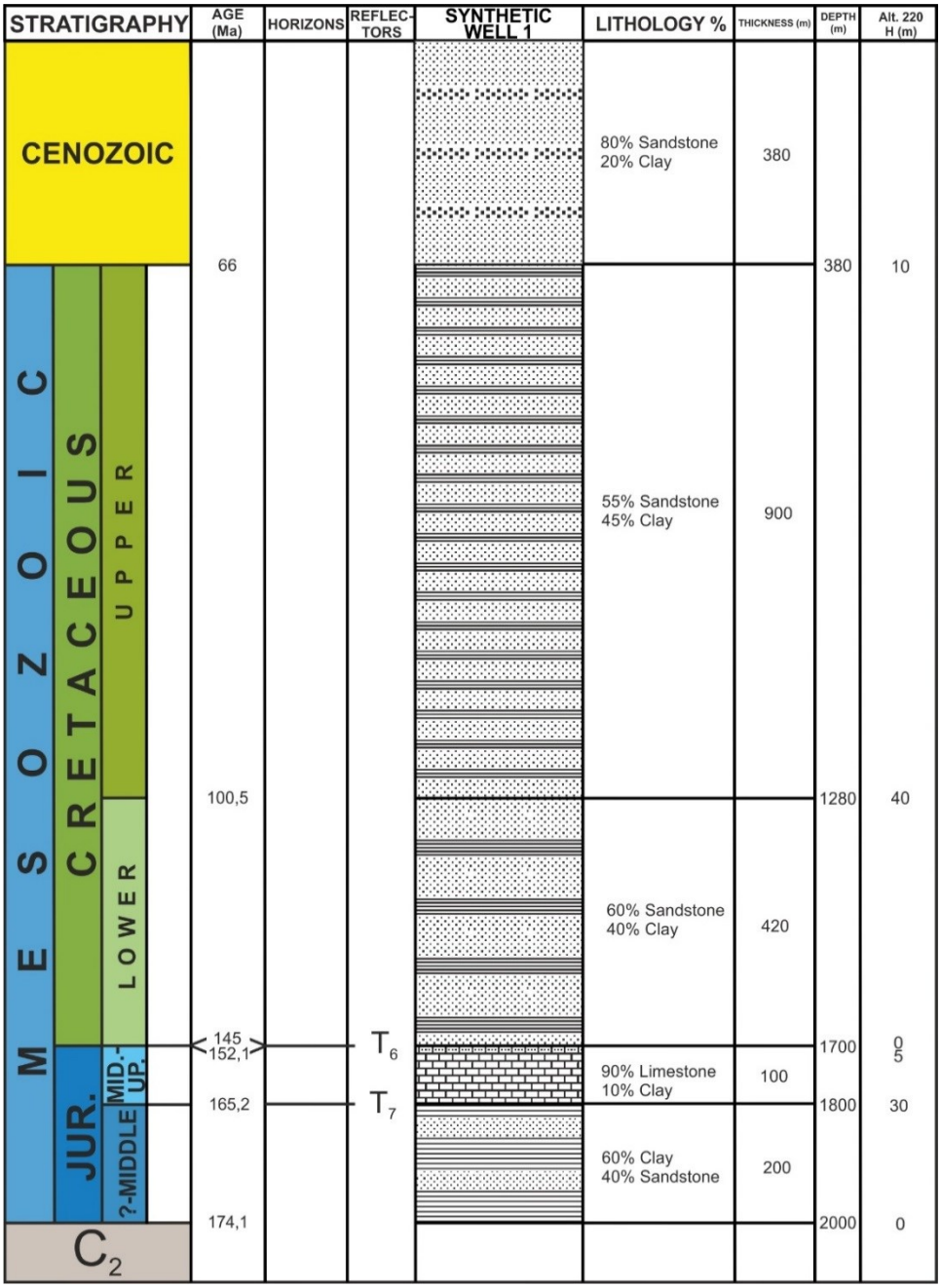

Fig. 4.23. Lithostratigraphic column of the Synthetic well 1.

The Synthetic well 1 column is very schematic, but allows showing the variations of thicknesses in the area and the absence of the Tithonian evaporite unit in a shortened Mesozoic section.

The subsidence curves of the Synthetic well 1 are thus not very detailed but the principal trends are still the same as in the previous wells. The main tectonic subsidence event is observed in the beginning of the Jurassic section for the Aalenian-Bathonian interval of time with a velocity of 12 m/Ma during 8.9 Ma (fig. 4.24). Then in the rest of Mesozoic, the subsidence became slower (0-5 m/Ma). As the Upper Cretaceous is undivided, the increase of velocity is averaged on a longer period and thus is smaller than for other wells. It is also the case for the Cenozoic uplift, which is small as averaged during 66 Ma.

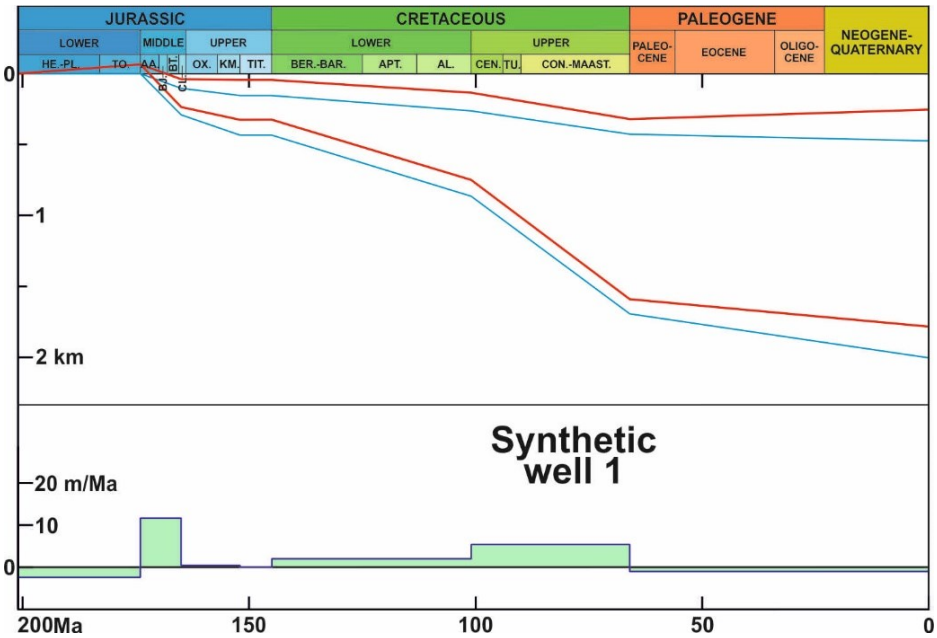

Fig. 4.24. Subsidence curves of the Synthetic well 1. Meaning of the curves see caption of fig. 4.13.

4.2.2.2. Kimerek 4 well

The first well of the Chardzhou step in the second selected area, is the Kimerek 4 well, located in the Karakul trough, very near the UKFFZ (see fig. 4.8). Kimerek 4 shows the mainly sandy-clayed section of the Kimerek graben – a huge Jurassic thickness anomaly (fig. 4.25). This narrow graben is well-seen on most of the isohypse maps (see fig. 4.21-B, E), bounded by faults and disappearing in the Cretaceous, as well as on the cross-sections E-E' (fig. 4.25) and Kuldjuktau-Farab (see fig. 4.15).

A geophysical model has been computed along a part of this section (fig. 4.26). It includes an intrusion in the Paleozoic sediments of the Kimerek graben, near the UKFFZ, shown on the map of ages of the pre-Jurassic (fig. 4.21-A). The intrusion drilled is composed of Upper Carboniferous-Lower Permian diorites (4.26) penetrated by Kimerek 4 for two metres (Babadjanov, 2008). The Jurassic Kimerek graben is overlying a wider area of thickened Paleozoic, located to the south of the UKFFZ, as seen by difference between the relief maps of the basement surface and of the bottom of the Jurassic (fig. 4.21-B, C) as well as on the geophysical model (fig. 4.26).

The Kimerek 4 column (fig. 4.27) was set up from several sources of data. The stratigraphy has been taken from the wells catalogue of «Uzbekgeofizika» but as there is no division inside the terrigenous Jurassic unit, this part of stratigraphy is not very precise. The lithology for the bottom part of the well (Toarcian) comes from the lithological description of the Jurassic terrigenous unit made by Mirkamalov (Mirkamalov et al., 2005). The rest of the terrigenous formation lithology comes from Shayakubov and Dalimov (1998). The lithology of the Jurassic carbonate, the Cretaceous and Cenozoic is issued from the Kimerek 6 well data (Safonova, 1985).

The Kimerek 4 well is 3405 m deep – one of the thickest well in the area. The Jurassic is 1698 m thick with 1402 m belonging to the terrigenous sequence (fig. 4.27).

A reconstruction along the line Kuldjuktau-Farab (Nugmanov, 2009b, fig. 4.15) shows a possible reverse fault and thus thinner layers deposited: the reconstructed terrigenous Jurassic would be then only around 960 m thick instead of 1402 m. We tried to get more details on the Jurassic of Kimerek 4 by looking to the detailed results of the well in reports and asked a specialist of IGIRNIGM (Oil and Gas Geology Institute). An inverted fault doubling a part of the terrigenous series (fig. 4.15) does not seem to exist in the Kimerek 4 well (Eydelnant N., 2015, personal communication) and seems to be a hypothesis of Nugmanov (2009b) to explain a part of the terrigenous sediments thickening. We thus kept the total thickness drilled but the distribution and ages of the formations inside the terrigenous unit is uncertain as the thicknesses proposed by different authors are not well in agreement.

Shayakubov and Dalimov (1998), in their schematic column of Kimerek 4 (see Chapter 2, fig. 2.10), distinguished the local formations: Sanjar (called here Kimerek suite, with an old stratigraphic age of Upper Triassic-Lower Jurassic), Gurud (Aalenian-Lower Bajocian), Degibadam (Upper Bajocian) and Baysun (Bathonian-Lower Callovian). The Tangiduval Formation (Lower-Middle Bathonian) is not indicated on the column of Shayakubov and Dalimov. (1998, fig. 2.10) when it seems to be individualized as Lower Bathonian in the section of Nugmanov (2009b, fig. 4.15).

In our lithostratigraphic column (fig. 4.27), we took the following distribution for the terrigenous Jurassic: a bottom part with clay and sandstone of 460 m of Toarcian age after Mirkamalov (Mirkamalov et al., 2005) as this sequence was recently well studied, then an undivided layer of 712 m of Aalenian-Bajocian (modified from Troitsky, 1967); a Bathonian-Lower Callovian interval (230 m, from Shayakubov and Dalimov, 1998) with appearance of some limestone.

The Middle Callovian-Kimmeridgian carbonate unit (296 m) is represented by limestone, Tithonian is missing. The Cretaceous sediments starting in the Berriasian and concerning all the stages, are 1455 m thick, composed of clay and sandstone, but some limestones are observed in the Turonian. The Cenozoic has a total thickness of 250 m with a thin Paleogene (in comparison to other wells of the Chardzhou step) constituted mostly of clay and sandstone, but marl and limestone also exist. The undivided Neogene-Quaternary sequence is represented by sandstone, sand, gravelite and clay.

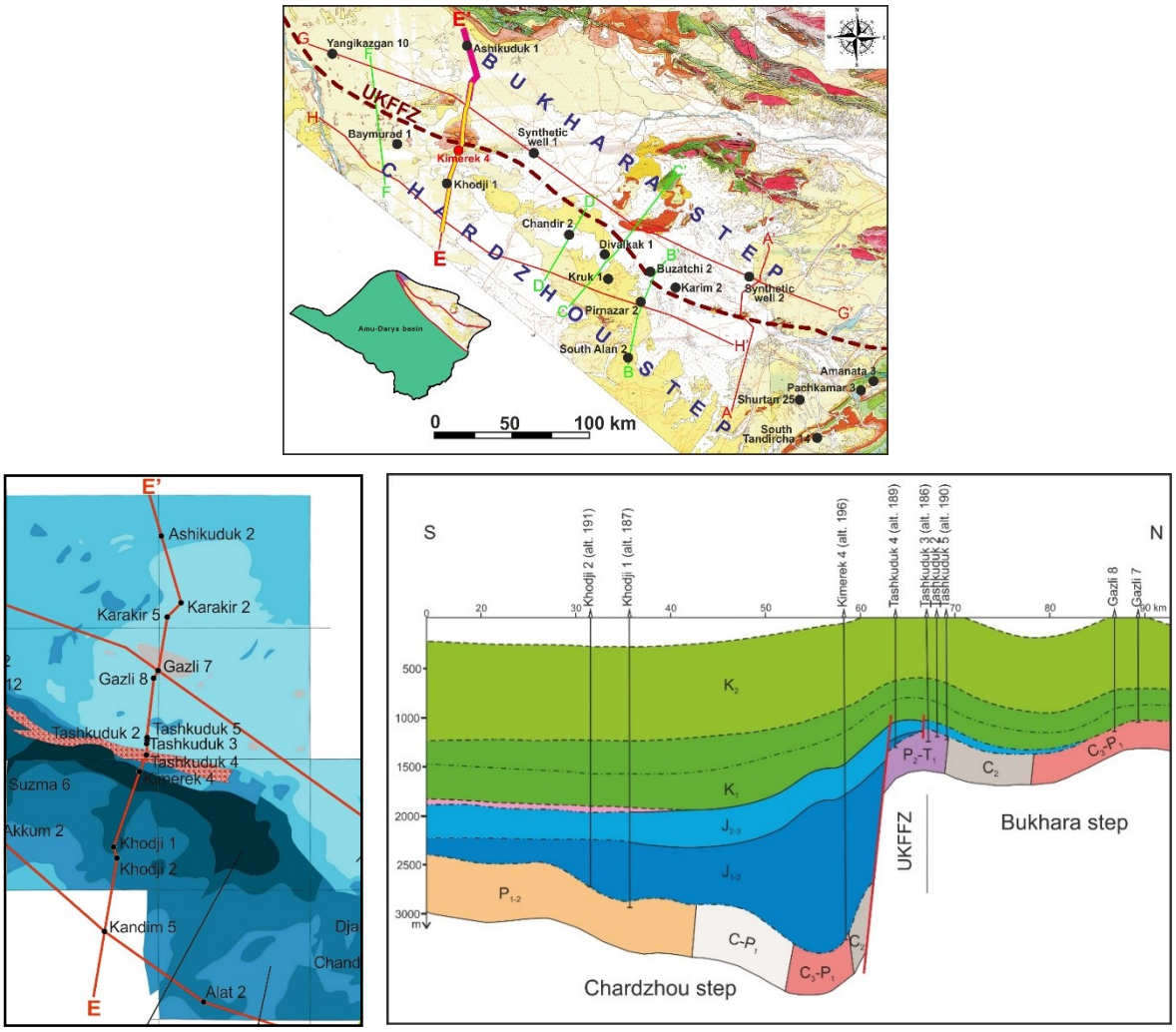

Fig. 4.25. Location of the Kimerek 4 well: on top map, with respect to the position of the E-E' line; on the left, with respect to the Kimerek graben corresponding to the darkest blue area with the thickest Jurassic terrigenous and carbonate layers (see the full schematic map in Chapters 2 and 3, modified after O. Mordvintsev, 2012 from Babadjanov, 2012); on the right, fragment of the E-E' line (location on top and left maps), showing the Kimerek graben structure. See Chapter 3 fig. 3.8, for details on the full line.

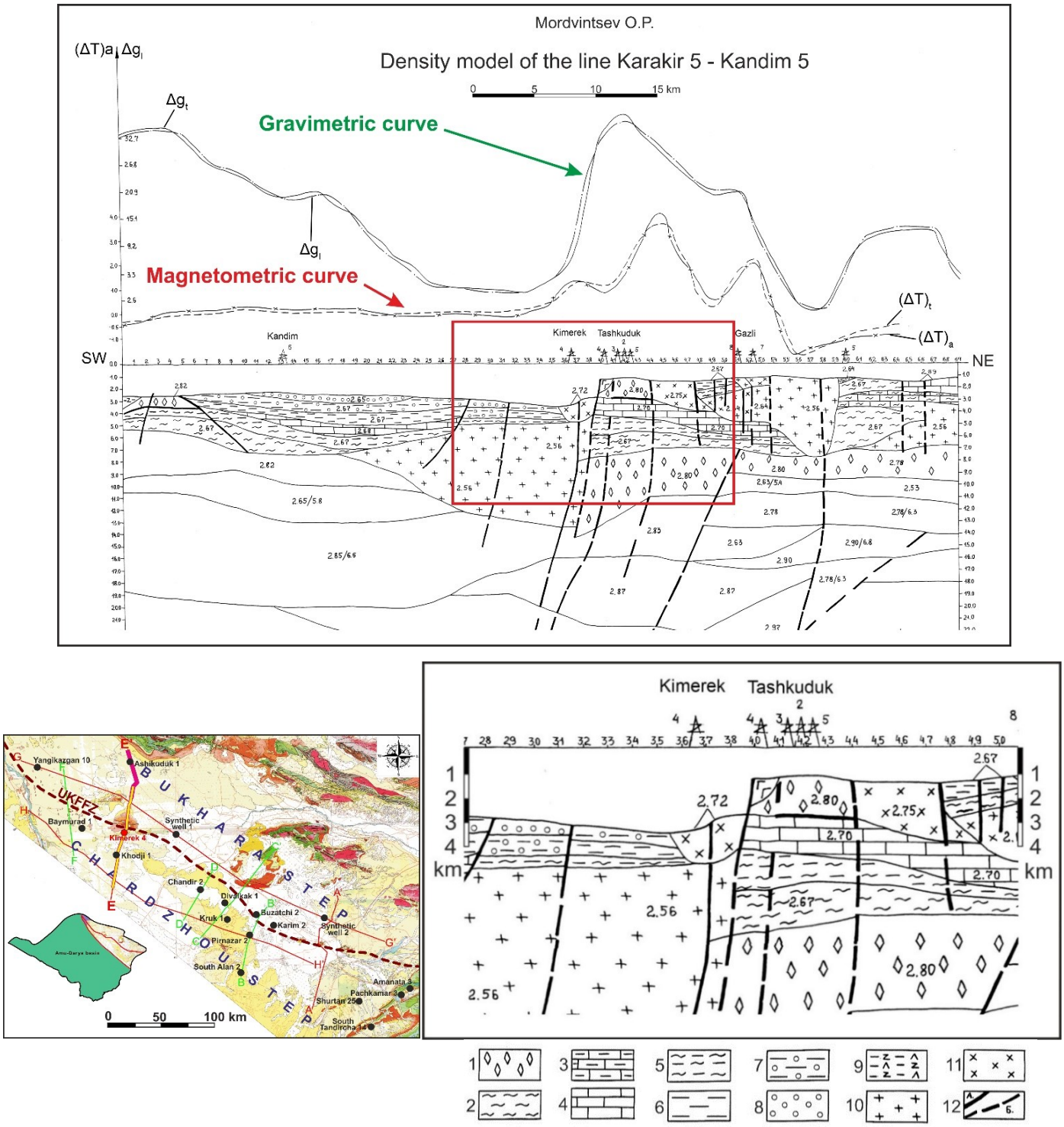

Fig. 4.26. Crustal scale geophysical model along a cross section of the Bukhara and Chardzhou steps, cutting the Kimerek graben (after O. Mordvintsev in Babadjanov, 2008). Location is similar to a part of the E-E' line, see above fig. 4.25 and marked by a yellow line on the left bottom map. Bottom right: enlargement of the central part (red rectangle) of the model. This density model shows an intrusion in the Paleozoic sediments of the Kimerek graben linked to the position of the UKFFZ, north of the Kimerek graben, the white area corresponds to the Meso-Cenozoic sediments. **1** – Crystalline basement rocks; **2** – Paleozoic terrigenous rocks; **3** – Carbonate-terrigenous rocks of D_3-C_1; **4** – D_3-C_1 carbonates; **5** - C_1-C_{1-2} terrigenous rocks; **6** – C_2, C_{2-3} sandy-shaly rocks; **7** – C_3-P_1, P_1 sandstone, siltstone, clay and shale; **8** – P_{1-2}-T conglomerate and sandstone; **9** – volcanogenous-terrigenous rocks with intermediate and acid effusives; **10** – granites; **11** – diorites; **12** – faults.

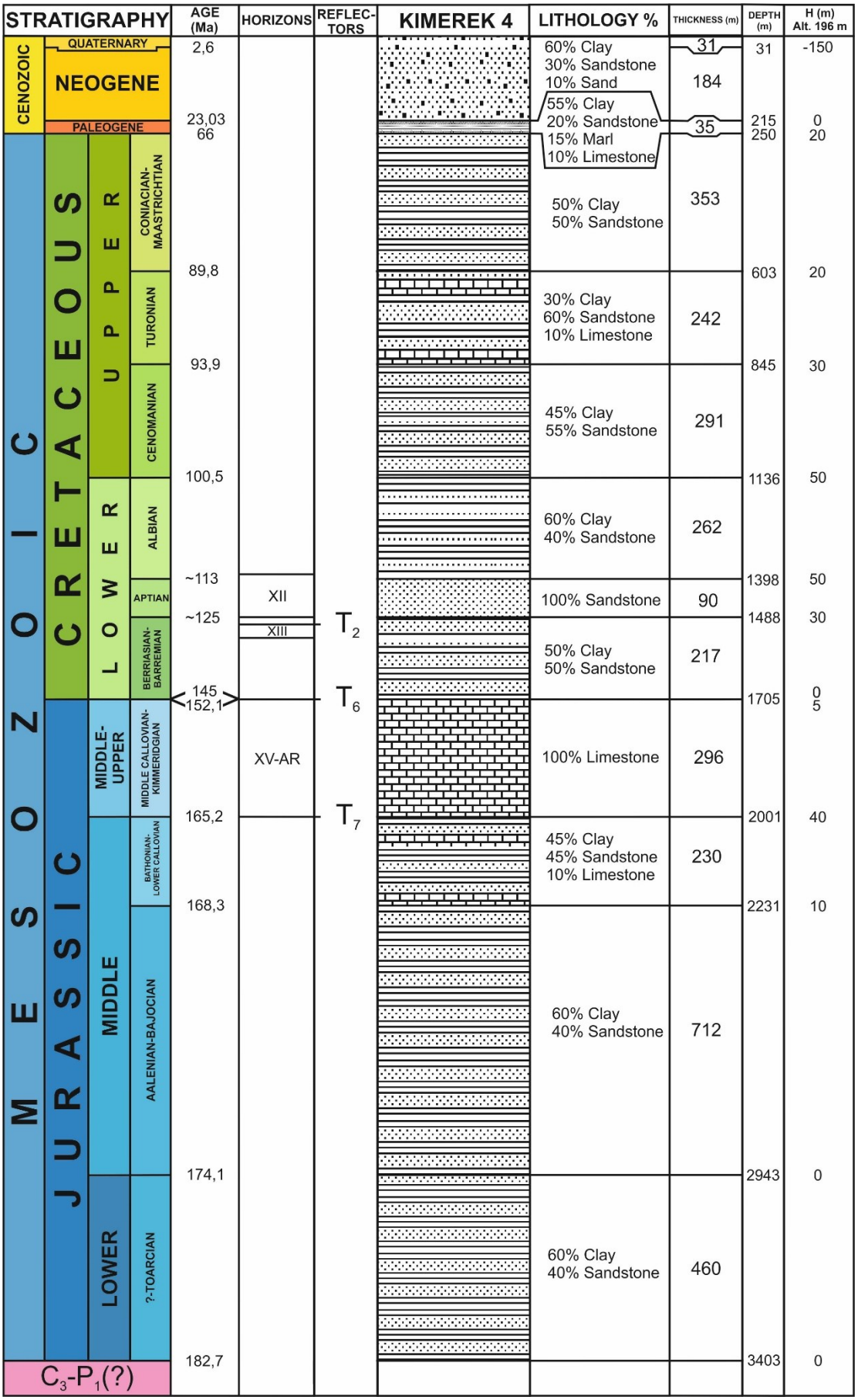

Fig. 4.27. Lithostratigraphic column of the Kimerek 4 well.

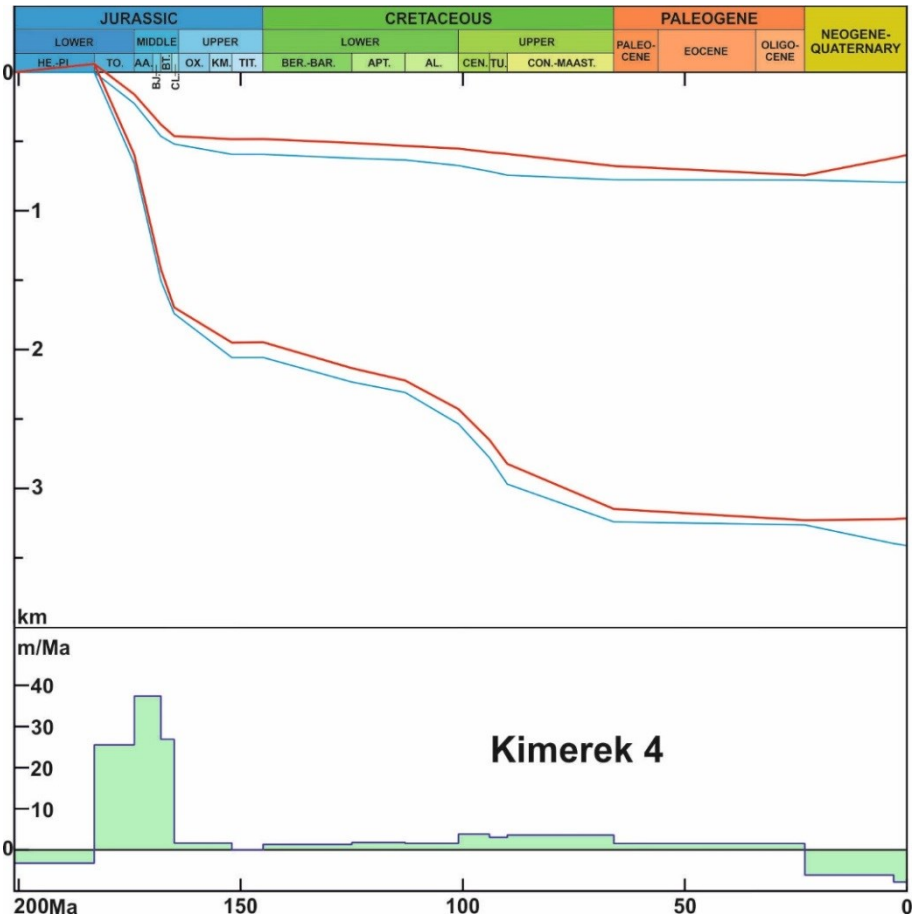

Fig. 4.28. Subsidence curves of the Kimerek 4 well. Meaning of the curves see caption of fig. 4.13.

The Lower-Middle Jurassic tectonic event is especially important for Kimerek 4 as the tectonic subsidence is high during 17.5 Ma (Toarcian-Lower Callovian), with velocities reaching 26-27 m/Ma during the Toarcian and Bathonian-Callovian and even 37 m/Ma during the Aalenian-Bajocian (fig. 4.28). This distribution is uncertain as the data used were controversial, nevertheless this period shows a clear rifting event of the Kimerek graben. The age of the first Lower Jurassic sediments could be older as in the Yangikazgan graben, the duration would be thus longer and velocities reduced. During the Upper Jurassic the subsidence is very slow and null during the Tithonian. The velocities increases slightly with the Lower Cretaceous with 1-2 m/Ma and 4-3 m/ma during the Cenomanian-Turonian and stays at this level during the remaining of the Upper Cretaceous. As the Paleogene is undivided the subsidence rate is averaged and slow before the final uplift at the end of the Cenozoic.

4.2.2.3. Khodji 1 well

The next well is Khodji 1. The Khodji field is located in the northern part of the Kandim high of the Chardzhou step (see fig. 4.8-B), south of the Kimerek graben. The relief of the main pre-Jurassic and Mesozoic surfaces in the limits of the Khodji area is rather smooth. Khodji 1 is located on the southwestern flank of the Khodji anticline, while the main dome is more to the northeast. The line E-E' crosses Khodji 1 (fig. 4.25) and the line Kuldjuktau-Farab, crosses the Khodji area (see above on fig. 4.15).

To construct the Khodji 1 well column we have used several sources of data. The stratigraphy was obtained from the wells catalogue of «Uzbekgeofizika», while the lithological data were taken from the synthetic section (Loginova, 1984) of the Western Khodji field, located few kilometres westwards. One interesting feature of this well is that it has penetrated 78 m of Paleozoic rocks, dated as Lower-Middle Permian (see fig. 4.21-A). According to the synthetic section of Western Khodji, the Jurassic is divided into the Bajocian-Lower Callovian terrigenous unit, the Middle Callovian-Kimmeridgian

carbonate unit and the Tithonian evaporite unit. The overlaying Cretaceous is also complete. The Cenozoic is represented by the Paleogene (Paleocene and Eocene stages, most part of the Paleogene thickness belonging to the Upper Eocene sequence) and an undivided sequence of the Neogene-Quaternary. Actually, in the synthetic section of Western Khodji, the terrigenous Jurassic unit is divided into the Degibadam (marked as Bajocian-Bathonian instead of Upper Bajocian) and Baysun (marked as Upper Bathonian-Lower Callovian) formations. The Tangiduval Formation is not mentioned as for Kimerek 4 (fig. 2.10). We suppose nevertheless that all the Jurassic units, from the Upper Bajocian to the Lower Callovian exist in the terrigenous Jurassic section of Khodji 1.

The Khodji 1 column is 3072 m thick (fig. 4.29, next page) with 935 m of Jurassic, while 1647 m belong to the Cretaceous; the Cenozoic here is thicker than in the previously described wells with 490 m, most part of which (337 m) belongs to the Paleogene sequence. The Jurassic terrigenous unit is represented by alternations of sandstone and clay where clays predominate. The carbonate unit is constituted of limestone and reefal limestone. The evaporite unit is expressed by anhydrites with some gypsum intercalations. The Cretaceous sequence is composed of alternating clay and sandstone layers. The Paleogene is composed of sandstone, clay, marl and limestone. According to the synthetic section of the Western Khodji field, the limestone sequence belongs to the so-called Bukhara limestone Formation. The undivided Neogene-Quaternary sequence consists of sandstone with some clay intercalations.

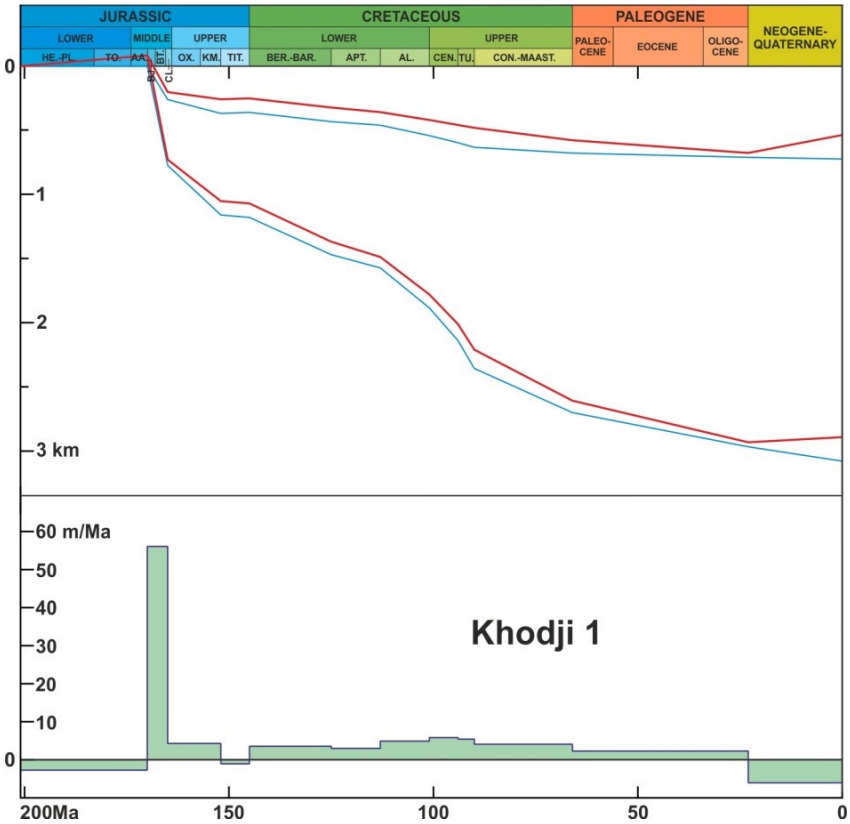

Fig. 4.30. Subsidence curves of the Khodji 1 well. Meaning of the curves see caption of fig. 4.13.

The Middle-Jurassic tectonic event is very sharp here as the age of the first deposits in Khodji 1 is supposed to be Bajocian-Lower Callovian (fig. 4.30). The period of deposits is thus short: 5.1 Ma with a high velocity of 56 m/Ma. This rate drastically decreases to 4 m/Ma during the Middle-Callovian-Kimmeridgian and is null (slightly negative) during the Tithonian. The tectonic subsidence activity reappears during all the Cretaceous, especially from the Albian to the Turonian with a maximum of 6 m/Ma during the Cenomanian. The Cenozoic being only divided into two parts, the velocities are averaged over long periods: 2 m/Ma during the Paleogene and an uplift at the end of the Cenozoic.

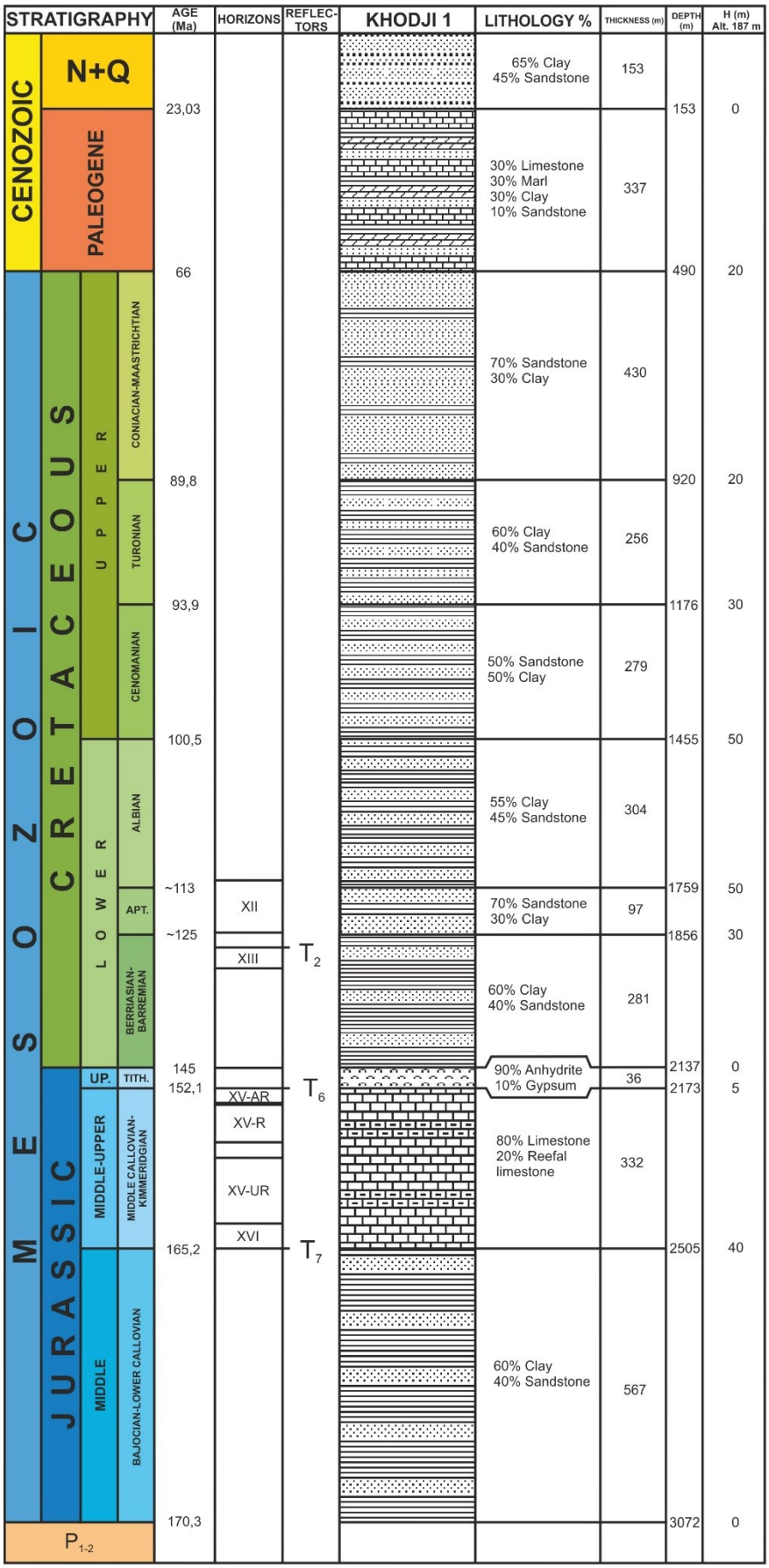

Fig. 4.29. Lithostratigraphic column of the Khodji 1 well.

4.2.2.4. Chandir 2 well

Chandir 2 is the easternmost well of the selected area, located in the central part of the Ispanli-Chandir high of the Chardzhou step (fig. 4.8-B). This well is one of the rare ones for which we have a complete data set. The stratigraphy was obtained from the wells catalogue of «Uzbekgeofizika» and the lithology from the synthetic section of the Chandir field (Storojenko, 1980). Chandir 2 is located in the main dome of the Chandir anticline, observed in the pre-Jurassic and Jurassic and still existing during the Cretaceous (fig. 4.21-B, F).

The well bottom is located in the pre-Jurassic, more precisely in the Middle Carboniferous, drilled by 11 m. According to the synthetic section of the field, the Jurassic starts in the Aalenian with an undivided Aalenian-Lower Callovian sequence and in the wells catalogue, this unit is marked only "terrigenous Jurassic", without any age. We thus kept this undivided age in our column too, followed by the two other Jurassic units. The Cretaceous concerns all the stages and starts with the Berriasian. The Cenozoic is represented by the Paleogene and an undivided Neogene-Quaternary sequence. The Paleogene, in its turn, is divided into the Paleocene and Eocene and the Oligocene is missing.

The Mesozoic-Cenozoic section of the Chandir 2 well is 2894 m long (fig. 4.31, next page) with 852 m of Jurassic and 1568 m of Cretaceous. The Cenozoic sediments are 474 m thick, where 320 m belongs to the Paleogene. Lithologically, most part of the Mesozoic section is represented by an alternation of sandstone and clay. The terrigenous Jurassic unit is expressed by a clayey section with few sandstone. The carbonate unit consists of different types of limestone and is divided into several horizons corresponding to the reefal type (see Chapter 2). We may suppose that the Chandir field is located in a stand-alone reef or bioherm as it is not yet located in the area of numerous reefs. The evaporite unit is represented by all its five members. The lower and upper anhydrite members are the thinnest. Most of the thickness belongs to the lower salt, middle anhydrite, upper salt members. The Cretaceous sequence shows mainly a sandy section with some clay intercalations and limestone inclusions in the Albian and Turonian. The Cenozoic section is mainly clastic. The Paleocene consists of the Bukhara limestone, overlain by a clayey Eocene. The Neogene-Quaternary sequence is constituted of sandstones.

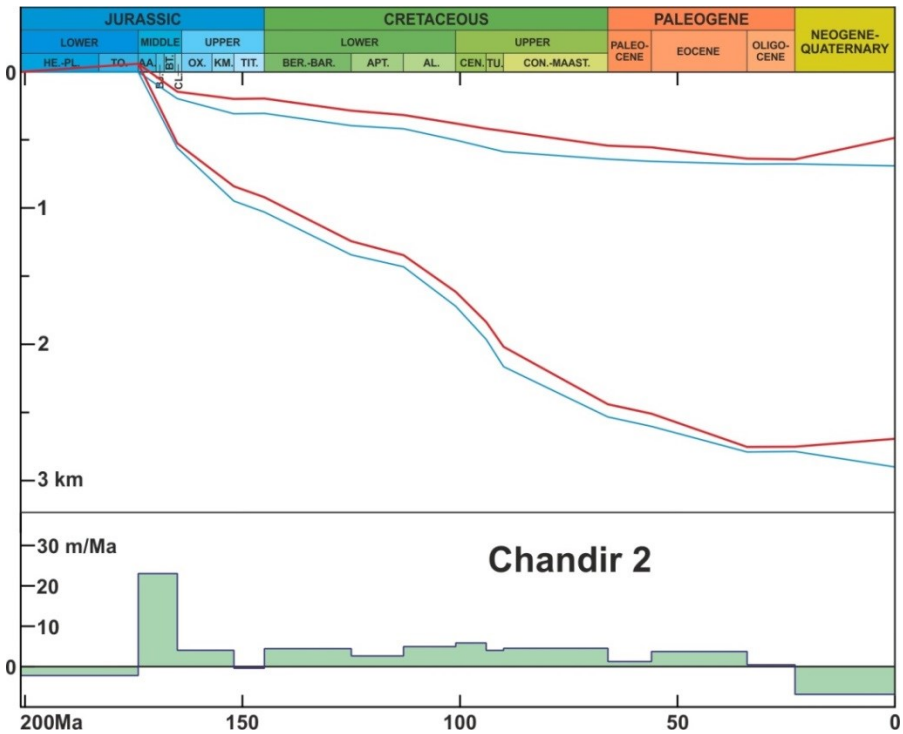

Fig. 4.32. Subsidence curves of the Chandir 2 well. Meaning of the curves see caption of fig. 4.13.

The main tectonic subsidence event of Chandir 2 is observed during the Aalenian-Lower Callovian interval of 8.9 Ma with a subsidence velocity of 23 m/Ma (fig. 4.32). Then the subsidence slows down before a new increase during all the Cretaceous: 3-5 m/Ma, and 6 m/Ma in the Cenomanian. The

Cenozoic is also characterized by a slow subsidence. A next decrease is observed during the Paleocene before a new increase during the Eocene (4 m/Ma) and the Late Cenozoic uplift.

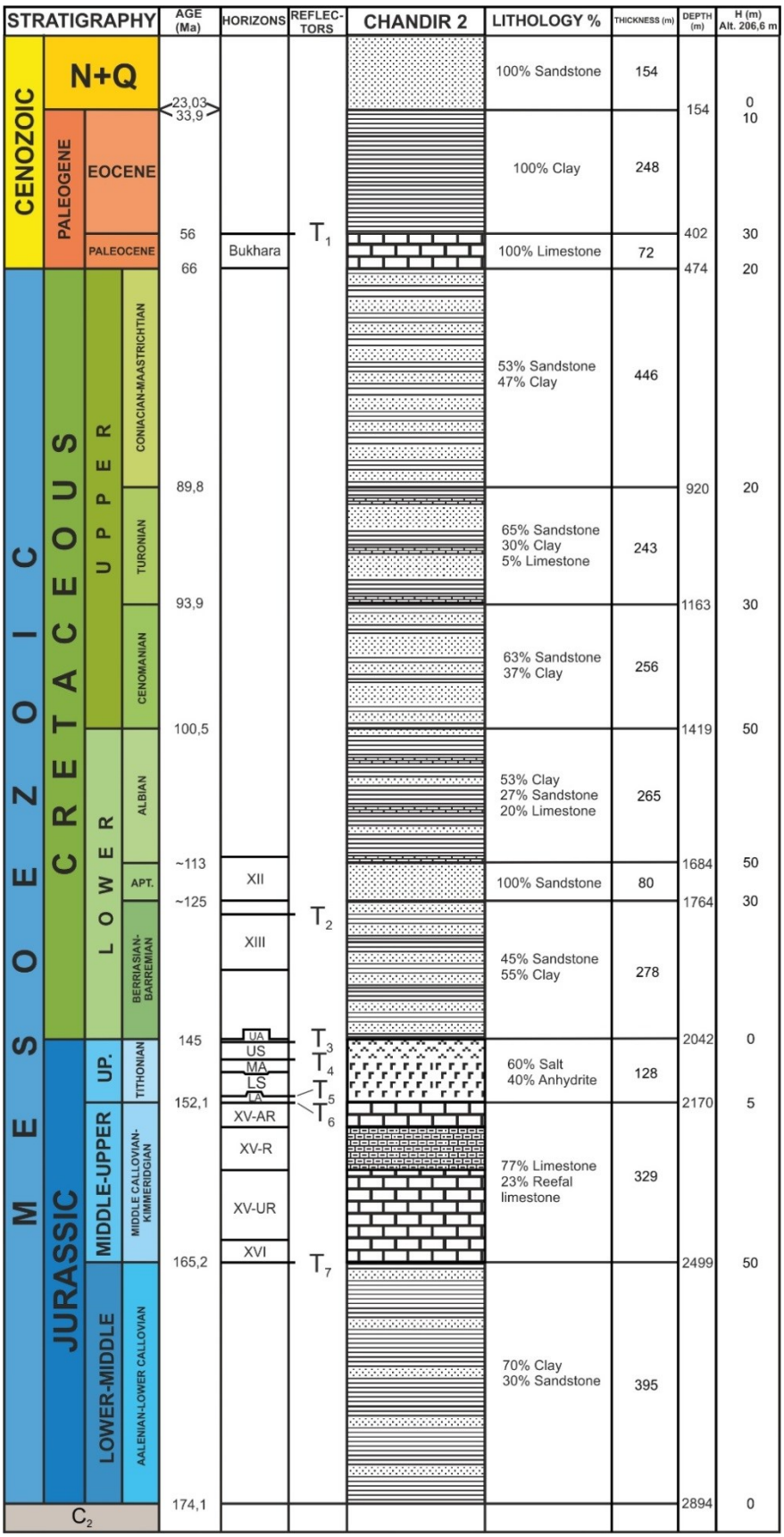

Fig. 4.31. Lithostratigraphic column of the Chandir 2 well.

4.2.3. Divalkak-South Alan area

The third selected area occupies the southern part of the Yambashi trough and the Mubarek system of folds in the Bukhara step, and in the Chardzhou step the eastern part of the Ispanli-Chandir high in the west, then in the east, the Beshkent trough as far as the Ayzovat and Girsan banks (see fig. 4.8-B). The Beshkent trough begins to the east of the Dengizkul high and extends towards the Southwestern Gissar.

The Divalkak-South Alan area concerns an important part of the wells we have selected for the subsidence analysis. There are Buzatchi 2, Karim 2 and the Synthetic well 2 in the Bukhara step and the Divalkak 1, Kruk 1, Pirnazar 2 and South Alan 2 wells in the Chardzhou step (fig. 4.33).

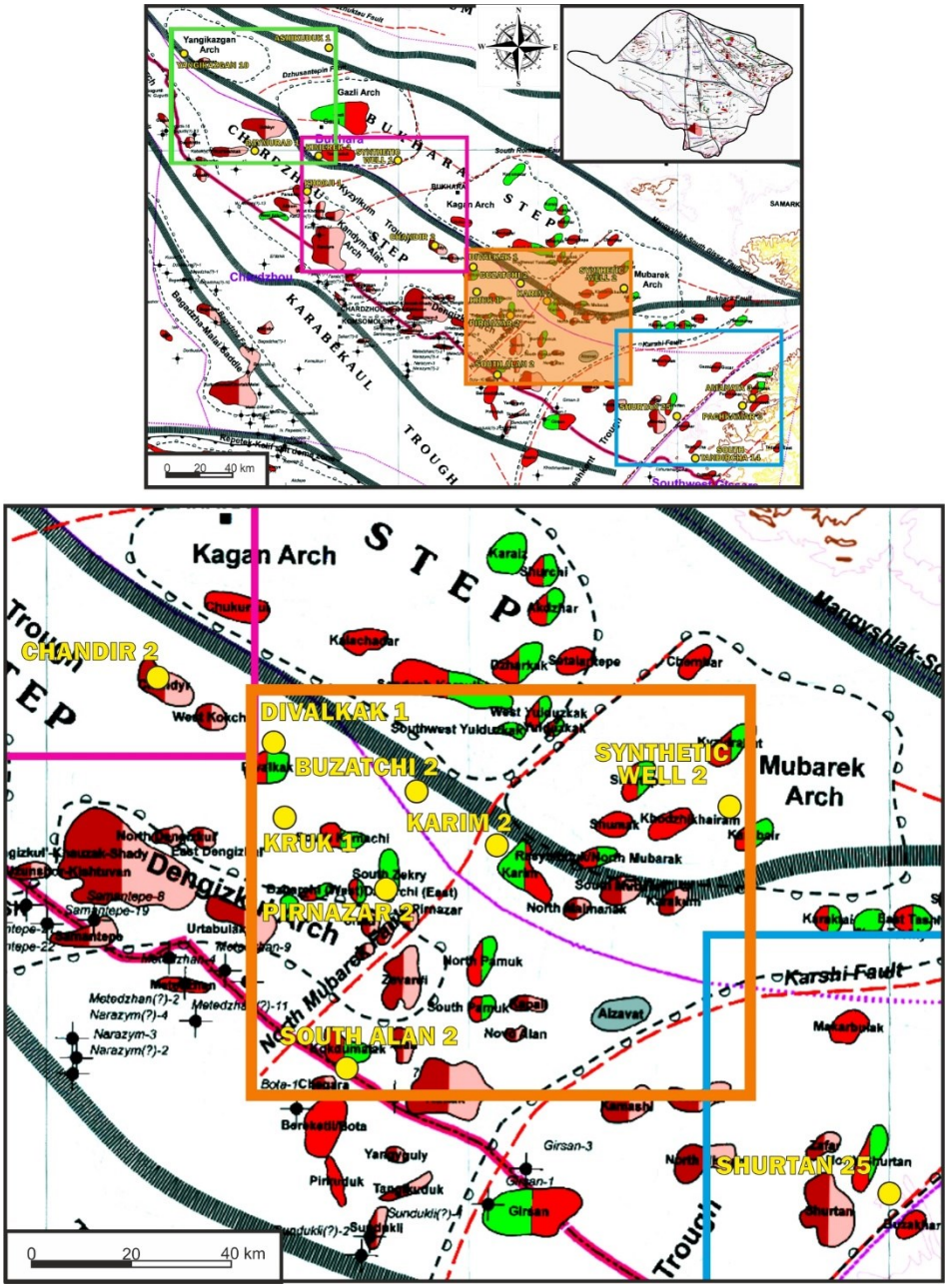

Fig. 4.33. Location of the wells studied in the Divalkak-South Alan area.
The purple solid line corresponds in the original background map (after Blackbourn, 2008, modified) to the boundary between the Bukhara and Chardzhou steps, the grey large line being the Bukhara fault.

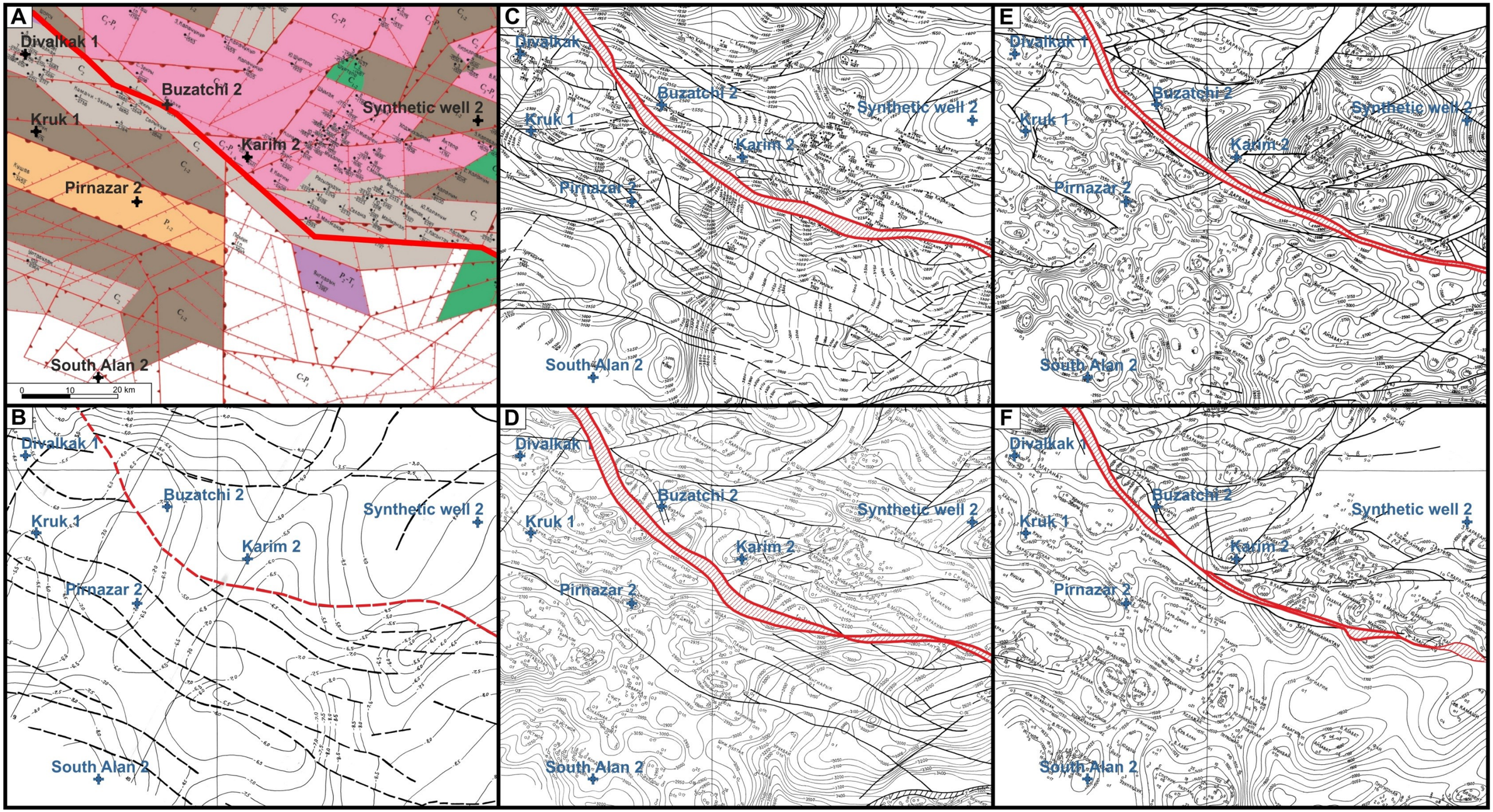

Fig. 4.34. Location of the wells studied in the third selected area, Divalkak-South Alan and of faults (in red) associated to the Uchbash-Karshi Flexure-Fault Zone.
A – age of the pre-Jurassic surface on a paleogeological scheme of the pre-Jurassic surface of the Bukhara-Khiva region. C. Carboniferous, P: Permian, T: Triassic; magmatism: intrusives in pink, effusives in dark green (after Babadjanov and Abdullaev, 2009, modified);
B-F: Isohypse maps (after Mordvintsev O. in Babadjanov, 2008, modified), **B** – relief of the crystalline basement, **C** – relief of the pre-Jurassic roof, **D** – relief of the Jurassic terrigenous roof, **E** – relief of the Jurassic carbonates roof, **F** – relief of the horizon XII roof in the Lower Cretaceous.

4.2.3.1. Buzatchi 2 well

The Buzatchi 2 well is the westernmost well of the Bukhara step in the selected area. It is located in the southern part of the Yambashi trough, very near the UKFFZ (see fig. 4.8).

To build the column of this well we have used the lithostratigraphic section of the Buzatchi 2 well (Gafurova, 1992) and the stratigraphic column from the wells catalogue of «Uzbekgeofizika».

The geological-geophysical line B-B' crosses the Buzatchi structure. Actually, this line crosses the Buzatchi 1 well, but as this well is very near Buzatchi 2, this line allows us to see the structure of the area (fig. 4.35). The UKFFZ is well seen on the seismic line, to the south of Buzatchi 1.

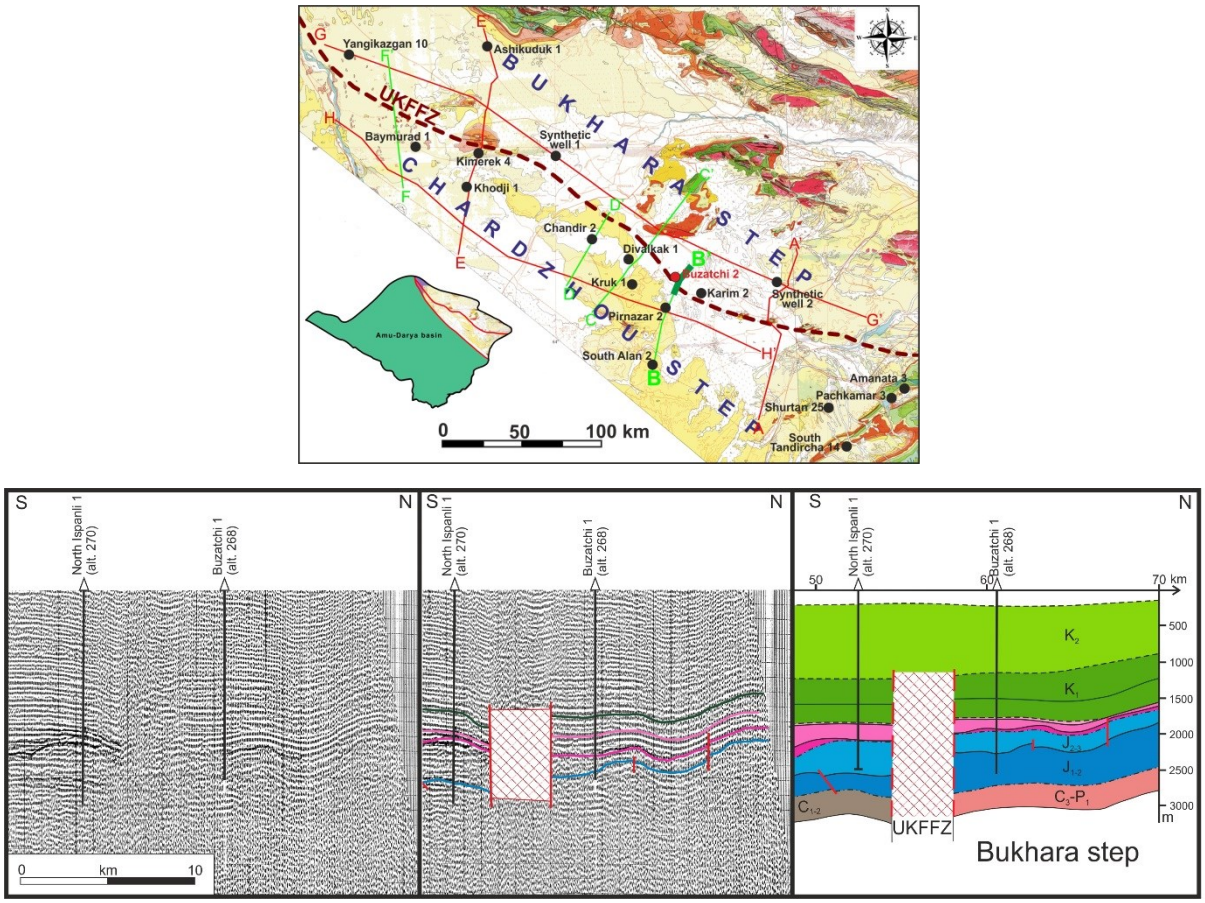

Fig. 4.35. Fragment of the B-B' line, crossing the Buzatchi structure. On the right, J_3 evaporites layers are in pink.

See Chapter 3 fig. 3.5, for details on the full line.

The Buzatchi 1 well does not reach the Paleozoic, but the Buzatchi 2 well does. Buzatchi 2 has penetrated Paleozoic rocks with 30 m of Upper Carboniferous-Lower Permian granites (see fig. 4.34-A). All the Jurassic units are well represented. Unfortunately, there was not any data about the age of the terrigenous formation, as in all sources of data for Buzatchi 2 it was marked as "terrigenous Jurassic" without any precision. We took a Bajocian age for the beginning of the Jurassic section, according to the presence of the XIX horizon in the Buzatchi 1 well, which corresponds to the upper part of the Bajocian and the horizon XVIII in the Buzatchi 2 well which corresponds to the Lower Bathonian. The carbonate unit is represented by the Middle Callovian-Kimmeridgian. The Tithonian ends the Jurassic section with a rather thick (in comparison with other areas of the Bukhara step) evaporite unit. The overlaying Cretaceous concerns all the stages from the Berriasian to the Maastrichtian. The Cenozoic is expressed by a Paleogene and Neogene-Quaternary sequence.

Several faults, almost parallel to the UKFFZ are observed in the Buzatchi area (see fig. 4. 34-C, F), they probably belong to the Uchbash-Karshi Flexure-Fault zone. This zone and faults create a horst-

like structure, where the Buzatchi 2 well is located. The Mesozoic-Cenozoic section of the Buzatchi 2 well is 2920 m long (fig. 4.36, following page). The Jurassic is 842 m thick and the Cretaceous is 1428 m. The Cenozoic is 650 m thick, including 320 m of Paleogene.

The terrigenous Jurassic unit is represented by sandstone. The carbonate unit consists of limestone and reefal limestone. One of the interesting points of this carbonate section is that it does not show the XV-a and XVI horizons. There only exist the reefal horizons, which allows us to consider the Buzatchi 2 section of the reefal type, despite it is in the Bukhara step where the reefs are not developed. On the section B-B' (fig. 4.35), north of Buzatchi 1, a small dome could correspond to a patch reef. The Tithonian evaporites cover the carbonates. Here, the salt-anhydrite unit is divided into the five salt and anhydrite members, the thickest ones are the lower and upper anhydrites. The Cretaceous sediments are represented, mainly, by an alternation of clay and sandstone with some layers of marl in the upper part of the section. The Paleogene consists of marl with some alternating layers of clay. The Neogene-Quaternary sequence is represented by sands and clay.

The section of the Buzatchi 2 well is not a typical section of the Bukhara step, as the Jurassic units are well developed with reefal limestone and rather thick evaporites. This can be explained by the very close location of this section with the UKFFZ and because the variation of the sedimentary thickness is less pronounced in this area (line B-B' fig. 4.29) between the Bukhara and Chardzhou steps.

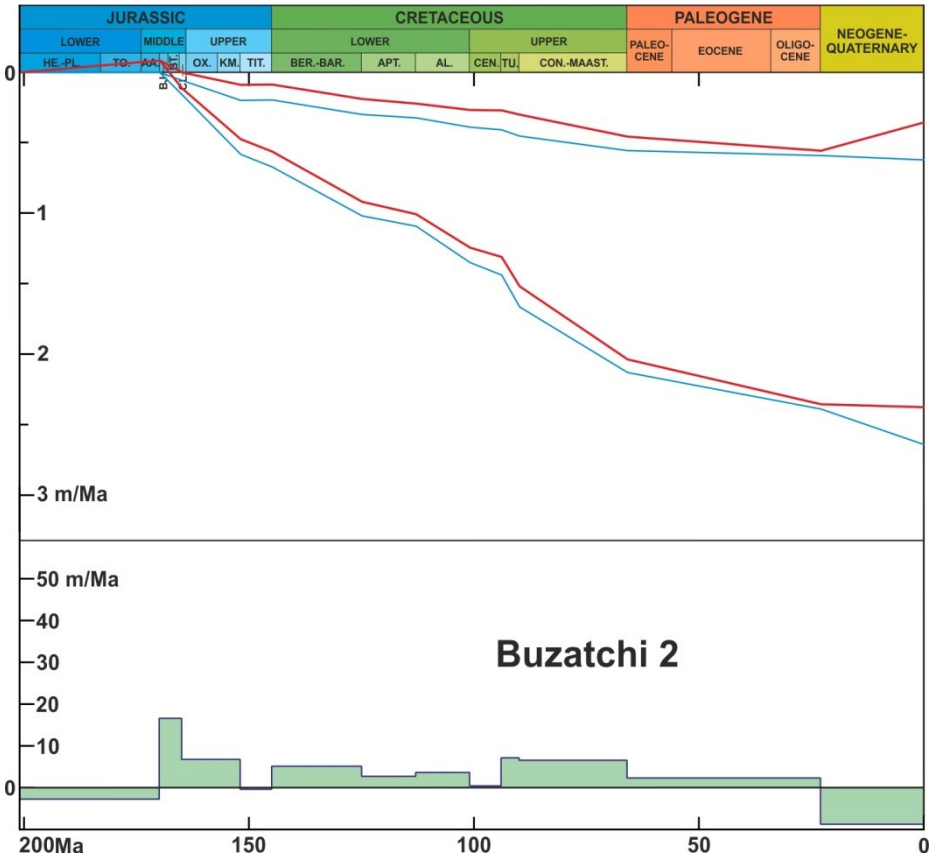

Fig. 4.37. Subsidence curves of the Buzatchi 2 well. Meaning of the curves see caption of fig. 4.13.

The principal tectonic subsidence event in the Buzatchi 2 (fig. 4.37) well evolution is fixed in the Bajocian-Lower Callovian interval of time of 5.1 Ma. This period is characterized by a subsidence velocity of 17 m/Ma. After that the subsidence reduced and to the end of the Jurassic (Tithonian) the subsidence is null or there is a slight uplift. The Cretaceous is characterized by a slow subsidence of 2-3 m/Ma with a stop during the Cenomanian. From the Turonian onwards, the remaining of the Upper Cretaceous is represented by velocities of 5-6 m/Ma. During the Paleogene the rate is reduced and averaged to 2 m/Ma, before the Late Cenozoic uplift.

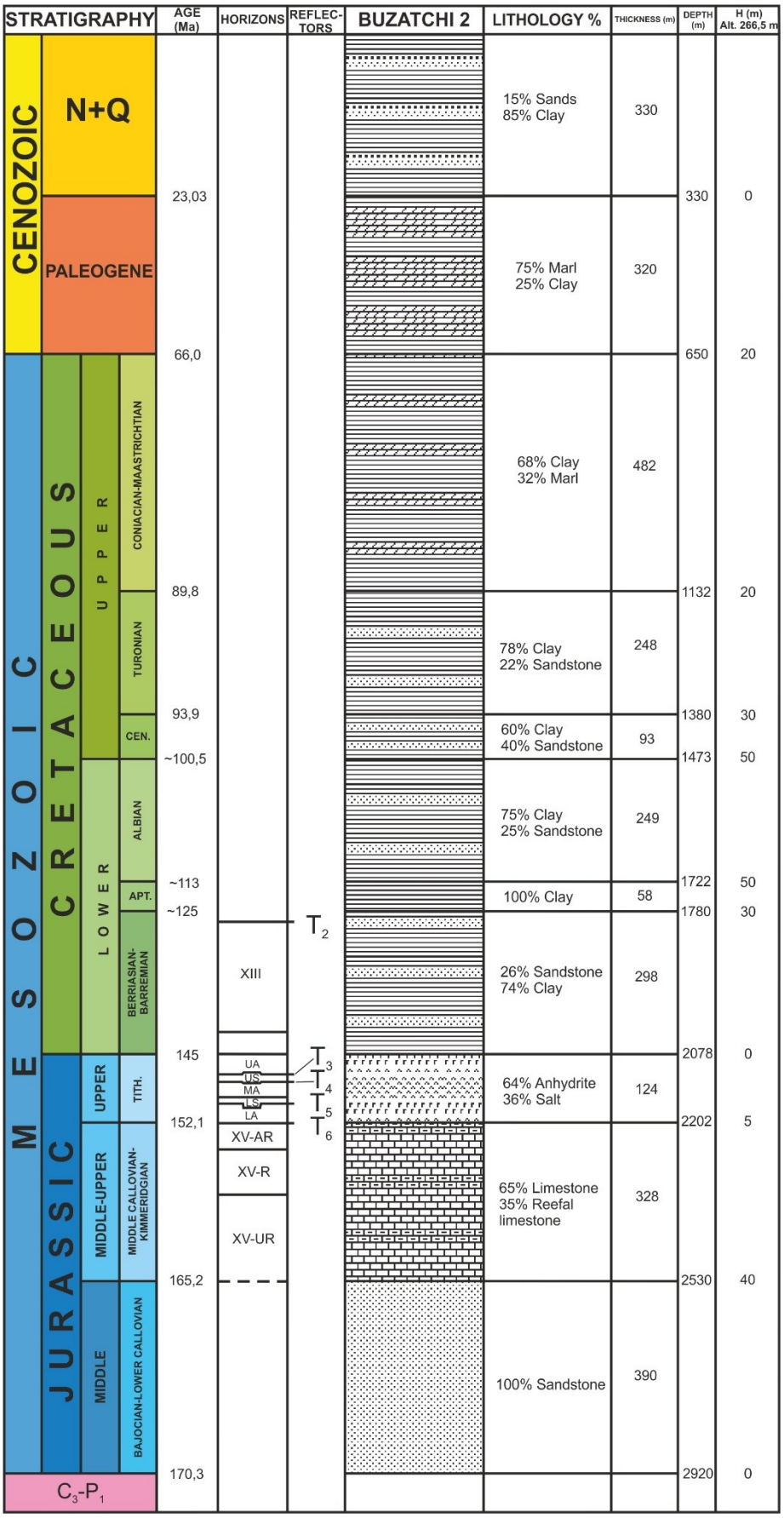

Fig. 4.36. Lithostratigraphic column of the Buzatchi 2 well

4.2.3.2. Karim 2 well

The next selected well for the Bukhara step, is Karim 2. As for the Buzatchi structure, the Karim field is located very near the UKFFZ, east of the Buzatchi field (see fig. 4.34, 4.35). It is located in the southern limits of the Yambashi trough: the same area as Buzatchi 2 (see fig. 4.8-B).

To establish the Karim 2 column we have used a synthetic section of the Karim field (Jukovsky, 1970). The stratigraphy of this well has been taken from the wells catalogue of «Uzbekgeofizika».

The main Paleozoic and Mesozoic surfaces are very tectonized in the Karim. Each side of the Karim field is limited by faults. The direction of these faults changes upwards the section (see fig. 4.34-C, F). We may suppose that this faulting is connected to the reactivation of the UKFFZ during the Mesozoic.

The section of Karim 2 goes from the Paleozoic to the Cenozoic. The Paleozoic is represented by Upper Carboniferous – Lower Permian intrusive rocks. The Jurassic concerns all the stages from the Bathonian (age taken from the synthetic section of Jukovsky, 1970), to the Tithonian. The Cretaceous starts with Berriasian sediments and exposes a complete section. The Cenozoic is represented by the Paleogene, consisting of the Paleocene and Eocene but no Oligocene, and by the Neogene-Quaternary sequence.

The section of the Karim 2 well is 2736 m thick (fig. 4.38). The Paleozoic takes 31 m. The Jurassic is 659 m thick, while the Cretaceous is 1589 m. The Paleogene is 217 m thick, where most part (140 m) belongs to the Eocene. The undivided Neogene-Quaternary sequence has a thickness of 240 m.

The terrigenous Jurassic is constituted of intercalated clay, sandstone, siltstone and argillite layers, where most part is composed of siltstone. The carbonate unit is represented, mainly, by limestone, but there are also reefal limestone and clayed limestone. It is interesting to note, that in this column, the carbonate unit shows a lagoonal type, while the carbonate unit of the Buzatchi field, which is westwards, but belongs to the same area, is of the reefal type. The evaporites show an abbreviated section; there are three members instead of five: the lower anhydrite, lower salt and upper anhydrite. The sediments of the Cretaceous are represented by sandstone, siltstone and clay. In the upper part of the section there are some unconsolidated rocks like pebble and gravelites. The Paleocene is constituted of the limestone of the Bukhara Formation. There are some gypsum intercalations within the limestone. The Eocene shows a siltstone-clayed section with some marl alternations. The undivided sequence of the Neogene-Quaternary is represented by intercalations of clay, sandstone and gravelite in the Neogene part of the section and by different sands and soil in the Quaternary part.

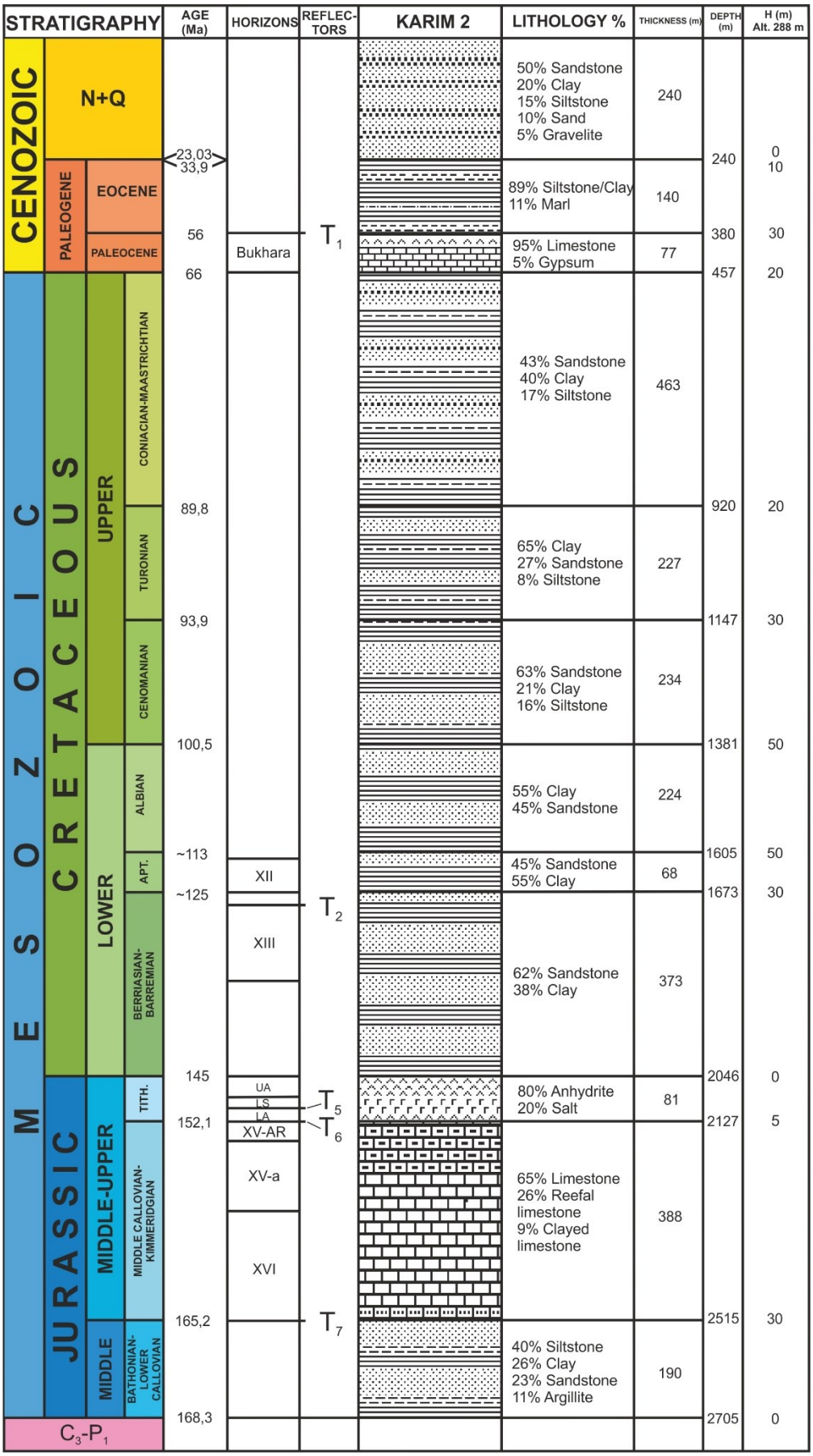

Fig. 4.38. Lithostratigraphic column of the Karim 2 well.

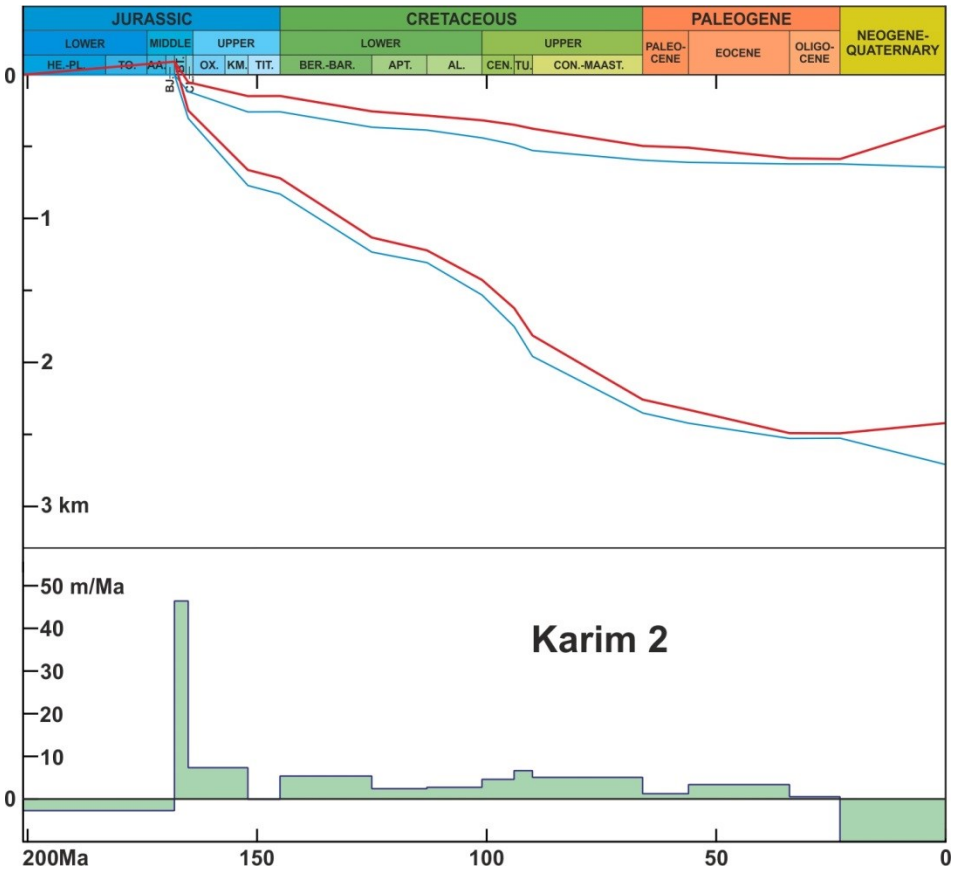

Fig. 4.39. Subsidence curves of the Karim 2 well. Meaning of the curves see caption of fig. 4.13.

The first and main tectonic subsidence event, shown by the Karim 2 well, occurs during the Bathonian-Lower Callovian (fig. 4.39). The high subsidence velocity of 46 m/Ma reached is due to the very short period of time (3.1 Ma) of this event as the beginning of the sedimentation was taken at the Bathonian. Then the subsidence of the area continued, but with a lesser velocity (7 m/Ma during the Middle-Callovian-Kimmeridgian), and stopping during the Tithonian. The subsidence rate increased again during the Cretaceous with average velocities of 2-5 m/Ma and an increase during the Turonian with 7 m/Ma. The Cenozoic is represented by a very slow subsidence (1-3 m/Ma) with a break in the Oligocene as its absence was identified in Karim 2. The Neogene-Quaternary features reflect the intensive uplift of the territory.

4.2.3.3. Synthetic well 2

As there was not well available with the stratigraphy and the lithology for the eastern part of the Bukhara step, we have reconstructed a second synthetic well there. It is located in the limits of the Mubarek fold system, not far west of the Karabair structure (fig. 4.8-B, fig. 4.40).

As a stratigraphic base we have used the NW-SE line G-G' (fig. 4.40). The lithology for the synthetic well has been taken from the structures of Karim and Khodjamubarek (which is located 27 km southwest from the Synthetic well 2, the section of Khodjamubarek was created by Zuev, 1997) even if the Synthetic well 2 is more to the north in the Bukhara step.

According to the isohypse maps (fig. 4.34), the Synthetic well 2 is located in a NE trending half-graben, which is well-seen in Figure 4.40. Upwards of the Cretaceous, the graben disappears.

The pre-Jurassic basement of the area has a Lower-Middle Carboniferous age. The Jurassic is represented by all the units, but not divided into stages. There are the Middle Jurassic terrigenous, the Middle-Upper Jurassic carbonate and the Upper Jurassic evaporite units. The Cretaceous concerns all the stages and an undivided Cenozoic sequence ends the section.

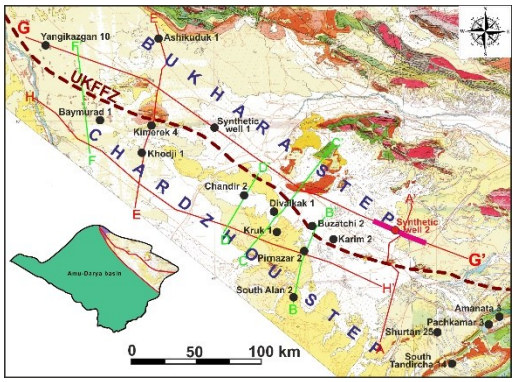

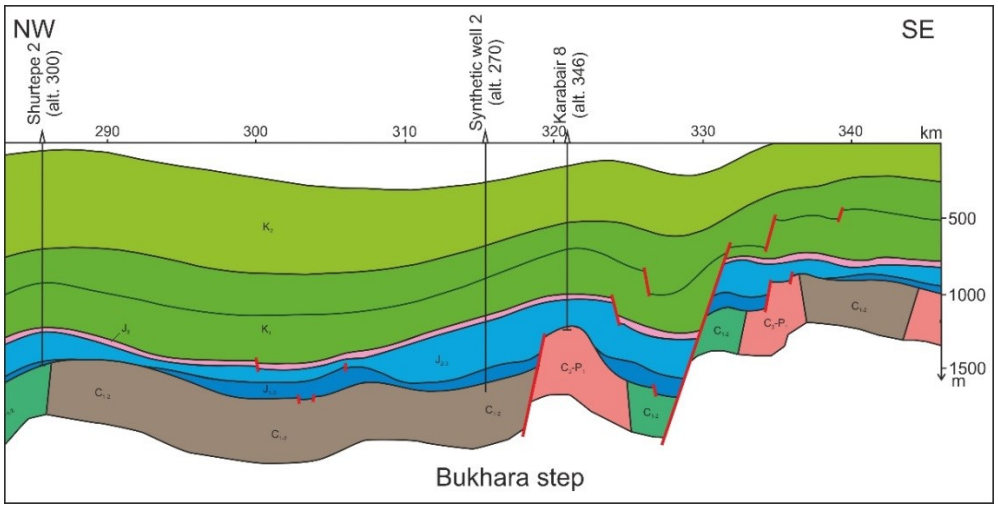

Fig. 4.40. Fragment of the NW-SE oriented G-G' line, exposing the Synthetic well 2.
See Chapter 3 fig. 3.10, for details on the full line.

The Synthetic well 2 is only 1550 m thick (fig. 4.41). The Jurassic is 410 m thick, where the thickest part is represented by the carbonate unit – 330 m. The Cretaceous has a thickness of 840 m and the Cenozoic is 300 m thick.

As we have taken Karim 2 as a basis for the lithology, both wells are similar. The terrigenous Jurassic is represented by a sandy-clayed section, where the sandstone takes most part of the section. The carbonate unit consists of different types of limestone, there is few reefal and clayed limestone. The presence of reefal carbonate in our column (fig. 4.41) is not representative of the real presence of reef at this location and is probably just an effect of using the lithology of field situated near the UKFFZ more to the south. The Upper Jurassic evaporites here are represented by anhydrites with very small salt intercalations. The Cretaceous section is constituted of intercalations of clay and sandstone with some siltstone inclusions. The Cenozoic consists of intercalated sands, soil, sandstone and clay.

The section of the Synthetic well 2 shows a complete, but shortened Mesozoic section, where all the units are represented but as it is not very detailed, the subsidence curves are schematic.

As the thickness of the first Middle Jurassic layer is thin, the Middle Callovian-Kimmeridgian interval appears to be the most important event of the subsidence history (fig. 4.42). But with a rate of only 8 m/Ma before a stop of subsidence during the Tithonian, it is really comparable to the velocities of this period of time observed for example for Buzatchi 2 or Karim 2, both situated in the southwest of the Synthetic well 2. Without any details, the Cretaceous and Cenozoic evolutions are too averaged to provide information on the evolution.

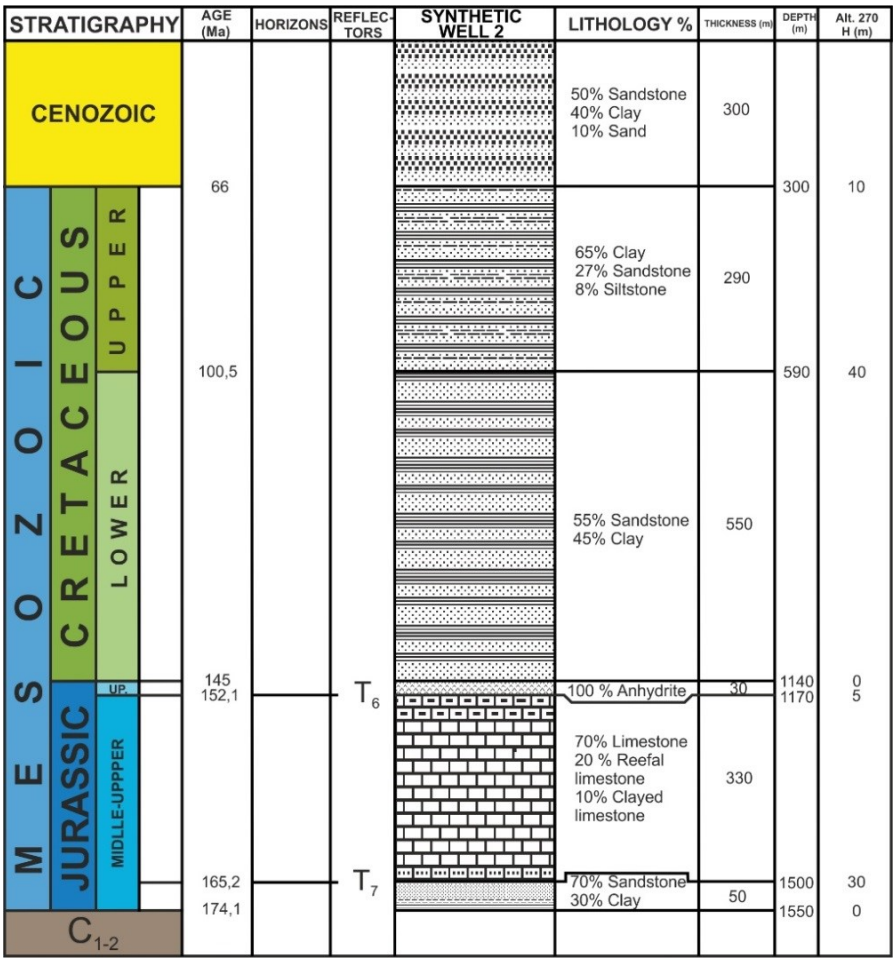

Fig. 4.41. Lithostratigraphic column of the Synthetic well 2.

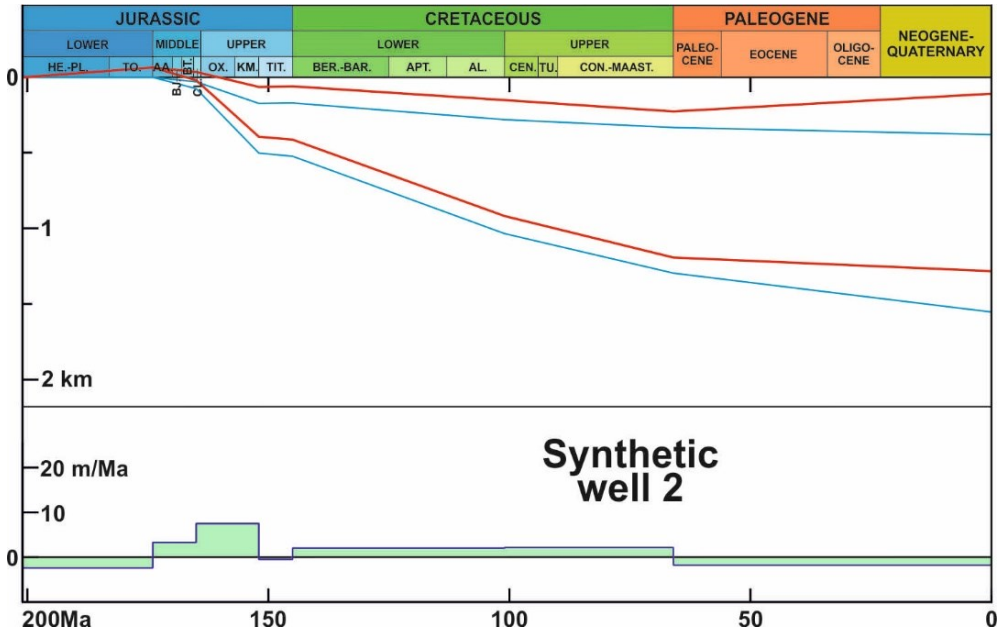

Fig. 4.42. Subsidence curves of the Synthetic well 2. Meaning of the curves see caption of fig. 4.13.

4.2.3.4. Divalkak 1 well

The Divalkak 1 well is the northwesternmost well of the Chardzhou step in the selected area. The Divalkak structure belongs to the Ispanli-Chandir high (see fig. 4.8-B).

As it is seen from the isohypse maps, the Divalkak structure is located in a fault-limited area (fig. 4.34-C, E). These faults create a well-seen triangle-like structure, which is traced up to the top of the carbonates surface. On the surface of the horizon XII of Lower Cretaceous these faults disappear.

A lithostratigraphic section exists for Divalkak 1 (Morozova, 1983) and was used to build our lithostratigraphic column (fig. 4.43). The Divalkak 1 well penetrated 15 m of Paleozoic represented by Middle Carboniferous rocks. The Jurassic starts with the Bajocian and concerns all the stages above it. The Bajocian age of the Jurassic bottom has been taken from the Matonat field synthetic section, which is few kilometres to the east of Divalkak (Matonat is located on the section C-C', see Chapter 3). The Cretaceous exposes a complete section, starting with the Berriasian. The Paleogene is divided into the Paleocene and Eocene, without the Oligocene. And the well is ended by the Neogene-Quaternary sequence.

The Mesozoic-Cenozoic section of Divalkak 1 is 2935 m thick (fig. 4.43) divide into 923 m of Jurassic, 1582 m of Cretaceous and 430 m of Cenozoic sediments, where 301 m belongs to the Paleogene.

From the lithological viewpoint the Bajocian-Lower Callovian siliciclastics are represented by sandstone, clay and siltstone. The Jurassic carbonate unit is composed of limestone, reefal limestone, clayed limestone and some clay; with its subdivisions it is showing a reefal type. The evaporite unit is represented by all the five evaporite members with clay intercalations. The Cretaceous is constituted by sandstone, clay and siltstone with limestone intercalations in the Albian and Turonian. We made the approximation in our reconstruction that the horizon XII is Aptian when in fact the base of the horizon could be Upper Barremian and the top is certainly Lower Albian in age. The Paleocene is represented by the Bukhara limestone Formation, while the Eocene consists of a clayed section with some marl. The Neogene-Quaternary is constituted of a mix of clay, sand, soil, siltstone and sandstone.

Divalkak 1 well is the first well from the selected ones, which is located within the barrier reef system. It exposes well the structure of the reefal type of the carbonate unit with all its subdivisions.

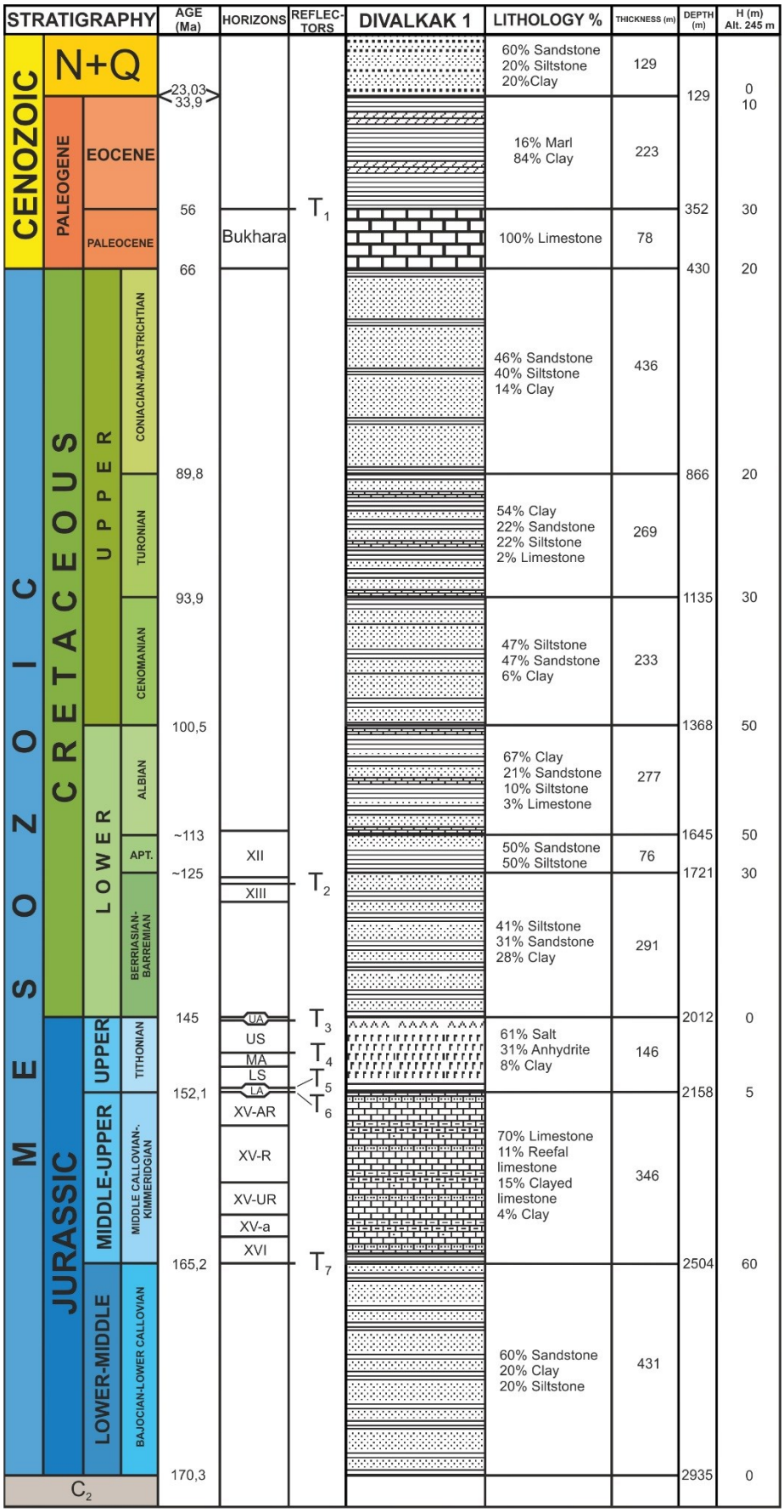

Fig. 4.43. Lithostratigraphic column of the Divalkak 1 well.

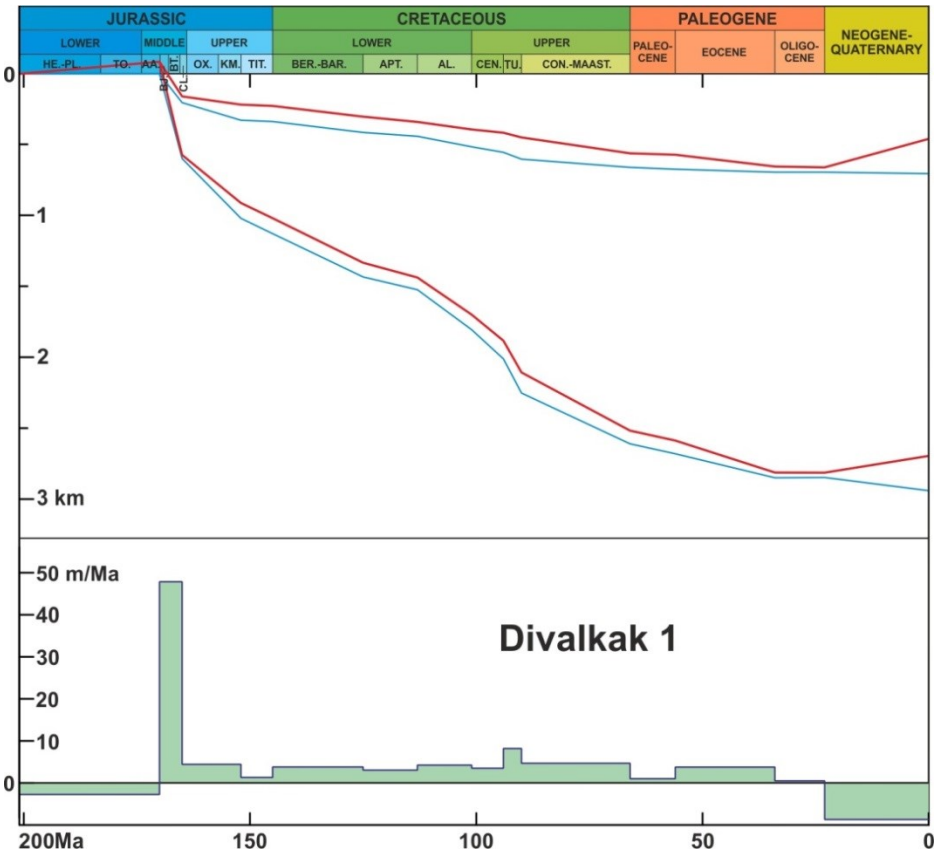

Fig. 4.44. Subsidence curves of the Divalkak 1 well. Meaning of the curves see caption of fig. 4.13.

The principal subsidence event in the Divalkak 1 well appeared in the Bajocian-Lower Callovian (fig. 4.44). The subsidence rate in this period (5.1 Ma) was 48 m/Ma. Then the subsidence has slowed to 1-4 m/Ma in the remaining of the Jurassic. The subsidence of the Cretaceous period is characterized by continuous but small velocities of 3-4 m/Ma, except an increase to 8 m/Ma in the Turonian. The beginning of the Cenozoic is represented by the subsidence velocities of 1 m/Ma in the Paleocene, increasing to 4 m/Ma in the Eocene and dropping to 0 in the end of the Paleogene as the Oligocene is absent. The Neogene-Quaternary shows the uprise of the area.

4.2.3.5. Kruk 1 well

The Kruk 1 well is located to the south of Divalkak 1, but is still belonging to the same Ispanli-Chandir high (see fig. 4.8-B).

The stratigraphic data used for this well come from the wells catalogue of «Uzbekgeofizika», while for the lithology we used the synthetic geological-geophysical section of the Kruk field (Isamuhamedova, 1987).

According to the pre-Mesozoic surface structure, Kruk 1 is located in an EW trending graben. But in the terrigenous Jurassic there are no fault in this area. Some faults, but NS trending appear again in the carbonate surface, then disappear in the Lower Cretaceous surface. In supplement, one big deep fault, which is almost parallel to the Chardzhou step trending, limits the Kruk structure to the south. This fault is observed in the depths maps of all the surfaces, except for the horizon XII of Lower Cretaceous (see fig. 4.34-B, F). These faults allow to suppose that the Kruk area was very active during the Mesozoic.

The Paleozoic is penetrated for 29 m and represented by Lower-Middle Carboniferous sediments. The Jurassic starts with the Aalenian and concerns all the stages up to the Tithonian. The Aalenian age of the Jurassic bottom has been taken from the synthetic section of the Kruk field

(Isamuhamedova, 1987). The Cretaceous also exposes a complete section. The Cenozoic is represented by Paleogene (no Oligocene) and Neogene-Quaternary sequences.

The thickness of the Mesozoic-Cenozoic section of the Kruk 1 well is 3420 m shared into 1357 m of Jurassic, 1668 m of Cretaceous, 288 m of Paleogene and 107 m for the Neogene-Quaternary sequence (fig. 4.45, next page). Lithologically, the Kruk 1 well section is almost the same as for Divalkak 1 as it is located in the reefal zone too. The terrigenous Jurassic is represented by a sandy-clayed section, where sandstone is prevailing. The carbonate Jurassic consists of limestone and reefal limestone exposing a reefal type. The interesting point of this section is that there are two reefal horizons, while in general there is only one. The salt-anhydrite unit consists of its five members. There are some clay intercalations within the evaporite unit. The thickest members are the upper salt and the middle anhydrite. Most part of the evaporite unit thickness belongs to the upper salt member. The Cretaceous is represented by a sandy-clayed section too, most part of the Cretaceous sediments being clayed. The Paleogene consists of the Bukhara limestone in the Paleocene and a clayed-sandy Eocene. The undivided sequence of the Neogene-Quaternary is constituted of intercalations of sands, clay, siltstone and sandstone.

The Kruk 1 well column has a rather thick section and one of interest is the presence of a second reefal limestone horizon in the carbonate Jurassic.

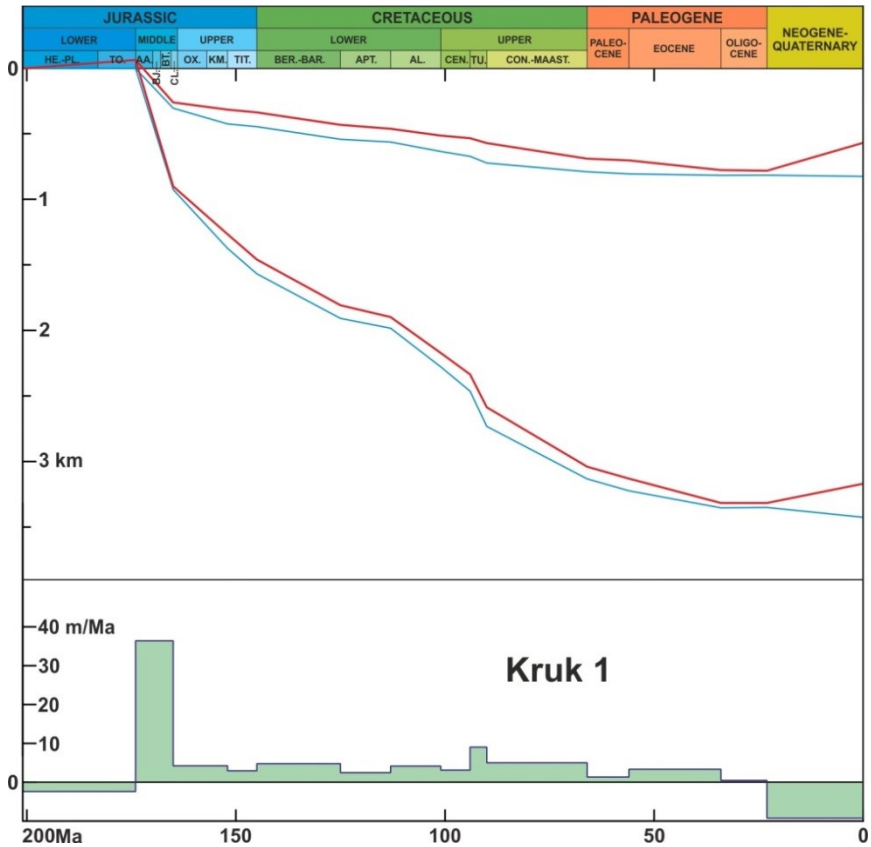

Fig. 4.46. Subsidence curves of the Kruk 1 well. Meaning of the curves see caption of fig. 4.13.

The main subsidence event is observed during the Aalenian-Lower Callovian interval with a high subsidence velocity of 36 m/Ma lasting during 8.9 Ma (fig. 4.46). Then the subsidence is continuous but slow during the remaining of the Mesozoic with velocities reduced a lot in a range of 3-5 m/Ma. A slight increase is observed during the Early Cretaceous and more pronounced during the Turonian reaching then a velocity of 9 m/Ma. Moving to the Cenozoic, the subsidence is very slow during the Paleocene before a last very slight increase during the Eocene (3 m/Ma). During the Neogene-Quaternary interval the curve of the tectonic subsidence rises and the velocity is negative, which marks the uplift of the area.

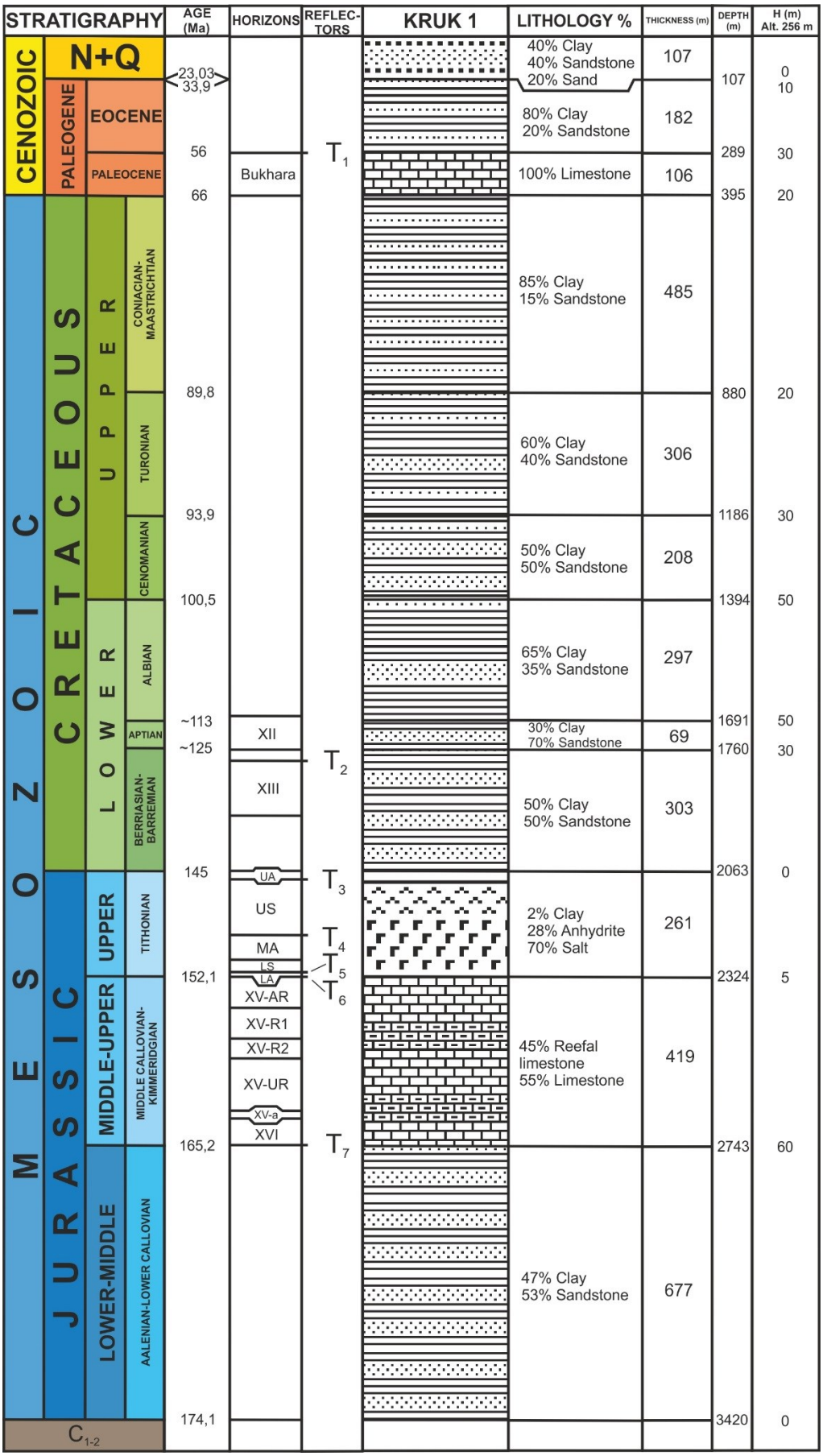

Fig. 4.45. Lithostratigraphic section of the Kruk 1 well.

4.2.3.6. Pirnazar 2 well

The Pirnazar 2 well is located to the southeast of Kruk 1. It belongs to the Ispanli-Chandir high, but is located in its very southeastern limit (see fig. 4.8-B). The information about this well was obtained from two sources. The first one, for the stratigraphy is the wells catalogue of «Uzbekgeofizika». The second one is the synthetic section of the Pirnazar-Markovskoye fields, established by Isamuhamedova (1983). The section of Pirnazar 2 only reaches the top of the Jurassic terrigenous unit but does not touch the pre-Jurassic level. The complete Jurassic thickness was derived from the depth of the pre-Jurassic surface in the line B-B' crossing this well (fig. 4.47).

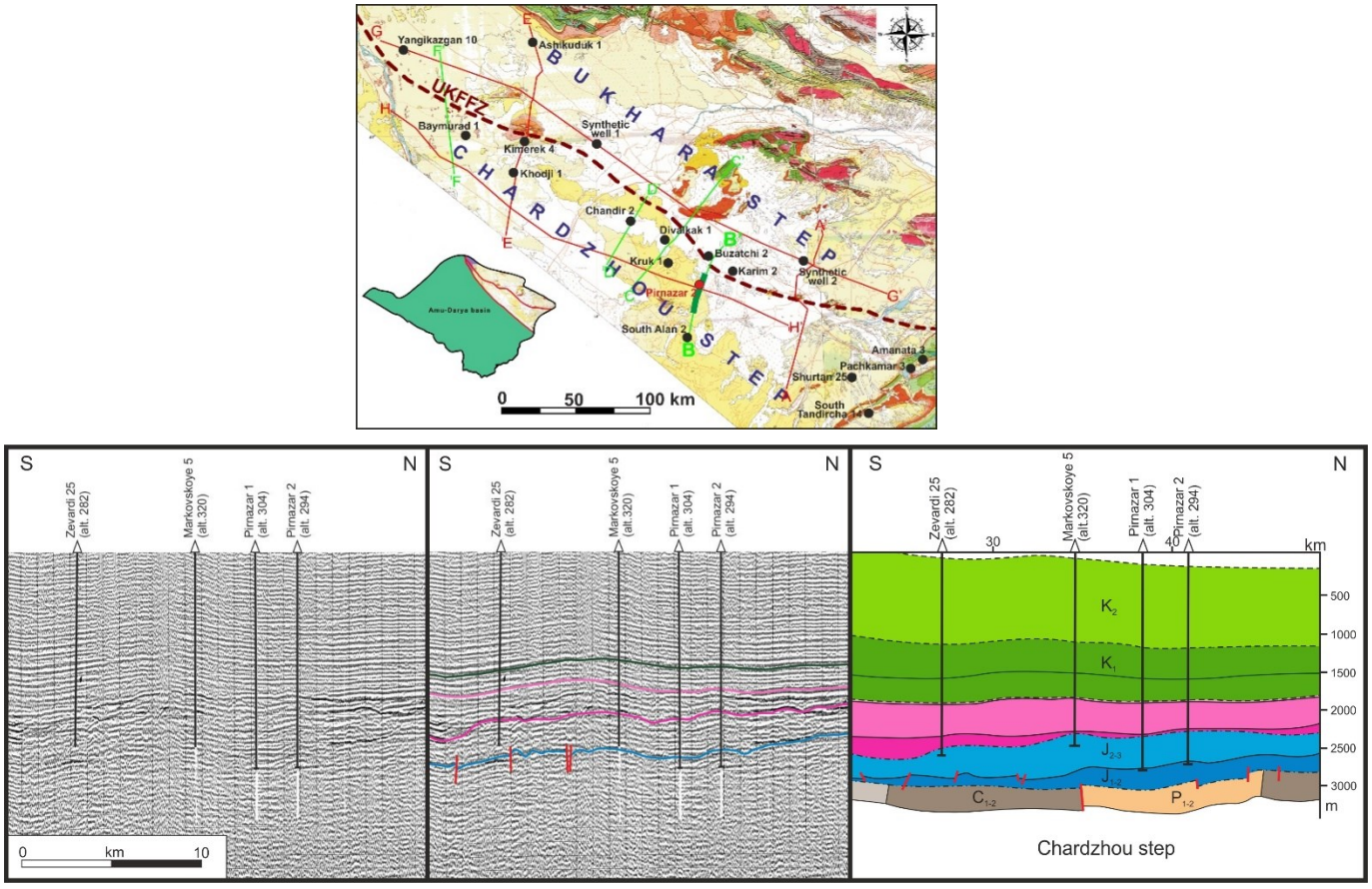

Fig.4.47. Fragment of the B-B' line, exposing the Pirnazar area.
See Chapter 3 fig. 3.5, for details on the full line.

As seen from the map of the age of the pre-Jurassic (fig. 4.34-A), the pre-Mesozoic level in the Pirnazar area has a Lower-Middle Permian age. There are some NW-SE trending faults, which frame the Pirnazar structure in the pre-Jurassic and disappear upwards the section.

The age of the Jurassic bottom is not specified in any source of data, except the synthetic section for the Pirnazar-Markovskoye field (Isamuhamedova, 1983), for which the Bathonian is the oldest age marked, we thus took the Bathonian for the beginning of the section. Besides the terrigenous unit, the Jurassic section contains the Middle Callovian-Kimmeridgian carbonates and the Tithonian evaporites. The Cretaceous shows all the stages, beginning in Berriasian. The Paleogene is represented only by the Paleocene and Eocene stages, the Oligocene is missing. An undivided Neogene-Quaternary sequence ends the Pirnazar 2 well section.

The complete column of Pirnazar 2 (well and the added part from the section) is 3300 m thick (fig. 4.48). The Pirnazar 2 well itself is 3060 m thick; the remaining 240 m were added from the section B-B' (fig. 4.47) based on isohypse map. The Jurassic has a thickness of 1061 m; the Cretaceous is 1763 m thick, while the Paleogene is 328 m thick and the Neogene-Quaternary sequence is 148 m.

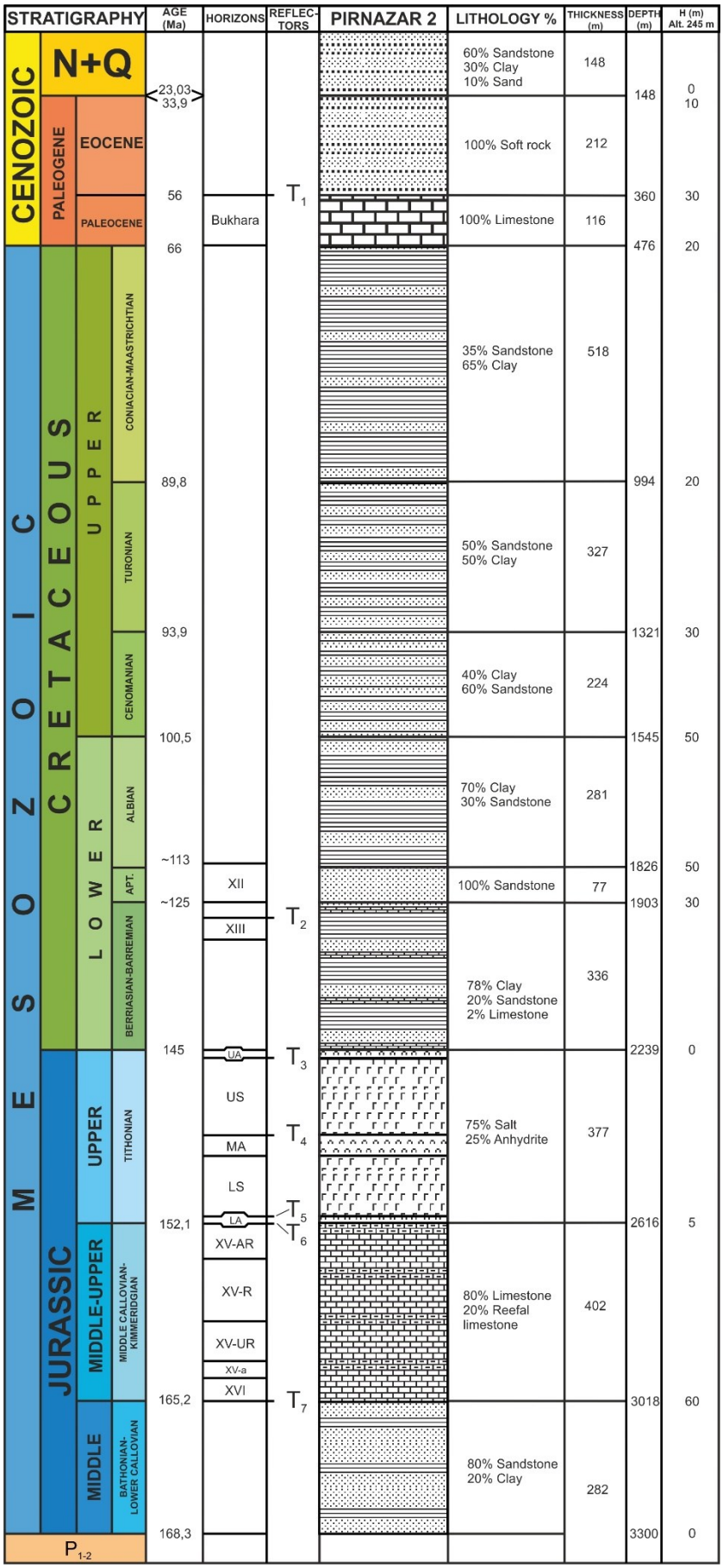

Fig. 4.48. Lithostratigraphic section of the Pirnazar 2 well.

The terrigenous Jurassic lithology was determined by approximation using the nearby wells and consists of an alternation of sandstone and clay in which sandstone is predominating. The carbonate unit is represented by different limestone types: limestone and reefal limestone. The structure of the carbonate unit corresponds to the reefal type. The evaporites are represented by all the five members, but, unlike the previously described wells, here the evaporite section is salty. The thickest parts of the evaporite unit belong to the lower and upper salt members, while the anhydrites are very thin. The overlaying Cretaceous consists of an alternation of sandstone and clay, with some limestone in the bottom of the section. The Cenozoic is represented by the Paleocene Bukhara limestone Formation and the Eocene clay. The Neogene-Quaternary sequence ends the Cenozoic section and consists of intercalations of sands, soil, argillite and clay.

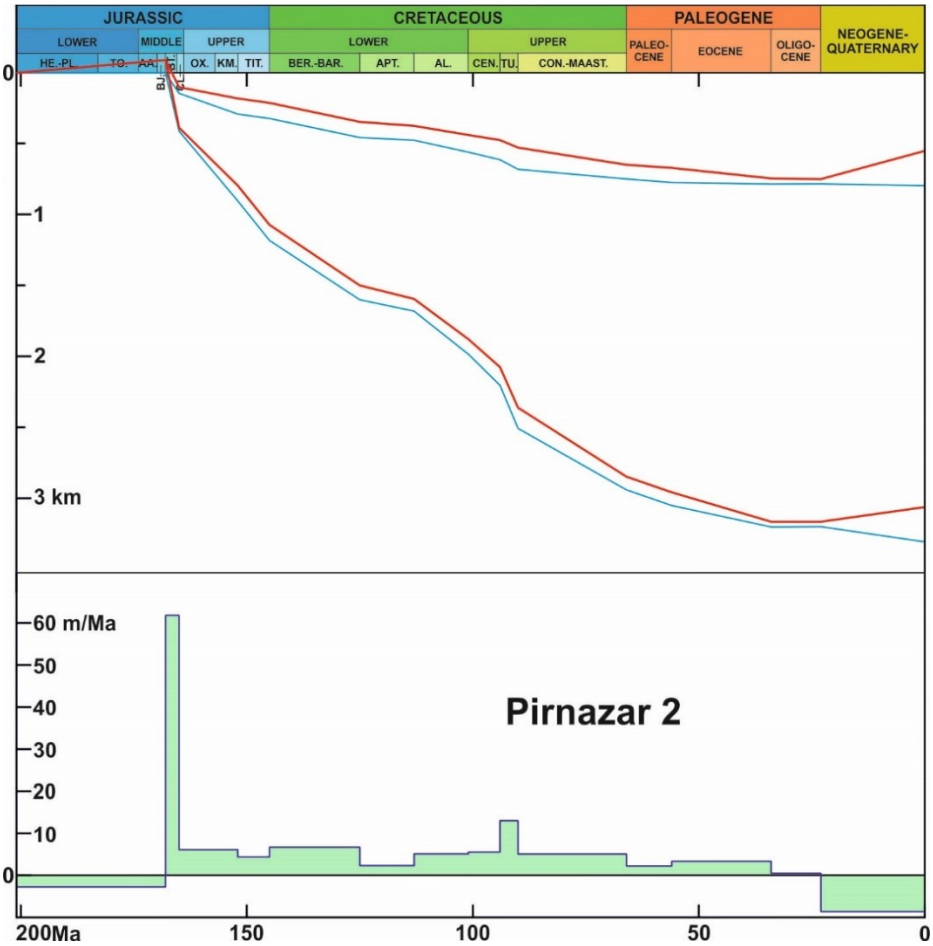

Fig. 4.49. Subsidence curves of the Pirnazar 2 well. Meaning of the curves see caption of fig. 4.13.

The maximal tectonic subsidence rate of all wells, chosen for the subsidence analysis, has been observed for Pirnazar 2 (fig. 4.49). Here, the subsidence velocity has reached 62 m/Ma as the deposition of sediments is supposed to be made in a short period of time: 3.1 Ma, during the Bathonian-Lower Callovian interval. We must remember that this age was chosen because we were lacking more precise data on the beginning of the Jurassic sedimentation. After this, the subsidence has decreased sharply and in the Middle Callovian-Kimmeridgian time the velocity was only 6 m/Ma. Moving to the end of the Jurassic, the subsidence has reduced more to 4 m/Ma in the Tithonian. The Cretaceous period is characterized by velocities ranging in the 2-7 m/Ma interval. As in the most part of the previous curves, the increasing of the subsidence in the Turonian is observed with here 13 m/Ma. The Paleogene is represented by slow subsidence, not exceeding 3 m/Ma. During the Neogene-Quaternary time, the usual uplift is observed.

4.2.3.7. South Alan 2 well

The last well in the selected area is South Alan 2. This well is located in the very south of the area, near the Uzbekistan-Turkmenistan border, in the Beshkent trough, which begins to the east of the Dengizkul high (see fig. 4.8).

The information about the South Alan 2 well comes from the wells catalogue of «Uzbekgeofizika» and from the synthetic section of the South Alan field (Loginova, 1992). The scheme of the pre-Jurassic age shows that a hypothetical Carboniferous-Lower Permian age (see fig. 4.34-A). According to the other surfaces relief maps, the South Alan structure is represented by a rather big anticline, well-seen in the carbonate surface (see fig. 4.34-E).Going towards the southeast of the Chardzhou step in the Beshkent area and its greater depths, this well is the first one of our selection not reaching the pre-Jurassic surface, the terrigenous unit is incomplete and the isohypse map or seismic line do not provide any information (fig. 4.34-C, 4.50).

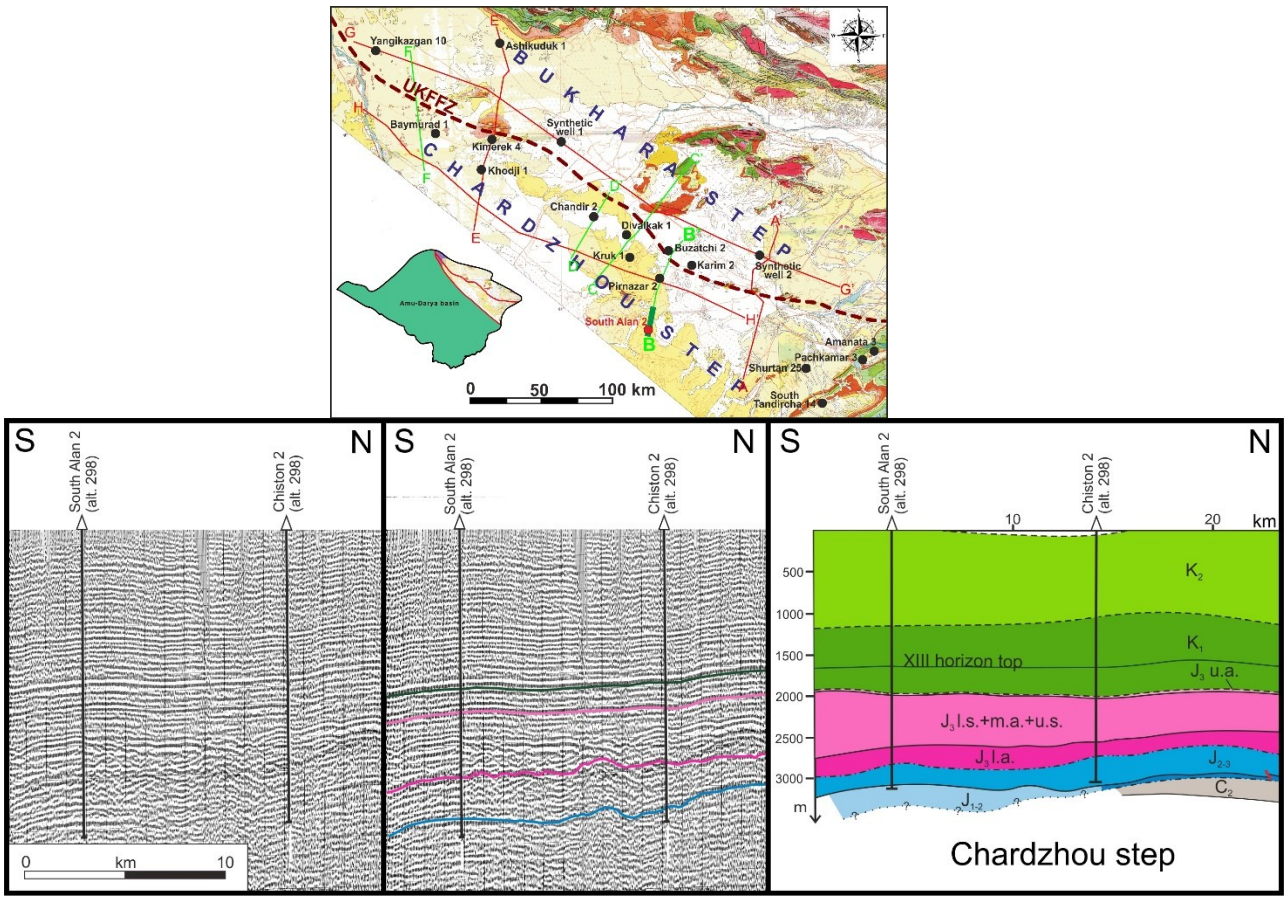

Fig. 4.50. Fragment of the B-B' line, showing the South Alan structure.
See Chapter 3 fig. 3.5, for details on the full line.

Except the small part of the Middle Jurassic terrigenous unit drilled by the well, the Jurassic concerns, the Middle Callovian-Kimmeridgian carbonate unit and the Tithonian evaporites. The Cretaceous represents a complete section, starting with the Berriasian. The Cenozoic section is divided into the Paleogene and Neogene-Quaternary sequence.

The South Alan 2 well is 3402 m long (fig. 4.51). The bottom of the well is situated 54 m below the top of the Middle Jurassic and the isohypse map of the terrigenous Jurassic bottom which is ending just to the north, indicates values around -3100 m (fig. 4.8-C), so a depth of 3400 m from the ground in adding the 300 m of altitude. We supposed that the terrigenous unit is thicker as the nearby Kokdumalak 15 well, located 2.3 km to the northwest, opened a part of the terrigenous unit with 298 m drilled and some general isopachs maps of the terrigenous unit show thicknesses greater than 500 m in this area (for example Ulmishek, 2004). So we supposed in our column a supplementary thickness of 593 m to the 54 m drilled, leading to a total thickness of 3950 m for the full column.

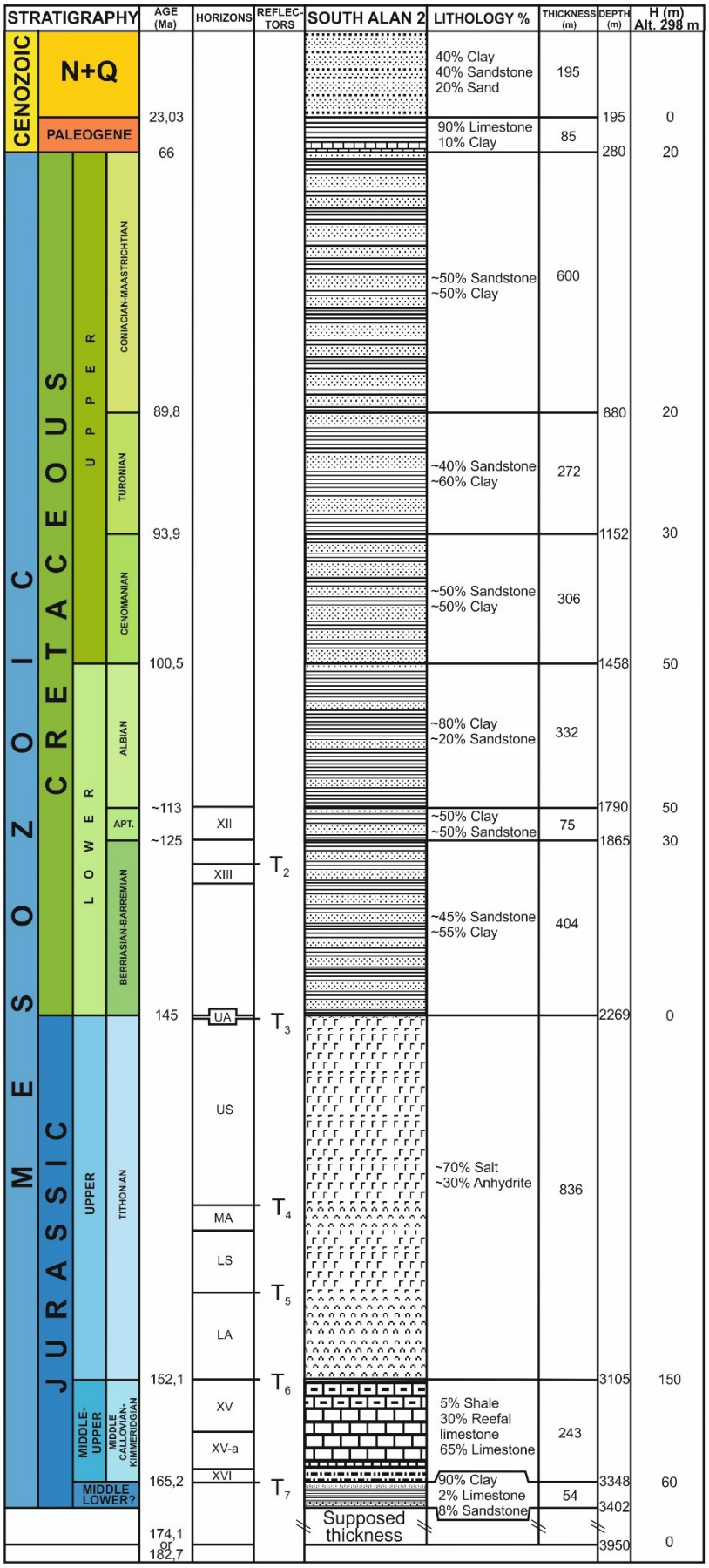

Fig. 4.51. Lithostratigraphic column of the South Alan 2 well.

The carbonate unit has a thickness of 243 m and the evaporites are 836 m thick. The Cretaceous is 1989 m thick and the Cenozoic reaches a thickness of 280 m (fig. 4.51).

Lithologically, the penetrated part of the terrigenous Jurassic unit is represented by an interbedded sequence of sandstone, clay and limestone. The carbonate unit consists of limestone, reefal limestone in the lower part and black shales at the top. These shales, called also the gamma-active pack, are a very good marker of the basinal type of the carbonate section and we supposed a more important bathymetry than for the other wells. The Tithonian evaporites are the thickest unit of the Jurassic in this well. Most part of the thickness belongs to the upper salt member, while the upper anhydrite is very thin. The overlaying Cretaceous beds are represented by intercalations of sandstone and clay, the clay is predominant. The Paleogene consists of limestone and some clay. The limestone corresponds to the Bukhara Formation of the Paleocene. The Neogene-Quaternary is represented by intercalations of sands, soils, gravelite, sandstone, clay and argillite.

The South Alan 2 well exposes a significant Jurassic salt thickening, which is connected to the salt-bearing basins in Turkmenistan and Tajikistan. The gamma-active pack, at the top of the carbonate unit, indicates that this section belongs to the basinal type of the carbonate unit.

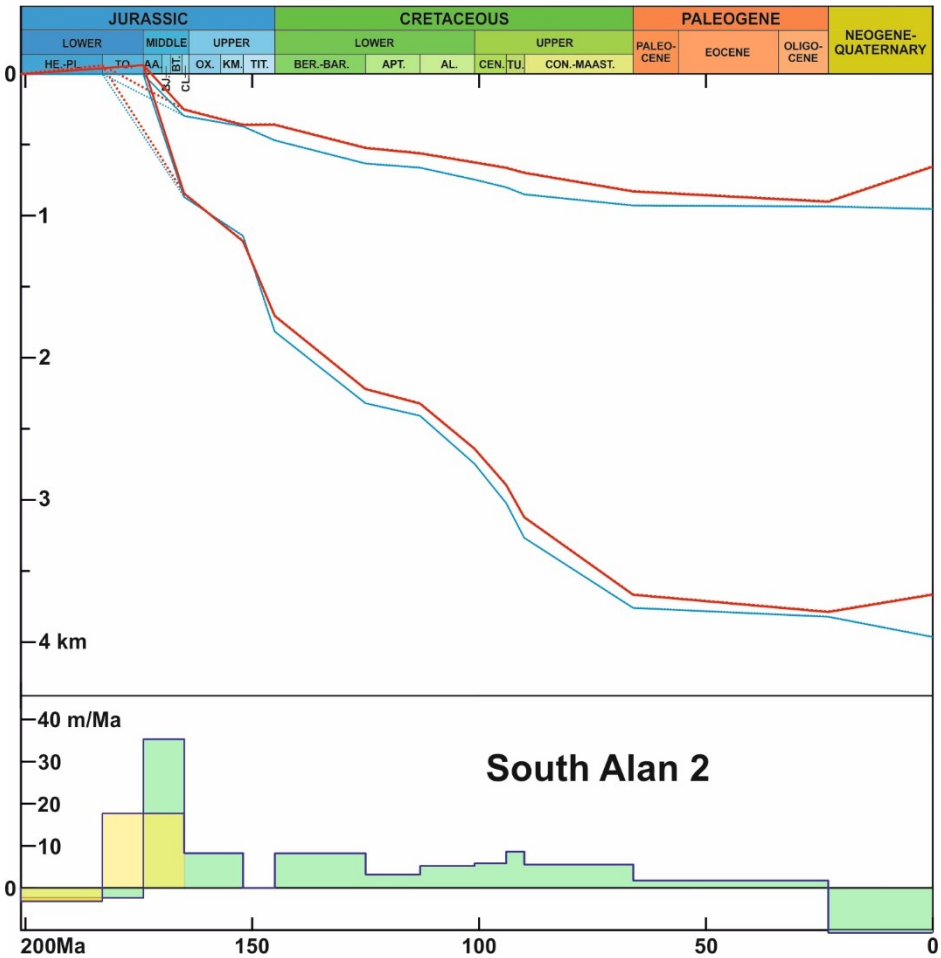

4.52. Subsidence curves of the South Alan 2 well. Meaning of the curves see caption of fig. 4.13. In the velocity diagram: green – Aalenian, yellow – Toarcian for the beginning of the Jurassic sedimentation. Two hypotheses are shown for the age of the beginning of the terrigenous Jurassic: Aalenian with continuous lines and green diagram for the Aalenian-Lower Callovian, and Toarcian with dotted lines and yellow part of the bottom diagram. From Middle Callovian onwards, curves and diagrams are identical for both hypotheses.

As the age of the first Jurassic sediments of South Alan 2 is not determined, we have calculated the tectonic subsidence rate for two hypotheses of ages only for the beginning of the sedimentation and the same supposed thickness of sediments (fig. 4.52). With a Toarcian-Lower Callovian age (in yellow) the velocity is 18 m/Ma during 17.5 Ma, with an Aalenian-Lower Callovian age (in green) the

velocity is 35 m/Ma during 8.9 Ma. From the Middle Callovian onwards, the evolution is the same for both hypotheses. The subsidence rates decreases to 8 m/Ma during the Middle Callovian-Kimmeridgian and is null during the Tithonian. The rate increases to 8 m/Ma during the undivided interval of the Berriasian-Barremian then decreases slightly in the range of 3-6 m/Ma during the remaining of the Cretaceous, except during the Turonian event with a rate of 9 m/Ma. In the Paleogene the subsidence is very slow as it is averaged, before the Late Cenozoic uplift.

4.2.4. Shurtan-Amanata, eastern area

The fourth selected area, covers the southeasternmost part of the Chardzhou step with the Beshkent trough and the Southwestern Gissar region (see fig. 4.8). This area concerns only 4 wells: a synthetic section based on the Shurtan 25 well; the South Tandircha 14, Pachkamar 3 and Amanata 3 wells (fig. 4.53). Shurtan 25 is located in the border zone between the Chardzhou step and the Southwestern Gissar; the South Tandircha 14 well is located in the limits of the Dehkanabad trough and the Pachkamar 3 and Amanata 3 well show the structure of the Karail-Pachkamar anticline zone. Unfortunately, we do not have a good map coverage of this area, as most of the isohypse maps stop in the Beshkent trough (fig. 4.54).

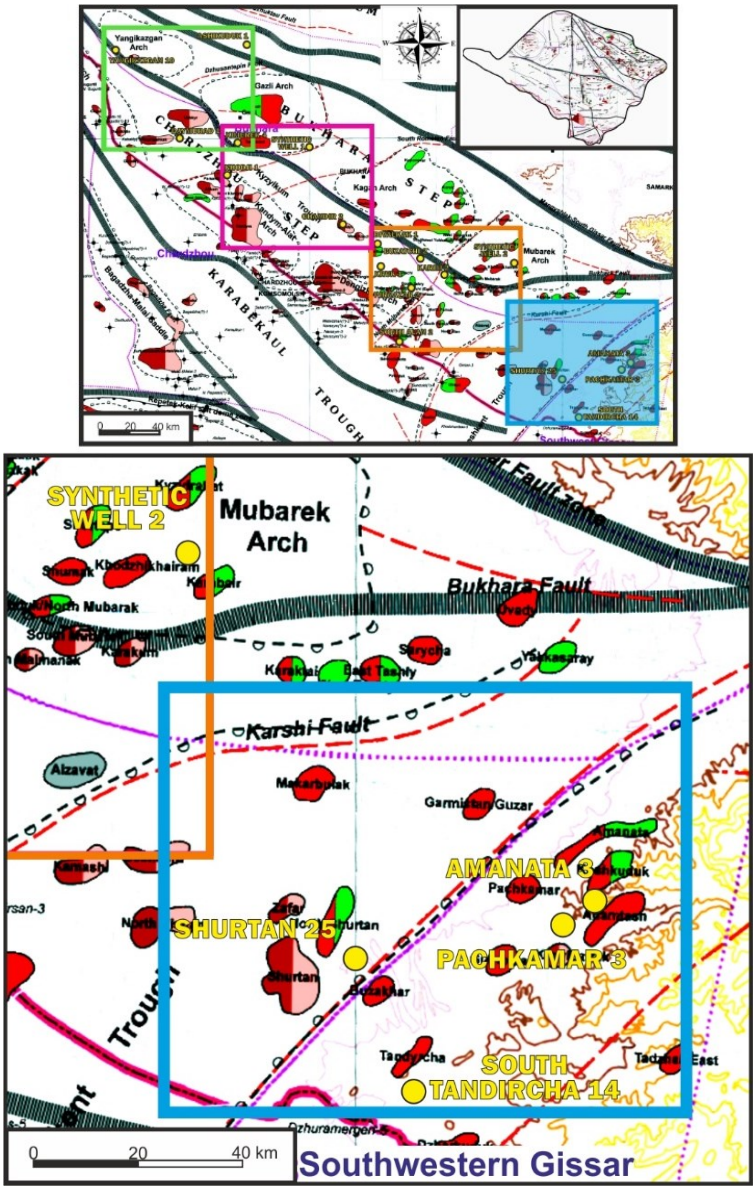

Fig. 4.53. Location of the wells studied in the Shurtan-Amanata area (background map after Blackbourn, 2008, modified).

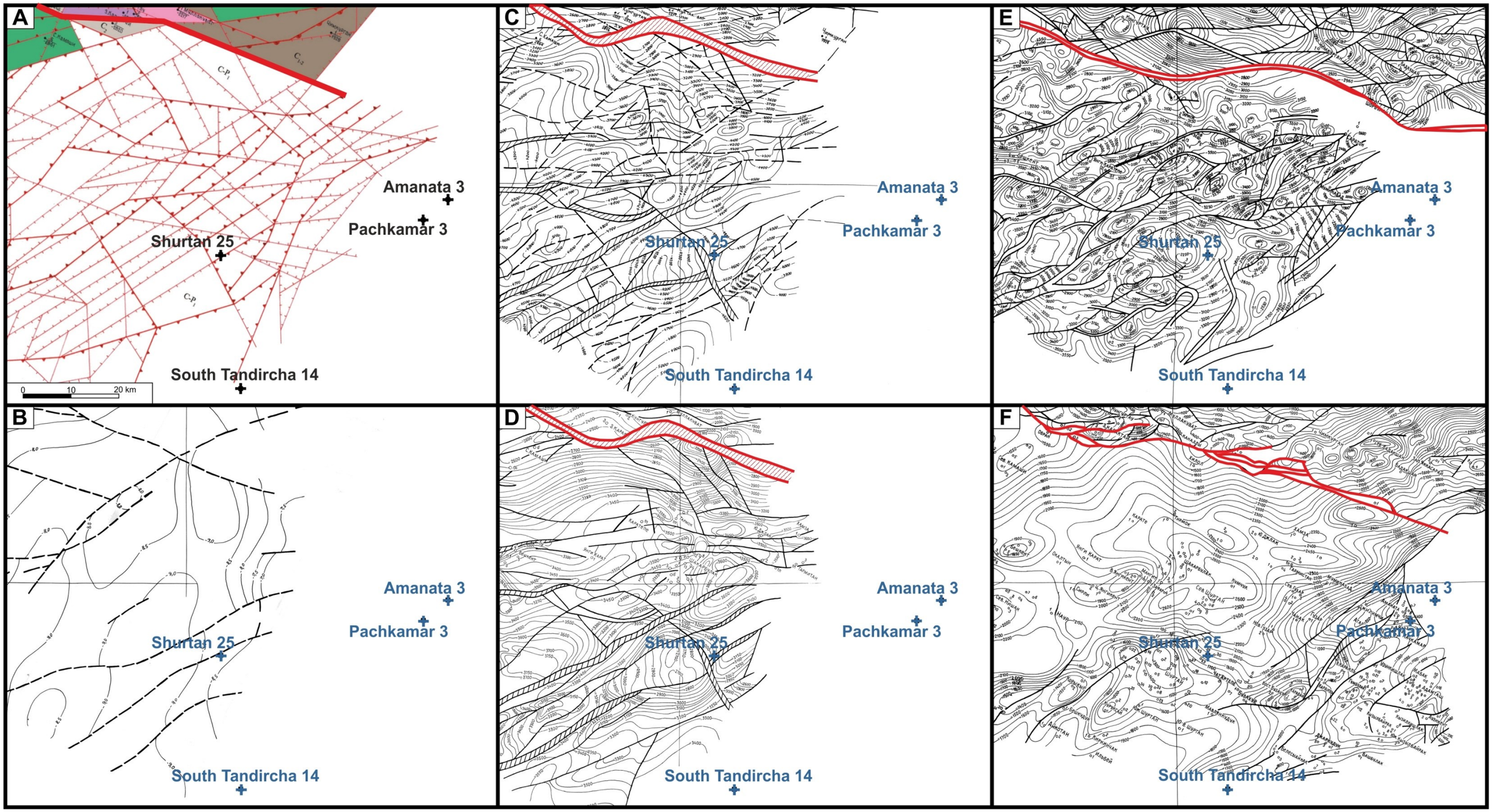

Fig. 4.54. Location of the wells studied in the southeastermost selected area, Shurtan-Amanata and of faults (in red) associated to the Uchbash-Karshi Flexure-Fault Zone.
A – age of the pre-Jurassic surface on a paleogeological scheme of the pre-Jurassic surface of the Bukhara-Khiva region. C. Carboniferous, P: Permian, Permo-Triassic (purple); magmatism: intrusives in pink, effusives in dark green (after Babadjanov and Abdullaev, 2009, modified);
B-F: Isohypse maps (after Mordvintsev O. in Babadjanov, 2008, modified), **B** – relief of the crystalline basement, **C** – relief of the pre-Jurassic roof, **D** – relief of the Jurassic terrigenous roof, **E** – relief of the Jurassic carbonates roof, **F** – relief of the horizon XII roof in the Lower Cretaceous.

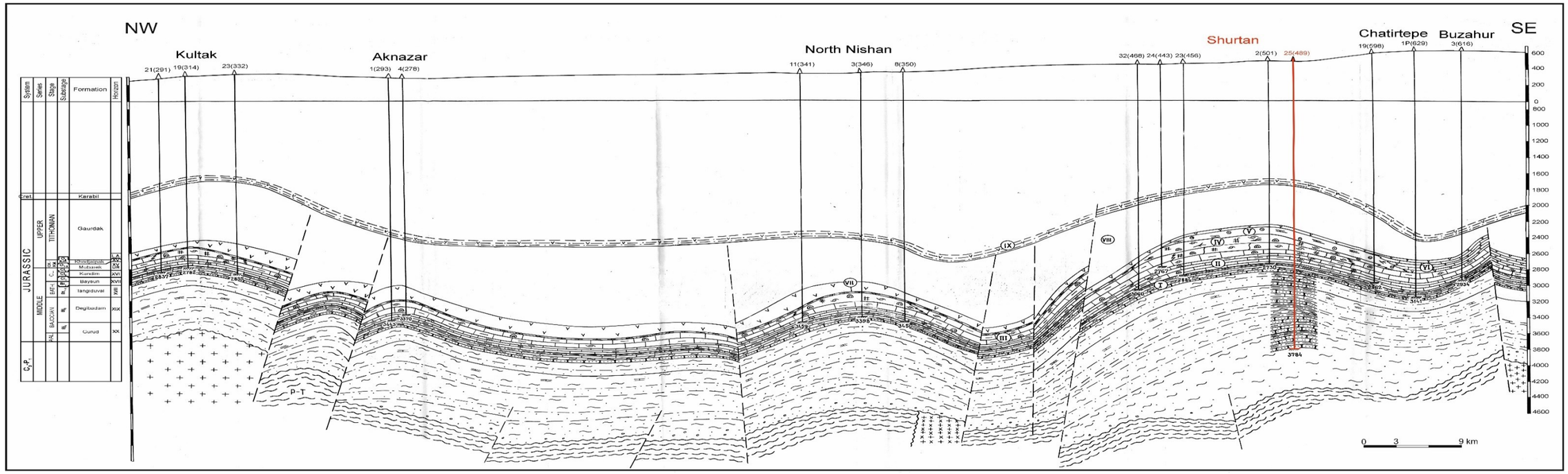

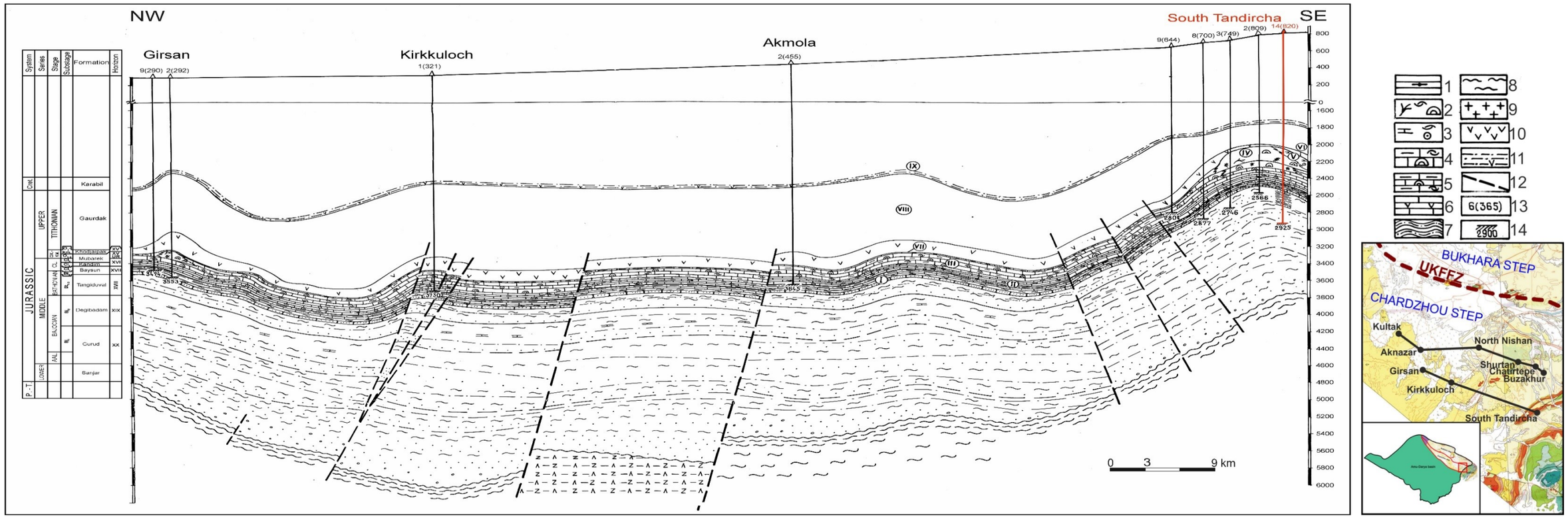

Fig. 4.55. Cross-sections of the Beshkent trough showing the wells Shurtan 25 and South Tandircha 14 and a hypothesis about the bottom depth of the terrigenous Jurassic along the sections (modified after Babadjanov, 2005).
Note that a part each section is not represented vertically: 0-780 m for the top section at and 0-1560 m for the bottom section which is much thicker. **1** – Strongly bituminous limestone; **2** –Massive, coral-algal limestone; **3** – Limestone accumulated, lumpy-algal, with detritus; **4, 5** – Thick-layered, pelitic, clayed limestone; **6** – Mixed limestone and anhydrite; **7** – C_3 metamorphic rocks; **8** – Metamorphic Paleozoic rocks; **9** – Granites; **10** – Lower Anhydrite; **11** – Red clay, sandstone and siltstone; **12** – Faults; **13** – Well (altitude); **14** – Well bottom. **I** – Baysun Formation; **II** – Kandim Formation; **III** – Mubarek Formation; **IV** – Urtabulak Formation; **V** – Kushab Formation; **VI** – Gardarya Formation; **VII** – Khodjaipak Formation; **VIII** – Gaurdak Formation; **IX** – Karabil Formation.

4.2.4.1. Shurtan 25 well synthetic column

Shurtan is one of the biggest oil and gas fields of the Bukhara-Khiva region. The terrigenous section of the Shurtan 25 well (from Babadjanov, 2005) is one of the stratotype sections for the Jurassic terrigenous of the Bukhara-Khiva region and is very precise. But, the lithostratigraphic section of this well stops upwards at the top of the carbonates. As we need the complete section, we have added the Jurassic evaporites, Cretaceous and Cenozoic stratigraphy from the Shurtan 5 well (from the wells catalogue of «Uzbekgeofizika»), which is located west of Shurtan 25. Indeed the depth of the top of the carbonates in the Shurtan 5 well (2771 m) is almost at the same depth than in Shurtan 25 (2770,3 m). To specify the lithological features of this uppart of the section we have used the synthetic section of the Shurtan field (Isamuhamedova, 1977).

All these data allow us to reconstruct the most complete and precise Mesozoic-Cenozoic section of all the wells we have selected for the analysis.

The Shurtan field is located in the Shurtan high (see fig. 4.8-B) in the easternmost part of the Beshkent trough, just at the limit between the Chardzhou step and the Southwestern Gissar.

There is no information about the pre-Jurassic in the sections and columns we used as well as on the scheme of the ages of the pre-Jurassic surface (fig. 4.54), indeed the Beshkent depression is the thickest area of the eastern part of the Chardzhou step and the pre-Jurassic has not been penetrated there. We used the NW-SE cross section Kultak-Buzahur (fig. 4.55) reconstructed by Abdullaev et al. in Babadjanov (2005) to make a hypothesis on the depth of the pre-Jurassic, taken here at 4600 m from the surface. The depths and structure along this section have been reconstructed mostly by geophysical data. Most part of the Jurassic section is also theoretical, as only the Shurtan 25 well has deeply drilled the Jurassic. One of the interesting features in most part of the sections of Figure 4.55 is the presence of the Khodjaipak Formation (roman number **VII** on the figure), which is the good marker of the basinal type of the Jurassic section in a great part of the Beshkent trough. Besides this, the Jurassic section of the Beshkent trough is represented as monotonous enough, without sharp drops of the thickness.

The Shurtan 25 well section starts with the Toarcian and concerns all the Jurassic stages up to the Tithonian. As it is the stratotype section, all these stages are well determined by their age. The overlaying Cretaceous also concerns all the stages, starting with the Berriasian sediments. The Cenozoic is represented by the Paleocene, without Eocene and Oligocene strata, and the Neogene-Quaternary sequence.

According to the structure of the carbonate unit showing up on the synthetic section of the Shurtan field (Isamuhamedova, 1977), the carbonates of Shurtan 25 expose the reefal type of the carbonate unit.

The section of the original Shurtan 25 well is 4217,2 m long, which makes it the longest section we have (fig. 4.56). We made the hypothesis to prolongate it down to 4600 m (after fig. 4.55). The Jurassic takes 1913.2 m with an addition of 383 m in our reconstruction. One of the interesting points of the Jurassic section is the very thick evaporite unit. The thickness of the Tithonian evaporites is 466,3 m and most part of this thickness belongs to the salt members. The Cretaceous is 1836 m thick. The Cenozoic thickness is 468 m and most part of it belongs to the Neogene-Quaternary pile.

From the viewpoint of the lithology, the terrigenous Jurassic exposes a sandy-clayed section, where the sandstone is strongly prevalent. The carbonate unit exposes the reefal type of the carbonate unit and consists of limestone, reefal limestone and clayed limestone. The Tithonian evaporites are constituted of the five members of intercalated salt and anhydrite. The thickest member is the upper salt, while the upper anhydrite is very thin.

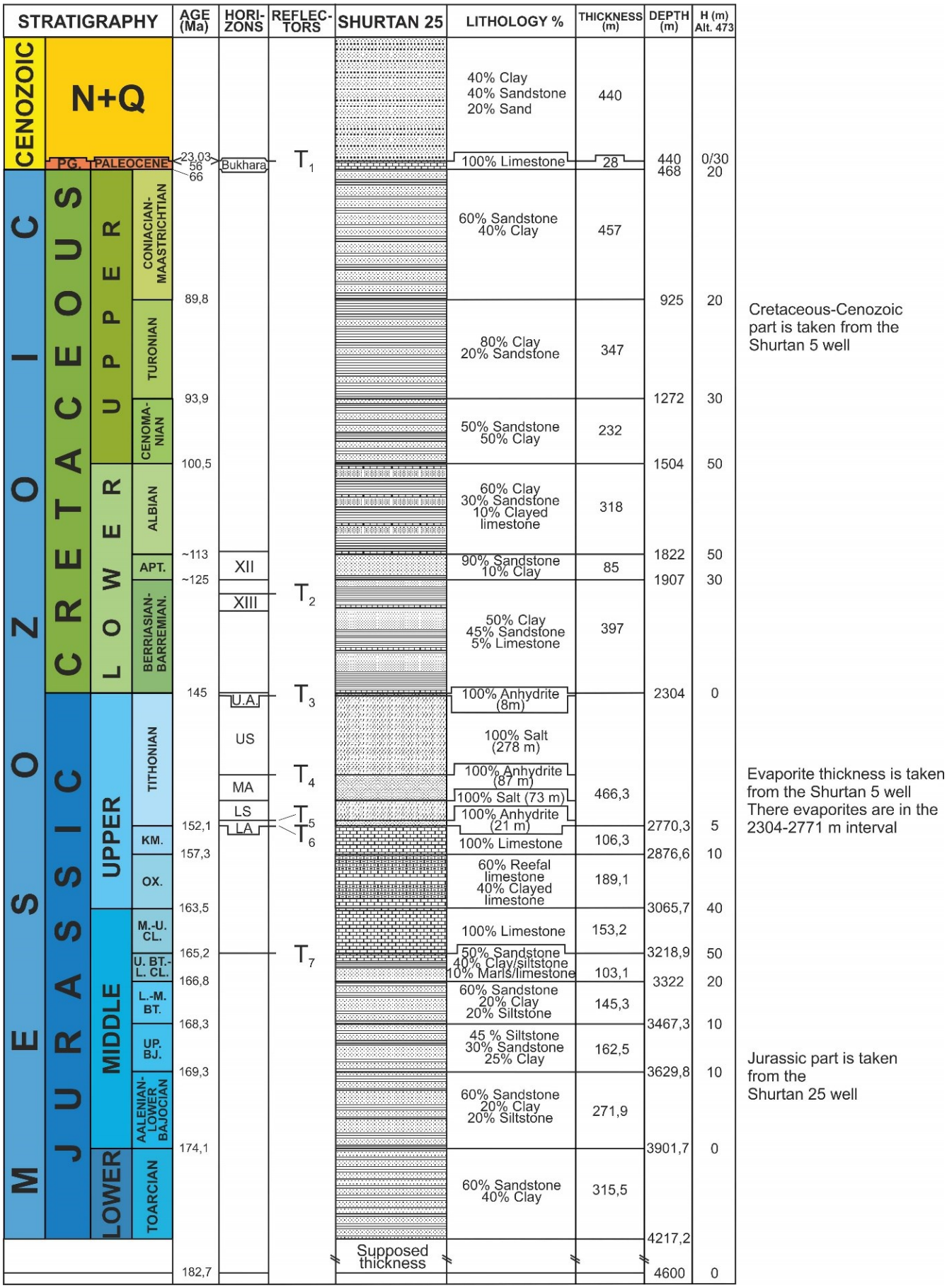

Fig. 4.56. Lithostratigraphic synthetic column of the Shurtan 25 well.

The lithology of the Cretaceous does not differ a lot from the same aged lithology from other wells. It is represented by alternations of sandstone and clay with some limestone and clayed limestone inclusions. The Paleogene layer, in comparison with other wells, is thin and represented by the Bukhara limestone. The Neogene-Quaternary consists of a mix of sand, pebble, sandstone, siltstone, soil and clay.

In brief, the Shurtan 25 well section is the thickest Jurassic section we have selected. At the same time it exposes a well divided lithostratigraphic Jurassic terrigenous unit. But the age of the first Jurassic sediments could possibly be older than Toarcian (Mirkamalov et al., 2005). Another interesting point is the evaporite unit thickening observed in this well. This thickening trends from the northwest of the Bukhara-Khiva area to the southeast and the Shurtan 25 well section confirms it. Another point is the very thin (in comparison with other wells) Paleogene sequence.

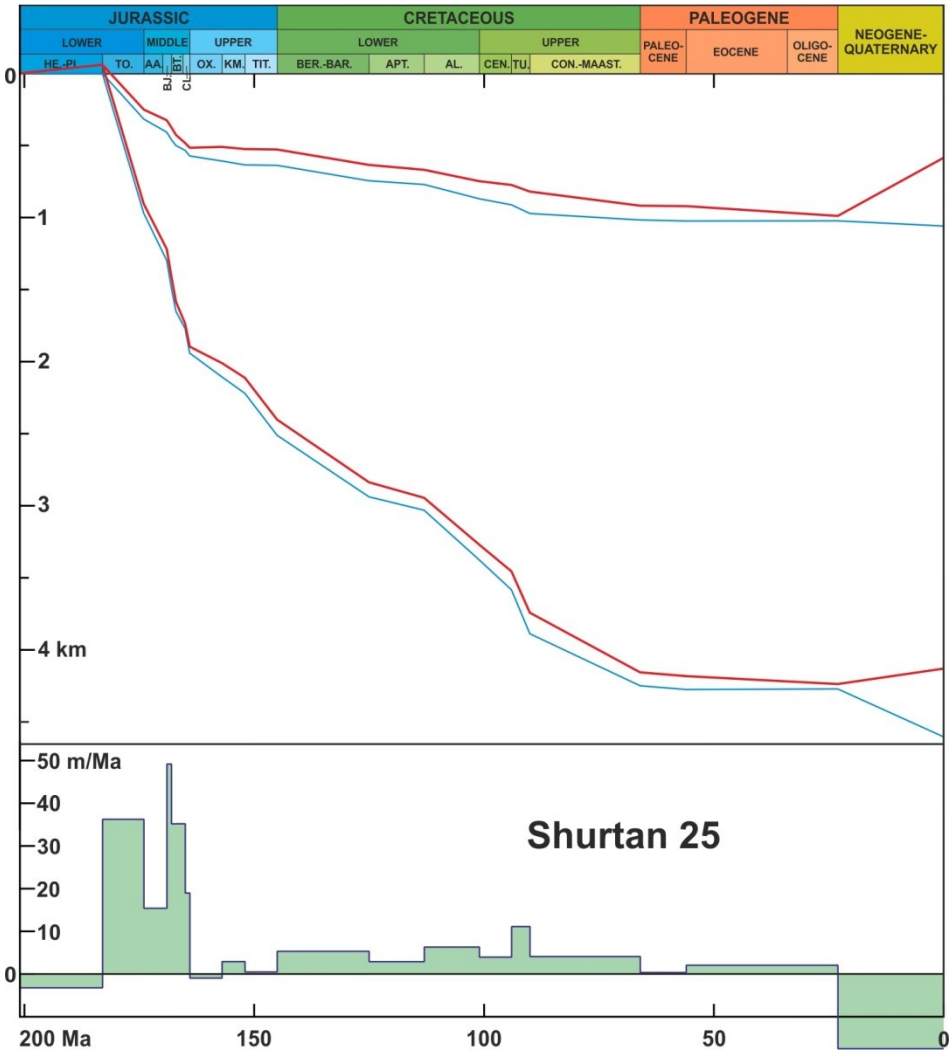

Fig. 4.57. Subsidence curves of the Shurtan 25 well. Meaning of the curves see caption of fig. 4.13.

As the section of the Shurtan 25 well is one of the most detailed sections we have reconstructed, its subsidence history is very detailed too (fig. 4.57). Nevertheless as we have only one well with such details, even if it is one stratotype section for the Jurassic terrigenous, we must be cautious in the interpretation of the ages which is not recent. Indeed precise ages over very short periods of time produce peaks in the subsidence diagrams, for example during the Upper Bajocian and the Lower-Middle Bathonian which are divided here.

The diagram of tectonic subsidence rates shows a main tectonic subsidence event from the Toarcian to the Middle Bathonian, with a duration of 19.2 Ma, divided into two main peaks. The first one with a

velocity reaching 36 m/Ma takes place during the Toarcian (8.6 Ma) and after a decreasing to 15 m/Ma during the Aalenian-Lower Bajocian (4.8 Ma), a second peak occurs from the Upper Bajocian to the Upper Callovian (5.8 Ma). Over this latter period, ages were determined sharply, the maximal tectonic susbidence velocity is reaching 49 m/Ma because a very short interval of one Ma is used for the Upper Bajocian then decreasing to 35 m/Ma over the Lower Bathonian-Lower Callovian interval, and 19 m/Ma during the Middle Upper Callovian. The subsidence is null during the Oxfordian and Tithonian or very reduced during the Kimmeridgian. During the Cretaceous a slow subsidence is observed with small increases during the Berriasian-Barremian (5 m/Ma), the Albian (6 m/Ma), and a bit more during the Turonian (11 m/Ma). The rate is null or reduced during the Cenozoic befre the late uplift.

4.2.4.2. South Tandircha 14 well.

South Tandircha 14 well is the southernmost well selected in the Southwestern Gissar area. It is located in the southern limit of the Dehkanabad trough, near the Uzbekistan border (see fig. 4.8).

We have used the wells catalogue of «Uzbekgeofizika» and the synthetic section of the South Tandircha field (anonymous, no date) as the source of data for South Tandircha 14 which is the longest well of this field. It does not touch the pre-Jurassic basement for which we have no information it comprises all the stages from the Lower Callovian to the Quaternary.

The thickness of the entire section of the South Tandircha 14 well is 4024 m. Being in the deepest parts of our area of investigation, the well does not reach the bottom of the Jurassic. We have used a reconstruction of a NW-SE cross section of the Beshkent trough from Girsan to Tandyrcha (modified from Babadjanov, 2005, fig. 4.55) to make a hypothesis on the depth of the pre-Jurassic basement. For the subsidence reconstruction we then used a total thickness of 4600 m. The Jurassic takes 1469 m from it in the real South Tandircha 14 well and we supposed a supplementary thickness of 576 m from the cross-section. The Cretaceous thickness is 2350 m and the Cenozoic is 205 m thick (fig. 4.58).

In the synthetic section of the South Tandircha field, the Jurassic bottom has an undetermined age: Lower?-Middle Jurassic and on the cross-section (fig. 4.55, after Babadjanov, 2005) the bottom layer is the Sanjar Formation of the Lower Jurassic. The age of the bottom is at least Aalenian, we assume a Toarcian age but it could be still older (Mirkamalov et al., 2005). One of the features of this section, as in the Shurtan section, is the thick evaporite and carbonate units. The evaporite thickening is usual for the southeastern areas of the Amu-Darya northern margin but in supplement the carbonate section of the South Tandircha 14 well is the thickest carbonate section among all the columns we have selected. According to its structure, it exposes the reefal type of the carbonate unit.

Lithologically, the terrigenous Jurassic unit is represented by a clayed-sandy section with some limestone at the top of the section. The carbonate unit mainly consists of limestone, reefal limestone and few clayed limestone. The Tithonian evaporite unit differs from the other evaporite sections as there are only four members instead of five, the upper anhydrite is missing. The upper salt is the thickest member and takes more than half of the entire evaporites thickness. The anhydrite members consist of gypsum despite their name of “anhydrite”. The Cretaceous is constituted of alternations of clay and sandstone with some limestone inclusions. The limit between the Berriasian-Barremian and Aptian is not well reflected in the lithological features of the section The Paleogene consists of alternating layers of limestone and gypsum. The Neogene-Quaternary consists of intercalations of clay, sandstone, siltstone and conglomerates.

The South Tandircha 14 well as the Shurtan 25 and Kimerek 4 columns is one of the thickest total sections, and of the thickest Jurassic we have selected. It is also the southernmost one towards the deep Amu-Darya basin. It does not expose the full terrigenous Jurassic the thickness of which is hypothesized by using a reconstructed cross-section of the Beshkent area. It has an unusual structure of the evaporite unit with only four members instead of five. Gypsum appears in the Paleogene section.

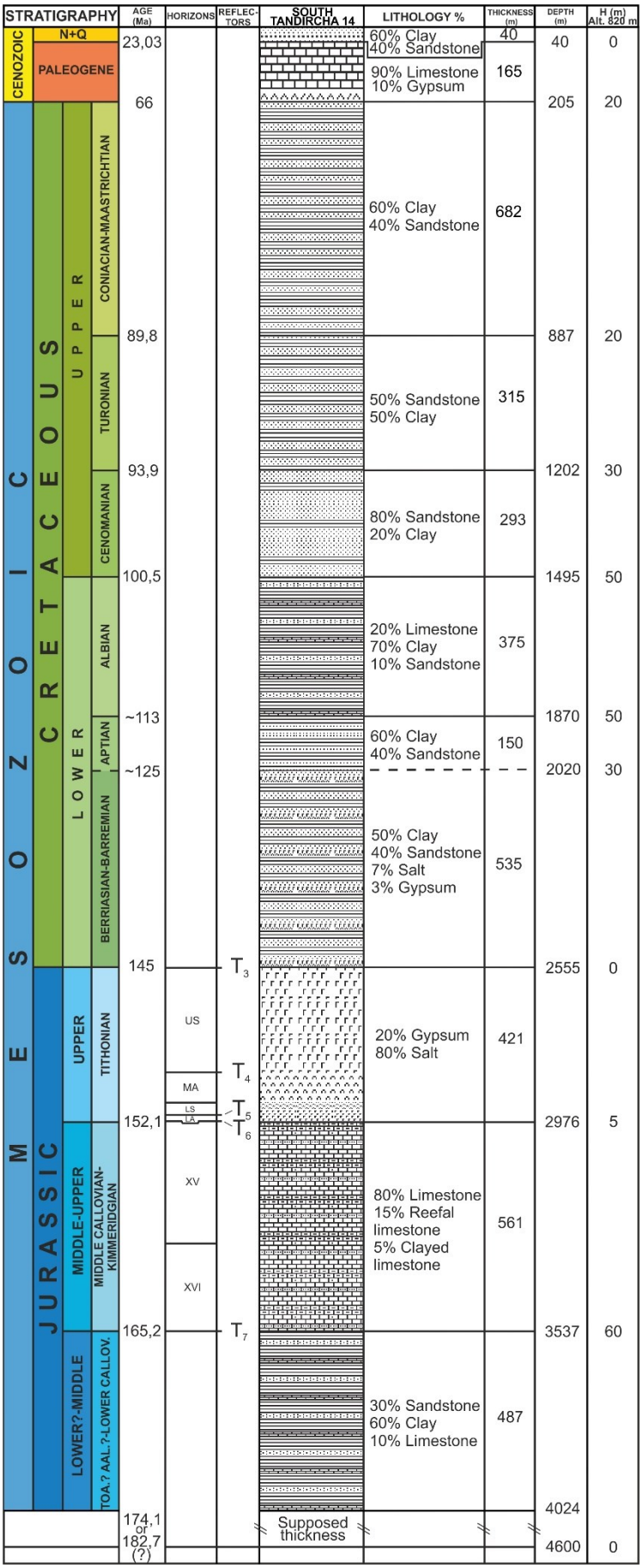

Fig. 4.58. Lithostratigraphic column of the South Tandircha 14 well.

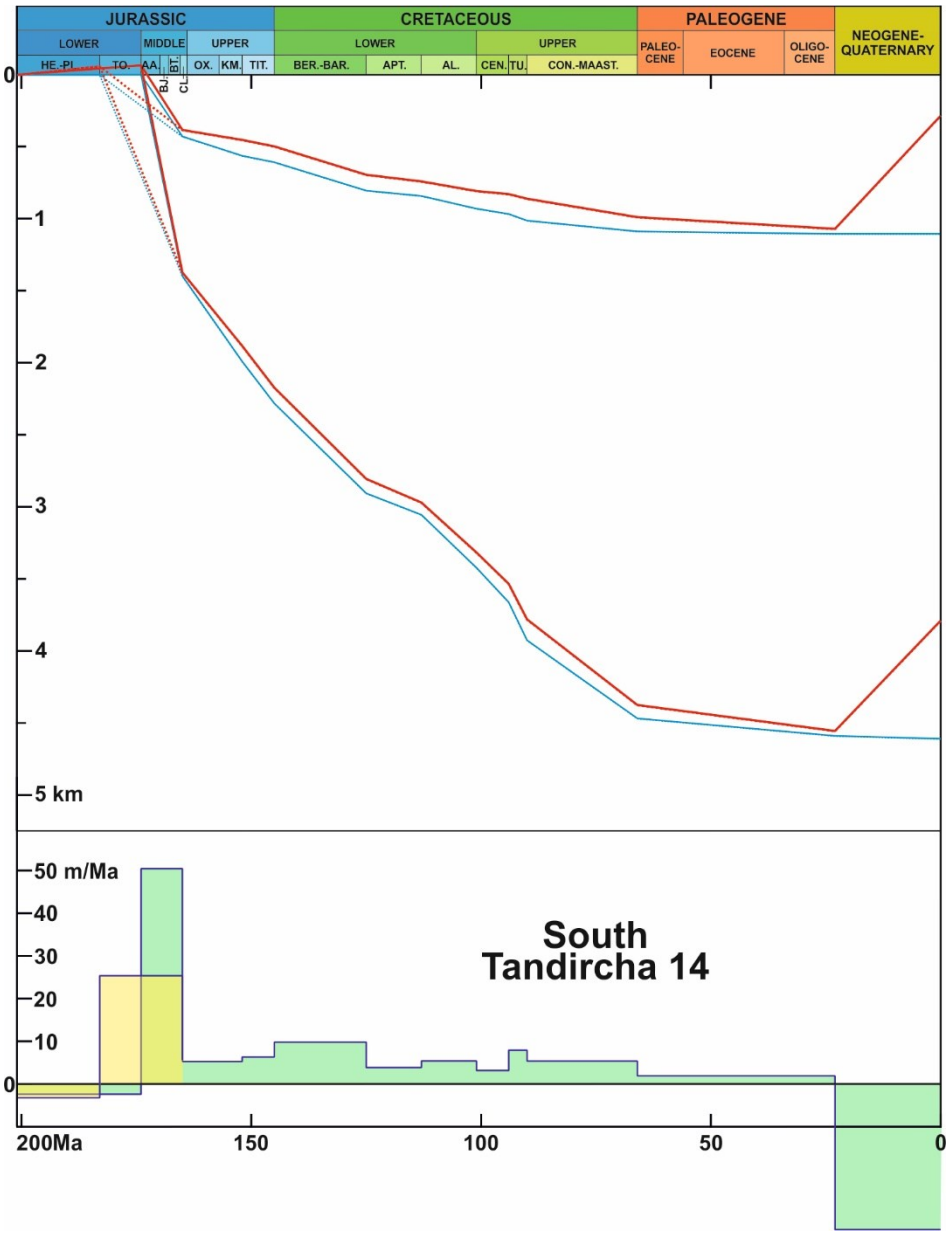

Fig. 4.59. Subsidence curves for the South Tandircha 14 well. Meaning of the curves see caption of fig. 4.13. In the velocity diagram: green – Aalenian, yellow – Toarcian for the beginning of the Jurassic sedimentation. Two hypotheses are shown for the age of the beginning of the terrigenous Jurassic: Aalenian with continuous lines and green diagram for the Aalenian-Lower Callovian, and Toarcian with dotted lines and yellow part of the bottom diagram. From Middle Callovian onwards, curves and diagrams are identical for both hypotheses.

The age of the Jurassic bottom of the South Tandircha 14 section is still under question. So we have calculated the subsidence velocities for two hypotheses: for a Toarcian or an Aalenian age (fig. 4.59). If the subsidence has started in the Toarcian, the subsidence velocity is of 25 m/Ma during 17.5 Ma, but if beginning in the Aalenian, the velocity increases to 50 m/Ma during 8.9 Ma till the Lower Callovian in both cases. During the Middle and Late Jurassic, the subsidence sharply decreases to 5-6 m/Ma. We must note, that during the Tithonian, when the subsidence usually stops, it continues here. This depends of the correction made for the bathymetry at the end of the Kimmeridgian. We supposed here a paleowater depth of 5 metres because we have reefal limestone in the Middle Callovian-Kimmeridgian strata. But if this reefal limestone of shallow water is present only in the lower part and if the surface is more clayey or with shale, we could suppose a deeper bathymetry as we took for South Alan 2, because we are near the basin. Doing so, the result would be to reduce the tectonic subsidence during the Tithonian, with only a filling of the depression by evaporites. The Cretaceous period is characterised by a slow continuous subsidence with velocities of 3-8 m/Ma the

higher values being observed during the Berriasian-Barremian (10 m/Ma) and (8 m/Ma) during the Turonian. The Cenozoic time is represented by a very slow subsidence of the area: 2 m/Ma during the Paleogene which is averaged and the sharp uplift in the Neogene-Quaternary as we have higher altitudes in the beginning of the Southwestern Gissar.

4.2.4.3. Pachkamar 3 well

The Pachkamar 3 well was selected to show the subsidence processes in the northern part of the Southwestern Gissar. This well is located in the limits of the Karail-Pachkamar and Adamtash anticline zones (see fig. 4.8) and we have a section crossing this area (fig. 4.60).

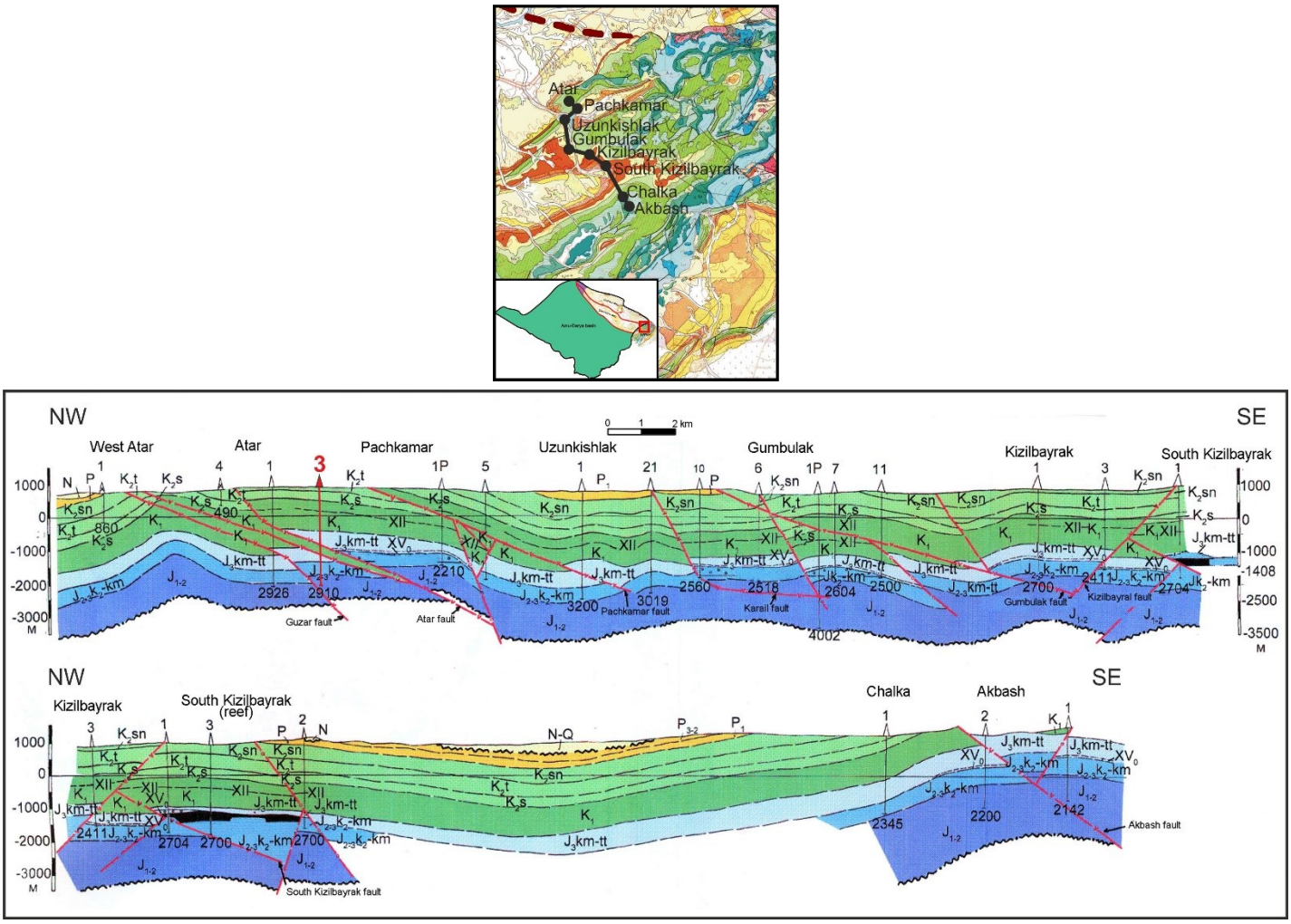

Fig. 4.60. Cross-section West Atar-Akbash showing the Pachkamar structure (modified after Nugmanov and Jdanova 1987-1999).

The stratigraphy of this well was obtained from the wells catalogue of «Uzbekgeofizika», while the lithology comes from the synthetic section of the Pachkamar-Amanata fields (Grudsky, 1988). We have no information about the pre-Jurassic of the area, as well as on the depths of the main surfaces as none of our maps covers this area.

The section of Pachkamar 3 concerns the Jurassic and the Cetaceous. The Jurassic is complete starting with the terrigenous unit of probably Middle Jurassic age. The Cretaceous exposes a shortened section from the Berriasian to the Turonian which is at the outcrop. The Berriasian-Barremian sequence is not separated from the Aptian.

The thickness of the Pachkamar 3 well is 2910 m. The Jurassic is 1663 m thick, from the cross-section (fig. 4.60), we supposed a supplementary thickness of 432 m of Middle Jurassic. There is an

abnormally thick Tithonian evaporite unit, reaching 949 m (fig. 4.61, next page). According to the cross-sections of the Pachkamar area (see fig. 4.60), this salt thickening is caused by tectonics, a thrusting and probably movements of salt along the faults. The lithostratigraphic column (fig. 4.61) is represented like in the well (949 m of evaporites) but for the subsidence calculation we took for the evaporite unit, an original thickness of 245 m (before salt movements) as in the Pachkamar-Amanata fields (Grudsky, 1988). Then we keep a total Jurassic thicknes of 1391 m (with the supplementary Middle Jurassic layer supposed and the thin evaporites). The Cretaceous which has been partly eroded during the uplift of the Southwestern Gissar has a thickness of 1247 m. To use more realistic porosities/densities as well as backstripped thicknesses of the strata, we supposed a paleo-burying of 1000 m for the column, corresponding to 1000 m of Late Cretaceous and Cenozoic sediments deposited then eroded during the uplift

Lithologically, the terrigenous Jurassic consists of clay and sandstone intercalated. The carbonate unit is represented by limestone, reefal limestone and clayed limestone. According to the presence of different carbonate horizons within the unit, the Pachkamar 3 well carbonate section corresponds to a lagoonal type of the carbonate unit. The evaporite unit is represented mainly by salt with a small gypsum layer at the top of the unit. The Cretaceous consists of sandy-clayed sediments with some limestone inclusions in the Lower Cretaceous.

The Pachkamar 3 section does not show the complete Mesozoic-Cenozoic section cut by erosion. It exposes a great Jurassic salt thickening probably caused by tectonics and halokinesis.

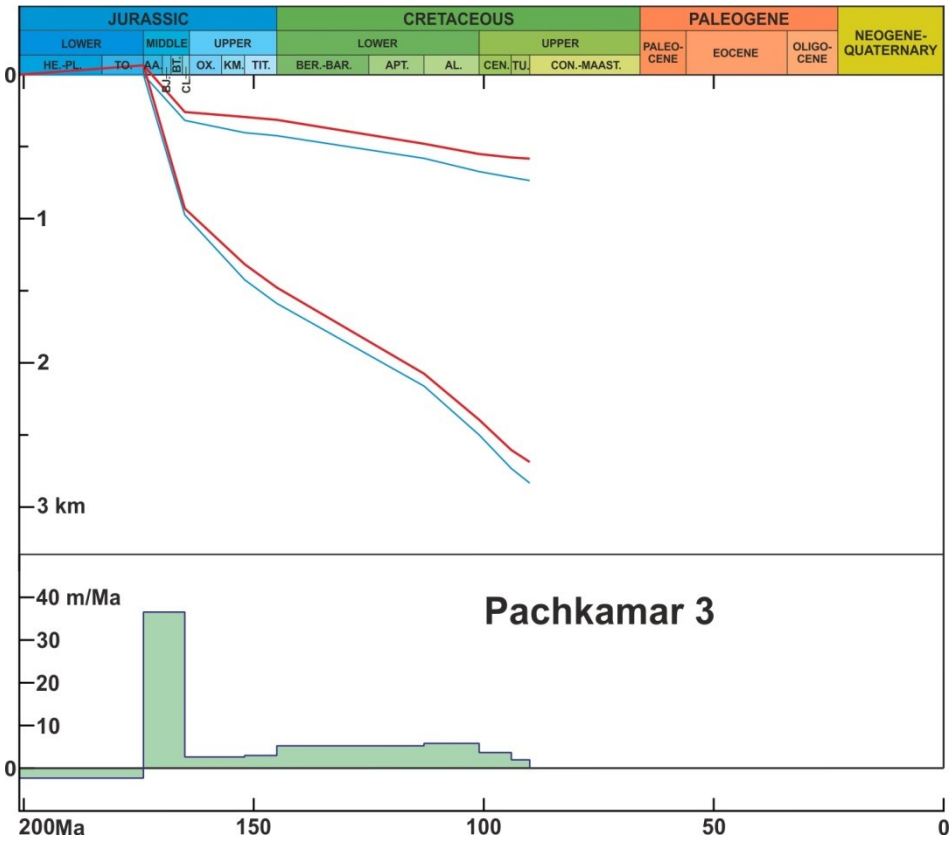

Fig. 4.62. Subsidence curves of the Pachkamar 3 well. Meaning of the curves see caption of fig. 4.13.

Pachkamar 3 presents a shortened section with only the Mesozoic strata (fig. 4.62). The main subsidence event is observed during the Aalenian-Lower Callovian, with a subsidence rate of 36 m/Ma, as we supposed that the Jurassic sedimentation begins in the Aalenian. In the Middle Callovian-Kimmeridgian the subsidence velocity sharply reduced to 3 m/Ma and stayed at the same level till the end of the Jurassic. Moving to the Lower Cretaceous the velocity of the subsidence increased slightly to 5-6 m/Ma (6 m/Ma during the Albian). Then it decreased as the Turonian is partly eroded as well as the final part of the section (Upper Cretaceous and Cenozoic), the altitude is 853 m.

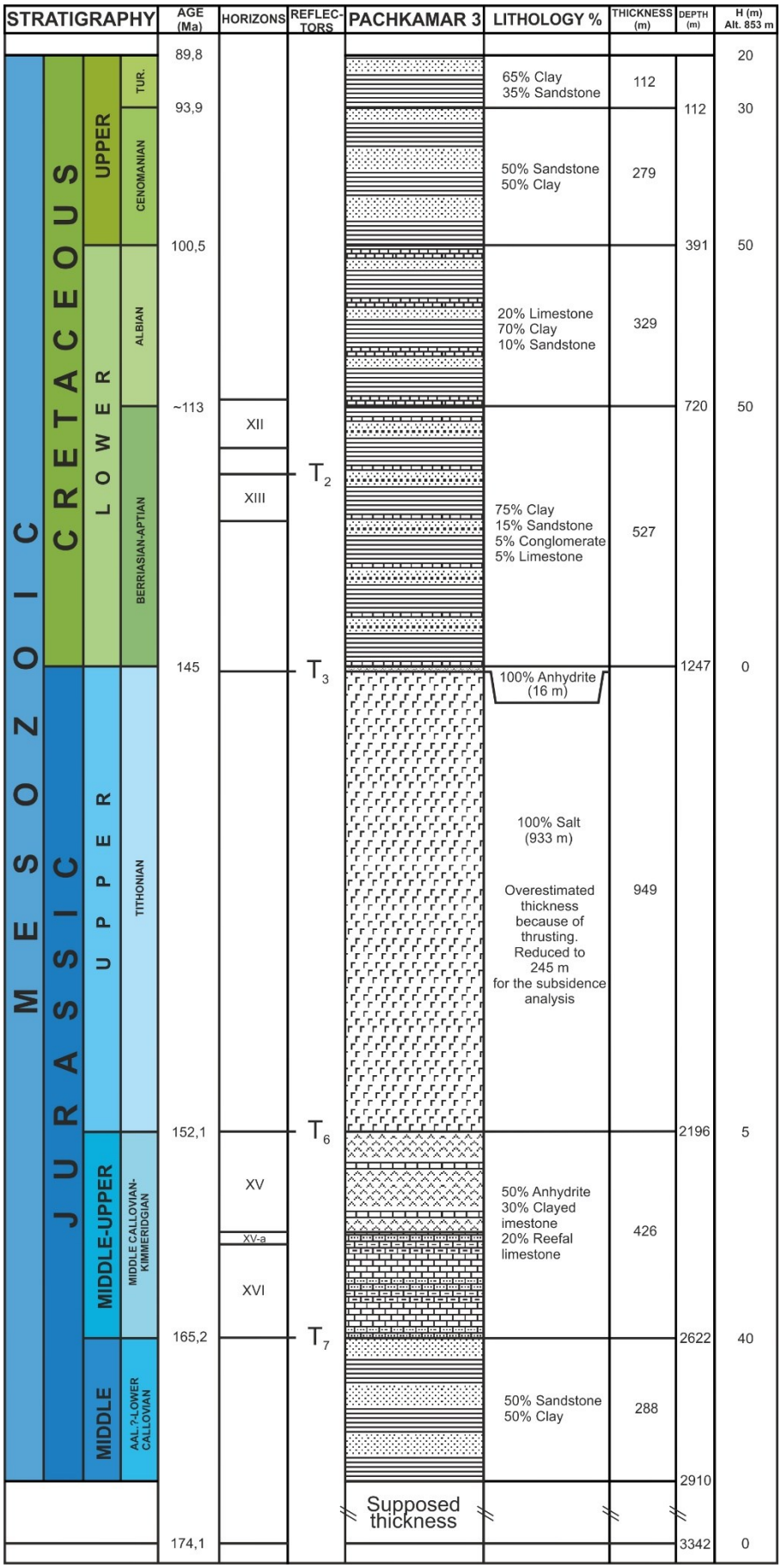

Fig. 4.61. Lithostratigraphic column of the Pachkamar 3 well.

4.2.4.4. Amanata 3 well

The Amanata 3 well is the easternmost well of all the wells selected. It is located in the same area as Pachkamar 3, a bit eastwards (see fig. 4.8). These two structures have a common synthetic geological-geophysical section (Grudsky, 1988) and the stratigraphic data for Amanata 3 were obtained from the wells catalogue.

As this well is located in the same area as Pachkamar, it exposes a similar section. This section is also incomplete – there is no Cenozoic cut by erosion, but, unlike Pachkamar 3, the Cretaceous section is complete and the Aptian is separated from the Berriasian-Barremian.

Amanata 3 does not reach the pre-Mesozoic for which we have no information. The well bottom is located in the terrigenous Jurassic rocks. The thickness of the entire real section of Amanata 3 is 2608 m (fig. 4.63). The Jurassic strata take 1094 m and the Cretaceous 1514 m. We supposed a supplementary thickness of Middle Jurassic of 73 m, in taking the same supposed total thickness of 720 m for the Aalenian-Lower Callovian layer than in Pachkamar 3. We supposed here a paleo-burying of 800 m for the column, with less erosion than for Pachkamar 3 as the Cretaceous is complete. There is an interesting point, which significantly differentiates Amanata 3 from Pachkamar 3, it is the thickness of the evaporite unit, which is only 49 m here. This could be explained by results of halokinesis, most part of the salt moving away of Amanata 3 or evaporites deposit was reduced there, in this lagoonal area. Unfortunately we do not have a cross-section showing Amanata 3 area to help to choose between these two hypotheses. The Cretaceous section is almost the same as in the Pachkamar area, except the presence of conglomerates at the bottom of the section.

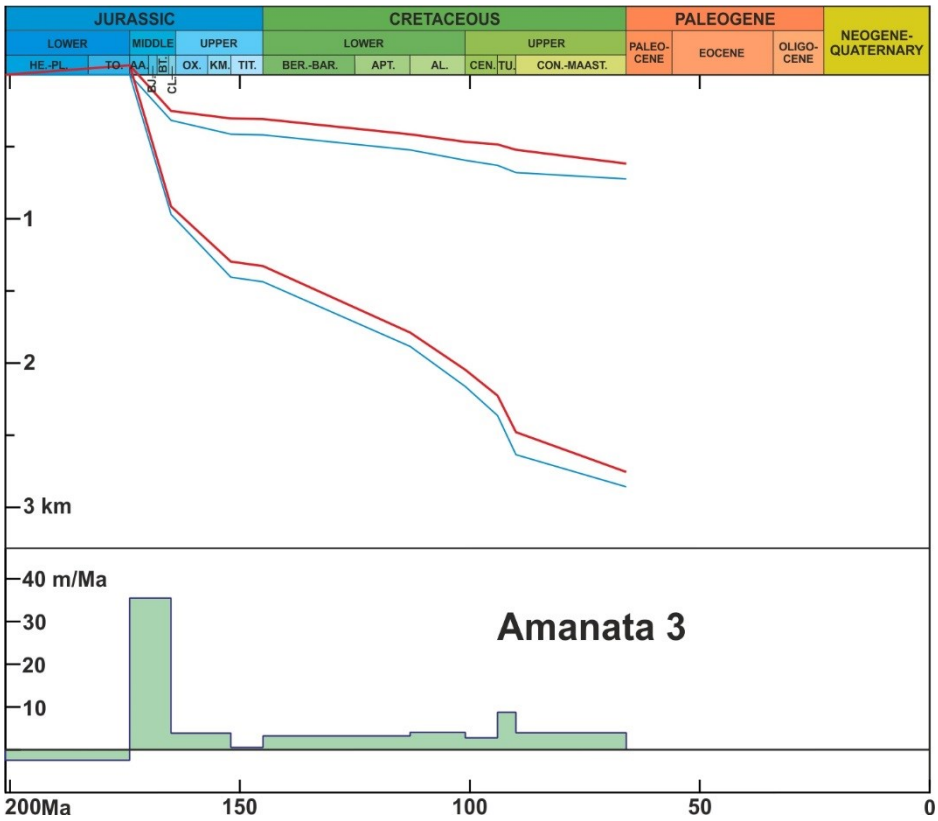

Fig. 4.64. Subsidence curves of the Amanata 3 well. Meaning of the curves see caption of fig. 4.13.

The main subsidence event for Amanata 3 is observed during the Aalenian-Lower Callovian time (fig. 4.64). In this interval of time, the velocity of the subsidence was 36 m/Ma, similar to the Pachkamar 3 results which is very close. In the Middle Callovian-Kimmeridgian the subsidence of the area became slower and almost stopped during the Tithonian. The subsidence increased again and was continuous during the Cretaceous, with a slight increase in the Albian and especially in the Turonian with a subsidence velocity of 9 m/Ma, then it decreased again.

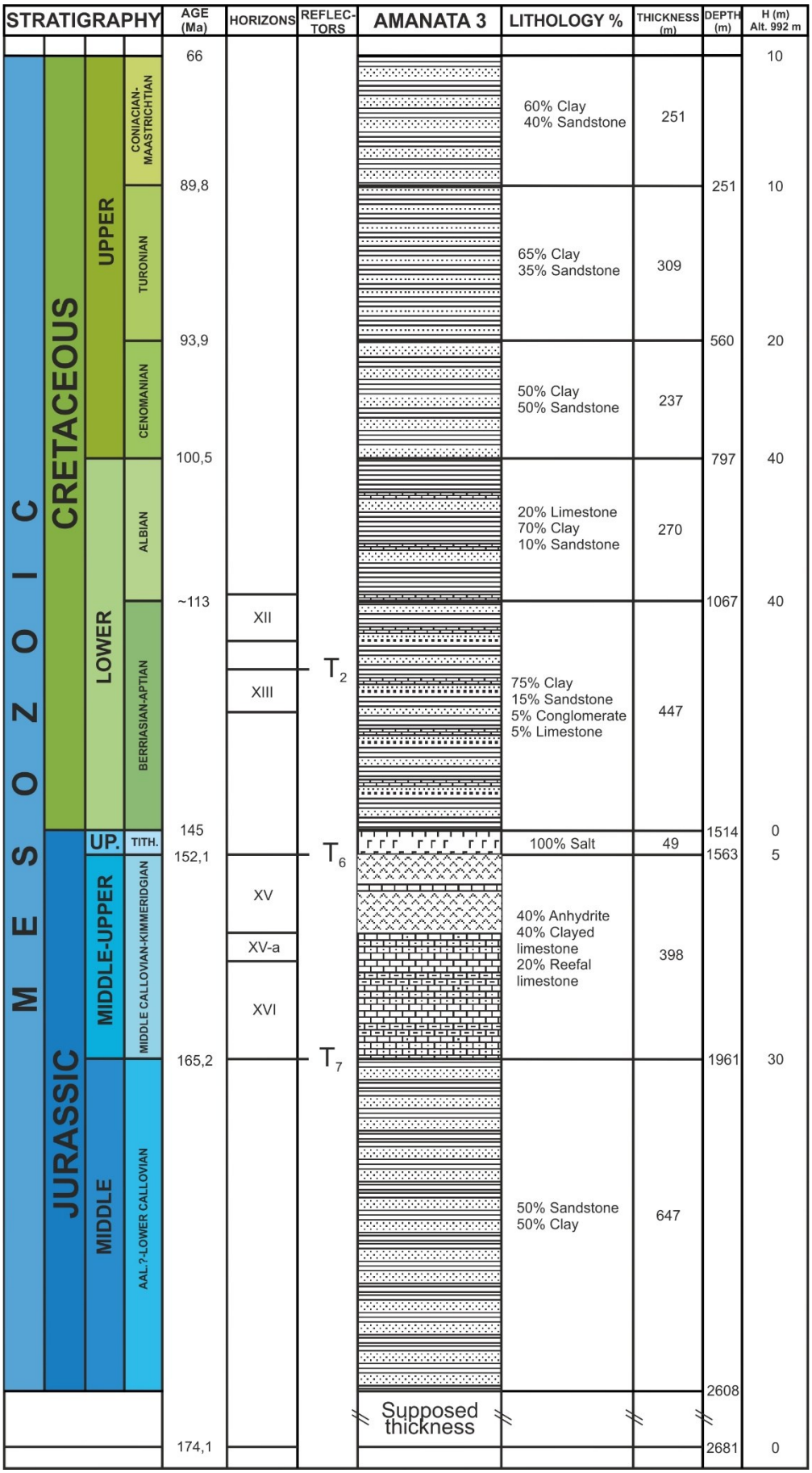

Fig. 4.63. Lithostratigraphic column of the Amanata 3 well.

4.3. Correlations of the studied wells and comparison of the tectonic subsidence rates

After to have seen the data and subsidence curves of each well studied, we will now compare the events identified, separately on the Bukhara and Chardzhou steps as well as in the Southwestern Gissar, at first for the Jurassic then the whole Mesozoic-Cenozoic. Then we will give a more general overview of the location of the subsidence through time.

4.3.1 Correlations of the Jurassic thicknesses and subsidence events

For a better understanding of the Jurassic evolution in the northern margin of the Amu-Darya basin, besides the subsidence analysis (fig. 4.65), we have made a correlation analysis of the Jurassic thickness (fig. 4.66).

A major tectonic subsidence event related to extension, occurs during the Jurassic. Its age boundaries are represented on the Figure 4.65 by the pink area. The end of this event has a very sharp boundary ending with the transition from the terrigenous unit to the carbonate unit, so from the Lower to the Middle Callovian. On the contrary the beginning of the event depends at first if the well is situated in an area of graben or only representing the general evolution either of the Bukhara or of the Chardzhou step and in supplement if situated in the northwest or the south east of the area. For the grabens, two areas were determined by the seismic analysis (see Chapter 3): the main Kimerek graben and a smaller one, the Yangikazgan graben. When green and yellow surfaces are superimposed for one well (fig. 4.65), we represented with green colour the event with a beginning at least with a certain recognized age and in yellow with a more hypothetical age chosen for the beginning.

As rates are represented, an increase of the duration of the event decreases its amplitude, the total amount of subsidence (surface) being kept. We must remind too that this tectonic subsidence is corrected from the sea-level variations which is homogeneous for all the wells, but also from the variations of bathymetries according to the wells and ages (hypotheses made for each well in our analysis, see the column of each well for the values taken). The oldest age, possibly identified by a spore-pollen assemblage, is the Pliensbachian for Yangikazgan 10, but it could be even older (end of Sinemurian). An equivalent age is proposed by some authors for the beginning of the terrigenous unit in the Beshkent trough (southeast of the Chardzhou step). A reliable Toarcian age is taken for Kimerek and Shurtan so it was supposed too for South Alan 2 and South Tandircha 14 which are in the basin area or on the edge.

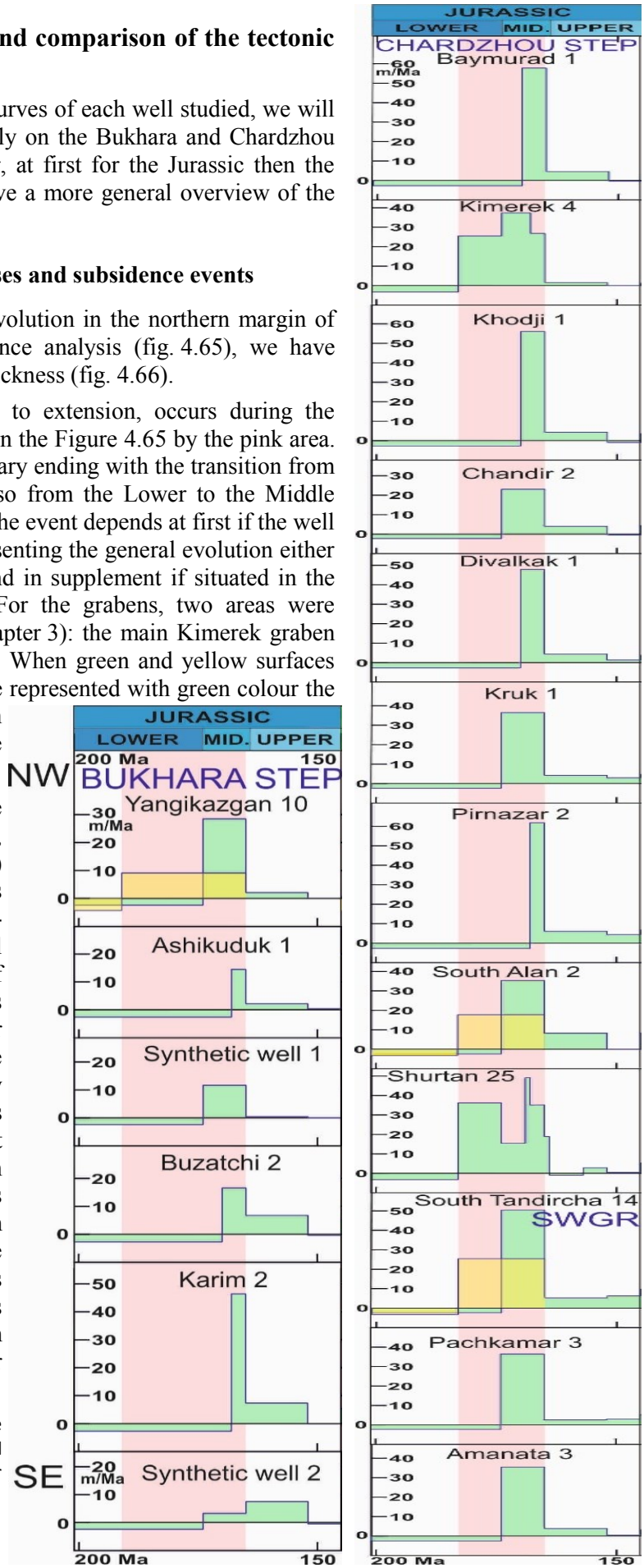

Fig. 4.65. Correlation scheme for the Jurassic of the tectonic subsidence rates corrected for se-level and bathymetry. Yellow areas, hypotheses with an older age.

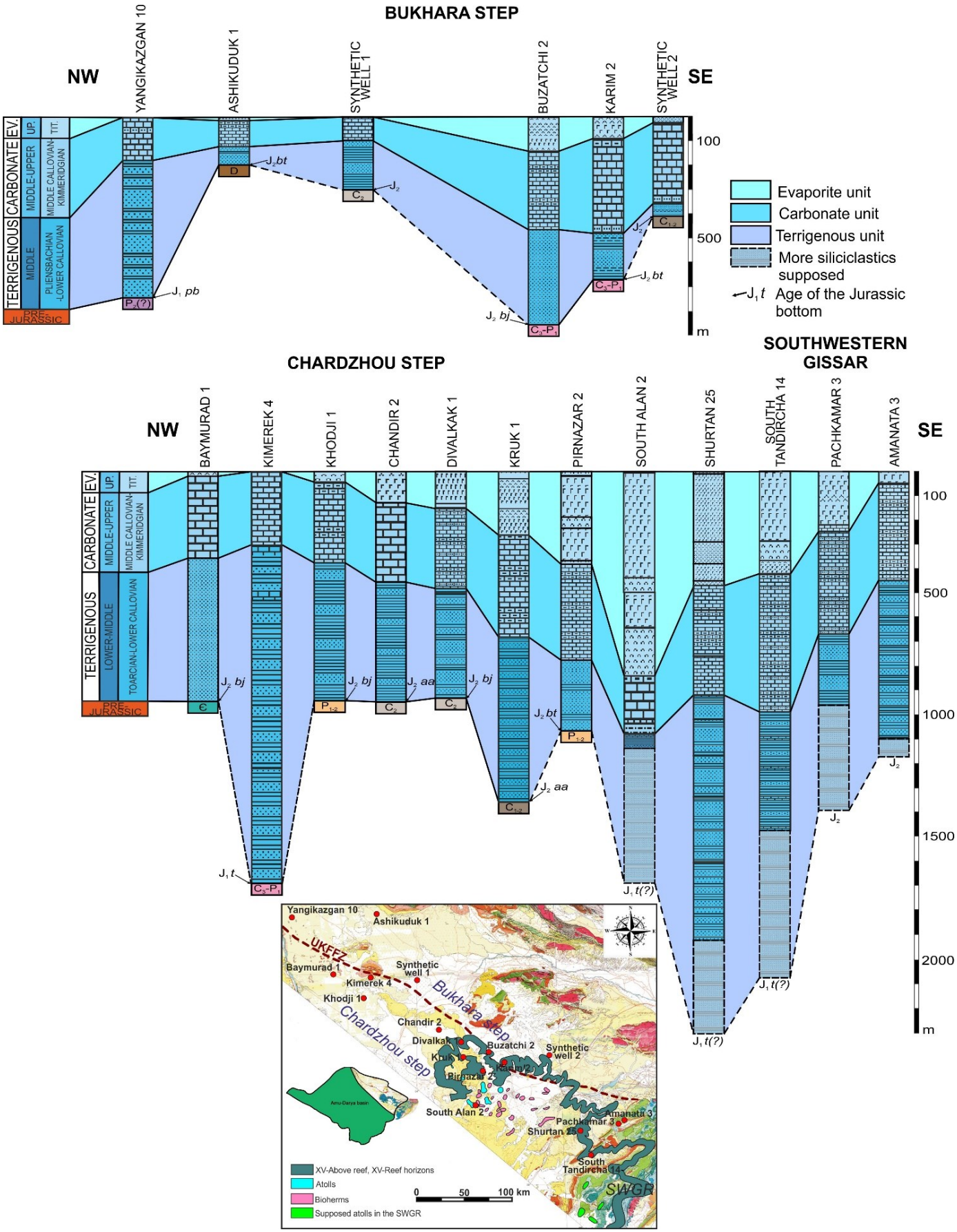

Fig. 4.66. Correlation scheme of the Jurassic thickness of the wells, chosen for the subsidence analysis.
The top of the evaporite unit is put at the horizontal, the distance between columns is not kept.
Pre-Jurassic: **€** - Cambrian; **D** – Devonian; **C_{1-2}** – Lower-Middle Carboniferous; **C_2** – Middle Carboniferous; **C_3-P_1** – Upper Carboniferous-Lower Permian, **P_{1-2}** – Lower-Upper Permian. Jurassic: **J_1 *pb*** – Pliensbachian; **J_1 *t*** – Toarcian; **J_2** – Undivided Middle Jurassic; **J_2 *aa*** – Aalenian; **J_2 *bj*** – Bajocian; **J_2 *bt*** – Bathonian. Bottom map, location of the wells according to the barrier reef system position. SWGR: Southwestern Gissar. Background = Geological map of Uzbekistan (1998); barrier reef system is modified after Babadjanov (2012).

For the other wells, the age of the first sediments is younger, with the Middle Jurassic either undefined or dated really Aalenian. When the wells are not situated in thick terrigenous areas the average age is Bajocian or Bathonian corresponding to an onlap and the marine transgression on probably higher areas on the edges of the terrigenous basin. When the identified age is young as the stages concern short period of time, the effect is to increase a lot the amplitude of peak but as it can be erroneous, the amplitude of the peaks must be considered cautiously. The evolution of Buzatchi 2 and Karim 2 is nearer a Chardzhou type than a Bukhara type as they are situated very near the Uchbash Karshi Flexure Fault zone and contains reefal carbonates. In fact they are situated between two NW-SE faults (fig. 4.33) and the boundary between the two steps is not clear in this area. The Shurtan 25 well was the best well dated, being a type section, but with also a possible overvaluation of the peaks. It is interesting to note that the Early-Middle Jurassic event is subdivided into two events: one in the Toarcian (or beginning before?) and one in the Upper Bajocian to Lower Callovian separated by a slight decrease of the rate. Unfortunately as this concerns only one well, this result cannot be extended to the whole area. We could suppose that the first event would follow an older (Permian-Triassic?) event (see fig. 4.72) and anyway in a generalized extensional area during the Toarcian (see Chapter 6) and the second event from the Late Bajocian onwards, would be more focused in the southeastern area to give birth to the Middle Upper Jurassic basin (see Chapter 6; Brunet et al., 2015).

Comparing the Bukhara and Chardzhou steps, it appears that the Early-Middle Jurassic rifting event is more important in the Chardzhou step and increasing from the northwest to the southeast (except inside the grabens area of Kimerek 4 and Yangikazgan 10 in which it is important). From the Middle Callovian onwards, the subsidence rates decrease drastically till the end of the Jurassic with only a thermal subsidence.

The correlations of the Jurassic columns (fig. 4.66) shows the geometry of the base of the evaporites representing the area with the more important bathymetries pre-existing (flexurally increased by the weight of the evaporites) as the top of the evaporite unit has been put at the horizontal, and as it was around to the zero level of deposition. The topography was acquired through the Middle Jurassic extensional event which developed by thermal subsidence during the deposits of the carbonates edging a deep marine basin. This basin was filled by the evaporites, the first anhydrite member levelling the rough topographies, but without a supplementary tectonic event. Indeed the correction of bathymetries allow to show that only a filling of pre-existing bathymetry is sufficient to explain the evaporites thickness (Brunet et al., 2015). Except in the southeast of the Bukhara step, the evaporites are almost absent of this northern step of the Amu-Darya basin margin.

Concerning the carbonate unit the main difference of thickness occurs between the wells situated in the reefal zone (from Divalkak 1 and even Chandir 2 with an isolated reef, going towards the southeast) with a decrease in South Alan 2 which is situated in the basinal area and more carbonate towards the Gissar and the southeast basin.

4.3.2 Correlation of the wells columns for the Cretaceous

The comparison of the Cretaceous columns (with the top of the Cretaceous put to the horizontal) shows a more homogeneous distribution even if the northwest-southeast increase trending is still observed. We must note that the Cretaceous columns are not complete towards the Gissar (Pachkamar 3 and Amanata 3) as the Cretaceous is outcropping and partly eroded.

The main subsidence observed during the Cretaceous will be shown in the next paragraph with the full diagrams of subsidence rates (fig. 4.68).

A difference exists between the thicknesses on the two steps during the Lower Cretaceous but almost disappeared during the Upper Cretaceous. It corresponds to a new Lower Cretaceous extensional event with an importance increasing towards the southeast of the Chardzhou step (fig. 4.68), when the evolution of the tectonic is similar for the two steps during the Late Cretaceous. We must note that for the subsidence analysis we considered most of the times that the XII horizon was Aptian in age. As one part of this horizon extends in the base of the Albian, for the subsidence rates, if one part of this thickness is Albian, the effect is to increase slightly the subsidence rate during the Albian.

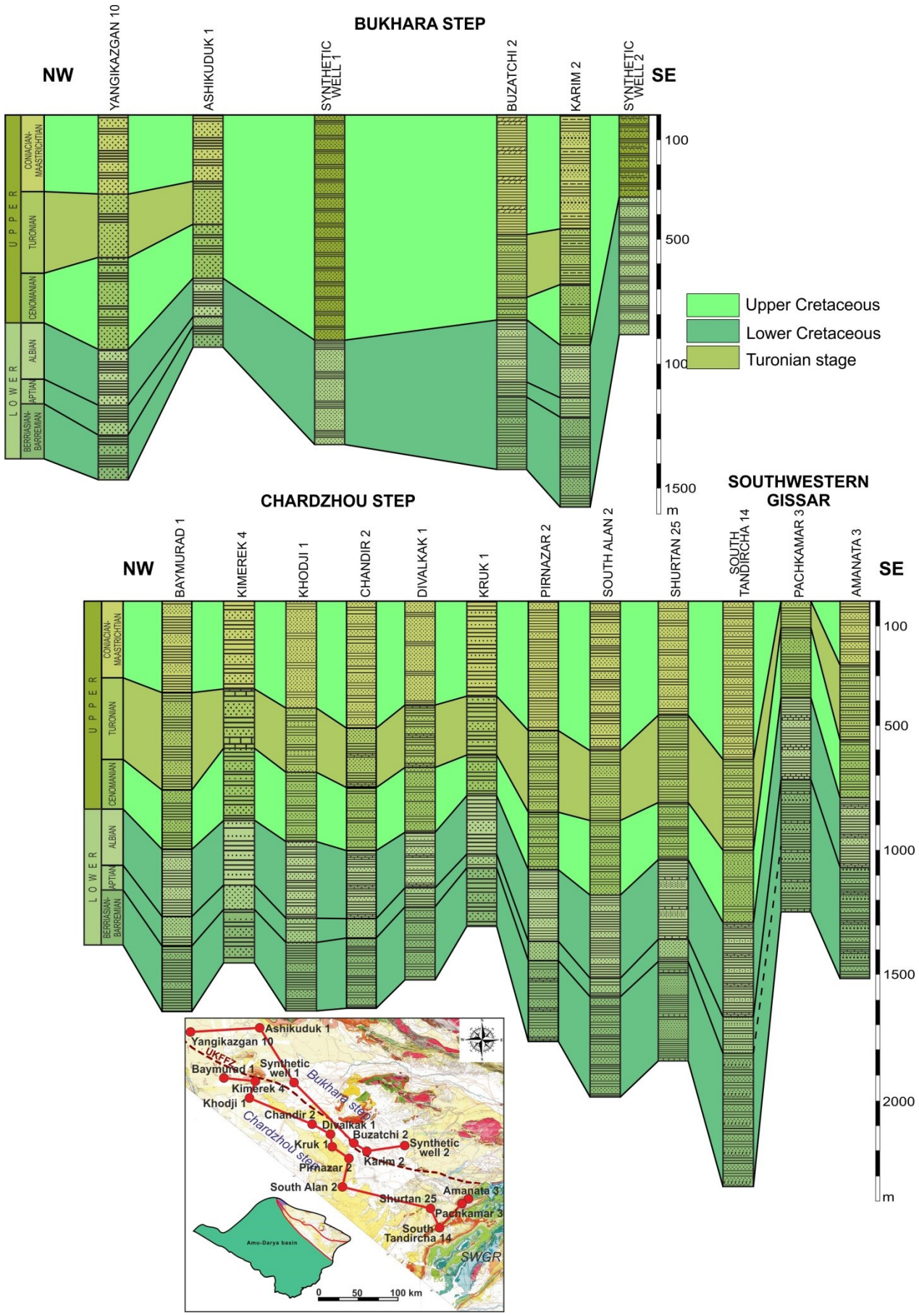

Fig. 4.67. Correlation scheme of the Cretaceous thickness of wells chosen for the subsidence analysis.

4.3.3 Correlations of the thicknesses and subsidence events during the Mesozoic and Cenozoic

We compare now the diagrams of subsidence rates (fig. 4.68) and the well columns (fig. 4.69) for the whole Mesozoic-Cenozoic evolution, allowing to see the relative importance of the subsidence events between them. The first Lower-Middle Jurassic event is the main one. We relate it to a period of rifting of the Amu-Darya basin and of the Tajik basin leading to the founding of the united large Mesozoic basin uniting these two basins (Brunet et al., 2015). In Chapter 6, this extensional period will be replaced in the general context of the southern part of Eurasia. This rifting event was followed by a period of slower thermal subsidence beginning around the Middle Late Callovian with the settling of the carbonate series, the deepening of the basin, then its filling by the evaporites. A new smaller event, also related to a probable extension, occurred during the Early Cretaceous. It is no well dated, in the Berriasian-Barremian interval as these stages are not divided in the lithostratigraphic columns. Two other events occurred in the Albian, probably also of extensional origin and during the Turonian. To relate this latter event to a geodynamic event is less evident. The origin of the following Upper Cretaceous continuous subsidence is also not fully clear. One part is of thermal origin but another part could be originated by a wider origin either thermal due by larger mantellic event or lithospheric flexural folding. At the end of the Cretaceous, the subsidence decreases before a new possible small event during the Eocene but the number of wells for which the Paleogene is subdivided is small. The end of the evolution is a Late Cenozoic uplift of the whole area due to the indentation of Pamir in the east and the uplift of the Gissar. The importance of the uplift event is thus increasing towards the east.

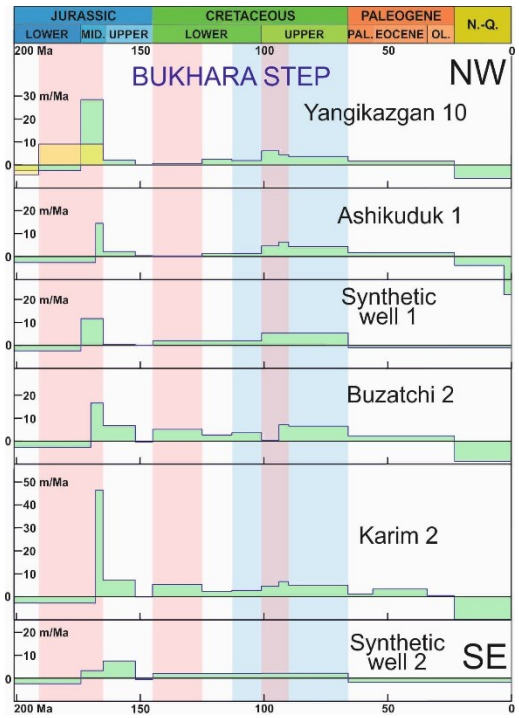

Fig. 4.68. Correlation scheme of the subsidence rates in the wells, chosen for the analysis, for the location see fig. 4.69, next page.

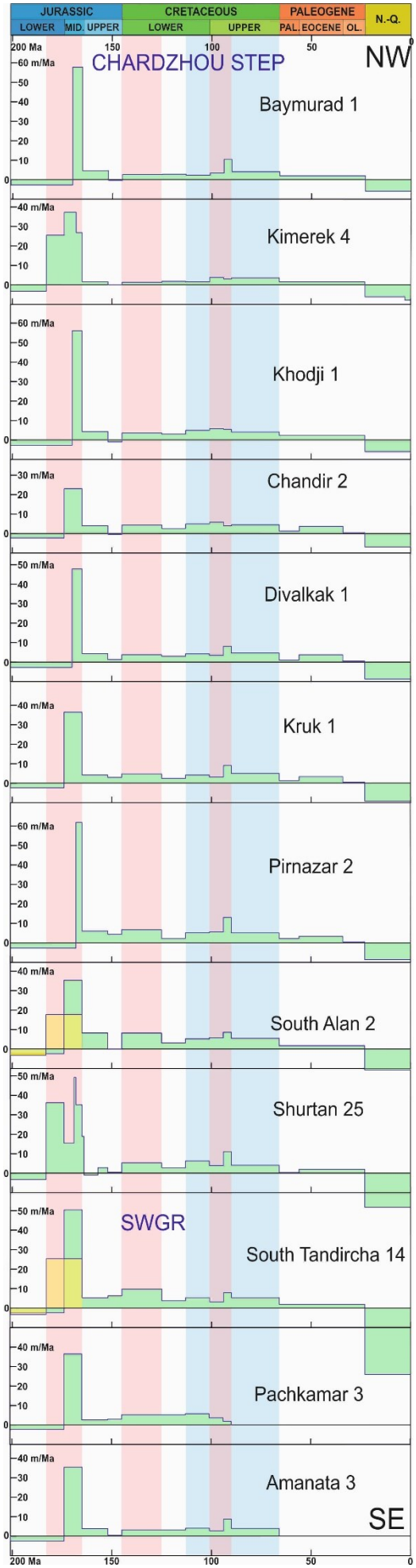

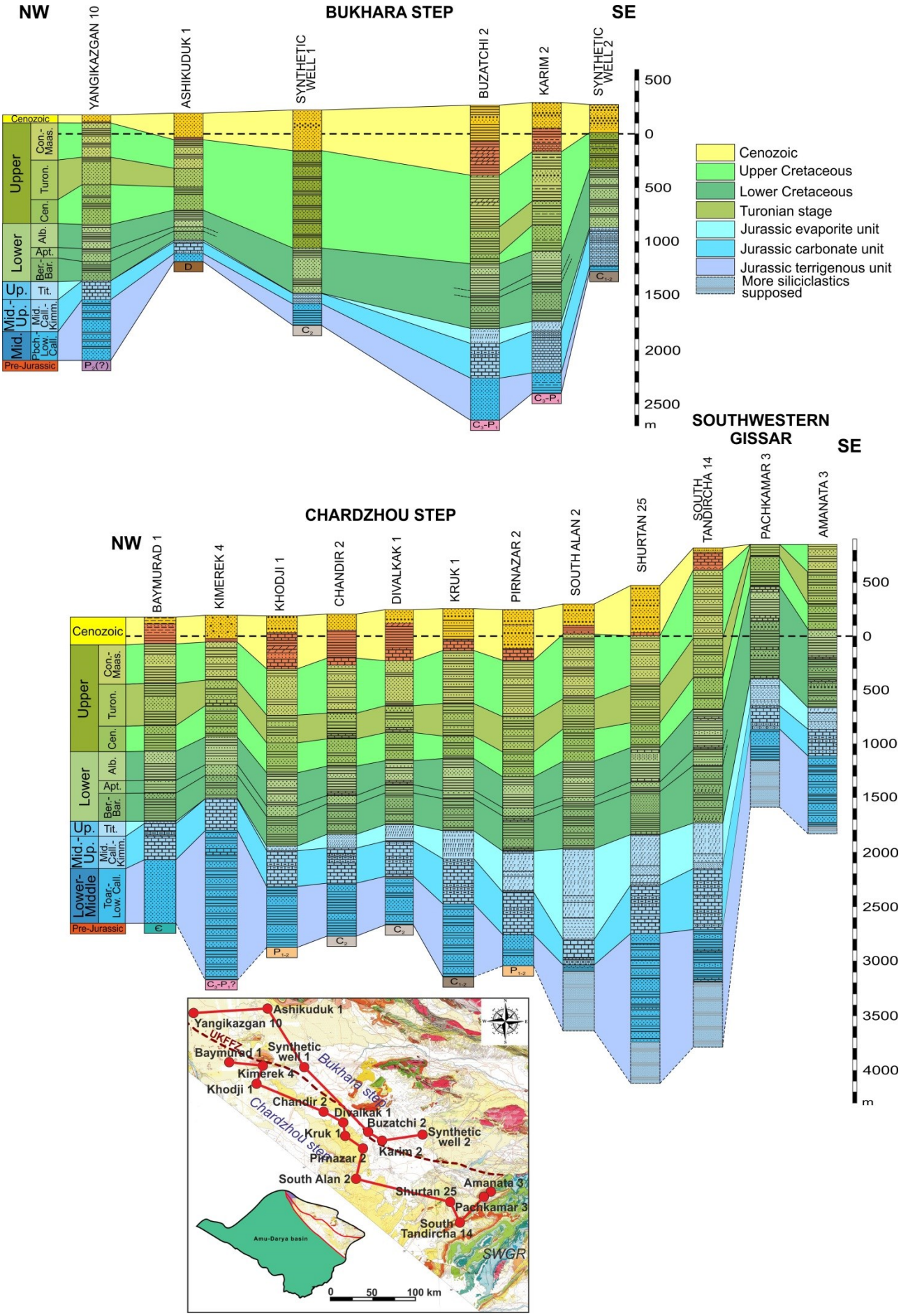

Fig. 4.69. Correlation of the thicknesses of the wells studied during the Mesozoic and the Cenozoic.

4.4 Evolution of the tectonic subsidence during the Meso-Cenozoic

We will now have a look to the series of isopach maps we have for the Mesozoic-Cenozoic: the isopach map of the Jurassic terrigenous and carbonates together (fig. 4.70) and a series of maps proposed by Nugmanov and Jdanova (2004) and Nugmanov (2009a) (fig. 4.71). We already discussed in Chapter 3 the three maps of the Jurassic and some differences in comparison to the well data. They allow anyway to have an overview of the total subsidence behaviour (with sediments but not corrected for the paleobathymetries) according to the different areas. Unfortunately no map is available for the evaporite unit.

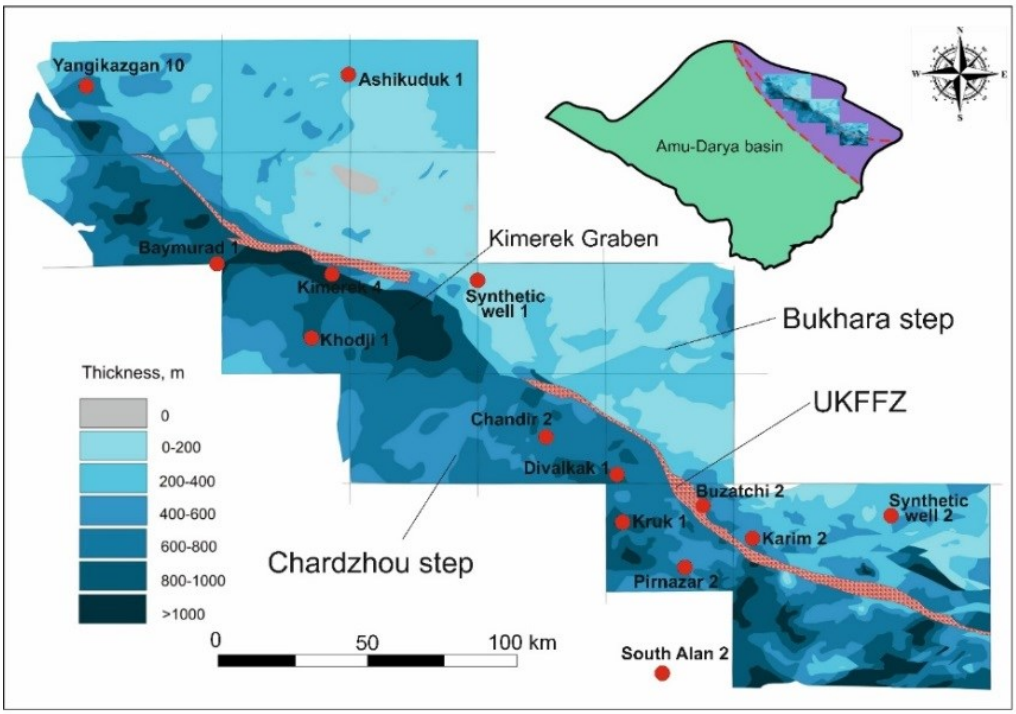

Fig. 4.70. Location of the wells studied on the thickness map of Jurassic terrigenous+carbonate units in the Bukhara-Khiva region.

The general trend is, as discussed before all along this thesis, an increase of subsidence from the Bukhara step in the northeast to the Chardzhou step in the southwest, and an increase trend from the NW to the SE, towards the Beshkent trough except during the Paleogene. The main orientations are NW-SE in the Bukhara region controlled by the Uchbash Karshi Flexure Fault zone becoming W-E in the east, in the Beshkent trough and Southwestern Gissar. For the Cretaceous the isopach maps show also an increase of subsidence towards the southeast but less difference between the two steps during the Late Cretaceous.

During the Paleogene two depocentres exist in the northwest of the Bukhara step and in the area of the Kimerek graben, more data would be necessary to explain that.

An interesting point that our analysis study of subsidence by well did not allow to show (Synthetic well 2 used only averaged values for the Cenozoic) is a localized subsidence during the Neogene to the northwest of Bukhara on the Bukhara step. This sub-basin is visible in the section G-G' (fig. 3.10). It could correspond, as the southeast thickening (fig. 3.11 line H-H', fig. 4.69 and 4.71), to a flexural bending, between highs (fig. 3.10, 4.8B) reactivated during the period of compression and thrusting uplifting Southwestern Gissar (see Chapter 6).

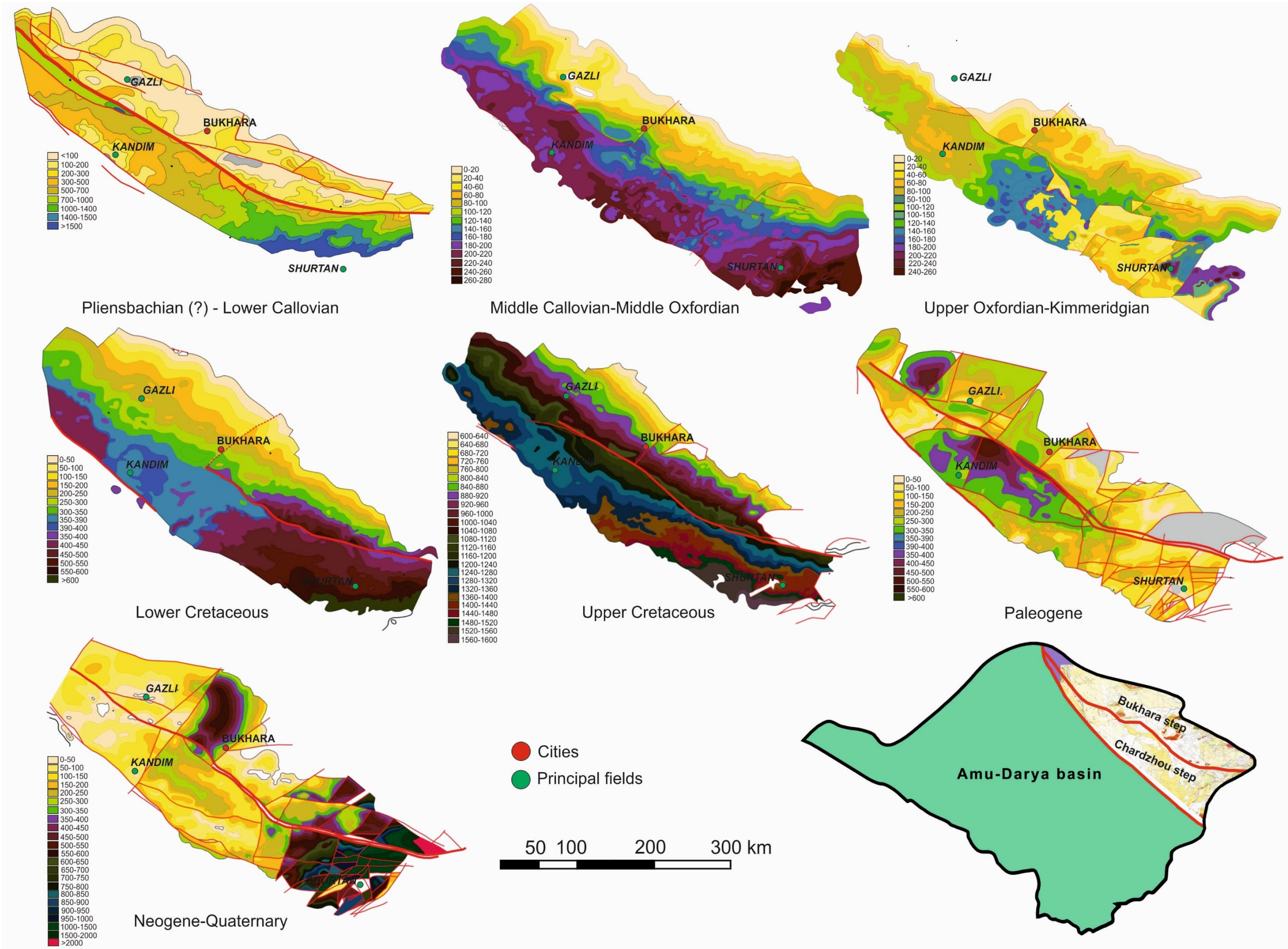

Fig. 4.71. Paleo-thickness maps of the Bukhara-Khiva region (modified after Nugmanov and Jdanova, 2004; Nugmanov, 2009a).

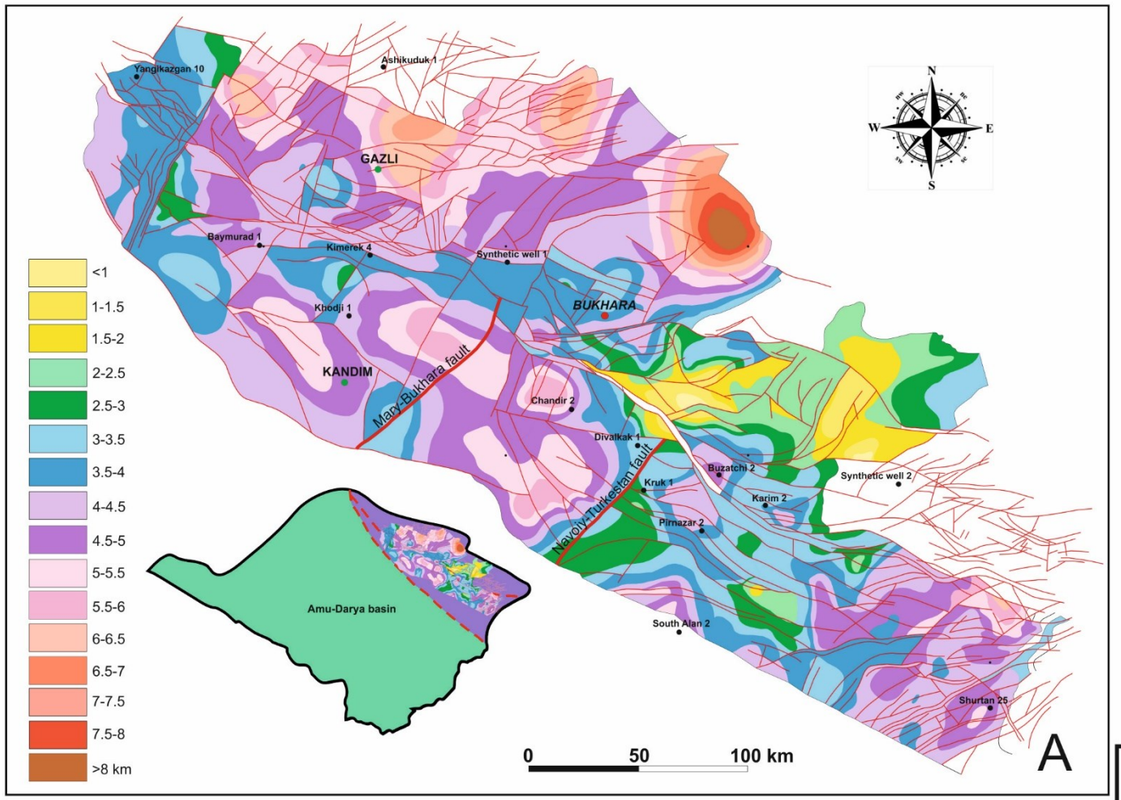
Yangikazgan 10
Ashikuduk 1
GAZLI
Baymurad 1
Kimerek 4
Synthetic well 1
Khodji 1
BUKHARA
KANDIM
Mary-Bukhara fault
Chandir 2
Divalkak 1
Navoiy-Turkestan fault
Kruk 1
Buzatchi 2
Karim 2
Synthetic well 2
Pirnazar 2
Amu-Darya basin
South Alan 2
Shurtan 25
<1
1-1.5
1.5-2
2-2.5
2.5-3
3-3.5
3.5-4
4-4.5
4.5-5
5-5.5
5.5-6
6-6.5
6.5-7
7-7.5
7.5-8
>8 km
0
50
100 km
A

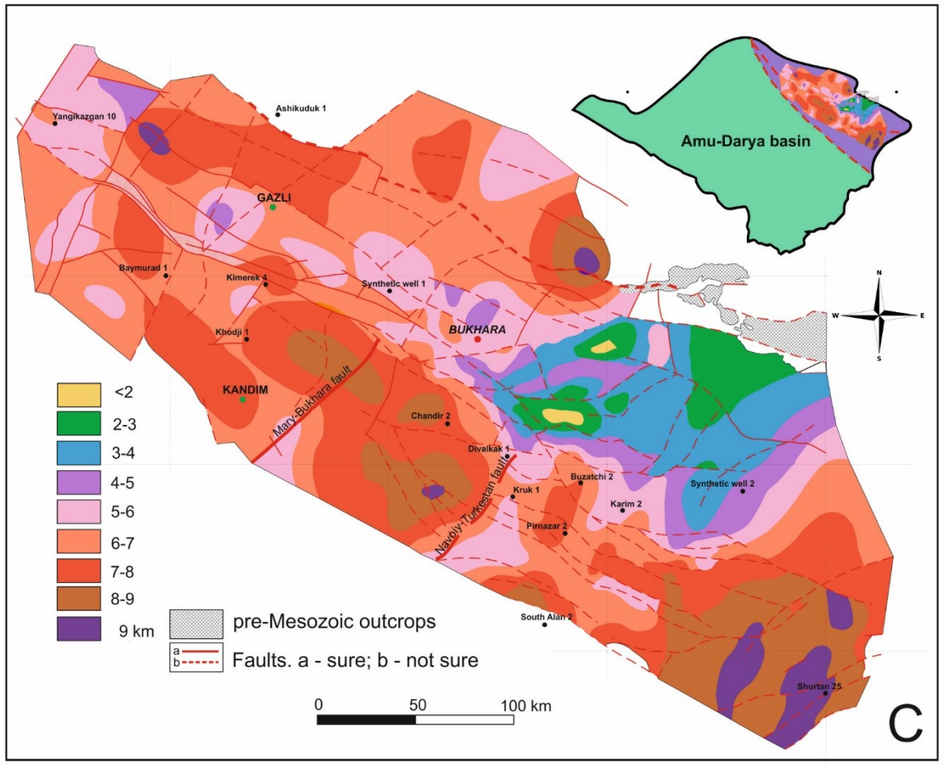
Yangikazgan 10
Ashikuduk 1
Amu-Darya basin
GAZLI
Baymurad 1
Kimerek 4
Synthetic well 1
Khodji 1
BUKHARA
KANDIM
Mary-Bukhara fault
Chandir 2
Divalkak 1
Navoiy-Turkestan fault
Kruk 1
Buzatchi 2
Karim 2
Synthetic well 2
Pirnazar 2
South Alan 2
Shurtan 25
<2
2-3
3-4
4-5
5-6
6-7
7-8
8-9
9 km
pre-Mesozoic outcrops
Faults. a - sure; b - not sure
0
50
100 km
C

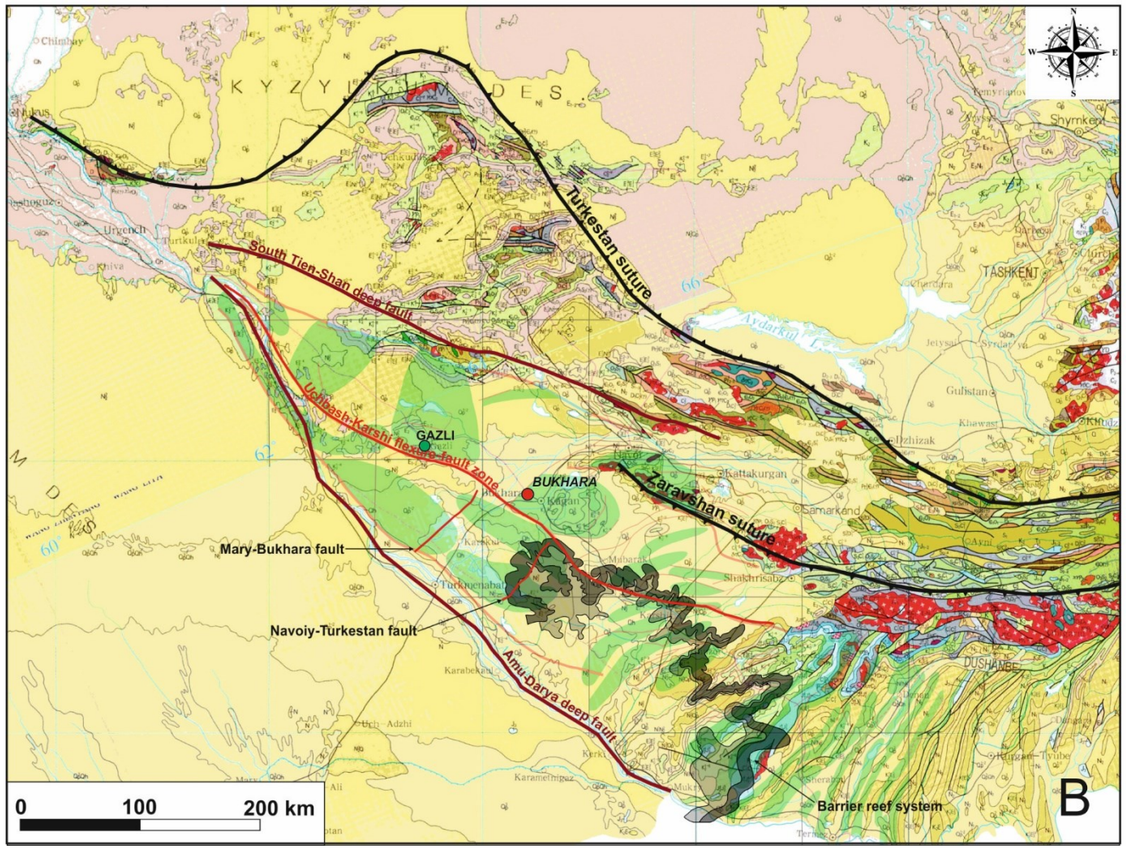
Turkestan suture
South Tien-Shan deep fault
Ushbosh-Karshi flexure-fault zone
GAZLI
BUKHARA
Zaravshan suture
Mary-Bukhara fault
Navoiy-Turkestan fault
Amu-Darya deep fault
Barrier reef system
TASHKENT
0
100
200 km
B

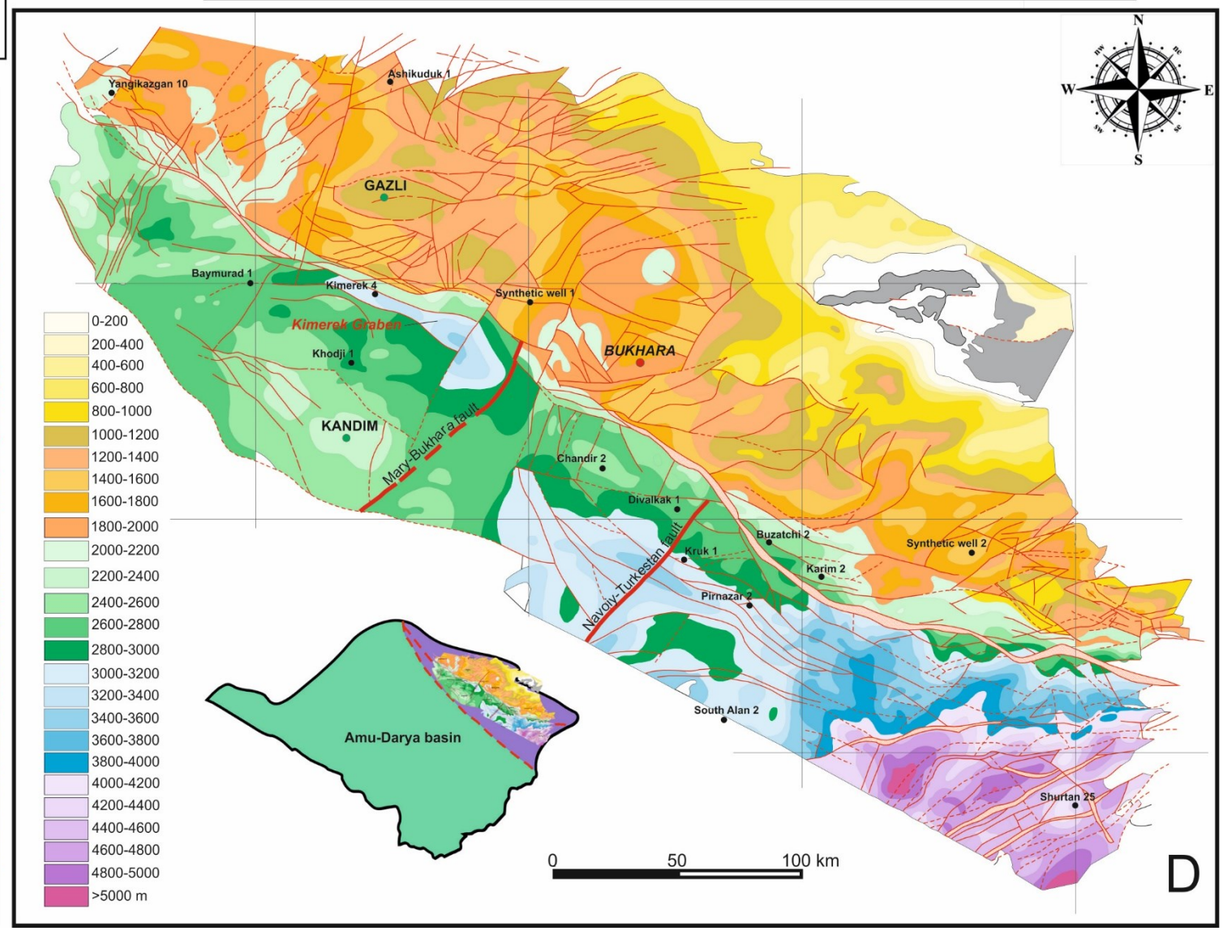
Yangikazgan 10
Ashikuduk 1
GAZLI
Baymurad 1
Kimerek 4
Synthetic well 1
Kimerek Graben
Khodji 1
BUKHARA
KANDIM
Mary-Bukhara fault
Chandir 2
Divalkak 1
Navoiy-Turkestan fault
Kruk 1
Buzatchi 2
Karim 2
Synthetic well 2
Pirnazar 2
South Alan 2
Shurtan 25
Amu-Darya basin
0-200
200-400
400-600
600-800
800-1000
1000-1200
1200-1400
1400-1600
1600-1800
1800-2000
2000-2200
2200-2400
2400-2600
2600-2800
2800-3000
3000-3200
3200-3400
3400-3600
3600-3800
3800-4000
4000-4200
4200-4400
4400-4600
4600-4800
4800-5000
>5000 m
0
50
100 km
D

With a more general overview in space and time of the Bukhara and Chardzhou steps, we compare the isopach map of the Paleozoic sediments, the isohypses maps of the basement depth and of the pre-Mesozoic surface to evidence the main structures controlling the subsidence evolution of the Bukhara Khiva region (fig. 4.72).

The isopachs of the Paleozoic show important thicknesses in pretty localized areas corresponding probably to Paleozoic grabens as those underlying other parts of the Amu-Darya basin. In the Bukhara-Khiva area they are probably located near the boundaries of former blocks collided during the Paleozoic (Brunet et al., 2015). We may identify the Yangikazgan graben and the Kimerek graben already discussed before. The important Jurassic Kimerek graben began its evolution in the Paleozoic and was reactivated during the Early-Middle Jurassic. During the Paleozoic the graben was extending much more towards the southeast, to the south and along the Uchbash Karshi Flexure Fault zone. As the map is stopping towards the southeast of the Bukhara-Khiva region, it is not clear to be sure if an important Paleozoic graben was already existing during the Paleozoic, below the Mesozoic-Cenozoic Beshkent trough and continuing to the south in the Murgab sub-basin of the large Amu-Darya basin (Brunet et al. 2015) and towards the south of the Gissar or the Afghan Tajik basin.

Comparing the Paleozoic isopachs to the structural map of highs (fig. 4.72B), we may see that a good number of the thick areas are corresponding to structural highs. We interpret it as the inversion of these Paleozoic grabens (Brunet et al., 2015) during the Eocimmerian event, inducing the strong unconformity underlying the Mesozoic sediments. Highs have also been reactivated during the Cenozoic compression. Some of these grabens, as the Kimerek one, were reactivated in extension during the Early-Middle Jurassic event.

Speaking now of the limits of the subsidence area, some structures (fig. 4.72, 4.73) show their leading role in the subsidence evolution of the area. At first it is the Uchbash Karshi Flexure Fault zone separating the Bukhara step slow subsiding from the Chardzhou step more subsiding as shown along this thesis. Some NE trending faults show also their role especially in two areas, one to the west of Bukhara in the area of the Mary-Bukhara regional fault (Mordvinstev and Mordvintsev, 2011) and going towards the east, the Navoiy-Turkestan fault.

The Mary-Bukhara fault, and in fact several other parallel NE faults in the same area are delimiting blocks mainly in the Chardzhou step but also in the Bukhara step but they are less evident to localize on the available maps.

The Navoiy Turkestan fault corresponds to the NW boundary and the turn of the supposed barrier reef, and also to the basinal area extending in the south-east as the reef borders the basin. At the same time, the evaporites filling the deep basin, it limits also the thickest part of the evaporites of the Gaurdak formation in the Amu-Darya basin (Brunet et al., 2015).

Fig. 4.72 (previous page) **A.** Isopach map of the pre-Mesozoic deposits; **B**. Main faults controlling the subsidence evolution. The location of the Upper Jurassic barrier reef and basin model is superimposed in grey and in green the structural highs of fig. 4.8B; **C**. Isohypse map of the basement ; **D**. Isohypse map of the pre-Jurassic roof; A, C and D are redrawn from Mordvintsev O. in Babadjanov, 2008. Location of the wells studied for the tectonic subsidence analysis is added on the isovalue maps.

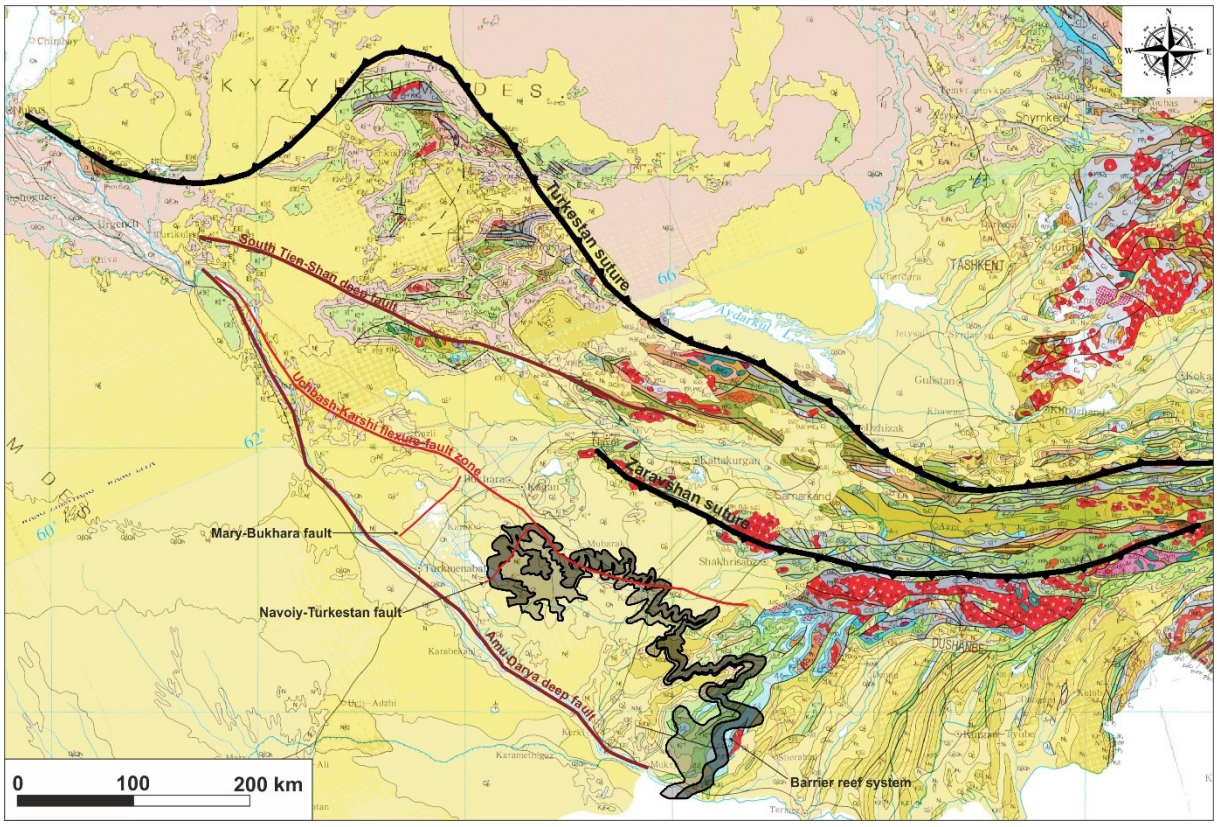

Fig. 4.73. Main faults controlling the subsidence evolution. The location of the Upper Jurassic barrier reef and basin model is superimposed in grey.

Chapter 5

Fault tectonic analysis

Chapter 5

Fault tectonic analysis

The fault tectonic analysis was used in this study of the southern Gissar Range. The tectonic events that have affected southern Gissar in Uzbekistan have produced a wide range of regional scale (folds, thrusts, strike-slip faults) and meso-scale (faults, joints, tension cracks) tectonic breaks. The analysis of these brittle features helps us to reconstruct the paleo-stress patterns during the Mesozoic. Furthermore, the results of this analysis in combination with the study of the subsidence will allow to more accurately reconstructing the tectonic evolution of the northern margin of the Amu-Darya basin.

5.1. Methodology

We used brittle tectonic analyses, including stress tensor inversion, to decipher the succession of deformational events that resulted in the present-day structure. The common steps in these analyses involve data collection in the field, data separation and age recognition, computation of stress fields, and finally characterization and classification of different events. The set of surface data consists of Soviet geological maps (scales 1:200 000 and 1:500 000) and of field data we collected during field campaigns performed from 2012 to 2014 in the Southwestern Gissar.

5.1.1. Paleostress reconstruction

One goal of the analysis of brittle tectonics is to reconstruct the state of paleostress associated with each tectonic period from the field study of fault populations. These methods are based on the use of measures of fault planes. Originally, graphical methods were based on the interpretation of the combined systems of different types of faults, which allowed defining a dihedral shear (Anderson, 1942). Modern methods, including the calculation of the average tensor constraint are used to calculate the restraint system for each set of fault populations.

The general idea is based on the inversion of reasoning of Wallace (1951) and Bott (1959). With the evolution of computer technology, in the seventies-eighties, the idea of solving the inverse problem has given rise to many numerical methods (Angelier, 1975; Carey, 1976; Angelier et al, 1982; Angelier, 1984; Michael; 1984; Reches, 1987, Angelier, 1990).

The determination of paleo-stress state is based on several assumptions. Inside the volume of rock, it is assumed that the stress field is uniform, and there is no movement guided by pre-existing plans and heterogeneities of materials or rotating block. It is considered that the streak represents the direction of the shear stress on the fault plane (fig. 5.1A). The stress state can be represented geometrically by an ellipsoid where axes constraints are the main σ1, σ2 and σ3 axes (fig. 5.1B) and analytically by a stress tensor which allows the necessary calculations.

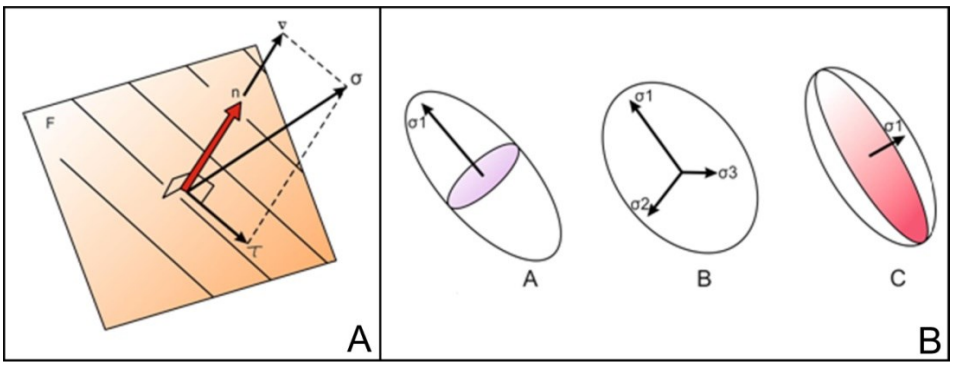

Fig. 5.1. State of stress on a fault plane.

A Fault plane and stress state (after Angelier, 1990): F = Fault plane with normal n; σ = Stress exerted on F decomposes into normal (υ) and tangential (or shear) normal stress (τ); **B** – Stress ellipsoids: A- ellipsoid of revolution "in cigar" around the axis σ1 (σ2 = σ3, so Φ = 0 (Φ = (σ2 - σ 3) / (σ1-σ3)); B- any ellipsoid (σ1> σ2> σ3, then 0 <Φ <1); C- ellipsoid of revolution around the σ3 axis (σ1 = σ2, so Φ = 1). From Al Abdalla (2008).

In the case of newly formed faults, it appears that:

- σ2 axis is parallel with the strike of the fault plane;
- σ1 axis makes an angle of approximately 30^0 with the strike of the plane of fault movement;
- σ3 forms an angle of approximately 60^0 with the strike of the plane of fault movement.

There are two main categories of faults:

1.- Conjugate faults: The geometry of fault populations depends on: (1) the orientation of the principal axes of stress (σ 1, σ 2 and σ 3), (2) materials, and (3) the shape of the ellipsoid constraints. These issues generally fall into two families of symmetric faults compared to planes containing the axes σ 1 and σ 2, which are called conjugate faults. These faults are very common in nature and they are a key to the analysis of field populations of faults;

2.- Inherited faults (fig. 5.4): whose orientation is random and the failure is based on the orientation of the fault relative to the main axes of the constraints of the form of the ellipsoid of constraints (therefore the ratio $\Phi = (\sigma 2 - \sigma 3)/(\sigma 1 - \sigma 3)$) and slip resistance on the fault plane.

There are three types of tectonic regimes: (1) normal, (2) strike-slip and (3) reverse (fig. 5.2). In the Anderson (1942) model, the newly formed combined natural faults in non-rational deformation exhibit symmetries between themselves and in relation to the vertical stress, which is σ1 axis for normal faults (fig. 5.3A), σ2 axis for strike-slip faults (fig. 5.3B) and σ3 axis for reverse faults (fig. 5.3C).

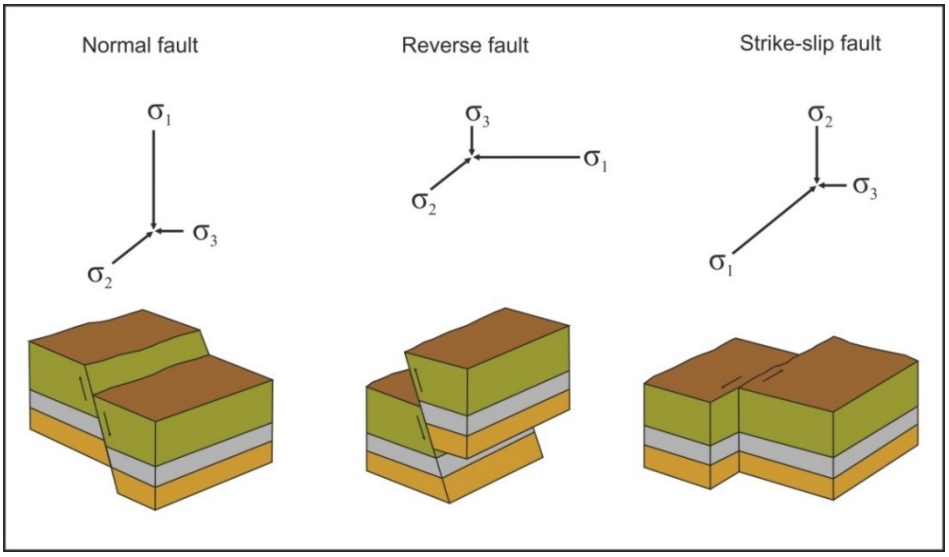

Fig. 5.2. The three different types of faults and stress patterns.

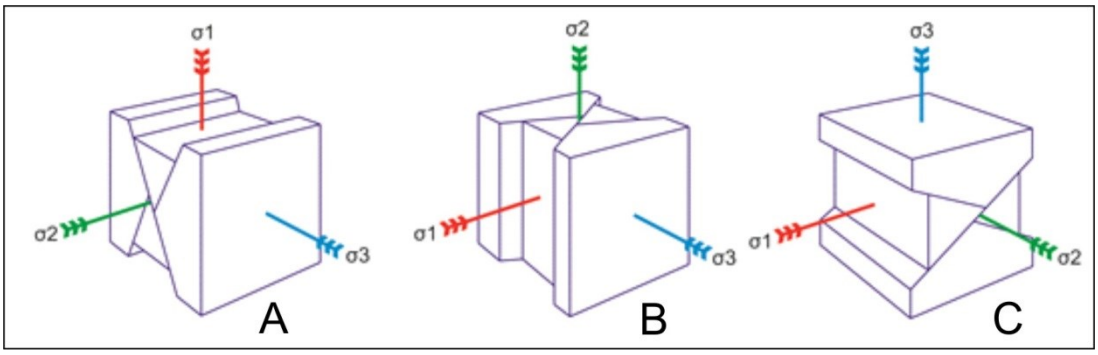

Fig. 5.3. Main types of conjugate systems of faults (from Anderson, 1942).
A-Conjugate systems of normal faults; B-conjugate systems of strike-slip faults; C-conjugate systems of reverse faults.

Fig. 5.4. Example of an inherited fault in the Sangardak river gorge (northern Southwestern Gissar).

5.1.2. Methods of analysis of a population of faults

The purpose of these methods is to rebuild systems from paleostress analysis in the field populations of faults streaks. The original Anderson models (1942), based on the results of rock mechanics, allow this in the case of newly formed combined position of σ1, σ2 and σ3 axes, and defined dihedral angle faults.

In our study, for the determination of the stress tensor, we use the Direct Inversion method, named INVD of Angelier (1990). The inversion is based on the slip-share angle (α) between the real stria (s) and the calculated relative shear stress (τ) (fig. 5.5) (Angelier, 1975, 1990).

A majority of the brittle structures that we collected are faults (normal, strike-slip, reverse, and oblique-slip faults). These data include the orientation of the fault planes, slickenside lineations, and senses of motion. The tension cracks are also common. Bedding attitudes were recorded at all sites in the sedimentary formations because they are an important key to reconstruct the pre-tilting configuration, where appropriate.

Many faults belong to simple conjugate-type patterns. Such associations facilitated a quick preliminary interpretation in the field. However, some of them could not unambiguously be interpreted in simple geometrical terms in the studied outcrops, because they may be the results of the reactivation on earlier fractures or any other mechanical discontinuities such as bedding planes and do not conform to simple, conjugate-like models.

The main goal for tectonic analysis of the fault population is the determination of the main characteristics of a paleo-stress tensor characterized by the three orthogonal principal stresses (σ1, σ2 and σ3 axes). These three stress axes are the axes of the stress ellipsoid.

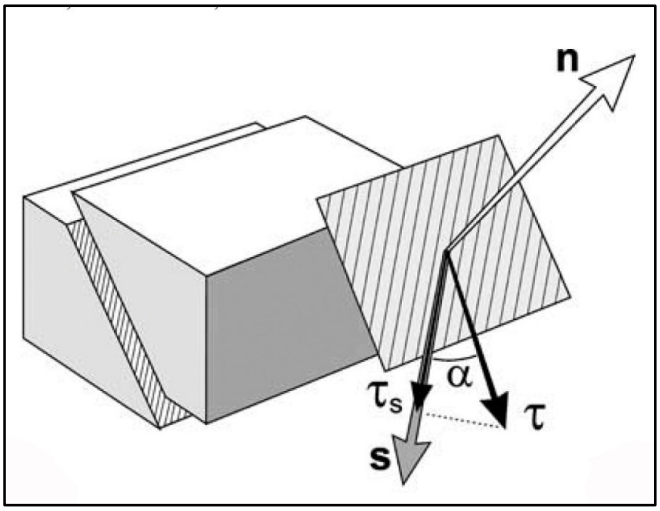

Fig. 5.5. Block diagram showing a reverse left-lateral fault.
Two unit vectors define the slip: n, normal to fault plane, and s, unit slip vector. By convention, n (open arrow) is chosen in the upper half-space, whereas s (grey arrow) indicates the motion of the lower block with respect to the upper one. Striations are as thin lines on fault plane. Black arrows indicate the shear stress, τ, and the SSSC vector, τs. The angle between the calculated shear stress and the actual slip is α (slip-shear angle) (from Angelier, 2002).

The analysis and computation of the fault populations for each site (especially if they contain different type of fault populations) pass through several steps:

1. Input whole faults, bedding plane and tension cracks into the software (Angelier, 1991);
2. Plot all the faults together on stereonets;
3. Separate the different fault types of faults (normal, strike-slip and reverse);
4. Make a computation of the fault population if the faults belong to a single tectonic event. If the faults belong to two or more system regime, we separate each population before computation;
5. Back-tilting the fault population and paleostress tensor if the faults are pre-tilting.

5.1.3. Fault slip analysis and measurements

A widespread difficulty in interpreting the measurements within the frame of poly-phase brittle tectonism was related to the heterogeneity of data sets in the studied area. Because of the large heterogeneity, computing an average stress regime was meaningless. We separated the data sets into more mechanically homogeneous subsets in order to reconstruct different stress fields that may correspond to distinct tectonic events.

5.1.3.1. Dating of meso-scale faults

In southern Gissar, meso-scale fault populations exist in the different stratigraphic succession and were formed at different times. Various criteria are used to establish a relative age relationship among structures, including crosscutting relationships and successive striae observed on fault surfaces, indicating fault reactivation under a new stress field.

Absolute dating

Absolute dating of tectonic events consists in founding the maximum accurate age of tectonic activity based on stratigraphic and structural criterion. The main criterions are: (1) the syndepositional faults, and (2) the angular unconformities.

The syndepositional faults are generally normal faults (fig. 5.6). These faults were formed during the deposition of the sediments. The identification of these faults is the thickness changes, on either side of the fault plane, and often internal thickness variations.

Fig. 5.6. An example of syndepositional fault in the Derbent gorge, central part of the Southwestern Gissar.

Growth faults are one of the safest ways for dating tectonic periods. They are mainly used to characterize extensive periods and assign a specific age in a population of normal faults. In our study we found several syndepositional faults mainly in the mid-late Jurassic carbonates.

The angular unconformity is a second reliable criterion for dating tectonic phases. Unlike growth faults, which essentially allow us to date the extensive periods, the angular unconformities also apply to compressive phases. But through our work we do not found any major regional angular unconformity in the Mesozoic stratigraphic succession.

Relative dating.

Inherited faults and lately formed faults

These faults are of two types: (1) newly formed if there is no pre-existing fracture and (2) reactivation of previous brittle structures as older faults, tension cracks, joints, or bedding planes. If the new fault does not destroy the remains of old structures, therefore the relative chronology between them can be indicating.

Criteria overlap

A fault or a family of faults is cut and offset by another fault or a fault population. This situation should be considered only if the timing is systematic in the fault population. It is generally easier to observe such a relative chronology for large faults, more particularly on the seismic profiles. At the level of the site, the use of this criterion is often difficult because the poly-phased tectonics obscure the relationship between the brittle structures.

Fault attitudes with respect to the folding (dip of the layers)

It is a criterion of relative chronology reliable and easy to use. It is a good way to determine the relative timing of formation of the fault population with respect to the folding. In our study we use the term pre-folding, or pre-tilting, faults for the faults that formed before the folding of the strata (fig. 5.7), and the term post-folding, or post-tilting, fault for those that formed after tilting (folding) of the strata (fig. 5.8).

The sedimentary layers have been subjected to both faulting and folding. It was thus indispensable to pay precise attention to geometrical and relative relationships between brittle structures and folds. To this end, we systematically back-tilted the strata to reconstruct the pre-folding orientation of structures in order to determine and separate brittle structures that formed before and after folding.

Fig. 5.7. An example of pre-tilting fault in the Derbent gorge, central part of the Southwestern Gissar.

5.1.3.2. Conjugate system of fault population

Conjugate faults are broadly contemporaneous faults which formed under similar stress conditions. The faults are arranged in a symmetrical trend in relation to the principal axes (σ1, σ2 and σ3 axes) of the applied stresses (fig. 5.3B).

The conjugate relationship is established when two sets of faults are present and where members of one set exhibit inconsistent cross-cutting relations with members of the other set, thereby suggesting contemporaneity (fig. 5.3A). The slip direction on each fault belonging to a conjugate should be at right angles to the line of intersection of the two faults.

Fig. 5.8. An example of post-tilting fault in the Derbent gorge, central part of the Southwestern Gissar.

The line of intersection is found by plotting the great circles for each fault plane. The line of intersection is taken as the direction of the intermediate stress axis; in addition the three principal stress axes (σ1, σ2 and σ3 axes) are commonly perpendicular to each other (fig. 5.3C).

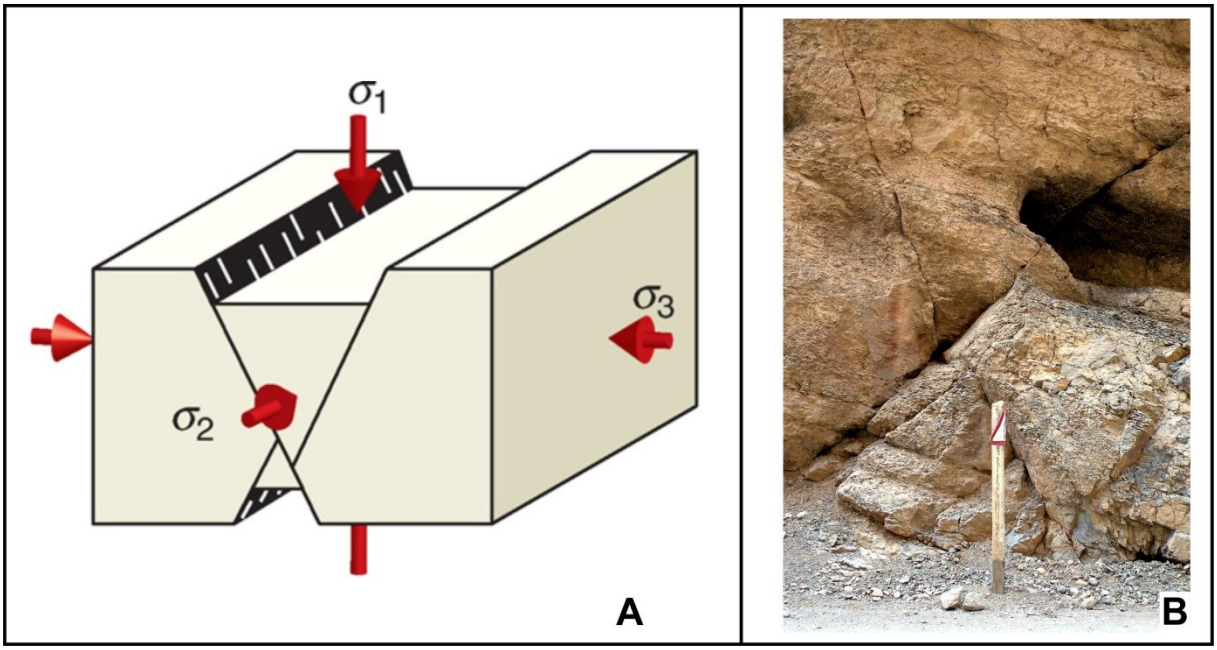

Fig. 5.9. Conjugate system of normal faults
A: schematic diagram of a conjugate set of normal faults with the 3 mean stress axes; B: Pre-tilting set of conjugate faults in the Derbent gorge (Southwestern Gissar).

In our study of the fault populations in each site we try to found conjugate fault systems, because there are helpful to identify that the fault systems formed before or after the folding of the strata (fig. 5.9, 5.10). The identification of the sets of pre- and post-folding conjugate fault systems is not simple especially if the fault population is pre-tilting type. Commonly, during the fieldwork we found different types of pre-tilting conjugate fault systems that in the present day appear as different fault types. Such as:

1. Pre-tilting conjugate of normal faults that appear in the present configuration as a left and right lateral strike-slip fault populations;
2. Pre-tilting conjugate of normal faults that appear in the present configuration as reverse and normal fault populations;
3. Pre-tilting conjugate system of strike-slip fault appears in the present configuration as strike-slip and reverses fault populations.

Also, according to the size of the fault and the displacement along the faults we may distinguish: (1) regional faults, which are generally very long (tens of kilometres) with large displacements (several hundred of metres to some kilometres) like the Uchbash-Karshi Flexure Fault Zone (UKFFZ) separating the Bukhara-Khiva regions, and (2) local faults, which are not very long with small displacements (fig. 5.11). These latter are the main purpose of our field investigation of brittle tectonics in Gissar.

Fig. 5.10. Pre-tilting conjugate fault system in the Derbent Gorge, Central part of Southwestern Gissar.

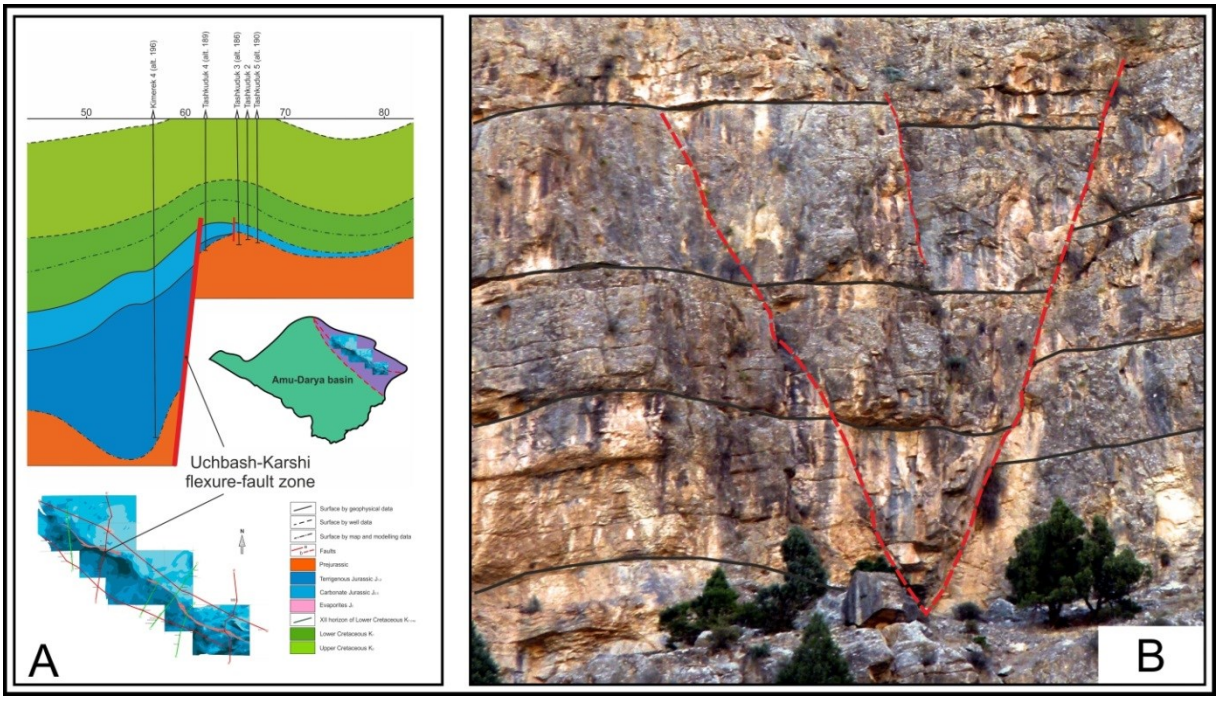

Fig. 5.11. Normal faults at different scales.
A: Regional fault with a huge displacement evidenced on a seismic line (fragment of the E-E' geological line);
B: Meso-scale faults in the Middle-Upper Jurassic carbonate (Sayrob Gorge, Southwestern Gissar).

5.1.3.3. Faults and displacement indicators

Faults in general are discontinuities along which movement has occurred. This is reflected in the plane of faults by striations or grooves that indicate the direction of movement of compartments faults. The identification of the fault striation needs careful and accurate work because several types of slickenside striation exist (fig. 5.12, 5.13). Many authors worked on brittle slickenside kinematic criteria type (e.g. Petit et al., 1983; Doblas, 1985, 1987; Petit and Laville, 1987; Mercier and Vergely, 1992).

On the ground, the direction, magnitude and direction of the inclination of striated plan and pitch streak (angle between the linear streaks with the horizontal in the plane of the fault) is measured with a compass. Measurement of fault planes and stratification structures are identified by (1) their azimuth (angle from 000^0 to 180^0) between the direction of the fault plane and the direction of magnetic north (clockwise) and value of the dip (angle from 00^0 to 90^0) between the fault plane and the horizontal, and (2) a dip direction (north, east, south or west).

The lineation on the fault plane is characterized by its pitch (angle from 00^0 to 90^0) on the fault plane between the streak and the horizontal and its dip direction. In the case of a low angle-dipping fault, the streak is indicated by the azimuth in degrees from a vertical plane containing the streak (angle of 000^0 to 180^0) (fig. 5.14, 5.15).

Fig. 5.12. Example of slickenside lineations on a strike-slip fault in the Jurassic carbonates of the Derbent gorge, central part of the Southwestern Gissar.

Fig. 5.13. Example of slickenside lineations on a strike-slip fault in the Jurassic carbonates of the Derbent gorge, central part of the Southwestern Gissar.

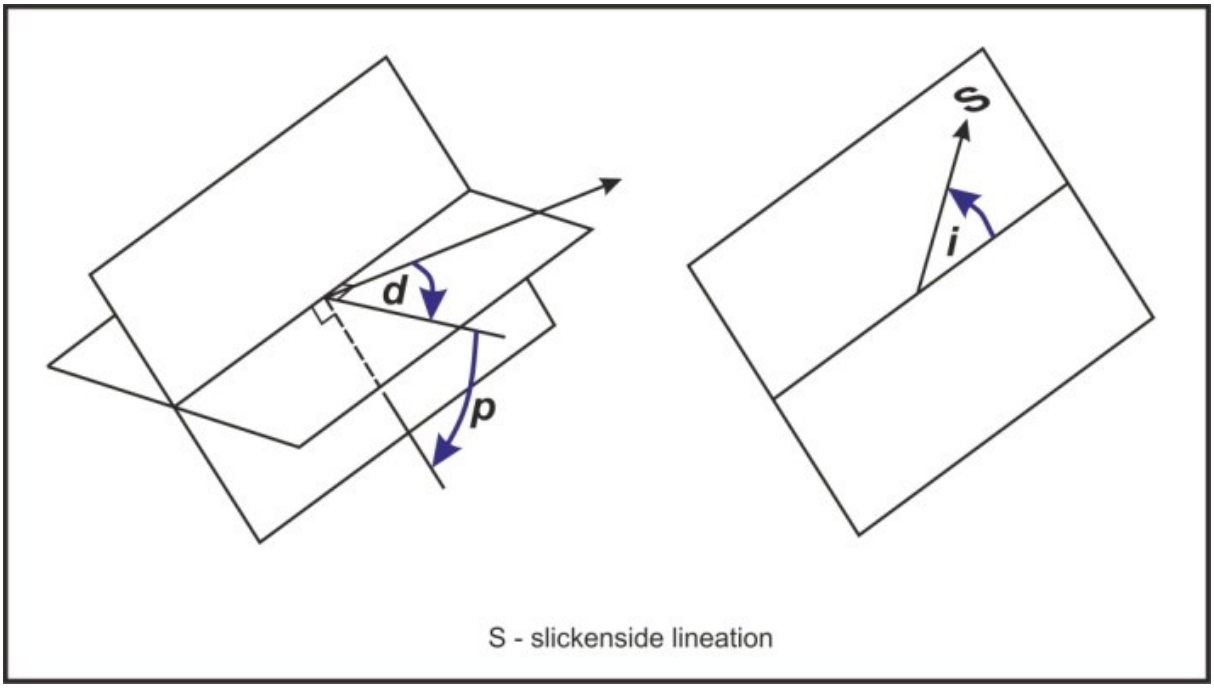

Fig. 5.14. Measurement of a fault plane
d: direction (000° to 180°, clockwise with respect to north); p: plunge (00° to 90°,); i: pitch (00° to 90° on the fault plane); S: slickenside lineation.

Fig. 5.15. Example of vertical displacement along a fault plane
(Langar Gorge, northwestern part of the Southwestern Gissar).

5.2. Field study

5.2.1. Area of investigation: the Southwestern Gissar region

The study area covers most of the Southwestern Gissar Range, approximately representing an area of 100000 km^2 (fig.5.16). The Southwestern Gissar is NE-oriented. It is constituted of 3-4 main parallel ranges bordered by major thrusts. The highest peaks reach of 4000 m in the north-eastern part of Gissar.

The south-western limit of the study area is the Uzbek-Turkmen border, which almost corresponds to the termination of the Southwestern Gissar Range. To the south-east the area is limited by the Surkhan-Darya River that constitutes the Uzbek-Afghan border. High mountains mark the north-eastern area of the range where Mesozoic rocks are almost absent. This latter high domain is generally called Gissar (s.s.). The area of investigation is included in the Kashkadarya and Surkhandarya provinces (see fig. 1.2).

5.2.2. Field work: the fault sites

In the field after a first examination we decide if the site is suitable for a detail analysis. Generally, in a first step we measure the bedding planes. In a second step we measure the faults, and possibly the other brittle features (joints, tension gashes, …).

For each fault we measure: (1) the direction of the fault plane, (2) the dip of the fault plane, and (3) the pitch or direction of the slickenside lineation(s). Then we specify the type of fault, i.e. normal, reverse, strike-slip (right or left lateral). In addition we describe the lithology of the formations and in most sites we collect samples for biostratigraphic study.

At first it was the data collecting in the Southwestern Gissar (fig. 5.16.).

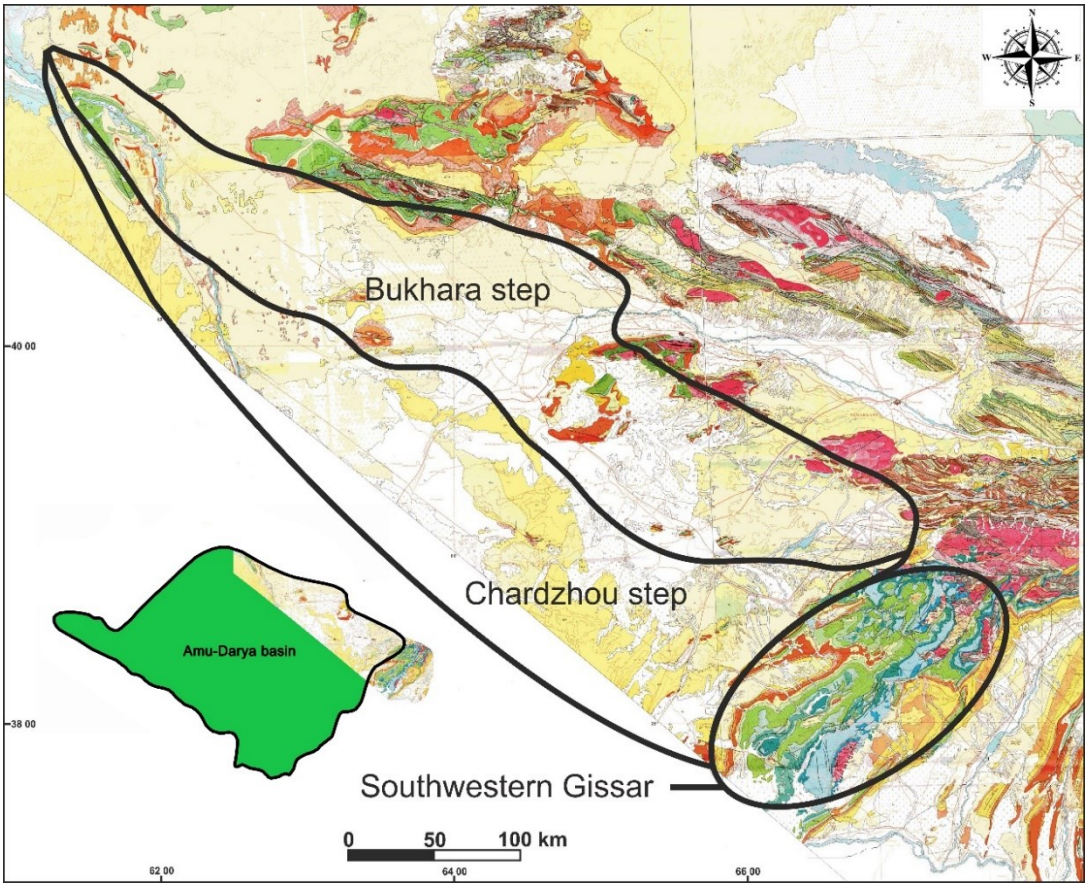

Fig. 5.16. Location of the Southwestern Gissar area (SWGR). Background: Geological map of Uzbekistan, 1:500000 (1988).

During a second stage we process the data collected on the field. The data processing is performed in the laboratory after the fieldwork. For this, as it was said before, we used the software INVD developed by Angelier (1990). This software allows computing and determining the paleo-stress tensor from a coherent population of fault.

The third point of the analysis was the data interpretation, which means the connection between the results of our work, we have obtained and the geological-tectonic events of the past.

Data collection

In the Southwestern Gissar we studied 6 sites located on the figure 5.17. After, we have chosen the most informative sites. They are the Derbent, Langar and Sayrob sites (fig. 5.18). The faults from all of these sites are situated in the upper part of the Jurassic carbonate (approx. Callovian in age), represented by the different types of limestones.

In the southeastern part of the area we studied sites in the Derbent gorge. South of Derbent we studied other sites in Sayrob, close from each other.

In the northwestern part of Southwestern Gissar we studied several sites near the Langar and Kizilkishlak villages.

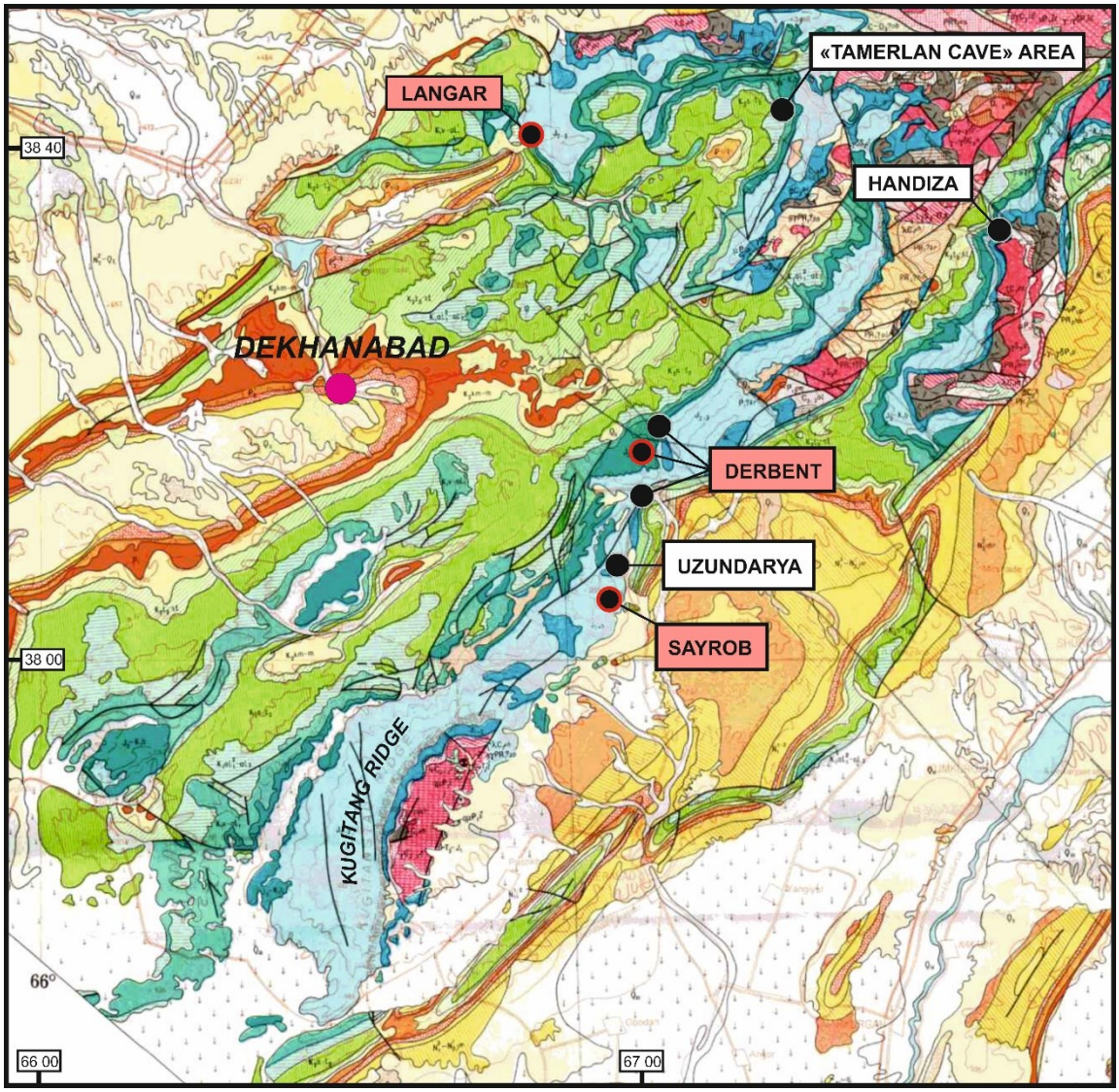

Fig. 5.17. Location of the studied sites (black dots). Black dots with red circles and pink box indicate the selected areas. Background: Geological map of Uzbekistan, 1:500000 (1998).

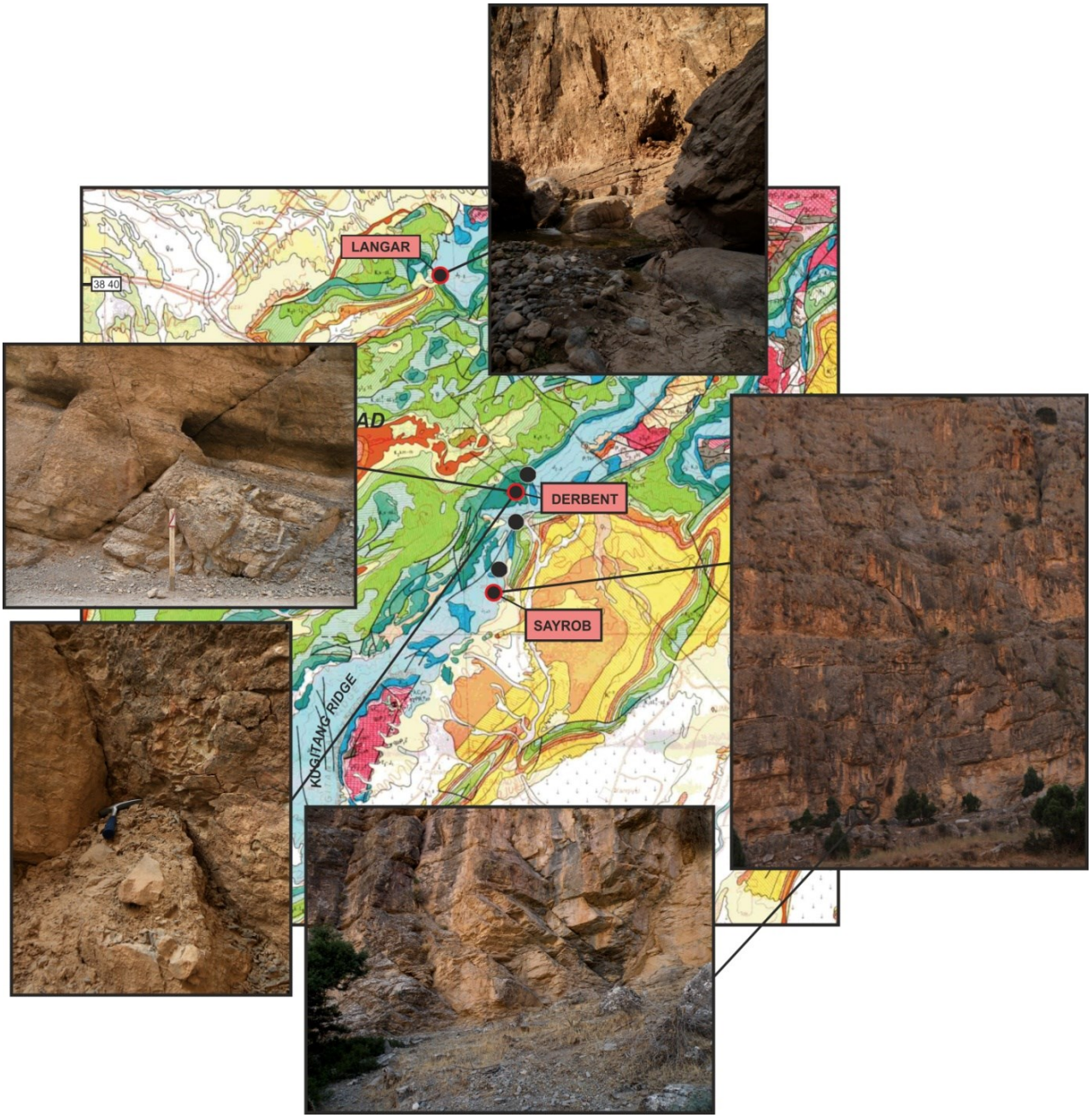

Fig. 5.18. Photos and location of the sites. Background: Geological map of Uzbekistan, 1:500000 (1988).

Data processing

After choosing the best sites, we have inserted their fault data into the software. In the data complex, except the main fault features also were the coordinates of the site, some stratigraphy description and a few words about tectonic conditions of the area. After some corrections and grouping information for each area we have calculated the paleo-stress directions.

Then we have obtained the diagrams showing the fault projections and tensor axes for each site (fig. 5.19., 5.20.).

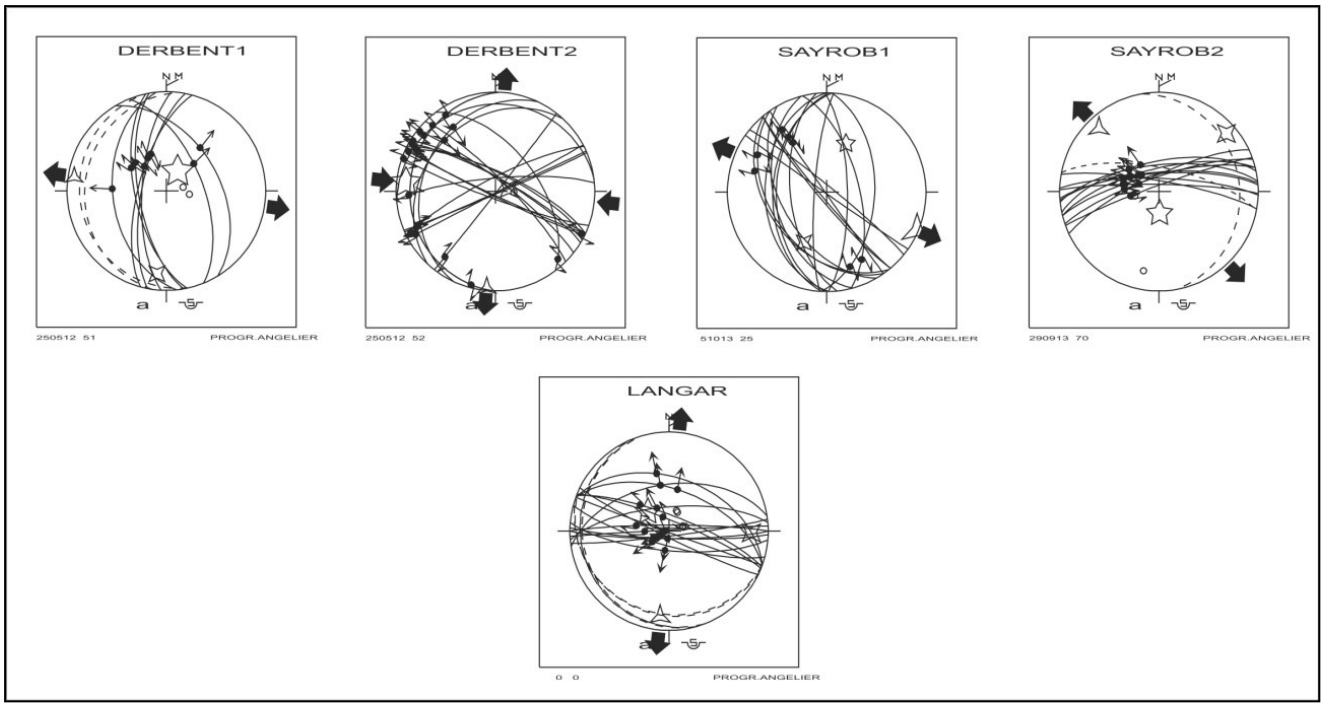

Fig. 5.19. Stereonets showing faults populations with the computed paleo-stress tensors.

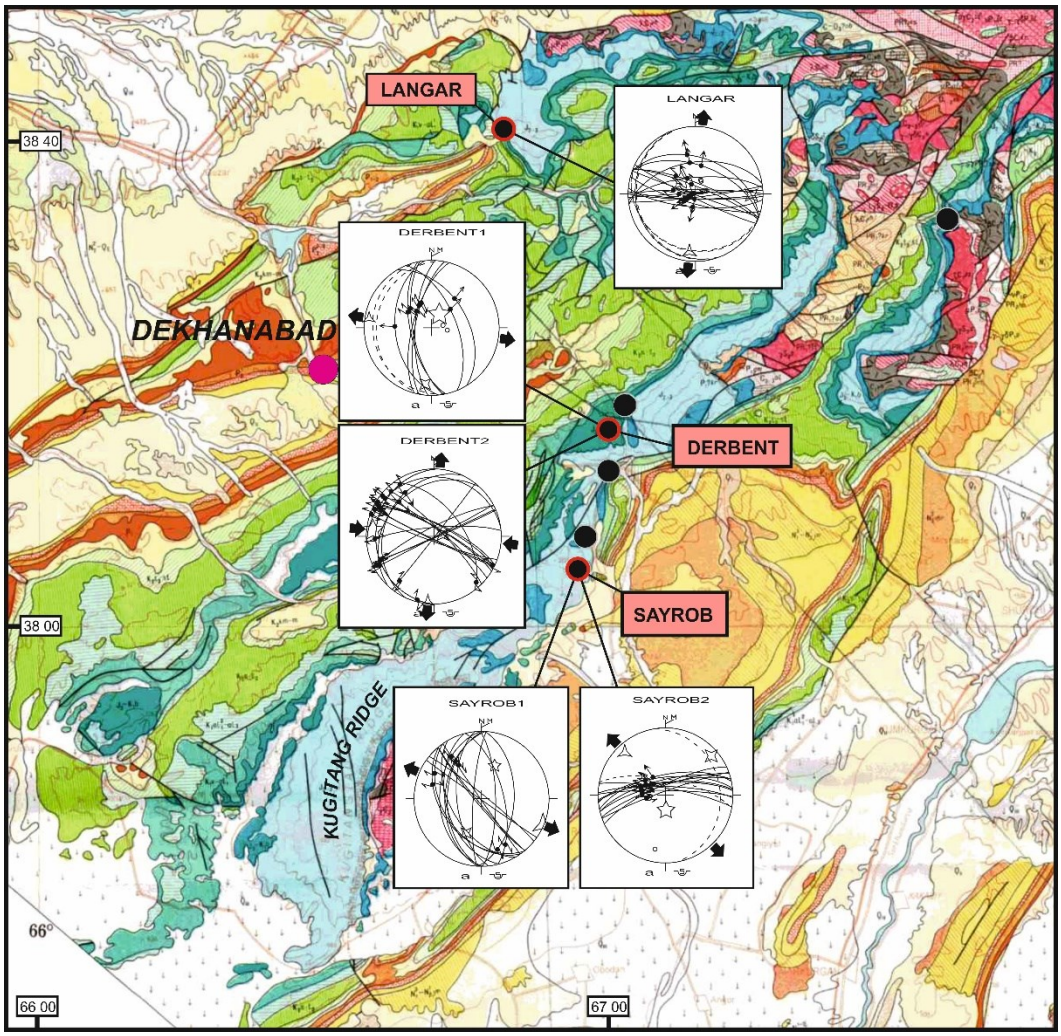

Fig. 5.20. Diagram locations. Background: Geological map of Uzbekistan, 1:500 000 (1998).

5.3. Study of the sites

5.3.1. Langar

The faults we measured in this area are situated in the so-called Langar Canyon, between the Kizilkishlak and Langar villages.

The limestone where is located the measured fault is dated from the top of the Middle Jurassic, more accurately from the Callovian (fig. 5.21).

The fault population is exclusively constituted of E-W to WSW-ENE striking normal faults. Most of them are north-dipping deep-slip normal faults.

The computation evidences a N-oriented σ3 axis in a pure extensional stress regime (fig. 5.22., table 5.1.).

Fig. 5.21. Langar 1 site.

σ_1		σ_2		σ_3		Φ
Strike	Pitch	Strike	Pitch	Strike	Pitch	
313	66	091	18	186	15	0,395

Tab. 5.1. Main stress axes parameters of the normal fault population of the Langar site.

In Langar we evidenced a roughly N-S oriented extension, probably pre-tilting, and poorly constrained in age. This stress regime well correlates with the large scale structure that suggests a major E-W to NW-SE trending normal fault passing near Langar and extending northwestwards to the Bukhara Step.

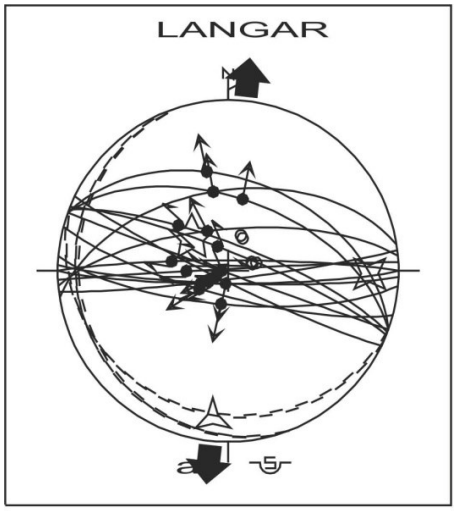

Fig. 5.22. Stereonet of the normal fault population of the Langar site.

5.3.2. Derbent

In the Derbent gorge, located few kilometres north of the Derbent village, we have measured several sites. The cliffs along the Machay River provide good outcrops all along the gorges.

All kind of fault populations, i.e. reverse, normal and strike-slip, are exposed in this area. Here we show only two, which are the most informative. The first one, called Derbent 1, is located in the southeastern part of the gorge, in the Callovian limestone (fig. 5.23).

Fig. 2.23. Conjugate fault system of the Derbent 1 site.

It is constituted by a population of conjugate normal faults. They are N- to NNW-oriented normal faults, westward and eastward dipping. We evidenced a well constrained E-W trending extension (fig. 5.24; table 5.2.).

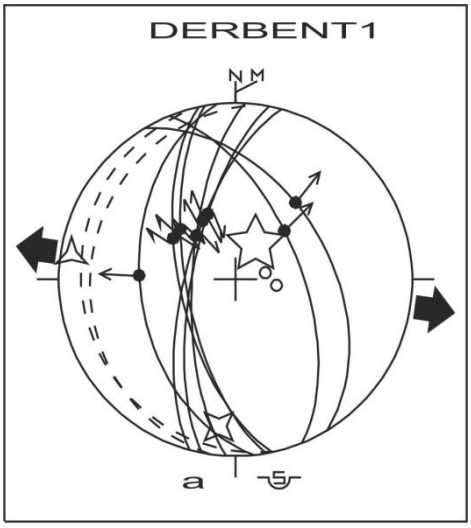

Fig. 5.24. Stereonet of the normal fault population of the site Derbent 1.

σ_1		σ_2		σ_3		Φ
Strike	Pitch	Strike	Pitch	Strike	Pitch	
030	71	187	17	279	07	0,041

Tab. 5.2. Main stress axes parameters of the paleostress tensor of the Derbent 1 normal fault population.

The Derbent 2 site is located in the gorge, just 150 m further north-west from Derbent 1. It is also in the Callovian carbonates, represented by well bedded limestone (fig. 5.25).

Fig. 5.25. The fault of the Derbent 2 site.

Derbent 2 displays a population of conjugate strike-slip faults. The right lateral faults strike NE-SW to E-W, while the left lateral faults are ESE- to SE- oriented (fig. 5.26; table 5.3).

In the Derbent gorge, the normal faults commonly exhibit syn-depositional features (fig. 5.25) allowing to accurately estimate the age of the extensional tectonics.

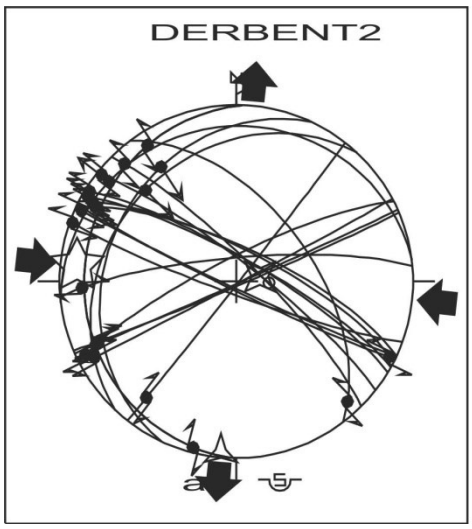

Fig. 5.26. Stereonet of the strike-slip fault population of the site Derbent 2.

σ_1		σ_2		σ_3		Φ
Strike	Pitch	Strike	Pitch	Strike	Pitch	
276	11	078	79	185	03	0,172

Tab.5.3. Main stress axes parameters of the paleostress tensor of the Derbent 2 strike-slip fault population.

5.3.3. Sayrob

The next area, where we have performed a fault tectonic analysis is called Sayrob. Sayrob is a small village located in south-eastern Gissar about 25 km south of Boysoun town. The sites are situated east of the village, in the cliff of a canyon. The sites are in the Callovian carbonate.

The first site, Sayrob 1, consists in a population of oblique normal faults, probably resulting from the reactivation of SE- to S-trending joints and former normal faults (fig. 5.27).

The result of the computation indicates a 113°-oriented σ3 axis (fig. 5.28, table 5.4). This ESE-trending extension probably succeeded to an E-W striking extension poorly expressed in this site where the dip-slip slickensides have been weathered.

The next site, Sayrob 2, is situated about 500 m from the previous one in the same canyon and cliff (fig. 5.29).

Here, we observed an ENE- to E-trending population of normal faults, probably pre-tilting (pre-folding) taking into account the attitude of the slickensides with respect to the bedding plane. Unfortunately only one set of normal faults (north dipping) exists in this site. Consequently, the paleostress axes are poorly constrained. However, the NE-oriented computed extension (fig. 5.30, table 5.5) is probably not too far from the true one taking into account the attitude of the slickenside with respect to the bedding plane. This extension is similar in direction to the one determined in Sayrob 1.

Fig. 5.27. Fault plane of the site Sayrob 1.

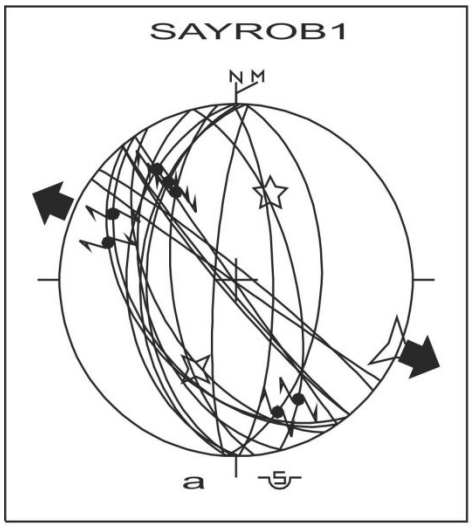

Fig. 5.28. Stereonet of the Sayrob 1 fault population.

σ_1		σ_2		σ_3		Φ
Strike	Pitch	Strike	Pitch	Strike	Pitch	
022	46	204	44	113	01	0,964

Tab. 5.4. Main stress axes parameters of the paleostress tensor computed from the Sayrob 1 fault population.

Fig. 5.29. Conjugate fault system of the Sayrob 2 site.

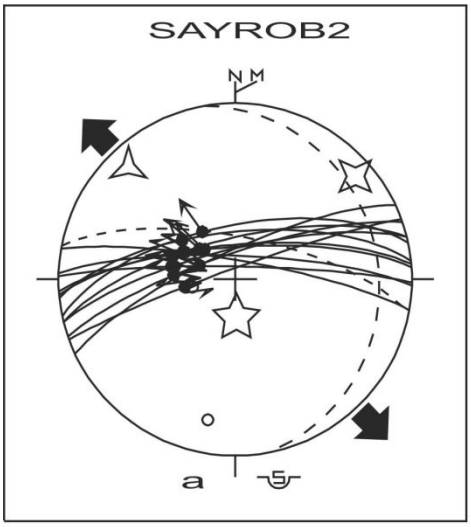

Fig. 5.30. Stereonet of the Sayrob 2 normal fault population.

σ_1		σ_2		σ_3		Φ
Strike	Pitch	Strike	Pitch	Strike	Pitch	
178	72	049	11	317	13	0,351

Tab. 5.5. Main stress axes parameters of the paleostress tensor of the Sayrob 2 fault population.

We may conclude that in this area of southern Gissar we evidenced a pre-folding NE-oriented extension. As no syn-depositional feature has been observed in these sites, the age of the faulting is still poorly determined in Callovian to Neogene interval.

Much more extensive faults studies in the Southwestern Gissar area would be necessary to get significant results for the fault tectonic analysis as here the data collected are not enough.

Chapter 6

Mesozoic-Cenozoic evolution of the northern margin of the Amu-Darya basin

Chapter 6

Mesozoic-Cenozoic evolution of the northern margin of the Amu-Darya basin

In the previous chapters of this thesis we have presented the tectono-stratigraphic evolution of the northern margin of the Amu-Darya basin. In the Uzbek part of the margin, the studied area comprises the Bukhara-Khiva and Southwestern Gissar regions. To fully understand the geological evolution during the Mesozoic-Cenozoic times we need to consider the tectono-stratigraphic evolution in the regional geodynamical context, including the entire South Tien-Shan region, the Amu-Darya basin itself and its margins. It is the purpose of this last chapter where we integrate the data we have obtained to present a picture of the regional evolution of the Amu-Darya basin and its northern margin from the Triassic to the Cretaceous.

The basinal sedimentary cover of the Amu-Darya basin unconformably overlies various older rocks. During Jurassic through Eocene time, sedimentation occurred in basins located on the southern margin of the Laurasia-Eurasia continent, north of the active margin of the Neo-Tethys. The Mesozoic evolution of Western Central Asia, on the contrary of the Paleozoic evolution, was poorly studied in the modern scientific literature, particularly the Amu-Darya basin. On the other hand, the Cenozoic evolution has been more extensively investigated, especially the Late Cenozoic Pamir and western Tien-Shan orogenies (Thomas et al., 1999; Burtman, 2000; Trifonov et al., 2011, among many others).

6.1. Pre-Jurassic evolution: the Late Paleozoic and Triassic tectonics

6.1.1. The Late Paleozoic collages and the mosaic of blocks

The Late Paleozoic-Triassic geodynamic evolution of Western Central Asia is characterized by a succession of collages of continental blocks associated with continent-continent collisions. Basically, two main periods of collision of blocks (or micro-continents) succeeded in this region from the Late Carboniferous to the Early-Middle Permian, and in Middle-Late Triassic respectively. Orogenic belts developed at the collisional boundaries between the blocks generating significant mountain belts covering vast areas of Western Central Asia. These Late Paleozoic and Triassic orogens sourced the surrounding platforms and basins, mainly during the Late Permian-Triassic and Early-Middle Jurassic periods.

The first period of collisions belong to the Hercynian cycle. It led to the creation of the Northern Pangea super-continent in the Permian time from a collage of continental plates and blocks (fig. 1.14 to 1.21). The main Late Paleozoic orogenic belts were the Tien-Shan and Uralian ranges, E- and N-trending respectively. These major orogens were connected in a poorly known area, currently located in the Aral-Ustyurt area, and deeply buried beneath the Mesozoic-Cenozoic sedimentary cover. In Southwestern Central Asia this long collisional suture zone separated the East European – Kazakh craton in the north (fig. 1.14) from a mosaic of continental blocks and micro-blocks in the south, including from east to west the Tarim, Alay, Afghan-Tajik, Amu-Darya and Karakum blocks (fig. 1.13 and 1.14), the last three belonging to the Turan domain (fig. 1.3, 1.14). The configuration of the blocks (geometry and names) constituting Southwestern Central Asia may change from one author to another in the geological literature.

The Bukhara-Khiva region, constituting the northern margin of the Amu-Darya basin, is situated on the northern border of the Turan domain (fig. 1.3). In this region the northern limit of the Turan domain is poorly determined and debated. The major Late Paleozoic regional suture zone is constituted by the ophiolitic belt of the Turkestan suture (fig. 1.8, 1.13). This main structural feature marks the limit between the Kazakh plate to the north and a hypothetic Alay block (or micro-continent or micro-plate) to the south (fig. 1.14). The so-called Late Paleozoic Southern Tien Shan Range develops south of this major regional suture and extends as far south as the hypothetical Zaravshan suture (fig. 1.8 and 1.13, 1.16). The nature of the Alay micro-plate is not really clear and still debated. Given the current state of knowledge it is difficult to determine whether or not this micro-plate has

been an independent block before the Late Paleozoic collision or was the northern promontory of the Turan domain that collided with the Kazakh plate (fig. 1.13 and 1.14). Figure 1.16 shows that the basement of the Chardzhou and Bukhara steps belongs to the northeastern Turan domain. However, the pre-Mesozoic basement of this northeastern part, occupies a complex location and probably includes several terranes or blocks.

6.1.2. The basement of the Amu-Darya and Tajik basins

A Late Paleozoic basement, unconformably covered by possibly Late Permian-Triassic sediments, underlies the Jurassic-Cenozoic Amu-Darya basin. This basin developed during the Mesozoic on the epi-Hercynian Turan Platform (called platform after the collage of blocks, see Chapter 1). The composition of the basement in the central part of the basin is poorly known. It probably results from the accretion of tectonic terranes as a consequence of the closure of oceanic domains during the Late Paleozoic. It is generally accepted that the basement of the Turan Platform comprises a mosaic of continental blocks that constituted micro-continents before the Late Paleozoic collages (including the Karakum, Amu Darya, and Afghan-Tajik blocks).

The Afghan-Tajik block, located east of the Amu-Darya block, underlies the Afghan-Tajik basin. It connects with the Amu-Darya block to the west (fig. 1.13). The relationships between these two blocks forming the Karakum - Amu Darya - Afghan-Tajik micro-continent (fig. 1.13) are hypothetical, mainly because of the deep burial beneath the Mesozoic sedimentary sequence of the Amu-Darya and Afghan-Tajik basins. Exposures in the Southern Gissar Range displayed Proterozoic basement rocks and Silurian to Carboniferous sediments interpreted as deposits of the margin of the northern Tajik micro-continent.

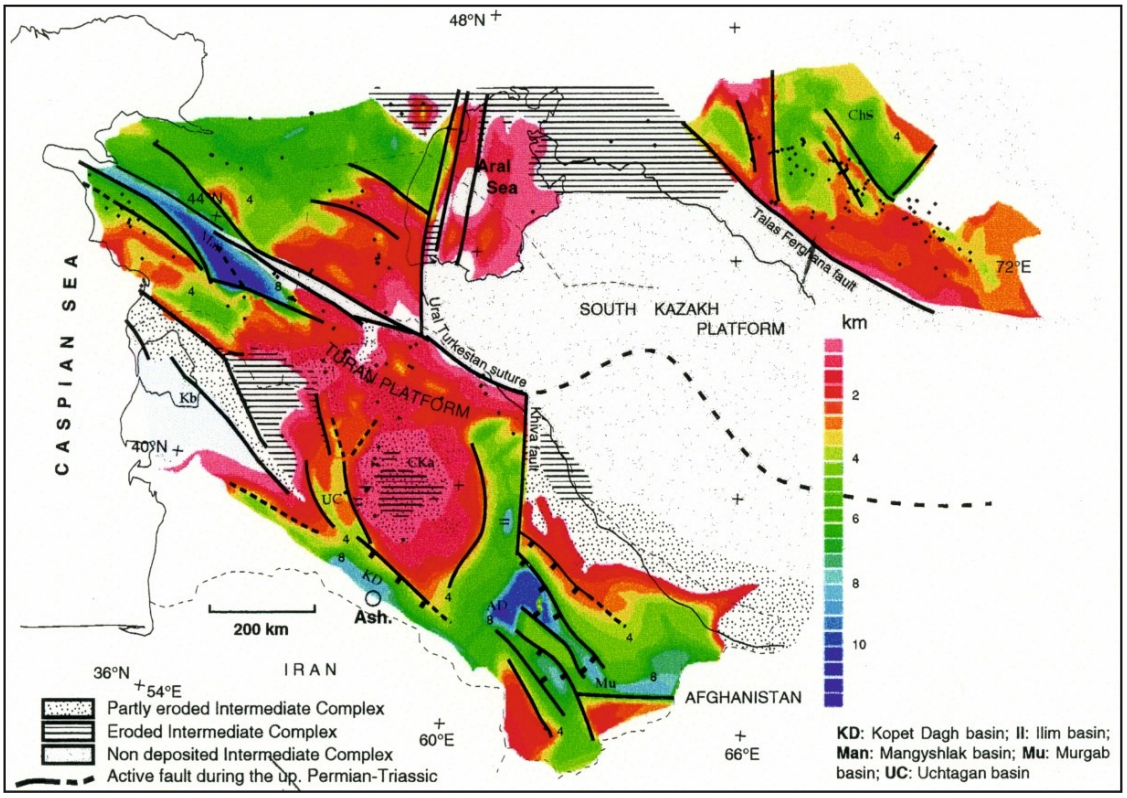

Fig. 6.1. Isopach map of the Late Permian-Triassic sediments
Number: Values of isopach contours in kilometre (from Thomas et al., 1999).

6.1.3. The Late Permian – Triassic post-orogenic rifts

Several post-collision sedimentary basins have been reported in the Turan Platform and Afghan-Tajik block (fig. 1.13 and 6.1). These basins are mainly determined by geophysical data. As noted in Chapter 2, more than 500 wells have reached the pre-Jurassic rocks in the Bukhara-Khiva region. Because of the deep burial, the location of these basins is poorly determined. They are generally considered as Late Permian to Triassic post-orogenic rifts where accumulated thick clastic sediments derived from the denudation of the Hercynian orogen.

The Late Permian to Triassic deposits have been only investigated in the inverted Turkestan ridge bounding the Amu-Darya basin to the south, and in northern Afghanistan where they are exposed in the northern flank of the Hindu-Kush (Montenat, 2009).

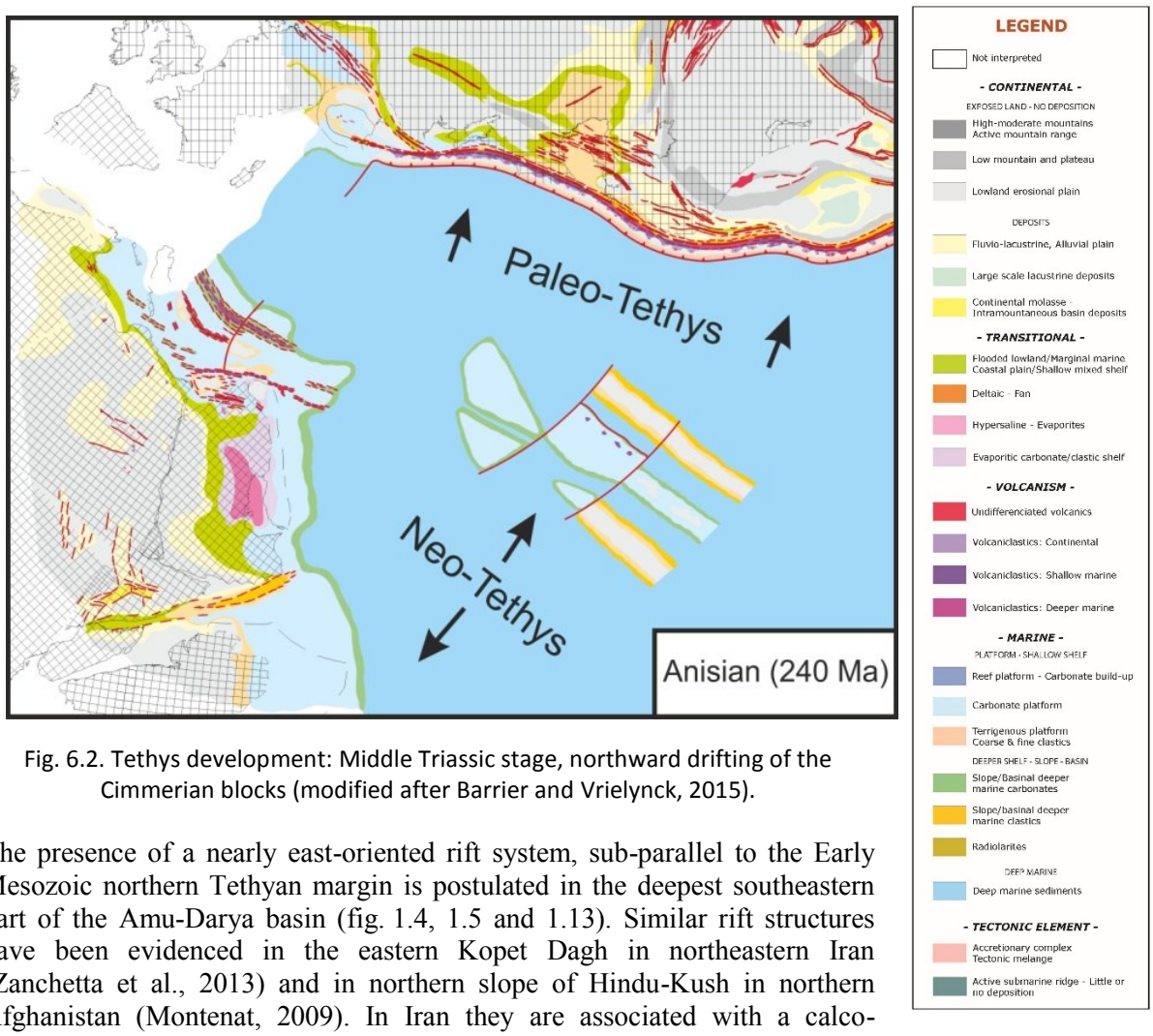

Fig. 6.2. Tethys development: Middle Triassic stage, northward drifting of the Cimmerian blocks (modified after Barrier and Vrielynck, 2015).

The presence of a nearly east-oriented rift system, sub-parallel to the Early Mesozoic northern Tethyan margin is postulated in the deepest southeastern part of the Amu-Darya basin (fig. 1.4, 1.5 and 1.13). Similar rift structures have been evidenced in the eastern Kopet Dagh in northeastern Iran (Zanchetta et al., 2013) and in northern slope of Hindu-Kush in northern Afghanistan (Montenat, 2009). In Iran they are associated with a calco-alcaline magmatic activity and filled up by volcanoclastic series. In northern Afghanistan, the North Hindu-Kush Rift also contains a thick Triassic marine volcanoclastic sequence.

These Late Permian to Middle-Late Triassic rifts are sub-parallel to the subduction zone that existed along the southern active margin of Northern Pangea (fig. 6.2). They are interpreted as back-arc basins developing behind this subduction zone where the Paleo-Tethys oceanic domain was subducting northwards beneath the Pangea margin. Other similar basins of same age developed further north in the Turan Platform and Tajik block (fig. 6.1 and 6.2). Several wells penetrated Permian and/or Triassic clastic deposits in the Bukhara and Chardzhou steps (fig. 6.3). Among them, are only 5 (Yangikazgan 4, Pamuk 1, Central Chukurkul 1, Shorsu 1 and Yangiarik 1P) crossing Triassic sediments. In these wells the Triassic and Permian sequence cannot be separated (fig. 6.3). It is why the presence of Triassic deposits is still questionable. According to Babadjanov and Abdullaev (2009)

these sediments exist, but according to Babadjanov (2008) the pre-Jurassic basement is represented only by the Permian sediments.

We postulate that these Late-Permian to Triassic back-arc activity originated the Amu-Darya and Tajik basins. The Late-Permian-Triassic rifting marks the beginning of extensional deformations in the southern margin of northern Pangea that will develop later with the Mesozoic basins.

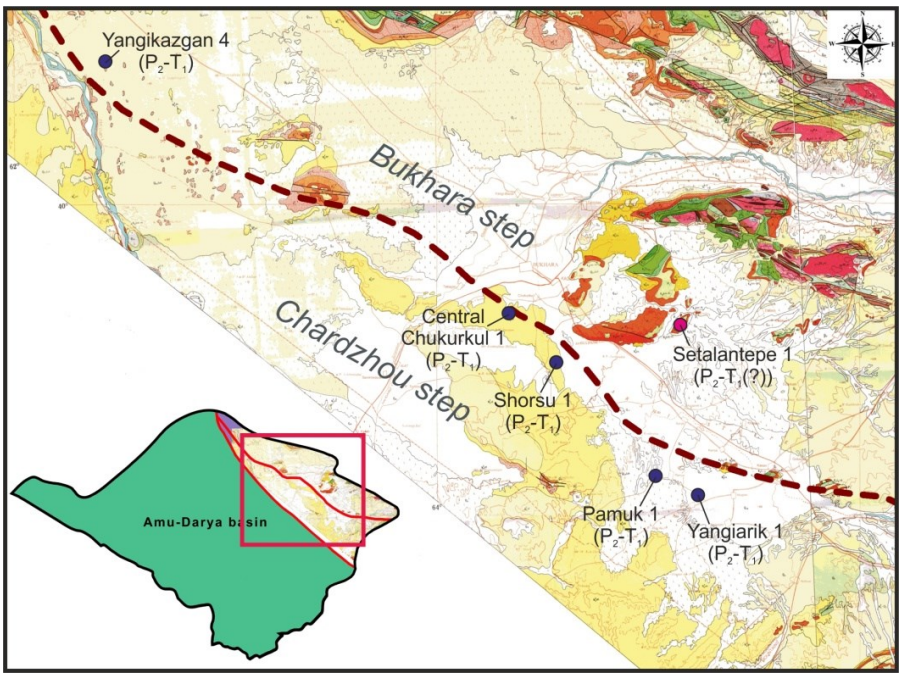

Fig. 6.3. Location of wells penetrated the Triassic sediments
Background: geological map of Uzbekistan, (1998).

6.1.4. The Middle-Late Triassic Cimmerian orogeny

The second main period of collision of blocks is Middle-Late Triassic in age. This regional phase is called Cimmerian orogeny, or more accurately Eo-Cimmerian orogeny for Middle-Late Triassic deformations. The Cimmerian orogeny results from the collision of the Cimmerian blocks with the southern margin of Northern Pangea. The Cimmerian blocks are continental blocks rifted from the northern Gondwanian margin in Early Permian (fig. 6.2). During the Late Permian – Early-Middle Jurassic these blocks drifted northwards (fig. 6.2). This north drifting was associated with the opening of the Neo-Tethys Ocean in the south and the coeval closure of the Paleo-Tethys oceanic domain in the north (fig. 6.2). This special configuration has led to the co-existing of two oceanic domains during the same period, the remains of Paleo-Tethys to the north, and the Neo-Tethys to the south. The Cimmerian blocks collided with the Northern Pangea margin during the Middle-Late Triassic, and in certain areas until the Early Jurassic. A consequence of the accretion of the Cimmerian blocks to the Pangea margin is the shift of the Neo-Tethys active margin towards the south (fig. 6.4).

The deformation related to the Eo-Cimmerian collisions did not directly affect the northern margin of the Amu-Darya margin because the main Eo-Cimmerian orogenic belt developed further south in the Afghanistan. The lack of good Permian-Triassic outcrops in Southern Gissar did not allow to really assess the Cimmerian deformations and more particularly the unconformity between the Late Permian-Triassic beds and the overlying pre-Jurassic ones. However, the Eo-Cimmerian is very important from the sedimentologic point of view. Indeed, the Cimmerian collision clearly controlled the deposition in the Amu-Darya and Tajik basins during the Early-Middle Jurassic times. In fact, the erosion of the Eo-Cimmerian orogen sourced the siliciclastic deposition during the whole Early Jurassic-Bajocian times in the Amu-Darya and Tajik basins (fig. 2.15-2.17, 6.4).

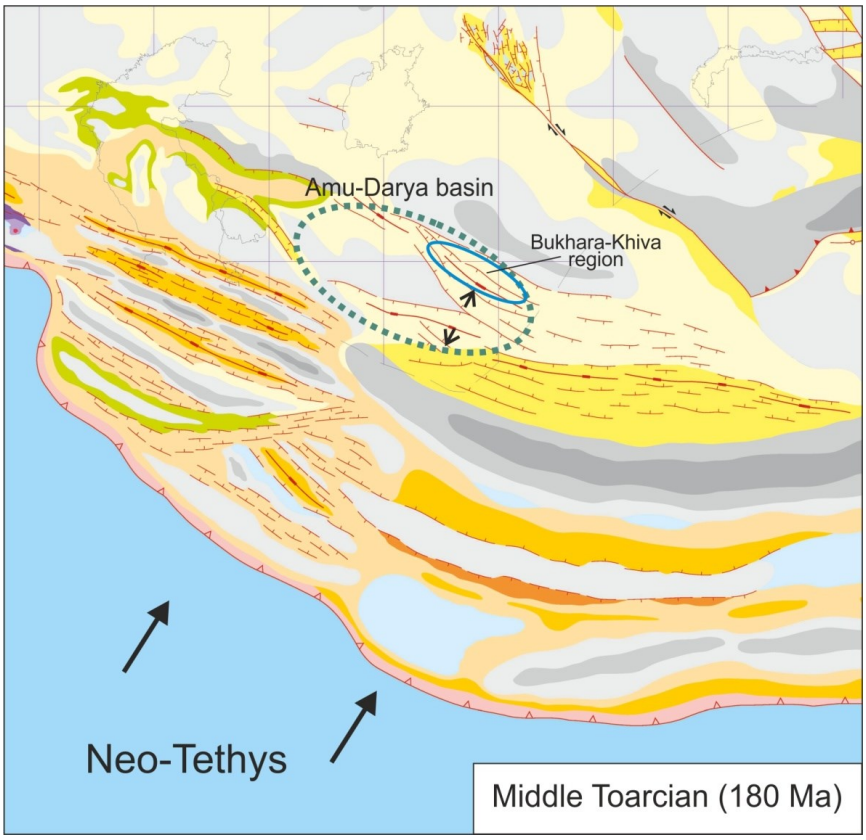

Fig. 6.4. Segment of the Southern Laurasia margin in Southwestern Central Asia during the Early Jurassic. The Amu-Darya basin and Bukhara-Khiva region are outlined (modified after Barrier and Vrielynck, 2015), for legend see Fig. 6.2.

6.2. Early-Middle Jurassic rifting

The beginning of the Jurassic is marked by major changes in both the tectonics and sedimentation in the northern margin of the Amu-Darya basin and in the basin as well.

6.2.1. Syn-rift sedimentation

Our results indicate that during the Early-Middle Jurassic the deposits in the Chardzhou step, and at lower level in the Bukhara step, are constituted of thick siliciclastic sections. Early to early Middle Jurassic (and possibly the uppermost Triassic) continental sediments mark the base of the Mesozoic sequence, unconformably overlying the pre-Jurassic formations. The Lower-Middle Jurassic sequence laps onto the basement and the Paleozoic sediments.

In the Amu-Darya basin the Jurassic sedimentation was relatively uniform, and was controlled by pronounced surrounding topographies. The deposits are mainly composed of continental clastics eroded from the Cimmerian mountain ranges erected during the Middle-Late Triassic. The Amu-Darya and Tajik basins were mainly sourced by the main Cimmerian Ranges located southwards in northern Afghanistan and northern Iran, while the Bukhara and Chardzhou steps were only sourced by reliefs located to the north and northeast (fig. 6.4.).

The Early to early Middle Jurassic environments were mainly non-marine and consist of flood plains, rivers, lakes and swamps. Coarse clastics are mainly confined to the basal Lower Jurassic section (and possible and locally uppermost Triassic) that commonly contains coal beds. These coaly deposits are probably Early Jurassic in age (Pliensbachian-Toarcian). Only thinner coal veins are present in the upper part of the continental clastic sequence.

The first marine clastic layers appear in the early Late Bajocian, partly connected to a global rise in sea level. According to Egamberdiev and Ishniyazov (1990), who reconstructed the paleo-environmental changes during the transgression in Southwestern Gissar, the lower part of the Middle Jurassic sedimentary cover was constituted of silty-sandy continental facies issued from paleo-rivers (fig. 2.17). Then, as the area was subsiding, the sea was transgressing from the south and the clastic input was decreasing, the lithology progressively graded from coarse to fine-grained deposits. On the Bukhara step the paleo-rivers gradually disappear. In the top of the siliciclastic sections the carbonate facies gradually appear.

Our results show that in the Bukhara-Khiva region the thickness of the siliciclastic deposits significantly increases southwestwards towards the centre of the Amu-Darya basin. The continental siliciclastic deposits sporadically filled up N- to NE-oriented valley in the Bukhara step, draining the sediments eroded from the Early-Middle Jurassic rejuvenated Tien-Shan Range. To the southwest, the input of clastics filled up the grabens that were developing in the Chardzhou step, and further south in the central part of the Amu-Darya basin.

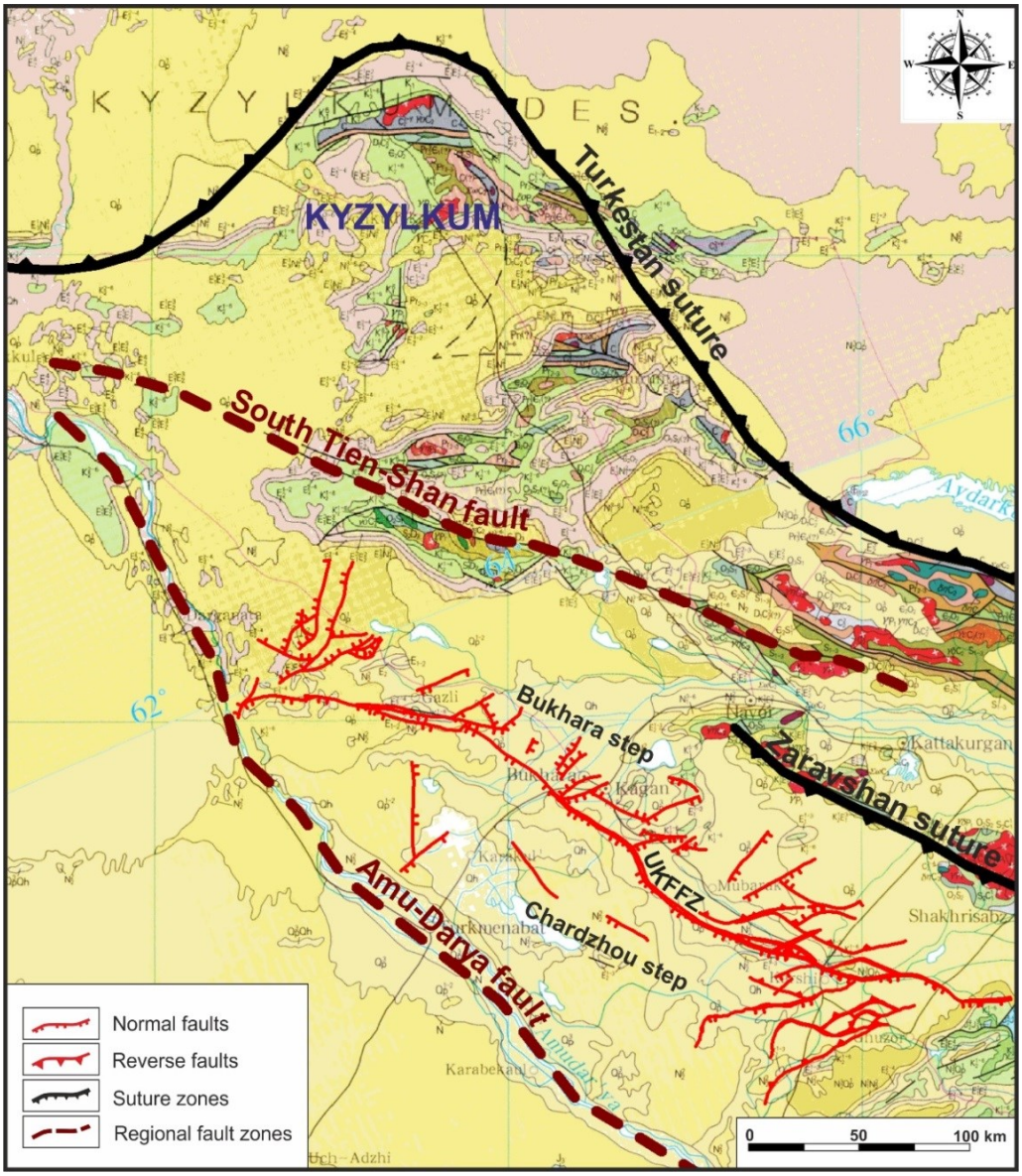

Fig. 6.5. Location of the normal faults active during the Jurassic, in the Bukhara-Khiva region, derived from this study; UKFFZ: Uchbash-Karshi Flexure-Fault zone.
Background: geological map of Uzbekistan (1998).

6.2.2. Early-Middle Jurassic Rifting

We evidence an extensional tectonic event lasting during the Early-Middle Jurassic times (fig. 4.65). The remote stress field that developed in the continental interior reactivated already existing weakness zones of the continental lithosphere. Some of these zones often correspond to the main suture zones, marking collisional areas, which constituted the Central Asian Orogenic Belt (Molnar and Tapponnier, 1975; Windley et al., 2007), i.e. the Tien-Shan Belt in Western Central Asia. Inherited structures related to the Carboniferous-Early Permian tectonic orogenic belts reworked (Hendrix et al., 1992; Allen and Vincent, 1997; Nikishin et al., 1998; Thomas et al., 1999; Allen et al., 2001; Brookfield and Hashmat, 2001; Ulmishek, 2004; De Grave et al., 2007; Jolivet, 2015). These inherited structures reworked as normal faults, or at least with a strong normal component, like the Paleozoic sutures of the Late Paleozoic Tien-Shan orogeny.

Such reactivations of Late Paleozoic structures have been evidenced in the Bukhara-Khiva region from the study of the seismic profiles and borehole data (see Chapter 3). Here, many pre-Jurassic faults were active during the Early-Middle Jurassic extension. According to our data most of these faults are located in the western and eastern parts of the Bukhara-Khiva region (fig. 6.4, 6.5). In the northern Amu-Darya margin, E- to SE-oriented normal faults (fig. 6.2 and 6.5) accommodated the extension with an increase of the subsidence rate from north to south (Thomas et al., 1995; Brunet et al., 2015). The South Tien-Shan Fault and the Zaravshan suture form the northern limit of the extensional domain where major normal faults and depocentres exist (fig. 6.5).

In the Bukhara-Khiva region the most significant example of such a fault reactivation is the Uchbash-Karshi Flexure-Fault Zone. The Jurassic thickness analysis and the reconstructed lines show that this Fault Zone was active during the Early-Middle Jurassic. However, it clearly appears that the activity of the Uchbash-Karshi Flexure-Fault Zone was complex and not homogenous during the Early-Middle Jurassic times. The different segments of the fault zone were active at different periods during the Jurassic and Cretaceous times. The eastern segment was the most active whereas the activity was much smaller and almost disappears in the western segment.

In the eastern part of the Bukhara-Khiva region in the Beshkent trough, the Uchbash-Karshi Flexure-Fault Zone was active during all the Jurassic (fig. 3.4) and Cretaceous times. The activity is evidenced by significant vertical displacements of the principal Mesozoic seismic horizons and by the thickness of the terrigenous deposits. To the west of the Beshkent trough, the activity of the fault zone declined during the upper part of the Middle Jurassic (fig. 3.5, 3.6) and finally disappeared in the Cretaceous. Then, the Uchbash-Karshi Flexure-Fault Zone was partly reactivated during the Late Jurassic and Early Cretaceous times.

The western part of the Bukhara-Khiva region is characterized by a more complicated behaviour of the Uchbash-Karshi Flexure-Fault Zone. The Kimerek graben, a main Early-Middle Jurassic graben of the Chardzhou step, developed in this area. In this graben the terrigenous sequence is abnormally thick. This graben is bordered to the north by the Uchbash-Karshi Flexure-Fault Zone that reworked as normal fault during the Early-Middle Jurassic Jurassic. In the Kimerek graben this fault zone is characterized by a large vertical displacement. Further west, in the westernmost part of the Bukhara-Khiva region, the western extension of the Uchbash-Karshi Flexure-Fault Zone was almost inactive during the Mesozoic (fig. 3.9) and only few normal faults displaying very small throws have been observed.

A similar chronology of the tectonic activity has been independently obtained from the analysis of the subsidence. In Chapter 4 we showed that the main period of subsidence was Early-Middle Jurassic in age (fig. 4.65, 4.68), and can be directly correlated with the activity of the main grabens in the Bukhara-Khiva region. Moreover, this extensional activity characterized by grabens filled with Early to early Middle Jurassic siliciclastic sediments have been also identified in the deeper part of the Amu-Darya basin from seismic data (Maksimov et al., 1986).

6.2.3. The Amu-Darya basin: an Early-Middle Jurassic extensional basin

The Neo-Tethys initiated its northward subduction beneath the newly active southern margin of northern Pangea after the cessation of the Cimmerian collisional process, as early as the Late Triassic (Berra and Angiolini, 2014; Barrier and Vrielynck, 2015). It is supposed that the extensional processes in the Amu-Darya and Tajik basins existed at least since the end of the collision (Hendrix et al., 1992; Hendrix, 2000; Jolivet et al., 2010, 2013; Johnson et al., 2015). It was generated by the oceanward migration of the bend of the slab of the downgoing Neo-Tethys oceanic lithosphere with respect to the overriding Laurasian continental lithosphere. Such rollbacks of the subducting oceanic plate are commonly observed in modern subduction zones.

The rollback process originated N- to NE-oriented extensional stress field behind the subduction zone in the overriding Laurasian plate (fig. 6.4). This extensional stress regime that developed during the Early-Middle Jurassic either reactivated the main Late Paleozoic to Triassic faults, or formed new normal faults.

New extensional basins were formed all along the southern Laurasian margin. Such similar extensional tectonics and basins have been described during this period as far west as Caucasus and northern Iran where the rifting of the Great Caucasus and South Caspian basin respectively developed (Brunet et al., 2003, 2010; Ershov et al., 2003…).

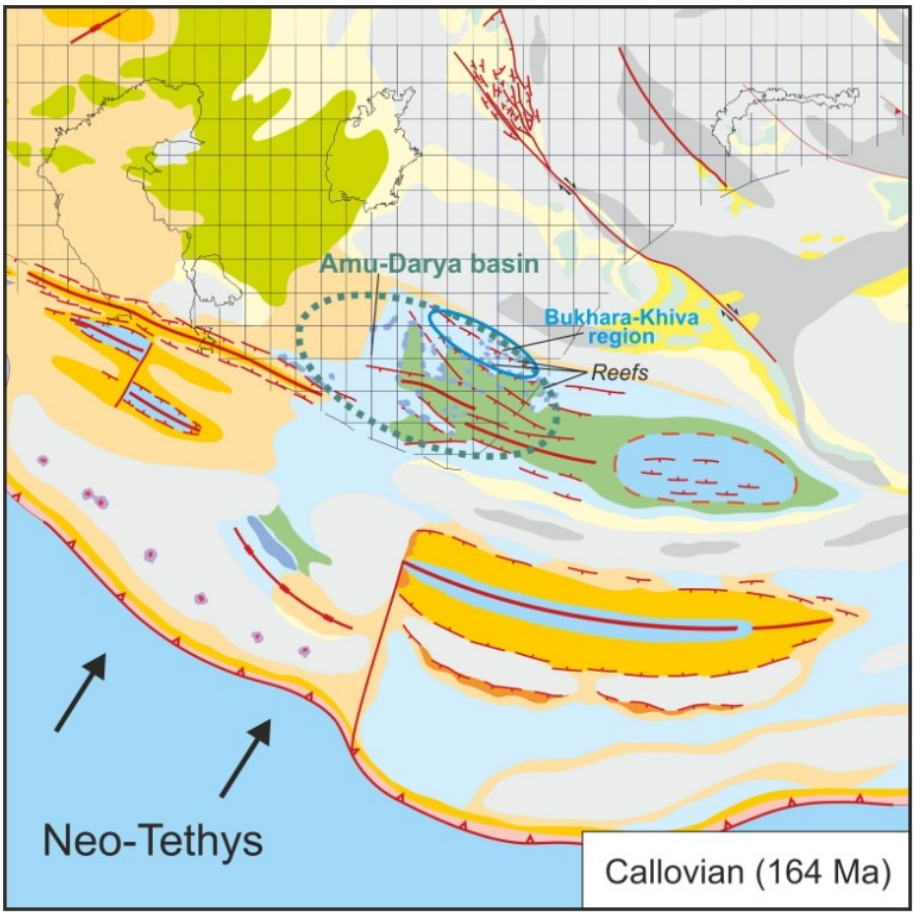

Fig. 6.6. Segment of the Southern Laurasia margin in Southwestern Central Asia during the Middle Jurassic. The Amu-Darya basin and Bukhara-Khiva region are outlined (modified after Barrier and Vrielynck, 2015), for legend see Fig. 6.2.

6.3. Middle-Late Jurassic post-rift evolution

At the end of the Middle Jurassic the northern margin of the Bukhara-Khiva region is marked by major changes concerning the climate, tectonic activity, and regional topography. These changes led to an important evolution of the Amu-Darya basin in term of sedimentation, subsidence and extension of the basin starting during the Middle Jurassic.

The first major change involves the sedimentation. During the lower part of the Middle Jurassic most of the mountain ranges resulting from the Middle-Late Triassic Cimmerian orogeny were almost eroded. The erosion considerably decreased in the landmasses involving a gradual decrease of the clastic input in the Amu-Darya basin during the Middle Jurassic. In the Middle Jurassic sections we observe a gradual replacement of siliciclastics by carbonates from the Bathonian onwards.

The second change concerns the climate that gradually switched from humid to arid during the Middle Jurassic. In practice, the clastic deposits rich in continental organic matters were progressively declining during this period while the carbonates were increasing.

The last main change is from tectonic origin. It is related to a decrease of the subsidence rate in the margin of the Amu-Darya basin (fig. 4.65) and in the basin as well (Brunet et al., 2015). The extensional tectonics that was developing in the Amu-Darya basin and surroundings since the Early Jurassic was decreasing during the Middle Jurassic. The youngest Jurassic syn-depositional normal faults have been evidenced in the lower part of the carbonates, i.e. in the Upper Callovian beds (see Chapter 5). The results of the subsidence analysis indicate a clear drop of the subsidence rate at the end of the Middle Jurassic (fig. 4.65, 4.68).

The major changes listed above associated to the transgression that initiated in the Bajocian-Bathonian limit led at the beginning of the Late Jurassic to the deposition of a carbonate sequence that transgressed northwards onto the Bukhara step.

Another point related to the subsidence and to the transgression is the disappearance of local highs during the lower part of the Middle Jurassic (fig. 2.16, 2.19 and 2.22). After the complete covering of the region by the sea in the Bathonian (fig. 2.22), the carbonate facies dominated in the Amu-Darya basin including the Bukhara-Khiva region (fig. 6.6).

The carbonate sedimentation commenced in the Bathonian (fig. 2.22) and continued till the Kimmeridgian time. From the Late Callovian and mainly during the Late Oxfordian-Kimmeridgian time, the Amu-Darya basin was topographically partitioned into the deep-water sea that occupied the southeastern basin and shallow-water shelfs on its margins (fig. 6.6). In the northern margin the Jurassic carbonate sections were studied in detail in Southwestern Gissar that displays good exposures and in the Bukhara and Chardzhou steps where many wells cross this unit. In the steps of the Bukhara-Khiva region the carbonates are mainly platform deposits showing ramp profiles and thinning towards the north.

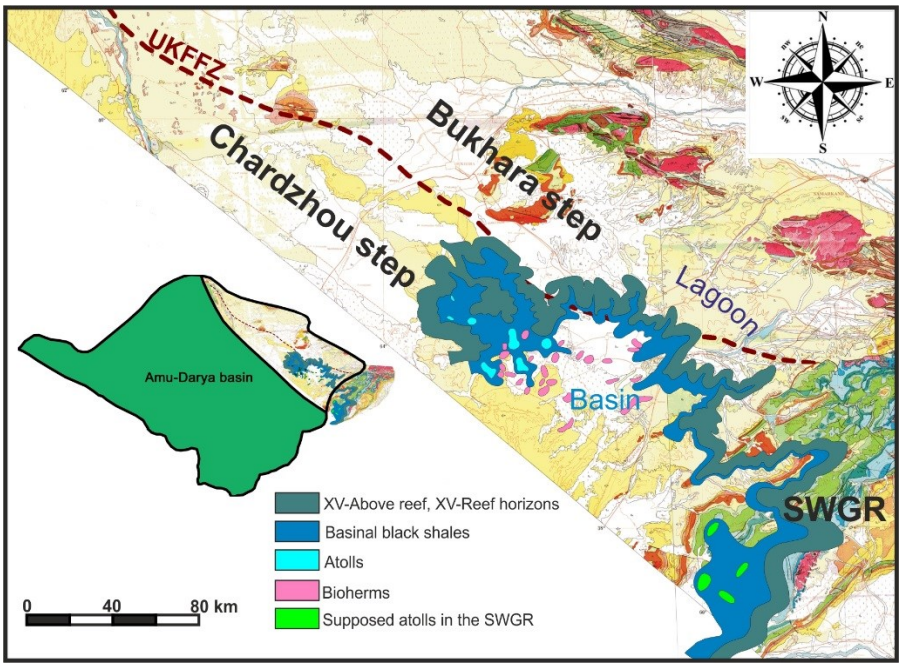

Fig. 6.7. Map of the carbonate types showing to the Oxfordian-Kimmeridgian reef systems (modified after Babadjanov, 2012). Background = geological map of Uzbekistan (1998).

The Middle Callovian-Middle Oxfordian interval is characterized by the deposition of different types of limestone with interbedded clayed layers all over the Bukhara-Khiva and Southwestern Gissar regions. In the southeastern part of the Bukhara-Khiva region appears a well-developed reefal systems (fig. 6.6 and 6.7). This system indicates a disparate development of the northern margin of the Amu-Darya basin during the Middle-Late Jurassic. The first patch reefs appear in the Middle Callovian time surrounded by inter reef bioclastic facies. Then, during the Late Oxfordian a complex of barrier reefs, pinnacle reefs and atolls developed in the Chardzhou step along the shelf edge and in marginal areas of the deeper water basin. The reefs often grew on Early-Middle Jurassic highs corresponding to paleo-horsts. Likely, the main reef alignments developed along the main Early Jurassic normal faults.

A number of solitary reef buildups (pinnacles and atolls) formed inside the deep-water basin. Basinwards, the reef-carbonate section grades into highly organic rich black shales that covers the basin floor and overlaps some of the reefs. These deep-water basinal facies are poorly known because they are deeply buried and have been penetrated in only a few wells, near the rreefal margin, but not in the middle of the deep basin.

During the Middle Callovian-Kimmeridgian period, the subsidence rate was low (fig. 4.65) and thermal subsidence occurred.

The evaporites of the Tithonian overlie the Jurassic carbonates all over the deeper part of the Amu-Darya basin, marking a new step in the sedimentation. These evaporites consist of alternating layers of salt and anhydrite, but most of the section belongs to the salts. The presence of evaporites marks a major change in the climate and regional paleogeography. At this time the subsidence was slow, of thermal type, and the thickness of evaporites deposited corresponds to the filling of the depression created before (Brunet et al., 2015). The arid conditions that will prevail during the beginning of the Early Cretaceous are now fully established. However, the deposition of evaporites does not constitute the end of the subsidence in the Amu-Darya basin that was continuing.

Figure 6.8 is a palinspastic reconstruction in Tithonian time displaying the extension of the evaporite basin, including the Amu-Darya and Tajik basins. The Tithonian paleogeography shows that the evaporite basin was mostly surrounded by emerged lands, including an active orogenic belt in the south. The basin could be only supplied in sea water from the west through a shoal located at the western end of the basin in the current Kopet-Dagh area.

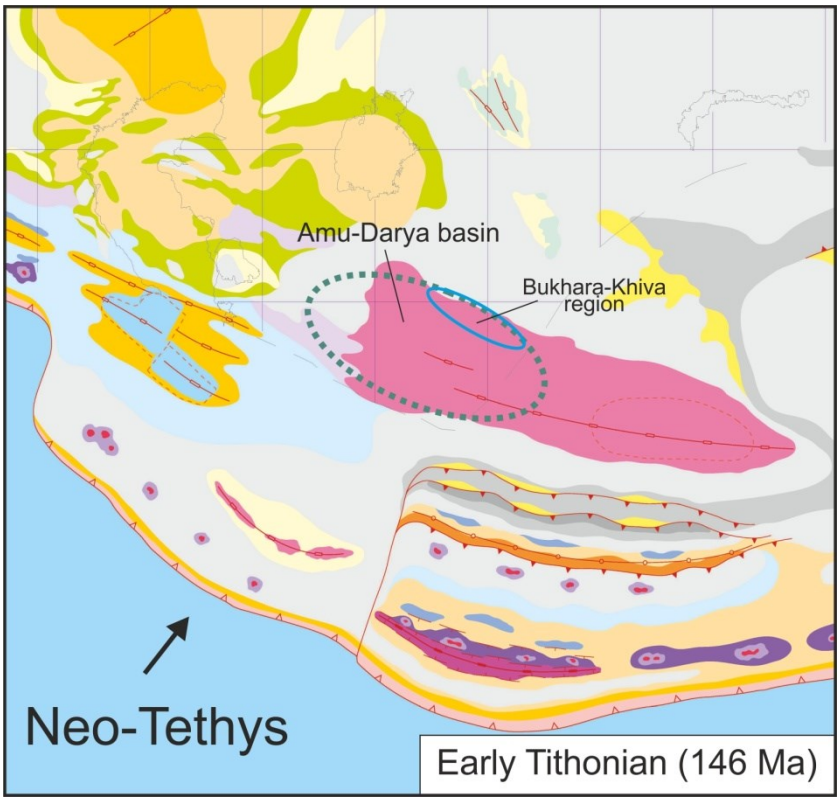

Fig. 6.8. Segment of the Southern Laurasia margin in Southwestern Central Asia during the Late Jurassic. The Amu-Darya basin and Bukhara-Khiva region are outlined (modified after Barrier and Vrielynck, 2015), for legend see Fig. 6.2.

In Kopet-Dagh the Upper Jurassic evaporites of the Amu-Darya basin grade into bedded and massive marine limestones in the Kimmeridgian and Tithonian (fig. 6.8). These shallow-water carbonates separated the open Tethys Sea to the south from the Amu-Darya evaporite lagoon to the north.

6.4. Cretaceous – Paleogene evolution

The tectonic regime in the Bukhara Khiva region and Amu-Darya basin is relatively stable during the Cretaceous and Paleocene times. Some accelerations of the subsidence related to minor tectonic events have been recorded in the Cretaceous sedimentary sequence (see Chapter 4, fig. 4.68) in Berriasian to Barremian, Albian and Turonian times.

6.4.1. Early Cretaceous tectonostratigraphy

In the Bukhara-Khiva region, as well as in the whole Amu-Darya basin, the evaporites are conformably overlain by Early Cretaceous continental red clastics. Coarse alluvial clastics transported from uplifts to the southwest compose the Berriasian to Hauterivian section in the northern Amu-Darya margin. On the basin margins these Lower Cretaceous continental red beds unconformably overlie the Paleozoic to Late Jurassic rocks. They are widespread in the whole Western Central Asia and extend as far northeast as the Talas-Fergana Fault, to the south they cover northern Afghanistan and to the west the Kopet-Dagh. From a regional point of view the continental red beds basin occupy an area wider than the Late Jurassic evaporite basin because it covered large areas of the southern part of the Western Central Asia platform.

The origin of these continental deposits is still debated. First of all, it is obvious that the Amu-Darya basin is no more supplied by sea water during the beginning of the Early Cretaceous. Uplifts developed south of the basin in Afghanistan and Central Iran during the uppermost Jurassic. This coastal range probably isolated the Amu-Darya and Tajik basins from the Neo-Tethys Ocean. In

addition, the beginning of the Early Cretaceous corresponds to a global low-stand of the sea level (fig. 4.7) thus making easier the regression on the continental shelf.

Secondly, we have to explain the clastic input that filled up the Early Cretaceous depression. In the Bukhara-Khiva region the clastics are sourced by highlands located in the northeast in the present western Tien-Shan region. During this period the Amu-Darya basin is also sourced by emerged lands located to the south probably resulting from the collision of blocks (Helmand and Lhasa blocks) with the southern Laurasia margin. It is not clear if the collision lasted until the beginning of the Early Cretaceous, but the increase of subsidence rate evidenced during the undivided period Berriasian-Barremian (see Chapter 4, fig. 4.68) in the northern Amu-Darya margin may suggest a tectonic reactivation of the basin.

To sum up, the deposition of the Early Cretaceous continental red clastics results from the interaction between a subsidence rate in the basin, the fall in eustatic global sea level, and the rate of sediment supply.

A marine transgression covered the entire Amu-Darya basin in the Late Barremian time. This transgression is a regional event that covered northern Afghanistan and the entire Central Iran in the south, and extended as far north as the Aral and north Caspian regions (fig. 6.9). In the platforms shallow water carbonates deposited whereas the sedimentation generally consists in shaly deposits in the basins. Then, the Aptian-Albian time is represented by a succession of well-dated marine shales, siltstones, sandstones, marly-limestones, and clays in the Amu-Darya basin (fig. 6.9). The Aptian is characterized by a moderate subsidence rate probably reflecting the thermal evolution of the Amu-Darya basin and margins then a possible reactivation during the Albian (fig. 4.68).

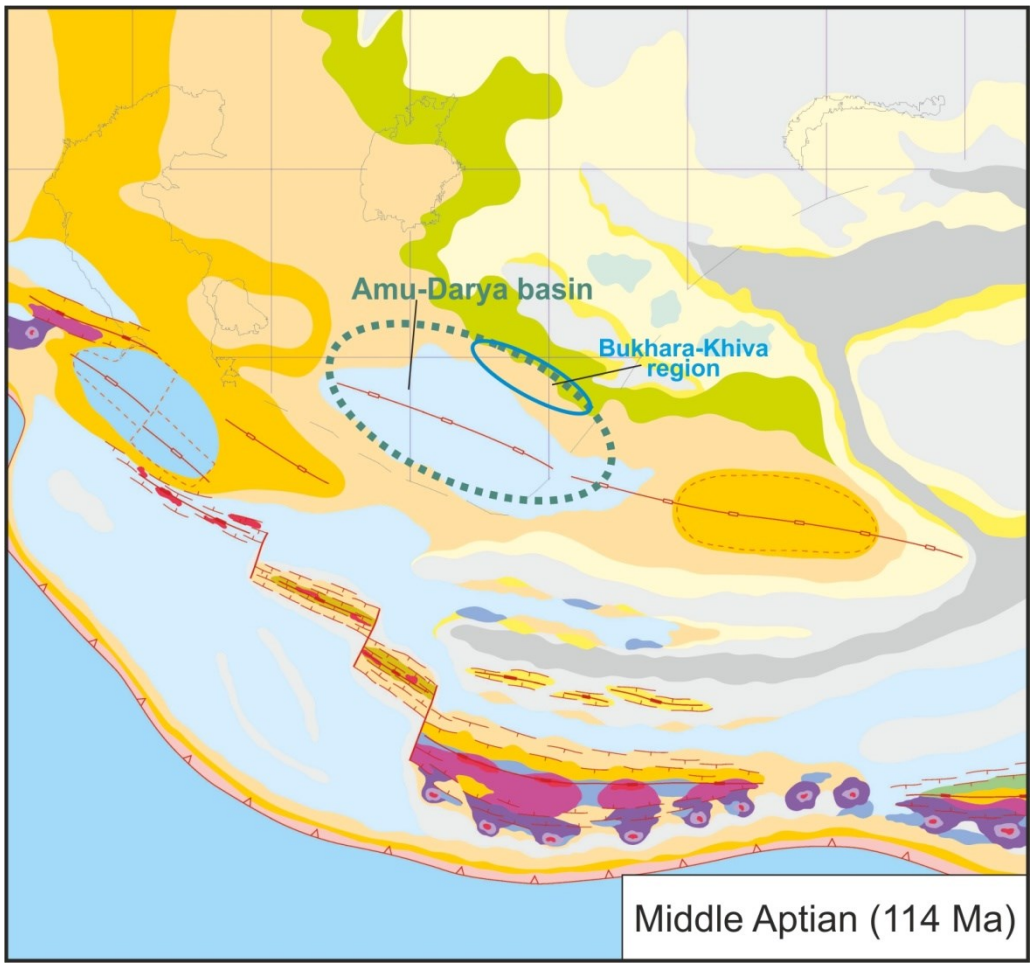

Fig. 6.9. Segment of the Southern Laurasia margin in Southwestern Central Asia during the Early Cretaceous (modified after Barrier and Vrielynck, 2015), for legend see Fig. 6.2.

6.4.2. Late Cretaceous-Paleogene subsidences

The Upper Cretaceous rocks are dominantly of marine origin. A thick accumulation of limestones and marls composes most of the Late Cretaceous section in the Amu-Darya basin. This thick Late Cretaceous sequence was deposited in a low-energy environment. Only the Cenomanian displays a significant clastic interval.

This about 75 Ma long period is characterized by low but continuous subsidence rate related to the thermal evolution of the Amu-Darya-Tajik basins, only interrupted by a surprising increase of the subsidence rate during the Turonian time.

The deposits of the Late Cretaceous in the Amu-Darya basin are generally characterized by accumulations of relatively deep-water clayed-marly formations. In the central Amu-Darya basin mainly deposited shales and siltstones while coarser sediments deposited on the margins. In Southern Gissar, belonging to the northern Amu-Darya margin, the Late Cretaceous is represented by siltstones, marly-limestones, limestones, and clays with interbedded layers of shelly limestone.

During the intercalated Cenomanian clastic interval deposited massive sandstones, siltstones and limestone with interbedded layers of gravels, and gypsum. This special clastic level marks a brief recovery of the erosion, possibly resulting from a regional tectonic uplift. The acceleration of the subsidence evidenced during the Turonian (see Chapter 4, fig. 4.68) could be linked to this event. Despite a possible problem of dating within the Cenomanian-Turonian interval, it appears that a discreet tectonic and unexplained event has affected the Amu-Darya region in the lower Late Cretaceous.

In the northern Amu-Darya basin the Paleogene rocks are Paleocene (fig. 6.10) to Middle Oligocene in age. Lower Paleocene clastics and carbonates are preserved only in the western and southern parts of the Amu-Darya basin. In Southern Gissar the Lower Paleocene lies on an erosional surface on chalky rocks. The Middle and Upper Paleocene Bukhara Formation is composed of shallow-water carbonates containing layers of clastics and anhydrites deposited in a lagoon under arid condition. The Bukhara Formation covers a vast region of the southern part of Western Central Asia.

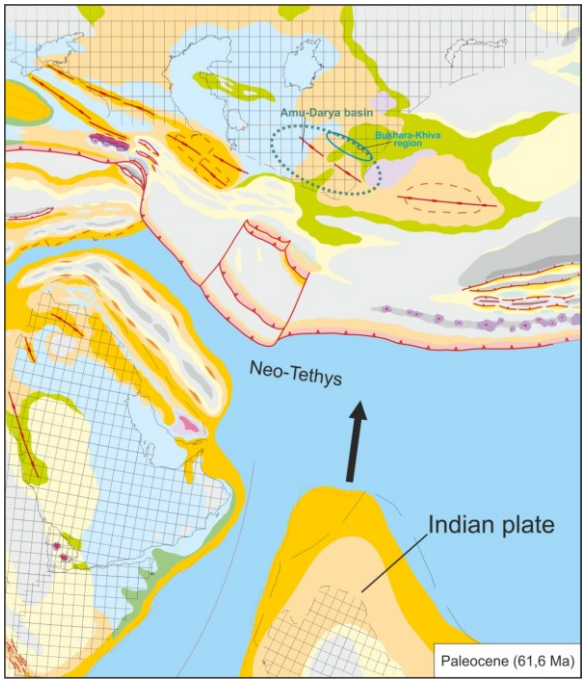

Fig. 6.10. Palinspastic reconstruction of the Tethysian domain and surrroundings at the Cretaceous-Paleogene boundary. Black arrow: India/Eurasia relative motion (modified after Barrier and Vrielynck, 2015), for legend see Fig. 6.2.

The overlying Eocene-Middle Oligocene sequence is mainly composed of shallow marine deposits including shales and siltstones. However, carbonates, marls, and sandstone layers are present throughout the sequence.

Interestingly, the India-Eurasia collision which initiated during the Early Eocene at about 55 Ma did not involve any significant compressive deformation in the Amu-Darya domain. The Amu-Darya – Tajik basins domain and surroundings remained a flat lowland until the Late Oligocene. In addition, during this period this vast area of southern Western Central Asia did not receive any strong clastic drift, showing that the main period of inversion started later at the end of Paleogene and the remote effects of the India-Eurasia collision were weak.

6.5. Neogene Pamir orogeny

The Alpine orogenic movements reached the area of the Amu-Darya basin in the Late Oligocene time, rather late with respect to the age (55 Ma) of the beginning of the India-Eurasia collision. The syn-orogenic upper Oligocene-Quaternary sequence reaches about 1 to 1.5 km in the centre of the Amu-Darya basin. It is as much as 5 to 7 km thick in the Tajik basin. During the collisions many Paleozoic and Mesozoic structures of Central Asia were reactivated (fig. 6.11). This has led to the inversion of the Paleozoic-Mesozoic structures of the Amu-Darya basin (Thomas et al., 1999). Tectonism progressively increased through the Pliocene and into Present.

In the Tien-Shan Range the main Cenozoic orogeny is Pliocene in age and formed most of the modern topography (Cobbold et al., 1996). The age estimation of the beginning of the deformation can be indirectly estimated by thermochronologic datings constraining the age of the uplift in the western Tien-Shan Range (Alay, Gissar, and Southwestern Gissar ranges). Two main phases of uplift were determined at 18-20 Ma and 13-8 Ma (Gagala, 2014).

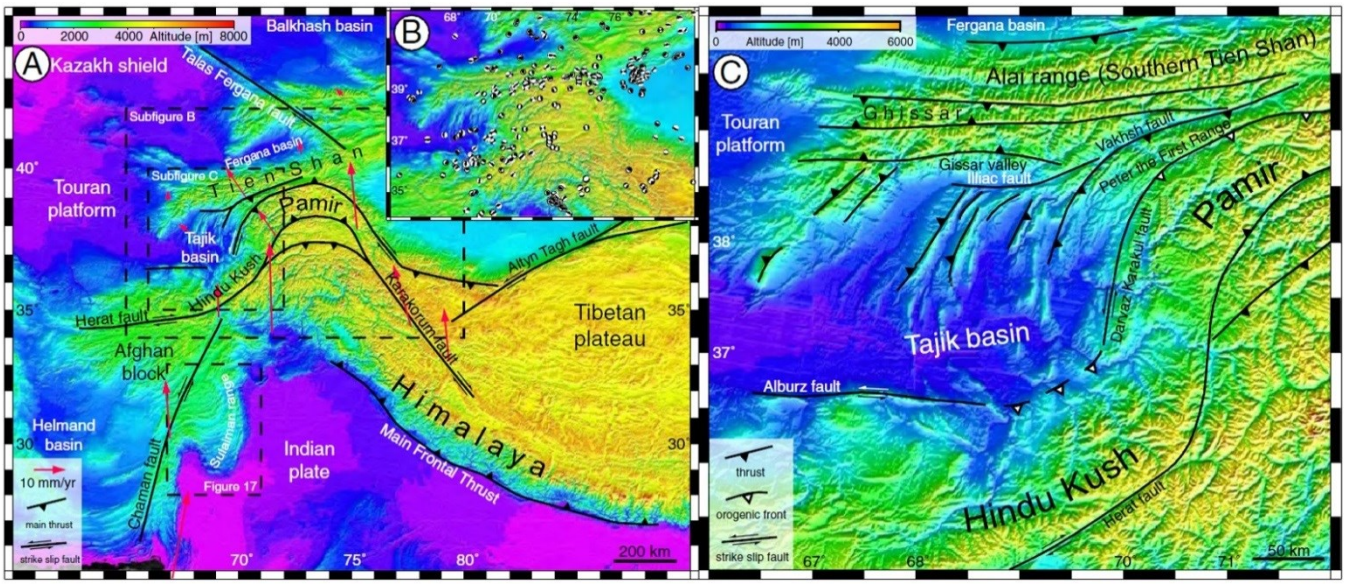

Fig. 6.11. A- Morphotectonic map of Central Asia with first-order faults. Red arrows: GPS-velocity vectors with respect to Eurasia (from Mohadjer et al., 2010); dashed lines: location of B and C insets; Structures compiled from Koulakov and Sobolev (2006) and Robinson et al. (2004). B- Map of seismicity in the Tajik basin area showing the high seismic activity north of Pamir and in Hindu–Kush. Focal mechanisms from Harvard catalogue. C- Topographic map of the Tajik basin with the main faults compiled from Coutand et al. (2002) and Thomas et al. (1994a). Topography from GINA (modified after Reiter et al., 2011).

The beginning of Alpine deformation in the Amu-Darya basin is marked by a widespread pre-Late Oligocene unconformity. The Upper Oligocene-Lower Miocene deposits are marine to lagoonal, mostly fine grained clastic rocks with gypsum beds indicating low reliefs and orogenic uplifts. On the

contrary, the Middle Miocene layers and the lower part of the Late Miocene sequence consist of coarser continental facies derived from the rising lands to the northeast and southeast.

The Upper Miocene to Pleistocene sequence of the whole basin is composed of a thick red bed sequence comprising silty-clay, and siltstone with interbedded layers of sandstones representing lacustrine and alluvial syn-orogenic clastic deposits. The basal Upper Pliocene molassic deposits consist in siltstone-clayed rocks with interlayers of sandstones. They are alluvial plain deposits unconformably overlaying eroded horizons of the Miocene, Paleogene and Upper Cretaceous sequences.

The Neogene evolution of the Amu-Darya-Tajik basins is linked to the indentation of Eurasia by the continental Pamir block (fig. 6.11 and 6.12). The northward movement of the Pamir block during the Miocene to Quaternary time (fig. 6.12) resulted in thrusting and folding of Mesozoic-Paleogene rocks of the Afghan-Tajik basin and Southwestern Gissar and the uplift of Western Tien-Shan. Although thrusting did not extend into the Bukhara and Chardzhou steps, the compression led to reactivation of inherited structures in the steps and in the Amu-Darya basin as well. Some local structural uplifts, mostly located along the margins of the basin, were produced during this stage (see Chapter 3).

Southwestern Gissar area is a thick-skinned fold and thrust belt. The Mesozoic-Cenozoic sediments of the Afghan-Tajik depression are underthrusted beneath the southeast-vergent frontal thrust of Southwestern Gissar. Tevelev and Georgievskii (2012) showed that the main tectonic activity in Southwestern Gissar is Late Pliocene-Quaternary in age.

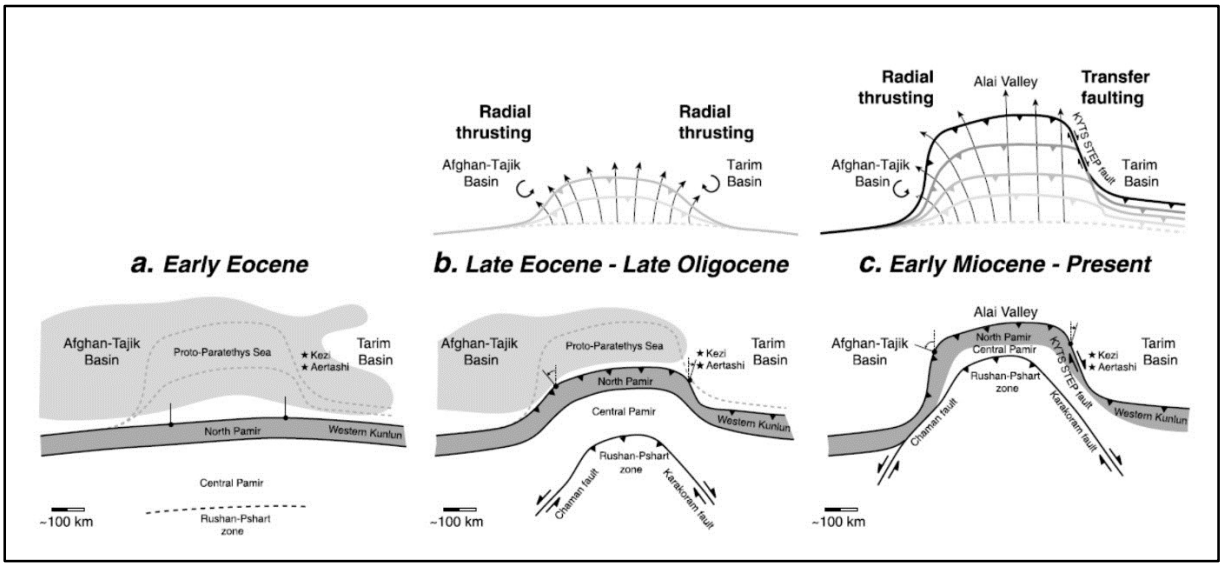

Fig. 6.12. Evolution of the Pamir indentation (modified after Cowgill, 2010 by Bosboom et al., 2014). The paleogeographic evolution is shown in the lower graphs. Approximate paleogeographic extent of the sea shaded in light grey, (b) before its final retreat in the Late Eocene. The upper graphs show the corresponding kinematic models.

The eastern boundary of the Turan-South Kazakh block deformation is controlled by the Pamir salient (Lukk et al., 1995; Searle, 1996; Thomas et al., 1996). The development of the Pamir orogeny during the Late Cenozoic is a direct result of the India-Eurasia collision. It is responsible for the modern and ongoing Southwestern Gissar orogeny. The first phase of tectonic evolution of Pamir was symmetric, with radial thrusting causing rotation on both sides until the Late Oligocene (fig. 6.12). In the Late Oligocene to Early Miocene, deformation became asymmetric with ceased clockwise rotation in the Tarim basin and continued anticlockwise rotation on the western side in the Afghan-Tajik basin, which affected the Southwestern Gissar (Bosboom et al., 2014) (fig. 6.12).

The indentation of the Eurasia by the Pamir salient (fig. 6.12) is the result of both the Eurasia-India collision and the southward subduction of a marginal basin embedded completely within the southern

Eurasian plate (Burtman and Molnar, 1993). The age and nature of the crust of this marginal basin subducting beneath the Pamir block is unknown. Several authors postulate that (1) the basin rifted during the Late Permian and opened in Early Mesozoic times, and (2) was floored by an oceanic crust (e.g. Cowgill, 2010; Bosboom et al., 2014; Barrier and Vrielynck, 2015). Whatever is the age and floor of the basin, this latter is subducting beneath the Pamir continental block, probably since the Late Oligocene. Unlike in Tibet, in Pamir most of the India-Eurasia convergence is consumed in the Eurasian plate itself in the intra-continental Pamir subduction zone rather than at the India-Eurasia boundary.

6.6. Conclusion

The works we developed in this thesis was part of a larger project dealing with Western Central Asia. The objective was a better understanding of the tectonic, stratigraphic and geodynamic evolution of this vast domain. Investigations based on analyses of sub-surface and geophysical data, and fieldworks were conducted in the basins and orogenic belts in cooperation with the Uzbek institutions.

The study of the northern margin of Amu-Darya basin integrated tectono-stratigraphic approaches. Complementary data concerning the Amu-Darya and Tajik basins and Western Tien-Shan were also considered. The main target was the Mesozoic, and more particularly the Jurassic. This period is of great interest because the Jurassic sequence constitutes in the Amu-Darya and Tajik basins a total petroleum system.

The study of the steps of the northern margin of the Amu-Darya basin was conducted together with joint projects addressing the sedimentology of the terrigenous, and carbonates and evaporites Jurassic units that developed in Southwestern Gissar where the complete Jurassic section is well exposed. The combination of collected surface and sub-surface data allowed reconstructing the tectonic and sedimentologic evolution of the northern margin of the Amu-Darya basin. This model was integrated on a larger scale in the Mesozoic geodynamic context.

It appears that the key point of the Mesozoic-Cenozoic tectonic evolution of the southern part of Western Central Asia is the relationship between the continental plates (northern Pangea, then Laurasia, and finally Eurasia) with the Tethys oceanic domains (Paleo-Tethys then Neo-Tethys). A series of tectonic events succeeded since the Late Permian at the active boundaries between the continental plates constituting Central Asia and the Tethyan oceanic domains. From the northward subduction of the Paleo-Tethys Ocean resulted the opening of Late Permian-Triassic back-arc basins; from the collision of the Cimmerian continental blocks with the northern Pangea margin in Triassic time high mountain ranges were erected that will source the basins during the Jurassic; from the subduction of the Neo-Tethys oceanic plate(s) a more diffuse rifting developed in the southern Laurasia margin; and finally from the Cenozoic India-Eurasia collision derived the Tien-Shan and Pamir orogenies both sourcing the Amu-Darya and Tajik basins in continental clastics, and deforming these basins.

References

References

Abdrakhmatov K.Y., Aldazhamov S.A., Hager B.H., Hamburger M.W., Herring T.A., Kalabaev K.B., Makarov V.I., Molnar P., Panasyuk S.V., Prilepin M.T., Reilinger R.E., Sadybakasov I.S., Souter B.J., Trapeznikov Y.A., Tsurkov V.Y. and Zubovich A.V., 1996. Relatively recent construction of the Tien-Shan inferred from GPS measurements of present-day crustal deformation rates. Nature, 384, 450–453.

Abdullaev G.S., 2004. Biostratigraphy, lithofacies and oil and gas perspectives of the Amu-Darya northern margin Jurassic carbonates. Abstract of the thesis, Geology and Geophysics Institute, archives, Tashkent, 39 p. (in Russian).

Abdullaev G.S. and Mirkamalov H.H., 2001. Stratigraphy of the Jurassic high-gamma activity rocks of the Bukhara-Khiva region and its importance for the modelisation of the carbonate formation. Geology and oil and gas perspectives of Uzbekistan, Tashkent, 13–24 (in Russian).

Abdullaev G.S. and Mirkamalov H.H., 2006. Volume and age of the Jurassic Gaurdak formation of the Southwestern Gissar and the Bukhara-Khiva region. Uzbekistan oil and gas journal, 2, 17–21 (in Russian).

Abdullaev R.N., Dalimov T.N., Muhin P.A. and Bazarbayev E.R., 1989. Rifting during the development of the Paleozoic folded areas. Science, Tashkent, 122 p. (in Russian).

Abdullaev G.S., Mirkamalov H.H. and Evseeva G.B., 2010. Oil and gas bearing reefal facies of the Jurassic carbonate unit of the Amu-Darya basin (Southern and Southwestern Uzbekistan) and their correlation with reef creation within the paleobasins of the Tethys. Materials of the "Theoretical and practical aspects of the oil and gas geology of Central Asian and the solutions for the modern problem of the domain", NGGI, Tashkent, 39–49 (in Russian).

Abidov A.A and Babadjanov T.L., 1999. Map of the tectonic regionalization of the oil and gas provinces of Uzbekistan, 1:1 000 000. Uzbekgeofizika, Tashkent.

Ahmedjanov M.A., Borisov O.M. and Fuzailov I.A., 1967. Structure of the paleozoic basement of Uzbekistan, vol. 1. Science, Tashkent (in Russian).

Al Abdalla A., 2008. Evolution tectonique de la Plate-forme Arabe en Syrie depuis le Mésozoïque. PhD thesis, Université Paris 6 (UPMC), 300 p.

Alexeiev D.V., Cook H. E., Buvtyshkin V.M. and Golub L.Y., 2009. Structural evolution of the Ural–Tian Shan junction: A view from Karatau ridge, South Kazakhstan. C. R. Geoscience, 341, 287–297.

Aliev S.A. and Cherkashina L.G., 1981. Report about regional seismic survey in the Bukhara-Khiva region, provided in 1978-1981. Uzbekgeofizika, Tashkent (in Russian).

Aliyev M.M., Krilov N.A., Genkina R.Z., Gofman E.A., Dubrovskaya E.N., Tsaturova A.A., Ammanoyazov K.N., Alimov K.N., Mirkamalov H.H., Maltseva A.K., Prozorovskaya E.L., Rostovtsev K.O. and Sqxarov A.S. 1983. Jurassic of the south USSR. Nauka, Moscow, 208 p.

Allen M.B. and Vincent S.J., 1997. Fault reactivation in the Junggar region, northwest China: the role of basement structures during Mesozoic-Cenozoic compression. Journal of the Geological Society, London, 154, 151–155.

Allen M.B., Alsop G.I., and Zhemchuzhnikov V.G., 2001. Dome and basin refolding associated with transpressive inversion along the Karatau Fault System, southern Kazakstan. Journal of the Geological Society, London, 158, 83–95.

Anderson E.M., 1942. The dynamic of faulting, 1st ed.. Olivier and Boyd, 206 p.

Angelier J., 1975. Sur l'analyse de mesures recueillies dans des sites faillés: l'utilité d'une confrontation entre les méthodes dynamiques et cinématiques. Comptes Rendus de l'Académie des Sciences, Paris, 281, 1805–1808.

Angelier J., 1984. Tectonic analyses of fault slip data sets. Journal of Geophysical Research, 89, 5835–8548.

Angelier J., 1990. Inversion of field data in fault tectonic to obtain the regional stress, III, A new rapid direct inversion method by analytical means. Geophysical Journal International, 103, 363–376.

Angelier J., 1991. Inversion directe et recherché 4-D: comparaison physique et mathématique de deux modes de détermination des tenseurs des pléocontraintes en tectonique de failles. C. R. Acad. Sci. Paris, t. 312, II, 1213-1218.

Angelier J., 2002. Inversion of earthquake focal mechanisms to obtain the seismotectonic stress: a new method free of choice among nodal planes. Geophysical Journal International, 150, 588-609.

Angelier J. Tarantola A., Valette B. and Manoussis S., 1982. Inversion of field data in fault tectonics to obtain the regional stress, I, Single phase fault populations: a new method of computing the stress tensor. Geophysical Journal of the Royal Astronomical Society, 69, 607–621.

Angevine C.L., Heller P.L. and Paola, C. 1990. Quantative sedimentary basin modelling. American Association of Petroleum Geologists Shortcourse Note Series #32, 247 p. (available at http://geofaculty.uwyo.edu/heller/shortcourse(90).htm).

Atlas of Geological Maps of Central Asia and Adjacent Areas (Li T.D., ed. in chief), 2008. 8 sheets, 1:2 500 000, Geological Publishing House, Beijing, China.

Babadjanov T.L., 2005. The studying of the pre-Jurassic complexes of the southeastern part of the paleorift system in the Bukhara-Khiva region. Uzbekgeofizika, report, Tashkent (in Russian).

Babadjanov T.L., 2008. The summarizing and re-interpretation of the data of the regional, searching and thematic geological-geophysical studies of pre-Jurassic complexes of the Bukhara-Khiva region, made in 1990-2004 years on the base of the modern geological ideas. Uzbekgeofizika JSC, report, Tashkent, 364 p. (in Russian).

Babadjanov T.L., 2012. The studying of the structure features of the North-East oriented flexure-break zones and their influence on the character of the sedimentation of the cover, diffusion of the main structural-material complexes of the intermediate structural stage and spacing of the oil and gas deposits. Uzbekgeofizika, report, Tashkent, 238 p. (in Russian).

Babadjanov T.L. and Abdullaev G.S. (eds), 2009. The structure features and oil and gas perspectives of the pre-Jurassic complexes of the Bukhara-Khiva region (Western Uzbekistan). Oil and Gas Institute, Tashkent, 120 p. (in Russian).

Babadjanov T.L. and Rubo V.V. 1991. Map of the tectonic regionalization of the central part of the Central Asia. Uzbekgeofizika, Tashkent.

Bai Y., Chen G., Sun Q., Sun Y., Li Y., Dong Y. and Sun D., 1987. Late Paleozoic polar wander path for the Tarim platform and its tectonic significance. Tectonophysics 139, 145–153.

Barrier E. and Brunet M.-F., 2011. GRI Total Tethys Nord: Central Asia. Unpublished report, UPMC, Paris, 116 p.

Barrier E. and Vrielynck B., 2015. Paleotectonic maps of Western Tethys surroundings: Middle East and Western Central Asia. Atlas of tectono-sedimentary maps from the Middle Permian to the Pliocene. Scale 1:17 000 000, 20 sheets, in preparation.

Berra F. and Angiolini L., 2014. The Evolution of the Tethys Region throughout the Phanerozoic: A Brief Tectonic Reconstruction, in L. Marlow, C. Kendall and L. Yose, eds., Petroleum systems of the Tethyan region: AAPG Memoir 106, 1–27.

Besse J., Courtillot V., Pozzi J.P., Westphal M. and Zhou Y.X., 1984. Paleomagnetic estimates of crustal shortening in the Himalayan thrusts and Zangbo suture. Nature, 311, 621–626.

Biske Yu.S. and Seltman R., 2010. Paleozoic Tian-Shan as a transitional region between the Rheic and Urals-Turkestan oceans. Gondwana Research, 17, 602–613.

Biske Y.S., Komissarov R.A. and Talashmanov Y.A., 1993. On Paleozoic horizontal movements on the northern margin of the Tarimsky continent from paleomagnetic data. Vestnik of Saint-Petersburg University, 7, 71–77.

Blackbourn G., 2008. Petroleum geology of the Amu Dar'ya Basin and adjacent regions of Turkmenistan and Uzbekistan. Blackbourn Geoconsulting (available at http://www.blackbourn.co.uk/reports/amu-darya.html and http://www.blackbourn.co.uk/databases/fsu-oilfield-database.html).

Bosboom R., Dupont-Nivet G., Huang W., Yang W.and Guo Z., 2014. Oligocene clockwise rotations along the eastern Pamir: Tectonic and paleogeographic implications. Tectonics, 33/2, 53–66.

Bott M. H. P., 1959. The mechanisms of oblique slip faulting. Geological Magagazine, 96, 109–117.

Brookfield M.E., 2000. Geological development and Phanerozoic crustal accretion in the western segment of the southern Tien Shan (Kyrgyzstan, Uzbekistan and Tajikistan), Tectonophysics, 328, 1–14.

Brookfield M.E. and Hashmat A., 2001. The geology and petroleum potential of the North Afghan platform and adjacent areas (northern Afghanistan, with parts of southern Turkmenistan, Uzbekistan and Tajikistan). Earth-Science Reviews, 55, 41–71.

Brunet M.-F., 1981. Etude quantitative de la subsidence du Bassin de Paris. Thèse 3e cycle Univ. Paris VI, Mém. Sci. Terre Univ. P. & M. Curie n° 81-21, 161 p.

Brunet M.-F., 1989. Méthode d'étude quantitative de la subsidence. In: Ass. Sédim. Français (ed.), Dynamique et méthodes d'étude des bassins sédimentaires. Technip, 87–98.

Brunet M.-F., Ershov A.V., Korotaev M. V., Kangarli T., Mamedov P.Z., Pravikova N.V., Mordvintsev D.O., Sidorova I. P., Koptev A.I. and Barrier E., 2013. Evolution of basins from Kura to Amu Darya. Abstract, Darius Programme, Central Asia Workshop 26-27 February 2013, Bonn – Germany, 14-15.

Brunet M.-F., Ershov A.V., Korotaev M.V., Mordvintsev D.O., Barrier E. and Sidorova I.P. 2014. Subsidence history of the Amu Darya basin and its geodynamic context. Darius Programme, final symposium: Evolution of the Black Sea to Central Asian Tethyan Realm since the Late Paleozoic, UPMC, Paris, France, Abstract volume, 42-43.

Brunet M.-F., Ershov A.V., Korotaev M.V., Barrier E., Mordvintsev D.O. and Sidorova I.P., 2015. Late Palaeozoic and Mesozoic evolution of the Amu Darya Basin (Turkmenistan, Uzbekistan). In: M.-F. Brunet, T. McCann and E. R. Sobel (eds), Geological Evolution of Central Asian Basins and the Western Tien Shan Range. Geological Society, London, Special Publications, 427, in preparation.

Brunet M.-F., Korotaev M.V., Ershov A.V. and Nikishin A.M., 2003. The South Caspian basin: a review of its evolution from subsidence modelling. In: Brunet M.-F. and Cloetingh S. (eds), Integrated PeriTethyan Basins Studies (Peri-Tethys Programme). Sedimentary Geology, 156 /1-4), 119-148.

Brunet M.-F., Shahidi A., Barrier E., Muller C. and Saidi A., 2010. South Caspian Basin opening: inferences from subsidence analysis in Northern Iran. In: B.A. Vining and S.C. Pickering (eds), Petroleum Geology: From Mature Basins to New Frontiers—Proceedings of the 7th Petroleum Geology Conference. The Geological Society of London, 2 vol. 1243 p., 1 CD interactive, Poster 1.

Bukharin A.K., 1999. Structural and formational regionalization of the Tien-Shan. Geology and mineral resources, 2, 3–12 (in Russian).

Burtman V.S., 1976. Structural Evolution of Paleozoic Fold Systems (Variscides of Tian-Shan and Caledonides of Northern Europe). Nauka, Moscow, 164 p.

Burtman V.S. 1978. Stationary network of continental faults and mobilism. Geotectonics, 12/3, 177-184.

Burtman V.S., 1980. Faults of Middle Asia. American Journal of Science, 280, 725–744.

Burtman V.S., Gurary G.S., Belenky A.V., Ignatiev A.V. and Audibert M., 1998. Turkestan Ocean in the Middle Paleozoic: A reconstruction using paleomagnetic data from the Tien Shan. Geotectonics, 1, 11–2.

Burtman V.S., 2000. Cenozoic crustal shortening between the Pamir and Tien Shan and a reconstruction of the Pamir–Tien Shan transition zone for the Cretaceous and Palaeogene. Tectonophysics, 319, 69–92.

Burtman V.S., 2006. Tien Shan and high Asia. Tectonics and Geodynamics in the Paleozoic. GEOS, Moscow, 214.

Buslov M.M., Saphonova I.Y., Watanabe T., Obut O.T., Fujiwara Y., Iwata K., Semakov N.N., Sugai Y., Smirnova L.V. and Kazansky A.Y., 2001. Evolution of the Paleo-Asian Ocean (Altai-Sayan Region, Central Asia) and collision of possible Gondwana derived terranes with the southern marginal part of the Siberian continent. Geoscience Journal, 5, 203–224.

Carey E., 1976. Analyse numérique d'un modèle mécanique élémentaire appliqué à l'étude d'une population de failles: calcul d'un tenseur moyen des contraintes à partir des stries de glissement. PhD thesis, Université Paris 6 (UPMC), 138 p.

Chen C.M., Lu H. F., Jia D., Cai D. S. and Wu S.M., 1999. Closing history of the southern Tianshan oceanic basin, western China: an oblique collisional orogeny. Tectonophysics, 302, 23–40.

Clarke J.W., 1988. Petroleum geology of the Amu-Dar'ya gas-oil province of Soviet Central Asia. Washington DC, United States Geological survey Open-File Report, 88–272, 59 p. (available at http://pubs.er.usgs.gov/publication/ofr88272).

Cobbold P.R., Sadybakasov E. and Thomas J.C., 1996. Cenozoic transgression and basin development, Kirghiz Tien-Shan, Central Asia. In: Roure F., Ellouz N., Shein V.S. and Skvotsov S. (eds), Geodynamic evolution of Sedimentary Basins, Technip., Paris, 181–202.

Coutand I., Strecker M.R., Arrowsmith J.R., Hilley G., Thiede R.C. and Korjenkov A., 2002. Late Cenozoic tectonic development of the intramontane Alai valley, (Pamir-Tien Shan region, central Asia: An example of intracontinental deformation due to the Indo-Eurasia collision. Tectonics, 21 (6), 3-1-3-19.

Cowgill E., 2010. Cenozoic right-slip faulting along the eastern margin of the Pamir salent,northwestern China. GSA Bull., 122, 1/2, 145-161.

Dalimov T.N., Ganiev I.N., Shpotova L.V. and Kadirov M.H., 1993. Geodynamics of the Tien-Shan. National University of Uzbekistan, Tashkent, 207 p. (in Russian).

De Grave J., Buslov M.M. and Van den Haute P., 2007. Distant effects of India-Eurasia convergence and Mesozoic intracontinental deformation in Central Asia: Constraints from apatite fission-track thermochronology. Journal of Asian Earth Sciences, 29, 188–204.

De Grave J., Van den Haute P., Buslov M.M., Dehandschutter B. and Glorie S., 2008. Apatite fission-track thermochronology applied to the Chulyshman Plateau, Siberian Altai Region. Radiation Measurements, 43 (1), 38–42.

Dikenshteyn G.H., Maksimov S.P., and Semenovich V.V. (eds), 1983. Petroleum provinces of the USSR. Moscow, Nedra, 272 p.

Doblas M., 1985. SC deformed rocks: the example of the Sierra de San Vicente sheared granitoids (Sierra de Gredos, Toledo, Spain). A.M. thesis, Harvard University, Cambridge, EEUU, 145 p. (unpublished).

Doblas M., 1987. Criterios del sentido del movimento en espejos de friccio'n: Classificacio'n y aplicacio'n a los granites cizallados de la Sierra de San Vicente (Sierra de Gredos). Estud. Geol., 43, 47–55.

Dyman T.S., Litinsky V.A. and Ulmishek G.F. 1999. Geology and Natural Gas Potential of Deep Sedimentary Basins in the Former Soviet Union. Denver, CO : U.S. Dept. of the Interior, U.S. Geological Survey Open-File Report 99-381, 36 p. (available at http://pubs.er.usgs.gov/publication/ofr99381).

Egamberdiev M.E. and Ishniyazov D.P., 1990. Comparative lithologic and facial-paleogeographic characteristics of lower-and middle Jurassic deposits of South Uzbekistan and North Afghanistan with hypothetical resources evaluation of coalfield. Report, Geology and Geophysics institute, Tashkent (in Russian).

Ershov A.V., Brunet M.-F., Nikishin A.M., Bolotov S.N., Nazarevich B.P. and Korotaev M.V., 2003. Northern Caucasus basin: thermal history and synthesis of subsidence models. In: Brunet M.-F. and Cloetingh S. (eds), Integrated PeriTethyan Basins Studies (Peri-Tethys Programme). Sedimentary Geology, 156/1-4, 95-118.

Fanti F., Contessi M., Nigarov A. and Esenov P., 2013. New Data on Two Large Dinosaur Tracksites from the Upper Jurassic of Eastern Turkmenistan (Central Asia). Ichnos, 20/2, 54–71.

Filippova I.B., Bush V.A. and Didenko A.N., 2001. Middle Paleozoic subduction belts: The leading factor in the formation of the Central Asian fold-and-thrust belt. Russian Journal of Earth Sciences, 3/6, 405–426.

Fürsich F.T., Brunet M.-F., Auxiètre J.-L. and Munsch H., 2015. Lower-Middle Jurassic facies patterns in the NW Afghan-Tajik Basin of southern Uzbekistan and their geodynamic context. In: M.-F. Brunet, T. McCann and E. R. Sobel (eds), Geological Evolution of Central Asian Basins and the Western Tien Shan Range. Geological Society, London, Special Publications, 427, http://doi.org/10.1144/SP427.9

Gafurova N., 1986. Baymurad field. Geological sections of wells, 1:10 000, Uzbekgeofizika, Tashkent.

Gafurova N., 1992. Buzatchi structure. Geological sections of wells, 1:10 000, Uzbekgeofizika, Tashkent.

Gagala L, 2014. Structural geometry and kinematics of the Tajik Depression, Central Asia: Neogene basin inversion in front of the Pamir salient. PhD Thesis, Technischen Universität Bergakademie Freiberg, Germany. 171p.

Gao J., Li M., Xiao X.C., Tang Y.Q. and He G.Q., 1998. Paleozoic Tectonic Evolution of the Tianshan Orogen, Northwestern China. Tectonophysics 287, 213–231.

Geological map of Uzbekistan, Shayakubov T. Sh. (ed.), 1998. Scale 1:500 000, State Committee for Geology and Mineral Resources of the Republic of Uzbekistan, Tashkent.

Grudsky P., 1988. Pachkamar-Amanata field. Synthetic geological-geophysical section, 1:2 000. Uzbekgeofizika, Tashkent.

Hendrix M.S., 2000. Evolution of Mesozoic sandstone compositions, southern Junggar, northern Tarim, and western Turpan basins, nortwestern China: a detrital record of the ancestral Tian Shan. Journal of Sedimentary Research, 70, 520–532.

Hendrix M.S., Graham S.A., Carroll A., Sobel E., McKnight C., Schulein B. and Wang Z., 1992. Sedimentary record and climatic implications of recurrent deformation in the Tian Shan: Evidence from Mesozoic strata of the north Tarim, south Dzungar, and Turpan basin, northwest China. Geological Society of America Bulletin, 104, 53–79.

Heubeck C., 2001. Assembly of Central Asia during the Middle and Late Paleozoic. Geological society of America, Memoir 194, 1–22.

International Commission on Stratigraphy, 2014. International Chronostratigraphic Chart (available at http://www.stratigraphy.org/index.php/ics-chart-timescale).

Isamuhamedova M., 1977. Shurtan field. Synthetic stratigraphic section, 1:2000, Uzbekgeofizika, Tashkent.

Isamuhamedova M., 1983. Pirnazar-Markovskoye field. Synthetic geological-geophysical section, 1:2000. Uzbekgeofizika, Tashkent.

Isamuhamedova M., 1987. Kruk field. Synthetic geological-geophysical section, 1:2000. Uzbekgeofizika, Tashkent.

Jackson J. and McKenzie D., 1984. Active tectonics of the Alpine-Himalayan belt between western Turkey and Pakistan. Geophys. J. R. Astron Soc., 77, 185–264.

Johnson C.L., Constenius K.C., Graham S.A., Mackey G., Menotti T., Payton A. and Tully J., 2015. Subsurface evidence for late Mesozoic extension in western Mongolia: tectonic and petroleum systems implications. Basin Research, 27, 3, 272-294.

Jolivet M., 2015. Mesozoic tectonic and topographic evolution of Central Asia and Tibet: a preliminary synthesis. In: M.-F. Brunet, T. McCann and E. R. Sobel (eds), Geological Evolution of Central Asian Basins and the Western Tien Shan Range. Geological Society, London, Special Publications, 427, http://doi.org/10.1144/SP427.6

Jolivet M., Arzhannikov S., Chauvet A., Arzhannikova A., Vassallo R., Kulagina N. and Akulova V., 2013. Accommodating large-scale intracontinental extension and compression in a single stress-field: A key example from the Baikal Rift System. Gondwana Research, 24, 918–935.

Jolivet M., Dominguez S., Charreau J., Chen Y., Li Y. and Wang Q., 2010. Mesozoic and Cenozoic tectonic history of the Central Chinese Tian Shan: Reactivated tectonic structures and active deformation. Tectonics, 29, TC6019, doi:10.1029/2010TC002712.

Jukovsky B., 1970. Karim field. Synthetic geological-geophysical section, 1:1000. Uzbekgeofizika, Tashkent.

Jukovsky B.L., 1993. Koshkuduk field. Synthetic geological-geophysical section, 1:2000. Uzbekgeofizika, Tashkent.

Khayitov N.Sh., 2006. Lithological-facial features and oil and gas perspectives of Lower Cretaceous sediments of Beshkent and Kashkadarya troughs. Thesis resume, Oil and Gas Institute, Tashkent, 28 (in Russian).

Khayitov N.Sh., 2013. Lithofacial and geochemical features of the oil and gas bearing Lower Cretaceous sediments in Uzbekistan. ISSN 2070-5379 Neftegasovaa geologia, Teoria i praktika, 8/4., http://www.ngtp.ru/rub/2013/49_2013.html (in Russian).

Kheraskova T.N., Bush V.A., Didenko A.N. and Samygin S.G., 2010. Breakup of Rodinia and early stages of evolution of the Paleoasian Ocean. Geotectonics, 44, 3–24.

Kim A.I., Salimova F.A., Abduasimova I.M. and Meshchankina N.A., 2007. Palaeontological atlas of Phanerozoic faunas and floras of Uzbekistan, volume II, Mesozoic and Cenozoic (Jurassic, Cretaceous, Palaeogene). Republic of Uzbekistan, State committee on geology and mineral resources, Tashkent, 261 p.

Kirshin A.V., 2007. Complex geological-geophysical researches of the Gissar block. Report, Oil and Gas Institute, Tashkent (in Russian).

Klett T.R., Ulmishek G.F., Wandrey C.J., Agena W.F. and U.S. Geological Survey-Afghanistan Ministry of Mines and Industry Joint Oil and Gas Resource Assessment Team, 2006. Assessment of Undiscovered Technically Recoverable Conventional Petroleum Resources of Northern Afghanistan. USGS Open-File Report 2006-1253, 237 p. and figures (available at http://pubs.usgs.gov/of/2006/1253/).

Klishevich V.L. and Khramov A.N., 1993. Reconstructions of Turkestan Paleo-ocean (Southern Tien Shan) for the Early Devonian. Geotectonics, 27, 326–335.

Klishevich V. and Khramov A., 1995. A paleogeodynamic model for the Urals–Tien Shan folded system for the Early Permian. Dokl. Ross. Akad. Nauk, 341/3, 381–385 (in Russian).

Klishevich V.L., Rzhevsky Y.S., Rodionov V.P. and Khramov A.N., 1992. Early Permian reconstruction of the Tien Shan region of Paleo-Tethys from paleomagnetic data. Soviet Geology, 12, 43–50 (in Russian).

Kominz M.A., Browning J.V., Miller K.G., Sugarman P.J., Mizintsevaw S. and Scotese C.R., 2008. Late Cretaceous to Miocene sea-level estimates from the New Jersey and Delaware coastal plain coreholes: an error analysis. Basin Research, 20, 211–226.

Koulakov I. and Sobolev S.V., 2006. A tomographic image of Indian lithosphere break-off beneath the Pamir-Hindukush region. Geoph. J. Intern., 164 (2), 425-440.

Koronovsky N.V., 2001. Isostasy. Soros educational journal, 11, 73–78 (in Russian).

Kravchenko K.N., 1979. Tectonic evolution of the Tien-Shan, Pamir and Karakorum. In: A. Farah and K.A. Dejong (eds), Geodynamics of Pakistan: Quetta, Geological Survey of Pakistan, 25–40.

Leith W., 1982. Rock assemblages in Central Asia and the evolution of the southern Asian margin. Tectonics, 3, 303–318.

Li G., 2011. World atlas of oil and gas basins. Wiley-Blackwell Editon, 196 p.

Loginova O., 1984. West Khodji field. Synthetic geological-geophysical section, 1:1000, Uzbekgeofizika, Tashkent.

Loginova O., 1992. South Alan field. Synthetic geological-geophysical section, 1:2000, Uzbekgeofizika, Tashkent.

Lukk A.A., Yunga S.L., Shevchenko V.I. and Hamburger M., 1995. Earthquake focal mechanisms, deformation state, and seismotectonics of the Pamir-Tien Shan region, central Asia. J. Geophys. Res., 100, B10, 20321–20343.

Maksimov S.P., Kleshchev K.A. and Shein, V.S. (eds), 1986. Geology and geodynamics of petroleum regions of the southern USSR. Moscow, Nedra, 232 p. (in Russian).

McCann T., 2015. The Jurassic of the Western Tien Shan: the Central Kyzylkum region, Uzbekistan. In: M.-F. Brunet, T. McCann and E.R. Sobel (eds), Geological Evolution of Central Asian Basins and the Western Tien Shan Range. Geological Society, London, Special Publications, 427, submitted.

McCann T., Nurtaev B., Kharin V. and Valdivia-Manchego M., 2013. Ordovician–Carboniferous tectono-sedimentary evolution of the North Nuratau region, Uzbekistan (Westernmost Tien Shan). Tectonophysics 590 (2013) 196–213.

McKenzie D., 1978. Some remarks on the development of sedimentary basins. Earth and Planet Sci. lett., 40, 25–32.

Mercier J. and Vergely P., 1992. Tectonique. Dunod, Paris, 214 p.

Michael A., 1984. Determination of stress from slip data: fault and folds. J. geophys. Res., B,89, 11 517–11 526.

Mirkamalov H.H., 1975. Sections and fauna of the Southwestern Gissar Cretaceous, Atlas, 36 p., Tashkent (in Russian).

Mirkamalov H.H., Abdullaev G.S., Evseeva G.B., Sudareva E.U., Ahmedova M.R., Haneeva F.R. and Muratova L.M., 2005. The studying of the Jurassic sediments of the Beshkent trough and nearby areas to precise its lithological-facial and stratigraphic structure and to determine its relations with the pre-Mesozoic complexes. Report, Oil and Gas Institute, Tashkent, 111 p. (in Russian).

Mitrofanova, Panova L.P. and Zueva S.A., 1981. Report about regional seismological survey in the northern part of the Kagan high and in the Karnabchul trough, provided in 1978-1981. Uzbekgeofizika, Tashkent (in Russian).

Mohadjer S., Bendick R., Ischuk A., Kuzikov S., Kostuk A., Saydullaev U., Lodi S., Makar D.M., Wasy A., Khan M.A., Molnar P., Bilham R. and Zubovich A.V., 2010. Partitioning of India-Eurasia convergence in the Pamir-Hindu Kush from GPS measurements. Geoph. Res. Intern., 37 (4), DOI:10.1029/2009GL041737.

Molnar P. and Tapponnier P., 1975. Cenozoic tectonics of Asia: Effects of a continental collision. Science, 189, 419–426.

Montenat C., 2009. The Mesozoic of Afghanistan. GeoArabia, 14/1, 147-210.

Mordvintsev O.P., 2004. Deep geological structure of the Western Uzbekistan. Thesis, Uzbekgeofizika, Tashkent, 290 p. (in Russian).

Mordvintsev O.P., 2008a. Map of the crystalline basement relief of the Bukhara-Khiva region, 1:200 000. Uzbekgeofizika, Tashkent.

Mordvintsev O.P., 2008b. Map of the pre-Jurassic thickness of the Bukhara-Khiva region, 1:200 000. Uzbekgeofizika, Tashkent.

Mordvintsev O.P., 2008c. Map of the pre-Jurassic relief of the Bukhara-Khiva region, 1:200 000. Uzbekgeofizika, Tashkent.

Mordvintsev O.P., 2012. Map of the Jurassic thickness (without salt-anhydrite pack) scale 1:100 000. Uzbekgeofizika, Tashkent.

Mordvintsev O.P. and Mordvintsev D.O., 2011. Nature of the 'anti Tien-Shan' flexure-fault zones and their role in the Central Asia-Kazakhstan region geological structure. Geology and mineral resources, 6, 41-46, Tashkent (in Russian).

Morozova N., 1983. Divalkak structure. Geological section of the Divalkak 1 well, Uzbekgeofizika, Tashkent.

Mukhin P.A., Abdullaev K.A., Minaev V.I., Khristov S.I. and Egamberdiev S.A., 1989. The Paleozoic geodynamics of Central Asia. International geological review, 30, 1073–1083.

Mukhin P.A., Karimov K.K. and Savchuk Y.S., 1991. Paleozoic geodynamics of Kyzylkum. Central Asia's Institute of geology and mineral resources, FAN, Tashkent, 146 p. (in Russian).

Müller, R.D., Sdrolias, M., Gaina, C., Steinberger, B. and Heine, C., 2008. Long-term sea-level fluctuations driven by ocean Basin dynamics. Science, 319, 1357–1362.

Natal'in B.A. and Şengör A.M.C., 2005. Late Palaeozoic to Triassic evolution of the Turan and Scythian platforms: The pre-history of the Palaeo-Tethyan closure. Tectonophysics, 404, 175–202.

Nikishin A.M., Cloetingh S., Bolotov S.N., Baraboshkin E.Y., Kopaevich L.F., Nazarevich B.P., Panov D.I., Brunet M.-F., Ershov A.V., Il'ina V.V., Kosova S.S. and Stephenson R.A., 1998. Scythian platform: chronostratigraphy and polyphase stages of tectonic history. In: S.Crasquin and E.Barrier (eds), Peri-Tethys Memoir 3 : Epicratonic Basins of Peri-Tethyan Platforms. Mémoires du Muséum national d'Histoire naturelle, 177, 151–162.

Nikolaev V.G., 2002. Afghan–Tajik depression: Architecture of sedimentary cover and evolution. Russian Journal of Earth Sciences, 4/6, 399–421.

Nugmanov A.H., 2009a. Paleotectonic scheme of the Jurassic Lower Kugitang carbonate sediments of the Bukhara-Khiva and Southwestern Gissar regions. Paleotectonic scheme of the Jurassic Upper Kugitang carbonate sediments of the Bukhara-Khiva and Southwestern Gissar regions. Oil and Gas Institute, Tashkent.

Nugmanov A.H. 2009b. Geological line Kuldjuktau-Farab. Oil and gas institute, Tashkent.

Nugmanov A.H and Jdanova E.N., 2004. Paleotectonic scheme of the Jurassic terrigenous sediments of the Bukhara-Khiva and Southwestern Gissar regions. Oil and Gas Institute, Tashkent.

Nurtaev B., Kharin V., McCann T. and Valdivia-Manchego M., 2013. The North Nuratau Fault Zone, Uzbekistan—Structure and evolution of Palaeozoic Suture Zone. Journal of Geodynamics, 64, 1–14.

Ostrovsky. S. 1965. Geological section of the Yangikazgan field. Geological Committee of UzSSR, Tashkent.

Pechersky D. and Didenko A., 1995. Paleo-Asian Ocean: Petromagnetic and Paleomagnetic Information on its Lithosphere. Moscow, 296 p. (in Russian).

Petit J.P. and Laville E., 1987. Morphology and microstructures of hydroplastic slickensides in sandstones. Geological Society, London, Special Publications, 29, 107–121.

Petit. J.P., Proust F. and Tapponnier P., 1983. Critères du sens du mouvement sur les miroirs de failles en roches non calcaires. Bull. Soc. Géol. Fr., 7, 589–608.

Pikovsky M. and Cherkashina L.G., 1971. Report about regional seismic survey by RCM in the central part of the Bukhara-Khiva oil and gas province, provided in 1970-1971. Uzbekgeofizika, Tashkent (in Russian).

Portnyagin E.A., 1974. Sheet dykes complex of the Southern Hissar. Doklady Akademii Nauk USSR, 219/4, 948–951 (in Russian).

Reches Z., 1987. Determination of the tectonic stress tensor from slip that obey the Coulomb yield criterion. Tectonics, 6, 849–861.

Reiter K., Kukowski N. and Ratschbacher L., 2011. The interaction of two indenters in analogue experiments and implications for curved fold-and-thrust belts. Earth and Planet. Sci. let., 302, 132-146.

Repman E.A. 1964. Age of the Gaurdak formation of the Southwestern Gissar region. Geology and Geophysics Institute scientific publications, 3, 204–206 (in Russian).

Ricou L.E., 1996. The plate tectonic history of the past Tethys Ocean. In: A.E.M. Nairn, L.E. Ricou, B. Vrielynck, and J. Dercourt (eds), The Ocean Basins and Margins, vol.8: The Tethys Ocean, Plenum Press, New York, 3–70.

Ruzhentsev S.V. and Mossakovsky A.A., 1996. Geodynamics and tectonic evolution of the Central Asian Paleozoic structures as the result of the interaction between the Pacific and Indo-Atlantic segments of the Earth. Geotectonics, 29, 294–311.

Safonova L., 1985. East Uchbash structure. Geological sections of wells, 1:10 000. Uzbekgeofizika, Tashkent.

Searle M.P., 1996. Geological evidence against large scale pre-Holocene offsets along the Karakoram fault: Implications for the limited extrusion of the Tibetan plateau. Tectonics, 15, 171–186.

Seltmann R., Konopelko D., Biske G., Divaev F. and Sergeev S., 2011. Hercynian postcollisional magmatism in the context of Paleozoic magmatic evolution of the Tien Shan orogenic belt. Journal of Asian Earth Sciences, 42, 821–838.

Şengör A.M.C. and Natal'in B.A., 2004. Phanerozoic analogues of Archean oceanic basement fragments: Altaid ophiolites and ophirags. In: T.M. Kusky (ed.), Precambrian Ophiolites and Related Rocks. Elsevier, Amsterdam, 675–726.

Şengör A.M.C., Natal'in B., van der Voo R. and Sunal G., 2014. A new look at the Altaids: A superorogenic complex in northern and central Asia as a factory of continental crust. Part II: palaeomagnetic data, reconstructions, crustal growth and global sea-level. Austrian Journal of Earth Sciences, 107/2, 131–181.

Séranne M., 2014. Cours M1 Bassins, Basin Dynamics Rifts2. (available at http://www.gm.univ-montp2.fr/spip.php?article1782 and http://www.gm.univ-montp2.fr/IMG/pdf/BasinDynamics-rifts2-3.pdf).

Shayakubov, T.Sh. and Dalimov T.N. (eds), 1998. Geology and mineral resources of the Republic of Uzbekistan. National University of Uzbekistan, Tashkent, 723 p. (in Russian).

Shein V., 1985. A geodynamic model for the petroliferous regions of the southern USSR. International Geology Review, 27/3, 253–266.

Sokolova I.M., Abryutina N.I., Makarov V.V., Kuldzhaev B.A., Rusinova G.V. and Petrov Al.A., 1993. Biomarkers in gas condensates of eastern Turkmenistan. Geokhimiya, 1, 123–130.

Steckler M.S. and Watts A.B., 1978. Subsidence of the atlantic-type continental margin off New York. Earth and Planetary Science Letters, 41, 1–13.

Storojenko N., 1980. Chandir field. Synthetic geological-geophysical section, 1:2000. Uzbekgeofizika, Tashkent.

Su W., Gao J., Klemd R., Li J.L., Zhang X., Li X.H., Chen N.S. and Zhang L., 2010. U-Pb zircon geochronology of Tianshan eclogites in NW China: Implication for the collision between the Yili and Tarim blocks of the southwestern Altaids. Eur. J. Mineral., 22/4, 473–478.

Tal-Virsky B.B. (ed.), 1967. Map of relief of Central Asia's west part infolded basement (scale 1:100 000). Tashkent.

Tal-Virsky B.B. and Fuzailov I.A. 1991. Map of magnetic anomaly of Central Asia, 1:1 500 000. National University of Uzbekistan, National technic University of Uzbekistan, Tashkent.

Talwani M., Belopolsky A. and Berry D.L., 1998. Geology and petroleum potential of Central Asia. The James A. Barker III Institute For Public Policy, Rice University, 25 p. (available at http://bakerinstitute.org/files/2682/).

Tevelev A.V. and Georgievskii B.V., 2012. Deformation History and Hydrocarbon Potential of the Southwestern Gissar Range (Southern Uzbekistan). Moscow University Geology Bulletin, 67/6, 340–352.

Thomas J.C., Cobbold P.R., Shein V.S. and Le Douaran S., 1995. Late Palaeozoic to recent development of sedimentary basins on the Turan and South Kazakh platforms, Central Asia. Paper presented at International Conference, Am. Ass. of Pet. Geol., Nice, 1995, France.

Thomas J.C., Cobbold P.R., Shein V.S. and Le Douaran S., 1999. Sedimentary record of late Paleozoic to Recent tectonism in central Asia – analysis of subsurface data from the Turan and south Kazak domains. Tectonophysics, 313, 243–263.

Thomas J.C., Perroud H., Cobbold P., Bazhenov M.L., Burtman V.S., Chauvin A. and Sadybakasov E., 1993. A paleomagnetic study of Tertiary formation of the Kirghiz Tien-Shan and its tectonic implications. J. Geophys. Res., 98, 9571-9589.

Trifonov V.G., Ivanova T.P. and Bachmanov D.M., 2011. Recent Mountain Building of the Central Alpine–Himalayan Belt. ISSN 0016_8521, Geotectonics, 46/5, 315–332.

Troisky V.I. 1967. Upper Triassic and Jurassic sediments of the southern Uzbekistan. Nedra, Leningrad, 312 p. (in Russian).

Troitsky V.I., 2005. Geodynamic regionalization of the Paleozoic structures of the Tien-Shan and Pamir. National University of Uzbekistan Newsletter, 1, Tashkent (in Russian).

Troitsky V.I., 2012. Oceanic basins and fold system of the Middle and High Asia, LAP, Lambert Academic Publishing (in Russian).

Tulyaganov H.T. and Yaskovich B.V., 1980. Explanatory report for the Geological map of the UzSSR, Tashkent, 157–175 (in Russian).

Ulmishek G.F., 2004. Petroleum Geology and Resources of the Amu-Darya Basin, Turkmenistan, Uzbekistan, Afghanistan, and Iran. U.S. Geological Survey Bulletin 2201–H, 32 p. (available at http://pubs.usgs.gov/bul/2201/H/).

Uzakov K.U., 1985. Lithological and biostratigraphical characteristics of the Upper Paleozoic sediments of the Bukhara-Karshi region. Uzbekistan geological oil and gas journal, 3.

Wallace R.E. 1951. Geometry of shearing stress and relation to faulting. J. Geol., 59, 118–130.

Wang B., Faure M., Shu L., Cluzel D., Charvet J., de Jong K. and Chen Y., 2008. Paleozoic Tectonic Evolution of the Yili Block, Western Chinese Tianshan. Bull. Soc. Géol. Fr., 179, 483–490.

Wang B., Shu L. S., Faure M., Jahn B. M., Cluzel D., Charvet J., Chung S.L. and Meffre S., 2011. Paleozoic tectonics of the Southern Tianshan: New insights from structural, chronological, and geochemical studies of the Heiyingshan ophiolitic melange (NW China). Tectonophysics, 497, 85–104.

Ward P. D., 1990. The Cretaceous/Tertiary extinctions in the marine realm. A 1990 perspective: Special Paper of the Geological Society of America, 247, 425–432.

Wilhem C., Windley B.F. and Stampfli G.M., 2012. The Altaids of Central Asia: A tectonic and evolutionary innovative review. Earth-Science Reviews, 113, 303–341.

Windley B.F., Alexeiev D., Xiao W., Kröner A., and Badarch G., 2007. Tectonic models for accretion of the Central Asian Orogenic Belt. Journal of the Geological Society, London, 164, 31–47.

Xiao, W. J., Huang B.C., Han C.M., Sun S. and Li J.L., 2010. A review of the western part of the Altaids: A key to understanding the architecture of accretionary orogens. Gondwana Res., 18/2–3, 253–273.

Yegorkin A.V., Abramson R.I. and Astaf'eva M.I. 1962. Report about the regional seismic survey by DSS method along the profile 081 Farab high – Babatag range. Uzbekgeofizika, Tashkent (in Russian).

Zanchetta S., Berra F., Zanchi A., Bergomi M., Caridroit M., Nicora A. and Heidarzadeh G., 2013. The record of the Late Palaeozoic active margin of the Palaeotethys in NE Iran: Constraints on the Cimmerian orogeny. Gondwana Research, 24, 1237–1266.

Zhang, L.F., Ai, Y.L., Li, X.P., Rubatto, D., Song, B., Williams, S., 2007. Triassic collision of western Tianshan orogenic belt, UHP eclogitic rocks. Lithos, 96, 266–280.

Zonenshain L.P., Kuz`min M.I. and Natapov L.V., 1990. Tectonics of lithosphere plates of the USSR territory. Moscow, Nedra. Part 1, 328 p. Part 2, 334 p.

Zuev S., 1997. Khodjamubarek structure. Synthetic geological section, 1:1000, Uzbekgeofizika, Tashkent.

Mordvintsev Dmitriy – Thèse de doctorat – 2015

Evolution tectono-stratigraphique de la marge nord du bassin de l'Amou-Daria en Ouzbékistan (régions de Boukhara-Khiva et du sud-ouest Ghissar)

Résumé :

L'objectif principal de cette thèse est la reconstruction de l'évolution tectonique et stratigraphique de la marge nord du bassin de l'Amou-Daria et du nord-ouest du bassin Afghan-Tadjik dans le sud-ouest de l'Ouzbékistan (régions de Boukhara-Khiva et SW Ghissar).

Nous avons utilisé des données géologiques-géophysiques pour construire 8 coupes géologiques-géophysiques. Deux de ces coupes sont parallèles à la région de Boukhara-Khiva, les six autres la recoupent du nord au sud. Les caractères principaux des surfaces pré-Mésozoïque et Mésozoiques ont été observés ainsi que les failles principales, hauts et dépressions.

Une autre partie de la thèse est consacrée à l'analyse de la subsidence, réalisée à partir de 18 puits choisis dans la région. La comparaison des taux de subsidence montre une subsidence tectonique active de la fin du Jurassique inférieur au Jurassique moyen et des événements mineurs au cours du Crétacé inférieur et du Turonien.

Une analyse de tectonique cassante, comprenant des travaux de terrain, a été menée dans la chaîne du SW Ghissar. Des populations de failles ont été mesurées dans les carbonates du Jurassique moyen-supérieur. Les résultats indiquent que les failles normales sont associées à une extension de direction NE qui s'est développée dans la marge nord du bassin de l'Amou-Daria au cours du Jurassique moyen supérieur.

Nos résultats montrent que l'évolution du bassin de l'Amou-Daria est liée au développement de la marge nord de l'océan néo-téthysien au Mésozoïque. La subduction vers le nord de la Néo-Téthys sous l'Eurasie durant le Jurassique a induit un régime extensif dans la plaque Touran chevauchante et l'ouverture du bassin de l'Amou-Daria.

Mots clés : Ouzbékistan ; tectonique ; subsidence ; sismique ; Ghissar ; Boukara-Khiva

Tectono-stratigraphic evolution of the northern margin of the Amu-Darya basin in Uzbekistan (Bukhara-Khiva and Southwestern Gissar regions)

Abstract:

The main aim of this thesis is reconstructing the tectono-stratigraphic evolution of the northern margin of the Amu-Darya basin and northwestern part of the Afghan-Tajik basin in southwestern Uzbekistan (Bukhara-Khiva and Southwestern Gissar regions).

We have used a complex of geological-geophysical data for the construction of 8 geological-geophysical sections. Two lines are parallel to the Bukhara-Khiva region, while other six cross it from the north to the south. The principal features of the pre-Mesozoic and Mesozoic surfaces were observed. The main faults, highs and lows were also determined.

Another part of the study is the tectonic subsidence analysis, performed through 18 wells, chosen for the area. The comparison of the tectonic subsidence rates shows an active tectonic subsidence during the late Early Jurassic to Middle Jurassic, and minor events during the Early Cretaceous and the Turonian.

The fault tectonic analysis, including fieldworks, has been performed in the Southwestern Gissar Mountains. We mainly analysed the faults population in the Middle-Late Jurassic carbonates. The results indicate that normal faulting developed during the Middle-Late Jurassic associated with the NE-trending extension that developed in the northern margin of the Amu-Darya basin.

All of the results show that the Amu-Darya basin evolution is strongly connected to the Mesozoic development of the northward subduction of the Tethys Oceanic domain beneath the Central Asia margin. During the Jurassic, the northward subduction of the Neo-Tethys beneath Eurasia generated extensional stress fields in the overriding Turan platform which originated the Amu-Darya basin.

Keywords : Uzbekistan ; tectonics ; subsidence ; seismics ; Gissar ; Bukhara-Khiva.